

# MOLECULAR MECHANISMS AND NEW THERAPEUTIC TARGETS IN EPITHELIAL TO MESENCHYMAL TRANSITION (EMT) AND FIBROSIS

EDITED BY: Cecilia Battistelli, Marc Diederich, Timothy Joseph Keane,  
Pilar Sandoval, Sergio Valente and Raffaele Strippoli  
PUBLISHED IN: Frontiers in Pharmacology





# frontiers

## Frontiers eBook Copyright Statement

The copyright in the text of individual articles in this eBook is the property of their respective authors or their respective institutions or funders. The copyright in graphics and images within each article may be subject to copyright of other parties. In both cases this is subject to a license granted to Frontiers.

The compilation of articles constituting this eBook is the property of Frontiers.

Each article within this eBook, and the eBook itself, are published under the most recent version of the Creative Commons CC-BY licence.

The version current at the date of publication of this eBook is CC-BY 4.0. If the CC-BY licence is updated, the licence granted by Frontiers is automatically updated to the new version.

When exercising any right under the CC-BY licence, Frontiers must be attributed as the original publisher of the article or eBook, as applicable.

Authors have the responsibility of ensuring that any graphics or other materials which are the property of others may be included in the CC-BY licence, but this should be checked before relying on the CC-BY licence to reproduce those materials. Any copyright notices relating to those materials must be complied with.

Copyright and source acknowledgement notices may not be removed and must be displayed in any copy, derivative work or partial copy which includes the elements in question.

All copyright, and all rights therein, are protected by national and international copyright laws. The above represents a summary only. For further information please read Frontiers' Conditions for Website Use and Copyright Statement, and the applicable CC-BY licence.

ISSN 1664-8714

ISBN 978-2-88963-502-3

DOI 10.3389/978-2-88963-502-3

## About Frontiers

Frontiers is more than just an open-access publisher of scholarly articles: it is a pioneering approach to the world of academia, radically improving the way scholarly research is managed. The grand vision of Frontiers is a world where all people have an equal opportunity to seek, share and generate knowledge. Frontiers provides immediate and permanent online open access to all its publications, but this alone is not enough to realize our grand goals.

## Frontiers Journal Series

The Frontiers Journal Series is a multi-tier and interdisciplinary set of open-access, online journals, promising a paradigm shift from the current review, selection and dissemination processes in academic publishing. All Frontiers journals are driven by researchers for researchers; therefore, they constitute a service to the scholarly community. At the same time, the Frontiers Journal Series operates on a revolutionary invention, the tiered publishing system, initially addressing specific communities of scholars, and gradually climbing up to broader public understanding, thus serving the interests of the lay society, too.

## Dedication to Quality

Each Frontiers article is a landmark of the highest quality, thanks to genuinely collaborative interactions between authors and review editors, who include some of the world's best academicians. Research must be certified by peers before entering a stream of knowledge that may eventually reach the public - and shape society; therefore, Frontiers only applies the most rigorous and unbiased reviews.

Frontiers revolutionizes research publishing by freely delivering the most outstanding research, evaluated with no bias from both the academic and social point of view. By applying the most advanced information technologies, Frontiers is catapulting scholarly publishing into a new generation.

## What are Frontiers Research Topics?

Frontiers Research Topics are very popular trademarks of the Frontiers Journals Series: they are collections of at least ten articles, all centered on a particular subject. With their unique mix of varied contributions from Original Research to Review Articles, Frontiers Research Topics unify the most influential researchers, the latest key findings and historical advances in a hot research area! Find out more on how to host your own Frontiers Research Topic or contribute to one as an author by contacting the Frontiers Editorial Office: [researchtopics@frontiersin.org](mailto:researchtopics@frontiersin.org)



# MOLECULAR MECHANISMS AND NEW THERAPEUTIC TARGETS IN EPITHELIAL TO MESENCHYMAL TRANSITION (EMT) AND FIBROSIS

Topic Editors:

**Cecilia Battistelli**, Sapienza University of Rome, Italy

**Marc Diederich**, Seoul National University, South Korea

**Timothy Joseph Keane**, Imperial College London, United Kingdom

**Pilar Sandoval**, Severo Ochoa Molecular Biology Center (CSIC-UAM), Spain

**Sergio Valente**, Sapienza University of Rome, Italy

**Raffaele Strippoli**, Sapienza University of Rome, Italy

**Citation:** Battistelli, C., Diederich, M., Keane, T. J., Sandoval, P., Valente, S., Strippoli, R., eds. (2020). Molecular Mechanisms and New Therapeutic Targets in Epithelial to Mesenchymal Transition (EMT) and Fibrosis. Lausanne: Frontiers Media SA. doi: 10.3389/978-2-88963-502-3

# Table of Contents

- 05 Editorial: Molecular Mechanisms and New Therapeutic Targets in Epithelial to Mesenchymal Transition (EMT) and Fibrosis**  
Cecilia Battistelli, Marc Diederich, Timothy Joseph Keane, Pilar Sandoval, Sergio Valente and Raffaele Strippoli
- 07 SMO Inhibition Modulates Cellular Plasticity and Invasiveness in Colorectal Cancer**  
Paolo Magistri, Cecilia Battistelli, Raffaele Strippoli, Niccolò Petrucciani, Teijo Pellinen, Lucia Rossi, Livia Mangogna, Paolo Aurello, Francesco D'Angelo, Marco Tripodi, Giovanni Ramacciato and Giuseppe Nigri
- 20 Tacrolimus Reverses UVB Irradiation-Induced Epidermal Langerhans Cell Reduction by Inhibiting TNF- $\alpha$  Secretion in Keratinocytes via Regulation of NF- $\kappa$ B/p65**  
JiaLi Xu, YaDong Feng, GuoXin Song, QiXing Gong, Li Yin, YingYing Hu, Dan Luo and ZhiQiang Yin
- 29 Downregulation of TLR4 by miR-181a Provides Negative Feedback Regulation to Lipopolysaccharide-Induced Inflammation**  
Kangfeng Jiang, Shuai Guo, Tao Zhang, Yaping Yang, Gan Zhao, Aftab Shaukat, Haichong Wu and Ganzhen Deng
- 42 Effects of Simultaneous Downregulation of PHD1 and Keap1 on Prevention and Reversal of Liver Fibrosis in Mice**  
Jing Liu, Wencai Li, Manoj H. Limbu, Yiping Li, Zhi Wang, Zhengyuan Cheng, Xiaoyi Zhang and Pingsheng Chen
- 51 Casein Kinase 1 $\delta/\epsilon$  Inhibitor, PF670462 Attenuates the Fibrogenic Effects of Transforming Growth Factor- $\beta$  in Pulmonary Fibrosis**  
Christine R. Keenan, Shenna Y. Langenbach, Fernando Jativa, Trudi Harris, Meina Li, Qianyu Chen, Yuxiu Xia, Bryan Gao, Michael J. Schuliga, Jade Jaffar, Danica Prodanovic, Yan Tu, Asres Berhan, Peter V. S. Lee, Glen P. Westall and Alastair G. Stewart
- 66 Fisetin Inhibited Growth and Metastasis of Triple-Negative Breast Cancer by Reversing Epithelial-to-Mesenchymal Transition via PTEN/Akt/GSK3 $\beta$  Signal Pathway**  
Jie Li, Xia Gong, Rong Jiang, Dan Lin, Tao Zhou, Aijie Zhang, Hongzhong Li, Xiang Zhang, Jingyuan Wan, Ge Kuang and Hongyuan Li
- 80 miR-374a Regulates Inflammatory Response in Diabetic Nephropathy by Targeting MCP-1 Expression**  
Zijun Yang, Zuishuang Guo, Ji Dong, Shifeng Sheng, Yulin Wang, Lu Yu, Hongru Wang and Lin Tang
- 88 P311, Friend, or Foe of Tissue Fibrosis?**  
Leslie Stradiot, Inge Mannaerts and Leo A. van Grunsven
- 101 Gremlin Regulates Tubular Epithelial to Mesenchymal Transition via VEGFR2: Potential Role in Renal Fibrosis**  
Laura Marquez-Exposito, Carolina Lavozy, Raul R. Rodrigues-Diez, Sandra Rayego-Mateos, Macarena Orejudo, Elena Cantero-Navarro, Alberto Ortiz, Jesús Egido, Rafael Selgas, Sergio Mezzano and Marta Ruiz-Ortega

- 116** *Low Expression of miR-466f-3p Sustains Epithelial to Mesenchymal Transition in Sonic Hedgehog Medulloblastoma Stem Cells Through Vegfa-Nrp2 Signaling Pathway*

Zein Mersini Besharat, Claudia Sabato, Agnese Po, Francesca Gianno, Luana Abballe, Maddalena Napolitano, Evelina Miele, Felice Giangaspero, Alessandra Vacca, Giuseppina Catanzaro and Elisabetta Ferretti
- 122** *Glutamyl-Prolyl-tRNA Synthetase Regulates Epithelial Expression of Mesenchymal Markers and Extracellular Matrix Proteins: Implications for Idiopathic Pulmonary Fibrosis*

Dae-Geun Song, Doyeun Kim, Jae Woo Jung, Seo Hee Nam, Ji Eon Kim, Hye-Jin Kim, Jong Hyun Kim, Cheol-Ho Pan, Sunghoon Kim and Jung Weon Lee
- 133** *Dual Tumor Suppressor and Tumor Promoter Action of Sirtuins in Determining Malignant Phenotype*

Vincenzo Carafa, Lucia Altucci and Angela Nebbioso
- 147** *Estrogens Modulate Somatostatin Receptors Expression and Synergize With the Somatostatin Analog Pasireotide in Prostate Cells*

Valentina Rossi, Erika Di Zazzo, Giovanni Galasso, Caterina De Rosa, Ciro Abbondanza, Antonio A. Sinisi, Lucia Altucci, Antimo Migliaccio and Gabriella Castoria
- 159** *Wedelolactone Attenuates Pulmonary Fibrosis Partly Through Activating AMPK and Regulating Raf-MAPKs Signaling Pathway*

Jin-yu Yang, Li-jun Tao, Bei Liu, Xin-yi You, Chao-feng Zhang, Hai-feng Xie and Ren-shi Li
- 171** *Therapeutic Targeting of Fibrotic Epithelial-Mesenchymal Transition—An Outstanding Challenge*

Attila Fintha, Ákos Gasparics, László Rosivall and Attila Sebe
- 182** *Natural Plants Compounds as Modulators of Epithelial-to-Mesenchymal Transition*

Lorena Avila-Carrasco, Pedro Majano, José Antonio Sánchez-Toméro, Rafael Selgas, Manuel López-Cabrera, Abelardo Aguilera and Guadalupe González Mateo
- 206** *TGF $\beta$  Impairs HNF1 $\alpha$  Functional Activity in Epithelial-to-Mesenchymal Transition Interfering With the Recruitment of CBP/p300 Acetyltransferases*

Francesca Bisceglia, Cecilia Battistelli, Valeria Noce, Claudia Montaldo, Agatino Zammataro, Raffaele Strippoli, Marco Tripodi, Laura Amicone and Alessandra Marchetti



# Editorial: Molecular Mechanisms and New Therapeutic Targets in Epithelial to Mesenchymal Transition (EMT) and Fibrosis

**Cecilia Battistelli<sup>1</sup>, Marc Diederich<sup>2</sup>, Timothy Joseph Keane<sup>3</sup>, Pilar Sandoval<sup>4</sup>, Sergio Valente<sup>5</sup> and Raffaele Strippoli<sup>1,6\*</sup>**

<sup>1</sup>Department of Molecular Medicine, Sapienza University of Rome, Rome, Italy, <sup>2</sup>Department of Pharmacy, Seoul National University, Seoul, South Korea, <sup>3</sup>Department of Materials, Imperial College London, London, United Kingdom, <sup>4</sup>Severo Ochoa Molecular Biology Center (CSIC-UAM), Madrid, Spain, <sup>5</sup>Department of Chemistry and Technologies of Drugs, Sapienza University of Rome, Rome, Italy, <sup>6</sup>National Institute for Infectious Diseases L. Spallanzani IRCCS, Rome, Italy

**Keywords:** natural compound, EMT, fibrosis, epigenetics, non-coding RNAs, therapeutic targets

## Editorial on the Research Topic

### Molecular Mechanisms and New Therapeutic Targets in Epithelial to Mesenchymal Transition (EMT) and Fibrosis

## OPEN ACCESS

### Edited by:

Dieter Steinhilber,  
Goethe University Frankfurt,  
Germany

### Reviewed by:

Melania Dovizio,  
Università degli Studi G. d'Annunzio  
Chieti e Pescara, Italy

### \*Correspondence:

Raffaele Strippoli  
raffaele.strippoli@uniroma1.it

### Specialty section:

This article was submitted to  
Inflammation Pharmacology,  
a section of the journal  
Frontiers in Pharmacology

**Received:** 06 November 2019

**Accepted:** 02 December 2019

**Published:** 16 January 2020

### Citation:

Battistelli C, Diederich M, Keane TJ,  
Sandoval P, Valente S and Strippoli R  
(2020) Editorial: Molecular  
Mechanisms and New Therapeutic  
Targets in Epithelial to Mesenchymal  
Transition (EMT) and Fibrosis.  
Front. Pharmacol. 10:1556.  
doi: 10.3389/fphar.2019.01556

Although the term “epithelial to mesenchymal transformation” was used for the first time by Betty Hay in 1968, the earliest description of the EMT process probably dates back to drawings made by the Nobel Prize Santiago Ramón y Cajal around 1890 (López-Novoa and Nieto, 2009).

After decades of studies, EMT is now considered a key physiopathological mechanism active in embryogenesis, in fibrotic diseases and in cancer. The scope of this research topic was to provide an updated overview of EMT processes and new therapeutic strategies aimed to target EMT processes. In this Topic, Fintha et al. provided a timely survey on the “fibroblast conversion” hypothesis (with a focus on renal fibrosis), where epithelial cell transdifferentiation plays a crucial role in the generation of myofibroblasts, the main cells implicated in organ fibrosis. The ‘fibroblast conversion’ hypothesis has been intensely debated over years, with some contradicting evidence in different experimental systems used.

The contribution of different molecular mechanisms to the initiation of EMT is elucidated by various research articles in this topic. TGFβ is universally known as the main extracellular biochemical EMT promoter. In this topic, the role of other extracellular mediators is discussed. The importance of the gremlin-VEGF2 axis in the genesis of renal fibrosis is discussed by Marquez-Esposito et al. Sonic Hedgehog (SHH) is an extracellular mediator with a role in cellular plasticity in various organs. Magistri et al. analyzed the effect of the inhibition of Smoothened (SMO), an intracellular mediator of SHH signaling, in the control of EMT and invasion in colon carcinoma. Besharat et al. analyzed the intracellular regulation of SHH and interference with VEGF-A/neuropilin signalling in EMT in medulloblastoma. In another study by Rossi et al., the EMT state of different prostate carcinoma cell lines was found differentially responsive to the combination of estrogens and somatostatin derivatives.

Biochemical extracellular mediators promote changes in cell plasticity by inducing specific intracellular pathways. In this topic, the role of pathways alternative to the TGFβ classical pathways,

such as SMADs, were analyzed. In particular, using a specific pharmacological inhibitor, Keenan et al. studied the role of casein kinase 1 delta and epsilon in pulmonary fibrosis. In a detailed review article, Stradiot et al. discussed the role of P311, an RNA binding protein implicated in the control of TGF $\beta$  translation in organ fibrosis. Moreover, Song et al. analyzed the role of glutamyl-prolyl-tRNA synthetase in the genesis of idiopathic pulmonary fibrosis. Liu et al. analyzed the role of two genes implicated in the oxidative response, PHD1 and KEAP, in controlling bleomycin -induced liver fibrosis in mice.

The changes of the cell proteome occurring during EMT are controlled by a limited number of master genes. Bisceglia et al. explored the mechanism by which the activity of HNF1, a master gene of epithelial differentiation, is impaired by TGF $\beta$  via altered recruitment of CBP-p300 acetyltransferase.

Recent studies unveiled the role of epigenetics in the control of EMT/MET dynamics and in general in cellular plasticity. A review article by Carafa et al. analyzed the dual role of sirtuins, class III histone deacetylases, in both promoting and limiting three main processes related to tumor transformation, i.e., EMT, invasion, and metastasis. Besides histone acetyltransferases and deacetylases, epigenetic control is exerted by non-coding RNAs. Among them, microRNAs may post-transcriptionally target the expression of genes relevant for cell plasticity. Jiang et al. analyzed the role of miR-181a in the downregulation of TLR4. TLR mediated activation of NF- $\kappa$ B p65 and ROS pathways controls LPS-induced lung inflammation, which is connected to EMT and fibrosis. Also, Yang et al. demonstrated that miR-374 regulates the inflammatory response in diabetic nephropathy targeting CCL2/MCP1 expression. The induction of this

chemokine contributes in turn to increased expression of inflammatory cytokines, such as TNF $\alpha$  and IL-6. Moreover, Besharat et al. analyzed the role of miR-466f-3p in the inhibition of EMT features in medulloblastoma.

Tightly connected with the analysis of molecular mechanisms is the search of new therapeutic targets to control and revert EMT and fibrosis. Emphasis has been given in this topic to natural compounds. Avila-Carrasco et al. provided an extensive survey of natural plant compounds reported to be active in targeting various pathways active in EMT. Other studies analyzed the effect of single derivatives. Wedelolactone, a major coumarin derivative of *E. prostrata*, was reported by Yang et al. to attenuate pulmonary fibrosis in a murine model by acting on AMPK and MAPK pathways. Also, fisetin, a natural flavonoid, was shown by Li et al. to reverse EMT features in triple negative breast cancer cell lines through regulation of (PI3K)-Akt-GSK-3 $\beta$  signaling pathway. Lastly, Xu et al. demonstrated that Tacrolimus, a calcineurin inhibitor, blocks TNF- $\alpha$  secretion and inflammation by interacting with NF- $\kappa$ B p65 activation in cultured epithelial tissue.

In summary, the broad coverage in this Topic provides several new perspectives on molecular aspects and novel therapeutic approaches aimed at counteracting and reversing EMT and fibrosis.

## AUTHOR CONTRIBUTIONS

All the authors have contributed to the composition and the revision of this Editorial Article.

## REFERENCE

- López-Novoa, J. M., and Nieto, M. A. (2009). Inflammation and EMT: an alliance towards organ fibrosis and cancer progression. *EMBO Mol. Med.* Sep1 (6–7), 303–314. doi: 10.1002/emmm.200900043

**Conflict of Interest:** The authors declare that the research was conducted in the absence of any commercial or financial relationships that could be construed as a potential conflict of interest.

Copyright © 2020 Battistelli, Diederich, Keane, Sandoval, Valente and Strippoli. This is an open-access article distributed under the terms of the Creative Commons Attribution License (CC BY). The use, distribution or reproduction in other forums is permitted, provided the original author(s) and the copyright owner(s) are credited and that the original publication in this journal is cited, in accordance with accepted academic practice. No use, distribution or reproduction is permitted which does not comply with these terms.



# SMO Inhibition Modulates Cellular Plasticity and Invasiveness in Colorectal Cancer

Paolo Magistri<sup>1†</sup>, Cecilia Battistelli<sup>2†</sup>, Raffaele Strippoli<sup>2†</sup>, Niccolò Petrucciani<sup>1</sup>, Teijo Pellinen<sup>3</sup>, Lucia Rossi<sup>2</sup>, Livia Mangogna<sup>1</sup>, Paolo Aurello<sup>1</sup>, Francesco D'Angelo<sup>1</sup>, Marco Tripodi<sup>2</sup>, Giovanni Ramacciato<sup>1</sup> and Giuseppe Nigri<sup>1\*</sup>

<sup>1</sup> Department of Medical and Surgical Sciences and Translational Medicine, Sapienza—University of Rome, Rome, Italy,

<sup>2</sup> Molecular Genetics Section, Department of Cellular Biotechnology and Hematology, Sapienza—University of Rome, Rome, Italy, <sup>3</sup> FIMM Institute for Molecular Medicine Finland, Helsinki, Finland

## OPEN ACCESS

### Edited by:

Giovanni Li Volti,  
Università degli Studi di Catania, Italy

### Reviewed by:

Richard T. Premont,  
Duke University, United States  
Barbara Stecca,  
Azienda Ospedaliero-Universitaria  
Careggi, Italy  
Massimo Donadelli,  
University of Verona, Italy

### \*Correspondence:

Giuseppe Nigri  
giuseppe.nigri@uniroma1.it

<sup>†</sup>These authors have contributed  
equally to this work.

### Specialty section:

This article was submitted to  
Experimental Pharmacology and Drug  
Discovery,  
a section of the journal  
Frontiers in Pharmacology

**Received:** 01 October 2017

**Accepted:** 15 December 2017

**Published:** 02 February 2018

### Citation:

Magistri P, Battistelli C, Strippoli R,  
Petrucciani N, Pellinen T, Rossi L,  
Mangogna L, Aurello P, D'Angelo F,  
Tripodi M, Ramacciato G and Nigri G  
(2018) SMO Inhibition Modulates  
Cellular Plasticity and Invasiveness in  
Colorectal Cancer.  
Front. Pharmacol. 8:956.  
doi: 10.3389/fphar.2017.00956

## HIGHLIGHTS

- Preliminary results of this work were presented at the 2016 Academic Surgical Congress, Jacksonville (FL), February 2–4 2016 (Original title: Selective Smo-Inhibition Interferes With Cellular Energetic Metabolism In Colorectal Cancer)
- This study was funded by “Sapienza—University of Rome” (Funds for young researchers) and “AIRC” (Italian Association for Cancer Research)
- Hedgehog inhibitor was kindly provided by Genentech, Inc.<sup>®</sup>.

Colon Cancer (CC) is the fourth most frequently diagnosed tumor and the second leading cause of death in the USA. Abnormalities of Hedgehog pathway have been demonstrated in several types of human cancers, however the role of Hedgehog (Hh) in CC remain controversial. In this study, we analyzed the association between increased mRNA expression of *GLI1* and *GLI2*, two Hh target genes, and CC survival and recurrence by gene expression microarray from a cohort of 382 CC patients. We found that patients with increased expression of *GLI1* showed a statistically significant reduction in survival. In order to demonstrate a causal role of Hh pathway activation in the pathogenesis of CC, we treated HCT 116, SW480 and SW620 CC cells lines with GDC-0449, a pharmacological inhibitor of Smoothened (SMO). Treatment with GDC-0449 markedly reduced expression of Hh target genes *GLI1*, *PTCH1*, *HIP1*, *MUC5AC*, thus indicating that this pathway is constitutively active in CC cell lines. Moreover, GDC-0449 partially reduced cell proliferation, which was associated with upregulation of p21 and downregulation of CycD1. Finally, treatment with the same drug reduced migration and three-dimensional invasion, which were associated with downregulation of Snail1, the EMT master gene, and with induction of the epithelial markers Cytokeratin-18 and E-cadherin. These results were confirmed by SMO genetic silencing. Notably, treatment with 5E1, a Sonic Hedgehog-specific mAb, markedly reduced the expression of Hedgehog target genes, as well as inhibited cell proliferation and mediated reversion toward an epithelial phenotype. This suggests the existence of a Hedgehog autocrine



signaling loop affecting cell plasticity and fostering cell proliferation and migration/invasion in CC cell lines. These discoveries encourage future investigations to better characterize the role of Hedgehog in cellular plasticity and invasion during the different steps of CC pathogenesis.

**Keywords:** colon cancer, hedgehog pathway, SMO inhibition, EMT, cell plasticity, cell invasiveness

## INTRODUCTION

In colon carcinoma (CC) as for other cancers, the understanding of cellular and molecular mechanisms involved in tumor progression is essential to provide the rationale for novel therapies. According to the 2016 NCCN Panel, CC is the fourth most frequently diagnosed tumor and the second leading cause of death in the USA. Incidence in Italy raised from 27.06% in 1970 to 52.65% in 2010 (Ciatto, 2007). Reactivation or alteration of molecular pathways that control cellular differentiation and proliferation play a role in the development and progression of both familiar and sporadic CC (Al-Sohaily et al., 2012; Bertrand et al., 2012). Numerous studies demonstrated that chemotherapy may be helpful both for primary and for metastatic tumors (Nappi et al., 2016). However, the persistence of cases of local recurrence in patients treated with current protocols impels to study the impact of novel pathways active in CC pathogenesis.

Hh pathway plays an important role in tissue development and organogenesis (Jiang and Hui, 2008; Rimkus et al., 2016). However, in mature organisms, Hh pathway remains selectively active, controlling cell proliferation and differentiation.

Hh ligands are expressed by various stromal and parenchymal tissues and act generally in a paracrine way by binding to the plasma membrane receptor Patched (PTCH1). Upon binding of Hh ligands to PTCH1, the G-protein-coupled receptor, Smoothened (SMO) is activated and promotes nuclear translocation of GLI family of zinc finger transcription factors. GLI activation induces the transcription of Hh target gene products, including ubiquitous genes such as GLI1, PTCH1, and Hh-interacting protein (HIP1) (Benvenuto et al., 2016; Rimkus et al., 2016). This canonical Hh signaling cascade plays a role in the normal gastrointestinal development, regulating the differentiation of normal intestinal villi and of the adjacent mesenchymal stromal cells. In particular, in the normal adult gastrointestinal tract, induction of the Hh pathway protects the differentiated epithelial cells of the villous surface at the top of the crypts of Lieberkuhn (the structural unit of the normal colon), counteracting the canonical Wnt signaling in the basal cells of the crypt. In the absence of Hh ligand, PTCH1 suppresses the activation of SMO.

Since Hh pathway is involved in the control of proliferation/differentiation status in many tissues, it is not surprising that Hh expression and activity are altered in tumors (Scales and de Sauvage, 2009).

Aberrant Hh signaling, which can be achieved by mutational inactivation of PTCH1, aberrant expression of its ligand, constitutive activation of SMO or gene amplification of GLI-associated transcription factors, has been implicated in the initiation and/or maintenance of different cancer types, including

basal cell carcinoma (BCC), lung, and brain tumors and rhabdomyosarcoma (Gupta et al., 2010).

The involvement of Hh pathway in the pathogenesis of CC and the potential relevance for therapy has been already addressed by different studies. It has been demonstrated that Hh-GLI activity in epithelial tumor cells of CC is essential for tumor growth, recurrence and metastasis, and regulates the behavior of human CC stem cells *in vivo* (Varnat et al., 2009). However, a randomized phase II trial using a pharmacological inhibitor of Hh failed to show an incremental benefit respect to standard treatments in a population of previously untreated patients with metastatic CC (Berlin et al., 2013). In spite of this, recent research based on *in vitro* and *in vivo* experimental systems, led to controversial results (Gerling et al., 2016; Kangwan et al., 2016; Lee T. Y. et al., 2016; Wang et al., 2016).

The aim of the present study was to analyze whether pharmacological inhibition of Hh pathway, and specifically of SMO, impacts epithelial plasticity and invasiveness in different CC cell lines, and to explore the molecular mechanisms involved. Starting from our evidence correlating Hh pathway effectors (i.e., GLI1 and GLI2) with CC patients survival, we first treated CC cell lines with a pharmacological SMO inhibitor, GDC-0449, a small molecule already approved by the US Food and Drug Administration (FDA) for the treatment of advanced basal cell carcinoma (BCC) (Dijkgraaf et al., 2011; Takebe et al., 2015). In addition, we investigated the effects of SMO-specific genetic silencing as well as 5E1, a Shh-specific Monoclonal Antibody (mAb). Our results show that Hh pathway impacts epithelial/mesenchymal features and invasion capability of CC cell lines.

## MATERIALS AND METHODS

### Cells

Primary (HCT 116, SW480) and metastatic (SW620) human CC cell lines were grown in DMEM supplemented with 10% FBS (GIBCO® Life Technology, Monza, Italy) and antibiotics. These cellular lines were reported to express detectable levels of SMO and GLI1 (Sun et al., 2013; Sécourt et al., 2016; Wang et al., 2017). MeT5A cells, a human mesothelium non-tumorigenic cell line were grown in M199 supplemented with 10% FBS (GIBCO® Life Technology, Monza, Italy) and antibiotics.

### RNA Extraction, Reverse Transcription (RT), and Real-Time Polymerase Chain Reaction (RT-qPCR)

RNA, extracted from cell cultures with ReliaPrep™ RNA Tissue Miniprep System (Promega, Madison, WI, USA), was



reverse transcribed with iScript™ c-DNA Synthesis Kit (Bio-Rad Laboratories, Inc., Hercules, CA, USA) according to the manufacturer's instructions. cDNAs were amplified by qPCR reaction using GoTaq® qPCR Master Mix (Promega, Madison, WI, USA). The specific primer pairs are listed in **Table 1**. Relative amounts, obtained with  $2^{-\Delta C_t}$  method, were normalized with respect to the housekeeping gene L32. Statistical significance was determined with a *t*-test with GraphPad Prism version 5.0 (La Jolla, CA, USA). Differences were considered significant at  $P < 0.05$  (\* $p < 0.05$ ; \*\* $p < 0.01$ ; \*\*\* $p < 0.001$ ).

## Antibodies and Chemicals

Monoclonal antibody against E-cadherin was from BD (Becton-Dickinson Laboratories, Mountain View, CA). Monoclonal antibodies against Snail1 and against GLI1 were from Cell signaling (Danvers, MA). Monoclonal antibody against pancreatic keratin was from Sigma (St Louis, MO). Polyclonal antibodies against SMO (N-19) and tubulin were from Santa Cruz biotechnology (Dallas, USA). GDC-0449, a Hedgehog/Smoothed pharmacological inhibitor, was a kind gift from Genentech (South San Francisco, CA). 5E1, Shh specific mAb was purchased by Developmental Studies Hybridoma Bank (Iowa City, Iowa, US) (Ericson et al., 1996).

## siRNA-Mediated SMO Knockdown

$200 \times 10^3$  cells were seeded on 12-well plates 24 h prior transfection. Cells were transfected with either 40 pmol ON-TARGETplus SMARTpool against human SMO (Dharmacon Ref#SO-2600349G) or the same amount of ON-TARGETplus NontargetingPool (Dharmacon Ref#D-001206-14-05) and  $2 \mu\text{l}$

Lipofectamine® RNAiMAX Reagent from Thermo Fisher Scientific (Waltham, MA USA) in 200  $\mu\text{l}$  Optimem from Gibco (Waltham, MA USA). 1 ml of supplemented medium per well was also added. Forty-eight hours after transfection, knockdown efficiency was determined by RT-PCR and western blot.

## Western Blotting

Monolayers of HCT 116 cells were lysed in modified RIPA buffer containing: 50 mM Tris-HCl, pH 7.4; 1% NP-40; 0.1% SDS; 0.25% Nadeoxycholate; 150 mM NaCl; 1 mM EDTA; 1 mM EGTA; 1 mM PMSF; 1  $\mu\text{g/ml}$  each of aprotinin, leupeptin, and pepstatin; and 25 mM NaF (all from Sigma). Equal amounts of proteins were resolved by SDS-PAGE. Proteins were transferred to nitrocellulose membranes, probed with antibodies and detected as in Battistelli et al. (2017).

## Scratch Assay

CC cell lines were pretreated with DMSO or 1  $\mu\text{M}$  GDC-0449 for 24 h in culture medium until reaching 100% confluency. A scratch wound was created on the cell surface using a micropipette tip in low serum (0.5% FBS) culture medium to inhibit cell proliferation. Micrographs were taken at time 0 and 24 h after the scratch. Cell devoid areas at time 0 and 24 h after the scratch were quantified through ImageJ software (NIH, Bethesda, MD, USA). Three independent experiments for each cell line were performed

## 3-Dimensional Invasion Assay and Immunofluorescence

3-dimensional invasion assays were performed as in Strippoli et al. (2015). HCT 116 cells ( $1.5 \times 10^5$ ) were treated with 1  $\mu\text{M}$  GDC-0449 or vehicle for 12 h and then seeded in triplicate in Ibidi 15-well chambers and allowed to attach for 3 h. 40% matrigel (40  $\mu\text{l}$ ) in serum-free medium was laid over the cells. After 1 h, 50  $\mu\text{l}$  full medium containing 20% serum (and GDC-0449 or vehicle) was added and cells incubated for 72 h. Cells were fixed with 4% paraformaldehyde (PFA), permeabilized with 0.25% Triton in PBS, and stained for 12 h with rhodamine-phalloidin (to stain F-actin) and Hoechst (to stain nuclei) in PBS. Confocal images were captured with a Leica SP5 fitted with a 40 $\times$  oil objective. Maximum projection images consist of 30 individual images with a z-distance of 120  $\mu\text{m}$ . Imaris image analysis software (Bitplane Scientific Software) was used to create a 3D view of the same cells and to quantify invading cells. Three independent experiments were performed.

## Statistical Analysis

Survival analysis significance was based on Logrank Test. Statistical significance of experiments performed with cell lines was determined with a *t*-test using GraphPad Prism version 5.0 (La Jolla, CA, USA). Differences were considered significant at  $P < 0.05$ .

**TABLE 1** | List of specific primer pairs for qRT-PCR used in this study.

Gene	Oligonucleotide sequence
L32 FW	GGAGCGACTGCTACGGAAG
L32 REV	GATACTGTCCAAAAGGCTGGAA
GLI1 FW	GACGCCATGTTCAACTCGATG
GLI1 REV	CAGACAGTCCTTCTGTCCCCAC
PTCH1 FW	GAGCAGATTCCAAGGGGAAGG
PTCH1 REV	ATGAGGAGGCCACAACCAA
HIP1 FW	AGAACTGCAAAATGTGAGCCAG
HIP1 REV	CTGATCAAGAATACCTGCCCTG
MUC5AC FW	CCATTGCTATTATGCCCTGTGT
MUC5AC REV	TGGTGACGGACAGTCACT
CYC D1 FW	CCTCTAAGATGAAGGAGACCA
CYC D1 REV	CAC TTGAGCTTGTTACCA
P21 FW	GAGGAGGCGCCATGTCAGAA
P21 REV	AGTCACCCTCCAGTGGTGTC
SNAIL1 FW	CACTATGCCGCGCTCTTTC
SNAIL1 REV	GCTGGAAGGTAAACTCTGGATTAGA
CK18 FW	CTGGAGACCGAGAACCGGA
CK18 REV	TCCGAGCCAGCTCGTCAT
SMO FW	TGAAGGCTGCACGAATGAGG
SMO REV	CTTGGGGTTGTCTGTCCGAA

## RESULTS

### GLI Altered Expression Correlates with Reduced Survival in CC Patients

To determine the clinical relevance of Hh-GLI pathway in CC, we examined the association between increased *GLI* mRNA expression and CC survival by exploring gene expression data microarray from a cohort of 382 CC patients in the cancer genome atlas (TCGA) database (Cerami et al., 2012; Gao et al., 2013).

Notably, patients with increased *GLI1* expression showed a statistically significant reduction in overall survival (OS) (Figure 1) and a trend toward reduced disease-free survival (DFS) (Figure S1A). Patients with increased *GLI2* expression showed tendency to reduced survival (Figure S1B). These findings support a role for *GLI1* and *GLI2* in CC pathogenesis, and prompted us to investigate if pharmacological inhibition of Hh pathway could affect the proliferation or the invasive capacity of CC cell lines.

### GDC-0449 Limits Cellular Proliferation of Several CC Cell Lines

We analyzed whether treatment with GDC-0449 affects the expression of Hh pathway specific genes in CC lines. We exposed HCT 116, SW480, primary CC lines, and SW620, a metastatic CC cell line, to GDC-0449 for 24 h at a concentration (1  $\mu$ M) that is compatible with cellular viability. As shown in Figures 2A–D, treatment with GDC-0449 significantly reduced the expression of *GLI1*, *PTCH1*, *HIP1*, and *MUC5AC*, four of the known Hh target genes, thus demonstrating that Hh pathway is constitutively active in all three cell lines. *GLI1* protein expression

upon treatment with GDC-0449 was shown in Figures S2A–C. Raw data of the original western blots shown in this study are displayed in Figures S5–S7.

Similar results were obtained by genetically silencing *SMO*, and by using 5E1, a mAb specifically binding to Shh (Figures 2E,F). The extent of *SMO* knockdown at mRNA level is shown in Figure S3A. Notably, the efficacy of 5E1 mAb, in the absence of exogenous stimulation, suggests the existence of an autocrine loop maintaining Hh pathway constitutively active in these cells.

Conversely in the MeT5A cell line, a non-tumorigenic mesothelium cell line, the same genes were found not responsive to the treatment with GDC-0449, therefore suggesting that these cells do not maintain a constitutively active *SMO*-*GLI* pathway (Figure S3B).

In order to evaluate the effect of *SMO* inhibition on cell proliferation, we exposed HCT 116, SW480, SW620, and MeT5A cells, to GDC-0449 for 24–48 h. At the concentration of 1  $\mu$ M, GDC-0449 significantly inhibited cell proliferation in HCT 116, SW480, and SW620 while causing negligible effect in MeT5A cells (Figures 3A–D.) At the molecular level, treatment with GDC-0449 reduced the expression of cell cycle promoters (*Cyclin D1*) while inducing the expression of cell cycle inhibitors (*p21*) in all of the three CC lines analyzed (Figures 3E,F). Accordingly, both genetic silencing of *SMO* and treatment with 5E1 mAb led to a reduction of *Cyclin D1* (Figure 3G), while increasing the expression of *p21* (Figure 3H). In contrast, no significant changes in the expression of these genes were detected when MeT5A were treated with GDC-0449 at the same concentrations (Figure S3C). These results demonstrate that activation of Hh pathway delivers proliferative signals in CC cell lines.

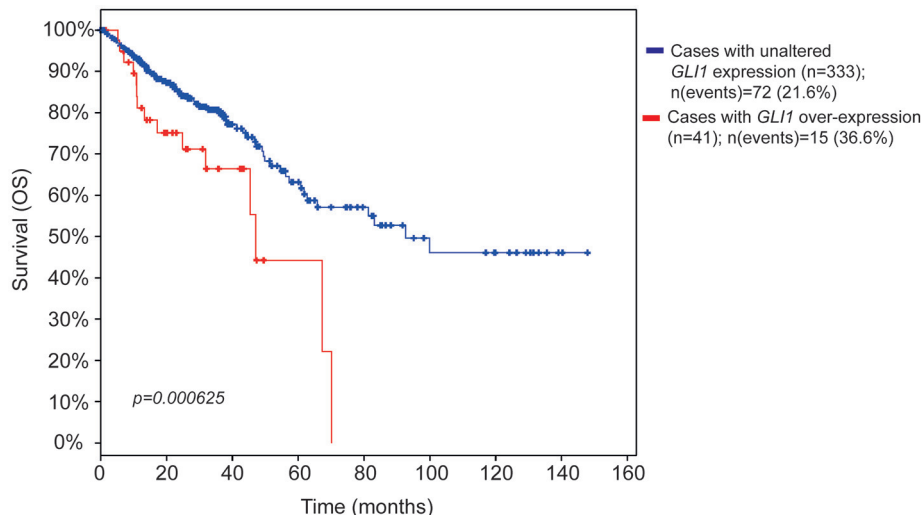


**FIGURE 1 |** Kaplan-Meier survival estimate plots for increased *GLI* mRNA expression in CC patients. The survival estimate was analyzed in <http://www.cbioportal.org> (Cerami et al., 2012; Gao et al., 2013) and is based on Colorectal adenocarcinoma TCGA provisional dataset, which is generated by <http://cancergenome.nih.gov/>. The cases were set to include tumor samples with mRNA data (RNA Seq V2,  $n = 382$  patients). The red line shows overall survival estimate for patients with increased *GLI1* expression (11% of the patients) as compared to patients with no alteration (blue line, the rest of the patients). Eight patients were missing in the survival analysis. The threshold for altered expression was set to z-score value = 1.2. The z-score value is used to define the cut-off for patient dichotomization in the TCGA datasets (see <http://www.cbioportal.org/>). The median months survival for the increased *GLI1* patient group and the reference group were 47.04 and 92.67, respectively. Survival analysis significance was based on Logrank Test.  $P < 0.05$  was considered significant.

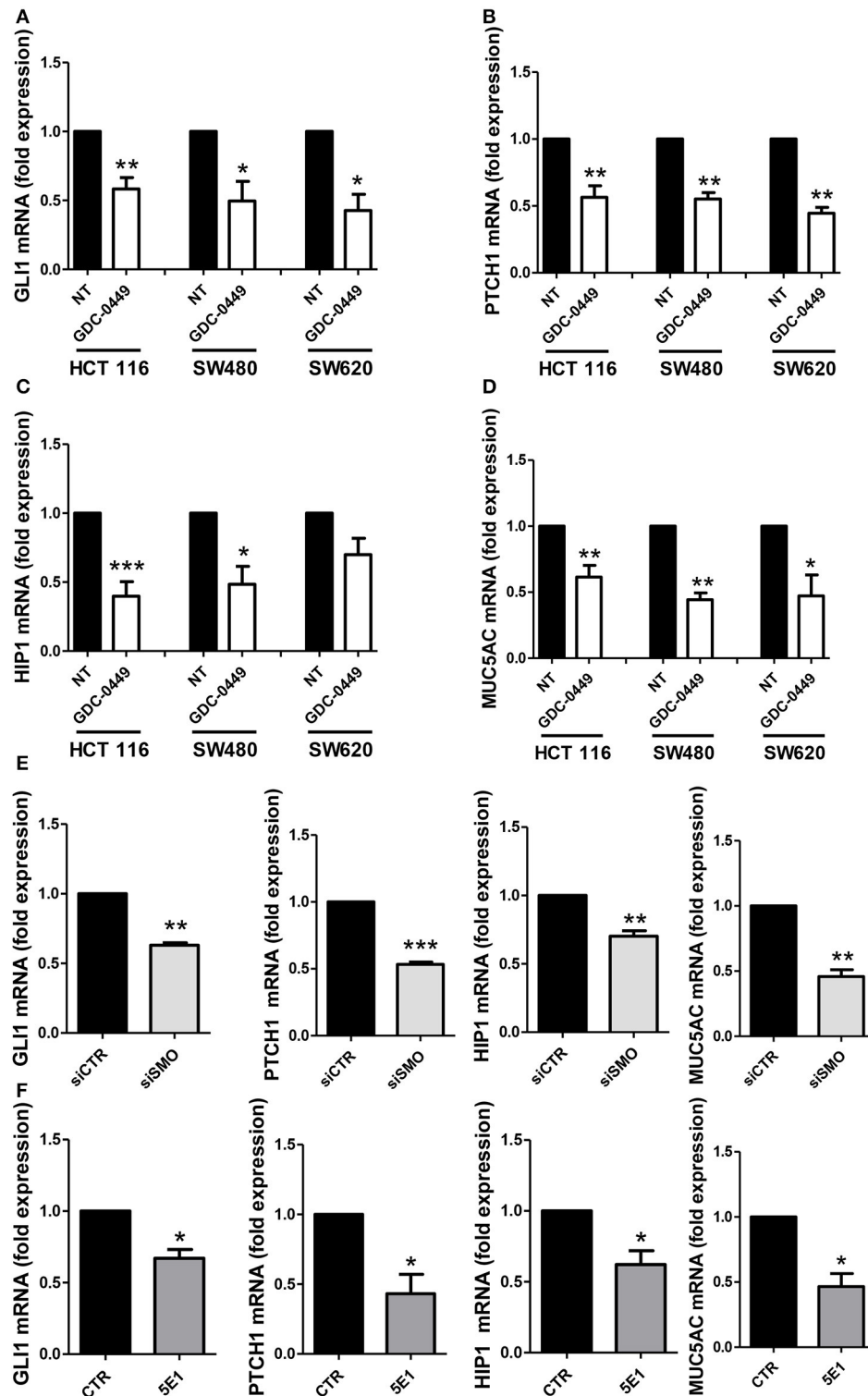


**FIGURE 2 |** Effect of Hh inhibition on Hh pathway-induced genes. HCT 116, SW480 and SW620 were treated with DMSO vehicle (NT) or with 1  $\mu$ M GDC-0449 for 24 h. Expression of *GLI1* (A), *PTCH1* (B), *HIP1* (C), *MUC5AC* (D) was evaluated on total RNA by qRT-PCR. Bars represent means  $\pm$  SEM of 7 experiments for HCT 116 cells, three experiments for SW480 and SW620 cells. Expression of *GLI1*, *PTCH1*, *HIP1*, *MUC5AC* in HCT 116 cells transfected with either control or specific SMO-targeting siRNAs (E). Expression of *GLI1*, *PTCH1*, *HIP1*, *MUC5AC* in HCT 116 cells treated with either isotype-control mAb or 5E1 mAb (F). Bars represent means  $\pm$  SEM of three experiments. \* $P < 0.05$ , \*\* $P < 0.01$ , \*\*\* $P < 0.001$ .

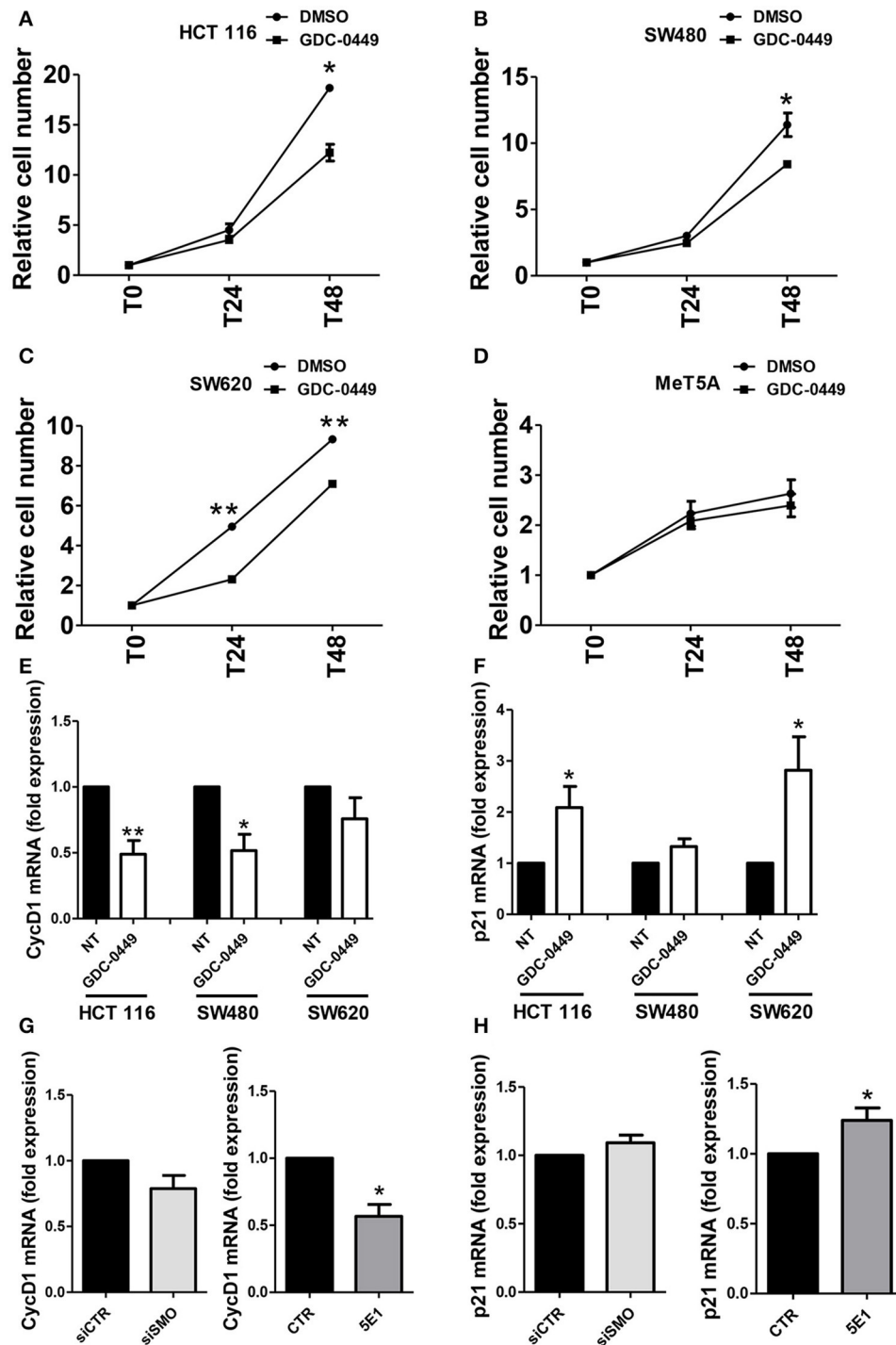


**FIGURE 3 |** Effect of Hh inhibition on cell proliferation. (A) HCT 116, (B) SW480, (C) SW620 or (D) MeT5A cells were treated with vehicle (DMSO) or with GDC-0449 (1  $\mu$ M) for 24–48 h. Cell proliferation was evaluated through microscopic count of living cells. Three independent experiments for each cell line were performed. Expression of *Cyclin D1* (E) and *p21* (F) was evaluated on total RNA by qRT-PCR. Bars represent means  $\pm$  SEM of 7 experiment for HCT 116 cells, three experiments for SW480 and SW620 cells. (G) Expression of *Cyclin D1* mRNA was evaluated in HCT 116 cells transfected with either control or specific SMO-targeting siRNAs (left), or in HCT 116 cells treated with either isotype-control mAb or 5E1 mAb (10  $\mu$ g/ml) (right). (H) Expression of *p21* mRNA was evaluated in HCT 116 cells transfected with either control or specific SMO-targeting siRNAs (left), or in HCT 116 cells treated with either isotype-control mAb or 5E1 mAb (10  $\mu$ g/ml) (right). Bars represent means  $\pm$  SEM of three independent experiments. \* $P$  < 0.05, \*\* $P$  < 0.01.

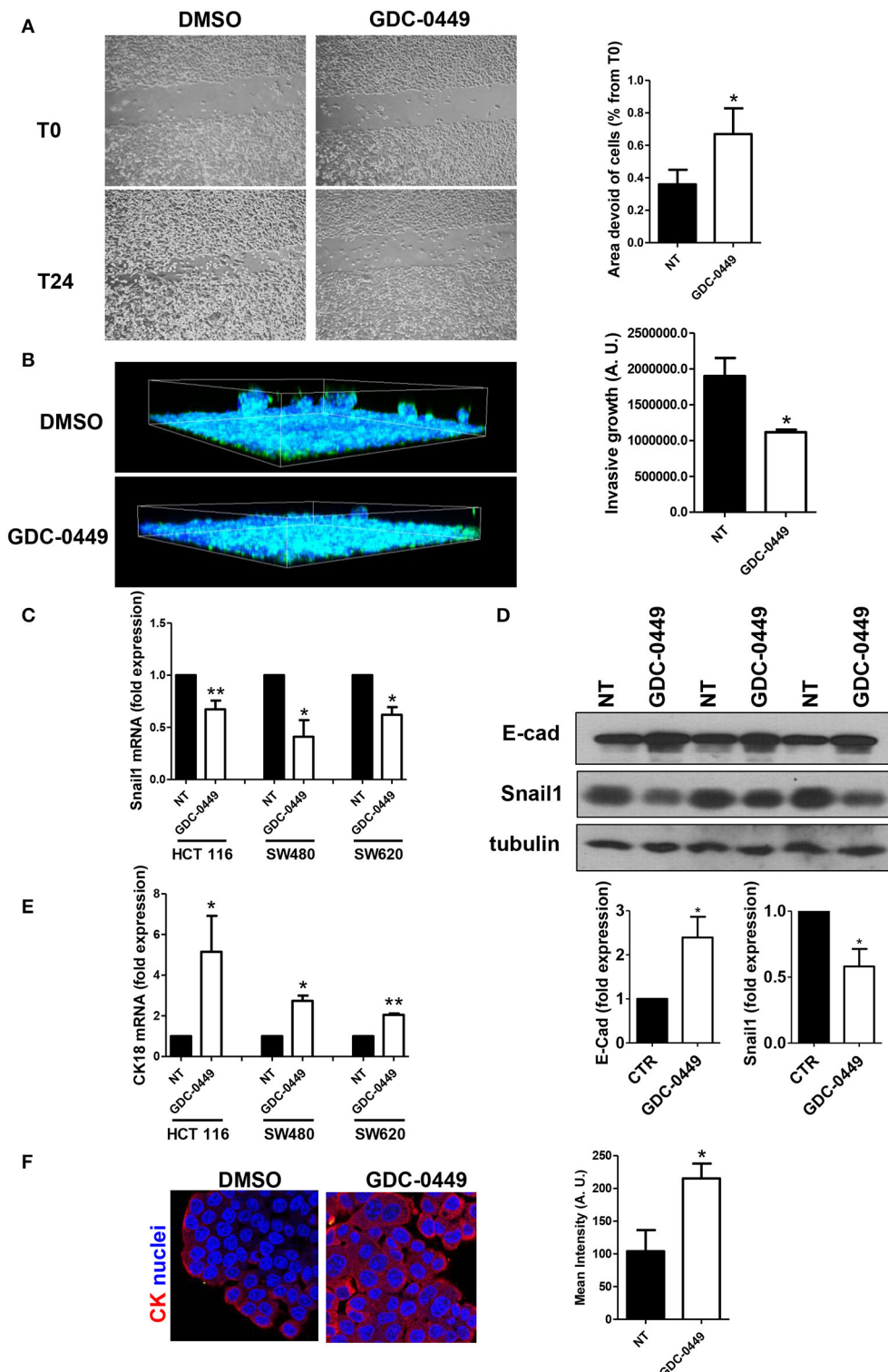


**FIGURE 4 |** Effect of Hh inhibition on cell directed migration and on EMT-MET dynamics. **(A)** HCT 116 cells were treated with vehicle (DMSO) or with GDC-0449 (1  $\mu$ M) in culture medium supplemented with 0.5% FCS. A scratch was performed and micrographs were taken 24 h after the scratch. Wound closure rate was quantified (right). Three independent experiments were performed. **(B)** HCT 116 cells were pretreated with GDC-0449 for 24 h and then overlaid with a Matrigel matrix. Invasion was monitored over 72 h. Three-dimensional invasion was enhanced by adding 20% FCS to the wells on top of Matrigel. Cells were stained with phalloidin (green) and Hoechst 33342 (cell nuclei, blue). Scale bar: 100  $\mu$ m. 3 dimensional invasion rate was quantified (right). Three independent experiments were performed. **(C,D)** Effect of GDC-0449 on genes related to EMT-MET dynamics. **(C)** HCT 116, SW480, and SW620 cells were treated with GDC-0449 (1  $\mu$ M) or

(Continued)



**FIGURE 4 |** DMSO for 24 h. Expression of *Snail1* mRNA was evaluated on total RNA by qRT-PCR. Bars represent means  $\pm$  SEM of 7 experiments for HCT 116 cells, three experiments for SW480 and SW620 cells. **(D)** Expression of *Snail1* and E-cadherin in cells treated as above by western blot on total protein lysates of HCT 116 cells treated as stated in the figure. Tubulin was used as a loading control. Three independent experiments were performed. Quantification of E-cadherin and *Snail1* protein expression is shown below. **(E)** Expression of *Cytokeratin 18* (CK18) mRNA from total RNA of HCT 116 cells treated as in **(C)**. **(F)** Cytokeratin expression and localization in HCT 116 cells was evaluated through immunofluorescence analysis. Nuclei were stained in blue with Hoechst. Quantification of Cytokeratin mean intensity is shown on the right. Two independent experiments were performed. \* $P < 0.05$ , \*\* $P < 0.01$ .

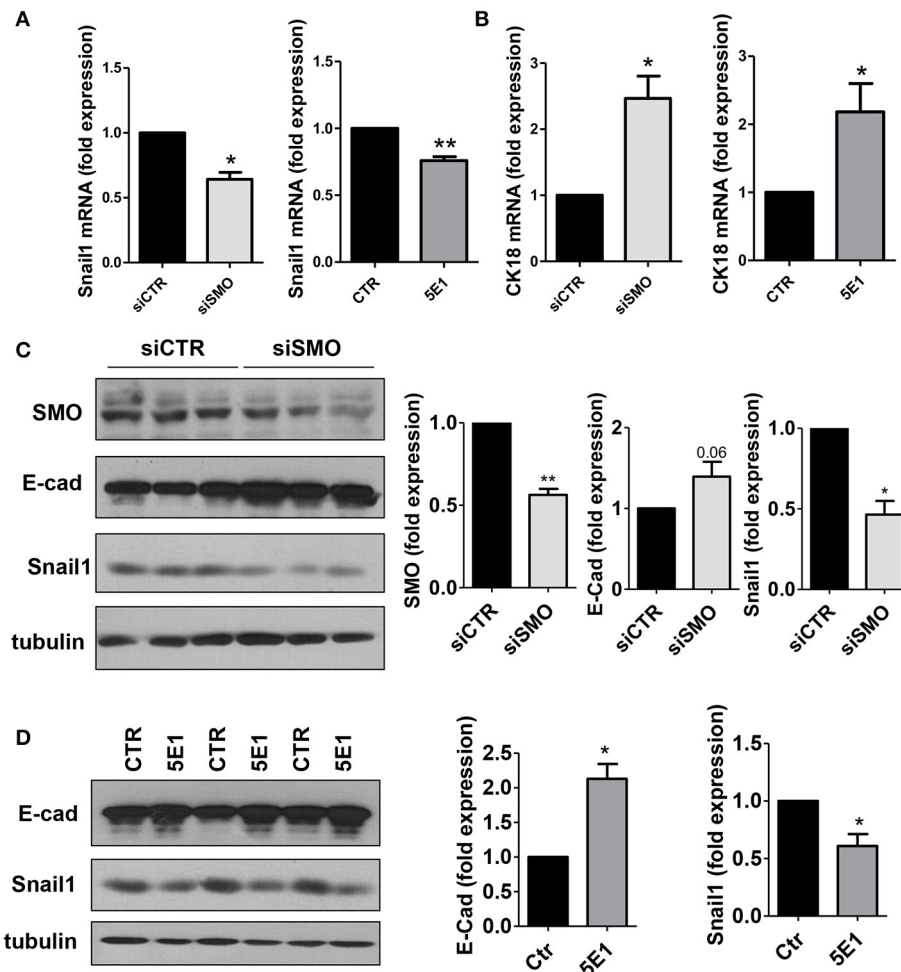


**FIGURE 5 |** **(A)** *Snail1* and **(B)** *Cytokeratin 18* expression was evaluated on total RNA by qRT-PCR from HCT 116 cells transfected with either control or specific *SMO*-targeting siRNAs (left), or from cells treated with either isotype-control mAb or 5E1 mAb (10  $\mu$ g/ml) (right) ( $n = 3$ ). **(C)** Western blot showing expression of *SMO*, E-cadherin, *Snail1* in HCT 116 cells transfected with either control or specific *SMO*-targeting siRNAs. Quantification of *SMO*, E-cadherin and *Snail1* is shown on the left. ( $n = 3$ ). **(D)** Western blot showing the expression of E-cadherin, *Snail1* in HCT 116 cells treated with either isotype-control mAb or 5E1 mAb (10  $\mu$ g/ml). Tubulin was used as loading control. E-cadherin and *Snail1* quantifications are shown on the right. Bars represent means  $\pm$  SEM of three independent experiments. \* $P < 0.05$ , \*\* $P < 0.01$ .

## GDC-0449 Inhibits Cell-Directed Motility and Invasion and Induces Met

We then analyzed whether GDC-0449 potentially inhibits tumor invasion. In order to analyze the effect of GDC-0449 in controlling cell directed motility, which is relevant for tumor invasion, we performed a scratch assay. Confluent HCT 116 monolayers were pre-treated with GDC-0449 for 24 h, a scratch was performed and the scratch closure was evaluated after 24 h.

As shown in **Figure 4A**, treatment with GDC-0449 significantly limited scratch closure.

Similar results were obtained by using SW480 and SW620 cells (**Figures S4A,B**). By contrast GDC-0449 treatment had no effect on the Hh-irresponsive cell line MeT5A (**Figure S4C**).

Notably, the use of a 3-dimensional invasion assay on Matrigel matrices highlighted also a reduced invasive capacity of GDC-0449-treated HCT 116 cells (**Figure 4B**).

At the molecular level, treatment with GDC-0449 markedly reduced the expression of Snail1, a main driver of EMT and tumor invasion, in all CC cell lines analyzed, while increasing the expression of the typical epithelial marker E-cadherin (Figures 4C,D). At the same time, Cytokeratin 18 (CK18) expression was increased both at mRNA and at protein level (Figures 4E,F). These results were confirmed by genetic silencing of SMO and by the use of 5E1 mAb (Figures 5A–D).

These data are in accordance with a data set from CC patients (Tables 2, 3), from the cancer genome atlas (TCGA) database (Cerami et al., 2012; Gao et al., 2013), where increased expression of Hh pathway genes (GLI1 and SMO) negatively correlates with protein expression of CDH1 (E-cadherin, epithelial marker) and positively correlate with CDH2 (N-Cadherin) and FN (Fibronectin), mesenchymal markers.

Overall, these results demonstrate that in primary and metastatic CC cell lines, the functional blockade of autocrine Hh pathway leads to a reduction of cellular growth and invasion through a reacquisition of epithelial-like features. These results may be helpful to more completely understand the complex biology of CC in light of future therapeutic strategies.

## DISCUSSION

The involvement of Hh in CC tumorigenesis is presently object of controversy. CC has a complex pathogenesis; during its progression, alterations of multiple genes and pathways are required. The observation that Hh pathway is tightly connected with other pathways that are often abnormally activated in CC, such as Wnt/ $\beta$ -catenin or Ras, strongly suggests its involvement in the multistep process of CC pathogenesis (Brechtel et al., 2014). In fact, recent evidence indicates that Hh signaling may act in CC in autocrine, paracrine or cancer stem cell fashion (Scales and de Sauvage, 2009).

Notably, RNA Seq analysis in 382 patients highlighted a significative correlation between GLI1 increased expression and reduced survival in CC patients. These data support the results obtained by other studies (Xu et al., 2012), and prompted us to overcome the correlative analysis in pinpointing a mechanism; this attempt implied to inhibit Hh pathway in CC cell lines.

We first evaluated the effect of GDC-0449, a specific SMO inhibitor, on Hh signaling in three primary and metastatic CC cell lines. In all cells analyzed, treatment with GDC-0449 significantly reduced the expression of four known target genes (*GLI1*, *PTCH1*, *HIP1*, *MUC5AC*), this implying a constitutive activation of Hh pathway. The activity of Hh pathway in CC cell lines has been already analyzed in other studies, with controversial results (Douard et al., 2006; Chatel et al., 2007; Alinger et al., 2009).

The observed discrepancies with some of these studies may be explained by the different cell lines analyzed (Alinger et al., 2009) or by the usage of semi-quantitative techniques (Chatel et al., 2007).

In our experimental system, treatment of all three lines with GDC-0449 also significantly reduced cell proliferation, whereas there was no effect in a not-responsive cell line used as a negative control.

**TABLE 2 |** Mean protein expression changes in CC patients with GLI1 mRNA overexpression.

Gene	Mean protein expression		Stddev. of protein expression		p-Value
	In GLI1 high group (n = 41)	In reference group (n = 333)	In GLI1 high group (n = 41)	In reference group (n = 333)	
FASN	−0.5	0.1	0.59	0.6	0.000001046
FOXM1	−0.36	0.02	0.38	0.56	0.000001847
CCNB1	−0.77	0.02	0.9	0.78	0.000009887
CCNE1	−0.26	0.06	0.36	0.46	0.00001511
RPS6	−0.45	0.04	0.59	0.52	0.00002737
MSH6	−0.49	−0.02	0.58	0.6	0.00004738
ACACB_PS79	−0.34	0.02	0.48	0.46	0.0001271
ACACA_PS79	−0.34	0.02	0.48	0.46	0.0001271
SLC1A5	−0.63	−0.04	0.82	0.62	0.0001453
CASP7	−0.49	0.13	0.82	1.16	0.0001513
ACACA	−0.43	0	0.61	0.62	0.0002158
DIRAS3	0.23	0.06	0.23	0.33	0.0003006
FN1	0.75	0.15	0.87	0.78	0.0003219
PEA15	0.28	0.07	0.3	0.31	0.0003356
COL6A1	0.73	0.08	1	0.59	0.0004711
ARID1A	−0.12	0	0.19	0.27	0.0004835
CDH2	0.15	0.03	0.18	0.25	0.0005421
EIF4E	−0.15	0.04	0.29	0.29	0.000731
CHEK2	−0.29	0.09	0.62	0.44	0.0009215
RPS6KA1	−0.16	0.09	0.4	0.43	0.0009856
CCNE2	−0.07	0.05	0.19	0.24	0.001171
SMAD1	−0.13	0.02	0.23	0.23	0.001174
FOXO3_PS318	0.18	−0.03	0.36	0.24	0.001343
MSH2	−0.07	0.12	0.32	0.32	0.001649
EEF2	−0.23	0.01	0.4	0.41	0.001656
ASNS	−0.13	0.15	0.46	0.57	0.001962
HSPA1A	0.82	0.23	1.04	0.86	0.002055
ITGA2	−0.23	0.07	0.52	0.46	0.002136
PCNA	−0.21	0.01	0.4	0.37	0.002343
CTNNA1	−1.06	−0.32	1.34	1.01	0.002551
TGM2	0.22	0.06	0.28	0.31	0.002916
RB1	−0.06	0.12	0.32	0.32	0.003076
BCL2	0.22	0.02	0.35	0.45	0.003119
ACVRL1	0.3	0.04	0.49	0.37	0.00349
ERBB3	−0.27	0.05	0.59	0.61	0.004059
BAP1	−0.32	−0.08	0.46	0.48	0.004078
RPS6KB1	−0.3	−0.08	0.43	0.37	0.004689
ANXA1	0.34	0.03	0.6	0.59	0.005383
CDH1	−0.93	−0.3	1.24	1	0.005527
CDKN1A	0.2	0.03	0.33	0.36	0.00556
BRD4	−0.42	−0.11	0.63	0.5	0.006666
STK11	0.11	0.04	0.14	0.15	0.006734
SQSTM1	−0.31	−0.02	0.59	0.52	0.006856
EIF4EBP1	−0.13	0.04	0.35	0.34	0.007095
BAK1	0.12	0.04	0.17	0.21	0.007894
NRAS	0.17	0.08	0.19	0.23	0.008201
PGR	0.23	0.11	0.24	0.31	0.008854
CDK1_PY15	−0.23	0	0.48	0.31	0.008911
MRE11A	0.15	0.04	0.23	0.17	0.009363
AR	0.18	0.06	0.27	0.26	0.0104
WWTR1	0.13	0.01	0.27	0.27	0.0138
G6PD	0.15	0.04	0.24	0.31	0.0142
TP53BP1	−0.4	−0.05	0.78	0.72	0.0145
BECN1	0.13	0.02	0.24	0.22	0.015
RBM15	−0.54	−0.11	0.98	0.62	0.0159

(Continued)



TABLE 2 | Continued

Gene	Mean protein expression		Stdev. of protein expression		p-Value
	In GLI1 high group (n = 41)	In reference group (n = 333)	In GLI1 high group (n = 41)	In reference group (n = 333)	
TFRC	-0.35	0.02	0.84	0.85	0.0159
EIF4G1	-0.66	-0.27	0.88	0.93	0.0181
ESR1	0.19	0.07	0.28	0.36	0.0188
CLDN7	-0.63	-0.07	1.32	1.04	0.019
XRCC5	-0.27	-0.02	0.59	0.5	0.0194
TSC2	-0.32	-0.06	0.62	0.49	0.023
GAPDH	-0.39	-0.06	0.81	0.74	0.0289
MS4A1	0.12	0.04	0.22	0.18	0.029
KIT	0.28	-0.07	0.88	0.9	0.0297
FOXO3	0.13	0.05	0.19	0.24	0.03
GSK3B	-0.06	0.05	0.28	0.24	0.0306
GSK3A	-0.06	0.05	0.28	0.24	0.0306
CCND1	0.07	-0.01	0.21	0.23	0.0366
CDKN1B	0.21	0.09	0.32	0.34	0.0376
MAPK8_PT183	0.27	0.02	0.68	0.39	0.0383
RAB11B	0.14	0.03	0.29	0.24	0.041
RAB11A	0.14	0.03	0.29	0.24	0.041
CASP8	-0.04	0.14	0.45	0.79	0.0414
YAP1	0.29	0.14	0.42	0.37	0.0445

Data was extracted from cBioPortal, Colorectal Adenocarcinoma (TCGA, Provisional),  $n(\text{patients}) = 382$ , z-score threshold = 1.2. The patient set was the same as in the survival analysis (see Figure 1). Protein measurements are based on antibody arrays (RPPA = Reverse Phase Protein Array), and the table shows only those proteins with significant p-value ( $p < 0.05$ ). The z-score threshold used was the same as in the survival analysis (see Figure 1), where z-score 1.2 resulted in the best separation of patient groups into Gli1 mRNA overexpressing and non-overexpressing patients.

At the molecular level, cell cycle inducers (Cyclin D1) were decreased, whereas cell cycle blockers (p21) were increased. Therefore, the use of GDC-0449 directly impacts cellular proliferation and potentially tumor growth. These results were confirmed by performing SMO genetic silencing and by using a 5E1 Shh-specific inhibitory mAb. The effect observed using 5E1 presupposes the existence of an autocrine activatory loop involving Shh-SMO-dependent canonical pathway activation. A previous report analyzing loss-of-function mutation in PTCH1 suggested a role of autocrine Hh signaling in colorectal tumorigenesis (Chung and Bunz, 2013). The autocrine loop observed by us in CC cell lines may complement other studies supporting a model in which paracrine Hh ligands released by CC cells take a role in instructing the stromal components of the tumor (Yauch et al., 2008).

Our results emphasize the role of canonical Hh signaling in CC cell lines, although we do not exclude that other pathways may play a role. Indeed, besides the canonical Hh-PTCH1-SMO-driven signals, ligand-independent pathways have been demonstrated (Merchant et al., 2004; Amakye et al., 2013). For instance, in tumors, GLI transcription may be decoupled from upstream Shh-PTCH1-SMO signaling being regulated by TGF- $\beta$  and KRAS (Nolan-Stevaux et al., 2009).

Treatment with GDC-0449 also led to reduced cellular motility in both a 2D and a 3D migration assays. These functional

TABLE 3 | Mean protein expression changes in CC patients with SMO mRNA overexpression.

Gene	Mean protein expression		Stdev. of protein expression		p-Value
	In SMO high group (n = 54)	In reference group (n = 325)	In SMO high group (n = 54)	In reference group (n = 325)	
RPS6KA1	-0.13	0.1	0.32	0.44	0.0001553
FN1	0.57	0.16	0.67	0.82	0.0005204
GAPDH	-0.42	-0.05	0.62	0.76	0.0006319
CLDN7	-0.61	-0.06	1.08	1.07	0.002821
CASP7	-0.36	0.13	0.98	1.15	0.003758
PTEN	-0.12	-0.03	0.21	0.22	0.006982
PEA15	0.21	0.08	0.29	0.32	0.008334
YAP1	0.32	0.13	0.43	0.36	0.0113
SYK	-0.21	0.03	0.59	0.54	0.0138
SLC1A5	-0.36	-0.07	0.76	0.65	0.0142
TFRC	-0.32	0.03	0.87	0.84	0.0172
VHL	-0.59	-0.18	1.04	1.21	0.0193
LCK	-0.06	0.09	0.37	0.47	0.0201
ERBB3	-0.17	0.04	0.51	0.62	0.0216
FOXO3_PS318	0.09	-0.02	0.29	0.26	0.0222
CTNNB1	-0.78	-0.34	1.15	1.05	0.0223
CDKN1B	0.2	0.08	0.32	0.34	0.0281
PECAM1	0.15	0.04	0.29	0.27	0.0282
MRE11A	0.11	0.04	0.2	0.17	0.0287
EEF2	-0.14	0	0.38	0.42	0.0304
RB1	0	0.11	0.3	0.33	0.0304
TSC2	-0.25	-0.07	0.52	0.51	0.0308
INPP4B	-0.17	0.01	0.5	0.63	0.0365
RBM15	-0.4	-0.12	0.82	0.65	0.0375
AR	0.16	0.06	0.31	0.25	0.0381
EGFR	-0.13	-0.05	0.21	0.25	0.0393
WWTR1	0.09	0.01	0.21	0.28	0.04
CDH1	-0.69	-0.32	1.11	1.03	0.0401
CDH2	0.1	0.03	0.2	0.25	0.0421
SMAD4	0.06	0	0.19	0.22	0.0448
SQSTM1	-0.2	-0.03	0.52	0.54	0.0451

Data was extracted from cBioPortal, Colorectal Adenocarcinoma (TCGA, Provisional),  $n(\text{patients}) = 382$ , z-score threshold = 1.2. Protein measurements are based on antibody arrays (RPPA = Reverse Phase Protein Array), and the table shows only those proteins with significant p-value ( $p < 0.05$ ). The z-score threshold 1.2 was selected based on optimal separation of patient groups into SMO mRNA overexpressing and non-overexpressing groups.

data correlated with an increased expression of epithelial markers (E-cadherin, Cytokeratin-18) and with a significant downregulation of Snail1, a main effector of TGF- $\beta$  pathway. With respect to cellular motility and Snail1 expression, our results appear equally provocative in the light of the fact that in several circumstances TGF- $\beta$  facilitates tumor invasiveness through induction of epithelial-mesenchymal transition (EMT). EMT is a complex phenotypic conversion of epithelial cells leading to the acquisition of a highly motile phenotype and other mesenchymal traits, and is a key mechanism by which pre-malignant epithelial cells acquire a highly invasive phenotype that leads to metastatic spreading. The evidence of EMT in CC *in vivo* was firstly demonstrated by Brabletz (Brabletz et al., 2005). Subsequently, genomics studies identified EMT as a major program in CC (Loboda et al., 2011). Moreover, expression of EMT-related genes correlated with poorer survival in CC, but not in other cancers (Tan et al., 2014).

Cell migration and invasiveness are driven by actin cytoskeleton dynamic polarization, which is controlled by the members of the Rho GTPase superfamily Rho, Rac, and Cdc42 (Ridley, 2015). At the same time, EMT dynamics, as well as the acquisition of stem-like phenotypes are characterized by selective activation of Rho GTPases (Yoon et al., 2017). Interestingly, recent studies link Hh pathway to Rho GTPases activation, providing potential molecular mechanisms for our observations (Peng et al., 2017).

Hh pathway has been shown to intersect and cooperate with other pathways by regulating the differentiation/proliferation status of the tissue. In the intestinal mucosa, Bone Morphogenetic Protein (BMP) and Hh pathways are preferentially activated in differentiated layers, whereas Notch and WNT pathways are activated in the basal cells of the crypt (Bertrand et al., 2012). Hh controls the expression of the Notch ligand Jagged2. Moreover, cross talks between TGF- $\beta$ -induced pathways and Hh have been demonstrated (Perrot et al., 2013). There is evidence of an interplay between Hh and TGF- $\beta$  pathways in both normal and malignant tissues. In particular, TGF- $\beta$  may induce GLI1 expression in a GLI2-dependent manner independently from SMO in breast cancer (Hu et al., 2008). Furthermore, pharmacologic blockade of TGF- $\beta$  signaling leads to a reduction of GLI1 expression in cyclophosphamide-resistant pancreatic adenocarcinoma (Dennler et al., 2007).

We hypothesize that in our cells Snail1 downregulation, mediated by Hh-pathway inhibition, contributes to the stabilization of an epithelial phenotype (underlined by the increase in E-cadherin and Cytokeratin 18 expression). Besides the well-known effect on tumor invasion, Snail1 downregulation may be effective in limiting chemoresistance, as recently demonstrated in CC (Lee T. Y. et al., 2016). Accordingly, Hh pathway inhibition by GDC-0449 was demonstrated to reduce the expression of a mesenchymal marker and to restore sensitivity to 5-fluorouracil in a 5-fluorouracil-resistant CC cell line (Liu et al., 2015).

While the role of Hh pathway in EMT induction in CC has already been demonstrated by Ruiz i Altaba and other groups (Varnat et al., 2009; Wang et al., 2012; Liu et al., 2015), our study firstly described the maintenance of an invasive “EMT like state” by an autocrine secretion of Hh ligands in CC cell lines. This cellular mechanism may play a role in promoting cellular invasion and metastatic spreading of CC to the liver, consistently with our previous findings on tumor-stroma interactions in liver neoplasms (Magistri et al., 2013). The impact of Hh pathway on CC tumorigenesis has been recently questioned in mouse models (Gerling et al., 2016; Lee J. J. et al., 2016). Using different experimental systems such as the AOM/DSS model of colitis-associated CC, it was demonstrated that Hh signaling is downregulated in CC, and that Hh pathway inhibition may

intensify colon inflammation (colitis) in mice, thus promoting tumorigenesis.

Conversely, other recent studies linked the same pathway activation to pro-tumor effects and to the acquisition of a cancer stem-like behavior (Kangwan et al., 2016; Wang et al., 2016).

Finally, it has been demonstrated that Hh active pathway may hamper tumor immunosurveillance (for example downregulating MHC1 expression in epithelial tumor cells), inhibiting the immune response against the tumor (Otsuka et al., 2015; Hanna and Shevde, 2016). Therefore, the interpretation of *in vivo* models is so far extremely challenging.

In conclusion, our *in vitro* study established a causal link between constitutive Hh activity and the acquisition of pro-invasive, mesenchymal-like properties in CC cell lines.

When looking for a possible translational relevance of these discoveries, one may hypothesize that subsets of colorectal tumors endowed with abnormal Hh signaling due to mutations, such as a recently reported PTCH1 loss-of-function mutation (Chung and Bunz, 2013), that may not have been represented in the cohorts previously treated with Hh inhibitors (Berlin et al., 2013), may benefit from drugs inhibiting Hh activity such as GDC-0449.

## AUTHOR CONTRIBUTIONS

PM, CB, and RS: equally contributed to the final manuscript and are responsible for study design, lab experiments, and manuscript drafting; GN, MT, and GR: supervised all the study process and revised the final manuscript; NP, LR, and FD: are responsible for literature review and data analysis; PA and LM: are responsible for lab experiments duplicates and statistical analysis. TP is responsible for the analysis of TCGA database.

## FUNDING

This study was funded by “Sapienza—University of Rome” (Funds for young researchers) and “AIRC” (Italian Association for Cancer Research) 2016 (n. 18843) (MT).

## ACKNOWLEDGMENTS

Authors want to thank Prof. Timothy Pawlik and Prof. Jason K. Sicklick for their passionate support and useful tips and Prof. Lucia Di Marcotullio for critically discussing the results.

## SUPPLEMENTARY MATERIAL

The Supplementary Material for this article can be found online at: <https://www.frontiersin.org/articles/10.3389/fphar.2017.00956/full#supplementary-material>

## REFERENCES

- Alinger, B., Kiesslich, T., Datz, C., Aberger, F., Strasser, F., Berr, F., et al. (2009). Hedgehog signaling is involved in differentiation of normal colonic tissue rather than in tumor proliferation. *Virchows Archiv.* 454, 369–379. doi: 10.1007/s00428-009-0753-7
- Al-Sohaily, S., Biankin, A., Leong, R., Kohonen-Corish, M., and Warusavitarne, J. (2012). Molecular pathways in colorectal cancer. *J. Gastroenterol. Hepatol.* 27, 1423–1431. doi: 10.1111/j.1440-1746.2012.07200.x
- Amakye, D., Jagani, Z., and Dorsch, M. (2013). Unraveling the therapeutic potential of the Hedgehog pathway in cancer. *Nat. Med.* 19, 1410–1422. doi: 10.1038/nm.3389

- Battistelli, C., Cicchini, C., Santangelo, L., Tramontano, A., Grassi, L., Gonzalez, F. J., et al. (2017). The Snail repressor recruits EZH2 to specific genomic sites through the enrollment of the lncRNA HOTAIR in epithelial-to-mesenchymal transition. *Oncogene* 36, 942–955. doi: 10.1038/onc.2016.260
- Benvenuto, M., Masuelli, L., De Smaele, E., Fantini, M., Mattera, R., Cucchi, D., et al. (2016). *In vitro* and *in vivo* inhibition of breast cancer cell growth by targeting the Hedgehog/GLI pathway with SMO (GDC-0449) or GLI (GANT-61) inhibitors. *Oncotarget* 7, 9250–9270. doi: 10.18632/oncotarget.7062
- Berlin, J., Bendell, J. C., Hart, L. L., Firdaus, I., Gore, I., Hermann, R. C., et al. (2013). A randomized phase II trial of vismodegib versus placebo with FOLFOX or FOLFIRI and bevacizumab in patients with previously untreated metastatic colorectal cancer. *Clin. Cancer Res.* 19, 258–267. doi: 10.1158/1078-0432.CCR-12-1800
- Bertrand, F. E., Angus, C. W., Partis, W. J., and Sigounas, G. (2012). Developmental pathways in colon cancer: crosstalk between WNT, BMP, Hedgehog and Notch. *Cell Cycle* 11, 4344–4351. doi: 10.4161/cc.22134
- Brabletz, T., Hlubek, F., Spaderna, S., Schmalhofer, O., Hiendlmeyer, E., Jung, A., et al. (2005). Invasion and metastasis in colorectal cancer: epithelial-mesenchymal transition, mesenchymal-epithelial transition, stem cells and beta-catenin. *Cells Tissues Organs* 179, 56–65. doi: 10.1159/000084509
- Brechbiel, J., Miller-Moslin, K., and Adjei, A. A. (2014). Crosstalk between hedgehog and other signaling pathways as a basis for combination therapies in cancer. *Cancer Treat. Rev.* 40, 750–759. doi: 10.1016/j.ctrv.2014.02.003
- Cerami, E., Gao, J., Dogrusoz, U., Gross, B. E., Sumer, S. O., Aksoy, B. A., et al. (2012). The cBio cancer genomics portal: an open platform for exploring multidimensional cancer genomics data. *Cancer Discov.* 2, 401–404. doi: 10.1158/2159-8290.CD-12-0095
- Chatel, G., Ganef, C., Boussif, N., Delacroix, L., Briquet, A., Nolens, G., et al. (2007). Hedgehog signaling pathway is inactive in colorectal cancer cell lines. *Int. J. Cancer* 121, 2622–2627. doi: 10.1002/ijc.22998
- Chung, J. H., and Bunz, F. (2013). A loss-of-function mutation in PTCH1 suggests a role for autocrine hedgehog signaling in colorectal tumorigenesis. *Oncotarget* 4, 2208–2211. doi: 10.18632/oncotarget.1651
- Ciatto, S. (2007). Current cancer profiles of the Italian regions: should cancer incidence be monitored at a national level? *Tumori* 93, 529–531.
- Dennler, S., André, J., Alexaki, I., Li, A., Magnaldo, T., ten Dijke, P., et al. (2007). Induction of sonic hedgehog mediators by transforming growth factor-beta: Smad3-dependent activation of Gli2 and Gli1 expression *in vitro* and *in vivo*. *Cancer Res.* 67, 6981–6986. doi: 10.1158/0008-5472.can-07-0491
- Dijkgraaf, G. J., Alicke, B., Weinmann, L., Januario, T., West, K., Modrusan, Z., et al. (2011). Small molecule inhibition of GDC-0449 refractory smoothened mutants and downstream mechanisms of drug resistance. *Cancer Res.* 71, 435–444. doi: 10.1158/0008-5472.CAN-10-2876
- Douard, R., Moutereau, S., Pernet, P., Chimingqi, M., Allory, Y., Manivet, P., et al. (2006). Sonic Hedgehog-dependent proliferation in a series of patients with colorectal cancer. *Surgery* 139, 665–670. doi: 10.1016/j.surg.2005.10.012
- Ericson, J., Morton, S., Kawakami, A., Roelink, H., and Jessell, T. M. (1996). Two critical periods of Sonic Hedgehog signaling required for the specification of motor neuron identity. *Cell* 87, 661–673.
- Gao, J., Aksoy, B. A., Dogrusoz, U., Dresdner, G., Gross, B., Sumer, S. O., et al. (2013). Integrative analysis of complex cancer genomics and clinical profiles using the cBioPortal. *Sci. Signal.* 6:p11. doi: 10.1126/scisignal.2004088
- Gerling, M., Buller, N. V., Kirn, L. M., Joost, S., Frings, O., Englert, B., et al. (2016). Stromal Hedgehog signalling is downregulated in colon cancer and its restoration restrains tumour growth. *Nat. Commun.* 7:12321. doi: 10.1038/ncomms12321
- Gupta, S., Takebe, N., and Lorusso, P. (2010). Targeting the Hedgehog pathway in cancer. *Ther. Adv. Med. Oncol.* 2, 237–250. doi: 10.1177/1758834010366430
- Hanna, A., and Shevde, L. A. (2016). Hedgehog signaling: modulation of cancer properties and tumor microenvironment. *Mol. Cancer* 15, 24. doi: 10.1186/s12943-016-0509-3
- Hu, M., Yao, J., Carroll, D. K., Weremowicz, S., Chen, H., Carrasco, D., et al. (2008). Regulation of *in situ* to invasive breast carcinoma transition. *Cancer Cell* 13, 394–406. doi: 10.1016/j.ccr.2008.03.007
- Jiang, J., and Hui, C. C. (2008). Hedgehog signaling in development and cancer. *Dev. Cell* 15, 801–812. doi: 10.1016/j.devcel.2008.11.010
- Kangwan, N., Kim, Y. J., Han, Y. M., Jeong, M., Park, J. M., Go, E. J., et al. (2016). Sonic hedgehog inhibitors prevent colitis-associated cancer via orchestrated mechanisms of IL-6/gp130 inhibition, 15-PGDH induction, Bcl-2 abrogation, and tumorsphere inhibition. *Oncotarget* 7, 7667–7682. doi: 10.18632/oncotarget.6765
- Lee, T. Y., Liu, C. L., Chang, Y. C., Nieh, S., Lin, Y. S., Jao, S. W., et al. (2016). Increased chemoresistance via snail-raf kinase inhibitor protein signaling in colorectal cancer in response to a nicotine derivative. *Oncotarget* 7, 23512–23520. doi: 10.18632/oncotarget.8049
- Lee, J. J., Rothenberg, M. E., Seeley, E. S., Zimdahl, B., Kawano, S., Lu, W. J., et al. (2016). Control of inflammation by stromal Hedgehog pathway activation restrains colitis. *Proc. Natl. Acad. Sci. U.S.A.* 113, E7545–E7553. doi: 10.1073/pnas.1616447113
- Liu, Y., Du, F., Zhao, Q., Jin, J., Ma, X., and Li, H. (2015). Acquisition of 5-fluorouracil resistance induces epithelial-mesenchymal transitions through the Hedgehog signaling pathway in HCT-8 colon cancer cells. *Oncol. Lett.* 9, 2675–2679. doi: 10.3892/ol.2015.3136
- Loboda, A., Nebozhyn, M. V., Watters, J. W., Buser, C. A., Shaw, P. M., Huang, P. S., et al. (2011). EMT is the dominant program in human colon cancer. *BMC Med. Genom.* 4:9. doi: 10.1186/1755-8794-4-9
- Magistri, P., Leonard, S. Y., Tang, C. M., Chan, J. C., Lee, T. E., and Sicklick, J. K. (2013). The glypican 3 hepatocellular carcinoma marker regulates human hepatic stellate cells via Hedgehog signaling. *J. Surg. Res.* 187, 377–385. doi: 10.1016/j.jss.2013.12.010
- Merchant, M., Vajdos, F. F., Ultsch, M., Maun, H. R., Wendt, U., Cannon, J., et al. (2004). Suppressor of fused regulates Gli activity through a dual binding mechanism. *Mol. Cell. Biol.* 24, 8627–8641. doi: 10.1128/MCB.24.19.8627-8641.2004
- Nappi, A., Nasti, G., Romano, C., Cassata, A., Silvestro, L., Ottaiano, A., et al. (2016). Multimodal treatment of recurrent colorectal cancer. *World Cancer Res. J.* 3:e719.
- Nolan-Steva, O., Lau, J., Truitt, M. L., Chu, G. C., Hebrok, M., Fernández-Zapico, M. E., et al. (2009). GLI1 is regulated through smoothened-independent mechanisms in neoplastic pancreatic ducts and mediates PDAC cell survival and transformation. *Genes Dev.* 23, 24–36. doi: 10.1101/gad.1753809
- Otsuka, A., Dreier, J., Cheng, P. F., Nägeli, M., Lehmann, H., Felderer, L., et al. (2015). Hedgehog pathway inhibitors promote adaptive immune responses in basal cell carcinoma. *Clin. Cancer Res.* 21, 1289–1297. doi: 10.1158/1078-0432.CCR-14-2110
- Peng, W. X., Zhu, S. L., Zhang, B. Y., Shi, Y. M., Feng, X. X., Liu, F., et al. (2017). Smoothened regulates migration of fibroblast-like synoviocytes in rheumatoid arthritis via activation of Rho GTPase signaling. *Front. Immunol.* 8:159. doi: 10.3389/fimmu.2017.00159
- Perrot, C. Y., Javelaud, D., and Mauviel, A. (2013). Overlapping activities of TGF-beta and Hedgehog signaling in cancer: therapeutic targets for cancer treatment. *Pharmacol. Ther.* 137, 183–199. doi: 10.1016/j.pharmthera.2012.10.002
- Ridley, A. J. (2015). Rho GTPase signalling in cell migration. *Curr. Opin. Cell Biol.* 36, 103–112. doi: 10.1016/j.ccb.2015.08.005
- Rimkus, T. K., Carpenter, R. L., Qasem, S., Chan, M., and Lo, H. W. (2016). Targeting the sonic hedgehog signaling pathway: review of smoothened and GLI inhibitors. *Cancers* 8:22. doi: 10.3390/cancers8020022
- Scales, S. J., and de Sauvage, F. J. (2009). Mechanisms of Hedgehog pathway activation in cancer and implications for therapy. *Trends Pharmacol. Sci.* 30, 303–312. doi: 10.1016/j.tips.2009.03.007
- Sénicourt, B., Boudjadi, S., Carrier, J. C., and Beaulieu, J. F. (2016). Neoeexpression of a functional primary cilium in colorectal cancer cells. *Heliyon* 2:e00109. doi: 10.1016/j.heliyon.2016.e00109
- Strippoli, R., Loureiro, J., Moreno, V., Benedicto, I., Perez Lozano, M. L., Barreiro, O., et al. (2015). Caveolin-1 deficiency induces a MEK-ERK1/2-Snail-1-dependent epithelial-mesenchymal transition and fibrosis during peritoneal dialysis. *EMBO Mol. Med.* 7, 102–123. doi: 10.15252/emmm.201404127
- Sun, K., Deng, H. J., Lei, S. T., Dong, J. Q., and Li, G. X. (2013). miRNA-338-3p suppresses cell growth of human colorectal carcinoma by targeting smoothened. *World J. Gastroenterol.* 19, 2197–2207. doi: 10.3748/wjg.v19.i14.2197
- Takebe, N., Miele, L., Harris, P. J., Jeong, W., Bando, H., Kahn, M., et al. (2015). Targeting notch, Hedgehog, and Wnt pathways in cancer stem cells: clinical update. *Nat. Rev. Clin. Oncol.* 12, 445–464. doi: 10.1038/nrclinonc.2015.61

- Tan, T. Z., Miow, Q. H., Miki, Y., Noda, T., Mori, S., Thiery, J. P., et al. (2014). Epithelial-mesenchymal transition spectrum quantification and its efficacy in deciphering survival and drug responses of cancer patients. *EMBO Mol. Med.* 6, 1279–1293. doi: 10.15252/emmm.201404208
- Varnat, F., Duquet, A., Malerba, M., Zbinden, M., Mas, C., Gervaz, P., et al. (2009). Human colon cancer epithelial cells harbour active HEDGEHOG-Gli signalling that is essential for tumour growth, recurrence, metastasis and stem cell survival and expansion. *EMBO Mol. Med.* 1, 338–351. doi: 10.1002/emmm.200900039
- Wang, D., Hu, G., Du, Y., Zhang, C., Lu, Q., Lv, N., et al. (2017). Aberrant activation of hedgehog signaling promotes cell proliferation via the transcriptional activation of forkhead Box M1 in colorectal cancer cells. *J. Exp. Clin. Cancer Res.* 36:23. doi: 10.1186/s13046-017-0491-7
- Wang, R., Wei, J., Zhang, S., Wu, X., Guo, J., Liu, M., et al. (2016). Peroxiredoxin 2 is essential for maintaining cancer stem cell-like phenotype through activation of Hedgehog signaling pathway in colon cancer. *Oncotarget* 7, 86816–86828. doi: 10.18632/oncotarget.13559
- Wang, T. P., Hsu, S. H., Feng, H. C., and Huang, R. F. (2012). Folate deprivation enhances invasiveness of human colon cancer cells mediated by activation of sonic hedgehog signaling through promoter hypomethylation and cross action with transcription nuclear factor-kappa B pathway. *Carcinogenesis* 33, 1158–1168. doi: 10.1093/carcin/bgs138
- Xu, M., Li, X., Liu, T., Leng, A., and Zhang, G. (2012). Prognostic value of hedgehog signaling pathway in patients with colon cancer. *Med. Oncol.* 29, 1010–1016. doi: 10.1007/s12032-011-9899-7
- Yauch, R. L., Gould, S. E., Scales, S. J., Tang, T., Tian, H., Ahn, C. P., et al. (2008). A paracrine requirement for hedgehog signalling in cancer. *Nature* 455, 406–410. doi: 10.1038/nature07275
- Yoon, C., Cho, S. J., Chang, K. K., Park, D. J., Ryeom, S., and Yoon, S. S. (2017). Role of Rac1 pathway in epithelial-to-mesenchymal transition and cancer stem-like cell phenotypes in gastric adenocarcinoma. *Mol. Cancer Res.* 15, 1106–1116. doi: 10.1158/1541-7786.MCR-17-0053

**Conflict of Interest Statement:** The authors declare that the research was conducted in the absence of any commercial or financial relationships that could be construed as a potential conflict of interest.

Copyright © 2018 Magistri, Battistelli, Strippoli, Petrucciani, Pellinen, Rossi, Mangogna, Aurello, D'Angelo, Tripodi, Ramacciato and Nigri. This is an open-access article distributed under the terms of the Creative Commons Attribution License (CC BY). The use, distribution or reproduction in other forums is permitted, provided the original author(s) and the copyright owner are credited and that the original publication in this journal is cited, in accordance with accepted academic practice. No use, distribution or reproduction is permitted which does not comply with these terms.



# Tacrolimus Reverses UVB Irradiation-Induced Epidermal Langerhans Cell Reduction by Inhibiting TNF- $\alpha$ Secretion in Keratinocytes via Regulation of NF- $\kappa$ B/p65

JiaLi Xu<sup>1</sup>, YaDong Feng<sup>2,3</sup>, GuoXin Song<sup>4</sup>, QiXing Gong<sup>4</sup>, Li Yin<sup>5,6</sup>, YingYing Hu<sup>5</sup>, Dan Luo<sup>5</sup> and ZhiQiang Yin<sup>5\*</sup>

<sup>1</sup> Department of Oncology, First Affiliated Hospital of Nanjing Medical University, Nanjing, China, <sup>2</sup> Department of Gastroenterology, First Affiliated Hospital of Nanjing Medical University, Nanjing, China, <sup>3</sup> Department of Gastroenterology, Zhongda Hospital, School of Medicine, Southeast University, Nanjing, China, <sup>4</sup> Department of Pathology, First Affiliated Hospital of Nanjing Medical University, Nanjing, China, <sup>5</sup> Department of Dermatology, First Affiliated Hospital of Nanjing Medical University, Nanjing, China, <sup>6</sup> Department of Dermatology, Affiliated Wuxi People's Hospital, Nanjing Medical University, Wuxi, China

## OPEN ACCESS

### Edited by:

Timothy Joseph Keane,  
Imperial College London,  
United Kingdom

### Reviewed by:

Claudio Ferrante,  
Università degli Studi "G. d'Annunzio"  
Chieti – Pescara, Italy  
Lucia Recinella,  
Università degli Studi "G. d'Annunzio"  
Chieti – Pescara, Italy

### \*Correspondence:

ZhiQiang Yin  
yzq2802@sina.com

### Specialty section:

This article was submitted to  
Inflammation Pharmacology,  
a section of the journal  
Frontiers in Pharmacology

Received: 30 November 2017

Accepted: 18 January 2018

Published: 22 February 2018

### Citation:

Xu J, Feng Y, Song G, Gong Q,  
Yin L, Hu Y, Luo D and Yin Z (2018)  
Tacrolimus Reverses UVB  
Irradiation-Induced Epidermal  
Langerhans Cell Reduction by  
Inhibiting TNF- $\alpha$  Secretion  
in Keratinocytes via Regulation  
of NF- $\kappa$ B/p65.  
Front. Pharmacol. 9:67.  
doi: 10.3389/fphar.2018.00067

**Background:** Topical calcineurin inhibitors including tacrolimus and pimecrolimus are used in the treatment of many inflammatory skin diseases mainly via blocking T-cell proliferation. Our previous studies found that pimecrolimus 1% cream could reverse high-dose ultraviolet B (UVB) irradiation-induced epidermal Langerhans cell (LC) reduction via inhibition of LC migration. We conducted this study to investigate the effects of topical tacrolimus 0.03% ointment on high-dose UVB-irradiated human epidermal LCs.

**Methods:** Twenty fresh human foreskin tissues were randomly divided into four groups as follows: *Control*, *Tacrolimus* (0.03%), *UVB* (180 mJ/cm<sup>2</sup>), and *UVB* (180 mJ/cm<sup>2</sup>) + *Tacrolimus* (0.03%). Four time points were set as follows: 0, 18, 24, and 48 h. We collected culture medium and tissues at each time point. The percentage of CD1a+ cells in the medium was detected by means of flow cytometry. Each tissue was prepared for immunohistochemistry, real-time quantitative PCR, and western blot. HaCaT cells were cultured and divided into four groups: *Control*, *Tacrolimus* (1  $\mu$ g/ml), *UVB* (30 mJ/cm<sup>2</sup>), and *UVB* (30 mJ/cm<sup>2</sup>) + *Tacrolimus* (1  $\mu$ g/ml). The cells were incubated for 24 h and prepared for real-time quantitative PCR and western blot.

**Results:** Topical tacrolimus significantly reversed high-dose UVB irradiation-induced epidermal LC reduction and CD1a+ cell increment in culture medium. Tacrolimus significantly inhibited UVB irradiation-induced tumor necrosis factor- $\alpha$  (TNF- $\alpha$ ) and nuclear factor kappa B (NF- $\kappa$ B)/p65 mRNA and protein expression in HaCaT cells. Tacrolimus also significantly inhibited high-dose UVB irradiation-induced TNF- $\alpha$  expression in cultured tissues. Finally, TNF- $\alpha$  antagonist (recombinant human TNF- $\alpha$  receptor II: IgG Fc fusion protein) could significantly reverse UVB irradiation-induced epidermal LC reduction.



**Conclusion:** Topical tacrolimus 0.03% could reverse UVB irradiation-induced epidermal LC reduction by inhibiting TNF- $\alpha$  secretion in keratinocytes via regulation of NF- $\kappa$ B/p65.

**Keywords:** tacrolimus, UVB, Langerhans cells, TNF- $\alpha$ , NF- $\kappa$ B

## INTRODUCTION

Topical calcineurin inhibitors (TCIs), including tacrolimus ointment and pimecrolimus cream, are widely used in the treatment of atopic dermatitis and many other inflammatory skin diseases, where the central therapeutic mechanism is to block T-cell proliferation and inhibit the activation of T-cells and thereby diminish inflammation (Yin et al., 2014; Nygaard et al., 2017). In contrast with topical corticosteroids, TCIs are not related to atrophy or increased percutaneous absorption after long-term use and have much lower possibility for systemic effects (Siegfried et al., 2016).

There is no evidence that TCIs have direct action on epidermal Langerhans cells (LCs). Epidermal LCs have the action of immunosurveillance and process antigen and migrate to local draining lymphnodes from epidermis, expressing CD1a (Rowden, 1980). Single high-dose ultraviolet B (UVB) irradiation can induce significant epidermal LC depletion in human skin, and the increased migration of LCs might be the main mechanism (Kölgen et al., 2002). UVB-induced apoptotic cells are phagocytosed by LCs *ex vivo*, which has an important anti-inflammatory effect in the resolution of UVB-induced cutaneous inflammation (Hatakeyama et al., 2017).

Our previous studies found that high-dose UVB irradiation significantly decreased the number of epidermal LCs, and pimecrolimus 1% cream could reverse these changes via inhibition of LCs migration by regulation of tumor necrosis factor- $\alpha$  (TNF- $\alpha$ ) and E-cadherin (Yin et al., 2012b, 2014). Whether topical tacrolimus (another kind of widely used TCI) can also inhibit LC migration in UVB-irradiated skin is still unclear.

Lan et al. (2005) reported UVB irradiation-induced secretion of TNF- $\alpha$  from keratinocytes, which could be inhibited by tacrolimus by downregulation of nuclear factor kappa B (NF- $\kappa$ B) expression. Wu et al. (2012) found that tacrolimus didn't affect the nuclear activation and translocation of NF- $\kappa$ B/p50; however, UVB irradiation-induced NF- $\kappa$ B/p65 nuclear expression was suppressed by tacrolimus. This study aimed to investigate the effect of topical tacrolimus 0.03% ointment on high-dose UVB-irradiated human epidermal LCs and the possible relation with TNF- $\alpha$  secretion and NF- $\kappa$ B/p65 regulation, which would contribute to further understanding of the mechanism of TCI action and treatment.

## MATERIALS AND METHODS

### Ethics Statement

This study was carried out in accordance with the recommendations of institutional guidelines and Local Ethics

Committee of the First Affiliated Hospital of Nanjing Medical University (approval number 2013-SRFA-074). Written informed consent was obtained from all subjects.

### Study Design

Twenty fresh human foreskin tissues were obtained from Department of Urology by circumcision, consented by the patients (age range 18–30 years). All subjects gave written informed consent in accordance with the Declaration of Helsinki. The tissues were randomly divided into four groups of five each, as follows: *Control*, *Tacrolimus* (tissues were applied once with topical tacrolimus 0.03% on the epidermis), *UVB* (tissues were irradiated once with 180 mJ/cm<sup>2</sup> UVB on the epidermis), and *UVB + Tacrolimus* (tissues were applied on the epidermis with topical tacrolimus 0.03% after 180 mJ/cm<sup>2</sup> UVB irradiation). The tissues were processed and cultured as previously described (Yin et al., 2012b). Recombinant human TNF- $\alpha$  receptor II: IgG Fc fusion protein (Yisaipu; CP Guojian Pharmaceutical Co., Ltd., Shanghai, China; 50  $\mu$ g/ml) was added into culture medium to block the effect of TNF- $\alpha$ .

The UVB source was a BLE-1T158 UV lamp (Spectronics Corp., Westbury, NY, United States) by which 180 mJ/cm<sup>2</sup> UVB was delivered once to the epidermis. After UVB irradiation or not, tacrolimus 0.03% ointment (Protopic; Astellas Toyama Co., Toyama, Japan) was applied on the epidermis. Ten minutes after application or irradiation, 1 ml culture medium was added to each well to immerse the whole tissue. All tissues were cultured at 37°C.

Four time points were set as follows: 0, 18, 24, and 48 h. For each group, each tissue was cut into four pieces corresponding to four time points. We collected culture medium and tissues at each time point, following which each tissue was cut into three parts. The percentage of CD1a+ cells in the medium was detected by means of flow cytometry. Each tissue was prepared for immunohistochemistry, real-time quantitative PCR, and western blot.

Keratinocyte line HaCaT cells were cultured as previously described (Zhou et al., 2013), and seeded in 12-well culture plates and divided into four groups, as follows: *Control*, *Tacrolimus* (Prograf; Astellas Ireland Co., Ltd., Killorglin, Co. Kerry, Ireland; 1  $\mu$ g/ml), *UVB* (30 mJ/cm<sup>2</sup>), and *UVB* (30 mJ/cm<sup>2</sup>) + *Tacrolimus* (1  $\mu$ g/ml). The cells were incubated for 24 h, and then prepared for real-time quantitative PCR and western blot. Experiments were repeated independently at least three times.

### Flow Cytometry

Detection of CD1a expression on cells in the culture medium was performed using anti-human CD1a-PE antibody (BioLegend,

Inc., San Diego, CA, United States) (Yin et al., 2014). A FACS Calibur<sup>TM</sup> Flow Cytometer (BD Biosciences, Franklin Lakes, NJ, United States) was used to gather data and images.

## Immunohistochemistry

Slides were prepared using a Ventana autoimmunostainer (Loche, United States) and available CD1a monoclonal antibody (Maixin-Bio, Fuzhou, Fujian, China) and active caspase-3 polyclonal antibody (Abcam, New Territories, Hong Kong, China). Detection utilized Polymer-HRP, with 3,3'-diaminobenzidine chromogen, and slides were visualized at 40× with a Nikon Eclipse microscope (Yin et al., 2012b). The number of typical CD1a positive epidermal LCs was counted for five successive fields in high magnification (HM, 400×). The number of LCs was calculated and expressed as CD1a+ LC/HM.

## Real-Time Quantitative PCR

Total mRNA was extracted from part (50 mg) of the aforementioned collected tissue, using TRIzol<sup>®</sup> Reagent (Invitrogen; Life Technologies Corp., Carlsbad, CA, United States). The HaCaT cells attached to the culture plates were washed three times using PBS and then dissolved in TRIzol<sup>®</sup> Reagent. First-strand cDNA was synthesized from 2 µg of total RNA. PCR amplification was performed in a total volume of 20 µl containing 1 µl template cDNA and 10 µl Real-Time PCR Master Mix (SYBR Green) (TOYOBO, Japan), and transcripts quantified using StepOnePlus<sup>TM</sup> Real-Time PCR System (Applied Biosystems, United States) (Yin et al., 2017).

All values were normalized to the expression of glyceraldehyde phosphate dehydrogenase (GAPDH). Primer sequences are shown in Table 1.

## Western Blot

The collected tissues and HaCaT cells were homogenized in cold lysis buffer containing protease inhibitor. Centrifugal separation was conducted at 4°C, at 14,000 rpm for 15 min. The upper layer of the solution was tested for protein using the Bradford method. SDS-PAGE was performed (Yin et al., 2017). The primary antibody was added as below: TNF-α, β-actin (Biosynthesis Bio, Beijing, China), and NF-κB/p65 (KeyGEN Biotech, Nanjing, Jiangsu, China), following the manufacturer's instructions. Differences in protein expression were examined using Gel-Pro 32 (Media Cybernetics, Rockville, MD, United States).

## Statistical Analysis

Data analysis was conducted by using GraphPad Prism for Windows (GraphPad Software, San Diego, CA, United States). All data were presented as mean ± SD. Data were tested for normality and statistical significance calculated using a Student's *t*-test, Mann-Whitney *U*-test, or Friedman's test, as appropriate (Yin et al., 2017). *P* < 0.05 was considered statistically significant.

## RESULTS

### Topical Tacrolimus Reverses High-Dose UVB Irradiation-Induced Epidermal Langerhans Cell Reduction

Immunohistochemistry showed that the number of epidermal CD1a+ LCs had no significant differences at different time points, for *Control* and *Tacrolimus* group. One hundred and eighty millijoules per centimeter squared UVB irradiation induced significant CD1a+ LC reduction at 18, 24, and 48 h (*P* < 0.01, respectively), which could be significantly reversed by topical tacrolimus 0.03% at 24 and 48 h (*P* < 0.05 and *P* < 0.01) (Figures 1A–D, upper panel, E).

The lower panel of Figures 1A,B show there were no obvious active caspase 3-positive cells in the epidermis for *Control* and *Tacrolimus* group. High-dose UVB irradiation induced obvious cell apoptosis in stratum spinosum and basal layer of epidermis, and UVB + *Tacrolimus* group seemed to have no visible difference in comparison with UVB group (Figures 1C,D, lower panel).

### Topical Tacrolimus Reverses High-Dose UVB Irradiation-Induced CD1a+ Cell Increment in Culture Medium

Flow cytometry (Figures 1F,G) showed 180 mJ/cm<sup>2</sup> UVB irradiation induced significant increment of the percentage of CD1a+ cells in culture medium at 18, 24, and 48 h (18 h, *P* < 0.05; 24 h, *P* < 0.001; 48 h, *P* < 0.01), compared with *Control* group. Topical tacrolimus had no direct effect on the percentage of CD1a+ cells in culture medium; however, it could reverse UVB

**TABLE 1 |** Primers for the target genes in real-time quantitative PCR.

Target genes	Primers
GAPDH (115 bp)	Sense: 5'-CATCTTCTTTTCGCTCGCCA-3' Antisense: 5'-TTAAAGCAGCCCTGGTGACC-3'
IL-18 (77 bp)	Sense: 5'-GGGAAGAGGAAAGGAACCTC-3' Antisense: 5'-CCATCTTTATTCCTGCGACA-3'
TNF-α (66 bp)	Sense: 5'-CCTCTTCTCCTTCTGATCG-3' Antisense: 5'-ATCACTCCAAAGTGCAGCAG-3'
E-cadherin (142 bp)	Sense: 5'-CAGCGTGTGTGACTGTGAAG-3' Antisense: 5'-AAACAGCAAGAGCAGCAGAA-3'
NF-κB/p65 (142 bp)	Sense: 5'-GCATCCAGACCAACAACAC-3' Antisense: 5'-ATGGGATGAGAAAGGACAGG-3'
IL-1β (115 bp)	Sense: 5'-AAGCTGAGGAAGATGCTGGT-3' Antisense: 5'-CGTTATCCCATGTGTGCGAAG-3'
CCR7 (141 bp)	Sense: 5'-GGGAGAGTGTGGTGTTCCT-3' Antisense: 5'-CCTGACATTTCCCTTGTCCT-3'
CCL19 (83 bp)	Sense: 5'-AAGACTGCTGCCTGTCTGTG-3' Antisense: 5'-GCCATCCTTGATGAGAAGGT-3'
MMP-9(81 bp)	Sense: 5'-CCGGACCAAGGATACAGTTT-3' Antisense: 5'-CGGCACTGAGGAATGATCTA-3'
ITGA6 (101 bp)	Sense: 5'-AACTGGAAAGGATTGTTTCG-3' Antisense: 5'-TGCTCAGTCTCTCCACCAAC-3'

Abbreviation: GAPDH, glyceraldehyde phosphate dehydrogenase; IL-18, interleukin-18; TNF-α, tumor necrosis factor-α; NF-κB, nuclear factor kappa B; IL-1β, Interleukin-1β; CCR7, C-C chemokine receptor type 7; CCL19, C-C motif ligand 19; MMP-9, matrix metalloproteinase 9; ITGA6, integrin alpha-6.



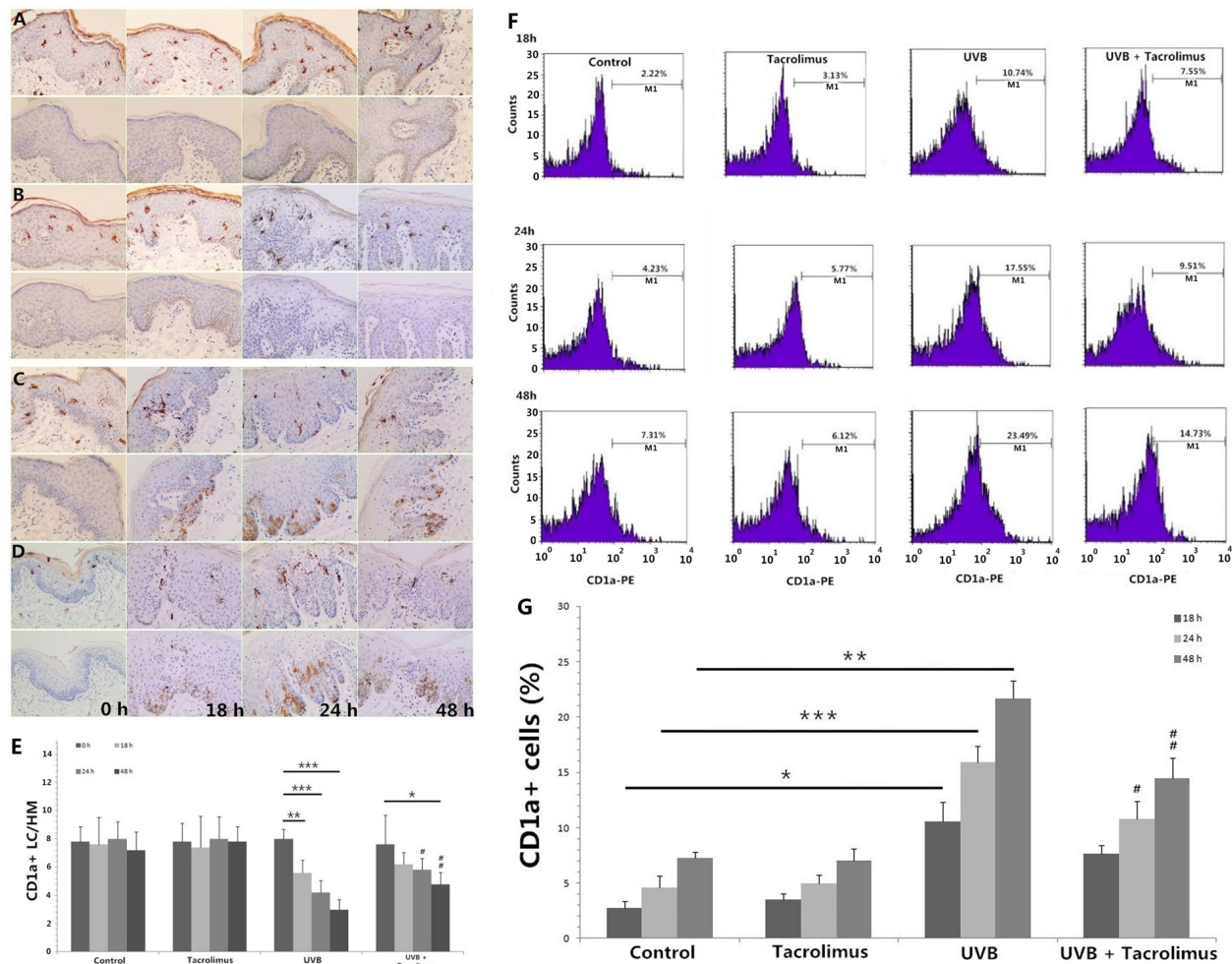


**FIGURE 1 |** Immunohistochemical staining of CD1a and active caspase 3 in foreskin tissues (A–E, HM  $\times$  400) and flow cytometry of CD1a expression on cells in the culture medium (F,G) at different time points. (A) Control group, (B) Tacrolimus group, (C) UVB group, (D) UVB + Tacrolimus group, (E) Topical tacrolimus significantly reversed 180 mJ/cm<sup>2</sup> UVB irradiation-induced marked epidermal CD1a+ LC reduction in tissues at 24 and 48 h, (F) Flow cytometry of CD1a, (G) Topical tacrolimus significantly inhibited UVB irradiation-induced marked CD1a+ cell increment in the culture medium at 24 and 48 h. Statistical significance indicated: \* $P < 0.05$ , \*\* $P < 0.01$ , \*\*\* $P < 0.001$ , # $P < 0.05$ , ## $P < 0.01$ , ### $P < 0.001$ . Abbreviation: UVB, ultraviolet B; LCs, Langerhans cells; HM, high magnification.

irradiation-induced CD1a+ cell increment (24 h,  $P < 0.05$ ; 48 h,  $P < 0.01$ ).

## Tacrolimus Inhibits UVB Irradiation-Induced TNF- $\alpha$ and NF- $\kappa$ B/p65 Expression in HaCaT Cells

We irradiated HaCaT cells with 30 mJ/cm<sup>2</sup> UVB and observed statistically significant increases in TNF- $\alpha$  and NF- $\kappa$ B/p65 but not interleukin-18 (IL-18) or E-cadherin mRNA after 24 h of incubation ( $P < 0.01$ , respectively) (Figure 2A). One microgram per milliliter tacrolimus had no direct effect on these cytokines and adhesion molecule mRNA expression in HaCaT cells; however, it could significantly inhibit UVB irradiation-induced TNF- $\alpha$  and NF- $\kappa$ B/p65 expression ( $P < 0.001$ , respectively) (Figure 2A), which was also confirmed at the protein level (Figures 2B,C).

## Topical Tacrolimus Inhibits High-Dose UVB Irradiation-Induced TNF- $\alpha$ Expression in Cultured Tissues

One hundred and eighty millijoules per centimeter squared UVB irradiation induced significant increases in TNF- $\alpha$  mRNA expression in cultured tissues at 18, 24, and 48 h (18 h,  $P < 0.001$ ; 24 h,  $P < 0.01$ ; 48 h,  $P < 0.01$ ) (Figure 3A), which was confirmed at the protein level (24 h,  $P < 0.01$ ; 48 h,  $P < 0.01$ ) (Figures 3B,C). Topical tacrolimus could significantly inhibit high-dose UVB irradiation-induced TNF- $\alpha$  mRNA expression (18 h,  $P < 0.001$ ; 24 h,  $P < 0.01$ ; 48 h,  $P < 0.05$ ) (Figure 3A), which was also confirmed at the protein level (24 h,  $P < 0.05$ ; 48 h,  $P < 0.05$ ) (Figures 3B,C). High-dose UVB irradiation also induced significant increases in matrix metalloproteinase 9 (MMP-9) mRNA expression in cultured tissues at 24 and 48 h (24 h,  $P < 0.001$ ; 48 h,  $P < 0.001$ ); however, it could not be

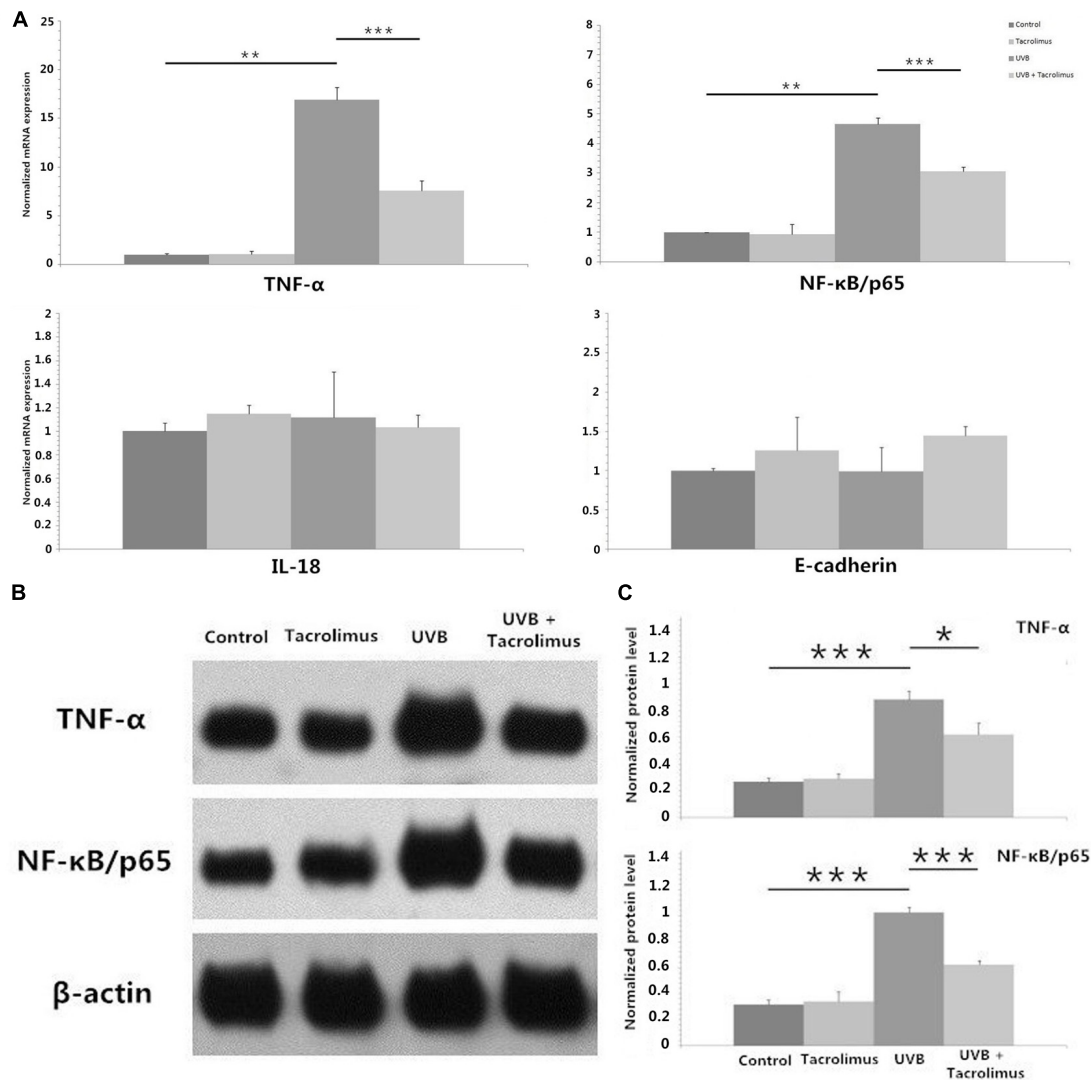


**FIGURE 2 |** Real-time quantitative PCR analyses of TNF- $\alpha$ , NF- $\kappa$ B/p65, IL-18, and E-cadherin mRNA expression in HaCaT cells (**A**) and western blot of TNF- $\alpha$  and NF- $\kappa$ B/p65 protein expression in HaCaT cells (**B,C**) after 24 h of incubation. (**A**) One microgram per milliliter tacrolimus significantly inhibited 30 mJ/cm<sup>2</sup> UVB irradiation-induced marked TNF- $\alpha$  and NF- $\kappa$ B/p65 mRNA expression. (**B**) Western blot of TNF- $\alpha$  and NF- $\kappa$ B/p65. (**C**) The inhibition of tacrolimus on UVB irradiation-induced TNF- $\alpha$  and NF- $\kappa$ B/p65 mRNA expression was confirmed at the protein level. Statistical significance indicated: \* $P$  < 0.05, \*\* $P$  < 0.01, \*\*\* $P$  < 0.001. Abbreviation: UVB, ultraviolet B; IL-18, interleukin-18; TNF- $\alpha$ , tumor necrosis factor- $\alpha$ ; NF- $\kappa$ B, nuclear factor kappa B.

regulated by topical tacrolimus (Figure 3A). Neither high-dose UVB single irradiation nor topical tacrolimus had direct effect on IL-1 $\beta$ , C-C chemokine receptor type 7 (CCR7), C-C motif ligand 19 (CCL19), and integrin alpha-6 (ITGA6) mRNA expression in tissues.

### TNF- $\alpha$ Antagonist Reverses High-Dose UVB Irradiation-Induced Epidermal Langerhans Cell Reduction and CD1a+ Cell Increment in Culture Medium

Figures 4A,B show that TNF- $\alpha$  antagonist (recombinant human TNF- $\alpha$  receptor II: IgG Fc fusion protein, 50  $\mu$ g/ml) significantly reversed high-dose UVB irradiation-induced epidermal LC

reduction at 24 h ( $P$  < 0.05), and inhibited UVB irradiation-induced significant increment of the percentage of CD1a+ cells in culture medium ( $P$  < 0.01) (Figures 4C,D).

## DISCUSSION

Langerhans cells represent the first line of immunological defense, which has been proved to belong to the macrophage lineage recently (Doebel et al., 2017). The proliferation, maturation, and migration of epidermal LCs can be affected by skin inflammation, and increased migration during inflammation can lead to a partial depletion of epidermal LCs. Adhesion between keratinocytes and LCs, mediated by E-cadherin, is

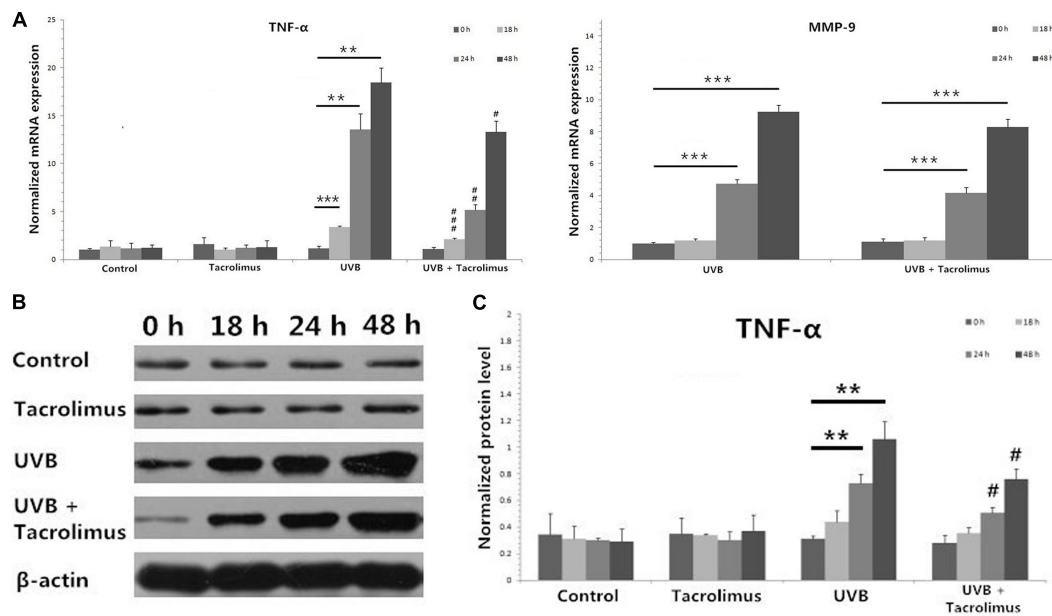


**FIGURE 3 |** Real-time quantitative PCR analyses of cultured tissues (A) and protein detection by using western blot (B,C) at different time points. (A) Topical tacrolimus significantly inhibited 180 mJ/cm<sup>2</sup> UVB irradiation-induced TNF-α mRNA expression in cultured tissues at 18, 24, and 48 h; however, it could not regulate UVB irradiation-induced significant increases in MMP-9 mRNA expression. (B) Western blot of TNF-α. (C) The inhibition of tacrolimus on UVB irradiation-induced TNF-α mRNA expression was confirmed at the protein level at 24 and 48 h. Statistical significance indicated: \**P* < 0.05, \*\**P* < 0.01, \*\*\**P* < 0.001, #*P* < 0.05, ##*P* < 0.01, ###*P* < 0.001. Abbreviation: UVB, ultraviolet B; TNF-α, tumor necrosis factor-α; MMP-9, matrix metalloproteinase 9.

important in the retention of LCs in the skin (Matthews et al., 2003). Epidermal LCs disengage from their adhesion with surrounding keratinocytes during the migration in part by downregulation of E-cadherin (Tang et al., 1993). Intradermal injection of antagonists against TNF-α, IL-1β, and IL-18 impairs epidermal LC migration (Cumberbatch et al., 1997, 2001). The increment of the expression of CCR7, CCL19, MMP-9, and ITGA6 also promotes LC migration from epidermis to dermis (Price et al., 1997; Randolph, 2001; Koch et al., 2006).

Previous studies observed that high-dose UVB irradiation could decrease the number of epidermal LCs, and found the possible mechanism was the increment of LC migration rather than LC apoptosis (Kölgen et al., 2002; Yin et al., 2012b). The cited study has also proved that high-dose UVB irradiation-induced epidermal LC reduction was related to LCs migration (Yin et al., 2014). Our study showed topical tacrolimus could reverse high-dose UVB irradiation-induced epidermal LC reduction by inhibiting TNF-α secretion in keratinocytes via regulation of NF-κB/p65. Anti-TNF-α treatment significantly reversed UVB irradiation-induced epidermal LC reduction and CD1a+ cell increment in culture medium. We thought the CD1a staining positive cells in the culture medium were mainly made up of migrated LCs and dermal dendritic cells, and the increased CD1a+ cells in the medium induced by UVB irradiation should most probable be LCs.

Epidermal LCs play important role in immunosurveillance, which is an important pathway against tumorigenesis. Epidermal immature LCs can discern and ingest antigen, then gradually

mature during migration. Interestingly, Modi et al. (2012) reported that LCs facilitated epithelial DNA damage and squamous cell carcinoma, suggesting the complex relation between immune cells and carcinogenesis. Lewis et al. (2015) also reported that LCs could facilitate UVB-induced epidermal carcinogenesis, which was counter to the concept of LCs as key players in tumor immunosurveillance that indicated the complexity of LC functions. Transforming growth factor beta-1 (TGF-β1) signaling promoted UVB-induced skin carcinogenesis that was mediated partly through its role in UVB-induced migration of dermal dendritic cell and cutaneous inflammation (Ravindran et al., 2014).

In 2006, the US Food and Drug Administration issued “black box” warnings for TCIs due to potential safety risks including skin cancers and lymphomas, which is still lack of evidence presently (Yin et al., 2012a). Voskamp et al. (2013) reported oral tacrolimus did not enhance UV irradiation-induced skin carcinogenesis. Mitamura et al. (2011) found both topical tacrolimus 0.03% and tacrolimus 0.1% could inhibit tumor induction in a mouse model of an initiation–promotion skin tumor. Topical tacrolimus did not enhance photocarcinogenesis or induce any dermal carcinogenicity in hairless mice (Lerche et al., 2008).

Pimecrolimus cream, another kind of TCI, did not affect LC number in healthy and atopic skin (Hoetzenecker et al., 2005; Yin et al., 2012b). In this study, tacrolimus 0.03% ointment used alone has also no obvious effect on human epidermal LC number; however, topical tacrolimus reverses high-dose UVB irradiation-induced epidermal LC reduction by inhibiting LC migration

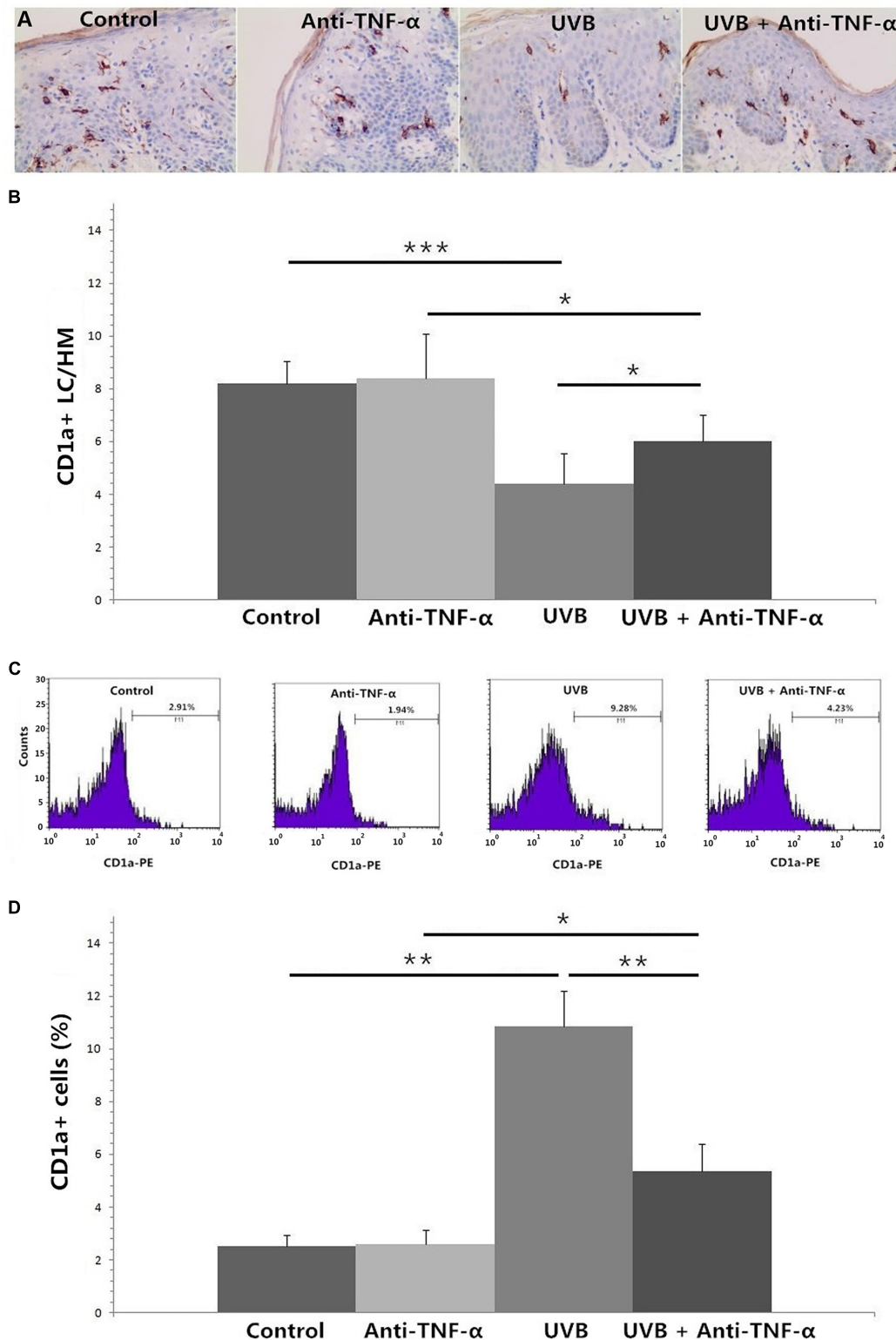


**FIGURE 4 |** Immunohistochemical staining of CD1a in foreskin tissues (**A,B**, HM  $\times$  400) and flow cytometry of CD1a expression on cells in the culture medium (**C,D**) after 24 h of incubation. (**A**) Less CD1a+ LCs were seen in epidermis after 180 mJ/cm<sup>2</sup> UVB irradiation. (**B**) TNF- $\alpha$  antagonist significantly reversed high-dose UVB irradiation-induced epidermal LC reduction at 24 h. (**C**) A higher percentage of CD1a+ cells in culture medium were observed in UVB group by using flow cytometry. (**D**) TNF- $\alpha$  antagonist significantly inhibited UVB irradiation-induced increment of the percentage of CD1a+ cells in culture medium. Statistical significance indicated: \* $P$  < 0.05, \*\* $P$  < 0.01, \*\*\* $P$  < 0.001. Abbreviation: UVB, ultraviolet; LCs, Langerhans cells; HM, high magnification; TNF- $\alpha$ , tumor necrosis factor- $\alpha$ .



via downregulation TNF- $\alpha$  secretion in epidermal keratinocytes. In light of the fact that LCs could facilitate UVB-induced epidermal carcinogenesis (Lewis et al., 2015), the regulation effect of tacrolimus ointment on UVB irradiation-induced LC migration would promote photocarcinogenesis or inhibit skin carcinogenesis, which needs further investigation.

## ETHICS STATEMENT

This study was carried out in accordance with the recommendations of institutional guidelines and Local Ethics Committee of the First Affiliated Hospital of Nanjing Medical University (approval number 2013-SRFA-074). All subjects gave written informed consent in accordance with the Declaration of Helsinki.

## REFERENCES

- Cumberbatch, M., Dearman, R.-J., Antonopoulos, C., Groves, R.-W., and Kimber, I. (2001). Interleukin (IL)-18 induces Langerhans cell migration by a tumour necrosis factor- $\alpha$ - and IL-1 $\beta$ -dependent mechanism. *Immunology* 102, 323–330. doi: 10.1046/j.1365-2567.2001.01187.x
- Cumberbatch, M., Dearman, R.-J., and Kimber, I. (1997). Langerhans cells require signals from both tumour necrosis factor- $\alpha$  and interleukin-1  $\beta$  for migration. *Immunology* 92, 388–395. doi: 10.1046/j.1365-2567.1997.00360.x
- Doebel, T., Voisin, B., and Nagao, K. (2017). Langerhans cells - the macrophage in dendritic cell clothing. *Trends Immunol.* 38, 817–828. doi: 10.1016/j.it.2017.06.008
- Hatakeyama, M., Fukunaga, A., Washio, K., Taguchi, K., Oda, Y., Ogura, K., et al. (2017). Anti-inflammatory role of Langerhans Cells and apoptotic keratinocytes in ultraviolet-B-induced cutaneous inflammation. *J. Immunol.* 199, 2937–2947. doi: 10.4049/jimmunol.1601681
- Hoetznecker, W., Ecker, R., Kopp, T., Stuetz, A., Stingl, G., and Elbe-Bürger, A. (2005). Pimecrolimus leads to an apoptosis-induced depletion of T cells but not Langerhans cells in patients with atopic dermatitis. *J. Allergy Clin. Immunol.* 115, 1276–1283. doi: 10.1016/j.jaci.2005.02.011
- Koch, S., Kohl, K., Klein, E., von Bubnoff, D., and Bieber, T. (2006). Skin homing of Langerhans cell precursors: adhesion, chemotaxis, and migration. *J. Allergy Clin. Immunol.* 117, 163–168. doi: 10.1016/j.jaci.2005.10.003
- Kölgen, W., Both, H., van Weelden, H., Guikers, K.-L., Bruijnzeel-Koomen, C.-A., Knol, E.-F., et al. (2002). Epidermal Langerhans cell depletion after artificial ultraviolet B irradiation of human skin *in vivo*: apoptosis versus migration. *J. Invest. Dermatol.* 118, 812–817. doi: 10.1046/j.1523-1747.2002.01742.x
- Lan, C.-C., Yu, H.-S., Wu, C.-S., Kuo, H.-Y., Chai, C.-Y., and Chen, G.-S. (2005). FK506 inhibits tumour necrosis factor- $\alpha$  secretion in human keratinocytes via regulation of nuclear factor- $\kappa$ B. *Br. J. Dermatol.* 153, 725–732. doi: 10.1111/j.1365-2133.2005.06779.x
- Lerche, C.-M., Philipsen, P.-A., Poulsen, T., and Wulf, H.-C. (2008). Topical tacrolimus in combination with simulated solar radiation does not enhance photocarcinogenesis in hairless mice. *Exp. Dermatol.* 17, 57–62.
- Lewis, J.-M., Bürgler, C.-D., Freudzon, M., Golubets, K., Gibson, J.-F., Filler, R.-B., et al. (2015). Langerhans cells facilitate UVB-induced epidermal carcinogenesis. *J. Invest. Dermatol.* 135, 2824–2833. doi: 10.1038/jid.2015.207
- Matthews, K., Leong, C.-M., Baxter, L., Inglis, E., Yun, K., Bäckström, B.-T., et al. (2003). Depletion of Langerhans cells in human papillomavirus type 16-infected skin is associated with E6-mediated down regulation of E-cadherin. *J. Virol.* 77, 8378–8385. doi: 10.1128/JVI.77.15.8378-8385.2003
- Mitamura, T., Doi, Y., Kawabe, M., Motomura, M., Oishi, Y., Yoshizawa, K., et al. (2011). Inhibitory potency of tacrolimus ointment on skin tumor induction in a mouse model of an initiation-promotion skin tumor. *J. Dermatol.* 38, 562–570. doi: 10.1111/j.1346-8138.2010.01046.x

## AUTHOR CONTRIBUTIONS

JX and YF were responsible for cell and tissue culture and qRT-PCR and western blot. GS and QG were responsible for immunohistochemistry. LY and YH were responsible for flow cytometry and data analysis. DL provided guidance to experiment design. ZY was responsible for the quality of the overall manuscript.

## FUNDING

This work was supported by the National Natural Science Foundation of China (81301387) and the Priority Academic Program Development of Jiangsu Higher Education Institutions (JX10231802).

- Modi, B.-G., Neustadter, J., Binda, E., Lewis, J., Filler, R.-B., Roberts, S.-J., et al. (2012). Langerhans cells facilitate epithelial DNA damage and squamous cell carcinoma. *Science* 335, 104–108. doi: 10.1126/science.1211600
- Nygaard, U., Deleuran, M., and Vestergaard, C. (2017). Emerging treatment options in atopic dermatitis: topical therapies. *Dermatology* doi: 10.1159/000484407 [Epub ahead of print].
- Price, A.-A., Cumberbatch, M., Kimber, I., and Ager, A. (1997). Alpha 6 integrins are required for Langerhans cell migration from the epidermis. *J. Exp. Med.* 186, 1725–1735. doi: 10.1084/jem.186.10.1725
- Randolph, G.-J. (2001). Dendritic cell migration to lymph nodes: cytokines, chemokines, and lipid mediators. *Semin. Immunol.* 13, 267–274. doi: 10.1006/smim.2001.0322
- Ravindran, A., Mohammed, J., Gunderson, A.-J., Cui, X., and Glick, A.-B. (2014). Tumor-promoting role of TGF $\beta$ 1 signaling in ultraviolet B-induced skin carcinogenesis is associated with cutaneous inflammation and lymph node migration of dermal dendritic cells. *Carcinogenesis* 35, 959–966. doi: 10.1093/carcin/bgt486
- Rowden, G. (1980). Expression of Ia antigens on Langerhans cells in mice, guinea pigs and man. *J. Invest. Dermatol.* 75, 22–31. doi: 10.1111/1523-1747.ep12521071
- Siegfried, E.-C., Jaworski, J.-C., Kaiser, J.-D., and Hebert, A.-A. (2016). Systematic review of published trials: long-term safety of topical corticosteroids and topical calcineurin inhibitors in pediatric patients with atopic dermatitis. *BMC. Pediatr.* 16:75. doi: 10.1186/s12887-016-0607-9
- Tang, A., Amagai, M., Granger, L.-G., Stanley, J.-R., and Udey, M.-C. (1993). Adhesion of epidermal Langerhans cells to keratinocytes mediated by E-cadherin. *Nature* 361, 82–85. doi: 10.1038/361082a0
- Voskamp, P., Bodmann, C.-A., Koehl, G.-E., Rebel, H.-G., Van Olderen, M.-G., Gaumann, A., et al. (2013). Dietary immunosuppressants do not enhance UV-induced skin carcinogenesis, and reveal discordance between p53-mutant early clones and carcinomas. *Cancer Prev. Res.* 6, 129–138. doi: 10.1158/1940-6207.CAPR-12-0361
- Wu, C.-S., Lan, C.-C., Kuo, H.-Y., Chai, C.-Y., Chen, W.-T., and Chen, G.-S. (2012). Differential regulation of nuclear factor- $\kappa$ B subunits on epidermal keratinocytes by ultraviolet B and tacrolimus. *Kaohsiung J. Med. Sci.* 28, 577–585. doi: 10.1016/j.kjms.2012.04.023
- Yin, L., Hu, Y.-Y., Xu, J.-L., Guo, J., Tu, J., and Yin, Z. (2017). Ultraviolet B inhibits IL-17A/TNF- $\alpha$ -stimulated activation of human dermal fibroblasts by decreasing the expression of IL-17RA and IL-17RC on fibroblasts. *Front. Immunol.* 8:91. doi: 10.3389/fimmu.2017.00091
- Yin, Z.-Q., Xu, J.-L., Lu, Y., and Luo, D. (2012a). Topical pimecrolimus 1% reverses long-term suberythral ultraviolet B-induced epidermal Langerhans cell reduction and morphologic changes in mice. *J. Drugs Dermatol.* 11, e25–e27.
- Yin, Z.-Q., Xu, J.-L., Zhang, Z.-H., and Luo, D. (2012b). Effects of topical pimecrolimus 1% on high-dose ultraviolet B-irradiated epidermal Langerhans

- cells. *Int. Immunopharmacol.* 14, 635–640. doi: 10.1016/j.intimp.2012.10.002
- Yin, Z.-Q., Xu, J.-L., Zhou, B.-R., Wu, D., Xu, Y., Zhang, J.-A., et al. (2014). Topical pimecrolimus inhibits high-dose UVB irradiation-induced epidermal Langerhans cell migration, via regulation of TNF- $\alpha$  and E-cadherin. *Drug Des. Devel. Ther.* 8, 1817–1825. doi: 10.2147/DDDT.S70790
- Zhou, B.-R., Zhang, J.-A., Zhang, Q., Permatasari, F., Xu, Y., Wu, D., et al. (2013). Palmitic acid induces production of proinflammatory cytokines interleukin-6, interleukin-1 $\beta$ , and tumor necrosis factor- $\alpha$  via a NF- $\kappa$ B-dependent mechanism in HaCaT keratinocytes. *Mediators Inflamm.* 2013:530429. doi: 10.1155/2013/530429

**Conflict of Interest Statement:** The authors declare that the research was conducted in the absence of any commercial or financial relationships that could be construed as a potential conflict of interest.

Copyright © 2018 Xu, Feng, Song, Gong, Yin, Hu, Luo and Yin. This is an open-access article distributed under the terms of the Creative Commons Attribution License (CC BY). The use, distribution or reproduction in other forums is permitted, provided the original author(s) and the copyright owner are credited and that the original publication in this journal is cited, in accordance with accepted academic practice. No use, distribution or reproduction is permitted which does not comply with these terms.



# Downregulation of TLR4 by miR-181a Provides Negative Feedback Regulation to Lipopolysaccharide-Induced Inflammation

Kangfeng Jiang, Shuai Guo, Tao Zhang, Yaping Yang, Gan Zhao, Aftab Shaikat, Haichong Wu and Ganzhen Deng\*

Department of Clinical Veterinary Medicine, College of Veterinary Medicine, Huazhong Agricultural University, Wuhan, China

## OPEN ACCESS

### Edited by:

Marc Diederich,  
Seoul National University,  
South Korea

### Reviewed by:

Parisa Kalantari,  
Tufts University School of Medicine,  
United States  
Amanda Jane Gibson,  
Royal Veterinary College,  
United Kingdom

### \*Correspondence:

Ganzhen Deng  
ganzhendeng@sohu.com

### Specialty section:

This article was submitted to  
Inflammation Pharmacology,  
a section of the journal  
Frontiers in Pharmacology

**Received:** 26 November 2017

**Accepted:** 09 February 2018

**Published:** 26 February 2018

### Citation:

Jiang K, Guo S, Zhang T, Yang Y,  
Zhao G, Shaikat A, Wu H and  
Deng G (2018) Downregulation  
of TLR4 by miR-181a Provides  
Negative Feedback Regulation  
to Lipopolysaccharide-Induced  
Inflammation.  
Front. Pharmacol. 9:142.  
doi: 10.3389/fphar.2018.00142

Acute lung injury (ALI) is a progressive clinical disease with a high mortality rate, and characterized by an excessive uncontrolled inflammatory response. MicroRNAs (miRNAs) play a critical role in various human inflammatory diseases, and have been recognized as important regulators of inflammation. However, the regulatory mechanisms mediated by miRNAs involved in Lipopolysaccharide (LPS)-induced inflammation in ALI remain hazy. In this study, we found that miR-181a expression in the lung tissues of ALI mice and LPS-stimulated RAW 264.7 macrophages is dramatically reduced. We also show that over-expression of miR-181a significantly decreased the production of inflammatory cytokines, such as IL-1 $\beta$ , IL-6, and TNF- $\alpha$ , whereas inhibition of miR-181a reversed this decrease. Moreover, miR-181a inhibits NF- $\kappa$ B activation and accumulation of reactive oxygen species (ROS) by targeting TLR4 expression. We further verify that miR-181a suppresses TLR4 expression by binding directly to the 3'-UTR of TLR4. Therefore, we provide the first evidence for the negative regulation of miR-181a in LPS-induced inflammation via the suppression of ROS generation and TLR4-NF- $\kappa$ B pathway.

**Keywords:** acute lung injury, miR-181a, LPS, NF- $\kappa$ B, ROS

## INTRODUCTION

Acute lung injury (ALI) is an excessive uncontrolled inflammatory response in lung tissues caused by various clinical disorders, including pneumonia, major trauma, and sepsis (Shen et al., 2009; Xiao et al., 2015; Yao et al., 2017). ALI is mainly characterized by the over-expression of inflammatory mediators and numerous neutrophils infiltration, which finally leads to pulmonary edema, hemorrhage, and even gas exchange impairment (Rubenfeld et al., 2005).

It is well established that inflammatory stimuli from microbial pathogens, such as endotoxin, are widely considered to be one of the causes of severe pneumonia (Rojas et al., 2005). Lipopolysaccharide (LPS), a potent endotoxin, is a major biologically active ingredient of the Gram-negative bacterial cell wall and plays a pivotal role in inflammatory responses (Dreyfuss and Ricard, 2005). Previous studies have demonstrated that LPS could induce ALI by activating TLR4/NF



- $\kappa$ B signaling pathway, which regulates the transcription of pro-inflammatory cytokines, such as IL-1 $\beta$ , IL-6, and TNF- $\alpha$  (Wu et al., 2016). These cytokines can induce innate immune response and cause serious injury to the lung tissues, ultimately result in ALI (Herold et al., 2011; Gandhi and Vliagoftis, 2015).

MicroRNAs (miRNAs) are a class of evolutionarily conserved, single strand and small non-coding RNA molecules, approximately 20–25 nucleotides (nts), which mainly regulate gene expression in a post-transcriptional level (Chen and Rajewsky, 2007; Leuenberger et al., 2016). Once in their mature form, miRNAs interact specifically with the 3'-untranslated regions (3'-UTRs) of target mRNAs, resulting in silencing of their functions through mRNA degradation or translational inhibition (Griffiths-Jones et al., 2006; Xu et al., 2016). A number of miRNAs have been demonstrated to have a notable impact on the magnitude of the inflammatory response by targeting signal transduction proteins or directly targeting mRNAs that encode pro-inflammatory cytokines following pathogenic microbes infection (O'Connell et al., 2012). Moreover, some studies also suggested that some miRNAs are involved in the Toll-like receptor (TLR) pathway, and it is likely that they modulate signaling transduction during the inflammatory response (Nahid et al., 2011). Recently, it has been reported that miR-181a is associated with tumor growth and immune response (Seoudi et al., 2012), and suppresses TNF- $\alpha$ -induced transcription of pro-inflammatory genes (Zhao et al., 2012). miR-181a also negatively regulates immune responses in DCs (Zhu et al., 2017), and influences differentiation of T helper cell and activation of macrophages (Ghorbani et al., 2017). More importantly, miR-181a could function as an apoptosis promoter in the pathogenesis of ALI (Li et al., 2016). These findings prompted us to investigate the role of miR-181a in immune responses to LPS both *in vivo* and *in vitro*. Here, we found that LPS treatment highly decreased the expression of miR-181a in lung tissues and macrophages. We also showed that transfection with miR-181a mimics or inhibitors resulted in a down-regulation or up-regulation in pro-inflammatory cytokines, such as IL-1 $\beta$ , IL-6, and TNF- $\alpha$ . Further experiments demonstrated that miR-181a decreased TLR4 expression by binding directly to the 3'-UTR of TLR4. This study revealed that miR-181a could be an important negative regulator of inflammation and shed new light on therapeutic approaches toward some inflammatory diseases including ALI.

## MATERIALS AND METHODS

### Reagents

Lipopolysaccharide (*Escherichia coli* 055:B5) was purchased from Sigma-Aldrich (St. Louis, MO, United States). Mouse TNF- $\alpha$ , IL-1 $\beta$ , and IL-6 enzyme-linked immunosorbent assay (ELISA) kits were purchased from ImmunoWay Biotechnology (Newark, DE, United States). The myeloperoxidase (MPO) determination kits were obtained from Nanjing Jiancheng Bioengineering Institute (Nanjing, China). Phospho-NF- $\kappa$ B p65 (Ser536) (93H1) Rabbit mAb, NF- $\kappa$ B p65 (D14E12) XP Rabbit mAb, Phospho-I $\kappa$ B $\alpha$  (Ser32) (14D4) Rabbit mAb, I $\kappa$ B $\alpha$  (L35A5) Mouse mAb, Phospho-IKK $\beta$  (Ser176/180) (16A6) Rabbit mAb,

IKK $\beta$  (D30C6) Rabbit mAb and TLR4,  $\beta$ -actin were provided by Cell Signaling Technology (Beverly, MA, United States). MyD88 (A0980) Rabbit pAb and TRAF6 (A0973) Rabbit pAb were purchased from ABclonal Biotechnology Co., Ltd. (Cambridge, MA, United States).

### Animals Experiments

BALB/c mice (25–30 g) were purchased from Experimental Animal Center of Huazhong Agricultural University (Wuhan, China). All animals were maintained in animal rooms at 22°C in a 12-h light/dark cycle and received food and water *ad libitum*. All animal experiments were performed in accordance with guidelines provided by the Laboratory Animal Research Center of Hubei province, and approved by the Ethical Committee on Animal Research at Huazhong Agricultural University (HZAUMO-2015-12). Mice were randomly divided into two groups ( $n = 12$ ): control group and LPS group. The method for creating the LPS-induced ALI model was described previously (Cai et al., 2012). Briefly, LPS was diluted to 10 mg/mL with phosphate-buffered saline (PBS). The mice were intratracheally administered with LPS at the dose of 10 mg/kg body mass, and the control group received equal amount of PBS. After 24 h, the mice were euthanized with sodium pentobarbital, three mice in each group were selected to measure the wet and dry weight of the lungs, three other mice were used to evaluate histological changes, and the remaining six mice were used to perform molecular biological analyses.

### Histological Analysis

For histological analysis, lung tissues were excised and fixed with 4% paraformaldehyde for 24 h. Sections (4  $\mu$ m) of the lungs were embedded in paraffin, sliced, and then stained with hematoxylin and eosin (H&E).

### Lung Wet to Dry Weight (W/D) Ratio and MPO Assays

The severity of pulmonary oedema was measured by calculating the W/D ratio of lung tissues. The lungs were excised, rinsed briefly in PBS, and then weighed to obtain the “wet” weight. Subsequently, the lung tissues were dried at 80°C for 24 h to obtain the “dry” weight. The lung W/D ratio was measured by dividing the wet weight by the dry weight. To detect the MPO activity, tissue samples were homogenized with reaction buffer ( $w/v$ , 1/9). The MPO activity was determined using an MPO determination kit according to the manufacturer's protocols.

### Cell Culture

The murine macrophage cell line RAW264.7 cells and the human embryonic kidney cell line HEK293T cells were purchased from American Type Culture Collection (ATCC, Manassas, VA, United States). RAW264.7 macrophages were cultured in DMEM (Invitrogen, Carlsbad, CA, United States) supplemented with 10% fetal bovine serum (FBS; Sigma, St. Louis, MO, United States), streptomycin (50  $\mu$ g/mL), and penicillin (50 U/mL) at 37°C in a 5% CO<sub>2</sub> incubator. HEK293T cells were grown in DMEM supplemented with 10% FBS.

## CCK-8 Assay

The viability of macrophages after treatment with LPS (2  $\mu$ g/mL) was assessed using a Cell Counting Kit-8 (CCK-8) assay kit purchased from Beyotime (Shanghai, China). In brief, macrophages were plated at a density of  $4 \times 10^4$  cells/well in 96-well plates for 1 h, and then the cells were treated with or without LPS for 0, 6, or 12 h. After treatment, 10  $\mu$ L of CCK8 solution was added to each well and continued incubate for another 3 h. Finally, the optical density (OD) was measured at 450 nm on a microplate reader (Bio-Rad Instruments, Hercules, CA, United States).

## Cell Transfection

Cultured cells were seeded at  $5 \times 10^5$  cells/well in 6-well plates (Corning Inc., Corning, NY, United States) for 12 h before transfection. The cells were transfected with miR-181a mimics, miR-181a inhibitors, siRNA or the negative controls using Lipofectamine 2000 (Invitrogen, Carlsbad, CA, United States) according to the manufacturer's instructions. The mimics, inhibitors, siRNA and corresponding negative controls were all synthesized by GenePharma (Shanghai, China). These sequences are shown in **Table 1**. The transfection efficiency was evaluated by qPCR assay.

## ELISA

24 h after transfection with miR-181a mimics or inhibitors or the respective controls, the cells were then stimulated with 2  $\mu$ g/mL LPS for 12 h. The levels of TNF- $\alpha$ , IL-1 $\beta$ , and IL-6 in the cell culture supernatants were measured with ELISA kits according to the manufacturer's protocols.

## RNA Isolation and qPCR Analysis

Total RNA was isolated using the TRIzol reagent (Invitrogen, United States) in accordance with the manufacturer's instructions. The concentration and purity of isolated RNA were evaluated by OD values at 260 and 280 nm using Q5000 (Quawell Technology, United States). The ratios of OD260 to OD280 for the samples were between 1.9 and 2.0. Typically, the ratio of OD260 to OD280 should range between 1.9 and 2.0 for good-quality RNA. Then all RNA samples were treated with RNase-free DNase to remove contaminating genomic DNA. For miRNA analysis, cDNA was synthesized by M-MLV reverse transcriptase with a special reverse transcription primer for

miRNAs. PCR was performed using a miRNAs real-time PCR kit (GenePharma, Shanghai, China) according to the instructions of the manufacturer. The primers for miR-181a and U6 snRNA were purchased from GenePharma. For mRNA analysis, cDNA was synthesized using a PrimeScript RT reagent kit (Takara, Dalian, China) according to the manufacturer's instructions. PCR was carried out using SYBR Green plus reagent kit (Roche, Basel, Switzerland) according to the instructions of the manufacturer. The sequences of the primers for PCR are as follows: TLR4, sense-TTCAGAGCCGTTGGTGTATC, antisense-CTCCATTCCAGGTAGGTGT; IL-1 $\beta$ , sense-CCTGGGCTGTCTGATGAGAG, antisense-TCCACGGGAAAGACACAGGTA; IL-6, sense-GGC GGATCGGATGTTGTGAT, antisense-GGACCCAGACAATC GGTTG; TNF- $\alpha$ , sense-CTTCTCATTCTGCTTGTG, antisense-ACTTGGTGGTTTGCTACG; GAPDH, sense-CAATG TGTCCGTCGTGGATCT; antisense-GTCCTCAGTGTAGCCC AAGATG. The relative expression levels of miR-181a and mRNAs were normalized to the endogenous references U6 snRNA and GAPDH following the  $2^{-\Delta\Delta C_t}$  method.

## Western Blot Analysis

Total protein was extracted with RIPA reagent (BioSharp, China) according to the manufacturer's recommended protocol. The total protein concentrations were determined using the Pierce BCA Protein Assay Kit (Thermo Fisher Scientific, Rockford, IL, United States). Protein samples (40  $\mu$ g) were separated by 10% SDS-polyacrylamide gel electrophoresis (SDS-PAGE), transferred onto polyvinylidene difluoride (PVDF) membranes, and probed with primary antibodies against the indicated proteins (1:1000) overnight. Membranes were then washed and exposed to horseradish peroxidase-conjugated secondary antibodies (1:4000), and visualized using enhanced chemiluminescence.

## Luciferase Reporter Assay

To study the effect of miR-181a on the LPS-induced activation of NF- $\kappa$ B, a NF- $\kappa$ B luciferase reporter gene assay was carried out as described previously (Du et al., 2011). Briefly, macrophages were co-transfected with pNF- $\kappa$ B-Luc, pRL-TK control vectors and miR-181a mimics along with indicated controls. After 24 h, the cells were stimulated with 2  $\mu$ g/mL LPS for another 12 h. The cells were lysed and analyzed for luciferase activities using the Dual-Luciferase Reporter Assay System (Promega, Madison, WI, United States) following the manufacturer's protocols.

The possible sites of binding between TLR4 and miR-181a were predicted using TargetScan<sup>1</sup> and miRanda<sup>2</sup>. To determine whether TLR4 is a direct target of miR-181a, we cloned 3'-UTR of TLR4 into a psiCHECK<sup>TM</sup>-2 vector (Promega, Madison, WI, United States) to generate a wild- or mutant-type TLR4 3'-UTR luciferase reporter vector. For the luciferase assay, HEK293T cells were co-transfected with the luciferase reporter vectors and miR-181a mimics or controls, respectively. After 24 h of transfection, the luciferase activities were measured.

**TABLE 1** | Sequences for miR-181a and TLR4 siRNA.

miR-181a mimics	Sense	5'-AACAUUCAACGCGUCGUGAGU-3'
	Antisense	5'-UCACCGACAGCGUUGAAUGUUUU-3'
Mimics NC	Sense	5'-UUCUCCGAACGUGUCACGUTT-3'
	Antisense	5'-ACGUGACACGUUCGGAGAATT-3'
miR-181a inhibitors	Sense	5'-ACUCACCGACAGCGUUGAAUGUU-3'
Inhibitors NC	Sense	5'-CAGUACUUUUGUGUAGUACAA-3'
TLR4 siRNA	Sense	5'-GGACAGCUUAUAACCUUAATT-3'
	Antisense	5'-UUAAGGUUAUAAGCUGUCCTT-3'
siRNA NC	Sense	5'-UUCUCCGAACGUGUCACGUTT-3'
	Antisense	5'-ACGUGACACGUUCGGAGAATT-3'

<sup>1</sup>www.targetscan.org

<sup>2</sup>www.microrna.org

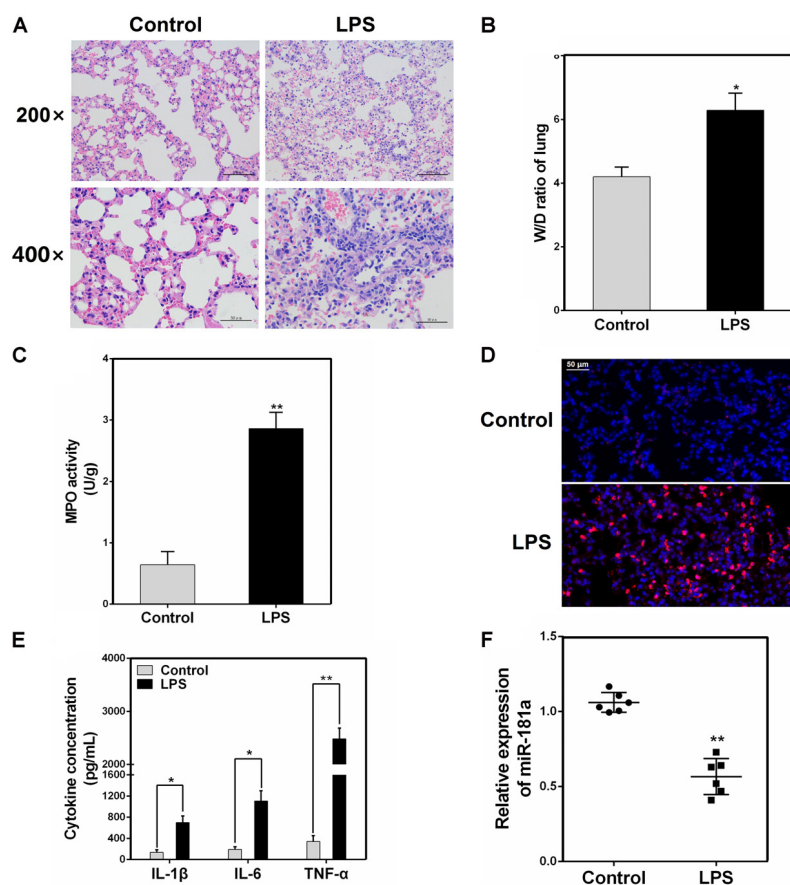


**FIGURE 1 |** miR-181a is down-regulated in the lung tissues of LPS-induced ALI mice. **(A)** Histopathological analysis of lung tissues. Mice were intratracheally administered with LPS for 24 h, and the degree of inflammation of lung samples was assessed with H&E staining ( $n = 3$ ). **(B)** Lung W/D ratio ( $n = 3$ ). **(C,D)** Infiltration of neutrophils into the lung tissues was measured by myeloperoxidase (MPO) immunofluorescence staining and MPO activity ( $n = 3$ ). **(E)** The levels of cytokines IL-1 $\beta$ , IL-6, and TNF- $\alpha$  was detected by ELISA ( $n = 3$ ). **(F)** The miR-181a expression was detected in the lung tissues of LPS treated mice by qPCR ( $n = 6$ ). U6 snRNA was used as an endogenous control. Data are expressed as mean  $\pm$  SEM of three independent experiments. \* $P < 0.05$ ; \*\* $P < 0.01$  (Student's  $t$ -test).

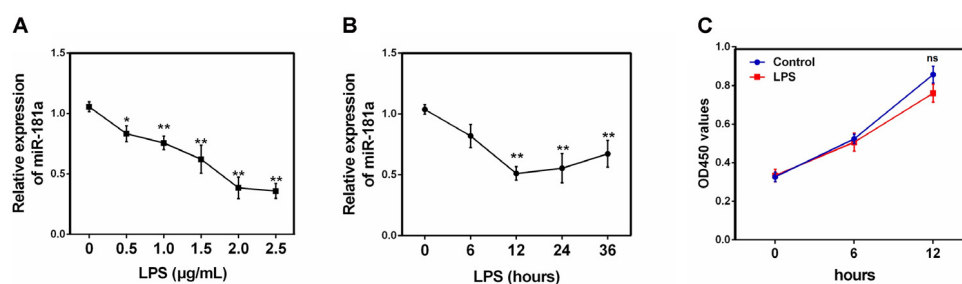


**FIGURE 2 |** miR-181a is down-regulated in LPS-stimulated RAW264.7 macrophages. **(A)** Macrophages were stimulated with different concentrations of LPS for 12 h. **(B)** Macrophages were stimulated with 2  $\mu$ g/mL LPS at different times as indicated. Cells were harvested, and miR-181a expression was measured by qPCR. The relative expression of miR-181a was normalized to U6 snRNA. **(C)** The viability of macrophages after treatment with LPS (2  $\mu$ g/mL) was assessed using a CCK-8 assay kit. Data are expressed as mean  $\pm$  SEM of three independent experiments. \* $P < 0.05$ ; \*\* $P < 0.01$  (Student's  $t$ -test).

## Reactive Oxygen Species (ROS) Assay

Intracellular ROS levels were detected using the fluorescent probe DCFH-DA (Beyotime, Shanghai, China). At the end of the treatment, cells were incubated with 10  $\mu$ M DCFH-DA at 37°C for 30 min in the dark. The fluorescence intensity were then

determined using an inverted fluorescence microscope (BX51TF, Olympus, Tokyo, Japan) or a flow cytometry (FACSCalibur, BD Biosciences, San Jose, CA, United States). For the fluorescence images, the integrated optical density (IOD) and area of cells were measured by Image-Pro Plus (IPP) 6.0 software (Media

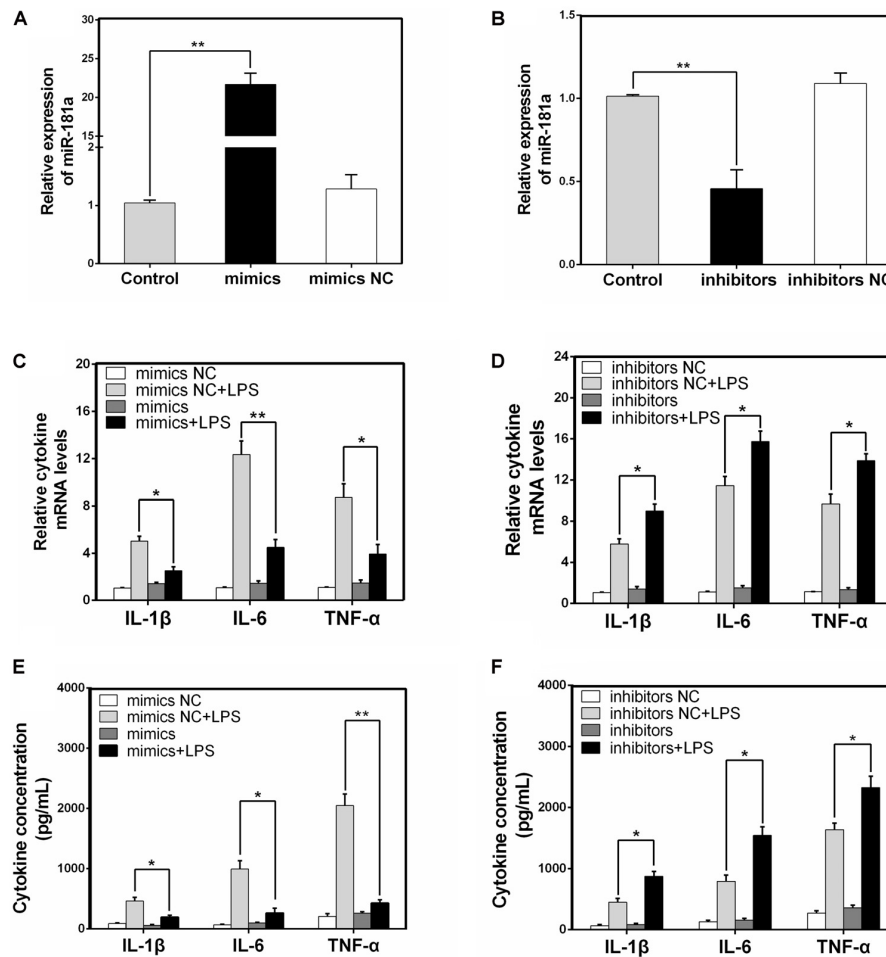


**FIGURE 3 |** miR-181a decreases the LPS-induced production of pro-inflammatory cytokines. **(A,B)** Macrophages were transfected with miR-181a mimics or inhibitors. At 24 h post-transfection, miR-181a levels were measured by qPCR. The relative expression of miR-181a was normalized to U6 snRNA. **(C,D)** Cells were transfected with 50 nM miR-181a mimics or 100 nM miR-181a inhibitors for 24 h, and then stimulated with 2  $\mu$ g/mL LPS for 12 h. The expression of cytokines IL-1 $\beta$ , IL-6, and TNF- $\alpha$  was determined by qPCR. GAPDH was used as an endogenous control. **(E,F)** The levels of cytokines IL-1 $\beta$ , IL-6, and TNF- $\alpha$  was detected by ELISA. Data are expressed as mean  $\pm$  SEM of three independent experiments. \* $P < 0.05$ ; \*\* $P < 0.01$  (Student's  $t$ -test).

Cybernetics, Silver Spring, MD, United States), and the ROS fluorescence intensity was expressed as IOD/area. For the flow cytometry, the intracellular mean fluorescence intensity was analyzed for more than 10000 cells of each sample by Flowjo software (Tree Star, San Carlos, CA, United States).

### Immunofluorescence Staining

Lung tissues were fixed in 4% paraformaldehyde for 24 h and then embedded in paraffin. Tissue samples were permeabilized with PBS containing 0.3% Triton X-100 and 10% BSA. RAW264.7 macrophages ( $1 \times 10^5$  cells/mL) were seeded onto a 12-well plates. After the cells were treated as indicated, immunofluorescence staining was performed. Sections of tissues or cells were incubated with special primary antibodies (1:100) overnight at 4°C and then incubated with FITC-labeled secondary antibodies (1:200) in the dark for 1 h at 25°C. Nuclei were stained using DAPI for 10 min, and fluorescent images were captured with an inverted fluorescence

microscope. The IOD and area of cells were measured by IPP 6.0 software, and the fluorescence intensity was expressed as IOD/area.

### Statistical Analysis

Data are expressed as mean  $\pm$  SEM. Statistical analysis was performed using the Student's  $t$ -test, with values of  $p < 0.05$  considered statistically significant.

## RESULTS

### The Expression of miR-181a Is Reduced in the Lung Tissues of LPS-Challenged Mice

We induced ALI in mice with LPS and then performed H&E staining. As shown in **Figures 1A,B**, the control group



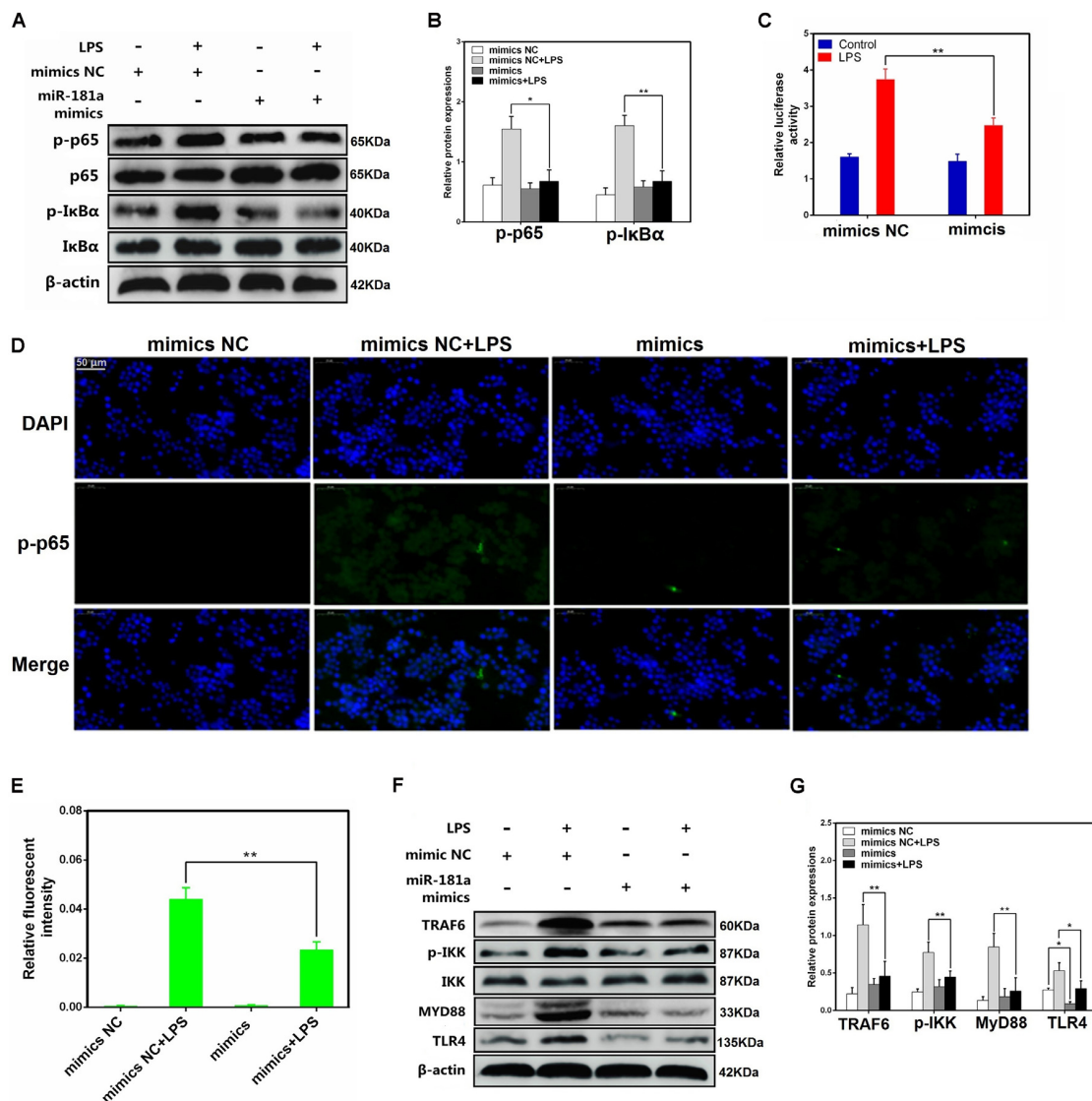


**FIGURE 4 |** miR-181a suppressed LPS-induced activation of NF-κB pathway. **(A)** Macrophages were transfected with miR-181a mimics or mimics NC for 24 h, then stimulated with 2 μg/mL LPS for 12 h. **(B)** The protein levels of NF-κB p65 and IκBα were measured by western blotting. β-actin was used as an internal control. **(C)** The NF-κB luciferase activity was measured by dual-luciferase assay. **(D)** Translocation of the p65 subunit from the cytoplasm into the nucleus was assessed by immunofluorescence staining (×400), scale bar = 50 μm. Blue spots represent cell nuclei, and green spots indicate p-p65 staining. **(E)** The IOD and area of cells were measured by IPP 6.0 software, and the fluorescence intensity of p-p65 was expressed as IOD/area. **(F)** Cells were treated as **(A)**, and the protein levels of upstream molecules of NF-κB pathway were measured by western blotting. **(B,G)** Gray values of the indicated proteins were measured by Image-Pro Plus (IPP) 6.0 software. Data are expressed as mean ± SEM of three independent experiments. \* $P < 0.05$ ; \*\* $P < 0.01$  (Student's *t*-test).

displayed the normal pulmonary histology. In contrast, the lung tissues from the LPS group showed remarkable lung injury, including hemorrhage, interstitial edema and infiltration of inflammatory cells. These results were also further confirmed by subsequent MPO and ELISA results (Figures 1C–E). Some miRNAs play a pivotal role in regulation of inflammation response triggered by LPS (Biswas and Lopez-Collazo, 2009). In order to explore whether miR-181a is involved in this immune reaction, we measured the expression of miR-181a in the lung tissues of ALI mice. qPCR assay showed that the level of miR-181a was markedly suppressed in lung tissues

of ALI mice when compared to that of the control group (Figure 1F).

### miR-181a Is Down-regulated in LPS-Stimulated Macrophages

To investigate the effect of miR-181a in LPS-induced inflammation in ALI, the expression of miR-181a in LPS-stimulated RAW 264.7 macrophages was also detected. As displayed in Figure 2A, miR-181a expression was significantly decreased upon LPS stimulation and the down-regulation of miR-181a expression was dose-dependent. Besides, we also tested



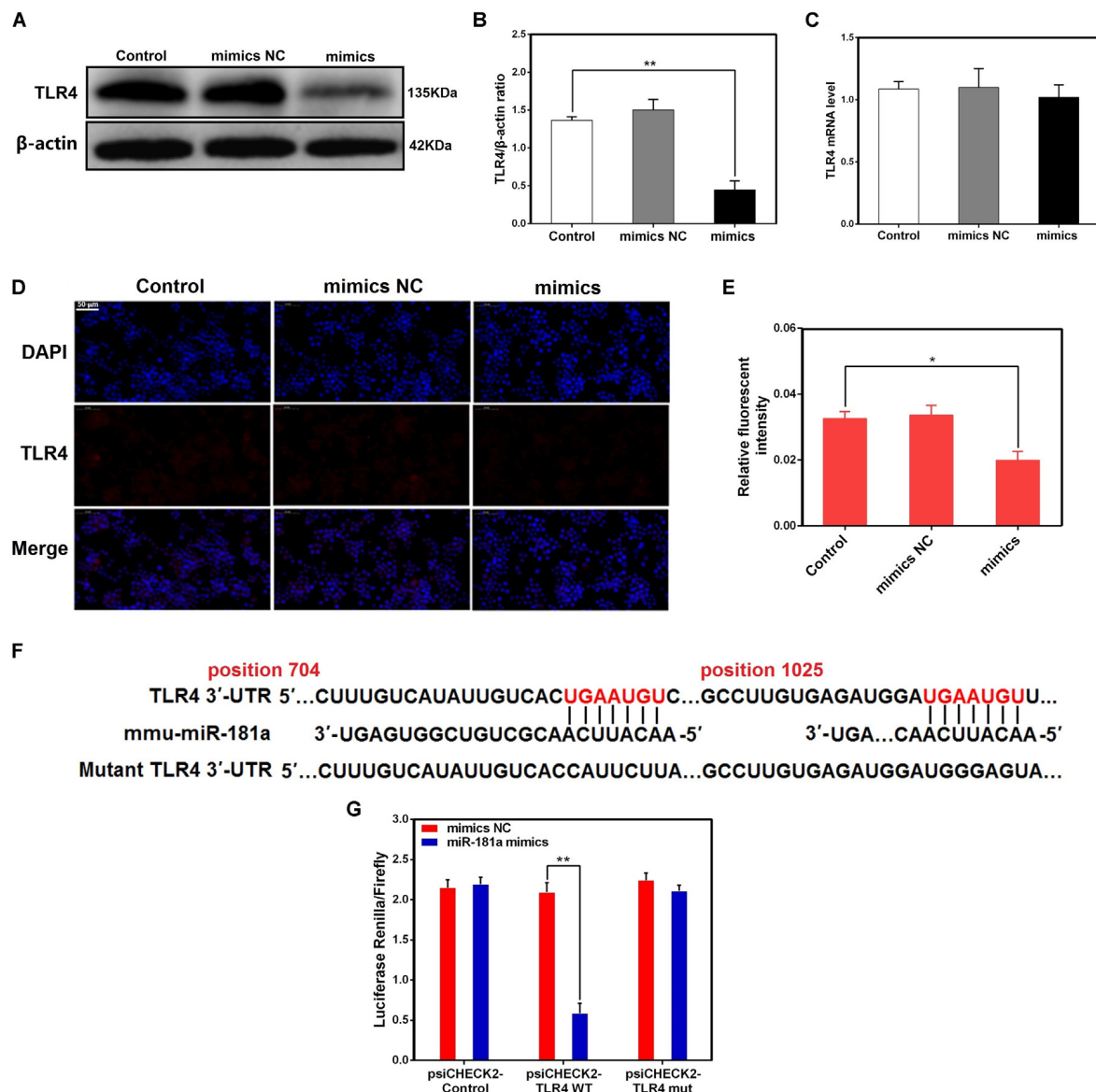


**FIGURE 5 |** TLR4 is a molecular target of miR-181a. **(A)** Macrophages were transfected with miR-181a mimics or mimics NC for 48 h, and the protein level of TLR4 was measured by western blotting.  $\beta$ -actin was used as an internal control. **(B)** Gray values of TLR4 protein were measured by IPP software. **(C)** Cells were treated as **(A)**, the mRNA level of TLR4 was detected by qPCR. GAPDH was used as an internal control. **(D)** Immunofluorescence staining was performed to identify the expression of TLR4 ( $\times 400$ ), scale bar = 50  $\mu$ m. Blue spots represent cell nuclei, and red spots indicate TLR4 staining. **(E)** The fluorescence intensity of TLR4. **(F)** The alignment of miR-181a and TLR4 3'-UTR by computational prediction via the TargetScan and miRanda. **(G)** The dual-luciferase reporter assay was performed in 293T cells. Cells were co-transfected with the wild- or mutant-type TLR4 3'-UTR luciferase reporter vectors, as well as miR-181a mimics or mimics NC. The ratio of Renilla activity/Firefly activity represents luciferase activity. Data are expressed as mean  $\pm$  SEM of three independent experiments. \* $P < 0.05$ ; \*\* $P < 0.01$  (Student's  $t$ -test).

miR-181a expression at different time points of LPS treatment. Results showed that LPS decreased miR-181a expression in a time-dependent manner and reached a nadir at 12 h (**Figure 2B**). In addition, CCK-8 assay demonstrated that the cell viabilities were not affected by LPS at the concentration (2  $\mu$ g/mL) used (**Figure 2C**). These results further confirm that miR-181a is involved in LPS-mediated immune response.

## miR-181a Decreases the LPS-Induced Production of Pro-inflammatory Cytokines

It is well-known that LPS could activate NF- $\kappa$ B pathway and subsequently lead to the secretion of inflammatory cytokines such as IL-1 $\beta$ , IL-6, and TNF- $\alpha$ , which all promote the development of ALI (Wu et al., 2017). To unravel the specific role of miR-181a in cytokines production in LPS-induced inflammatory

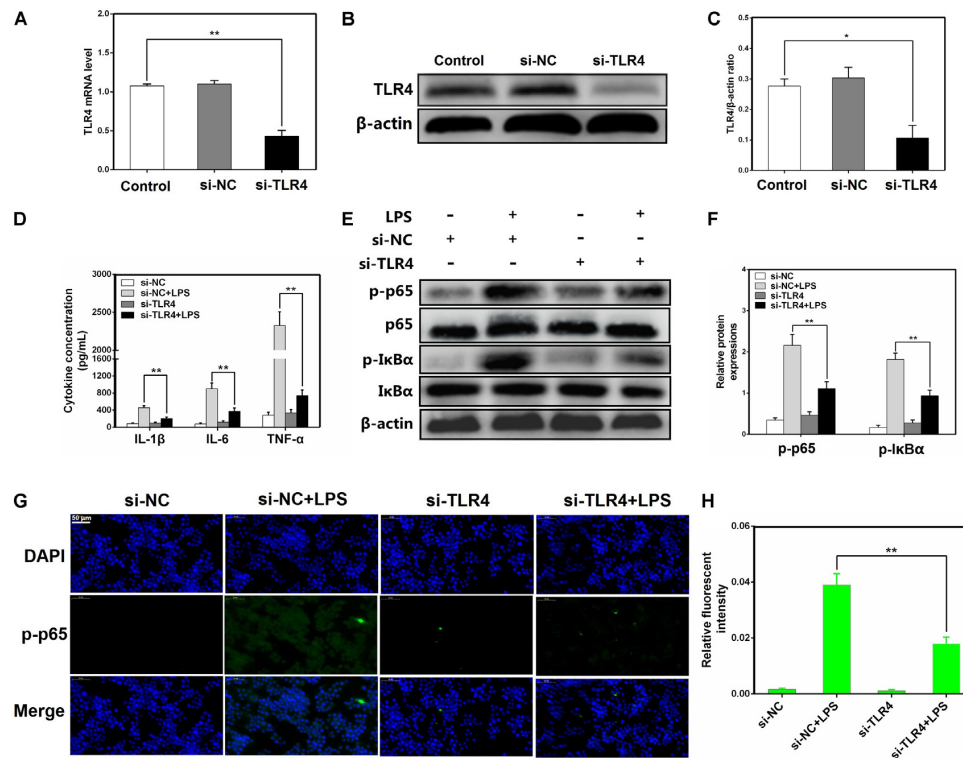


**FIGURE 6 |** Knockdown of TLR4 alleviates LPS-induced inflammatory responses. **(A)** Macrophages were transfected with the siRNA specific for TLR4 (si-TLR4) or the negative control siRNA (si-NC) at a concentration of 200 nM for 24 or 48 h, and the mRNA level of TLR4 was measured by qPCR. GAPDH was used as an internal control. **(B)** The protein level of TLR4 was determined by western blotting.  $\beta$ -actin was used as an internal control. **(D)** Cells were transfected with 200 nM si-TLR4 or si-NC for 24 h, and then stimulated with 2  $\mu$ g/mL LPS for 12 h. The levels of cytokines IL-1 $\beta$ , IL-6, and TNF- $\alpha$  were detected by ELISA. **(E)** The protein levels of NF- $\kappa$ B p65 and I $\kappa$ B $\alpha$  were measured by western blotting.  $\beta$ -actin was used as an internal control. **(G)** Translocation of the p65 subunit from the cytoplasm into the nucleus was assessed by immunofluorescence staining ( $\times 400$ ), scale bar = 50  $\mu$ m. Blue spots represent cell nuclei, and green spots indicate p-p65 staining. **(H)** The fluorescence intensity of p-p65. **(C,F)** Gray values of the indicated proteins were measured by IPP 6.0 software. Data are expressed as mean  $\pm$  SEM of three independent experiments. \* $P < 0.05$ ; \*\* $P < 0.01$  (Student's *t*-test).

response, macrophages were transiently transfected with miR-181a mimics or inhibitors. Twenty-four hours after transfection, the transfection efficacy was assessed by qPCR, and the results confirmed that transfection with miR-181a mimics or inhibitors led to a dramatical increase or decrease in miR-181a expression (Figures 3A,B). Subsequently, the cells were stimulated with 2  $\mu$ g/mL LPS for another 12 h and the levels of inflammatory cytokines were detected by qPCR and ELISA. As shown in Figures 3C–F, over-expression or inhibition of miR-181a significantly decreased or increased the LPS-induced secretion of pro-inflammatory cytokines. These results indicate that miR-181a play an anti-inflammatory role in the LPS-induced inflammatory response.

### miR-181a Suppressed LPS-Induced Activation of NF- $\kappa$ B Pathway

It has been generally accepted that the expression levels of inflammatory cytokines are regulated by multiple signaling pathways, such as NF- $\kappa$ B pathway. NF- $\kappa$ B, a crucial nuclear transcription factor, plays an important role in LPS-induced ALI (Jiang et al., 2017b). To further vindicate the mechanism of

miR-181a in cytokines inhibition, we then determined the ability of miR-181a to modulate the activation of NF- $\kappa$ B pathway in macrophages. The protein levels of NF- $\kappa$ B p65 and I $\kappa$ B $\alpha$  were detected using western blotting. As shown in Figures 4A,B, the phosphorylated p65 and I $\kappa$ B $\alpha$  proteins were significantly increased in the LPS group. In contrast, their levels were dramatically reduced while over-expression of miR-181a. We also studied the effect of miR-181a in NF- $\kappa$ B activation by dual-luciferase assay, and the results showed that miR-181a inhibited NF- $\kappa$ B activation (Figure 4C). Similarly, immunofluorescence results confirmed that miR-181a mimics induced a decrease in the nuclear translocation of NF- $\kappa$ B p65 after 12 h of LPS stimulation when compared to the control mimics (Figures 4D,E). To find out the possible target of miR-181a, we next detected the expression of upstream molecules of NF- $\kappa$ B pathway. Western blot results showed that LPS-induced TLR4, MyD88, TRAF6 and phosphorylated IKK $\alpha$ / $\beta$  levels were markedly inhibited. However, the TLR4 expression was also decreased by miR-181a mimics in the absence of LPS compared with the control mimics (Figures 4F,G). These data suggests that miR-181a could suppress LPS-induced activation of NF- $\kappa$ B pathway, likely through decreasing TLR4 expression.

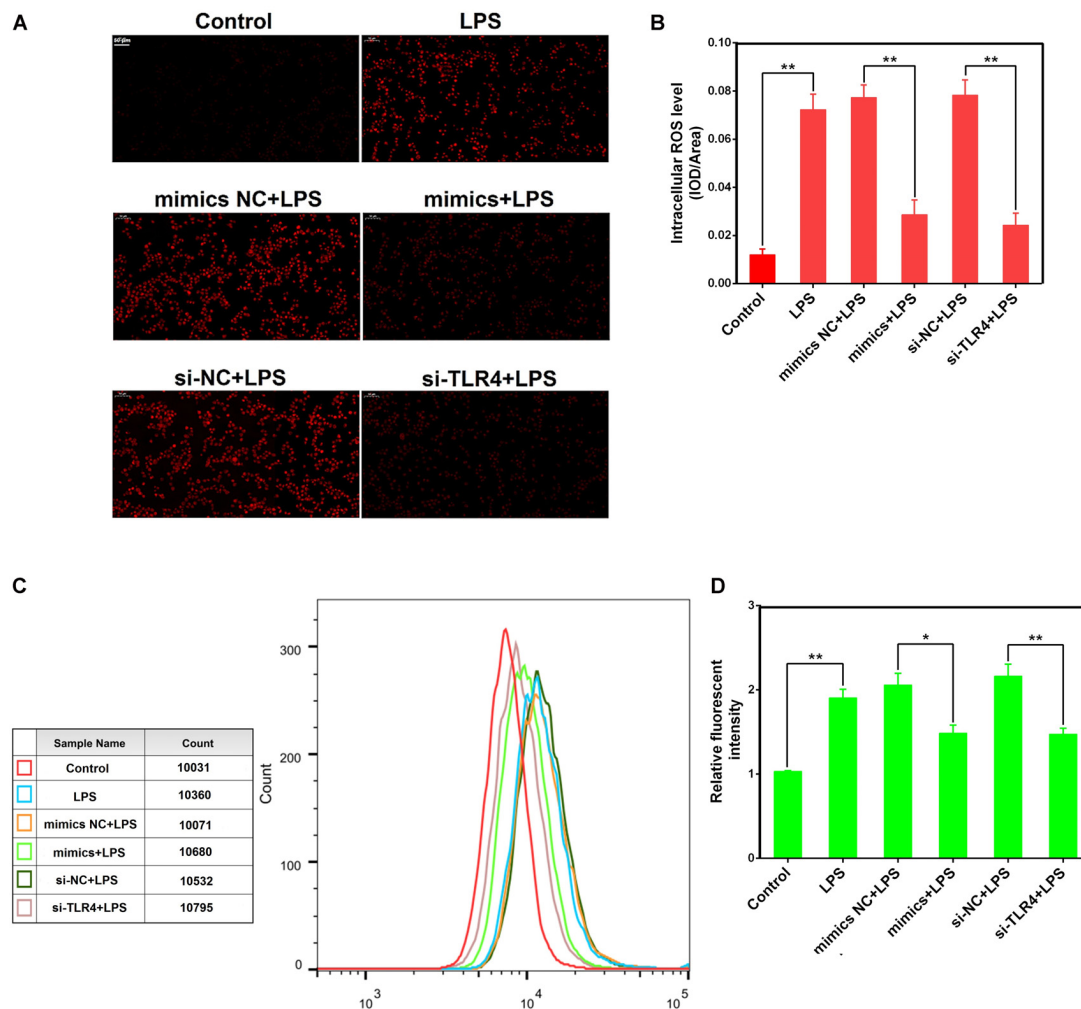


**FIGURE 7 |** miR-181a reduces LPS-induced intracellular ROS accumulation in macrophages. Macrophages were transfected with miR-181a mimics or si-TLR4 or the respective controls for 24 h, then incubated with 10  $\mu$ M DCFH-DA for 30 min followed by stimulation with 2  $\mu$ g/mL LPS for an additional 30 min. **(A)** Qualitative characterization of ROS were viewed using an inverted fluorescence microscope. **(B)** The IOD and area of cells were measured by IPP 6.0 software, and the ROS fluorescence intensity was expressed as IOD/area. **(C)** The ROS levels of cells were detected using flow cytometry. **(D)** The relative fluorescence intensity was analyzed by FlowJo software. Data are expressed as mean  $\pm$  SEM of three independent experiments. \* $P < 0.05$ ; \*\* $P < 0.01$  (Student's *t*-test).

## TLR4 Is a Molecular Target of miR-181a

We transfected macrophages with miR-181a mimics or negative controls and then examined the expression of TLR4. As displayed in **Figures 5A–E**, transfection with miR-181a mimics restrained the protein level of TLR4 but not the mRNA level, indicating that miR-181a may function at the translational level. In addition, bioinformatic softwares (TargetScan and miRanda) showed that there are two putative binding sites between miR-181a and the 3'-UTR of TLR4 (**Figure 5F**). To further confirm that miR-181a is able to directly bind to TLR4 mRNA, a luciferase reporter assay was performed. Briefly, the wild- or mutant-type TLR4 3'-UTR luciferase reporter vectors were transfected into HEK293T cells, and then treated with miR-181a mimics or control mimics. We found that miR-181a mimics markedly decreased the luciferase activity for the wild-type 3'-UTR of TLR4 but showed no inhibition effect for the mutated 3'-UTR of TLR4

(**Figure 5G**). These results imply that miR-181a inhibits TLR4 expression by directly binding the 3'-UTR of TLR4 mRNA.

## Knockdown of TLR4 Alleviates LPS-Induced Inflammatory Responses

TLR4 has been shown to play an essential role in LPS-mediated NF- $\kappa$ B activation (Guijarro Muñoz et al., 2014; Jiang et al., 2017a). To further elucidate the mechanisms by which miR-181a regulates LPS-induced inflammatory responses, a siRNA specific for TLR4 (si-TLR4) was used to knock down TLR4 expression in macrophages, and then, the expression level of TLR4 was measured by qPCR and western blotting. Following transfection, TLR4 mRNA and the protein levels were significantly reduced (**Figures 6A–C**). Moreover, the production of the pro-inflammatory cytokines including IL-1 $\beta$ , IL-6, and TNF- $\alpha$  was also repressed (**Figure 6D**). Knockdown of TLR4

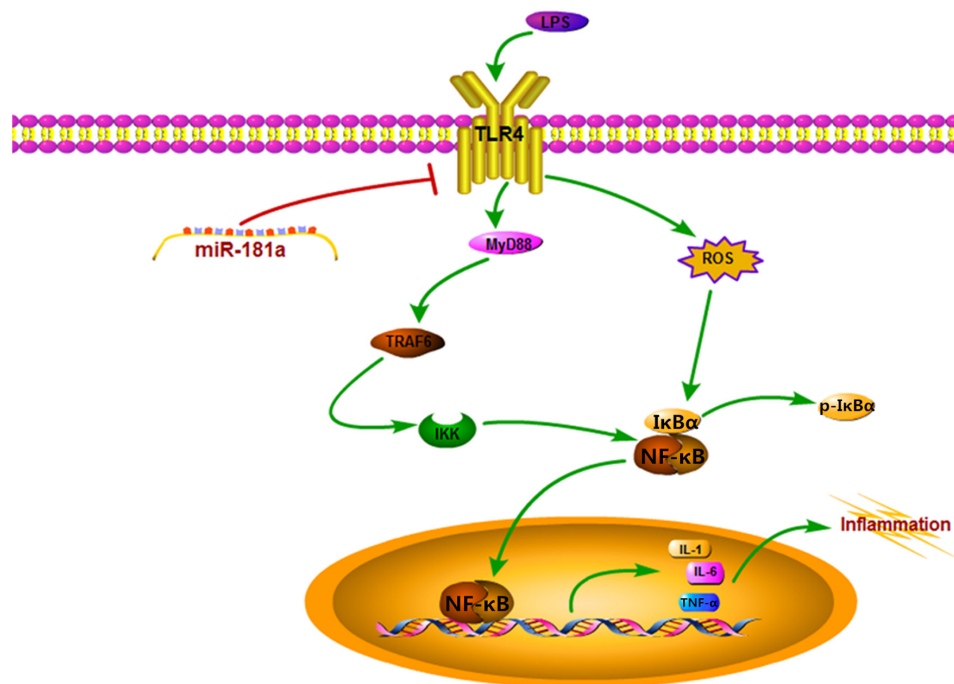


**FIGURE 8 |** Schematic diagram of signaling pathways related to anti-inflammatory effects of miR-181a on LPS-induced inflammation.

also significantly inhibited the phosphorylation of NF- $\kappa$ B p65 and I $\kappa$ B $\alpha$ , consistent with the above results (**Figures 6E–H**). Taken together, these findings strongly demonstrate miR-181a is implicated in the negative regulation of LPS-induced inflammation through inhibiting TLR4-NF- $\kappa$ B pathway.

### miR-181a Reduces LPS-Induced Intracellular ROS Accumulation in Macrophages

Reactive oxygen species were involved in LPS-mediated immune response, and contributes to the exacerbation of inflammation (Zou et al., 2013). We observed that miR-181a mimics significantly restrained the accumulation of intracellular ROS in LPS-stimulated macrophages compared with mimics NC. Similarly, si-TLR4 also significantly decreased ROS production compared to si-NC (**Figures 7A–D**). These results reveal that miR-181a could also alleviate the inflammatory response mediated by inhibition of the ROS production (**Figure 8**).

## DISCUSSION

Acute lung injury is a type of severe inflammatory disease, which is hard to treat and poor prognosis (Matthay and Zimmerman, 2005). Although multiple promising pharmacological interventions have been studied in patients with ALI, the mortality rate is still as high as 30–70% (Rubenfeld et al., 2005). Therefore, there is a need to develop a new therapeutic strategy for the treatment of ALI. miRNAs are an important class of small endogenous non-coding RNAs that play a

regulatory role in various basic biological processes, such as cell proliferation, differentiation, apoptosis, and inflammation (Cheng et al., 2005; Ochs et al., 2011). It was found recently that some miRNAs can serve as a negative feedback regulator of inflammatory response, through targeting signaling proteins involved in signal transmission (Case et al., 2011; Iyer et al., 2012).

miR-181a belongs to the miR-181 family, and its nucleic acid sequence is highly conserved in mammals (Ji et al., 2009). Previous research has shown that miR-181a is mainly involved in modulation of tumor cell growth, and acts as a tumor suppressor in human glioma cells (Shi et al., 2008). More notably, anti-inflammatory function of miR-181a has been identified in some recent studies. miR-181a suppresses TNF- $\alpha$ -induced transcription of pro-inflammatory genes in liver epithelial cells by targeting p300/CBP-associated factor (Zhao et al., 2012), and inhibits oxidized low-density lipoprotein-stimulated inflammatory responses in dendritic cells by targeting c-Fos (Wu et al., 2012). Moreover, the immunoregulatory effect of miR-181a in differentiation of T helper cell and activation of macrophages has also been proposed (Ghorbani et al., 2017). However, we are not certain whether miR-181a has an anti-inflammatory effect in LPS-induced inflammation in ALI. Therefore, we employed an *in vivo* ALI model as well as an *in vitro* inflammation model using RAW 264.7 macrophages to explore the possible role of miR-181a in inflammatory response induced by LPS. In the current study, we found that exposure to LPS led to severe pathological lesions, including alveolar damage and inflammatory cell infiltration. Subsequently, we demonstrated that miR-181a is down-regulated in the lung tissues of LPS-challenged mice, consistent with a



previous study (Cai et al., 2012). However, this finding is contrary to another published report which has suggested that miR-181a is up-regulated in the lung tissues (Li et al., 2016). A possible explanation for this might be that we used a lower dose of LPS (10 mg/kg) in the present study. Furthermore, down-regulation of miR-181a in macrophages stimulated with LPS in a dose- and time-dependent manner was also found, indicating miR-181a may have an important biological function in LPS-induced inflammation.

It is well recognized that innate immune system can recognize conserved pathogen associated molecular patterns (PAMPs) through pattern recognition receptors (PRRs), and is the main contributor to inflammation caused by pathogenic microbial infection (Akira and Hemmi, 2003; Zhou et al., 2014). TLR4 is one of the best studied PRR families expressed in macrophages and other immune cells, and evidence suggests that several PAMPs such as LPS can stimulate TLR4, which ultimately leads to the secretion of inflammatory mediators from macrophages (Shi et al., 2006; Lu et al., 2008). In the present study, we identified that over-expression or inhibition of miR-181a significantly decreased or increased the LPS-induced production of IL-1 $\beta$ , IL-6, and TNF- $\alpha$  in macrophages. NF- $\kappa$ B is a type of critical nuclear transcriptional regulatory factor responsible for the production of pro-inflammatory cytokines, which induce a cascade of inflammatory responses and related lung damage (Lawrence, 2009; Shen et al., 2009). Intriguingly, the activation of NF- $\kappa$ B pathway by LPS was also repressed following transfection with miR-181a mimics. The observations showed that miR-181a likely provided a negative feedback to inflammation stimulated by LPS.

In order to explore the programmed feedback mechanism of miR-181a regulating inflammation, it is essential to study its target genes. TLR4 plays an essential role for the LPS triggered-NF- $\kappa$ B activation (Guijarromuñoz et al., 2014). Knock-out of TLR4 could attenuate the pro-inflammatory state of diabetes in mice (Devaraj et al., 2011). More importantly, TLR4 possesses a central role in initiating changes in miRNAs expression in answer to invading pathogens (Curtale et al., 2013). Therefore understanding the regulatory effect of miRNA in TLR4 gene expression is vital for future development of therapeutic agents against inflammatory diseases. In present study, we found that miR-181a mimics dramatically decreased the TLR4 protein level. Furthermore, bioinformatics predictions made with TargetScan and miRanda showed that TLR4 is a putative target of miR-181a. To further validate that TLR4 is a molecular target of miR-181a, the luciferase reporter assay was performed. Luciferase activity was significantly reduced when co-transfected miR-181a mimics with wild-type TLR4 3'-UTR vector, whereas no significant change was observed with mutant-type TLR4 3'-UTR vector.

These results imply that miR-181a is able to bind to TLR4 mRNA directly and inhibits its translation. Moreover, TLR4 expression was also silenced using si-TLR4 so as to further verify whether TLR4 is involved in the anti-inflammatory effect of miR-181a. Our results showed that knock-down of TLR4 ameliorated inflammatory response and NF- $\kappa$ B p65 phosphorylation under LPS stimulation. Collectively, these data strongly demonstrate that the TLR4 was the very target of miR-181a following LPS stimulation.

It is well-known that inflammation induced by endotoxin such as LPS was closely associated with ROS generation (Patrino et al., 2015). ROS, which are mainly produced by NADPH oxidase, are commonly considered cytotoxic and can even induce cell damage in high levels (Ray et al., 2012). Previous studies also have shown that ROS were implicated in TLR4-mediated immune reactions (Zhang et al., 2016; Pan et al., 2017), and elicited a cascade of inflammatory events, such as activation of NF- $\kappa$ B (Yu et al., 2015; Singh et al., 2016). In the present study, miR-181a mimics markedly suppressed the intracellular ROS accumulation in LPS-induced macrophages. As expected, si-TLR4 also decreased ROS production. These results suggest that miR-181a could also alleviate LPS-induced inflammation through reducing TLR4-mediated ROS production.

## CONCLUSION

The results of our study not only demonstrates that miR-181a targets TLR4 directly to regulate the activation of NF- $\kappa$ B and subsequent secretion of inflammatory cytokines in response to LPS stimulation, but also reveal further that this miRNA represses the intracellular ROS accumulation. All these findings indicates, that miR-181a may be a negative regulator of LPS-stimulated inflammation via the suppression of ROS generation and TLR4-NF- $\kappa$ B pathway.

## AUTHOR CONTRIBUTIONS

KJ and GZ conceived and designed the experiments. TZ and YY carried out the experiments. SG, HW, and AS analyzed the data. KJ and GD wrote the manuscript. All authors agreed to be responsible for the content of the work.

## FUNDING

This study was supported by the National Natural Science Foundation of China (Nos. 31772816 and 31472254).

## REFERENCES

- Akira, S., and Hemmi, H. (2003). Recognition of pathogen-associated molecular patterns by TLR family. *Immunol. Lett.* 85, 85–95. doi: 10.1016/S0165-2478(02)00228-6
- Biswas, S. K., and Lopez-Collazo, E. (2009). Endotoxin tolerance: new mechanisms, molecules and clinical significance. *Trends Immunol.* 30, 475–487. doi: 10.1016/j.it.2009.07.009
- Cai, Z. G., Zhang, S. M., Zhang, Y., Zhou, Y. Y., Wu, H. B., and Xu, X. P. (2012). MicroRNAs are dynamically regulated and play an important role in LPS-induced lung injury. *Can. J. Physiol. Pharmacol.* 90, 37–43. doi: 10.1139/y11-095
- Case, S. R., Martin, R. J., Jiang, D., Minor, M. N., and Chu, H. W. (2011). MicroRNA-21 inhibits toll-like receptor 2 agonist-induced lung inflammation in mice. *Exp. Lung Res.* 37, 500–508. doi: 10.3109/01902148.2011.596895



- Chen, K., and Rajewsky, N. (2007). The evolution of gene regulation by transcription factors and microRNAs. *Nat. Rev. Genet.* 8, 93–103. doi: 10.1038/nrg1990
- Cheng, A. M., Byrom, M. W., Shelton, J., and Ford, L. P. (2005). Antisense inhibition of human miRNAs and indications for an involvement of miRNA in cell growth and apoptosis. *Nucleic Acids Res.* 33, 1290–1297. doi: 10.1093/nar/gki200
- Curtale, G., Mirolo, M., Renzi, T. A., Rossato, M., Bazzoni, F., and Locati, M. (2013). Negative regulation of Toll-like receptor 4 signaling by IL-10-dependent microRNA-146b. *Proc. Natl. Acad. Sci. U.S.A.* 110, 11499–11504. doi: 10.1073/pnas.1219852110
- Devaraj, S., Tobias, P., and Jialal, I. (2011). Knockout of toll-like receptor-4 attenuates the pro-inflammatory state of diabetes. *Cytokine* 55, 441–445. doi: 10.1016/j.cyto.2011.03.023
- Dreyfuss, D., and Ricard, J. D. (2005). Acute lung injury and bacterial infection. *Clin. Chest Med.* 26, 105–112. doi: 10.1016/j.ccm.2004.10.014
- Du, R. H., Li, E. G., Cao, Y., Song, Y. C., and Tan, R. X. (2011). Fumigaclavine C inhibits tumor necrosis factor  $\alpha$  production via suppression of toll-like receptor 4 and nuclear factor  $\kappa$ B activation in macrophages. *Life Sci.* 89, 235–240. doi: 10.1016/j.lfs.2011.06.015
- Gandhi, V. D., and Vliagoftis, H. (2015). Airway epithelium interactions with aeroallergens: role of secreted cytokines and chemokines in innate immunity. *Front. Immunol.* 6:147. doi: 10.3389/fimmu.2015.00147
- Ghorbani, S., Talebi, F., Fuk Chan, W., Masoumi, F., Voigani, M., Power, C., et al. (2017). MicroRNA-181 variants regulate T cell phenotype in the context of autoimmune neuroinflammation. *Front. Immunol.* 8:758. doi: 10.3389/fimmu.2017.00758
- Griffiths-Jones, S., Grocock, R. J., van Dongen, S., Bateman, A., and Enright, A. J. (2006). miRBase: microRNA sequences, targets and gene nomenclature. *Nucleic Acids Res.* 34, D140–D144. doi: 10.1093/nar/gkj112
- Guijarro Muñoz, I., Compte, M., Álvarezciénfuegos, A., Álvarezvallina, L., and Sanz, L. (2014). Lipopolysaccharide activates toll-like receptor 4 (TLR4)-mediated NF- $\kappa$ B signaling pathway and proinflammatory response in human pericytes. *J. Biol. Chem.* 289, 2457–2468. doi: 10.1074/jbc.M113.521161
- Herold, S., Mayer, K., and Lohmeyer, J. (2011). Acute lung injury: how macrophages orchestrate resolution of inflammation and tissue repair. *Front. Immunol.* 2:65. doi: 10.3389/fimmu.2011.00065
- Iyer, A., Zurolo, E., Prabowo, A., Fluiters, K., Spliet, W. G., van Rijen, P. C., et al. (2012). MicroRNA-146a: a key regulator of astrocyte-mediated inflammatory response. *PLoS One* 7:e44789. doi: 10.1371/journal.pone.0044789
- Ji, J., Yamashita, T., Budhu, A., Forgues, M., Jia, H. L., Li, C., et al. (2009). Identification of microRNA-181 by genome-wide screening as a critical player in EpCAM-positive hepatic cancer stem cells. *Hepatology* 50, 472–480. doi: 10.1002/hep.22989
- Jiang, K., Ma, X., Guo, S., Zhang, T., Zhao, G., Wu, H., et al. (2017a). Anti-inflammatory effects of rosmarinic acid in lipopolysaccharide-induced mastitis in mice. *Inflammation*. doi: 10.1007/s10753-017-0700-8 [Epub ahead of print].
- Jiang, K., Zhang, T., Yin, N., Ma, X., Zhao, G., Wu, H., et al. (2017b). Geraniol alleviates LPS-induced acute lung injury in mice via inhibiting inflammation and apoptosis. *Oncotarget* 8, 71038–71053. doi: 10.18632/oncotarget.20298
- Lawrence, T. (2009). The nuclear factor NF- $\kappa$ B pathway in inflammation. *Cold Spring Harb. Perspect. Biol.* 1:a001651. doi: 10.1101/cshperspect.a001651
- Leuenberger, C., Schuoler, C., Bye, H., Mignan, C., Rechsteiner, T., Hillinger, S., et al. (2016). MicroRNA-223 controls the expression of histone deacetylase 2: a novel axis in COPD. *J. Mol. Med.* 94, 725–734. doi: 10.1007/s00109-016-1388-1
- Li, W., Qiu, X., Jiang, H., Han, Y., Wei, D., and Liu, J. (2016). Downregulation of miR-181a protects mice from LPS-induced acute lung injury by targeting Bcl-2. *Biomed. Pharmacother.* 84, 1375–1382. doi: 10.1016/j.biopha.2016.10.065
- Lu, Y. C., Yeh, W. C., and Ohashi, P. S. (2008). LPS/TLR4 signal transduction pathway. *Cytokine* 42, 145–151. doi: 10.1016/j.cyto.2008.01.006
- Matthay, M. A., and Zimmerman, G. A. (2005). Acute lung injury and the acute respiratory distress syndrome: four decades of inquiry into pathogenesis and rational management. *Am. J. Respir. Cell Mol. Biol.* 33, 319–327. doi: 10.1165/rmb.F305
- Nahid, M. A., Satoh, M., and Chan, E. K. (2011). MicroRNA in TLR signaling and endotoxin tolerance. *Cell. Mol. Immunol.* 8, 388–403. doi: 10.1038/cmi.2011.26
- Ochs, M. J., Steinhilber, D., and Suess, B. (2011). MicroRNA involved in inflammation: control of eicosanoid pathway. *Front. Pharmacol.* 2:39. doi: 10.3389/fphar.2011.00039
- O'Connell, R. M., Rao, D. S., and Baltimore, D. (2012). microRNA regulation of inflammatory responses. *Annu. Rev. Immunol.* 30, 295–312. doi: 10.1146/annurev-immunol-020711-075013
- Pan, N., Lu, L. Y., Li, M., Wang, G. H., Sun, F. Y., Sun, H. S., et al. (2017). Xylometal B alleviates cerebral infarction and neurologic deficits in a mouse stroke model by suppressing the ROS/TLR4/NF- $\kappa$ B inflammatory signaling pathway. *Acta Pharmacol. Sin.* 38, 1236–1247. doi: 10.1038/aps.2017.22
- Patruno, A., Fornasari, E., Stefano, A. D., Cerasa, L. S., Marinelli, L., Baldassarre, L., et al. (2015). Synthesis of a novel cyclic prodrug of S-Allyl-glutathione able to attenuate LPS-induced ROS production through the inhibition of MAPK pathways in U937 cells. *Mol. Pharm.* 12, 66–74. doi: 10.1021/mp500431r
- Ray, P. D., Huang, B. W., and Tsuiji, Y. (2012). Reactive oxygen species (ROS) homeostasis and redox regulation in cellular signaling. *Cell. Signal.* 24, 981–990. doi: 10.1016/j.cellsig.2012.01.008
- Rojas, M., Woods, C. R., Mora, A. L., Xu, J., and Brigham, K. L. (2005). Endotoxin-induced lung injury in mice: structural, functional, and biochemical responses. *Am. J. Physiol. Lung Cell Mol. Physiol.* 288, L333–L341. doi: 10.1152/ajplung.00334.2004
- Rubenfeld, G. D., Caldwell, E., Peabody, E., Weaver, J., Martin, D. P., Neff, M., et al. (2005). Incidence and outcomes of acute lung injury. *N. Engl. J. Med.* 353, 1685–1693. doi: 10.1056/NEJMoa050333
- Seoudi, A. M., Lashine, Y. A., and Abdelaziz, A. I. (2012). MicroRNA-181a – a tale of discrepancies. *Expert Rev. Mol. Med.* 14, e5. doi: 10.1017/s1462399411002122
- Shen, W., Gan, J., Xu, S., Jiang, G., and Wu, H. (2009). Penicillamine hydrochloride attenuates LPS-induced acute lung injury involvement of NF- $\kappa$ B pathway. *Pharmacol. Res.* 60, 296–302. doi: 10.1016/j.phrs.2009.04.007
- Shi, H., Kokoeva, M. V., Inouye, K., Tzamelis, I., Yin, H., and Flier, J. S. (2006). TLR4 links innate immunity and fatty acid-induced insulin resistance. *J. Clin. Invest.* 116, 3015–3025. doi: 10.1172/JCI28898
- Shi, L., Cheng, Z., Zhang, J., Li, R., Zhao, P., Fu, Z., et al. (2008). hsa-mir-181a and hsa-mir-181b function as tumor suppressors in human glioma cells. *Brain Res.* 1236, 185–193. doi: 10.1016/j.brainres.2008.07.085
- Singh, A., Singh, V., Tiwari, R. L., Chandra, T., Kumar, A., Dikshit, M., et al. (2016). The IRAK-ERK-p67phox-Nox-2 axis mediates TLR4, 2-induced ROS production for IL-1 $\beta$  transcription and processing in monocytes. *Cell. Mol. Immunol.* 13, 745–763. doi: 10.1038/cmi.2015.62
- Wu, C., Gong, Y., Yuan, J., Zhang, W., Zhao, G., Li, H., et al. (2012). microRNA-181a represses ox-LDL-stimulated inflammatory response in dendritic cell by targeting c-Fos. *J. Lipid Res.* 53, 2355–2363. doi: 10.1194/jlr.M028878
- Wu, H., Jiang, K., Yin, N., Ma, X., Zhao, G., Qiu, C., et al. (2017). Thymol mitigates lipopolysaccharide-induced endometritis by regulating the TLR4- and ROS-mediated NF- $\kappa$ B signaling pathways. *Oncotarget* 8, 20042–20055. doi: 10.18632/oncotarget.15373
- Wu, H., Zhao, G., Jiang, K., Chen, X., Zhu, Z., Qiu, C., et al. (2016). Plantamajoside ameliorates lipopolysaccharide-induced acute lung injury via suppressing NF- $\kappa$ B and MAPK activation. *Int. Immunopharmacol.* 35, 315–322. doi: 10.1016/j.intimp.2016.04.013
- Xiao, J., Tang, J., Chen, Q., Tang, D., Liu, M., Luo, M., et al. (2015). miR-429 regulates alveolar macrophage inflammatory cytokine production and is involved in LPS-induced acute lung injury. *Biochem. J.* 471, 281–291. doi: 10.1042/bj20131510
- Xu, D. D., Zhou, P. J., Wang, Y., Zhang, Y., Zhang, R., Zhang, L., et al. (2016). miR-150 suppresses the proliferation and tumorigenicity of leukemia stem cells by targeting the nanog signaling pathway. *Front. Pharmacol.* 7:439. doi: 10.3389/fphar.2016.00439
- Yao, H., Sun, Y., Song, S., Qi, Y., Tao, X., Xu, L., et al. (2017). Protective effects of dioscin against lipopolysaccharide-induced acute lung injury through inhibition of oxidative stress and inflammation. *Front. Pharmacol.* 8:120. doi: 10.3389/fphar.2017.00120
- Yu, J., Lu, Y., Li, Y., Xiao, L., Xing, Y., Li, Y., et al. (2015). Role of S100A1 in hypoxia-induced inflammatory response in cardiomyocytes via TLR4/ROS/NF- $\kappa$ B pathway. *J. Pharm. Pharmacol.* 67, 1240–1250. doi: 10.1111/jphp.12415

- Zhang, X., Wang, C., Shan, S., Liu, X., Jiang, Z., and Ren, T. (2016). TLR4/ROS/miRNA-21 pathway underlies lipopolysaccharide instructed primary tumor outgrowth in lung cancer patients. *Oncotarget* 7, 42172–42182. doi: 10.18632/oncotarget.9902
- Zhao, J., Gong, A.-Y., Zhou, R., Liu, J., Eischeid, A. N., and Chen, X.-M. (2012). Downregulation of PCAF by miR-181a/b provides feedback regulation to TNF- $\alpha$ -induced transcription of proinflammatory genes in liver epithelial cells. *J. Immunol.* 188, 1266–1274. doi: 10.4049/jimmunol.110.1976
- Zhou, A., Li, S., Wu, J., Khan, F. A., and Zhang, S. (2014). Interplay between microRNAs and host pathogen recognition receptors (PRRs) signaling pathways in response to viral infection. *Virus Res.* 184, 1–6. doi: 10.1016/j.virusres.2014.01.019
- Zhu, J., Wang, F. L., Wang, H. B., Dong, N., Zhu, X. M., Wu, Y., et al. (2017). TNF- $\alpha$  mRNA is negatively regulated by microRNA-181a-5p in maturation of dendritic cells induced by high mobility group box-1 protein. *Sci. Rep.* 7:12239. doi: 10.1038/s41598-017-12492-3
- Zou, J., Feng, D., Ling, W. H., and Duan, R. D. (2013). Lycopene suppresses proinflammatory response in lipopolysaccharide-stimulated macrophages by inhibiting ROS-induced trafficking of TLR4 to lipid raft-like domains. *J. Nutr. Biochem.* 24, 1117–1122. doi: 10.1016/j.jnutbio.2012.08.011

**Conflict of Interest Statement:** The authors declare that the research was conducted in the absence of any commercial or financial relationships that could be construed as a potential conflict of interest.

Copyright © 2018 Jiang, Guo, Zhang, Yang, Zhao, Shaukat, Wu and Deng. This is an open-access article distributed under the terms of the Creative Commons Attribution License (CC BY). The use, distribution or reproduction in other forums is permitted, provided the original author(s) and the copyright owner are credited and that the original publication in this journal is cited, in accordance with accepted academic practice. No use, distribution or reproduction is permitted which does not comply with these terms.



# Effects of Simultaneous Downregulation of PHD1 and Keap1 on Prevention and Reversal of Liver Fibrosis in Mice

Jing Liu<sup>1</sup>, Wencai Li<sup>1</sup>, Manoj H. Limbu<sup>2</sup>, Yiping Li<sup>2</sup>, Zhi Wang<sup>2</sup>, Zhengyuan Cheng<sup>2</sup>, Xiaoyi Zhang<sup>2</sup> and Pingsheng Chen<sup>2\*</sup>

<sup>1</sup> Department of Pathology, The First Affiliated Hospital of Zhengzhou University, Zhengzhou, China, <sup>2</sup> Department of Pathology and Pathophysiology, School of Medicine, Southeast University, Nanjing, China

## OPEN ACCESS

### Edited by:

Raffaele Strippoli,  
Sapienza Università di Roma, Italy

### Reviewed by:

Brian Gregory George Oliver,  
University of Technology Sydney,  
Australia

Christoph Eugen Hagemeyer,  
Monash University, Australia

### \*Correspondence:

Pingsheng Chen  
101006524bingli@sina.cn

### Specialty section:

This article was submitted to  
Translational Pharmacology,  
a section of the journal  
Frontiers in Pharmacology

**Received:** 08 March 2018

**Accepted:** 08 May 2018

**Published:** 30 May 2018

### Citation:

Liu J, Li W, Limbu MH, Li Y, Wang Z, Cheng Z, Zhang X and Chen P (2018) Effects of Simultaneous Downregulation of PHD1 and Keap1 on Prevention and Reversal of Liver Fibrosis in Mice. *Front. Pharmacol.* 9:555. doi: 10.3389/fphar.2018.00555

**Background and Aim:** To investigate whether double-knockdown of PHD1 and Keap1 in mice could enhance the resolution of carbon tetrachloride (CCl<sub>4</sub>)-induced liver fibrosis.

**Methods:** The liver fibrosis model of mice was established by intraperitoneal injection of 25% CCl<sub>4</sub> in olive oil (4 ul/g) twice a week for 8 weeks. PHD1shRNA and Keap1shRNA eukaryotic expression plasmids were simultaneously administered from the beginning of the first to fourth week (preventive group) or from the fifth to eighth week of CCl<sub>4</sub> injection (therapeutic group) via hydrodynamic-based tail vein injection. Successful transfection was confirmed with the expression of red fluorescent protein and green fluorescent protein in hepatocytes. Western blot was used for determining the expression of PHD1 and Keap1, HE, Sirius red, and Masson staining for evaluating the histopathological stages of fibrosis. Immunohistochemical techniques were applied to evaluate the expression of α-SMA.

**Results:** The fluorescence of red and green were observed mainly in hepatocytes, and downregulation of PHD1 and Keap1 expression in liver was detected by western blot. Meanwhile, double-knockdown of PHD1 and Keap1 in mice alleviated liver fibrosis, and the effect was further enhanced especially in the preventive group. Immunocytochemical staining showed decreased expression of α-SMA when both PHD1 and Keap1 were knockdown.

**Conclusion:** Downregulation of PHD1 and Keap1 expression in the liver could be achieved via hydrodynamic injection of PHD1shRNA and Keap1shRNA, thereby, preventing liver fibrosis.

**Keywords:** liver fibrosis, hepatocytes, PHD1, Keap1, hypoxia, oxidative stress

## INTRODUCTION

Liver fibrosis is a type of liver scarring from compensatory response to various chronic liver injuries resulting in disruption of extracellular matrix, cell populations, and cytokines. As a metabolically active organ, liver is extremely sensitive to hypoxia and hypoxia in liver fibrosis is mainly due to sinusoidal stenosis, neovascularization, collagen deposition, and abnormal hepatic vascular

network. It has been postulated that liver injury are often accompanied by hypoxia (Onori et al., 2000). In recent years, studies have shown that oxidative stress plays an important role in the development of liver fibrosis (Yang et al., 2013) and often factors involved in liver fibrosis are accompanied by increased oxidation or decreased antioxidant. The inter relationship between oxidative stress and liver fibrosis are currently among the hot topic of research. PHD1 and Keap1 are the intracellular oxygen sensor and oxidative stress sensor respectively, and we have used the *in vitro* shRNA technology to interfere with their functions in the hepatocytes, and thereby reducing hepatocytes hypoxia and oxidative stress (Liu et al., 2017). In this study, PHD1shRNA and Keap1shRNA plasmids were simultaneously transfected into the mice with liver fibrosis via hydrodynamic injection, and the subsequent effects of PHD1 and Keap1 on the prevention and reversal of liver fibrosis were observed.

## MATERIALS AND METHODS

### PHD1shRNA and Keap1shRNA Plasmid Construction

The plasmids pGPU6/RFP/Neo-PHD1shRNA and pGPU6/RFP/Neo-PHD1shNC were both designed by GenePharma (Shanghai, China). For silencing Keap1 gene expression, the plasmid Plvx/GFP/puro-Keap1shRNA was designed by Hanbio Biotechnology (Shanghai, China). The purity and quantity of the DNA were measured by spectrophotometry (Thermo, United States) at 260/280 nm.

### Establishment of CCl<sub>4</sub>-Induced Liver Fibrosis Model

Sixty healthy male ICR mice, 6 weeks old, each weighing about 16–20 g were purchased from Yangzhou University Animal Experiment Center. Mice were housed at temperature of 20–28°C, relative humidity of 60–70% with normal ventilation and 12 h light and dark cycle. During whole period of experiment, mice were provided free access to sterile deionized water and standard normal food. This study was carried out in accordance with the recommendations of the European Council Directive of the 24<sup>th</sup> November 1986 (86/609/EEC). All procedures were approved by the Animal Research Ethics Committee at the Medical School of the Southeast University (Nanjing, China).

Mice were divided into the following six groups, and 10 in each group: (1) Blank control group were administered normal saline, twice a week for 8 weeks. (2) CCl<sub>4</sub> model group were administered 5  $\mu$ L/g of 25% CCl<sub>4</sub> in olive oil, twice a week for 8 weeks. (3) PHD1shNC group were treated CCl<sub>4</sub> similar to model group for 8 weeks along with PHD1shNC empty plasmid hydrodynamic injection once a week from week 1 to week 4. (4) Single transfection group (PHD1shRNA group) were treated same as model group along with PHD1shRNA injection once weekly from week 1 to week 4. (5) Co-transfection preventive group was similar to model group along with co-injection of PHD1shRNA and Keap1shRNA once weekly from week 1 to

week 4. (6) Co-transfection therapeutic group were treated similar to model group along with co-injection of PHD1shRNA and Keap1shRNA plasmid once weekly from week 4 to week 8.

After 8 weeks, mice were killed with intraperitoneally injection of pentobarbital solution. Livers were dissected and washed in PBS and photographs photographed. At the same time, heart, spleen, lung, kidney, and other organs were preserved for the follow-up experiments. Half of tissues were fixed in a 10% formalin. Part of the tissues were embedded in OCT (optimal cutting temperature compound) for frozen sections, and the rest were snap frozen in liquid nitrogen and stored at –80°C for WB.

### Hydrodynamic Injection of PHD1shRNA and Keap1 shRNA Plasmids

Hundred  $\mu$ g each of PHD1shRNA and Keap1shRNA plasmid DNA were mixed in a 2 mL solution of 0.9% sodium chloride and was injected through the tail vein of mice within 6 to 7 s, the frequency of injection was once a week for 4 weeks (Maruyama et al., 2002; Chen et al., 2004; Zender et al., 2005). The mice were sacrificed 24 h after the last injection, and frozen sections were prepared from the tissues of liver, heart, spleen, lung, and kidney and then washed in a cold acetone for 10 min. After being allowed to dry, the cells were washed in PBS for 5 min for three times, and DAPI (4',6-diamidino-2-phenylindole) staining for 5 min was done next. Finally, the sections were observed under fluorescence microscope for the expression of RFP (red fluorescence protein) and GFP (green fluorescence protein) for determining if the transfection was successful. The protein expression levels of PHD1 and Keap1 *in vivo* were detected by WB using a polyclonal antibody to PHD1 (Abcam, United States) and Keap1 (Proteintech, United States).

### Body Weight and Liver Index

Body weight were recorded before each intraperitoneal injection of CCl<sub>4</sub> and were also calculated after 8 weeks. Liver index was calculated according to the following formula: liver index = wet weight of liver/body weight  $\times$  100%.

### Liver Function

Intraocular venous blood was collected and centrifuged at 3000 rpm/min for 5 min. The supernatants were collected and measured for ALT, AST, and ALP levels by automatic blood biochemical analyzer.

### Liver Histology and Immunohistochemical Staining

The sections were cut into 3–5  $\mu$ m thick slices with a microtome, and stained with hematoxylin and eosin (H&E), Masson dyes, and sirius red.

According to Scheuer's program (Scheuer, 1991), liver fibrosis were graded into S0~S4 stages, S0: no fibrosis. S1: the portal area, periportal fibrosis, limiting plate fibrosis or intralobular fibrosis, neither of which affects the structural integrity of the lobules. S2: fibrous septum formation due to bridging necrosis but lobular structure is preserved. S3: a large number



of fibrous septum dividing hepatic lobules, causing distortion of lobular structure, but no cirrhosis formation. S4: early cirrhosis, extensive destruction of liver parenchyma, diffuse fibrogenesis, and pseudolobule formation. The semiquantitative scoring system (SSS) for liver fibrosis was done according to the Chevallier's protocol (Chevallier et al., 1994).

Next, the expression of  $\alpha$ -SMA in liver tissue was detected by immunohistochemistry. Paraffin sections were antigen-retrieved, blocked with 5% BSA, and then was incubated with primary antibody  $\alpha$ -SMA (Proteintech, United States) for overnight. Next, section were incubated with secondary antibody for 20 min at 37°C, then coloration with 3, 3-Diaminobenzidine (DAB) was done, next, the nuclei were counterstained with hematoxylin, and then were observed under the light microscope and subjected to semi-quantitative analysis using Image J software.

## Statistical Analysis

All the results are expressed as mean  $\pm$  SD. One-way analysis of variance (ANOVA) and the Student's *t*-test were used to evaluate the difference between groups. SPSS16.0 software was used for statistical analysis of data. A *p*-value < 0.05 was considered significant.

## RESULTS

### Fluorescence Observation of Each Organ Sections

PHD1shRNA and Keap1shRNA plasmids were injected into mice via tail vein and then observed by fluorescence microscopy (Figure 1). Obvious red and green fluorescence were observed in liver tissues. DAPI staining of nuclei suggested that most of the fluorescence existed within the hepatocytes. The fluorescence in other organs were weak and some were even undetectable. Thus, successful targeted transfection of hepatocytes were achieved using hydrodynamic injection.

### PHD1 and Keap1 Protein Expression

PHD1shRNA and Keap1shRNA plasmids were successfully targeted to the hepatocytes via tail vein, and expression of PHD1 and Keap1 were detected by using western blot (Figure 2). Compared with that in the blank control group, the expression of Keap1 in the model group was increased significantly, however, the expression of PHD1 only changed by little. There were no significant differences in the PHD1 and Keap1 levels between PHD1shNC group and the model group (*p* > 0.05), and we found that the levels of PHD1 and Keap1 in the single transfection group were decreased, while those in the co-transfection group were further reduced.

### Mouse Liver Morphology

The Figure 3 showed that the liver in the blank group was smooth, ruddy and soft textured, while the model group had obvious adhesion with the surrounding tissues, the edges were blunt and the surface were granular, the changes in the PHD1shNC group were similar to that of the model group. The liver from the co-transfection preventive group showed no obvious changes, even though the color was not as ruddy as that of blank group, the lesions were less severe than the model group. The pathological changes in the single-transfection group and co-transfection therapeutic group were little more severe than in the preventive group.

### Mice Weight and Liver Index

As shown in Table 1, the model group had weight reduction (*p* < 0.01) than the blank control group. There were no significant differences in the weight between the single transfection group and the co-transfection preventive group, but both had increased weight when compared to the model group (*p* < 0.05). However, the weight of the co-transfection therapeutic group was slightly higher than those of the model group, but was

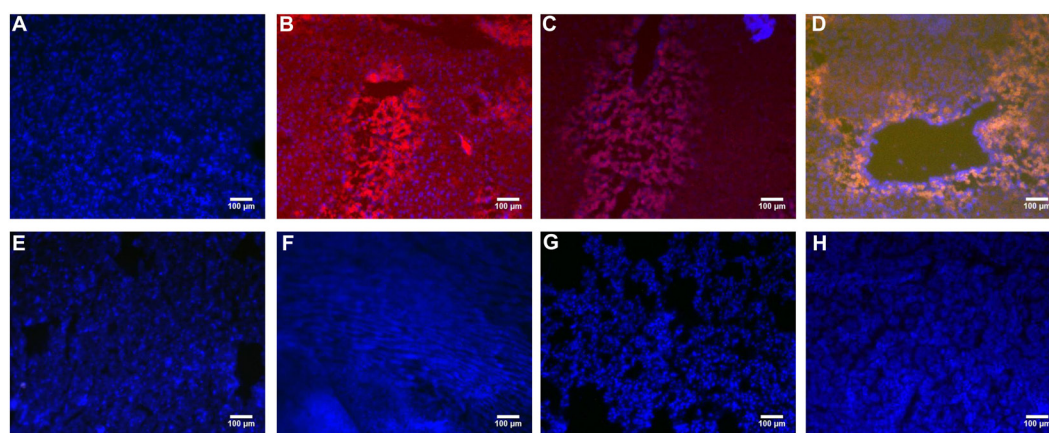
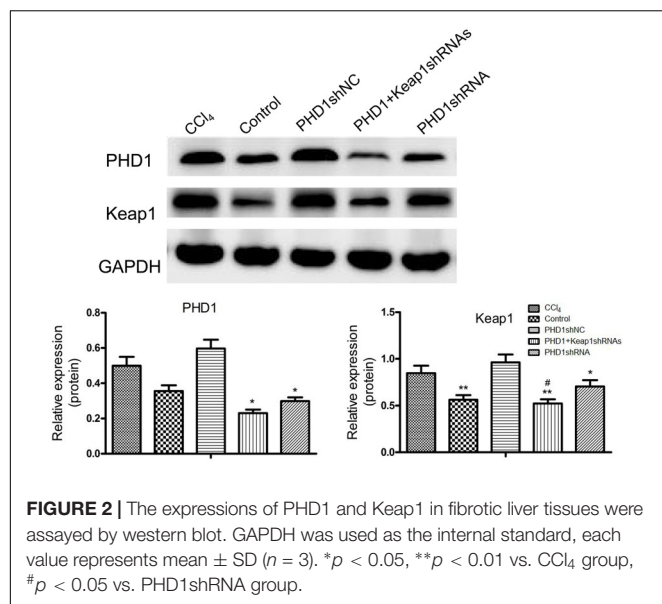


**FIGURE 1 |** The PHD1shRNA, PHD1shNC, PHD1+Keap1shRNAs expression vectors were injected into CCl<sub>4</sub>-treated mice, respectively. The fluorescence from the fibrotic liver of blank control group (A), PHD1shRNA group (B), PHD1shNC group (C), PHD1+Keap1shRNAs-transfected group (D), and from Heart (E), Lung (F), Spleen (G), Kidney (H) of PHD1+Keap1shRNAs-transfected group were observed by fluorescent microscope. DAPI staining for cell nuclei in the same field.





not statistically significant ( $p > 0.05$ ). Compared to the blank group, the liver index of model group increased significantly ( $p < 0.05$ ), however, there were no significant differences between the PHDshNC group and the model group, and there was also no significant difference between co-transfection group and single transfection group ( $p > 0.05$ ). The liver index in the co-transfection preventive group were lower than those in the model group ( $p < 0.05$ ), but the single transfection group and the co-transfection therapeutic group did not reach statistical significance when compared to the model group ( $p > 0.05$ ).

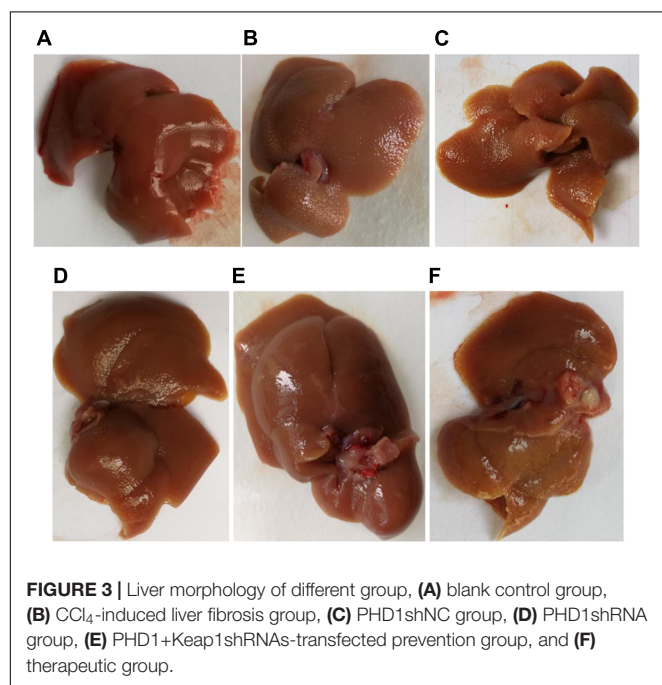


**TABLE 1 |** The weight and liver index in different groups.

Group	Weight		Liver index (%)
	0 week	8 week	
Blank control	27.83 $\pm$ 1.52	43.25 $\pm$ 1.06	4.27 $\pm$ 0.62
CCl <sub>4</sub>	27.66 $\pm$ 1.25	35.05 $\pm$ 0.91 <sup>▼▼</sup>	7.70 $\pm$ 1.45 <sup>▼</sup>
PHD1shNC	27.67 $\pm$ 1.75	36.05 $\pm$ 0.97	6.60 $\pm$ 1.02
PHD1shRNA	27.5 $\pm$ 1.80	37.95 $\pm$ 0.89*	6.10 $\pm$ 0.94
PHD1+Keap1shRNAs co-transfection preventive group	27.5 $\pm$ 2.29	39.02 $\pm$ 1.79*	5.10 $\pm$ 0.60*
PHD1+Keap1shRNAs co-transfection therapeutic group	27.66 $\pm$ 2.25	36.72 $\pm$ 1.19	6.20 $\pm$ 0.83

\* $p < 0.05$  vs. CCl<sub>4</sub>, <sup>▼</sup> $p < 0.01$ , <sup>▼▼</sup> $p < 0.001$  vs. blank control.

## Liver Functions

As shown in Table 2, liver functions test showed that when compared to the blank group, the levels of serum ALT and AST in the model group were significantly increased, while the levels in the PHDshNC group were not significantly different from those in the model group ( $p > 0.05$ ). The levels in the single transfection group were decreased than that in the model group, while the decrease in the co-transfection preventive group were more obvious (statistically significant when compared to single transfection group), which indicated that co-inhibition of PHD1 and Keap1 expression could better prevent liver injury in mice. However, the reduction in the co-transfection therapeutic group was not as effective as that of preventive group. The level of ALP in the model group was higher than that in the blank control group and the ALP in the co-transfection preventive group was lower than that in the model group, but the ALP levels of all six groups were within the normal range.

## Liver Fibrosis Grades and Scores

According to the results of HE (Figure 4), Masson (Figure 5) and Sirius red staining (Figure 6), the degree of liver fibrosis was graded and scored for each group in Table 3. The liver

**TABLE 2 |** The ALT, AST, ALP levels of different groups.

Group	ALT	AST	ALP
Blank control	39 $\pm$ 3.94	36 $\pm$ 3.28	38 $\pm$ 6.16
CCl <sub>4</sub>	436 $\pm$ 61.15 <sup>▼▼▼</sup>	316 $\pm$ 48.18 <sup>▼▼▼</sup>	62 $\pm$ 5.66 <sup>▼▼</sup>
PHD1shNC	368 $\pm$ 45.44	262 $\pm$ 42.68	52 $\pm$ 4.99
PHD1shRNA	222 $\pm$ 22.05**	99 $\pm$ 12.85**	56 $\pm$ 5.22
PHD1+Keap1shRNAs co-transfection preventive group	145 $\pm$ 16.98***	71 $\pm$ 7.6***	42 $\pm$ 4.57**
PHD1+Keap1shRNAs co-transfection therapeutic group	193 $\pm$ 24.86**	78 $\pm$ 11.23**	60 $\pm$ 7.66

\* $p < 0.05$ , \*\* $p < 0.01$ , \*\*\* $p < 0.001$  vs. CCl<sub>4</sub>, # $p < 0.05$ , ## $p < 0.01$  vs. PHD1shRNA, <sup>▼</sup> $p < 0.01$ , <sup>▼▼</sup> $p < 0.01$ , <sup>▼▼▼</sup> $p < 0.001$  vs. blank control.

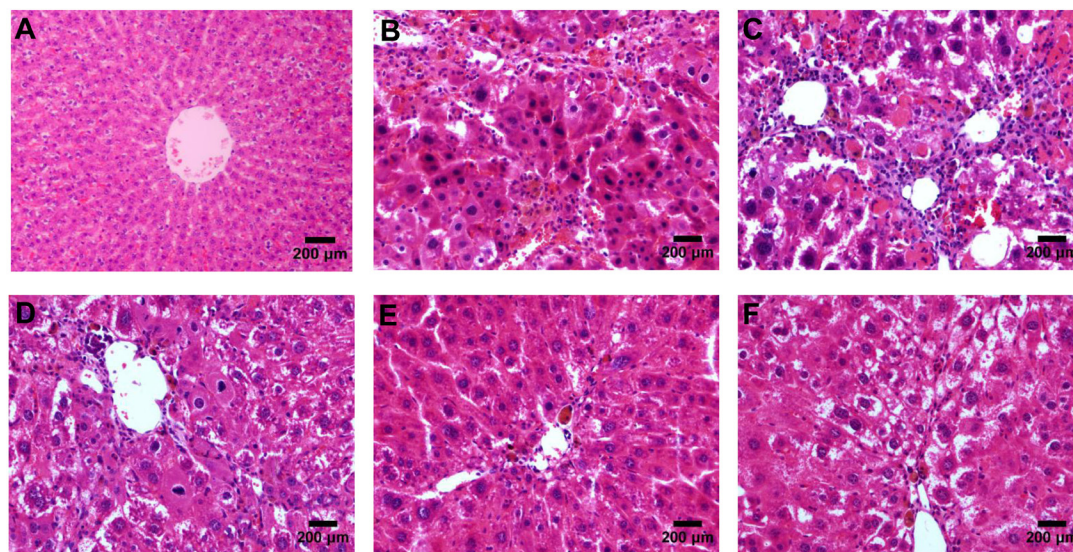


**FIGURE 4 |** HE staining of liver tissues, (A) blank control group, (B) the CCl<sub>4</sub>-induced liver fibrosis group, (C) PHD1shNC group, (D) PHD1shRNA group, (E) PHD1+Keap1shRNAs co-transfected prevention group, and (F) treatment group.

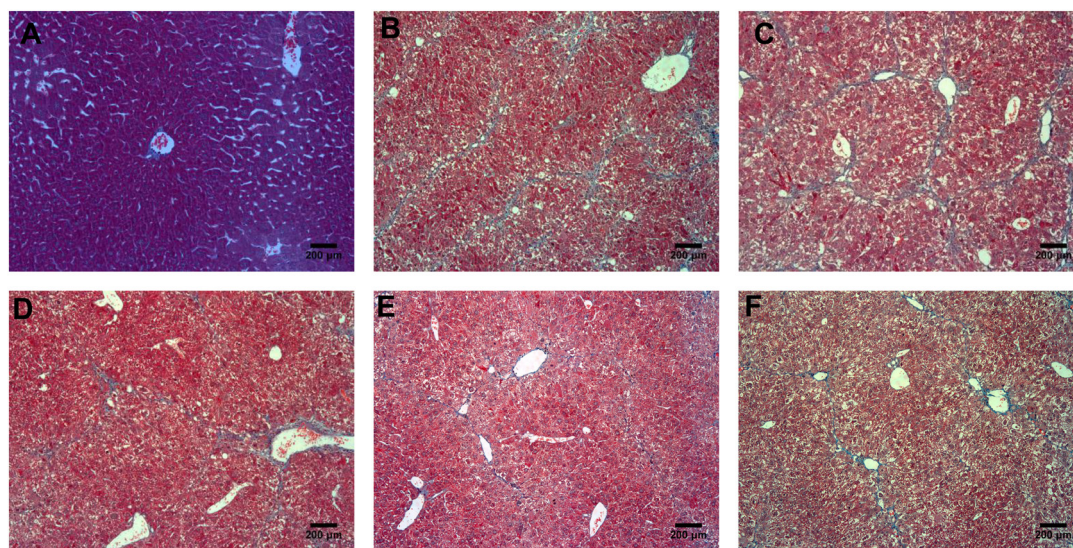


**FIGURE 5 |** Masson staining of liver tissues, (A) normal control group, (B) the CCl<sub>4</sub>-induced liver fibrosis group, (C) PHD1shNC group, (D) PHD1shRNA group, (E) PHD1+Keap1shRNAs co-transfected prevention group, and (F) treatment group.

fibrosis stage in model group and PHDshNC group were mostly S3~S4 phases, and the single transfection group were mostly S1~S2 phases. Most of the co-transfection preventive groups were S1 phase while most of the co-transfection therapeutic group were S2~S3 phases. Scores between PHD1shNC group and the model group had no significant differences, while scores of single transfection group, co-transfection preventive group and co-transfection therapeutic group were lower than that of model group. Whereas, scores of co-transfection therapeutic group was higher than in the co-transfection preventive group.

### a-SMA Expression in Liver Tissue

a-SMA is an indicator of HSCs activation. In normal liver, a-SMA was mainly expressed on the walls of central vein, periportal, and outside the vessel walls. In the model group, a-SMA was strongly expressed in the fibrous septa and perivascular areas, while there were no significant differences between the PHDshNC group and model group ( $p > 0.05$ ) (Figure 7). Compared to the model group, a-SMA expression in the co-transfection preventive group was weaker ( $p < 0.01$ ) and mainly around the incomplete fibrous speta. In addition, the expression of a-SMA in co-transfection therapeutic group was



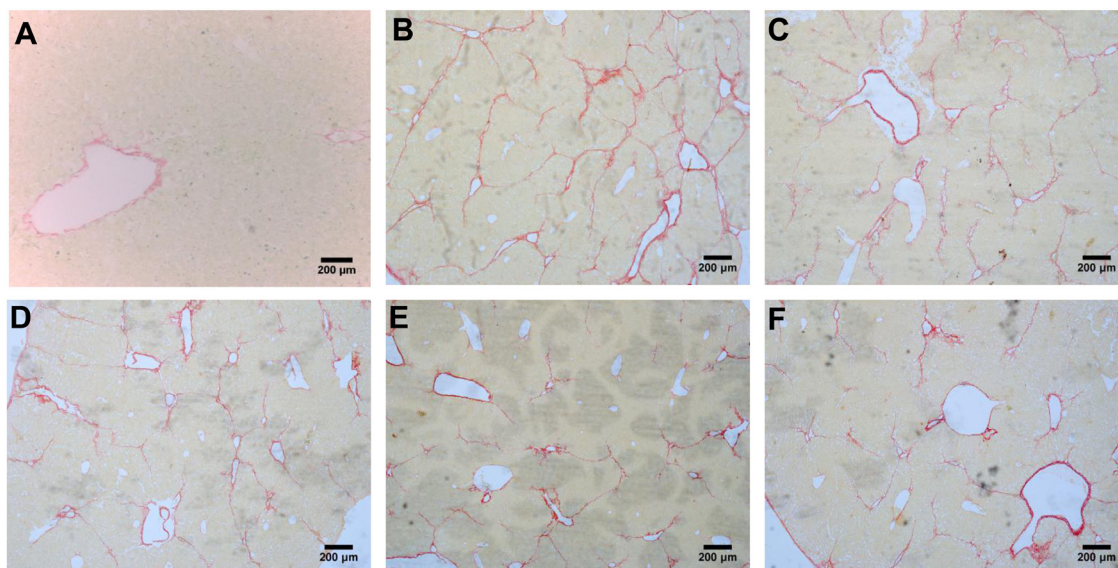


**FIGURE 6 |** Sirius red staining of liver tissues, (A) blank control group, (B) the CCl<sub>4</sub>-induced liver fibrosis group, (C) PHD1shNC group, (D) PHD1shRNA group, (E) PHD1+Keap1shRNAs co-transfected prevention group, and (F) treatment group.

**TABLE 3 |** The grades and scores of liver fibrosis in different groups.

Group	Quantity	Staging	Scoring
Blank control group	10	S0	0
CCl <sub>4</sub> model group	10	S3~S4	20.6 ± 3.78
PHD1shNC empty plasmid group	10	S3~S4	18.7 ± 3.43
PHD1 shRNA group	10	Mostly S1~S2, little for the S3	9.8 ± 1.79*
PHD1+Keap1shRNAs co-transfection preventive group	10	Mostly S1, little for the S2	6.5 ± 1.19**#
PHD1+Keap1shRNAs co-transfection therapeutic group	10	S2~S3	11.5 ± 2.11*

\* $p < 0.05$ , \*\* $p < 0.01$  vs. CCl<sub>4</sub>, # $p < 0.05$  vs. PHD1shRNA.

significantly decreased. Therefore, the above results indicates that the activation of HSCs can specifically be inhibited by downregulating the expression of PHD1 and Keap1 in rats with hepatic fibrosis.

## DISCUSSION

Liver fibrosis is a pathological process caused by chronic liver injury. There are many factors such as viral hepatitis, alcohol and drugs which results in chronic liver injury (Begriche et al., 2011). CCl<sub>4</sub> is a hepatotoxin widely used for establishing animal models of liver fibrosis. It acts on hepatocytes directly by causing tissue necrosis. In this study, the injection of 25% CCl<sub>4</sub> in olive oil at the dose of 5 μL/g for 8 weeks resulted in severe liver injury in the model

group. The liver histology of model group showed disruption of normal hepatic architecture, infiltration of inflammatory cells, necrosis, broad fibrous septa with pseudolobules. Thus, it concluded that CCl<sub>4</sub> induced hepatic fibrosis was successfully established.

In recent years, gene therapy has become a hot topic of research in the treatment of liver fibrosis. RNAi is one of the most widely studied techniques in gene therapy, and shRNA has been widely used *in vivo* experiment for its high efficiency and strong stability. However, owing to the complexity of the human body and lack of specific target, it leads to adverse effects. Therefore, the key to the treatment of liver fibrosis would be to design an effective and specific targeted gene delivery system. Currently, the effective vectors for gene delivery are mainly divided into viral vectors and non-viral vectors. However, viral vectors have some limitations in clinical application due to their immunogenicity and carcinogenic properties. On the other hand, non-viral vectors in the recent years has been studied extensively with considerable progress in targeted anti-fibrotic approach in the treatment of liver fibrosis. Asialoglycoprotein receptor is an efficient endocytic vector present in the liver parenchymal cells and it is widely used in targeted drug therapy of liver disease. Sato et al. (2007) reported that by injecting galactosylated liposomes encapsulated siRNA into the tail vein of mice can achieve an effective gene silencing in the liver cells of those mice. However, it has been reported that cationic liposome/DNA complexes injection through the tail vein are associated with certain degree of hepatotoxicity (Tousignant et al., 2000; Loisel et al., 2001; Kawakami et al., 2006). Moreover, during the study of targeted drugs via receptor-mediation, the receptor density and its binding activity vector/drug interaction and vector/internal environment interactions must also be put into consideration.

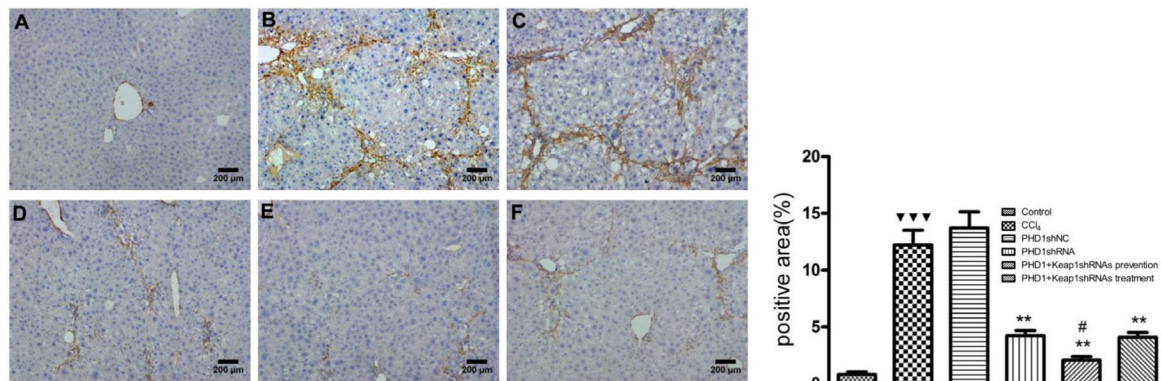


**FIGURE 7 |** The expression of  $\alpha$ -SMA were measured by immunohistochemical staining. (A) blank control group, (B) the CCl<sub>4</sub>-induced liver fibrosis group, (C) PHD1shNC group, (D) PHD1shRNA group, (E) PHD1+Keap1shRNAs co-transfected preventive group, and (F) therapeutic group. Each value represents mean  $\pm$  SD ( $n = 3$ ). \*\* $p < 0.01$  vs. CCl<sub>4</sub> group, # $p < 0.05$  vs. PHD1shRNA group, \*\*\* $p < 0.001$  vs. control.

It should also be considered that low transport efficiency of non-viral vectors is the biggest bottleneck preventing its widespread application.

Hydrodynamic injection is the solution for the above mentioned shortcoming of non viral vectors (Song et al., 2002), which was discovered by Liu et al. (1999) and Zhang et al. (1999). Dynamic CT scans monitoring has already confirmed that the hydrodynamic injection could achieve better liver targeting effects (Yokoo et al., 2015). Hydrodynamic injection of siRNA or shRNA naked plasmid could inhibit the genes expression in the liver (McCaffrey et al., 2002; Song et al., 2003), Abe et al. (2016) also has recently found that by mediating MMP-13 expression via hydrodynamic injection could effectively inhibit liver fibrosis in rats. In addition, hydrodynamic injection of HbeAg-negative cccDNA into C57BL/6J mice resulted in a nearly 100% HBV infection in the initial stage (Wang et al., 2017). Clinical trials in human has also shown that hydrodynamic injection of thrombopoietin plasmids through human portal vein could markedly increase platelet count (Khorsandi et al., 2008).

It is believed that the rapid injection of large volume of plasmid solution leads to the transient right heart failure which results into a temporary systemic circulatory congestions, and increasing the contact time between the DNA and intrahepatic cells. Moreover, rapid injection of the DNA also minimizes its rapid degradation in the blood, thereby allowing prolong contact of the DNAs with the cells (Maruyama et al., 2002). Pressure also has the key role in allowing the liver cells to absorb DNA plasmids. Speed and volume of injection also directly affects the efficiency of DNA transfection, therefore, slow rate of injection and reduced volume reduces the efficiency of gene expression. Studies have shown that injecting the DNA volume of about 8% of total body weight within 7 s could achieve maximum expression level (Liu et al., 1999; Zhang et al., 1999). However, due to the limitation of animal tolerance, the volume of DNA injected hits plateau after the volume of 100  $\mu$ g (Zhang et al., 1999). Moreover, a study has found that the expression of exogenous genes in the liver peaks within 8–24 h

after hydrodynamic injections and decreases significantly within 6 days, but higher levels can still be detected. The safety and efficacy of hydrodynamic injection has also been reported by a large number of researchers in recent years (Kamimura et al., 2009, 2013, 2014), and although hydrodynamic injection has been reported to cause a slight increase in ALT, it is transient and regresses to normal range within days (Suda et al., 2008; Yokoo et al., 2013).

Based on hydrodynamic injection technique, in this experiment, plasmid solution was injected at the concentration of 100  $\mu$ g/2 mL within 6 s, and once every 5 days. The results showed that hydrodynamic injection resulted in high expression of RFP and GFP only in the liver but not in other tissues such as heart, spleen, lung, and kidney. Western blot also showed good targeted interference effect in the liver tissues. Compared to single transfection group, co-transfection group could better reduce PHD1 and Keap1 protein levels, and were consistent with the results of our *in vitro* experiments (Liu et al., 2017).

The results of liver function tests and histopathology showed that the anti-fibrotic effect in the co-transfection group was significantly better than that in the single transfection group, while there were no significant difference between PHD1shNC group and CCl<sub>4</sub> model group. In addition, the degree of hepatocyte injury and fibrosis in mice from both preventive group and therapeutic group were lesser than the model group, but the preventive group showed significantly reduced liver fibrosis damage than the treatment group. Thus, this indicates that interfering with the expression of PHD1 and Keap1 in the hepatocytes has obvious preventive effect against the CCl<sub>4</sub>-induced hepatic fibrosis.

Damaged hepatocytes releases various cytokines and activates HSCs which is marked by expression of  $\alpha$ -SMA. Therefore, inhibiting HSCs activation could be the key to anti fibrotic process (Yu et al., 2012; Su et al., 2013). Our study found that  $\alpha$ -SMA expression in the co-transfection preventive group was relatively decreased than in the single transfection group and also

lower than in the therapeutic group. Therefore, it shows that the interference of PHD1 and Keap1 in hepatocytes *in vivo* could indirectly inhibit the activation of HSCs, and could synergistically effect each other.

PHD1shRNA and Keap1shRNA plasmids injections via hydrodynamic injection could offer a novel strategy in the prophylaxis of liver fibrosis, however, there are still some shortcomings such as difficulty in its operation and discrepancies in its effects among individuals. Therefore, further detailed study about this method is necessary. Since fibrosis could still be seen in the co-transfection preventive group, which suggests that co-transfection does not completely prevent fibrosis. As liver fibrosis is a complex process involving different types of cells, cytokines and signaling pathways, and it may also cross react with other genes while interfering with PHD1 and Keap1 genes. Therefore, it is imperative to

develop safe and combined multi-gene and multi-factor targeted therapy.

## AUTHOR CONTRIBUTIONS

JL, YL, and PC: conceived and designed the experiments. JL, ML, ZW, ZC, and XZ: performed the experiments. JL and YL: analyzed the data and wrote the paper. YL, WL, and PC: revised the paper.

## FUNDING

This work was financially supported by the National Natural Science Foundation of China (Grant No. 81370868).

## REFERENCES

- Abe, H., Kamimura, K., Kobayashi, Y., Ohtsuka, M., Miura, H., Ohashi, R., et al. (2016). Effective prevention of liver fibrosis by liver-targeted hydrodynamic gene delivery of matrix metalloproteinase-13 in a rat liver fibrosis model. *Mol. Ther. Nucleic Acids* 5:e276. doi: 10.1038/mtna.2015.49
- Begrache, K., Massart, J., Robin, M. A., Borgne-Sanchez, A., and Fromenty, B. (2011). Drug-induced toxicity on mitochondria and lipid metabolism: mechanistic diversity and deleterious consequences for the liver. *J. Hepatol.* 54, 773–794. doi: 10.1016/j.jhep.2010.11.006
- Chen, C., Zhang, J., Li, J., Huang, J., Yang, C., Huang, G., et al. (2004). Hydrodynamic-based *in vivo* transfection of retinoic X receptor- $\alpha$  gene can enhance vitamin A-induced attenuation of liver fibrosis in mice. *Liver Int.* 24, 679–686. doi: 10.1111/j.1478-3231.2004.0977.x
- Chevallier, M., Guerret, S., Chossegros, P., Gerard, F., and Grimaud, J. A. (1994). A histological semiquantitative scoring system for evaluation of hepatic fibrosis in needle liver biopsy specimens: comparison with morphometric studies. *Hepatology* 20, 349–355. doi: 10.1002/hep.1840200213
- Kamimura, K., Kanefuji, T., Yokoo, T., Abe, H., Suda, T., Kobayashi, Y., et al. (2014). Safety assessment of liver-targeted hydrodynamic gene delivery in dogs. *PLoS One* 9:e107203. doi: 10.1371/journal.pone.0107203
- Kamimura, K., Suda, T., Xu, W., Zhang, G., and Liu, D. (2009). Image-guided, lobe-specific hydrodynamic gene delivery to swine liver. *Mol. Ther.* 17, 491–499. doi: 10.1038/mt.2008.294
- Kamimura, K., Suda, T., Zhang, G., Aoyagi, Y., and Liu, D. (2013). Parameters affecting image-guided, hydrodynamic gene delivery to swine liver. *Mol. Ther. Nucleic Acids* 2:e128. doi: 10.1038/mtna.2013.52
- Kawakami, S., Ito, Y., Charoensit, P., Yamashita, F., and Hashida, M. (2006). Evaluation of proinflammatory cytokine production induced by linear and branched polyethylenimine/plasmid DNA complexes in mice. *J. Pharmacol. Exp. Ther.* 317, 1382–1390. doi: 10.1124/jpet.105.100669
- Khorsandi, S. E., Bachellier, P., Weber, J. C., Greget, M., Jaecq, D., Zacharoulis, D., et al. (2008). Minimally invasive and selective hydrodynamic gene therapy of liver segments in the pig and human. *Cancer Gene Ther.* 15, 225–230. doi: 10.1038/sj.cgt.7701119
- Liu, F., Song, Y., and Liu, D. (1999). Hydrodynamics-based transfection in animals by systemic administration of plasmid DNA. *Gene Ther.* 6, 1258–1266. doi: 10.1038/sj.gt.3300947
- Liu, J., Li, Y., Liu, L., Wang, Z., Shi, C., Cheng, Z., et al. (2017). Double knockdown of PHD1 and Keap1 attenuated hypoxia-induced injuries in hepatocytes. *Front. Physiol.* 8:291. doi: 10.3389/fphys.2017.00291
- Loisel, S., Le Gall, C., Doucet, L., Ferec, C., and Floch, V. (2001). Contribution of plasmid DNA to hepatotoxicity after systemic administration of lipoplexes. *Hum. Gene Ther.* 12, 685–696. doi: 10.1089/104303401300057405
- Maruyama, H., Higuchi, N., Nishikawa, Y., Kameda, S., Iino, N., Kazama, J. J., et al. (2002). High-level expression of naked DNA delivered to rat liver via tail vein injection. *J. Gene Med.* 4, 333–341. doi: 10.1002/jgm.281
- McCaffrey, A. P., Meuse, L., Pham, T. T., Conklin, D. S., Hannon, G. J., and Kay, M. A. (2002). RNA interference in adult mice. *Nature* 418, 38–39. doi: 10.1038/418038a
- Onori, P., Morini, S., Franchitto, A., Sferri, R., Alvaro, D., and Gaudio, E. (2000). Hepatic microvascular features in experimental cirrhosis: a structural and morphometrical study in CCl<sub>4</sub>-treated rats. *J. Hepatol.* 33, 555–563. doi: 10.1016/S0168-8278(00)80007-0
- Sato, A., Takagi, M., Shimamoto, A., Kawakami, S., and Hashida, M. (2007). Small interfering RNA delivery to the liver by intravenous administration of galactosylated cationic liposomes in mice. *Biomaterials* 28, 1434–1442. doi: 10.1016/j.biomaterials.2006.11.010
- Scheuer, P. J. (1991). Classification of chronic viral hepatitis: a need for reassessment. *J. Hepatol.* 13, 372–374. doi: 10.1016/0168-8278(91)90084-O
- Song, E., Lee, S. K., Wang, J., Ince, N., Ouyang, N., Min, J., et al. (2003). RNA interference targeting Fas protects mice from fulminant hepatitis. *Nat. Med.* 9, 347–351. doi: 10.1038/nm828
- Song, Y. K., Liu, F., Zhang, G., and Liu, D. (2002). Hydrodynamics-based transfection: simple and efficient method for introducing and expressing transgenes in animals by intravenous injection of DNA. *Methods Enzymol.* 346, 92–105. doi: 10.1016/S0076-6879(02)46050-8
- Su, L. J., Chang, C. C., Yang, C. H., Hsieh, S. J., Wu, Y. C., Lai, J. M., et al. (2013). *Graptopetalum paraguayense* ameliorates chemical-induced rat hepatic fibrosis *in vivo* and inactivates stellate cells and Kupffer cells *in vitro*. *PLoS One* 8:e53988. doi: 10.1371/journal.pone.0053988
- Suda, T., Suda, K., and Liu, D. (2008). Computer-assisted hydrodynamic gene delivery. *Mol. Ther.* 16, 1098–1104. doi: 10.1038/mt.2008.66
- Tousignant, J. D., Gates, A. L., Ingram, L. A., Johnson, C. L., Nietupski, J. B., Cheng, S. H., et al. (2000). Comprehensive analysis of the acute toxicities induced by systemic administration of cationic lipid: plasmid DNA complexes in mice. *Hum. Gene Ther.* 11, 2493–2513. doi: 10.1089/10430340050207984
- Wang, L., Cao, M., Wei, Q. L., Zhao, Z. H., Xiang, Q., Wang, H. J., et al. (2017). A new model mimicking persistent HBV e antigen-negative infection using covalently closed circular DNA in immunocompetent mice. *PLoS One* 12:e0175992. doi: 10.1371/journal.pone.0175992
- Yang, J. J., Tao, H., Huang, C., and Li, J. (2013). Nuclear erythroid 2-related factor 2: a novel potential therapeutic target for liver fibrosis. *Food Chem. Toxicol.* 59, 421–427. doi: 10.1016/j.fct.2013.06.018
- Yokoo, T., Kamimura, K., Suda, T., Kanefuji, T., Oda, M., Zhang, G., et al. (2013). Novel electric power-driven hydrodynamic injection system for gene delivery: safety and efficacy of human factor IX delivery in rats. *Gene Ther.* 20, 816–823. doi: 10.1038/gt.2013.2
- Yokoo, T., Kanefuji, T., Suda, T., Kamimura, K., Liu, D., and Terai, S. (2015). Site-specific impact of a regional hydrodynamic injection: computed tomography study during hydrodynamic injection targeting the swine liver. *Pharmaceutics* 7, 334–343. doi: 10.3390/pharmaceutics7030334



- Yu, F., Su, L., Ji, S., Zhang, S., Yu, P., Zheng, Y., et al. (2012). Inhibition of hepatic stellate cell activation and liver fibrosis by fat-specific protein 27. *Mol. Cell Biochem.* 369, 35–43. doi: 10.1007/s11010-012-1366-z
- Zender, L., Hutker, S., Mundt, B., Waltemathe, M., Klein, C., Trautwein, C., et al. (2005). NFkappaB-mediated upregulation of bcl-xl restrains TRAIL-mediated apoptosis in murine viral hepatitis. *Hepatology* 41, 280–288. doi: 10.1002/hep.20566
- Zhang, G., Budker, V., and Wolff, J. A. (1999). High levels of foreign gene expression in hepatocytes after tail vein injections of naked plasmid DNA. *Hum. Gene Ther.* 10, 1735–1737. doi: 10.1089/10430349950017734

**Conflict of Interest Statement:** The authors declare that the research was conducted in the absence of any commercial or financial relationships that could be construed as a potential conflict of interest.

Copyright © 2018 Liu, Li, Limbu, Li, Wang, Cheng, Zhang and Chen. This is an open-access article distributed under the terms of the Creative Commons Attribution License (CC BY). The use, distribution or reproduction in other forums is permitted, provided the original author(s) and the copyright owner are credited and that the original publication in this journal is cited, in accordance with accepted academic practice. No use, distribution or reproduction is permitted which does not comply with these terms.



# Casein Kinase 1 $\delta/\epsilon$ Inhibitor, PF670462 Attenuates the Fibrogenic Effects of Transforming Growth Factor- $\beta$ in Pulmonary Fibrosis

Christine R. Keenan<sup>1†</sup>, Shenna Y. Langenbach<sup>1†</sup>, Fernando Jativa<sup>1,2</sup>, Trudi Harris<sup>1</sup>, Meina Li<sup>1</sup>, Qianyu Chen<sup>1</sup>, Yuxiu Xia<sup>1</sup>, Bryan Gao<sup>1,3</sup>, Michael J. Schuliga<sup>1</sup>, Jade Jaffar<sup>4</sup>, Danica Prodanovic<sup>1</sup>, Yan Tu<sup>1</sup>, Asres Berhan<sup>1</sup>, Peter V. S. Lee<sup>2</sup>, Glen P. Westall<sup>4</sup> and Alastair G. Stewart<sup>1,3\*</sup>

## OPEN ACCESS

### Edited by:

Suowen Xu,  
University of Rochester, United States

### Reviewed by:

Christian Stockmann,  
Institut National de la Santé et de la  
Recherche Médicale (INSERM),  
France  
Erzsébet Bartolák-Suki,  
Boston University, United States  
Vassilis Aidinis,  
Alexander Fleming Biomedical  
Sciences Research Center, Greece

### \*Correspondence:

Alastair G. Stewart  
astew@unimelb.edu.au

<sup>†</sup>These authors have contributed  
equally to this work.

### Specialty section:

This article was submitted to  
Translational Pharmacology,  
a section of the journal  
Frontiers in Pharmacology

Received: 26 February 2018

Accepted: 18 June 2018

Published: 10 July 2018

### Citation:

Keenan CR, Langenbach SY, Jativa F,  
Harris T, Li M, Chen Q, Xia Y, Gao B,  
Schuliga MJ, Jaffar J, Prodanovic D,  
Tu Y, Berhan A, Lee PVS, Westall GP  
and Stewart AG (2018) Casein Kinase  
1 $\delta/\epsilon$  Inhibitor, PF670462 Attenuates  
the Fibrogenic Effects of Transforming  
Growth Factor- $\beta$  in Pulmonary  
Fibrosis. *Front. Pharmacol.* 9:738.  
doi: 10.3389/fphar.2018.00738

<sup>1</sup> Lung Health Research Centre, Department of Pharmacology and Therapeutics, University of Melbourne, Parkville, VIC, Australia, <sup>2</sup> Department of Biomedical Engineering, University of Melbourne, Parkville, VIC, Australia, <sup>3</sup> ARC Centre for Personalised Therapeutics Technologies, Parkville, VIC, Australia, <sup>4</sup> Department of Allergy, Immunology and Respiratory Medicine, The Alfred Hospital, Monash University, Melbourne, VIC, Australia

Transforming growth factor-beta (TGF- $\beta$ ) is a major mediator of fibrotic diseases, including idiopathic pulmonary fibrosis (IPF). However, therapeutic global inhibition of TGF- $\beta$  is limited by unwanted immunosuppression and mitral valve defects. We performed an extensive literature search to uncover a little-known connection between TGF- $\beta$  signaling and casein kinase (CK) activity. We have examined the abundance of CK1  $\delta$  and  $\epsilon$  (CK1 $\delta/\epsilon$ ) in lung tissue from IPF patients and non-diseased controls, and investigated whether inhibition of CK1 $\delta/\epsilon$  with PF670462 inhibits pulmonary fibrosis. CK1 $\delta/\epsilon$  levels in lung tissue from IPF patients and non-diseased controls were assessed by immunohistochemistry. Anti-fibrotic effects of the CK1 $\delta/\epsilon$  inhibitor PF670462 were assessed in pre-clinical models, including acute and chronic bleomycin mouse models and *in vitro* experiments on spheroids made from primary human lung fibroblast cells from IPF and control donors, and human A549 alveolar-like adenocarcinoma-derived epithelial cells. Increased expression of CK1 $\delta$  and  $\epsilon$  in IPF lungs compared to non-diseased controls was accompanied by increased levels of the product, phospho-period 2. *In vitro*, PF670462 prevented TGF- $\beta$ -induced epithelial-mesenchymal transition. The stiffness of IPF-derived spheroids was reduced by PF670462 and TGF- $\beta$ -induced fibrogenic gene expression was inhibited. The CK1 $\delta/\epsilon$  inhibitor PF670462 administered systemically or locally by inhalation prevented both acute and chronic bleomycin-induced pulmonary fibrosis in mice. PF670462 administered in a 'therapeutic' regimen (day 7 onward) prevented bleomycin-induced lung collagen accumulation. Elevated expression and activity of CK1  $\delta$  and  $\epsilon$  in IPF and anti-fibrogenic effects of the dual CK1 $\delta/\epsilon$  inhibitor, PF670462, support CK1 $\delta/\epsilon$  as novel therapeutic targets for IPF.

**Keywords: PF-670462, TGF- $\beta$ , lung, mechanobiology, collagen, epithelial mesenchymal transition, myofibroblast, anti-fibrotic**

## INTRODUCTION

Fibrosis, a common feature of most chronic diseases, contributes to up to 45% of deaths in the industrialized world (Friedman et al., 2013). Idiopathic pulmonary fibrosis (IPF) is an irreversible, progressive and usually fatal lung disease characterized by fibrosis of the lung parenchyma and progressive loss of lung function, with a median survival following diagnosis of 2.5–3.5 years (Ley et al., 2011). Drug targeting of IPF is hampered by a lack of understanding of its pathogenesis (Spagnolo et al., 2014). Current evidence suggests that dysregulated repair of injured alveolar epithelial cells leads to the subepithelial accumulation of activated myofibroblasts through the proliferation and migration of interstitial fibroblasts, epithelial-mesenchymal transition (EMT), and recruitment of circulating fibrocytes, leading to fibroplasia and excessive deposition of collagen within the lung interstitium and alveolar space (Fernandez and Eickelberg, 2012). The proliferation and migration of mesothelial cells and pericytes also contribute to the development of fibroblast foci that form a complex, three-dimensional reticulum from the pleural surface into the lung parenchyma. The quantitative contribution of these respective sources of activated fibroblasts to the overall fibroplasia is controversial (see reviews: Kage and Borok, 2012; Bartis and Thickett, 2014; Bartis et al., 2014; Wolters et al., 2014; Mora et al., 2017), but unresolved in this condition which remains idiopathic. Patients experience dyspnea and cough due to progressive fibrosis and stiffening of the lungs. The mechanical changes lead to increased lung elasticity, restrictive ventilation impairment, and ultimately to respiratory failure (Raghu et al., 2011).

Transforming growth factor-beta (TGF- $\beta$ ) makes a major contribution to fibrotic disease through, *inter alia*, induction of EMT and activation of myofibroblasts (Leask and Abraham, 2004). The 3 isoforms of TGF- $\beta$  (TGF- $\beta_{1-3}$ ) share similar biological activity, but differ in expression patterns. TGF- $\beta_1$  is the only isoform shown to be differentially expressed in epithelial cells from advanced pulmonary fibrosis (Khalil et al., 1996). Transient pulmonary overexpression of TGF- $\beta_1$  is sufficient to phenocopy progressive lung fibrosis in mice (Sime et al., 1997; Coker et al., 2001). TGF- $\beta_1$  and associated down-stream signaling pathways therefore present as prominent therapeutic targets for the treatment of pulmonary fibrosis.

Induction of fibrosis by TGF- $\beta_1$  is mediated by ALK5-dependent pathways (Biernacka et al., 2011). However, global inhibition of TGF- $\beta_1$  signaling through the inhibition of ALK5 receptor kinase activity is not a feasible therapeutic approach, as it results in autoimmune colitis (Shull et al., 1992; Kulkarni et al., 1993) and mitral valve damage (Anderton et al., 2011). In contrast, the modulators of TGF- $\beta_1$  expression and activity, nintedanib and pirfenidone, are sufficiently well-tolerated for their chronic use in IPF. Thus, partial abrogation of TGF- $\beta_1$  activity presents a clinically tractable approach to the treatment of fibrosis (LaChapelle et al., 2018). Our efforts to identify the mechanism of TGF- $\beta$ -induced glucocorticoid insensitivity (Salem et al., 2012; Keenan et al., 2014; Xia et al., 2017) lead to a comprehensive literature review that revealed a little-known connection between TGF- $\beta_1$  signaling and casein kinase (CK) activity (Hall et al., 1996). CK1 $\epsilon$  physically interacts with

Smad3 to mediate some TGF- $\beta$  signals, including upregulation of the fibrogen, plasminogen-activator inhibitor-1 (Waddell et al., 2004). Since CK1 $\epsilon$  shares much functional redundancy with CK1 $\delta$  due to 98% homology in the kinase domains (Fish et al., 1995), in the current study, we sought to investigate whether CK1 $\delta$  and/or  $\epsilon$  are dysregulated in the lungs of patients with IPF. Furthermore, we investigate whether PF670462, a dual inhibitor of casein kinase 1 $\delta/\epsilon$  activity with Ki values of 10 and 50 nM respectively (Badura et al., 2007; Wager et al., 2014), has anti-fibrotic effects in pre-clinical models of pulmonary fibrosis. This dual CK1 $\delta/\epsilon$  inhibitor has effects on the circadian clock by blocking the phosphorylation of the CLOCK (circadian locomotor output cycles kaput) repressor, Period (Badura et al., 2007; Wager et al., 2014). The Period protein (Per-2) acts to repress CLOCK genes, including ARNTL which encodes the transcription factor, BMal1 (Dierickx et al., 2018). The phosphorylation of Per-2 by CK1 $\delta$  inactivates its transrepressive activity. Conversely, inhibition of CK1 $\delta$  leads to an initial increase in Per-2 with more repression of ARNTL. We have therefore used ARNTL expression in the current study to establish an effective blockade of CK1 $\delta$ . Further interest in our study is provided by findings implicating CLOCK and related CLOCK-dependent genes in airway inflammation and fibrosis (Durrington et al., 2014). In order to avoid the confounding influence of central CLOCK disruption, we have established the anti-fibrogenic effectiveness of inhaled PF670462, demonstrating the feasibility of lung-selective therapy.

## MATERIALS AND METHODS

### Cell Culture

Primary human parenchymal fibroblast cells (pFbs) were cultured from parenchyma of lung resection specimens from non-transplanted lungs of donors without chronic respiratory disease and those of IPF patients diagnosed by multidisciplinary review (HREC #336/13; Alfred Hospital, Melbourne VIC, Australia), as previously described (Schuliga et al., 2009, 2017). Donor characteristics of specimens used for cell culture are shown in **Table 1**. pFbs were passaged in Dulbecco's Modified Eagle's Media (DMEM) containing 10% (v/v) heat-inactivated fetal calf serum (FCS), 15 mM HEPES, 0.2% (v/v) sodium bicarbonate, 2 mM L-glutamine, 1% (v/v) non-essential amino acids, 1% (v/v) sodium pyruvate, 2.5  $\mu$ g/mL amphotericin, 5 IU/mL penicillin and 50  $\mu$ g/mL streptomycin. Primary fibroblast 3D spheroids were generated by seeding cells into 96 well round bottom plates coated with 0.5% poly(2-hydroxyethyl methacrylate) (poly-HEMA) to minimize cellular adhesion to plastic, and by incubating cells to allow aggregation into cellular spheroids over a period of 24–48 h.

A549 alveolar epithelial-like adenocarcinoma-derived cells (ATCC, Manassas, VA, United States) were cultured in DMEM containing 5% (v/v) FCS, 15 mM HEPES, 0.2% (v/v) sodium bicarbonate, 2 mM L-glutamine, 1% (v/v) non-essential amino acids, 1% (v/v) sodium pyruvate, 5 IU/mL penicillin and 50  $\mu$ g/mL streptomycin as previously described (Salem et al., 2012; Keenan et al., 2014).

**TABLE 1** | Characteristics of lung tissue obtained from IPF and non-IPF donors for CK1 $\delta/\epsilon$  immunohistochemistry.

Age	Sex	FEV1 (% pred)	FVC (% pred)	TLCO (% pred)	Smoking history (pack yrs)
<b>Control patients</b>					
47.4 $\pm$ 16.7 (mean $\pm$ SD)	2M/2F/2 unknown	unknown	unknown	unknown	4Ex/1 current/1 unknown
<b>IPF patients (diagnosed by interdisciplinary review)</b>					
60.5 $\pm$ 4.6 (mean $\pm$ SD)	4M/2F	62.3 $\pm$ 13.6 (mean $\pm$ SD)	53.3 $\pm$ 16.4 (mean $\pm$ SD)	14.8 $\pm$ 1.6 (mean $\pm$ SD)	4 current/2 never

Prior to experimentation, pFb and A549 cells were incubated in serum-free DMEM containing 0.25% bovine serum albumin (BSA) and insulin-transferrin-selenium-containing supplement (Monomed A; CSL, Parkville, Melbourne, VIC, Australia). Where indicated, cells were treated with PF670462 (0.3 – 10  $\mu$ M) (Abcam, Australia) prior to 100 pM TGF- $\beta_1$  (R&D Systems, Minneapolis, MN, United States) or 300 pM bFGF (Promega, Madison, WI, United States). Pirfenidone, PF670462 (Abcam, Australia), and nintedanib (Focus Bioscience, Australia) were made as 10 mM – 100 mM stock solutions in 100% DMSO and diluted to the required concentration in medium or saline containing 0.1% DMSO (final concentration). For intraperitoneal administration of PF670462 it was initially dissolved in 100% DMSO and prepared for injection by 1:10 dilution in Arachis oil (Sigma). For inhalational studies PF670462 was dissolved in the indicated concentrations in saline for injection.

## Cell Stiffness Measurement

The micropipette aspiration technique was used to measure the Young's tensile modulus ( $E$ ) of 3D spheroids, as previously described (Guevorkian et al., 2010, #39; Schuliga et al., 2013, #38). The stiffness of individual fibroblast cells was also assessed following dissociation from plastic culture vessels using trypsin. The micropipette aspiration was performed in a temperature control chamber (Warner Instrument CL-100) to maintain the cells at 37°C. Briefly, the tips of the custom-made glass micropipettes (8  $\mu$ m diameter), were pre-coated with silicone using Sigmacote (Sigma, United Kingdom) to prevent cell adhesion. Suction pressure was applied to the cell/cell aggregate by controlling the water level in a water reservoir. The suction pressure was applied in 1 cm H<sub>2</sub>O (0.098 kPa) increments and kept stable for 60 s at each increment. The maximum suction pressure was 6 cm H<sub>2</sub>O (0.588 kPa). The aspirated length in the micropipette was measured from a brightfield image taken by a Leica DMI6000B microscope at the end of each pressure increment. The apparent Young's modulus of the cell (or cell stiffness) was calculated using a model that assumes the cell is a homogeneous, isotropic, elastic and incompressible half-space medium (Theret et al., 1988, #40). Young's Modulus  $E$  was calculated according to Equation 1 where  $D_p$  is the inner

diameter of the micropipette and  $L$  the aspiration length, as shown in **Figure 3**.  $\Delta P$  represents the aspiration pressure and  $\phi$  is the wall function with a typical value of 2.1, as described previously (Hochmuth, 2000).

$$E = \frac{3D_p\Delta P}{4\pi L\phi} \quad (1)$$

## Immunohistochemistry

CK1 $\delta$  and  $\epsilon$  expression was assessed by immunohistochemistry (IHC) in lung tissue specimens from IPF patients and non-diseased controls. Sections were obtained from end stage IPF patients undergoing lung transplantation and from controls without IPF. Donor characteristics for the IHC studies are provided in **Table 2**.

Paraffin-embedded IPF and non IPF lung tissue was obtained from Alfred Health from the Alfred Tissue Biobank for Interstitial Lung Disease (HREC#336/13, Alfred Hospital, Melbourne, VIC, Australia). Sections of parenchymal lung tissue were immunostained for one of CK1 $\delta$  (rabbit, 1:400, Abcam, Cambridge, United Kingdom), CK1 $\epsilon$  (rabbit, 1:25, Proteintech Group, Chicago, IL, United States) or positive control pan-actin (rabbit, 1:400, Cell Signaling, Danvers, MA, United States). Immunohistochemistry was completed by using the Vectastain ABC kit (Biotinylated goat anti rabbit, 1:200, streptavidin HRP layer 1:100, Vectalabs, United States) and 3, 3'-diaminobenzidine development for visualization (Dako chromagen substrate kit, United States). Sections were counterstained with haematoxylin (Grale Scientific, Australia). On serial sections, a Masson's Trichrome stain was also performed to provide indicative levels of fibrosis in IPF and non-IPF sections the reagents required include Bouin's fixative solution Scott's tap water, Mayer's Haematoxylin, Trajan Scientific; Celestine Blue, Biebrich Scarlet/Acid Fuchsin; Phosphotungstic acid, Sigma; Aniline blue solution (aust biostain)]. Selected sections were also stained with anti- $\alpha$ -smooth muscle actin (mouse monoclonal 1:400, Dako Cytomation). The CK1 $\delta$  and CK1 $\epsilon$  staining was qualitatively scored from 0 to 5 by an experienced operator and confirmed by an additional operator (each blinded to group allocations),

**TABLE 2** | Donor characteristics for human primary fibroblast cultures.

Age	Sex	FEV1 (% pred)	FVC (% pred)	TLCO (% pred)	Smoking history (pack yrs)
<b>Control patients</b>					
50.2 $\pm$ 14.6 (mean $\pm$ SD)	7M/5F/1 unknown	unknown	unknown	unknown	7 unknown; 5 ex; 1 current
<b>IPF patients (diagnosed by interdisciplinary review)</b>					
58.0 $\pm$ 8.2 (mean $\pm$ SD)	7M/1F	53.8 $\pm$ 16.2 (mean $\pm$ SD)	48.7 $\pm$ 18.6 (mean $\pm$ SD)	22.0 $\pm$ 9.4 (mean $\pm$ SD)	2 Never/4 ex/2 unknown



with 0 denoting no staining and 5 indicating heavy uniform and extensive staining.

## Immunofluorescence

A549 cells for immunofluorescence staining were seeded in ibiTreat 8-chamber slides (Ibidi) and left to adhere overnight. Cells were then serum-starved for 16 h prior to pre-incubation with PF670462 (0.3 – 10  $\mu$ M) for 30 min then TGF- $\beta$  (100 pM) for 48 h. Cells were fixed in 10% neutral buffered formalin (Grate Scientific) for 15 min and non-specific binding sites were blocked by incubation with 5% normal goat serum/0.3% Triton X-100 in PBS for 1 h. E-Cadherin expression was detected using a rabbit monoclonal antibody (1:200, Clone 24E10; Cat#3195, Cell Signaling) followed by an AlexaFluor-488 conjugated anti-Rabbit F(ab')<sub>2</sub> fragment secondary (1:500, Cat#4412, Cell Signaling). Specific binding was confirmed using an isotype control antibody (protein content matched to respective primary antibodies, Clone DA1E rabbit IgG; Cat#3900, Cell Signaling). Cell nuclei were then stained with DAPI. Cells were imaged using a Leica SP5 confocal microscope (Biological Optical Microscopy Platform, University of Melbourne). Cell morphology and immunofluorescent staining was quantified using the Operetta High Content Imaging System (Biological Optical Microscopy Platform, University of Melbourne).

## Bleomycin-Model of Pulmonary Fibrosis

All animal experiments were carried out in accordance with ethical guidelines from the University of Melbourne Animal Ethics Committee (AEEC#1513736.1). Six- to eight-week old 20–25 g C57Bl/6 mice (ARC, Perth, WA, Australia) received 35  $\mu$ L of saline or bleomycin (105 mU per mouse) on day 0 by intranasal administration, as previously described (Langenbach et al., 2007). Acute and chronic bleomycin mouse models were used to assess the effect of PF670462 on pulmonary fibrosis *in vivo*. PF670462 was administered systemically by intraperitoneal injection or locally to the lungs by inhalation of an aerosol generated using an oxygen concentrator connected to a Hudson nebuliser operating at 5 L/min for 15 min. Mice that did not receive PF670462 treatment received vehicle (intraperitoneal administration, 10% DMSO, 90% peanut oil; inhalational administration, normal saline). In the 3-day model, PF670462 administration commenced on day -1 (day prior to bleomycin) and continued to day 3. In the 14-day model PF670462 was administered from day 3 to day 14. In the 21-day model considered to reflect the peak of fibrosis (Langenbach et al., 2007), PF670462 administration commenced on day 8 and continued to day 21. Mice were allowed food and water *ad libitum* for the duration of all studies. At the end of each study, bronchoalveolar lavage (BAL) was performed from which viable cells were enumerated (cells that show no nuclear staining after incubation on ice for 30 s in acridine orange/ethidium bromide/saline resuspension of the cell pellet sedimented by centrifugation at 1000  $\times$  g, 5 min 4°C) with the aid of an epifluorescence microscope (Zeiss Axioshop, Germany). Acellular protein content in the supernatant of the sedimented BAL cell pellet was determined by the Bradford protein assay using BSA as a standard, as previously described

(Langenbach et al., 2007), lungs were dissected and snap frozen. Hydroxyproline content, phosphorylated p38 MAP kinase levels and gene expression were determined from pulverized frozen lung tissue, as previously described (Langenbach et al., 2007; Salem et al., 2012).

## Lung Dry Mass and Hydroxyproline Determination

Frozen mouse lung tissue was pulverized in a mortar and pestle chilled by liquid N<sub>2</sub>. The lung fragments were weighed and then lyophilized and re-weighed to determine dry mass as previously described (Langenbach et al., 2007). Briefly, hydroxyproline content was then determined from 8 mg of lyophilized mouse lung tissue by hydrolysis in 6M HCL for 16 h at 130°C. Ten microliters of the hydrolysate was added to a well of a 96 well plate containing 10  $\mu$ L of citrate buffer, to which 100  $\mu$ L of the chromagen chloramine T (Sigma-Aldrich, United States) was added for 20 min at ambient temperature prior to the addition of 100  $\mu$ M 4-(dimethylamino)benzaldehyde (DMAB, Fluka, Switzerland). The absorbance was measured at 560 nm in a multiscan plate reader after being allowed to cool for 10 min following 20 min incubation at 65°C, with further information as previously detailed (Langenbach et al., 2007).

## Protein Analysis and Immunoassay

Total protein content in acellular BAL fluid, generated by centrifugation at 1000  $\times$  g, 5 min 4°C, was assessed using the Bradford protein assay method (BioRad, Australia) with BSA as a standard. Levels of phosphorylated p38 MAP kinase were determined in lyophilized mouse lung tissue by western blotting, as previously described (Salem et al., 2012). A limited number of BAL samples from the 3-day systemic treatment study were submitted to immunoassay for IL-6, which was carried out according to the Manufacturer's instructions (murine OptiEIA kit, Becton Dickinson, Australia).

## Analysis of Gene Expression

Total RNA was extracted from pulverized mouse lung or cultured cells using illustra RNAspin Mini RNA Isolation Kit (GE Healthcare). RNA extracts were reverse transcribed into cDNA using High-Capacity RNA-to-cDNA Kit (Applied Biosystems). Real-time PCR was then performed using a QuantStudio 6 Flex Real-Time PCR System using iTaq Universal SYBR green supermix and the following thermal protocol: 50°C (2 min), 95°C (10 min), then 40 cycles of 95°C (15 s), 60°C (1 min). The threshold cycle (CT) values determined for target genes were normalized against those obtained for 18S ribosomal RNA (18S rRNA), which was included as internal control. The generation of specific PCR products was confirmed by dissociation curve analysis. Primer sequences used are shown in Table 3.

## Statistical Analysis

Data are presented as mean  $\pm$  SEM or SD (Tables 1, 2), as indicated. Statistical comparisons among multiple groups were made by 1-way ANOVA with Dunnett's *post hoc* test or two-way ANOVA with Bonferroni *post hoc* test. In cases in which data



**TABLE 3 |** Primer sequences for RT-qPCR.

Gene	Forward primer	Reverse primer
<b>Human</b>		
18S rRNA	CGC CGC TAG AGG TGA AAT TC	TTG GCA AAT GCT TTC GCT C
COL1A	GTG CTA AAG GTG CCA ATG GT	ACC AGG TTC ACC GCT GTT AC
CTGF	TGT GTG ACG AGC CCA AGG A	TCT GGG CCA AAC GTG TCT TC
E-Cad	ACC ACA AAT CCA GTG AAC AAC G	CAA GCC CTT TGC TGT TTT CAA
N-Cad	CGA GAA AAA GTG CAA CAG TAT ACG TTA A	GCC TTC CAT GTC TGT AGC TTG A
PAI-1	TCAGGCTGACTTCACGAGTCTTT	CTGCGCGACGTGGAGAG
VIM	AAT CCA AGT TTG CTG ACC TCT CTG	GGG CGT CAT TGT TCC GG
<b>Mouse</b>		
18s rRNA	TCC GGC GAG GGA GCC TG	CCT GCT GCC TTC CTT GGA T
ARG2	CAT AAT ACA GGG TTG CTG TC	CTT CTC TTG TCT GAC CAA AAC
COL1A	ACG GCT GCA CGA GTC ACA C	GGC AGG CGG GAG GTC TT
COL3	GTT CTA GAG GAT GGC TGT ACT AAA CAC A	TTG CCT TGC GTG TTT GAT ATT C
CTGF	GTC AAG CTG CCT GGG AAA TG	CTT GGG CTC GTC ACA CAC C
IFN- $\gamma$ 2	AAG GAT GCC ATC GAG AAG	GTC ATG TTC TCC CAG ACC
IL-6	CTG CAA GAG ACT TCC ATC CAG TT	TTG TCA CCA GCA TCA GTC CC
MMP-2	ATC ATT GGT TAC ACA CCT GAC CTG	GCA AAA GCA TCA TCC ACG G
PAI-1	AGC AAC AAG TTC AAC TAC AC	CTT CCA TTG TCT GAT GAG TTC
TIMP-1	GAT ATG CCC ACA AGT CCC AGA	GGC CCG TGA TGA GAA ACT CTT
TIMP-2	GAC GTA GTG ATC AGA GCC AAA GC	CCC GGA ATC CAC CTC CTT

were non-normally distributed, a Mann–Whitney  $U$  test was applied (Figure 1). A  $P$ -value of less than 0.05 was considered to be statistically significant. All statistical analyses were performed using GraphPad Prism version 5 or later.

## RESULTS

### CK1 $\delta$ and $\epsilon$ Are Highly Upregulated in the Lungs of IPF Patients

The distribution and level of immunoreactive CK1 $\delta$  and CK1 $\epsilon$  are altered in IPF (Figure 1), with each showing a striking increase in level at the cellular level (i.e., independent of the increase in tissue area per field of view). Expression is evident in multiple cell types, based on location and cell shape. Moreover, one of the biologically important substrates for CK1 $\delta$  and CK1 $\epsilon$ , Period-2 showed increased levels of expression and phosphorylation in IPF parenchymal sections, consistent with inferred increased net activity of the CK1 $\delta/\epsilon$  isoforms (Figure 1).

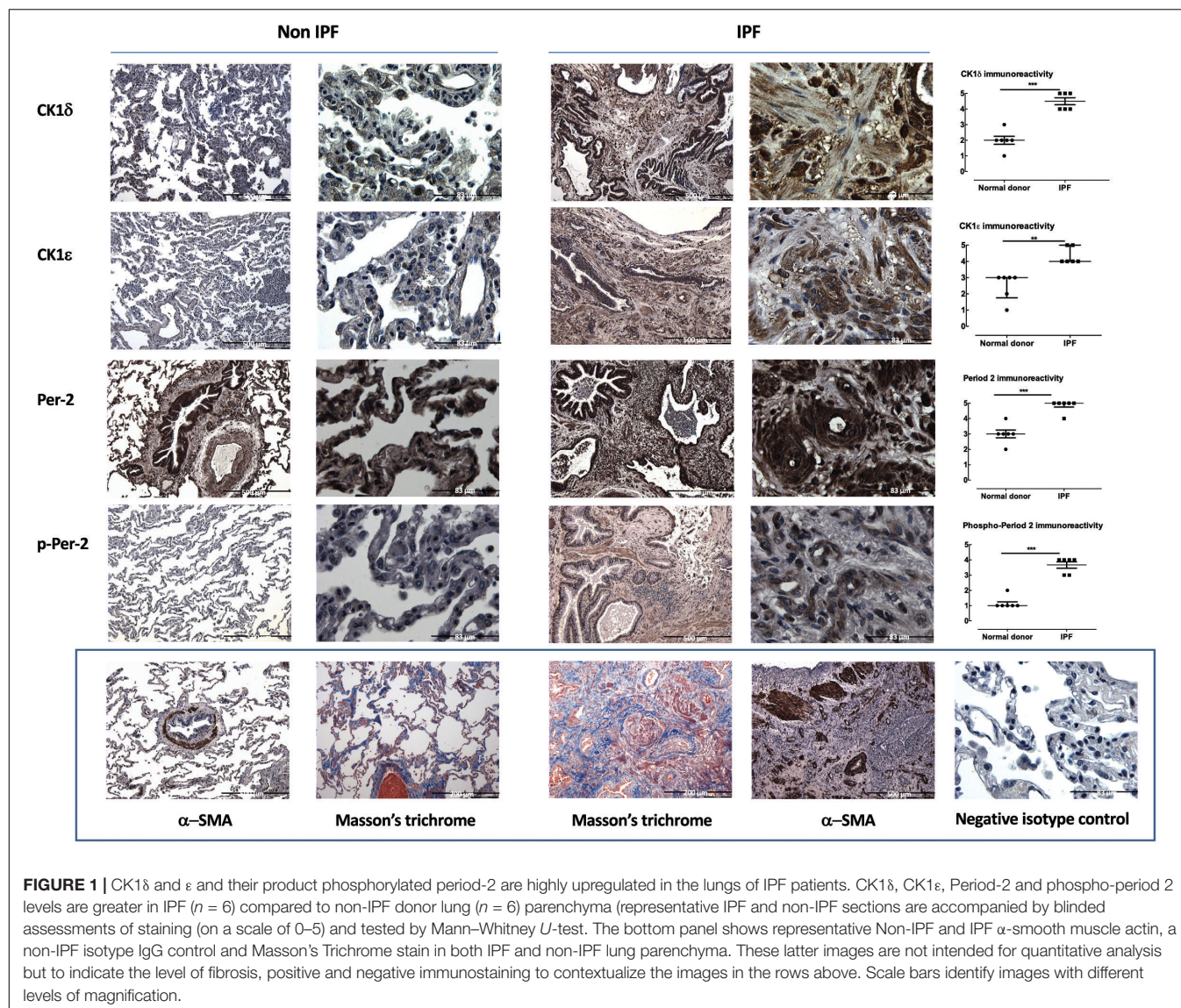
As TGF- $\beta$  induces fibrosis through both the activation of fibroblasts and the induction of EMT (Leask and Abraham, 2004), we next sought to establish whether PF670462 modulated TGF- $\beta$ -activated fibrogenic pathways.

### PF670462 Softens Primary Human Fibroblast Spheroids

A three-dimensional *in vitro* model to resemble fibroblast foci seen in fibrotic lesions was developed with cell spheroids formed from primary cells from IPF donors and non-diseased controls, the morphology of which is shown in Figure 2. Cells aggregated into spheroids and were incubated over 48 h, with most remodeling occurring during the first 24 h and minimal

change in spheroid volume (measured by area of a cross-sectional plane) in the final 24 h. There was no difference in the size of spheroids from IPF or non-diseased control donors during or at the conclusion of the spheroid remodeling (Figure 2). Both non-diseased and IPF derived spheroids showed CK1 $\delta$  immunoreactivity compared to the negative IgG isotype control. For contrast,  $\alpha$ -smooth muscle actin was also used as a positive control, and indicated the presence of myofibroblasts within the spheroids (Figure 2).

Fibroblasts from normal and IPF patients are known to be responsive to the stiffness of their mechanical microenvironment, with increases in contractile and proliferative phenotype observed when cells are in contact with stiffer extracellular matrix (Marinkovic et al., 2013). Stiffness can be measured by aspiration of cells and spheroids into the barrel of a micropipette using a pressure gradient. The lesser the displacement into the barrel for a given amount of pressure the “stiffer” the material. Importantly, whilst we observed no difference in mechanical stiffness in individual cells derived from IPF or non-IPF donors, cell spheroids generated from IPF fibroblasts showed significantly higher stiffness compared to non-IPF donors (Figure 3), suggesting that the stiffening is an emergent property that may enhance the pro-fibrotic phenotype of these cells when culture = d as spheroids. Exposure to the fibrogen TGF- $\beta$  for 48 h increased the stiffness of non-IPF spheroids ( $P < 0.05$ ,  $n = 5$ ), but not to the level of stiffness of IPF spheroids (Figure 3). Pretreatment with PF670462 (3  $\mu$ M) for 30 min prior to TGF- $\beta$  exposure reduced the level of stiffness in IPF spheroids ( $P < 0.05$ ,  $n = 6$ ) (Figure 3). Thus, PF670462 softens IPF fibroblast spheroids and thereby potentially interferes with the positive-feedback cycle of stiffness-induced stiffening.



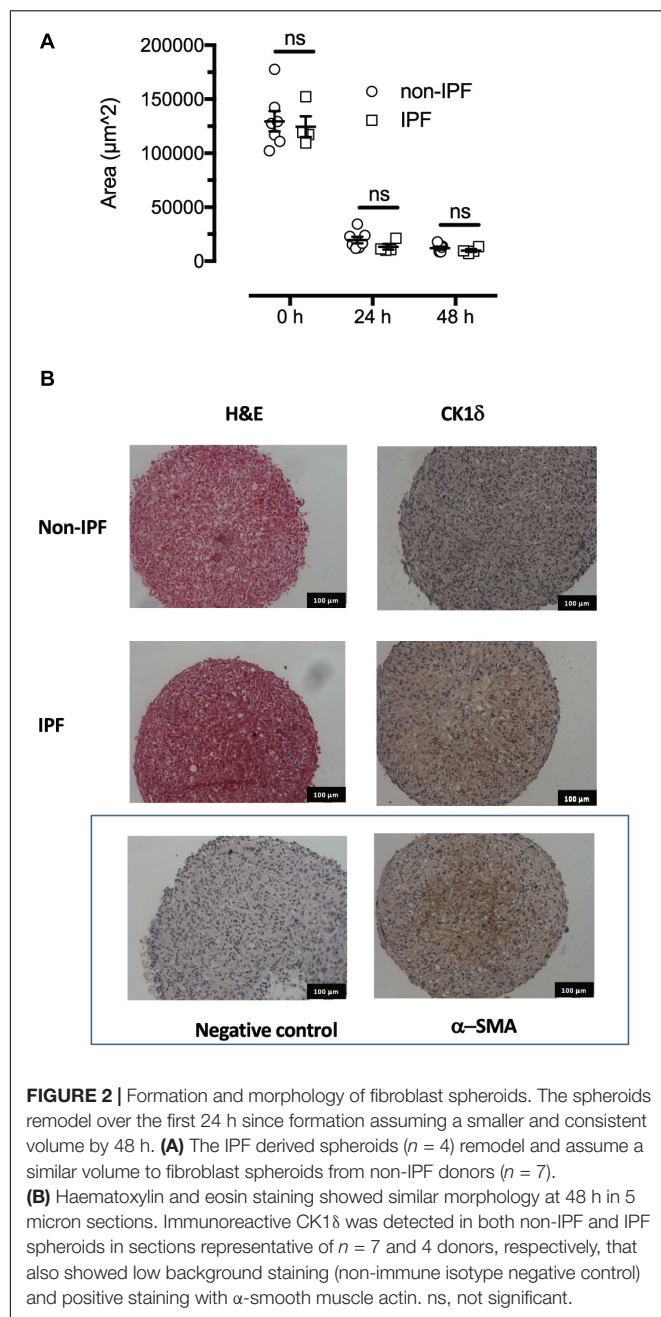
## PF670462 Inhibits Fibrogenic Gene Expression in 2D and 3D Culture Systems

We used fibroblast monolayers and spheroids to examine the effect of PF670462 on TGF- $\beta_1$  fibrogenic gene activation. Two IPF cultures and one non-diseased control culture that did not respond to TGF- $\beta_1$  stimulation were excluded from further analysis in this and other fibroblast studies. IPF fibroblast cultures showed enhanced TGF- $\beta$  induction of the genes *COL1A* and *CTGF* compared to non-IPF derived fibroblasts, whereas fibroblast spheroids showed decreased gene induction compared with fibroblast monolayers regardless of disease status of donors (**Figure 3A**). Pretreatment with PF670462 inhibited the TGF- $\beta$ -induced increase in *COL1A* and *CTGF* mRNA in fibroblast monolayers and spheroids from both IPF and non-diseased control donors (**Figure 3C**). TGF- $\beta_1$  itself showed no effect on fibroblast cell proliferation (data not shown). Basic fibroblast

growth factor (bFGF)-induced mitogenesis was only marginally reduced by PF670462 at 10  $\mu$ M (**Figure 3D**), suggesting that inhibition of fibroblast proliferation is not a major anti-fibrotic mechanism for PF670462.

We also sought to examine the effects of PF670462 in comparison with two clinically used anti-fibrotic agents indicated for IPE, nintedanib and pirfenidone. Non-IPF fibroblasts were incubated with nintedanib (0.3  $\mu$ M), a concentration chosen for its proximity to the  $C_{max}$  of  $\sim 70$  nM when taken orally at 150 mg twice daily (Ogura et al., 2015) and to avoid overt cytotoxicity noted at 3  $\mu$ M. Pirfenidone was used at a concentration of 100  $\mu$ M also chosen for its proximity to the reported  $C_{max}$  of  $\sim 70$   $\mu$ M when 801 mg is taken orally in the fasted state as a single tablet (Pan et al., 2017). The concentration of PF670462 was chosen based on our previous concentration-response analyses, since  $C_{max}$  is not known, and indeed likely to be irrelevant for the efficacy of an inhalational agent. Pirfenidone (100  $\mu$ M) caused a





significant and pronounced reduction in TGF- $\beta$ -induced Col1A mRNA levels without affecting either CTGF or  $\alpha$ SMA expression. Nintedanib significantly reduced Col1 A and  $\alpha$ SMA, but not CTGF. In contrast, 1  $\mu$ M PF670462 reduced expression of each of these fibrogenic genes (Table 4).

### PF670462 Inhibits Epithelial-Mesenchymal Transition of Alveolar Epithelial Cells

We investigated whether PF670462 modulates TGF- $\beta$  signaling of EMT in A549 cells, measuring regulation of the

EMT-associated genes *N*-Cadherin (*N*-Cad), Vimentin (*Vim*) and *E*-Cadherin (*E*-Cad) after 24 h of TGF- $\beta$  exposure, with no change being detected at the 4 h timepoint (Figure 4A). These delayed gene expression changes were inhibited by PF670462 in a concentration-dependent manner, reaching a maximum effect at 10  $\mu$ M (Figure 4A). To confirm a functional effect of PF670462 in preventing TGF- $\beta$  induced EMT, *E*-cadherin was immunostained. PF670462 concentration-dependently inhibited TGF- $\beta$ -induced loss of *E*-cadherin expression, reaching a maximum effect at 3–10  $\mu$ M PF670462 (Figures 4B,C).

We also undertook comparative assessment of the activity of nintedanib, pirfenidone and PF670462 on markers of EMT in A549 cells (Figure 5). PF670462 concentration-dependently and fully prevented all of the TGF- $\beta$  effects. Pirfenidone was without any significant effects up to 100  $\mu$ M, whereas nintedanib showed activity on *N*-Cad, *E*-Cad and PAI-1 at the highest concentration of 1  $\mu$ M.

### PF670462 Attenuates Bleomycin-Induced Fibrosis in Acute and Chronic Mouse Models

Since CK1 $\delta$  and  $\epsilon$  have been implicated in TGF- $\beta$  signaling and showed greatly increased levels and activity in IPF lungs, we examined the effect of the dual CK1 $\delta/\epsilon$  inhibitor PF670462 in preventing and therapeutically treating bleomycin-induced pulmonary fibrosis in mice. We first assessed early fibrogenic responses in mice, 3 days after transnasal pulmonary bleomycin exposure. The increase in p38 MAPK phosphorylation was prevented by systemic PF670462 (30 mg/kg/day i.p. from day  $-1$  to 3) (Figure 6A), a dosing regimen based on preclinical work showing that this daily i.p. dose was sufficient to cause a phase shift in the central CLOCK (Sprouse et al., 2010). This latter finding has been confirmed in a number of studies (Badura et al., 2007; Walton et al., 2009; Meng et al., 2010; Kennaway et al., 2015) and applied in others, to examine the impact of CK1 $\delta$  inhibitors on drug seeking behavior (Bryant et al., 2009; Perreau-Lenz et al., 2012). Although PF670462 is known to be subject to rapid hepatic metabolism and has a quoted T1/2 of less than 30 min (Wager et al., 2014), it is evident from the cited findings that peripheral blood levels are sufficient to achieve inhibition of the central CLOCK, and are therefore sufficient to block the target in peripheral tissues, as further indicated by control of hepatic CLOCK genes (Kennaway et al., 2015). Fibrogenic gene induction was reduced (IL-6, TIMP-1) or prevented (COL-1A, COL-3) by PF670462 treatment and BAL levels of immunoreactive IL-6 (Figure 6B). We also demonstrate the suppression of ARNTL expression, which itself is partially suppressed by bleomycin.

To evaluate the anti-fibrotic potential of PF670462, treatment was commenced at day 3 (peak of inflammation) continuing until day 13 before *post mortem* at day 14. Lung collagen was assessed by measurement of the collagen-specific modified amino acid, hydroxyproline. PF670462 (30 mg/kg/day, i.p.) attenuated bleomycin-induced accumulation of hydroxyproline and the number of infiltrating immune cells measured in the BAL fluid (Figure 6C).

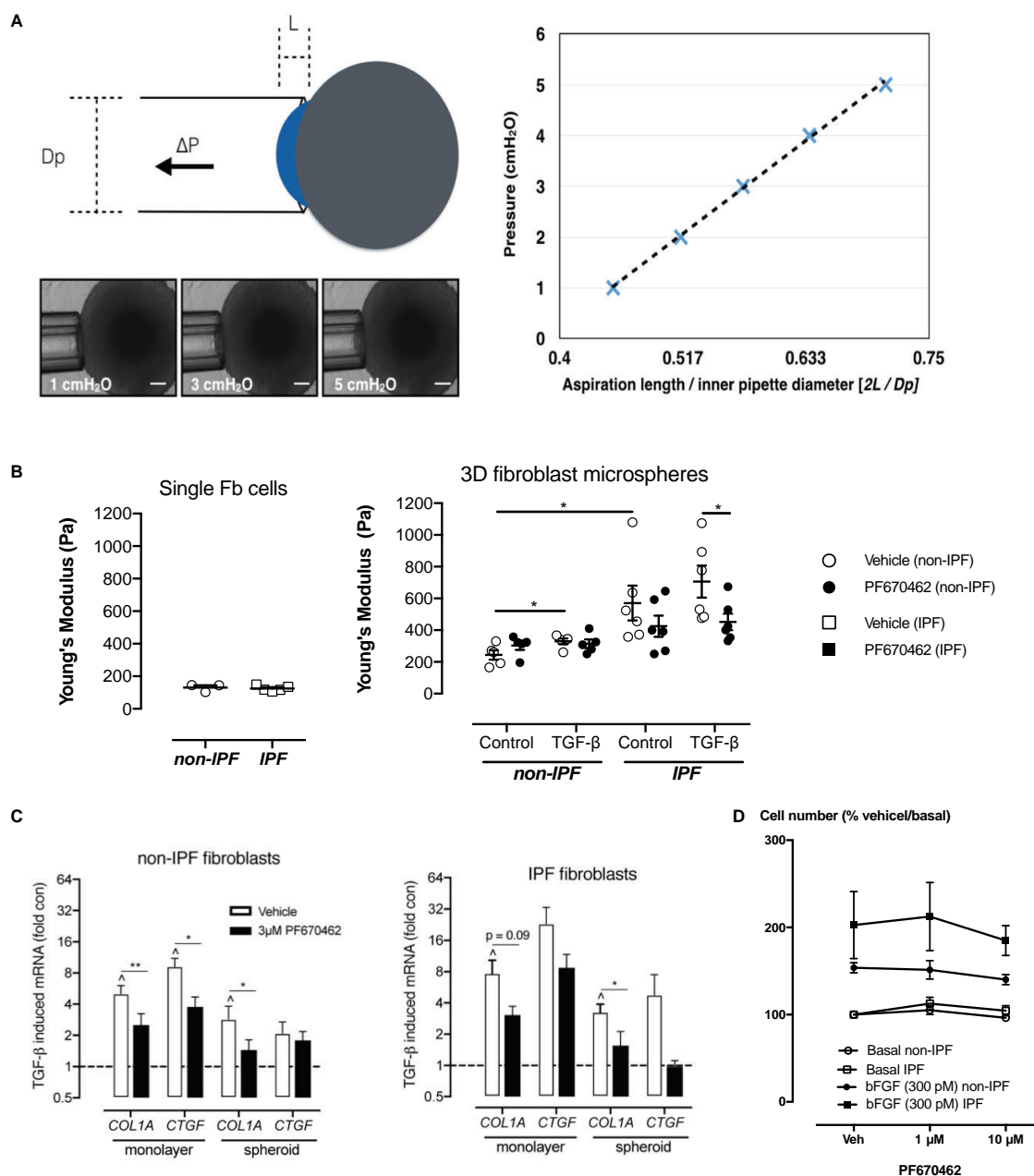


**FIGURE 3 | (A)** Measurement of Young's modulus. With increasing pressure ( $P$ ) the spheroid travels a distance ( $L$ ) through the micropipette barrel of inner diameter ( $D_p$ ). A representative spheroid is shown with aspiration at 3 different pressures. The normalized distance ( $2L/D_p$ ) is linearly related to the applied pressure and the slope of the linear regression defines the Young's modulus. Scale bars indicate 100  $\mu$ m. **(B)** Spheroid stiffness was measured by micropipette aspiration and quantified to measure the Young's Modulus of stiffness in single cells (non-IPF,  $n = 3$ ; IPF,  $n = 5$ ) and in microspheres (non-IPF,  $n = 6$ ; IPF,  $n = 6$ ). **(C)** The effects of PF670462 on TGF- $\beta$  (100 pM)-induced COL1A and CTGF mRNA expression from pFb monolayers and microspheres from IPF and non-IPF pFbs are presented as the means and SEM of (for monolayer expression: non-IPF,  $n = 3$ ; IPF,  $n = 5$ ) and (for spheroid expression: non-IPF,  $n = 9$ ; IPF,  $n = 6$ ). **(D)** Cell number expressed as a percentage of the basal cell number in the presence and absence of vehicle (Veh) or PF670462 in cells from non-IPF or IPF donors in the presence and absence of the mitogen, bFGF ( $n = 6$ ). \* $P < 0.05$ , \*\* $P < 0.01$  from two-way ANOVA with Bonferroni *post hoc* test or 1-way ANOVA with Dunnett's *post hoc* test.  $^{\wedge}P < 0.05$  from one-sample *t*-test compared to 1.0.

To further restrict the potential for a PF670462 treatment effect on inflammation, we delayed treatment until day 7 post-bleomycin, extending the period day 21 to allow sufficient time

for an anti-fibrotic effect of this delayed treatment to be detected. Using this 'therapeutic' treatment regimen, bleomycin-induced increases in lung collagen (hydroxyproline), oedema (lung wet

**TABLE 4 |** Modulation of TGF- $\beta$  induced gene expression in non-IPF lung fibroblasts.

Gene	mRNA expression (% TGF- $\beta$ level)		
	Nintedanib 0.3 $\mu$ M	Pirfenidone 30 $\mu$ M	PF670462 1 $\mu$ M
CTGF	70.2 $\pm$ 20.5 (10) ns	75.6 $\pm$ 20.0 (11) ns	56.5 $\pm$ 14.7 (7)*
Col1A	51.9 $\pm$ 15.8 (8)*	21.1 $\pm$ 5.0 (9)*	33.9 $\pm$ 12.5 (5)*
$\alpha$ SMA	64.4 $\pm$ 15.0 (10)*	72.0 $\pm$ 18.2 (11) ns	71.2 $\pm$ 9.9 (7)*

Mean and SEM of (n) observations. \* $P < 0.05$ , paired Students *t*-test vs. level of gene expression detected in vehicle incubated TGF- $\beta$  exposed cultures (100%).

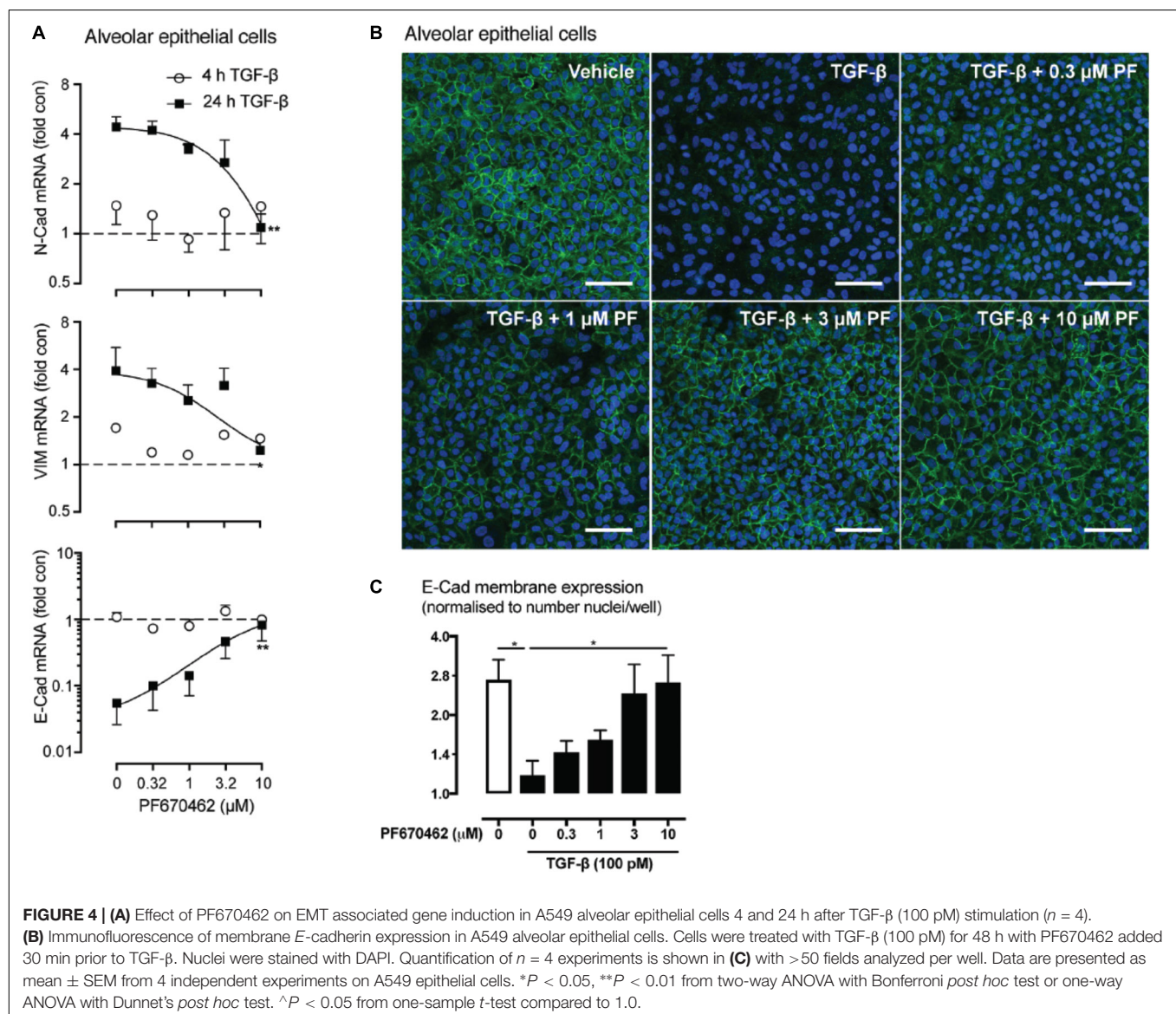
weight), BAL fluid infiltrating cells and protein were reduced by PF670462 treatment (**Figure 6D**).

In a separate study in female mice, aerosolised PF670462 (0.3–3.0 mg/ml, 15 min/once daily) corresponding to estimated deposited doses of  $\sim 1$ –10  $\mu$ g/day (Oldham and Robinson, 2007)

from day 8–20, also reduced hydroxyproline content, BALF cell influx, and fibrogenic gene expression at day 21 (**Figure 7**), albeit that the effects of PF670462 did not show dose-related effects on these measures over this range of exposures.

## DISCUSSION

In this study, we have demonstrated striking up-regulation of CK1 $\delta$  and  $\epsilon$  in the lungs of IPF patients. Furthermore, in 4 separate studies we show that the dual CK1 $\delta/\epsilon$  inhibitor PF670462 exhibits anti-fibrotic effects in early and later phases of the fibrogenic response to bleomycin. In late 2014 the first two drugs were approved by the Food and Drug Administration (United States) for the treatment of IPF. Hitherto, treatment relied on azathioprine, systemic glucocorticoids and N-acetyl cysteine, which have since been found to shorten survival





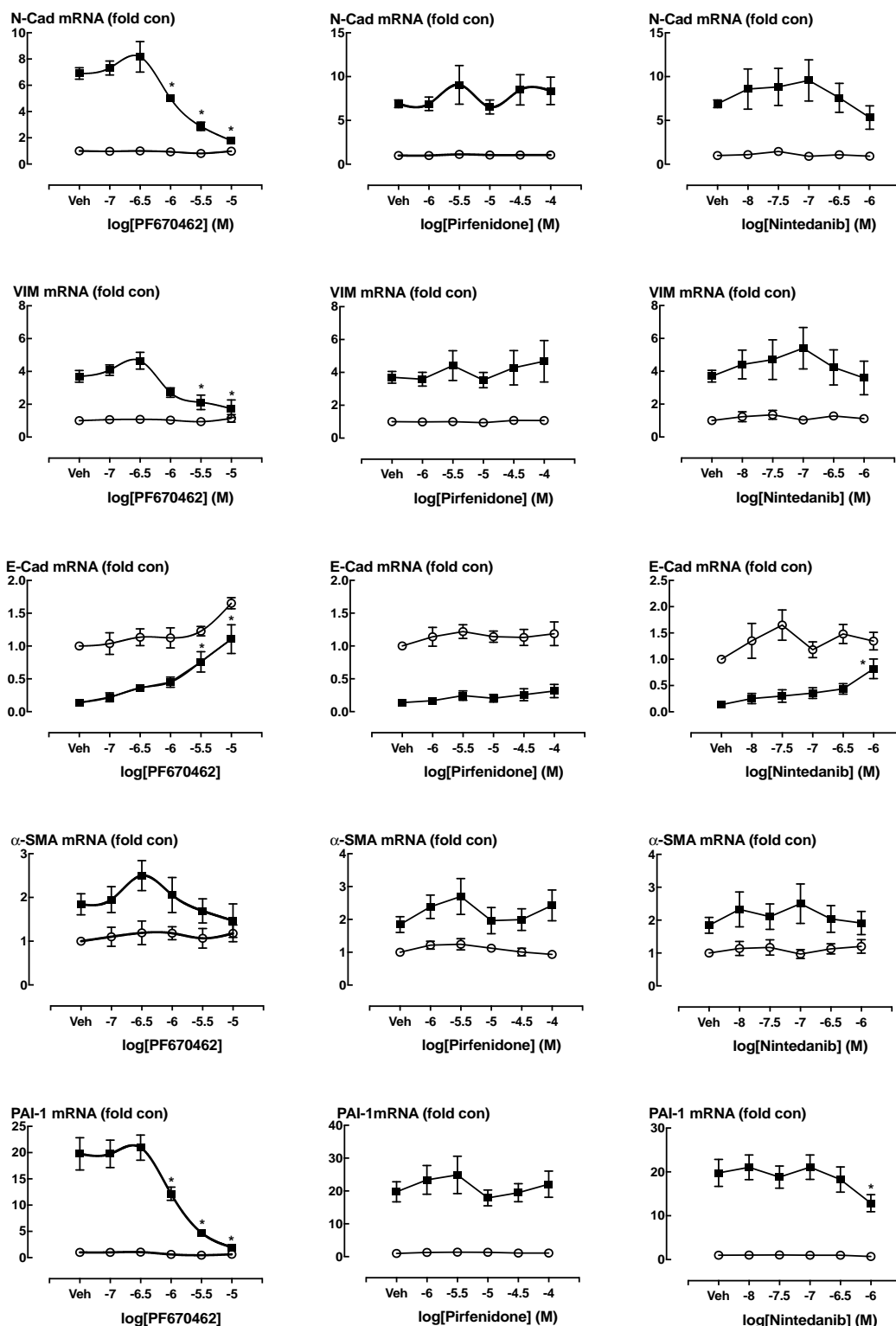


**FIGURE 5 |** The EMT gene expression at baseline and in the presence of TGF- $\beta$  (100 pM, 24 h incubation) was measured in the presence of vehicle (Veh, 0.1% DMSO) or over a range of concentrations of PF670462 (0.1 – 10  $\mu$ M), Pirfenidone (1 – 100  $\mu$ M) or nintedanib (10 – 1000 nM) in. Data are presented as mean and SEM of  $n = 4$  independent experiments and show the TGF- $\beta$  induced fold increase in the expression of genes that change during EMT or in response to TGF- $\beta$  in A549 cells, including *N*-cadherin (*N*-Cad), Vimentin (*Vim*), *E*-Cadherin (*E*-Cad),  $\alpha$ -smooth muscle actin ( $\alpha$ -SMA) plasminogen-activator inhibitor-1 (PAI-1). Data were analyzed by two-way ANOVA with repeated measures, followed by comparisons at individual concentrations using Bonferroni's correction for multiple comparisons. \* $P < 0.05$ .

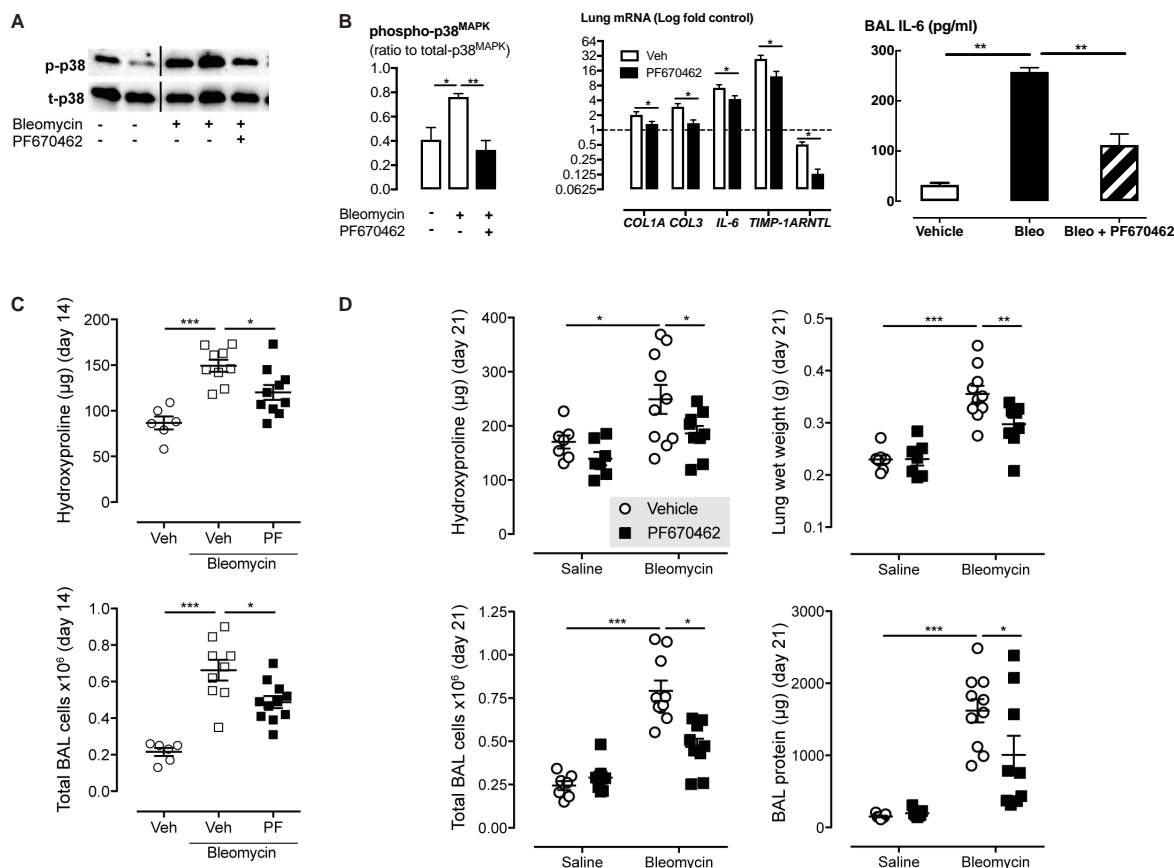


**FIGURE 6 |** The dual CK1 $\delta$ / $\epsilon$  inhibitor PF670462 prevents and attenuates bleomycin-induced pulmonary fibrogenesis in mice. Male C57Bl/6 mice received an intranasal dose of bleomycin or saline on day 0. PF670462 (30 mg/kg/day, i.p.). (A,B) p38<sup>MAPK</sup> phosphorylation and fibrogenic gene expression in lungs from mice treated with PF670462 from day -1 to 3 as measured on day 3 ( $n = 5$  per group). Western blots of 2 representative mice are shown and data from all mice quantitated and tested. (C) Hydroxyproline content and bronchoalveolar lavage (BAL) cell number in lungs from female mice treated with PF670462 from day 3–13, as measured on day 14 ( $n = 6$  sal,  $n = 12$  bleo groups). (D) Hydroxyproline content and wet weight of lungs and BAL cell number and protein content from female mice treated with PF670462 from day 7–21 as measured on day 21 ( $n = 7$  sal,  $n = 9$ –10 bleo groups). Data are presented as mean  $\pm$  SEM. \* $P < 0.05$ , \*\* $P < 0.01$ , \*\*\* $P < 0.001$  from one-way ANOVA with Dunnett's *post hoc* test, or two-way ANOVA with Bonferroni *post hoc* test.

(Idiopathic Pulmonary Fibrosis Clinical Research Network et al., 2012). Treatment with nintedanib over extended periods reduces the decline in lung function compared to placebo (Richeldi et al., 2014). Nintedanib is a tyrosine kinase inhibitor that inhibits the ATP binding site of a host of tyrosine kinase receptors, including those for PDGF, FGF and VEGF. Pirfenidone, on the other hand, has anti-inflammatory, anti-fibrotic and antioxidant effects through an as yet undefined receptor that involves inhibition of TGF- $\beta$  production, reduced fibroblast activation, and a decrease in extracellular matrix production (King et al., 2014; Selvaggio and Noble, 2016). Importantly, as both of these orally administered drugs have significant systemic adverse-effects, there remains great scope for further therapeutic gains from new agents, delivered by inhalation to minimize systemic adverse effects.

The bleomycin mouse model of fibrosis has been criticized for poor predictive value (Mercer et al., 2015). However, the use of a “therapeutic” drug dosing regimen, in which

drugs are administered after the inflammatory phase of the model (as in the current study), is thought to be more predictive of clinical outcome (Moeller et al., 2008). Indeed, the impact on collagen deposition of PF670462 treatment (either systemically 30 mg/kg/day or by aerosol 1  $\mu$ g/day) once daily in the bleomycin mouse model is comparable with reports of the twice daily impact of dosing of 400 mg/kg/day of pirfenidone (Kakugawa et al., 2004). Pirfenidone is known to modulate TGF- $\beta$  pathways, but there is no discrete molecular target against which the drug class can be further optimized. PF670462 may be more suitable than pirfenidone as a TGF- $\beta$  modulator, as its potency enables inhalational delivery, thereby limiting the systemic adverse effects. Head-to-head studies in the murine model of fibrogenesis may add weight to the existing contrasts on *in vitro* fibrogenesis models using cultured human cells.

Two features of PF670462 support its suitability as a TGF- $\beta$  modulator. Firstly, PF670462 shows selectivity for inhibition

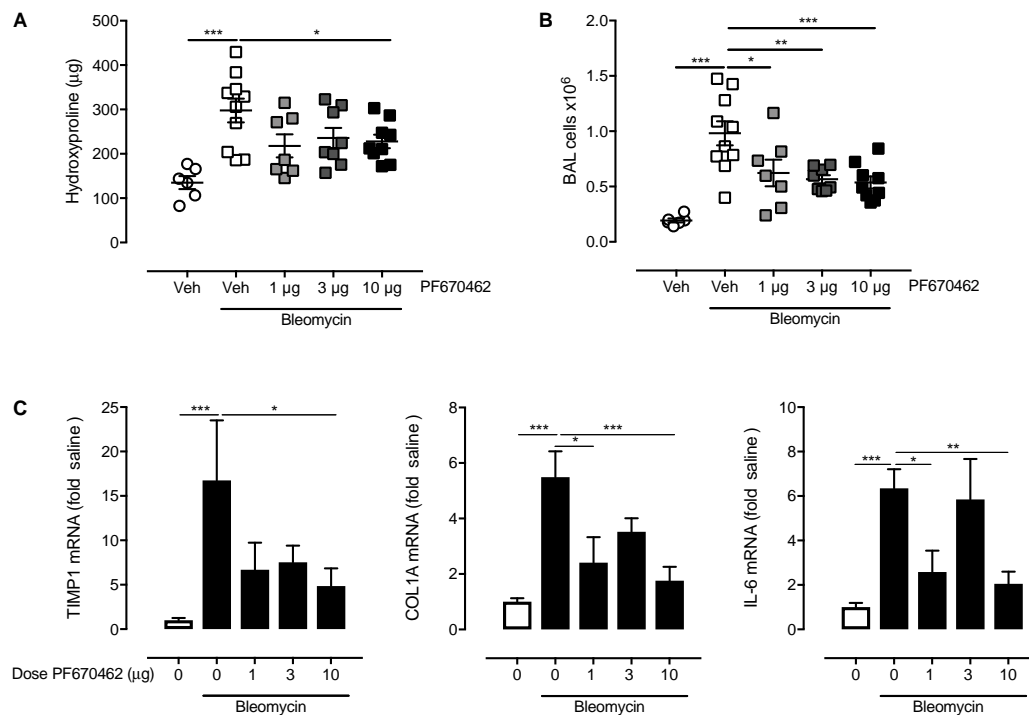


**FIGURE 7 |** Effect of inhaled PF670462 (day 8–21) on bleomycin-induced collagen deposition and BAL cell recruitment in mouse lungs. Female C57Bl/6 mice received intranasal bleomycin or saline on day 0. PF670462 was administered on days 8–20 by the daily inhalation of aerosol of increasing concentration from 0.3 to 3 mg/mL, for a period of 15 min once daily. Collagen content (**A**; measured by assessment of lung hydroxyproline content), Bronchoalveolar lavage (BAL) cell number (**B**) and lung fibrogenic gene expression (**C**) were assessed on day 21. Data are presented as mean  $\pm$  SEM ( $n = 6$  sal,  $n = 9$ –10 bleo groups). \* $P < 0.05$ , \*\* $P < 0.01$ , \*\*\* $P < 0.001$  from one-way ANOVA with Dunnett's *post hoc* test.

of CK1 $\delta/\epsilon$  –dependent as opposed to other actions of TGF- $\beta$ , as expected from its selectivity for CK1 $\delta$  over the TGF- $\beta$  receptor kinase, ALK5. This selectivity avoids compromising TGF- $\beta$  dependent Treg cell populations, the loss of which are implicated in gut autoimmune colitis resulting from global TGF- $\beta$  inhibition, as discussed in our recent review on safety of TGF- $\beta$  modulation (LaChapelle et al., 2018). Secondly, the greatly diminished systemic exposure achieved by inhalational usage reduces the risk of cardiac or gut autoimmune defects, and minimizes the risk of disruption to central circadian rhythm.

Studies on the mechanism of PF670462 suggest suppression of EMT, in addition to regulatory effects on lung fibroblasts, presenting a pharmacological profile that is distinct to nintedanib, which reduces (myo)fibroblast activity, with limited effect on EMT (Wollin et al., 2015). We acknowledge limitations in the utility of A549 cells to represent native alveolar epithelial cells. Nevertheless, A549 cells recapitulate the hallmarks of EMT that are observed in *in vivo* studies in reporter mice and human IPF patients (Kasai et al., 2005; Kim et al., 2006), and our data unequivocally indicate modulation of TGF- $\beta$  effects.

As TGF- $\beta$  is a very well validated key target in fibrosis, there is considerable interest in investigating selective targeting strategies. Recent efforts have identified that targeting the  $\alpha_v\beta_6$  integrin, that is strongly upregulated at fibrogenic sites,

reduces fibrosis-related TGF- $\beta$  activation whilst avoiding TGF- $\beta$  suppression in healthy tissue (Horan et al., 2008; Puthawala et al., 2008). This strategy seems promising. BG00011 (aka STX-100), a humanized monoclonal antibody targeting the  $\alpha_v\beta_6$  integrin, is currently in phase 2 clinical trials (NCT01371305). PF670462, as a small molecule, has many advantages over a monoclonal antibody, including ease and route of administration, and lower cost of goods. Furthermore, our observation of local efficacy following inhalation in the bleomycin-mouse model enables minimization of the systemic adverse-effects of targeting TGF- $\beta$  pathways.

Our results suggest that PF670462 or similar CK1 $\delta/\epsilon$  inhibitors could provide a promising new approach for the treatment of pulmonary fibrosis. The beneficial actions of PF670462 in highly relevant 3D spheroid models using both non-diseased and IPF-derived fibroblasts, considered together with the impact of the ‘therapeutic’ dosing regimen in the mouse studies, support arguments for further preclinical development of PF670462 or other agents targeting CK1 $\delta/\epsilon$ . Minimization of the systemic adverse-effects of targeting TGF- $\beta$  pathways will be important in the development of this agent. The potential impact of the inevitable off-target effects of small molecule kinase inhibitors CK1 $\delta/\epsilon$  will be minimized by their inhalational use. There are predictable on-target adverse effects of systemic CK1 $\delta/\epsilon$  inhibitors, including modulation of circadian rhythm

(Badura et al., 2007; Meng et al., 2010). Inhalational use of CK1 $\delta/\epsilon$  inhibitors will minimize unwanted systemic actions, as will the low oral availability of PF670462 that is subject to rapid first-pass hepatic metabolism (Wager et al., 2014). Although we propose that CK1 $\delta/\epsilon$  is playing a role in selected fibrogenic TGF- $\beta$  signaling, recent findings demonstrating the *Clock* <sup>$\Delta$ 19</sup> mice that lack circadian variation in anti-oxidant enzymes, show greater fibrogenic response to bleomycin (Pekovic-Vaughan et al., 2014), raises the potential for additional benefits of CK1 $\delta/\epsilon$  inhibitors to those of modulating downstream TGF- $\beta$  signaling.

## CONCLUSION

Our evidence indicates that both CK1 $\delta$  and  $\epsilon$  are highly up-regulated in IPF lungs and their inhibition with the dual kinase inhibitor PF670462 has broad anti-fibrotic efficacy in pre-clinical models. We therefore suggest that PF670462 or other inhibitors of CK1 $\delta/\epsilon$  are promising candidates for development as inhalational anti-fibrotic agents.

## DATASETS ARE AVAILABLE ON REQUEST

The raw data supporting the conclusions of this manuscript will be made available by the authors, without undue reservation, to any qualified researcher.

## REFERENCES

- Anderton, M. J., Mellor, H. R., Bell, A., Sadler, C., Pass, M., Powell, S., et al. (2011). Induction of heart valve lesions by small-molecule ALK5 inhibitors. *Toxicol. Pathol.* 39, 916–924. doi: 10.1177/0192623311416259
- Badura, L., Swanson, T., Adamowicz, W., Adams, J., Cianfroga, J., Fisher, K., et al. (2007). An inhibitor of casein kinase I epsilon induces phase delays in circadian rhythms under free-running and entrained conditions. *J. Pharmacol. Exp. Ther.* 322, 730–738. doi: 10.1124/jpet.107.122846
- Bartis, D., Mise, N., Mahida, R. Y., Eickelberg, O., and Thickett, D. R. (2014). Epithelial-mesenchymal transition in lung development and disease: does it exist and is it important? *Thorax* 69, 760–765. doi: 10.1136/thoraxjnl-2013-204608
- Bartis, D., and Thickett, D. R. (2014). Authors' response: epithelial-mesenchymal Transition (EMT) is a common molecular programme in epithelial cells which can be triggered by injury. *Thorax* 69:769. doi: 10.1136/thoraxjnl-2014-205647
- Biernacka, A., Dobaczewski, M., and Frangogiannis, N. G. (2011). TGF-beta signaling in fibrosis. *Growth Factors* 29, 196–202. doi: 10.1007/s00213-008-1417-z
- Bryant, C. D., Graham, M. E., Distler, M. G., Munoz, M. B., Li, D., Vezina, P., et al. (2009). A role for casein kinase 1 epsilon in the locomotor stimulant response to methamphetamine. *Psychopharmacology* 203, 703–711. doi: 10.1007/s00213-008-1417-z
- Coker, R., Laurent, G., Jeffery, P., Du Bois, R., Black, C., and McAnulty, R. (2001). Localisation of transforming growth factor  $\beta$ 1 and  $\beta$ 3 mRNA transcripts in normal and fibrotic human lung. *Thorax* 56, 549–556. doi: 10.1136/thorax.56.7.549
- Dierickx, P., Van Laake, L. W., and Geijsen, N. (2018). Circadian clocks: from stem cells to tissue homeostasis and regeneration. *EMBO Rep.* 19, 18–28. doi: 10.15252/embr.201745130
- Durrington, H. J., Farrow, S. N., Loudon, A. S., and Ray, D. W. (2014). The circadian clock and asthma. *Thorax* 69, 90–92. doi: 10.1136/thoraxjnl-2013-203482
- Fernandez, I. E., and Eickelberg, O. (2012). New cellular and molecular mechanisms of lung injury and fibrosis in idiopathic pulmonary fibrosis. *Lancet* 380, 680–688. doi: 10.1016/S0140-6736(12)61144-1
- Fish, K. J., Cegielska, A., Getman, M. E., Landes, G. M., and Virshup, D. M. (1995). Isolation and characterization of human casein kinase I epsilon (CKI), a novel member of the CKI gene family. *J. Biol. Chem.* 270, 14875–14883. doi: 10.1074/jbc.270.25.14875
- Friedman, S. L., Sheppard, D., Duffield, J. S., and Violette, S. (2013). Therapy for fibrotic diseases: nearing the starting line. *Sci. Transl. Med.* 5:167sr1. doi: 10.1126/scitranslmed.3004700
- Guevorkian, K., Colbert, M. J., Durth, M., Dufour, S., and Brochard-Wyart, F. (2010). Aspiration of biological viscoelastic drops. *Phys. Rev. Lett.* 104:218101. doi: 10.1103/PhysRevLett.104.218101
- Hall, F. L., Benya, P. D., Padilla, S. R., Carbonaro-Hall, D., Williams, R., Buckley, S., et al. (1996). Transforming growth factor-beta type-II receptor signalling: intrinsic/associated casein kinase activity, receptor interactions and functional effects of blocking antibodies. *Biochem. J.* 316(Pt 1), 303–310. doi: 10.1042/bj3160303
- Hochmuth, R. M. (2000). Micropipette aspiration of living cells. *J. Biomech.* 33, 15–22. doi: 10.1016/S0021-9290(99)00175-X
- Horan, G. S., Wood, S., Ona, V., Li, D. J., Lukashev, M. E., Weinreb, P. H., et al. (2008). Partial inhibition of integrin  $\alpha$ (v) $\beta$ 6 prevents pulmonary fibrosis without exacerbating inflammation. *Am. J. Respir. Crit. Care Med.* 177, 56–65. doi: 10.1164/rccm.200706-805OC
- Idiopathic Pulmonary Fibrosis Clinical Research Network, Raghu, G., Anstrom, K. J., King, T. E. Jr., Lasky, J. A., et al. (2012). Prednisone, azathioprine, and N-acetylcysteine for pulmonary fibrosis. *N. Engl. J. Med.* 366, 1968–1977. doi: 10.1056/NEJMoa1113354
- Kage, H., and Borok, Z. (2012). EMT and interstitial lung disease: a mysterious relationship. *Curr. Opin. Pulm. Med.* 18, 517–523. doi: 10.1097/MCP.0b013e3283566721
- Kakugawa, T., Mukae, H., Hayashi, T., Ishii, H., Abe, K., Fujii, T., et al. (2004). Pirfenidone attenuates expression of HSP47 in murine bleomycin-induced

## AUTHOR CONTRIBUTIONS

CK, SL, DP, ML, TH, MS, YT, FJ, YX, and BG acquired and analyzed the data. CK, SL, PL, and AS interpreted the data. JJ and GW provided the human lung specimens from IPF and non-IPF donors from which TH generated primary human fibroblast cell cultures. AS conceived the study. CK and AS wrote and AS revised the manuscript. All authors edited and approved submission of the manuscript.

## FUNDING

This work was funded in part by grants from NHMRC (Australia): #1045372; #1137171 and #1059665, and the Australian Research Council LP160100635 and ARC Centre for Personalised Therapeutics Technologies IC170100016 (AS).

## ACKNOWLEDGMENTS

We thank the Departments of Respiratory Medicine, Surgery, and Anatomical Pathology, Alfred Hospital, Australia, and Prof. Catriona MacClean for assistance in obtaining human lung tissue and Prof Judith Black for provision of two lung fibroblast cell lines derived from IPF donors. We also acknowledge the assistance of Ellie Cho from the Biological Optical Microscopy Platform, University of Melbourne.

- pulmonary fibrosis. *Eur. Respir. J.* 24, 57–65. doi: 10.1183/09031936.04.00120803
- Kasai, H., Allen, J. T., Mason, R. M., Kamimura, T., and Zhang, Z. (2005). TGF- $\beta$ 1 induces human alveolar epithelial to mesenchymal cell transition (EMT). *Respir. Res.* 6:56.
- Keenan, C. R., Mok, J. S., Harris, T., Xia, Y., Salem, S., and Stewart, A. G. (2014). Bronchial epithelial cells are rendered insensitive to glucocorticoid transactivation by transforming growth factor- $\beta$ 1. *Respir. Res.* 15:55. doi: 10.1186/1465-9921-15-55
- Kennaway, D. J., Varcoe, T. J., Voultsios, A., Salkeld, M. D., Rattanaray, L., and Boden, M. J. (2015). Acute inhibition of casein kinase 1delta/epsilon rapidly delays peripheral clock gene rhythms. *Mol. Cell. Biochem.* 398, 195–206. doi: 10.1007/s11010-014-2219-8
- Khalil, N., O'Connor, R. N., Flanders, K. C., and Unruh, H. (1996). TGF- $\beta$  1, but not TGF- $\beta$  2 or TGF- $\beta$  3, is differentially present in epithelial cells of advanced pulmonary fibrosis: an immunohistochemical study. *Am. J. Respir. Cell Mol. Biol.* 14, 131–138. doi: 10.1165/ajrcmb.14.2.8630262
- Kim, K. K., Kugler, M. C., Wolters, P. J., Robillard, L., Galvez, M. G., Brumwell, A. N., et al. (2006). Alveolar epithelial cell mesenchymal transition develops in vivo during pulmonary fibrosis and is regulated by the extracellular matrix. *Proc. Natl. Acad. Sci. U.S.A.* 103, 13180–13185. doi: 10.1073/pnas.0605669103
- King, T. E. Jr., Bradford, W. Z., Castro-Bernardini, S., Fagan, E. A., Glaspole, I., Glassberg, M. K., et al. (2014). A phase 3 trial of pirfenidone in patients with idiopathic pulmonary fibrosis. *N. Engl. J. Med.* 370, 2083–2092. doi: 10.1056/NEJMoa1402582
- Kulkarni, A. B., Huh, C. G., Becker, D., Geiser, A., Lyght, M., Flanders, K. C., et al. (1993). Transforming growth factor  $\beta$  1 null mutation in mice causes excessive inflammatory response and early death. *Proc. Natl. Acad. Sci. U.S.A.* 90, 770–774. doi: 10.1073/pnas.90.2.770
- LaChapelle, P., Li, M., Douglass, J., and Stewart, A. G. (2018). Safer approaches to therapeutic modulation of TGF- $\beta$  signaling for respiratory disease. *Pharmacol. Ther.* 187, 98–113. doi: 10.1016/j.pharmthera.2018.02.010
- Langenbach, S. Y., Wheaton, B. J., Fernandes, D. J., Jones, C., Sutherland, T. E., Wraith, B. C., et al. (2007). Resistance of fibrogenic responses to glucocorticoid and 2-methoxyestradiol in bleomycin-induced lung fibrosis in mice. *Can. J. Physiol. Pharmacol.* 85, 727–738. doi: 10.1139/Y07-065
- Leask, A., and Abraham, D. J. (2004). TGF- $\beta$  signaling and the fibrotic response. *FASEB J.* 18, 816–827. doi: 10.1096/fj.03-1273rev
- Ley, B., Collard, H. R., and King, T. E. Jr. (2011). Clinical course and prediction of survival in idiopathic pulmonary fibrosis. *Am. J. Respir. Crit. Care Med.* 183, 431–440. doi: 10.1164/rccm.201006-0894CI
- Marinkovic, A., Liu, F., and Tschumperlin, D. J. (2013). Matrices of physiologic stiffness potently inactivate idiopathic pulmonary fibrosis fibroblasts. *Am. J. Respir. Cell Mol. Biol.* 48, 422–430. doi: 10.1165/rcmb.2012-0335OC
- Meng, Q. J., Maywood, E. S., Bechtold, D. A., Lu, W. Q., Li, J., Gibbs, J. E., et al. (2010). Entrainment of disrupted circadian behavior through inhibition of casein kinase 1 (CK1) enzymes. *Proc. Natl. Acad. Sci. U.S.A.* 107, 15240–15245. doi: 10.1073/pnas.1005101107
- Mercer, P. F., Abbott-Banner, K., Adcock, I. M., and Knowles, R. G. (2015). Translational models of lung disease. *Clin. Sci.* 128, 235–256. doi: 10.1042/CS20140373
- Moeller, A., Ask, K., Warburton, D., Gaudie, J., and Kolb, M. (2008). The bleomycin animal model: a useful tool to investigate treatment options for idiopathic pulmonary fibrosis? *Int. J. Biochem. Cell Biol.* 40, 362–382. doi: 10.1016/j.biocel.2007.08.011
- Mora, A. L., Rojas, M., Pardo, A., and Selman, M. (2017). Emerging therapies for idiopathic pulmonary fibrosis, a progressive age-related disease. *Nat. Rev. Drug Discov.* 16, 755–772. doi: 10.1038/nrd.2017.170
- Ogura, T., Taniguchi, H., Azuma, A., Inoue, Y., Kondoh, Y., Hasegawa, Y., et al. (2015). Safety and pharmacokinetics of nintedanib and pirfenidone in idiopathic pulmonary fibrosis. *Eur. Respir. J.* 45, 1382–1392. doi: 10.1183/09031936.00198013
- Oldham, M. J., and Robinson, R. J. (2007). Predicted tracheobronchial and pulmonary deposition in a murine asthma model. *Anatom. Record* 290, 1309–1314. doi: 10.1002/ar.20593
- Pan, L., Belloni, P., Ding, H. T., Wang, J., Rubino, C. M., and Putnam, W. S. (2017). A pharmacokinetic bioequivalence study comparing pirfenidone tablet and capsule dosage forms in healthy adult volunteers. *Adv. Ther.* 34, 2071–2082. doi: 10.1007/s12325-017-0594-8
- Pekovic-Vaughan, V., Gibbs, J., Yoshitane, H., Yang, N., Pathirana, D., Guo, B., et al. (2014). The circadian clock regulates rhythmic activation of the NRF2/glutathione-mediated antioxidant defense pathway to modulate pulmonary fibrosis. *Genes Develop.* 28, 548–560. doi: 10.1101/gad.237081.113
- Perreault-Lenz, S., Vengeliene, V., Noori, H. R., Merlo-Pich, E. V., Corsi, M. A., Corti, C., et al. (2012). Inhibition of the casein-kinase-1-epsilon/delta/prevents relapse-like alcohol drinking. *Neuropsychopharmacology* 37, 2121–2131. doi: 10.1038/npp.2012.62
- Puthawala, K., Hadjiangelis, N., Jacoby, S. C., Bayongan, E., Zhao, Z., Yang, Z., et al. (2008). Inhibition of integrin  $\alpha(v)\beta6$ , an activator of latent transforming growth factor- $\beta$ , prevents radiation-induced lung fibrosis. *Am. J. Respir. Crit. Care Med.* 177, 82–90. doi: 10.1164/rccm.200706-806OC
- Raghu, G., Collard, H. R., Egan, J. J., Martinez, F. J., Behr, J., Brown, K. K., et al. (2011). An official ATS/ERS/JRS/ALAT statement: idiopathic pulmonary fibrosis: evidence-based guidelines for diagnosis and management. *Am. J. Respir. Crit. Care Med.* 183, 788–824. doi: 10.1164/rccm.2009-040GL
- Richeldi, L., du Bois, R. M., Raghu, G., Azuma, A., Brown, K. K., Costabel, U., et al. (2014). Efficacy and safety of nintedanib in idiopathic pulmonary fibrosis. *N. Engl. J. Med.* 370, 2071–2082. doi: 10.1056/NEJMoa1402584
- Salem, S., Harris, T., Mok, J. S., Li, M. Y., Keenan, C. R., Schuliga, M. J., et al. (2012). Transforming growth factor- $\beta$  impairs glucocorticoid activity in the A549 lung adenocarcinoma cell line. *Br. J. Pharmacol.* 166, 2036–2048. doi: 10.1111/j.1476-5381.2012.01885.x
- Schuliga, M., Jaffar, J., Berhan, A., Langenbach, S., Harris, T., Waters, D., et al. (2017). Annexin A2 contributes to lung injury and fibrosis by augmenting factor Xa fibrogenic activity. *Am. J. Physiol. Lung Cell. Mol. Physiol.* 312, L772–L782. doi: 10.1152/ajplung.00553.2016
- Schuliga, M., Javed, A., Harris, T., Xia, Y., Qin, C., Wang, Z., et al. (2013). Transforming growth factor- $\beta$ -induced differentiation of airway smooth muscle cells is inhibited by fibroblast growth factor-2. *Am. J. Respir. Cell Mol. Biol.* 48, 346–353. doi: 10.1165/rcmb.2012-0151OC
- Schuliga, M. J., See, I., Ong, S. C., Soon, L., Camoretti-Mercado, B., Harris, T., et al. (2009). Fibrillar collagen clamps lung mesenchymal cells in a nonproliferative and noncontractile phenotype. *Am. J. Respir. Cell Mol. Biol.* 41, 731–741. doi: 10.1165/rcmb.2008-0361OC
- Selvaggio, A. S., and Noble, P. W. (2016). Pirfenidone initiates a new era in the treatment of idiopathic pulmonary fibrosis. *Annu. Rev. Med.* 67, 487–495. doi: 10.1146/annurev-med-120214-013614
- Shull, M. M., Ormsby, I., Kier, A. B., Pawlowski, S., Diebold, R. J., Yin, M., et al. (1992). Targeted disruption of the mouse transforming growth factor- $\beta$  1 gene results in multifocal inflammatory disease. *Nature* 359, 693–699. doi: 10.1038/359693a0
- Sime, P. J., Xing, Z., Graham, F. L., Csaky, K. G., and Gaudie, J. (1997). Adenovector-mediated gene transfer of active transforming growth factor- $\beta$  1 induces prolonged severe fibrosis in rat lung. *J. Clin. Invest.* 100, 768–776. doi: 10.1172/JCI119590
- Spagnolo, P., Rossi, G., and Cavazza, A. (2014). Pathogenesis of idiopathic pulmonary fibrosis and its clinical implications. *Exp. Rev. Clin. Immunol.* 10, 1005–1017. doi: 10.1586/1744666X.2014.917050
- Sproule, J., Reynolds, L., Kleiman, R., Tate, B., Swanson, T. A., and Pickard, G. E. (2010). Chronic treatment with a selective inhibitor of casein kinase I delta/epsilon yields cumulative phase delays in circadian rhythms. *Psychopharmacology* 210, 569–576. doi: 10.1007/s00213-010-1860-5
- Theret, D. P., Levesque, M. J., Sato, M., Nerem, R. M., and Wheeler, L. T. (1988). The application of a homogeneous half-space model in the analysis of endothelial cell micropipette measurements. *J. Biomech. Eng.* 110, 190–199. doi: 10.1115/1.3108430
- Waddell, D. S., Liberati, N. T., Guo, X., Frederick, J. P., and Wang, X. F. (2004). Casein kinase I epsilon plays a functional role in the transforming growth factor- $\beta$  signaling pathway. *J. Biol. Chem.* 279, 29236–29246. doi: 10.1074/jbc.M400880200
- Wager, T. T., Chandrasekaran, R. Y., Bradley, J., Rubitski, D., Berke, H., Mente, S., et al. (2014). Casein kinase Idelta/epsilon inhibitor PF-5006739 attenuates opioid drug-seeking behavior. *ACS Chem. Neurosci.* 5, 1253–1265. doi: 10.1021/cn500201x



- Walton, K. M., Fisher, K., Rubitski, D., Marconi, M., Meng, Q. J., Sladek, M., et al. (2009). Selective inhibition of casein kinase 1 epsilon minimally alters circadian clock period. *J. Pharmacol. Exp. Ther.* 330, 430–439. doi: 10.1124/jpet.109.151415
- Wollin, L., Wex, E., Pautsch, A., Schnapp, G., Hostettler, K. E., Stowasser, S., et al. (2015). Mode of action of nintedanib in the treatment of idiopathic pulmonary fibrosis. *Eur. Respir. J.* 45, 1434–1445. doi: 10.1183/09031936.00174914
- Wolters, P. J., Collard, H. R., and Jones, K. D. (2014). Pathogenesis of idiopathic pulmonary fibrosis. *Annu. Rev. Pathol.* 9, 157–179. doi: 10.1146/annurev-pathol-012513-104706
- Xia, Y. C., Radwan, A., Keenan, C. R., Langenbach, S. Y., Li, M., Radojicic, D., et al. (2017). Glucocorticoid insensitivity in virally infected airway epithelial cells is dependent on transforming growth factor-beta activity. *PLoS Pathog.* 13:e1006138. doi: 10.1371/journal.ppat.1006138

**Conflict of Interest Statement:** AS, CK, and TH are co-inventors on a patent protecting the use and formulation of inhaled PF670462 in respiratory disease.

The remaining authors declare that the research was conducted in the absence of any commercial or financial relationships that could be construed as a potential conflict of interest.

Copyright © 2018 Keenan, Langenbach, Jativa, Harris, Li, Chen, Xia, Gao, Schuliga, Jaffar, Prodanovic, Tu, Berhan, Lee, Westall and Stewart. This is an open-access article distributed under the terms of the Creative Commons Attribution License (CC BY). The use, distribution or reproduction in other forums is permitted, provided the original author(s) and the copyright owner(s) are credited and that the original publication in this journal is cited, in accordance with accepted academic practice. No use, distribution or reproduction is permitted which does not comply with these terms.



# Fisetin Inhibited Growth and Metastasis of Triple-Negative Breast Cancer by Reversing Epithelial-to-Mesenchymal Transition via PTEN/Akt/GSK3 $\beta$ Signal Pathway

Jie Li<sup>1,2,3†</sup>, Xia Gong<sup>4†</sup>, Rong Jiang<sup>5</sup>, Dan Lin<sup>3</sup>, Tao Zhou<sup>3</sup>, Aijie Zhang<sup>1</sup>, Hongzhong Li<sup>2</sup>, Xiang Zhang<sup>1</sup>, Jingyuan Wan<sup>3\*</sup>, Ge Kuang<sup>3\*</sup> and Hongyuan Li<sup>1\*</sup>

<sup>1</sup> Department of Endocrine and Breast Surgery, The First Affiliated Hospital of Chongqing Medical University, Chongqing, China, <sup>2</sup> Molecular Oncology and Epigenetics Laboratory, The First Affiliated Hospital of Chongqing Medical University, Chongqing, China, <sup>3</sup> Chongqing Key Laboratory of Biochemistry and Molecular Pharmacology, Chongqing Medical University, Chongqing, China, <sup>4</sup> Department of Anatomy, Chongqing Medical University, Chongqing, China, <sup>5</sup> Laboratory of Stem Cell and Tissue Engineering, Chongqing Medical University, Chongqing, China

## OPEN ACCESS

### Edited by:

Cecilia Battistelli,  
Sapienza Università di Roma, Italy

### Reviewed by:

Sonia Emanuele,  
Università degli Studi di Palermo, Italy  
Martina Schmidt,  
University of Groningen, Netherlands

### \*Correspondence:

Jingyuan Wan  
jywan@cqmu.edu.cn  
Ge Kuang  
kuangge72@aliyun.com  
Hongyuan Li  
hongy\_li@hotmail.com

<sup>†</sup> These authors are joint first authors  
and have contributed equally to this  
work.

### Specialty section:

This article was submitted to  
Experimental Pharmacology  
and Drug Discovery,  
a section of the journal  
Frontiers in Pharmacology

**Received:** 01 April 2018

**Accepted:** 26 June 2018

**Published:** 31 July 2018

### Citation:

Li J, Gong X, Jiang R, Lin D, Zhou T, Zhang A, Li H, Zhang X, Wan J, Kuang G and Li H (2018) Fisetin Inhibited Growth and Metastasis of Triple-Negative Breast Cancer by Reversing Epithelial-to-Mesenchymal Transition via PTEN/Akt/GSK3 $\beta$  Signal Pathway. *Front. Pharmacol.* 9:772. doi: 10.3389/fphar.2018.00772

Triple negative breast cancer (TNBC), characterized by its highly aggressive and metastatic features, is associated with poor prognosis and high mortality partly due to lack of effective treatment. Fisetin, a natural flavonoid compound, has been demonstrated to possess anti-cancer effects in various cancers. However, the effects and mechanisms of fisetin on metastasis of TNBC remain uncovered. In this study, we found that fisetin dose-dependently inhibited cell proliferation, migration and invasion in TNBC cell lines MDA-MB-231 and BT549 cells. In addition, fisetin reversed epithelial to mesenchymal transition (EMT) as evaluated by cell morphology and EMT markers in MDA-MB-231 and BT549 cells. Furthermore, fisetin suppressed phosphoinositol 3-kinase (PI3K)-Akt-GSK-3 $\beta$  signaling pathway but upregulated the expression of PTEN mRNA and protein in a concentration-dependent manner. Further, silence of PTEN by siRNA abolished these benefits of fisetin on proliferation and metastasis of TNBCs. *In vivo*, using the metastatic breast cancer xenograft model bearing MDA-MB-231 cells, we found that fisetin dramatically inhibited growth of primary breast tumor and reduced lung metastasis, meanwhile, the expression of EMT molecules and PTEN/Akt/GSK-3 $\beta$  in primary and metastatic tissues changed in the same way as those *in vitro* experiments. In conclusion, all these results indicated that fisetin could effectively suppress proliferation and metastasis of TNBC and reverse EMT process, which might be mediated by PTEN/Akt/GSK-3 $\beta$  signaling pathway.

**Keywords:** fisetin, triple negative breast cancer, EMT, PTEN, AKT

## INTRODUCTION

Breast cancer is the most common malignant tumor in women, and it is the most important reason causing cancer death among women, either in developed countries or developing countries. In 2012, there were 1,383,500 women who were diagnosed with breast cancer all over the world, and about 458,400 of them died because of breast cancer (Torre et al., 2015). Although plenty of drugs

and synthetic treatment strategies have been utilized extensively in clinic, the incidence rate of treatment failure and cancer recurrence still remains at a high level, overwhelmingly because of cancer metastasis (Wculek and Malanchi, 2015). Thus, it can be seen that metastatic breast cancer is an increasing threat for global women's health. To explore the mechanisms of metastasis and find the new drugs to aim directly at it may provide a better prognosis for patients.

Epithelial to mesenchymal transition (EMT) is a common phenotypic conversion involved in both normal physiological and pathological processes including embryonic development, wounded tissues plerosis, and the tumor metastasis and dissemination (Takebe et al., 2011; Nieto et al., 2016). EMT makes it possible for cancer cells to detach from the primary tumor site and encroach into the surrounding normal tissues, lymphatic and blood system, where they are disseminated to distant sites to form the metastatic lesion (Nickel and Stadler, 2015). During the EMT process of tumor metastasis, the cancer cells complete the shift from the adhesive, non-mobile, oval epithelial phenotype to the mobile, invasive long spindle mesenchymal phenotype, meanwhile, the epithelial cell markers like E-cadherin and Claudin were down-regulated but the mesenchymal cell markers such as N-cadherin and Vimentin were up-regulated (Banyard and Bielenberg, 2015). There are plenty of transcriptional factors like Slug, Snail, ZEB, Twist and signaling molecules such as Wnt, Notch, TGF- $\beta$ , and ErbB to be involved in the regulation of EMT (Takebe et al., 2011; Moyret-Lalle et al., 2014). Besides cancer metastasis, a series of researches have confirmed that EMT also has connection with emergence of drug resistance and acquisition of cancer stem cells feature, which make the treatment of cancer sink into a more difficult situation (Huang et al., 2015).

Along with the continual incidence of drug resistance and the serious adverse effects of the routine agents for chemotherapy in the treatment of cancers, more and more studies transfer their focus on the potential of natural plant compounds (Rasool et al., 2015). Fisetin (3,3',4',7-tetrahydroxyflavone, **Figure 1A**) is one of the major flavonoids that can be extracted from many fruits and vegetables like strawberry, apple, persimmon, grape, onion, and cucumber (Khan et al., 2013). It has been reported that fisetin exerted a series of pharmacological functions including anti-oxidant, anti-inflammatory, anti-angiogenesis, and anti-tumor (Bhat et al., 2012; Pal et al., 2016; Rengarajan and Yaacob, 2016; Sechi et al., 2016). In addition, several researches have shown that fisetin exhibited dramatically inhibitory effects on tumor progression by suppressing cancer cell growth, migration, invasion, and autophagy process and promoting cell cycle arrest and apoptosis in various of cancers, such as nasopharyngeal carcinoma, melanoma, lung cancer, breast cancer, bladder cancer, hepatocellular carcinoma, and prostate cancer (Li et al., 2011, 2014; Khan et al., 2012, 2014; Yang et al., 2012; Syed et al., 2014; Kang et al., 2015; Maurya and Trigun, 2017). However, the effects and underlying mechanisms of fisetin on the growth and metastasis of triple-negative breast cancer (TNBC) still remain unclear.

In this study, we chose two fibroblastic human TNBC cell lines MDA-MB-231 and BT549, which are utilized extensively

as highly aggressive breast cancer cell lines (Lehmann and Pietenpol, 2014), to investigate the potential effects and mechanisms of fisetin on the growth and metastasis of TNBC *in vitro* and *in vivo*.

## MATERIALS AND METHODS

### Reagents and Antibodies

Fisetin (purity > 99%) was bought from Push Bio-Technology (Chengdu, China). 3-(4,5 dimethylthiazol-2-yl)-2,5-diphenyltetrazolium bromide (MTT) was purchased from Sigma (St. Louis, United States). Vectastain ABC kit was obtained from Vector (Burlingame, CA, United States). The liquid DAB+ Substrate Chromogen System was purchased from Dako (California, United States). Dulbecco's Modified Eagle's (DMEM) medium, trypsin-EDTA, phosphate buffer saline (PBS) and penicillin/streptomycin were bought from Hyclone (Los Angeles, CA, United States). Fetal bovine serum (FBS) was the product of Gibco (Grand Island, NY, United States). RNA extraction, PrimeScript RT and PCR reagent kits were bought from TaKaRa (Dalian, China). Primary antibodies used in this study including anti-Vimentin, anti-E-cadherin, anti-Claudin, anti-N-cadherin, anti-Slug, anti-Snail, anti-PTEN, anti-p-Akt, anti-Akt, anti-p-GSK-3 $\beta$  were obtained from Cell Signaling Technology (New England Biolabs, Ipswich, MA, United States), anti-Ki67 was from Abcam (Cambridge, United Kingdom). Secondary antibody (rabbit monoclonal IgG) was from Abcam (Cambridge, United Kingdom). Anti-GAPDH was from Santa Cruz Biotechnology (Santa Cruz, CA, United States). Anti-F-actin-Red 555 was from Invitrogen (Carlsbad, CA, United States).

### Cell Culture and Treatment

Human TNBC cell lines MDA-MB-231 and BT549 were obtained from the American Type Culture Collection (ATCC) (Manassas, VA, United States) and cultured in Dulbecco's Modified Eagle Media (DMEM) medium with 10% fetal bovine serum (FBS) and 1% penicillin/streptomycin in a humidified atmosphere of 5% CO<sub>2</sub> at 37°C. The cells were treated with fisetin in different concentrations (10, 30, and 100  $\mu$ M) for indicated time.

### Cell Viability Assay

The effect of fisetin on cell viability was assessed using the 3-(4,5-dimethylthiazol-2-yl)-2,5-diphenyl-2H-tetrazolium bromide (MTT) assay. Exponentially growing MDA-MB-231 and BT549 cells were seeded at  $8 \times 10^3$  cells per well in 96-well culture plates, and cultured for 12 h before treatment with a series of concentrations (10, 30, and 100  $\mu$ M, respectively) of fisetin. Each concentration set 3 replicates. Blank control cells were treated with DMEM alone. After incubation for 72 h, 20  $\mu$ L of 5 mg/mL MTT was added to each well and incubated for another 4 h. After that, the medium containing MTT was removed and replaced by 120  $\mu$ L/well of DMSO to solubilize the blue formazan crystals. Absorbance at 490 nm was detected with an automated microplate reader (ELx800, BioTek, United States).

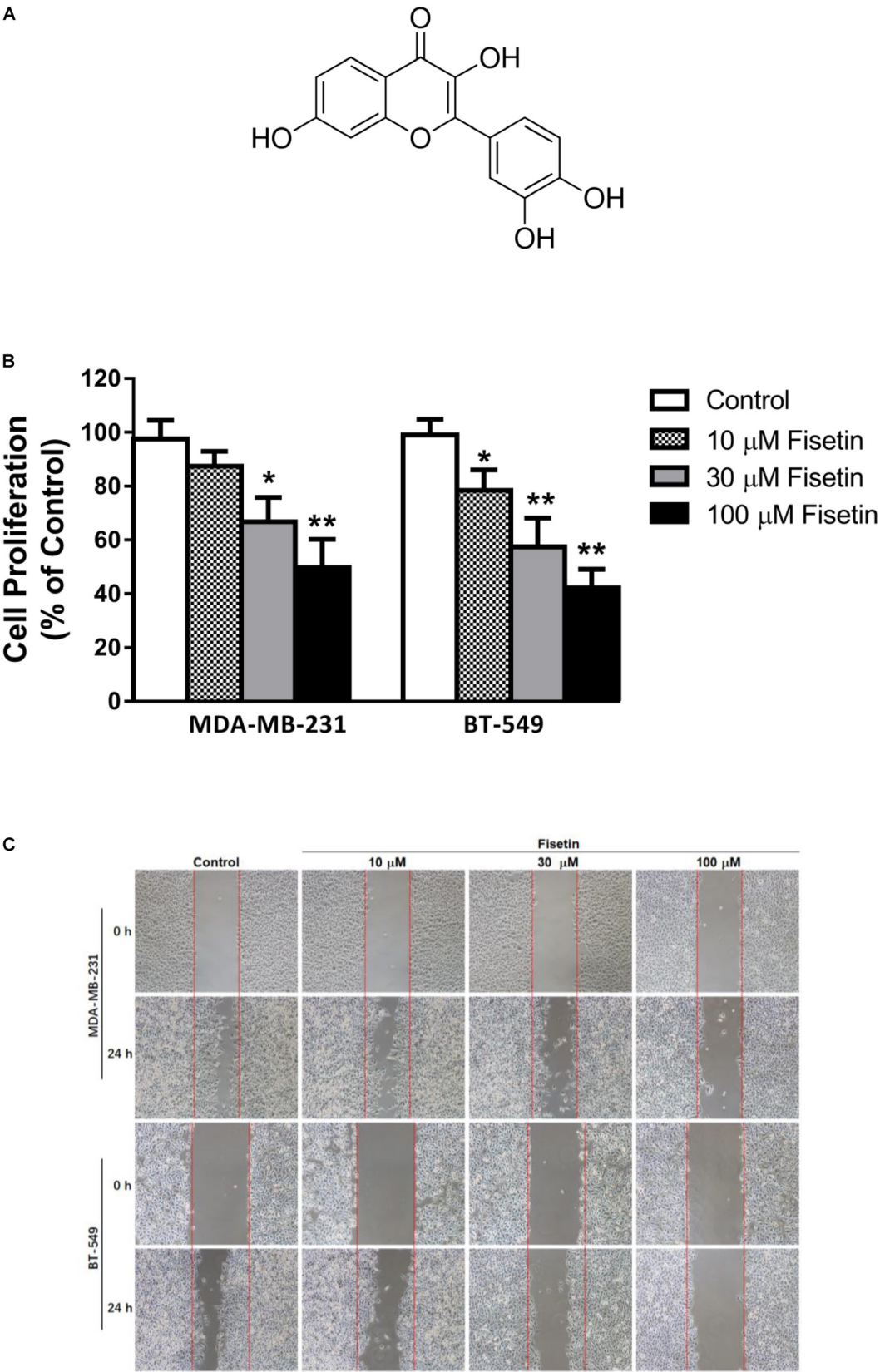


**FIGURE 1** | Continued



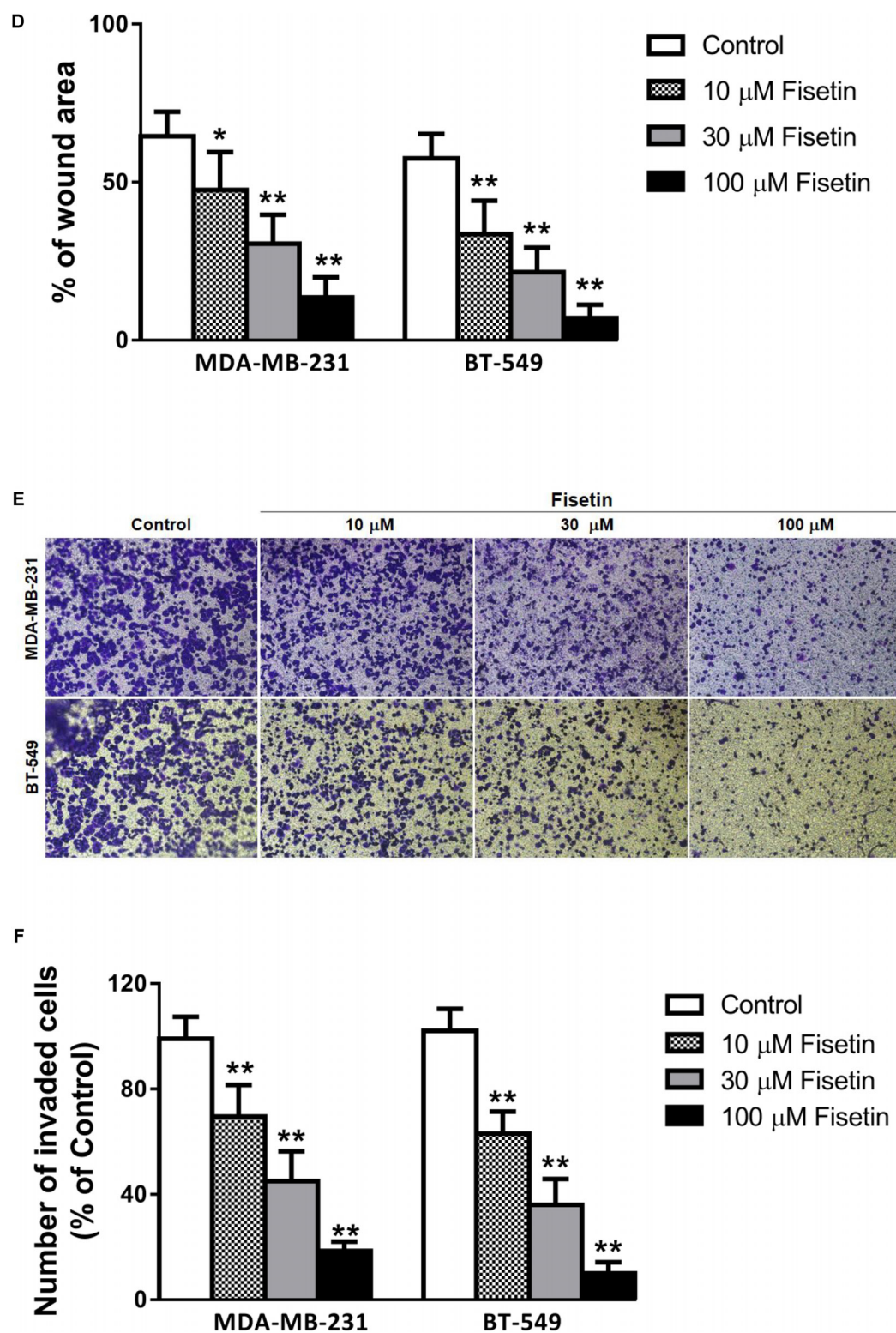


**FIGURE 1 |** Fisetin suppresses the proliferation, migration and invasion of TNBC cells *in vitro*. Triple-negative breast cancer (TNBC) cell lines MDA-MB-231 and BT549 were treated with various concentrations of fisetin (10, 30, and 100  $\mu$ M) for indicated time. **(A)** Chemical structure of fisetin. **(B)** The cell proliferation was determined by MTT assay at 72 h after fisetin treatment. **(C)** The cell migration was determined by wound-healing assay. **(D)** Quantification of the migrated cells. **(E)** The cell invasion was determined by transwell invasion assay. **(F)** Quantification of the invasive cells. The results are shown as the mean  $\pm$  SD of three experiments, \* $P$  < 0.05, \*\* $P$  < 0.01 compared with control.

## Wound Healing Assay

MDA-MB-231 and BT549 cells were seeded into six-well plates in culture medium and allowed to grow to 100% confluence. A sterile toothpick was used to scrap the center of wells to create wounds. The scraped cells were washed out with PBS and the remaining cells continued to be cultured in the absence or presence of different concentrations of fisetin. After 24 h, cells were observed and the gap distance of the wound was measured. Two time points (0 and 24 h after scrap) were selected to capture the wound healing of MDA-MB-231 and BT549 cells by a light microscope (Nikon, Japan).

## Transwell Invasion Assay

The invasion of MDA-MB-231 and BT549 cells was measured using the Matrigel-coated Transwell chamber (Corning, MA, United States). Briefly, cells at a density of  $2.5 \times 10^5$  cells/well were seeded onto the upper chambers in a serum-free medium with or without series concentrations of fisetin, the lower chamber was filled with DMEM medium supplemented with 10% FBS. Following incubation for 24 h, the cells on top surface were scraped, and the cells on the lower surface of the membranes were fixed with 4% paraformaldehyde for 10 min and stained using 0.25% crystal violet for 15 min. The invaded cells were counted at 200 $\times$  magnifications using a microscope (Nikon, Japan).

## Immunofluorescent (IF) Staining

For IF analysis, MDA-MB-231 and BT549 cells treated by series concentrations of fisetin were fixed in 4% paraformaldehyde for 10 min, permeabilized with 0.05% Triton X-100 for 10 min at room temperature and incubated with primary antibodies overnight at 4°C. The cells were then incubated with fluorescein-conjugated secondary antibodies for 1 h at room temperature in darkness. At last DAPI was added to counterstain the nucleus. The primary tumor tissues were stained in the same way, except that tissues were immersed in blocking solution containing 1% BSA in PBS after permeabilized. Images of cells and tissues were captured using fluorescence microscope (Nikon, Japan).

## Western Blot Analysis

MDA-MB-231 and BT549 cells were cultured in absence or presence of series concentrations of fisetin for 24 h, then harvested and lysed in RIPA buffer to isolate the total protein. After incubation for 30 min on ice, lysates were centrifugated at 12,000 g for 5 min and the supernatants were collected and stored at  $-80^{\circ}\text{C}$ . The protein concentration was detected by using the BCA kit according to the manufacturer's instructions. Equal amounts of denatured proteins (30  $\mu\text{g}$ ) were electrophoresed on 10% SDS gel and subsequently transferred to polyvinylidene fluoride (PVDF) membranes. After being blocked in Tris-Buffered Saline containing 0.1% Tween-20 (TBST) for 1 h, the membranes were incubated with an optimal dilution of the desired primary monoclonal antibodies at 4°C overnight. After washing with TBST for three times, the membranes were incubated with an optimal dilution of the appropriate secondary antibodies conjugated with horseradish peroxidase (HRP) for 2 h at the room temperature. At last use the enhanced

chemiluminescent system and X-ray to make the membranes visualization.

## Quantitative Reverse Transcription-Polymerase Chain Reaction (qRT-PCR)

Briefly, total RNA was extracted from cells following the manufacturer's instruction of the RNA extraction kit. Total RNA (1  $\mu\text{l}$ ) was reverse transcribed to complementary DNA (cDNA) by using the PrimeScript RT reagent Kit. At last qPCR was performed by using the PCR kit following the instruction. The specific primer sequences we used were as following: E-cadherin: 5'-TCCTGGGCAGAGTGAATTTTGAAGA-3' (forward), 5'-AAACGGA GGCCTGATGGGG-3' (reverse); Claudin: 5'-CCTCCTGG GAGTGATAGCAAT-3' (forward), 5'-GGCAACTAAAATAGC CAGACCT-3' (reverse); Vimentin: 5'-TACAGGAAGCTGCTGG AAGG-3' (forward), 5'-ACCAGAGGGAGTGAATCCAG-3' (reverse); N-Cadherin: 5'-AGCCAACCTTAACTGAGGAGT-3' (forward), 5'-GGCAAGTTGATTGGAGGGATG-3' (reverse); Snail: 5'-TCGGAAGCCTAACTACAGCGA-3' (forward), 5'-AGATGAGCATTTGGCAGCGAG-3' (reverse); Slug: 5'-GGGG AGAAGCCTTTTCTTG-3' (forward), 5'-TCCTCATGTT TGTGCAGGAG-3' (reverse); PTEN: 5'-TGGATTGCACTTAG ACTTGACCT-3' (forward), 5'-GCGGTGTCATAATGTCTC TCAG-3' (reverse); GAPDH: 5'-TGTTGCCATCAATGACC CCTT-3' (forward), 5'-CTCCACGACGTACTCAGCG-3' (reverse). GAPDH primers were used as internal control and equal loading.

## Transient Transfection of siRNA

Briefly, cells were seeded into 24-well plates and incubated to about 50% confluence, then MDA-MB-231 cells were transfected with Ad-siPTEN or Ad-RFP, respectively. After 48 h transfection, the levels of PTEN protein and mRNA were analyzed by Western blotting and qRT-PCR, respectively.

## Immunohistochemistry (IHC) Staining

Tissue sections were cut into 5  $\mu\text{m}$  thick after fixed with 4% paraformaldehyde and embedded. Then, tissues were deparaffinized, rehydrated, antigen repaired, and blocked with 5% goat serum. Endogenous peroxidases were quenched by incubating with hydrogen peroxide, followed by incubating with primary antibodies at 4°C overnight and HRP-conjugated second antibodies sequentially. Finally, the sections were visualized with DAB staining and imaged.

## Xenograft Model

Four to five-week-old female nude mice were obtained from the Animal Ethics Committee of Chongqing Medical University and housed in specific pathogen free (SPF) laboratory environment. The protocol was reviewed and approved by the Animal Ethics Committee of Chongqing Medical University. We chose MDA-MB-231 cells for determining the effects of fisetin *in vivo*. Female nude mice were injected subcutaneously with  $1 \times 10^6$  MDA-MB-231 cells into bilateral gluteal regions. When the tumor reached

100 mm<sup>3</sup> in volume, mice were divided randomly into sham-treated group and fisetin-treated group. The former received PBS served as control and the latter received 100 mg/kg fisetin in an intraperitoneal injection way every 3 days. Tumor sizes were measured every 3 days. After 4 weeks, all mice were sacrificed under anesthesia, and the tumors and lungs were excised, weighted, and counted for the tumor nodules on the lung. The fixed tumor tissues were further analyzed.

## Statistical Analysis

All experiments were repeated at least three times. Data was expressed as mean  $\pm$  SD. Student's *t*-test and one-way ANOVA analysis were used to analyze the variances between groups. *P* < 0.05 was considered statistically significant.

## RESULTS

### Fisetin Suppressed the Proliferation, Migration and Invasion of TNBC Cells *in Vitro*

To examine the anticancer effect of fisetin on TNBC cells, we treated the highly aggressive MDA-MB-231 cells and BT549 cells with fisetin in different concentration (10, 30, and 100  $\mu$ M, respectively). Firstly, we assessed its proliferative activities through MTT assay at 72 h. It can be observed that fisetin inhibited the cancer cells proliferation in a dose-dependent way (Figure 1B). Then we used wound-healing and transwell assay to determine whether fisetin had the potential to inhibit breast cancer cells migration and invasion. Fisetin could concentration-dependently slow down the wound healing process comparing to the control group (Figures 1C,D), and a similar effect was observed in transwell assay, the invaded cells were decreased in fisetin-treated groups when compared with the control group (Figures 1E,F). All these results suggested that fisetin had the anticancer capability through influencing the proliferation, migration and invasion of TNBC cells.

### Fisetin Reversed EMT in TNBC Cells *in Vitro*

Epithelial to mesenchymal transition is an important process related to the metastasis of tumor cells. For the inhibitory function of fisetin on invasion and migration in MDA-MB-231 and BT549 cells, we explored whether fisetin might achieve it through regulating the EMT process. Therefore, to determine the relationship between fisetin and EMT, we used 10, 30, and 100  $\mu$ M of fisetin to treat MDA-MB-231 and BT549 cells, followed by exploring the shift of cell morphology and evaluating the expression of EMT markers. The two TNBC cell lines presented a long spindle mesenchymal-like feature, while treated with fisetin, cancer cells were changed into oval epithelial-like type (Figure 2A). The immunofluorescence results showed a visible up-regulation of E-cadherin and down-regulation of Vimentin at the concentration of 30  $\mu$ M fisetin, and the cytoskeletal protein F-actin in the cytoplasm was remodeled (Figures 2B,C), suggesting that our hypothesis might be right, in

which fisetin had the potential to suppress EMT. So furthermore, we quantitatively detected the expression of EMT markers by Western blot and qRT-PCR. These two assays demonstrated that both at the protein and mRNA levels, the epithelial markers E-cadherin and Claudin were up-regulated but the mesenchymal markers N-cadherin and Vimentin changed in the opposite way, at the same time, the EMT related transcription factor Snail but not Slug was down-regulated (Figures 2D,E).

### Fisetin Suppressed PI3K-Akt-GSK-3 $\beta$ Signal Pathway but Upregulated PTEN Expression *in Vitro*

As PI3K/Akt/GSK-3 $\beta$  signaling pathway plays an important role in promoting the process of EMT and mediating the metastasis of cancer, and PTEN can act as a phosphatase to dephosphorylate Akt, so we detected the expression of the key members in this PTEN-Akt-GSK-3 signaling molecules. Immunofluorescent staining results showed that the expression of p-Akt was downregulated, but PTEN was upregulated after being treated with 30  $\mu$ M fisetin comparing to the control group (Figures 3A,B). Moreover, the result of western blot in Figure 3C showed that comparing to the control group, both in the two cell lines, the protein level of PTEN was upregulated by fisetin in a dose-dependent way, while the expression of p-Akt and p-GSK-3 $\beta$  was decreased in the same way. Consonantly, using the qRT-PCR method to assay the expression of PTEN mRNA, we found that fisetin dose-dependently unregulated the expression of PTEN mRNA in two TNBC cell lines (Figure 3D).

### Silencing of PTEN Abrogated the Effects of Fisetin on TNBC Cells Proliferation and Metastasis as Well as EMT

To evaluate whether the antitumor effects of fisetin is mainly correlated with the upregulation of PTEN which can inhibit Akt signaling, the expression of PTEN was silenced with Ad-si PTEN in MDA-MB-231 cells. As shown in Figure 4A, the decrease of PTEN and increase of p-Akt and p-GSK-3 $\beta$  were observed in Ad-si PTEN transfected MDA-MB-231 cells treated by fisetin (100  $\mu$ M) when compared with Ad-RFP control group. Moreover, using western blot method, we found that those beneficial changes of fisetin on EMT markers E-cadherin, Claudin, N-Cadherin, Vimentin and related transcription factor Snail, were also abrogated by PTEN silence (Figure 4B). Intriguingly, anti-proliferation (Figure 4C), anti-migration (Figure 4D), and anti-invasion (Figure 4E) effects of 100  $\mu$ M fisetin was counteracted by the silence of PTEN.

### Fisetin Inhibited the Growth and Metastasis of TNBC *in Vivo*

To evaluate the anti-proliferation and anti-metastasis potential of fisetin *in vivo*, we used the xenograft metastasis tumor model bearing MDA-MB-231 cells. Results indicated that the primary tumors isolated from fisetin-fed mice exhibited a dramatic decrease in tumor growth volume (Figure 5A) and weight (Figure 5B) comparing with the control group. IHC staining of Ki-67 on the primary tumor tissues also clarified that fisetin could



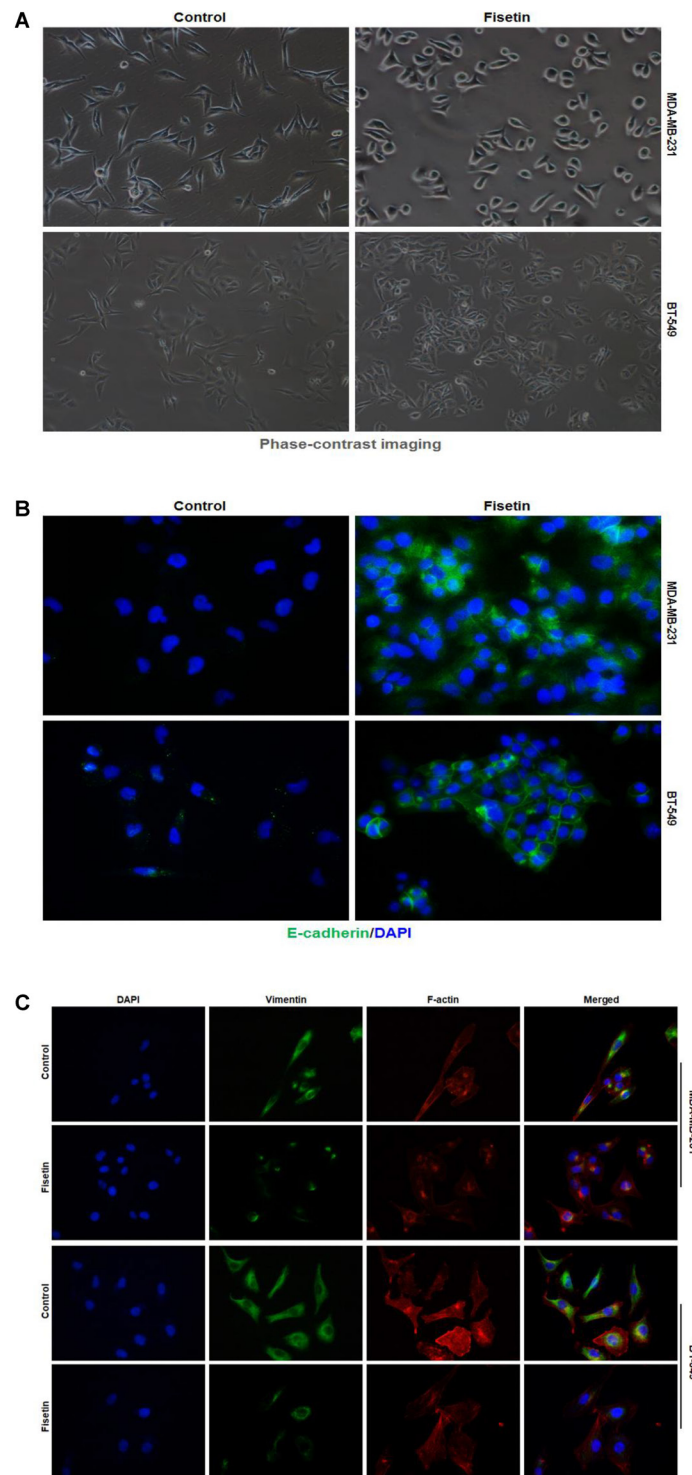


**FIGURE 2 |** Continued

significantly reduce the area of cancer nests and decrease the proliferation ability of breast cancer cells (**Figure 5C**). Moreover, we found the number of the prominent metastatic nodules on the surface of lungs were less in fisetin-treated mice than control

mice (**Figure 5D**). HE staining of lung tissue sections isolated from mice received orthotopic transplantation also showed that fisetin dramatically suppressed TNBC cells metastases to the lung (**Figure 5E**).



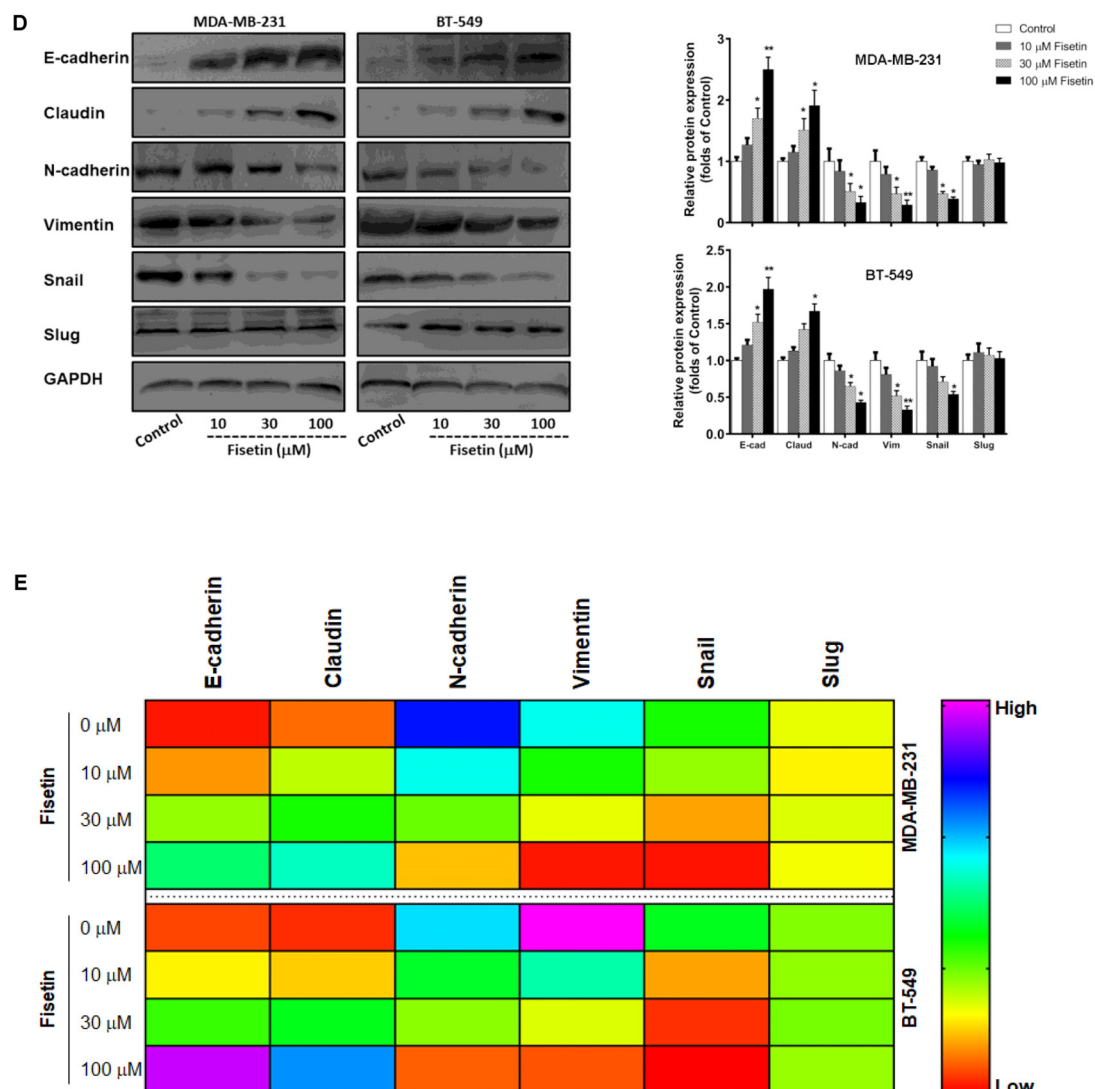


**FIGURE 2 |** Fisetin reverses EMT in TNBC cells *in vitro*. TNBC cell lines MDA-MB-231 and BT549 were treated with vehicle or fisetin for 24 h. **(A)** The morphology of the cells treated with vehicle or 30 μM fisetin was observed by phase-contrast microscopy. **(B)** E-cadherin and **(C)** Vimentin and F-actin expression were evaluated by immunofluorescence in TNBC cells treated by vehicle or 30 μM fisetin. The cells pretreated with vehicle or various concentrations of fisetin (10, 30, and 100 μM, respectively) were subjected to western blot for the indicated proteins **(D)** and qRT-PCR for the indicated mRNA **(E)**. The results are shown as the mean ± SD of three experiments, \* $P < 0.05$ , \*\* $P < 0.01$  compared with control.

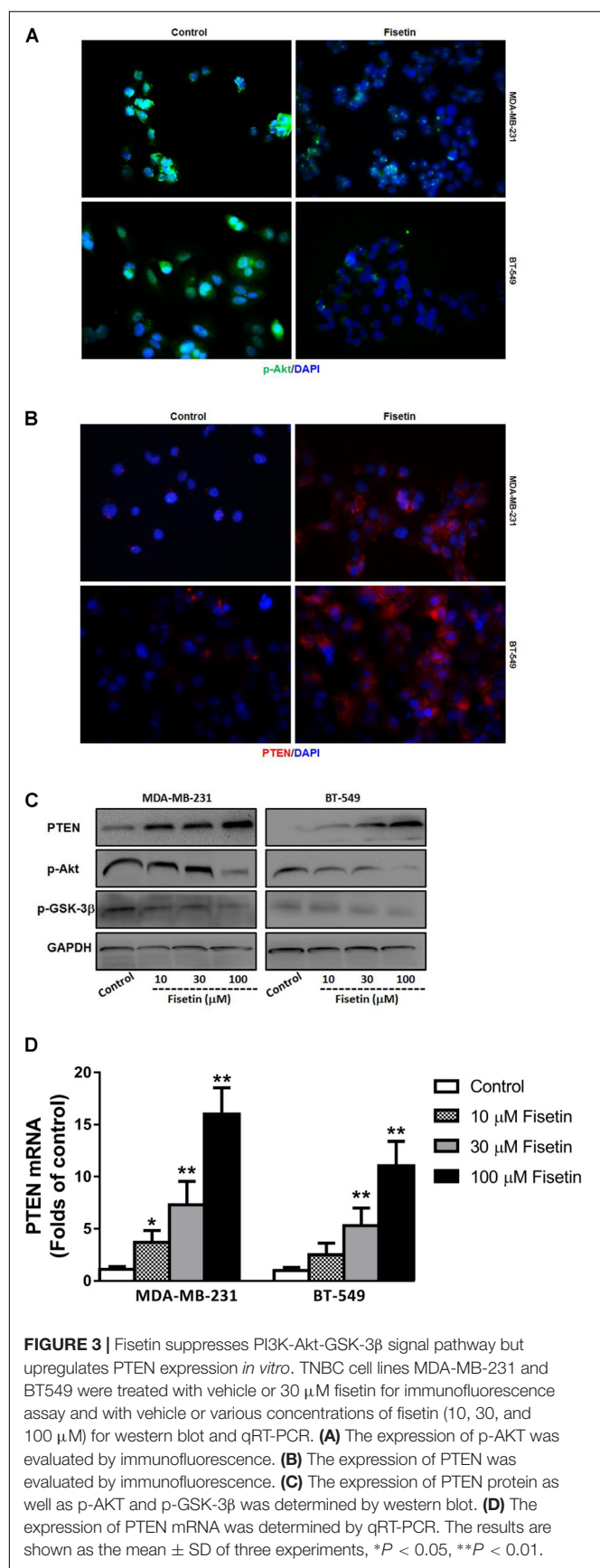
## Fisetin Inhibited PTEN-Akt-GSK-3β Signaling Pathway and Reversed EMT *in Vivo*

To confirm the pathophysiological relevance of our *in vitro* observations, we examined the related signal molecules in tumor tissues of xenografted model implanted with MDA-MB-231 cells. In agreement with the *in vitro* results, IHC analysis of the xenograft primary tumor tissues revealed an apparent down-regulation of p-Akt (**Figure 6A**) and upregulation of PTEN (**Figure 6B**) in fisetin-treated group. In addition, immunofluorescent analysis showed that mesenchymal marker molecule Vimentin and transcription factor Snail were significantly inhibited by fisetin compared with xenografted

model mice (**Figure 6C**). Coincident with the results above, western blot analysis showed that PTEN as well as the epithelial markers E-cadherin and Claudin were increased but p-Akt and p-GSK3β and the mesenchymal markers N-cadherin, Vimentin with the EMT transcription factor Snail were decreased in the orthotopic tumor tissues of mice after fisetin treatment (**Figures 6D,E**).

## DISCUSSION

Nowadays, breast cancer is no longer considered as a single disease but a systemic diseases, and the complete diagnosis dependent on the histopathology report of the tumor which



assess the presence or absence of the hormone receptors for estrogen (ER), progesterone (PR), and the human epidermal growth factor receptor-2 (HER-2) (Shaikh et al., 2016). Therefore, it is a heterogeneous disease which can be divided into many different subtypes including luminal A and B, HER2-enriched, basal-like, and normal breast-like (Tao et al., 2014). These factors are the basis for us to choose therapy strategy, because some of these factors have been associated with the survival rate of patients and their clinical outcome after treatment (Hernandez-Aya and Gonzalez-Angulo, 2013). However, in all of the molecular subtypes, triple-negative breast cancer (TNBC) which is characterized by a loss of ER, PR and HER-2 is the most tough situation and the total number of the patients approximately accounts for 10–20% of all breast cancer patients that is not a small percentage that can be ignored (Boyle, 2012). Patients with TNBC usually have a poor prognosis and high rates of metastasis because of the lack of targets for endocrinotherapy and targeted therapy (Li et al., 2016), chemotherapy is the major treatment they can take after surgery. However, the generation of chemoresistance leads the anti-cancer treatment into a dilemma. Fisetin, a structurally distinct chemical substance that belongs to the flavonoid group of polyphenols, has been reported to exert the beneficial effects on anti-cancer (Murtaza et al., 2009; Szliszka et al., 2011; Chou et al., 2013). In breast cancer, there are several studies confirm that fisetin can induce cell cycle arrest, caspase-dependent apoptosis, inhibit autophagy, and enhance cytotoxicity of chemotherapeutic agents (Yang et al., 2012; Smith et al., 2016). As indicated in this study, fisetin effectively inhibited the proliferation, migration and invasion of MDA-MB-231 and BT549 cells, and suppressed the growth and lung metastasis of breast cancer in the xenograft model bearing MDA-MB-231 cells, indicating that fisetin may be used as an effective drug for treatment of metastatic TNBC patients.

Triple negative breast cancer, a subtype of breast cancer characterized by its highly aggressive and metastatic features, has been proved to have close relationship with EMT. The promotion of EMT programs apparently drives TNBC metastasis partly by eliciting cytoskeleton rebuilding from apical-basolateral polarities characteristic of epithelial cells to the synthesis of actin stress fibers characteristic of mesenchymal cells (Taylor et al., 2013), during which, the morphology, motility and polarity all perform a dramatic shift, and at the molecule level, the epithelial markers E-cadherin and Claudin are lost and the mesenchymal markers Vimentin and N-cadherin are gained (Ombrato and Malanchi, 2014). When the EMT process was inhibited by miRNAs or the silence of the transcription factors, metastasis of TNBC was reversed at the same time (Rhodes et al., 2014; Lv et al., 2016). As have been proved that fisetin had the certain potential on inhibition of migration and invasion in TNBC, we supposed whether the anti-metastasis function was associated with EMT. So in the present study, we detected the EMT related biomarkers in MDA-MB-231 and BT549 cells, and found that after being treated with fisetin, both of the two cell lines acquired epithelial features and lost mesenchymal phenotype, which was coincident with the previous reports describing that fisetin-inhibited EMT in nasopharyngeal

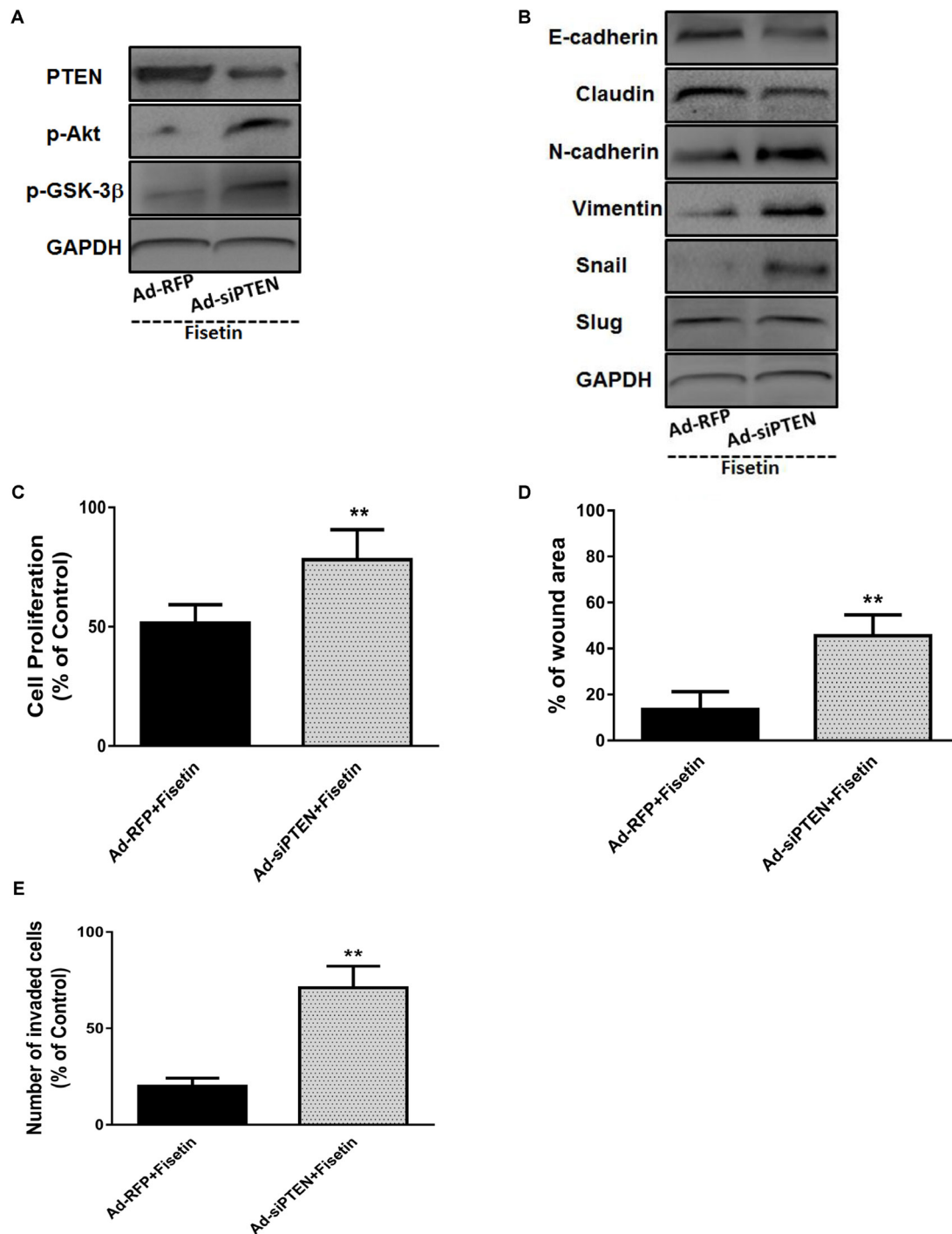


**FIGURE 4 |** Silencing of PTEN abrogates the effects of fisetin on TNBC cells proliferation and metastasis as well as EMT. TNBC cell line MDA-MB-231 cells were transfected with Ad-RFP or Ad-siPTEN, and subsequently treated with fisetin (100  $\mu$ M). **(A)** The expression of PTEN and p-AKT and p-GSK-3 $\beta$  protein was determined by western blot. **(B)** EMT molecule markers were determined by western blot. **(C)** The cell proliferation was determined by MTT assay. **(D)** The cell migration was determined by wound-healing assay. **(E)** The cell invasion was determined by transwell invasion assay. The results are shown as the mean  $\pm$  SD of three experiments, \* $P$  < 0.05, \*\* $P$  < 0.01 compared with control.

carcinoma cells and prostate cancer cells, respectively (Khan et al., 2014; Li et al., 2014). *In vivo* experiments, we also got the same results in primary tumor and metastatic lung tissues.

Furthermore, we detected the expression of two major EMT-related transcription factors Snail and Slug and found that fisetin also dose-dependently inhibited the expression of Snail.

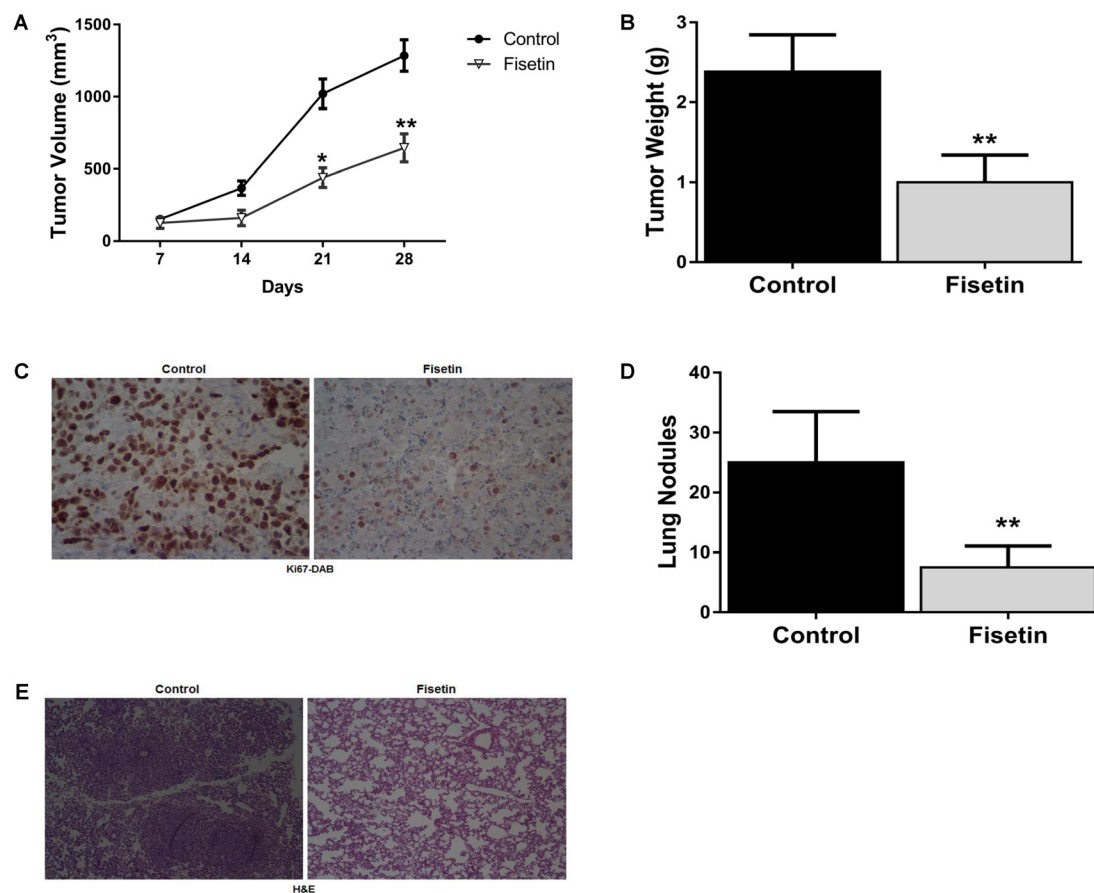


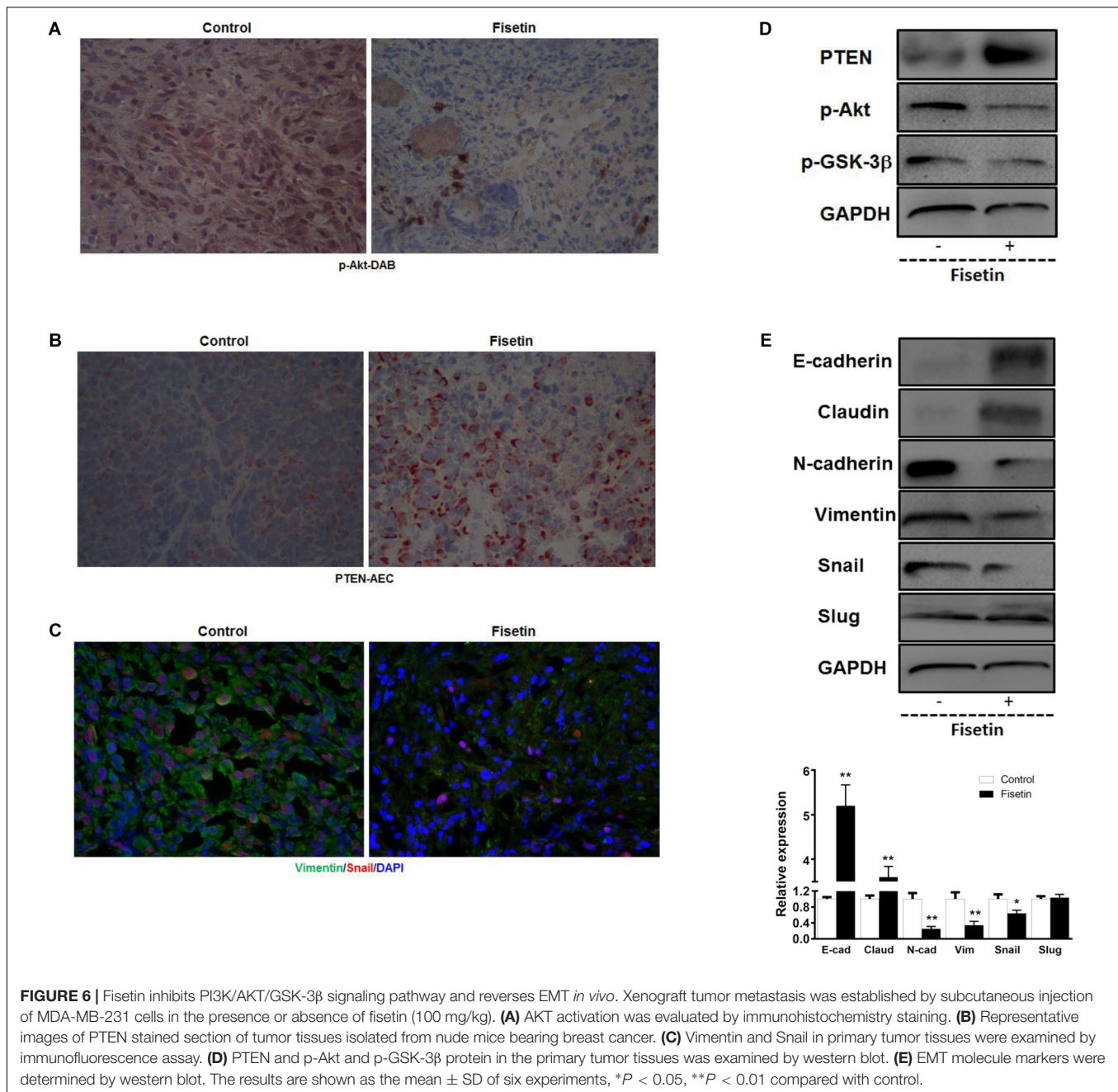
**FIGURE 5 |** Fisetin inhibits the growth and metastasis of TNBC *in vivo*. Xenograft breast cancer model was established by subcutaneous injection of MDA-MB-231 cells in the presence or absence of fisetin (100 mg/kg). **(A)** Tumor growth curve was recorded. **(B)** Tumor weight was measured. **(C)** The expression of Ki67 in the primary tumor tissues was evaluated by immunohistochemistry staining. **(D)** Metastatic tumor nodules on the surface of lungs were counted. **(E)** Representative images of HE staining in the metastatic nodules of lungs. The results are shown as the mean  $\pm$  SD of six experiments, \* $P < 0.05$ , \*\* $P < 0.01$  compared with control.

All these data demonstrated that the inhibitory effect of fisetin on metastasis of TNBC is closely connected with reversion of EMT.

Cancer metastasis and EMT are complicated processes regulated by numerous chiasmatic signaling pathways such as Wnt/ $\beta$ -catenin, hedgehog, and PI3K/Akt signaling pathways. Among these signal pathways, PI3K/Akt pathway is one of the major regulators. In breast cancer, a number of researches have reported that once PI3K/Akt pathway is inhibited, cancer metastasis will be suppressed at the same time (Ren et al., 2014; Chang et al., 2016). Akt can be activated by the lipid kinase PI3K through generating the second messenger PIP3 (phosphatidylinositol-3,4,5- triphosphate). GSK-3 $\beta$  is an important downstream molecule of Akt, which has close relationship with cellular proliferation, migration, apoptosis, cell cycle and glucose regulation (Ali et al., 2001; Umezawa et al., 2016). Activation of the PI3K-Akt-GSK-3 $\beta$  signaling pathway makes the downstream transcription factor Snail more stable to repress the expression of gene CDH 1 encoding E-cadherin, promoting EMT process (Lamouille et al., 2014). PTEN (phosphatase and tensin homolog deleted on chromosome

10) is a well-known tumor suppressing gene and the deletion or mutation of PTEN is usually involved in tumor development (Keniry and Parsons, 2008). PTEN emerges the anti-cancer effects partly because it can negatively regulate PI3Ks via dephosphorylating PIP3 into PIP2 (phosphatidylinositol- 4,5- biphosphate) (Chalhoub and Baker, 2009). PTEN level and function are regulated transcriptionally, post-transcriptionally, and post-translationally. On transcriptional level, it can be positively regulated by a wealth of transcription factors, such as early growth response protein 1 (EGFR-1), peroxisome proliferator activated receptor  $\gamma$  (PPAR- $\gamma$ ), and tumor protein 53 (Tp53), which can directly bind to PTEN promoter region, while other transcription factors show the negative regulation of PTEN in several cancer models, such as mitogen activated protein kinase kinase-4 (MKK4), transforming growth factor  $\beta$  (TGF- $\beta$ ), and the polycomb group (PcG) protein BMI1 (Bermudez Brito et al., 2015). In breast cancer, PTEN expression also can be suppressed by promoter methylation (Garcia et al., 2004). Histone modifications is another epigenetic mechanism by which PTEN expression can be suppressed (Mirmohammadsadegh





et al., 2006). On post-transcriptionally level, miRNAs play an important role on the regulation of PTEN expression. Dong et al. (2014) have demonstrated that the upregulated miR-21 reduced the PTEN expression in TNBC. In this study, using MDA-MB-231 and BT549 cells, we firstly demonstrated the expression of PTEN could be dose-dependently up-regulated by fisetin at mRNA and protein levels, along with the reduction of p-Akt and p-GSK-3 $\beta$  activation. And *in vivo*, with the breast cancer xenograft model bearing MDA-MB-231 cells, we further found that fisetin also apparently up-regulated the expression of PTEN and inhibited p-Akt in primary tumor tissues. According to this arresting discovery, coupled with the subtle relationship between

PTEN-Akt-GSK-3 $\beta$  signaling and EMT and tumor metastasis, we speculated that the anti-metastasis effect of fisetin on breast cancer was mediated by PTEN-Akt-GSK-3 $\beta$  signaling pathway, and in which, PTEN was the most important kernel molecule. To prove this hypothesis, we used siRNA to make PTEN silenced in MDA-MB-231 cells before fisetin intervention, and found that the restraint effects of fisetin on metastasis and EMT was counteracted, implying that up-regulation of PTEN expression is the key point to the inhibitory function of fisetin on tumor metastasis and EMT. But how PTEN was upregulated by fisetin should be further researched. It may through suppressing the negative transcription factors or miRNAs, or promoting the

positive transcription factors, or interfering in the epigenetic modification way.

## CONCLUSION

Our present study authenticated that the natural flavonoid fisetin manifested a potential agonistic activity on metastasis of TNBC, which might be the results from reversing of EMT by inhibition of PTEN-Akt-GSK-3 $\beta$  signaling pathway. These findings provided supporting evidence to make fisetin to be recognized as a novel potential therapeutic agent for the treatment of TNBC patients with metastatic breast cancer.

## REFERENCES

- Ali, A., Hoeflich, K. P., and Woodgett, J. R. (2001). Glycogen synthase kinase-3: properties, functions, and regulation. *Chem. Rev.* 101, 2527–2540. doi: 10.1021/cr000110o
- Banyard, J., and Bielenberg, D. R. (2015). The role of EMT and MET in cancer dissemination. *Connect. Tissue Res.* 56, 403–413. doi: 10.3109/03008207.2015.1060970
- Bermudez Brito, M., Goulielmaki, E., and Papakonstanti, E. A. (2015). Focus on PTEN Regulation. *Front. Oncol.* 5:166. doi: 10.3389/fonc.2015.00166
- Bhat, T. A., Nambiar, D., Pal, A., Agarwal, R., and Singh, R. P. (2012). Fisetin inhibits various attributes of angiogenesis in vitro and in vivo—implications for angioprevention. *Carcinogenesis* 33, 385–393. doi: 10.1093/carcin/bgr282
- Boyle, P. (2012). Triple-negative breast cancer: epidemiological considerations and recommendations. *Ann. Oncol.* 23(Suppl. 6), vi7–vi12. doi: 10.1093/annonc/mds187
- Chalhoub, N., and Baker, S. J. (2009). PTEN and the PI3-kinase pathway in cancer. *Annu. Rev. Pathol.* 4, 127–150. doi: 10.1146/annurev.pathol.4.110807.092311
- Chang, C. H., Ou, T. T., Yang, M. Y., Huang, C. C., and Wang, C. J. (2016). *Nelumbo nucifera* Gaertn leaves extract inhibits the angiogenesis and metastasis of breast cancer cells by downregulation connective tissue growth factor (CTGF) mediated PI3K/AKT/ERK signaling. *J. Ethnopharmacol.* 188, 111–122. doi: 10.1016/j.jep.2016.05.012
- Chou, R. H., Hsieh, S. C., Yu, Y. L., Huang, M. H., Huang, Y. C., and Hsieh, Y. H. (2013). Fisetin inhibits migration and invasion of human cervical cancer cells by down-regulating urokinase plasminogen activator expression through suppressing the p38 MAPK-dependent NF-kappaB signaling pathway. *PLoS One* 8:e71983. doi: 10.1371/journal.pone.0071983
- Dong, G., Liang, X., Wang, D., Gao, H., Wang, L., Wang, L., et al. (2014). High expression of miR-21 in triple-negative breast cancers was correlated with a poor prognosis and promoted tumor cell in vitro proliferation. *Med. Oncol.* 31:57. doi: 10.1007/s12032-014-0057-x
- Garcia, J. M., Silva, J., Pena, C., Garcia, V., Rodriguez, R., Cruz, M. A., et al. (2004). Promoter methylation of the PTEN gene is a common molecular change in breast cancer. *Genes Chromosomes Cancer* 41, 117–124. doi: 10.1002/gcc.20062
- Hernandez-Aya, L. F., and Gonzalez-Angulo, A. M. (2013). Adjuvant systemic therapies in breast cancer. *Surg. Clin. North Am.* 93, 473–491. doi: 10.1016/j.suc.2012.12.002
- Huang, J., Li, H., and Ren, G. (2015). Epithelial-mesenchymal transition and drug resistance in breast cancer (Review). *Int. J. Oncol.* 47, 840–848. doi: 10.3892/ijo.2015.3084
- Kang, K. A., Piao, M. J., and Hyun, J. W. (2015). Fisetin induces apoptosis in human nonsmall lung cancer cells via a mitochondria-mediated pathway. *In Vitro Cell. Dev. Biol. Anim.* 51, 300–309. doi: 10.1007/s11626-014-9830-6
- Keniry, M., and Parsons, R. (2008). The role of PTEN signaling perturbations in cancer and in targeted therapy. *Oncogene* 27, 5477–5485. doi: 10.1038/onc.2008.248
- Khan, M. I., Adhami, V. M., Lall, R. K., Sechi, M., Joshi, D. C., Haidar, O. M., et al. (2014). YB-1 expression promotes epithelial-to-mesenchymal transition in prostate cancer that is inhibited by a small molecule fisetin. *Oncotarget* 5, 2462–2474. doi: 10.18632/oncotarget.1790

## AUTHOR CONTRIBUTIONS

All authors listed have contributed to the work and approved it for publication. JW, GK, and HL conceived and designed the experiments. JL, XG, RJ, DL, HL, and TZ performed the experiments. XG, JW, GK, and JL analyzed the data. JL, JW, and HL wrote the paper.

## FUNDING

This research was supported by grants from the National Natural Science Foundation of China (No. 81472475).

- Khan, N., Afaq, F., Khusro, F. H., Mustafa Adhami, V., Suh, Y., and Mukhtar, H. (2012). Dual inhibition of phosphatidylinositol 3-kinase/Akt and mammalian target of rapamycin signaling in human nonsmall cell lung cancer cells by a dietary flavonoid fisetin. *Int. J. Cancer* 130, 1695–1705. doi: 10.1002/ijc.26178
- Khan, N., Syed, D. N., Ahmad, N., and Mukhtar, H. (2013). Fisetin: a dietary antioxidant for health promotion. *Antioxid. Redox Signal.* 19, 151–162. doi: 10.1089/ars.2012.4901
- Lamouille, S., Xu, J., and Derynck, R. (2014). Molecular mechanisms of epithelial-mesenchymal transition. *Nat. Rev. Mol. Cell Biol.* 15, 178–196. doi: 10.1038/nrm3758
- Lehmann, B. D., and Pietenpol, J. A. (2014). Identification and use of biomarkers in treatment strategies for triple-negative breast cancer subtypes. *J. Pathol.* 232, 142–150. doi: 10.1002/path.4280
- Li, J., Cheng, Y., Qu, W., Sun, Y., Wang, Z., Wang, H., et al. (2011). Fisetin, a dietary flavonoid, induces cell cycle arrest and apoptosis through activation of p53 and inhibition of NF-kappa B pathways in bladder cancer cells. *Basic Clin. Pharmacol. Toxicol.* 108, 84–93. doi: 10.1111/j.1742-7843.2010.00613.x
- Li, P., Sun, T., Yuan, Q., Pan, G., Zhang, J., and Sun, D. (2016). The expressions of NEDD9 and E-cadherin correlate with metastasis and poor prognosis in triple-negative breast cancer patients. *Oncotargets Ther.* 9, 5751–5759. doi: 10.2147/OTT.S113768
- Li, R., Zhao, Y., Chen, J., Shao, S., and Zhang, X. (2014). Fisetin inhibits migration, invasion and epithelial-mesenchymal transition of LMP1-positive nasopharyngeal carcinoma cells. *Mol. Med. Rep.* 9, 413–418. doi: 10.3892/mmr.2013.1836
- Lv, Z. D., Kong, B., Liu, X. P., Jin, L. Y., Dong, Q., Li, F. N., et al. (2016). miR-655 suppresses epithelial-to-mesenchymal transition by targeting Prrx1 in triple-negative breast cancer. *J. Cell. Mol. Med.* 20, 864–873. doi: 10.1111/jcmm.12770
- Maurya, B. K., and Trigun, S. K. (2017). Fisetin attenuates AKT associated growth promoting events in aflatoxinb1 induced hepatocellular carcinoma. *Anticancer Agents Med. Chem.* doi: 10.2174/1871520618666171229223335 [Epub ahead of print].
- Mirmohammadsadegh, A., Marini, A., Nambiar, S., Hassan, M., Tannapfel, A., Ruzicka, T., et al. (2006). Epigenetic silencing of the PTEN gene in melanoma. *Cancer Res.* 66, 6546–6552. doi: 10.1158/0008-5472.CAN-06-0384
- Moyret-Lalle, C., Ruiz, E., and Puisieux, A. (2014). Epithelial-mesenchymal transition transcription factors and miRNAs: “plastic surgeons” of breast cancer. *World J. Clin. Oncol.* 5, 311–322. doi: 10.5306/wjco.v5.i3.311
- Murtaza, I., Adhami, V. M., Hafeez, B. B., Saleem, M., and Mukhtar, H. (2009). Fisetin, a natural flavonoid, targets chemoresistant human pancreatic cancer AsPC-1 cells through DR3-mediated inhibition of NF-kappaB. *Int. J. Cancer* 125, 2465–2473. doi: 10.1002/ijc.24628
- Nickel, A., and Stadler, S. C. (2015). Role of epigenetic mechanisms in epithelial-to-mesenchymal transition of breast cancer cells. *Transl. Res.* 165, 126–142. doi: 10.1016/j.trsl.2014.04.001
- Nieto, M. A., Huang, R. Y., Jackson, R. A., and Thiery, J. P. (2016). EMT: 2016. *Cell* 166, 21–45. doi: 10.1016/j.cell.2016.06.028
- Omrato, L., and Malanchi, I. (2014). The EMT universe: space between cancer cell dissemination and metastasis. *Crit. Rev. Oncog.* 19, 349–361. doi: 10.1615/CritRevOncog.2014011802

- Pal, H. C., Pearlman, R. L., and Afaq, F. (2016). Fisetin and its role in chronic diseases. *Adv. Exp. Med. Biol.* 928, 213–244. doi: 10.1007/978-3-319-41334-1\_10
- Rasool, M., Malik, A., and Manan, A. (2015). Roles of natural compounds from medicinal plants in cancer treatment: structure. *Med. Chem.* 11, 618–628. doi: 10.2174/1573406411666150430120038
- Ren, W., Liu, Y., Wan, S., Fei, C., Wang, W., Chen, Y., et al. (2014). BMP9 inhibits proliferation and metastasis of HER2-positive SK-BR-3 breast cancer cells through ERK1/2 and PI3K/AKT pathways. *PLoS One* 9:e96816. doi: 10.1371/journal.pone.0096816
- Rengarajan, T., and Yaacob, N. S. (2016). The flavonoid fisetin as an anticancer agent targeting the growth signaling pathways. *Eur. J. Pharmacol.* 789, 8–16. doi: 10.1016/j.ejphar.2016.07.001
- Rhodes, L. V., Tate, C. R., Segar, H. C., Burks, H. E., Phamduy, T. B., Hoang, V., et al. (2014). Suppression of triple-negative breast cancer metastasis by pan-DAC inhibitor panobinostat via inhibition of ZEB family of EMT master regulators. *Breast Cancer Res. Treat.* 145, 593–604. doi: 10.1007/s10549-014-2979-6
- Sechi, M., Syed, D. N., Pala, N., Mariani, A., Marceddu, S., Brunetti, A., et al. (2016). Nanoencapsulation of dietary flavonoid fisetin: formulation and in vitro antioxidant and alpha-glucosidase inhibition activities. *Mater. Sci. Eng. C Mater. Biol. Appl.* 68, 594–602. doi: 10.1016/j.msec.2016.06.042
- Shaikh, F., Jamal, Q., Baig, S., Hadi, N. I., Majeed, N. (2016). Correlation of hormone receptor and HER2/neu expression with clinicopathologic. *Asian Pac. J. Cancer Prev.* 17, 3363–3367.
- Smith, M. L., Murphy, K., Doucette, C. D., Greenshields, A. L., and Hoskin, D. W. (2016). The dietary flavonoid fisetin causes cell cycle arrest, caspase-dependent apoptosis, and enhanced cytotoxicity of chemotherapeutic drugs in triple-negative breast cancer cells. *J. Cell. Biochem.* 117, 1913–1925. doi: 10.1002/jcb.25490
- Syed, D. N., Chamcheu, J. C., Khan, M. I., Sechi, M., Lall, R. K., Adhami, V. M., et al. (2014). Fisetin inhibits human melanoma cell growth through direct binding to p70S6K and mTOR: findings from 3-D melanoma skin equivalents and computational modeling. *Biochem. Pharmacol.* 89, 349–360. doi: 10.1016/j.bcp.2014.03.007
- Szliszka, E., Helewski, K. J., Mizgala, E., and Krol, W. (2011). The dietary flavonol fisetin enhances the apoptosis-inducing potential of TRAIL in prostate cancer cells. *Int. J. Oncol.* 39, 771–779.
- Takebe, N., Warren, R. Q., and Ivy, S. P. (2011). Breast cancer growth and metastasis: interplay between cancer stem cells, embryonic signaling pathways and epithelial-to-mesenchymal transition. *Breast Cancer Res.* 13:211. doi: 10.1186/bcr2876
- Tao, Z., Shi, A., Lu, C., Song, T., Zhang, Z., and Zhao, J. (2014). Breast cancer: epidemiology and etiology. *Cell Biochem. Biophys.* 72, 333–338. doi: 10.1007/s12013-014-0459-6
- Taylor, M. A., Davuluri, G., Parvani, J. G., Schiemann, B. J., Wendt, M. K., Plow, E. F., et al. (2013). Upregulated WAVE3 expression is essential for TGF-beta-mediated EMT and metastasis of triple-negative breast cancer cells. *Breast Cancer Res. Treat.* 142, 341–353. doi: 10.1007/s10549-013-2753-1
- Torre, L. A., Bray, F., Siegel, R. L., Ferlay, J., Lortet-Tieulent, J., and Jemal, A. (2015). Global cancer statistics, 2012. *CA Cancer J. Clin.* 65, 87–108. doi: 10.3322/caac.21262
- Umezawa, Y., Kurosu, T., Akiyama, H. (2016). Down regulation of Chk1 by p53 plays a role in synergistic induction of apoptosis by chemotherapeutics and inhibitors for Jak2 or BCR/ABL in hematopoietic cells. *Oncotarget* 7, 44448–44461. doi: 10.18632/oncotarget.9844
- Wculek, S. K., and Malanchi, I. (2015). Neutrophils support lung colonization of metastasis-initiating breast cancer cells. *Nature* 528, 413–417. doi: 10.1038/nature16140
- Yang, P. M., Tseng, H. H., Peng, C. W., Chen, W. S., and Chiu, S. J. (2012). Dietary flavonoid fisetin targets caspase-3-deficient human breast cancer MCF-7 cells by induction of caspase-7-associated apoptosis and inhibition of autophagy. *Int. J. Oncol.* 40, 469–478.

**Conflict of Interest Statement:** The authors declare that the research was conducted in the absence of any commercial or financial relationships that could be construed as a potential conflict of interest.

Copyright © 2018 Li, Gong, Jiang, Lin, Zhou, Zhang, Li, Zhang, Wan, Kuang and Li. This is an open-access article distributed under the terms of the Creative Commons Attribution License (CC BY). The use, distribution or reproduction in other forums is permitted, provided the original author(s) and the copyright owner(s) are credited and that the original publication in this journal is cited, in accordance with accepted academic practice. No use, distribution or reproduction is permitted which does not comply with these terms.



# miR-374a Regulates Inflammatory Response in Diabetic Nephropathy by Targeting MCP-1 Expression

Zijun Yang<sup>1†</sup>, Zuishuang Guo<sup>1†</sup>, Ji Dong<sup>2</sup>, Shifeng Sheng<sup>1</sup>, Yulin Wang<sup>1</sup>, Lu Yu<sup>1</sup>, Hongru Wang<sup>1</sup> and Lin Tang<sup>1\*</sup>

<sup>1</sup> Department of Nephropathy, The First Affiliated Hospital of Zhengzhou University, Zhengzhou, China, <sup>2</sup> Henan Medical College, Zhengzhou, China

## OPEN ACCESS

### Edited by:

Cecilia Battistelli,  
Sapienza Università di Roma, Italy

### Reviewed by:

Melania Dovizio,  
Università degli Studi "G. d'Annunzio"  
Chieti - Pescara, Italy  
Emanuela Marcantoni,  
New York University, United States

### \*Correspondence:

Lin Tang  
tanglin@zzu.edu.cn

<sup>†</sup>These authors have contributed  
equally to this work as co-first authors

### Specialty section:

This article was submitted to  
Inflammation Pharmacology,  
a section of the journal  
Frontiers in Pharmacology

Received: 05 May 2018

Accepted: 23 July 2018

Published: 10 August 2018

### Citation:

Yang Z, Guo Z, Dong J, Sheng S,  
Wang Y, Yu L, Wang H and Tang L  
(2018) miR-374a Regulates  
Inflammatory Response in Diabetic  
Nephropathy by Targeting MCP-1  
Expression. *Front. Pharmacol.* 9:900.  
doi: 10.3389/fphar.2018.00900

The microRNA (mir)-374a has been implicated in several types of human cancer; however, its role in diabetic nephropathy (DN) remains unclear. Monocyte chemoattractant protein (MCP)-1 is a chemokine that recruits macrophages to inflammatory sites and is important for the development and progression of DN. However, the relationship between miR-374a and MCP-1 in DN is unknown. We addressed this in the present study by examining the expression of these factors in kidney tissue samples from DN patients and through loss- and gain-of-function experiments using HK2 human renal tubular epithelial cells. We found that miR-374a was downregulated whereas MCP-1 was upregulated in DN tissue. A bioinformatics analysis revealed that MCP-1 is a putative target of miR-374a. To confirm this relationship, HK2 cells treated with normal glucose (5.6 mmol/l D-glucose), high glucose (HG) (30 mmol/l D-glucose), or high osmotic pressure solution (5.6 mmol/l D-glucose + 24.4 mmol/l D-mannitol) were transfected with miR-374a mimic or inhibitor. miR-374a mimic reduced MCP-1 mRNA expression and migration of co-cultured U937 cells, whereas miR-374a inhibition had the opposite effects. Additionally, interleukin-6 and -18 and tumor necrosis factor- $\alpha$  levels were downregulated by transfection of miR-374a mimic. On the other hand, MCP-1 overexpression reversed the inhibitory effects of miR-374a in HK2 cells. Thus, miR-374a suppresses the inflammatory response in DN through negative regulation of MCP-1 expression. These findings suggest that therapeutic strategies that target the miR-374a/MCP-1 axis can be an effective treatment for DN.

**Keywords:** miR-374a, diabetic nephropathy, MCP-1, inflammatory response, high glucose

## INTRODUCTION

Diabetic nephropathy (DN) is one of the major microvascular complications associated with diabetic patients. Approximately 15–25% of type 1 diabetes and 30–40% of type 2 diabetes develop DN, which is the main cause of end-stage renal disease (ESRD) (Scherthaner and Scherthaner, 2013). The United States Renal Data System reported that type 2 DN accounts for 35–50% of ESRD cases (Collins et al., 2014). There are currently no treatments for DN other than symptomatic relief such as blood pressure and glucose control, administration of renin-angiotensin-aldosterone inhibitors, and dialysis and kidney transplantation. None of these treatments has reduced the high



morbidity and mortality rates associated with DN, resulting in a significant health care burden for society (Lopez-Vargas et al., 2016). Patients undergoing dialysis have a mortality rate of 20% per year, and transplantation is restricted by the lack of renal allografts (DeFronzo et al., 2017). Clarifying the mechanism underlying DN and developing novel and effective therapeutic strategies is critical for improving disease outcome.

Recent studies have demonstrated an important role for inflammation in the development and progression of DN (Feng et al., 2015; Sancar-Bas et al., 2015; Zheng and Zheng, 2016). Glomerular sclerosis and interstitial fibrosis are the major pathological changes associated with DN, and renal biopsies suggest that macrophage infiltration and elevated levels of inflammatory cytokines are closely associated with kidney fibrosis. Inflammatory factors can activate myofibroblasts at injury sites in the kidney while inducing the differentiation of mesangial cells, glomeruli, and renal tubular epithelial cells into fibroblasts, resulting in enhanced extracellular matrix (ECM) production and deposition, which in turn promote tubulointerstitial fibrosis (Kanasaki et al., 2013; Maeshima et al., 2014).

Elevated levels of monocyte chemoattractant protein (MCP)-1 in type 1 and 2 DN patients have been linked to DN development (Banba et al., 2000) through recruitment of macrophages and monocytes to inflammatory sites and upregulation of cytokines such as interleukin (IL)-1, -6, -8, and tumor necrosis factor (TNF)- $\alpha$ . MCP-1 expression is induced by hyperglycemia, lipid metabolism, advanced glycation end products, overstimulation of the renin-angiotensin system, oxidative stress, and nuclear factor (NF)- $\kappa$ B signaling (Wei et al., 2015) in DN patients.

MicroRNAs (miRNAs) are endogenous non-coding RNAs 20–25 nucleotides in length that negatively regulate gene expression in animals and plants by targeting the 3' untranslated region (3'-UTR) of target mRNA (Cai et al., 2013). Aberrant miRNA expression has been reported in several kidney conditions including DN, polycystic kidney disease, renal fibrosis, drug-induced kidney injury, and kidney transplantation (Cardenas-Gonzalez et al., 2017; Celen et al., 2017; Cho et al., 2017; Huttenhofer and Mayer, 2017; Wonnacott et al., 2017; Yheskel and Patel, 2017; Zununi et al., 2017). miRNAs participate in positive or negative feedback loops by targeting NF- $\kappa$ B, I $\kappa$ B, inhibitor of I $\kappa$ B kinase (IKK) (Ma et al., 2011). Members of the miR-184, -29, and -200 families as well as miR-192 and miR-21 have also been implicated in fibrotic processes in DN (Kato and Natarajan, 2014, 2015; McClelland et al., 2014; Rudnicki et al., 2015; Zanchi et al., 2017).

miR-374a has been reported to be involved in many types of cancer. For example, miR-374a suppresses lung adenocarcinoma cell proliferation and invasion by targeting transforming growth factor (TGF)- $\alpha$  gene expression (Wu et al., 2016), whereas in gastric cancer, miR-374a level is increased and targets SRC kinase signaling inhibitor 1 to promote cell proliferation, migration, and invasion (Xu et al., 2015). miR-374a also negatively regulates WNT5A, Wnt inhibitory factor 1, and phosphatase and tensin homolog to promote breast cancer epithelial-to-mesenchymal transition and metastasis *in vitro* and *in vivo* (Cai et al., 2013).

However, the molecular mechanism and function of miR-374a in DN is not known.

We addressed this in the present study by examining the expression of miR-374a and MCP-1 in kidney tissue samples from DN patients and performing loss- and gain-of-function experiments using HK2 human renal tubular epithelial cells. We found that miR-374a is downregulated in DN tissues and HK2 cells treated with high glucose (HG). We also confirmed that miR-374a suppresses the production of cytokines including IL-6 and -18, TNF- $\alpha$ , and MCP-1. These results indicate that miR-374a inhibits the inflammatory response via modulation of MCP-1 during DN progression.

## MATERIALS AND METHODS

### Clinical Samples and Immunohistochemistry

Human DN ( $n = 10$ ) and adjacent non-cancerous ( $n = 5$ ) tissue samples (3–5 cm from the tumor edge) were obtained from patients without diabetes mellitus or any other type of kidney disease who underwent surgical resection for kidney tumors at the First Affiliated Hospital of Zhengzhou University. The clinical characteristics of DN patients are shown in **Supplementary Table 1**. This study was approved by the Ethics Committee of the First Affiliated Hospital of Zhengzhou University. Kidney tissue sections approximately 4  $\mu$ m thick and embedded in paraffin were labeled with an antibody against MCP-1 using a commercial kit (Abcam, Cambridge, MA, United States). Brown positive staining in DN ( $n = 10$ ) and adjacent non-cancerous tissue ( $n = 5$ ) was semi-quantitatively scored based on density and area by an independent investigator in a blinded fashion.

### Hematoxylin and Eosin (HE) Staining

Kidney tissue samples were immersed in 4% paraformaldehyde for 4 h and then transferred to 70% ethanol. Individual lobes of renal biopsy specimens were placed in processing cassettes, dehydrated through a graded series of alcohol, and embedded in paraffin. The renal tissue blocks were cut into sections 4  $\mu$ m thick that were deparaffinized in xylene, rehydrated with decreasing concentrations of ethanol, washed in phosphate-buffered saline, and stained with HE. The sections were then dehydrated in increasing concentrations of ethanol and xylene and mounted for microscopic observation.

### Plasmid Construction and Luciferase Reporter Assay

The 3'-UTR sequence of MCP-1 was predicted to interact with miR-374a by bioinformatics analysis with TargetScan, Microna, and PicTar programs. Mutant (MT) and wild-type (WT) MCP-1 3'-UTR sequences were synthesized and inserted into the pmirGLO vector. pmirGLO-WT-MCP-1-3'-UTR or pmirGLO-MT-MCP-1-3'-UTR constructs were co-transfected into 293T cells with miR-374a mimic or a scrambled sequence (negative control). After 48 h, firefly and Renilla luciferase activities were measured using the Dual Luciferase Reporter Assay kit (Promega,

Beijing, China) according to the manufacturer's instructions. The assay was performed in triplicate.

## Cell Culture and Treatment

HK2 or U937 cells (Chinese Academy of Sciences Shanghai Cell Bank, Shanghai, China) were cultured in Dulbecco's modified Eagle's medium (DMEM) supplemented with 5.6 mmol/l glucose, 10% fetal bovine serum, 100 U/ml penicillin, and 100 µg/ml streptomycin in a 5% CO<sub>2</sub> incubator at 37°C. The cells were trypsinized and seeded in 6-well culture plates at a density of  $1 \times 10^6$ /ml and grown to over 80% confluence; cultures were

synchronized with serum-free medium for 12 h and used for experiments when they reached 70–80% confluence. HK2 cells were treated with normal glucose (NG; 5.6 mmol/l D-glucose), HG (30 mmol/l D-glucose), or high osmotic pressure solution (HO; 5.6 mmol/l D-glucose + 24.4 mmol/l D-mannitol).

## Quantitative Real-Time (qRT)-PCR

Total RNA was extracted and reverse transcribed into cDNA that was used as a template for qRT-PCR on a DNA Engine Opticon system (Fuzhong Bio-Company, Shanghai, China) in 96-well plates under the following reaction conditions: 95°C for

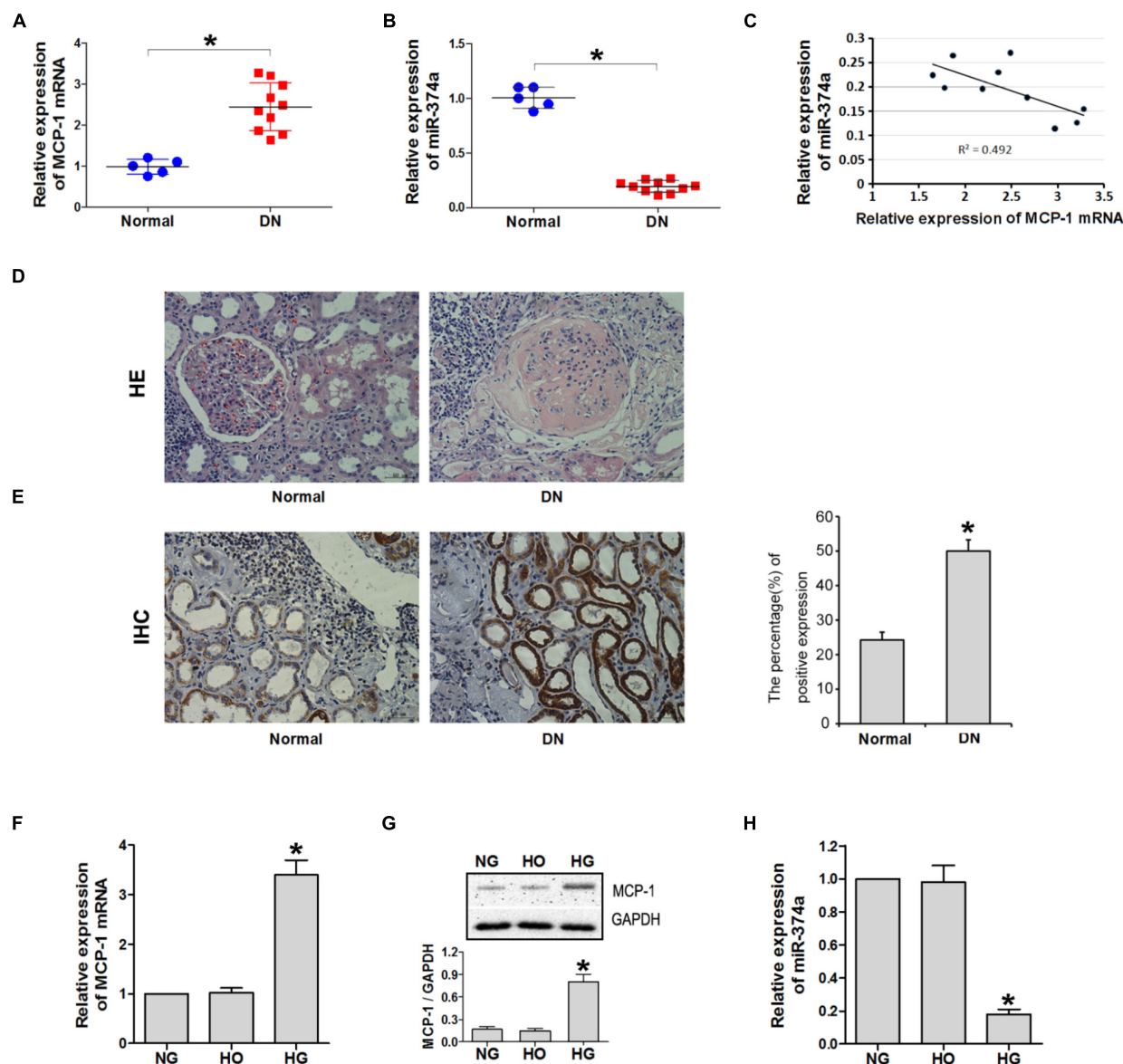


**FIGURE 1 |** MCP-1 and miR-374a expression in DN tissues. qRT-PCR analysis of MCP-1 mRNA (A) and miR-374a (B) levels in DN tissues. (C) Spearman's correlation analysis demonstrating an inverse correlation between miR-374a and MCP-1 mRNA levels. \* $P < 0.05$ . (D) Histological analysis of normal ( $n = 5$ ) and DN ( $n = 10$ ) tissues, as determined by HE staining. (E) Upregulation of MCP-1 in DN tissue, as determined by immunohistochemistry. HG induced MCP-1 but suppressed miR-374a in HK2 cells. (F) qRT-PCR and (G) western blot analysis of MCP-1 expression in HK2 cells treated with NG, HG, or HO for 24 h. \* $P < 0.05$  vs. NG or HO group ( $n = 3$ ). (H) miR-374a expression in each group as determined by qRT-PCR. \* $P < 0.05$  vs. NG group ( $n = 3$ ).

10 min, and 40 cycles at 95°C for 15 s and 60°C for 1 min. Glyceraldehyde 3-phosphate dehydrogenase (GAPDH) was used as an internal control to determine the relative expression levels of target genes; U6 small nuclear RNA served as an endogenous control for miR-374a. The  $2^{-\Delta\Delta C_t}$  method was used to normalize and calculate fold changes in gene expression.

## Western Blot Analysis

Cells were harvested and lysed in radioimmunoprecipitation assay buffer containing protease and phosphatase inhibitors and centrifuged at 12,000 rpm for 20 min at 4°C. Protein concentration was measured with the bicinchoninic acid assay (BCA). Briefly, 20  $\mu$ l of protein sample were added to 200  $\mu$ l BCA reagent, and absorbance at 590 nm was measured on a microplate reader. A standard curve was generated from the measured values and used to determine protein content. Protein samples in loading buffer were boiled at 100°C for 5 min and resolved by 12% sodium dodecyl sulfate polyacrylamide gel electrophoresis, and electrotransferred to a polyvinylidene difluoride membrane that was blocked with 5% skimmed milk and probed with a primary antibody against MCP-1 (Abcam; 1:500) for 12 h at 4°C. After washing, the membrane was incubated with an appropriate secondary antibody at room temperature for 2 h; 3'-diaminobenzidine was used for visualization. The ChemiDoc MP Imaging System (Bio-Rad, Shanghai, China) was used for densitometric analysis. GAPDH (Santa Cruz Biotechnology, Santa Cruz, CA, United States; 1:1000) was used as the loading control.

## Enzyme-Linked Immunosorbent Assay (ELISA)

After establishing the co-culture system, cells were cultured under the various treatment conditions. IL-6 and -18 and TNF- $\alpha$  levels in the culture supernatant were measured by ELISA using the appropriate ELISA kit (R&D Systems, Minneapolis, MN, United States) according to the manufacturer's instructions.

## Transwell Migration Assay

Corning 24-well Transwell co-culture plates (pore size: 5  $\mu$ m) were used to evaluate cell migration. The co-culture system was

divided into two compartments separated by a microporous membrane that permitted diffusion of soluble molecules and chemotactic agents and the interaction of cells in the different layers. Before the experiment, HK2 cells were inoculated in the lower compartment at a density of  $1 \times 10^5$  cells/ml, while 600  $\mu$ l culture medium were added to the lower chamber. Cells were synchronized with serum-free DMEM/F12 for 12 h before the experiment. U937 cells were inoculated into the upper chamber at a density of  $5 \times 10^4$  cells/ml; 200  $\mu$ l of culture medium were added to the cells, which were synchronized 12 h before the experiment. The cells remaining on the upper surface of the membrane were removed with a cotton swab, and those that had migrated through the 5- $\mu$ m-diameter pores and had adhered to the lower surface of the membrane were fixed with 4% paraformaldehyde, stained with crystal violet, and photographed under a light microscope.

## Cell Transfection

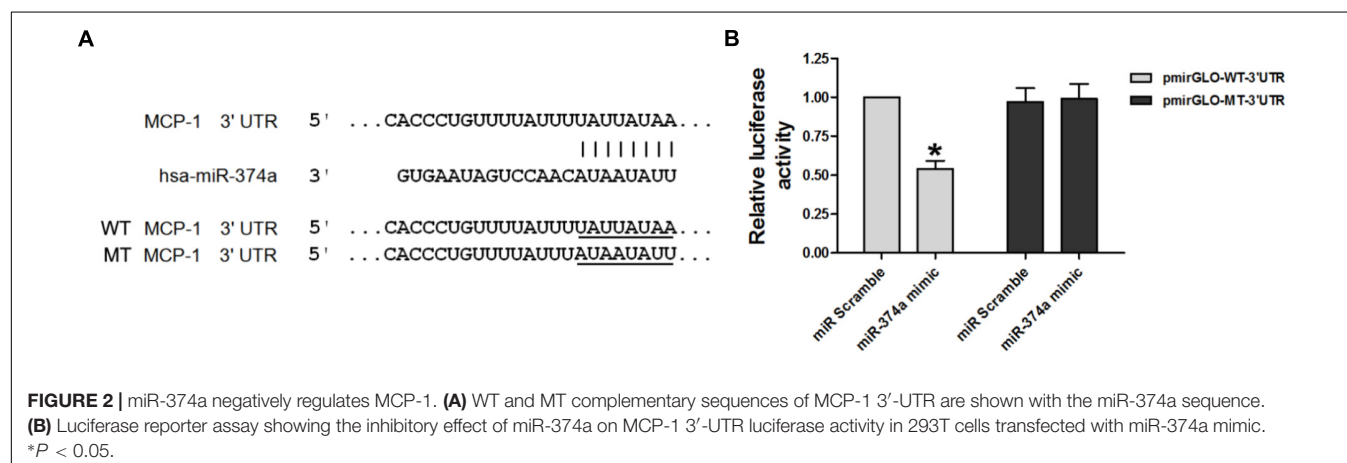
HK2 cells were seeded in 6-well plates. When they reached 50–80% confluence, they were transfected with miR-374a mimic or inhibitor (GenePharma, Shanghai, China) using Lipofectamine 2000 (Invitrogen, Carlsbad, CA, United States) according to the manufacturer's instructions. After 6 h, the cells were treated with NG, HG, or HO. Protein and RNA were extracted for analyses.

## Overexpression of MCP-1

The pcDNA3.1-MCP-1 vector lacking the 3'-UTR was constructed and transfected into HK2 cells using Lipofectamine 2000.

## Statistical Analysis

Data are expressed as mean  $\pm$  SD. Means of multiple groups were compared by one-way analysis of variance. The statistical significance of differences between two groups was evaluated with the least significant difference test.  $P < 0.05$  was considered statistically significant. The relationship between two variables was evaluated by Spearman's correlation analysis. Statistical analyses were performed using SPSS v.18.0 software (SPSS Inc., Chicago, IL, United States).



## RESULTS

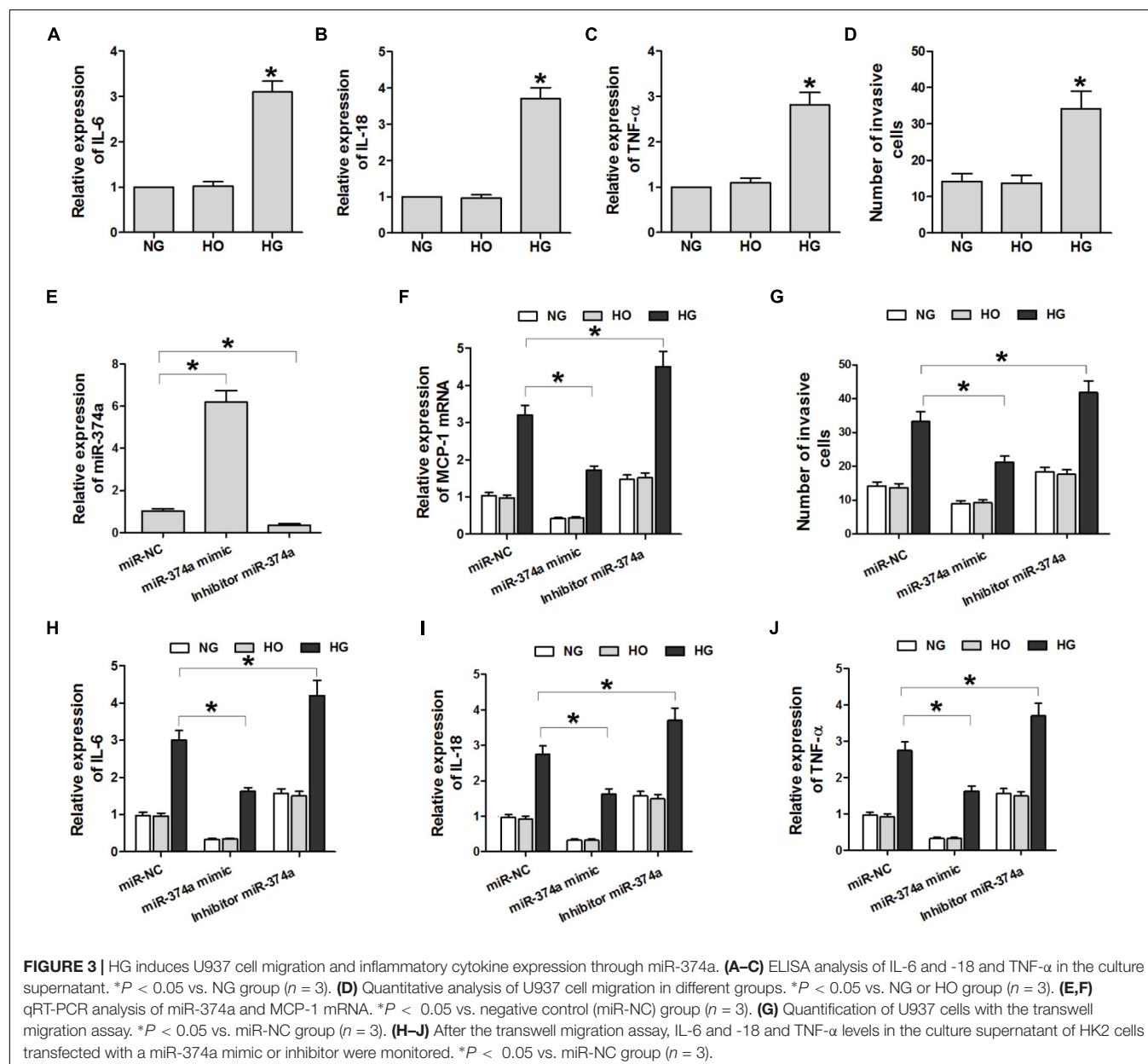
### HG Induces MCP-1 but Suppresses miR-374a Expression

MCP-1 mRNA and miR-374a levels were detected in DN ( $n = 10$ ) and adjacent non-cancerous ( $n = 5$ ) tissues by qRT-PCR. MCP-1 was upregulated whereas miR-374a was downregulated in DN relative to control tissue (Figures 1A,B); there was a negative linear correlation between their expression levels (Figure 1C). A histological analysis revealed that DN tissue had abnormal architecture, as evidenced by glomerular swelling and vacuolization in the endothelial lining (Figure 1D). An immunohistochemical analysis confirmed upregulation of MCP-1 in DN tissue (Figure 1E). MCP-1 and miR-374a levels in the

supernatant of HK2 cell cultures incubated with NG, HG, and HO were evaluated by qRT-PCR and western blotting. After 24 h of HG stimulation, MCP-1 mRNA and protein levels were almost 3-fold higher than in the NG or HO group (Figures 1F,G). In contrast, miR-374a was downregulated approximately 5 fold in the HG as compared to the NG or HO group after 24 h (Figure 1H). These results suggest a regulatory relationship between MCP-1 and miR-374a in DN.

### MCP-1 Is a Direct Target of miR-374a

Given the negative correlation between the expression levels of miR-374a and MCP-1, we investigated whether MCP-1 is a target of miR-374a regulation. A bioinformatics analysis with TargetScan, Microna, and PicTar programs identified a





short complementary sequence shared by miR-374a and MCP-1 (Figure 2A). We carried out a luciferase reporter assay to determine whether miR-374a regulates MCP-1 expression by transfecting WT-MCP-1-3'UTR and MT-MCP-1-3'UTR plasmid constructs into 293T cells along with a miR-374a mimic or scrambled control sequence. The results showed that miR-374a mimic suppressed the transcriptional activity of the luciferase-WT-MCP-1-3'-UTR reporter by approximately 50% relative to the control group. However, the activity of MT-MCP-1-3'UTR harboring a mutated miR-374a binding site was not suppressed by miR-374a mimic (Figure 2B). These results indicate that miR-374a inhibits MCP-1 expression through a direct regulatory mechanism.

## HG Induces U937 Cell Migration and Expression of Inflammatory Cytokines via miR-374a

To determine whether miR-374a suppresses the inflammatory response in DN by targeting MCP-1 expression, we carried out a transwell migration assay with U937 and HK2 cells seeded in the top and bottom chambers, respectively. The cells were treated with NG, HG, or HO and IL-6 and -18 and TNF- $\alpha$  levels in the supernatant were determined by ELISA and the number of U937 cells in the supernatant was counted. IL-6 and -18 and TNF- $\alpha$  levels were higher in the HG group than in the NG and HO groups (Figures 3A–C). In addition, HK2 cells treated with HG induced the migration of U937 cells as compared to the NG and HO groups (Figure 3D). Thus, HG induces U937 cell migration and promotes inflammatory cytokine expression.

To investigate the effect of miR-374a on the production of inflammatory cytokines in U937 cells, miR-374a mimic or inhibitor was overexpressed in HK2 cells. The inhibitor significantly reduced miR-374a expression (Figure 3E). Compared to the negative control group, miR-374a mimic suppressed the HG-induced upregulation of MCP-1 transcript and IL-6 and -18 and TNF- $\alpha$  proteins, whereas miR-374a inhibitor had the opposite effect (Figures 3F,H–J). Similarly, miR-374a mimic suppressed HG-induced migration of U937

cells, which was reversed by miR-374a inhibitor (Figures 3F,G). These data suggest that increased miR-374a expression suppresses the inflammatory response in DN.

## MCP-1 Overexpression Antagonizes the Effect of miR-374a Mimic

To confirm the regulatory relationship between miR-374a and MCP-1, we overexpressed MCP-1 lacking the 3'-UTR in HK2 cells transfected with miR-374a mimic (Figure 4A). MCP-1 overexpression was not suppressed by miR-374a mimic (Figure 4A). Furthermore, the migration of U937 cells was not blocked under HG conditions upon co-transfection of pcDNA3.1-MCP-1 and miR-374a mimic (Figure 4B), which also did not affect the production of IL-6 and -18 and TNF- $\alpha$  in the HK2 and U937 cell co-culture system with HG (Figure 4C). These results confirm that miR-374a negatively regulates MCP-1 expression through binding to the 3'-UTR region.

## DISCUSSION

In this study, we demonstrated that miR-374a expression was lower in DN as compared to normal tissues and is negatively correlated with that of MCP-1. Overexpression of miR-374a suppressed MCP-1 expression; IL-6 and -18 and TNF- $\alpha$  production; and cell invasion, whereas miR-374a inhibition had the opposite effects. The results of the luciferase reporter assay showed that miR-374a directly targets the 3'-UTR of MCP-1 transcript. On the other hand, MCP-1 overexpression antagonized the inhibitory effect of miR-374a mimic on the inflammatory response, suggesting that MCP-1 is a downstream target of miR-374a during DN. This is the first report describing miR-374a function and its relationship to MCP-1 in DN.

Previous studies have reported that miRNAs regulate gene expression during DN progression (Long et al., 2010; Wang et al., 2010) by targeting signaling pathways related to mechanical stress, oxidative stress, generation of advanced glycation end products and their receptors, renin-angiotensin-aldosterone system (RAAS) activation, and autophagy (Wang et al., 2008;

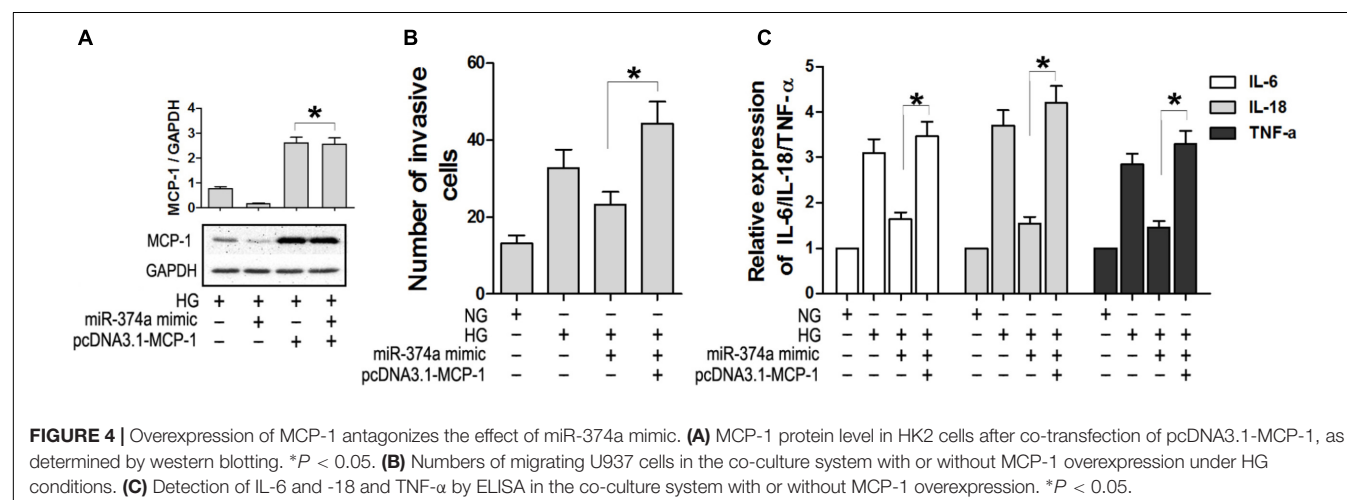


**FIGURE 4 |** Overexpression of MCP-1 antagonizes the effect of miR-374a mimic. **(A)** MCP-1 protein level in HK2 cells after co-transfection of pcDNA3.1-MCP-1, as determined by western blotting. \* $P < 0.05$ . **(B)** Numbers of migrating U937 cells in the co-culture system with or without MCP-1 overexpression under HG conditions. **(C)** Detection of IL-6 and -18 and TNF- $\alpha$  by ELISA in the co-culture system with or without MCP-1 overexpression. \* $P < 0.05$ .

Macconi et al., 2012; Fiorentino et al., 2013; Li et al., 2013; Tekirdag et al., 2013). For example, miR-184 was shown to promote tubulointerstitial fibrosis as a downstream effector of albuminuria through lipid phosphate phosphatase 3 (Zanchi et al., 2017). Hyperglycemia influenced pathogenic processes during DN through an miR-23b/GTPase activating protein (SH3 domain)-binding protein 2 feedback circuit involving p38 mitogen-activated protein kinase (MAPK) and p53 (Zhao et al., 2016). Proteinuria, genetics, ethnicity, hypoxia, ischemia, and inflammation have been proposed as factors contributing to DN (Fernandez et al., 2012). miRNAs also regulate inflammation by targeting TGF- $\beta$ -activated kinase 1/MAPK kinase kinase 7-binding protein 2/3, and inhibitor of NF- $\kappa$ B kinase subunit- $\alpha$  (Zhu et al., 2012), while miR-155 and -146 were shown to regulate inflammatory responses through NF- $\kappa$ B signaling (Mann et al., 2017). Our results also provide evidence for the involvement of miR-374a in the inflammatory response, although the detailed mechanism remains to be elucidated.

MCP-1 is a ligand of CC chemokine receptor 2 that acts as a chemotactic factor for monocytes/macrophages and activated T cells (Boels et al., 2017). MCP-1 levels in peripheral blood of diabetes mellitus patients were positively correlated with urinary albumin excretion rate, and MCP-1 mRNA and protein levels are higher in DN than in normal renal tissue (Giunti et al., 2010). There are several mechanisms by which MCP-1 may contribute to DN. Firstly, direct stimulation by HG could lead to upregulation of MCP-1. Secondly, the general existence of blood lipid metabolism disorder in DN and high levels of low-density lipoprotein and its metabolite could induce MCP-1 production by mesangial cells (Rutledge et al., 2010). Thirdly, endothelial and mesangial cells may produce MCP-1 in response to IL-1, TNF- $\alpha$ , and platelet-derived growth factor stimulation (Fufaa et al., 2015). Fourthly, activated RAAS could regulate MCP-1 by increasing macrophage infiltration and ECM accumulation through NF- $\kappa$ B signaling (Yang et al., 2016).

In this study, we confirmed the regulation of MCP-1 by miR-374a in HK2 cells, which suggests an important role for this signaling pathway in the development and progression of DN. In cells expressing miR-146a and -146b, I $\kappa$ B phosphorylation on serine 32—which is essential for its degradation—was reduced to 40 or 20% of control levels in an experiment that directly demonstrated the negative regulation of NF- $\kappa$ B by miR-146 (Ma et al., 2011). Advanced oxidation protein product-induced MCP-1 expression has been linked to the IKK/NF- $\kappa$ B signaling pathway (Zhao et al., 2015). Based on these findings, we propose

that miR-374a interacts with MCP-1 via the NF- $\kappa$ B signaling pathway in DN.

## CONCLUSION

Our results indicate that MCP-1 is a direct downstream target of miR-374a in DN. Thus, therapeutic strategies targeting this axis may be effective for the treatment of DN.

## ETHICS STATEMENT

This study was carried out in accordance with the recommendations of the Institutional Review Board and Ethics Committee of the First Affiliated Hospital of Zhengzhou University, with written, informed consent from all subjects in accordance with the Declaration of Helsinki. The protocol was approved by the Institutional Review Board and Ethics Committee of the First Affiliated Hospital of Zhengzhou University.

## AUTHOR CONTRIBUTIONS

LT conceived and designed the study. SS, YW, LY, and HW performed the experiments. JD analyzed the data. ZY and ZG wrote the paper and contributed equally to this work. LT and JD reviewed and edited the manuscript. All authors read and approved the final manuscript.

## FUNDING

This work was supported by grants for National Natural Science Foundation of China (No. 81300605) and the Key Project of Medical Science and Technology of Henan Province (201501010).

## SUPPLEMENTARY MATERIAL

The Supplementary Material for this article can be found online at: <https://www.frontiersin.org/articles/10.3389/fphar.2018.00900/full#supplementary-material>

## REFERENCES

- Banba, N., Nakamura, T., Matsumura, M., Kuroda, H., Hattori, Y., and Kasai, K. (2000). Possible relationship of monocyte chemoattractant protein-1 with diabetic nephropathy. *Kidney Int.* 58, 684–690. doi: 10.1046/j.1523-1755.2000.00214.x
- Boels, M., Koudijs, A., Avramut, M. C., Sol, W., Wang, G., van Oeveren-Rietdijk, A. M., et al. (2017). Systemic monocyte chemotactic protein-1 inhibition modifies renal macrophages and restores glomerular endothelial glycocalyx and barrier function in diabetic nephropathy. *Am. J. Pathol.* 187, 2430–2440. doi: 10.1016/j.ajpath.2017.07.020
- Cai, J., Guan, H., Fang, L., Yang, Y., Zhu, X., Yuan, J., et al. (2013). MicroRNA-374a activates Wnt/beta-catenin signaling to promote breast cancer metastasis. *J. Clin. Invest.* 123, 566–579. doi: 10.1172/JCI65871
- Cardenas-Gonzalez, M., Srivastava, A., Pavkovic, M., Bijol, V., Rennke, H. G., Stillman, I. E., et al. (2017). Identification, confirmation, and replication of novel urinary microRNA biomarkers in lupus nephritis and diabetic nephropathy. *Clin. Chem.* 63, 1515–1526. doi: 10.1373/clinchem.2017.274175
- Celen, E., Ertosun, M. G., Kocak, H., Dinckan, A., and Yoldas, B. (2017). Expression profile of microRNA biogenesis components in renal transplant patients. *Transplant. Proc.* 49, 472–476. doi: 10.1016/j.transproceed.2017.01.019

- Cho, Y. E., Kim, S. H., Lee, B. H., and Baek, M. C. (2017). Circulating plasma and exosomal micrornas as indicators of drug-induced organ injury in rodent models. *Biomol Ther* 25, 367–373. doi: 10.4062/biomolther.2016.174
- Collins, A. J., Foley, R. N., Chavers, B., Gilbertson, D., Herzog, C., Ishani, A., et al. (2014). US renal data system 2013 annual data report. *Am. J. Kidney Dis.* 63(1 Suppl.):A7. doi: 10.1053/j.ajkd.2013.11.001
- DeFronzo, R. A., Norton, L., and Abdul-Ghani, M. (2017). Renal, metabolic and cardiovascular considerations of SGLT2 inhibition. *Nat. Rev. Nephrol.* 13, 11–26. doi: 10.1038/nrneph.2016.170
- Feng, Y., Yang, S., Ma, Y., Bai, X. Y., and Chen, X. (2015). Role of toll-like receptors in diabetic renal lesions in a miniature pig model. *Sci. Adv.* 1:e1400183. doi: 10.1126/sciadv.1400183
- Fernandez, F. B., Elewa, U., Sanchez-Nino, M. D., Rojas-Rivera, J. E., Martin-Cleary, C., Egido, J., et al. (2012). 2012 update on diabetic kidney disease: the expanding spectrum, novel pathogenic insights and recent clinical trials. *Minerva Med.* 103, 219–234.
- Fiorentino, L., Cavallera, M., Mavilio, M., Conserva, F., Menghini, R., Gesualdo, L., et al. (2013). Regulation of TIMP3 in diabetic nephropathy: a role for microRNAs. *Acta Diabetol.* 50, 965–969. doi: 10.1007/s00592-013-0492-8
- Fufaa, G. D., Weil, E. J., Nelson, R. G., Hanson, R. L., Knowler, W. C., Rovin, B. H., et al. (2015). Urinary monocyte chemoattractant protein-1 and hepcidin and early diabetic nephropathy lesions in type 1 diabetes mellitus. *Nephrol. Dial. Transplant.* 30, 599–606. doi: 10.1093/ndt/gfv012
- Giunti, S., Barutta, F., Perin, P. C., and Gruden, G. (2010). Targeting the MCP-1/CCR2 system in diabetic kidney disease. *Curr. Vasc. Pharmacol.* 8, 849–860.
- Huttenhofer, A., and Mayer, G. (2017). Circulating miRNAs as biomarkers of kidney disease. *Clin. Kidney J.* 10, 27–29. doi: 10.1093/ckj/sfw075
- Kanasaki, K., Taduri, G., and Koya, D. (2013). Diabetic nephropathy: the role of inflammation in fibroblast activation and kidney fibrosis. *Front. Endocrinol.* 4, 7. doi: 10.3389/fendo.2013.00007
- Kato, M., and Natarajan, R. (2014). Diabetic nephropathy—emerging epigenetic mechanisms. *Nat. Rev. Nephrol.* 10, 517–530. doi: 10.1038/nrneph.2014.116
- Kato, M., and Natarajan, R. (2015). MicroRNAs in diabetic nephropathy: functions, biomarkers, and therapeutic targets. *Ann. N. Y. Acad. Sci.* 1353, 72–88. doi: 10.1111/nyas.12758
- Li, D., Lu, Z., Jia, J., Zheng, Z., and Lin, S. (2013). Curcumin ameliorates podocytic adhesive capacity damage under mechanical stress by inhibiting miR-124 expression. *Kidney Blood Press. Res.* 38, 61–71. doi: 10.1159/000355755
- Long, J., Wang, Y., Wang, W., Chang, B. H., and Danesh, F. R. (2010). Identification of microRNA-93 as a novel regulator of vascular endothelial growth factor in hyperglycemic conditions. *J. Biol. Chem.* 285, 23457–23465. doi: 10.1074/jbc.M110.136168
- Lopez-Vargas, P. A., Tong, A., Howell, M., and Craig, J. C. (2016). Educational interventions for patients with ckd: a systematic review. *Am. J. Kidney Dis.* 68, 353–370. doi: 10.1053/j.ajkd.2016.01.022
- Ma, X., Becker, B. L., Barker, J. R., and Li, Y. (2011). MicroRNAs in NF-kappaB signaling. *J. Mol. Cell Biol.* 3, 159–166. doi: 10.1093/jmcb/mjr007
- Macconi, D., Tomasoni, S., Romagnani, P., Trionfini, P., Sangalli, F., Mazzinghi, B., et al. (2012). MicroRNA-324-3p promotes renal fibrosis and is a target of ACE inhibition. *J. Am. Soc. Nephrol.* 23, 1496–1505. doi: 10.1681/ASN.2011121144
- Maeshima, A., Mishima, K., Yamashita, S., Nakasatomi, M., Miya, M., Sakurai, N., et al. (2014). Follistatin, an activin antagonist, ameliorates renal interstitial fibrosis in a rat model of unilateral ureteral obstruction. *Biomed. Res. Int.* 2014, 376191. doi: 10.1155/2014/376191
- Mann, M., Mehta, A., Zhao, J. L., Lee, K., Marinov, G. K., Garcia-Flores, Y., et al. (2017). An NF-kappaB-microRNA regulatory network tunes macrophage inflammatory responses. *Nat. Commun.* 8:851. doi: 10.1038/s41467-017-00972-z
- McClelland, A., Hagiwara, S., and Kantharidis, P. (2014). Where are we in diabetic nephropathy: microRNAs and biomarkers? *Curr. Opin. Nephrol. Hypertens.* 23, 80–86. doi: 10.1097/01.mnh.0000437612.50040.ae
- Rudnicki, M., Beckers, A., Neuwirt, H., and Vandesompele, J. (2015). RNA expression signatures and posttranscriptional regulation in diabetic nephropathy. *Nephrol. Dial. Transplant.* 30(Suppl. 4), iv35–iv42. doi: 10.1093/ndt/gfv079
- Rutledge, J. C., Ng, K. F., Aung, H. H., and Wilson, D. W. (2010). Role of triglyceride-rich lipoproteins in diabetic nephropathy. *Nat. Rev. Nephrol.* 6, 361–370. doi: 10.1038/nrneph.2010.59
- Sancar-Bas, S., Gezginici-Oktayoglu, S., and Bolkent, S. (2015). Exendin-4 attenuates renal tubular injury by decreasing oxidative stress and inflammation in streptozotocin-induced diabetic mice. *Growth Factors* 33, 419–429. doi: 10.3109/08977194.2015.1125349
- Scherthner, G., and Scherthner, G. H. (2013). Diabetic nephropathy: new approaches for improving glycemic control and reducing risk. *J. Nephrol.* 26, 975–985. doi: 10.5301/jn.5000281
- Tekirdag, K. A., Korkmaz, G., Ozturk, D. G., Agami, R., and Gozuacik, D. (2013). MIR181A regulates starvation- and rapamycin-induced autophagy through targeting of ATG5. *Autophagy* 9, 374–385. doi: 10.4161/auto.23117
- Wang, B., Herman-Edelstein, M., Koh, P., Burns, W., Jandeleit-Dahm, K., Watson, A., et al. (2010). E-cadherin expression is regulated by miR-192/215 by a mechanism that is independent of the profibrotic effects of transforming growth factor-beta. *Diabetes Metab. Res. Rev.* 59, 1794–1802. doi: 10.2337/db09-1736
- Wang, Q., Wang, Y., Minto, A. W., Wang, J., Shi, Q., Li, X., et al. (2008). MicroRNA-377 is up-regulated and can lead to increased fibronectin production in diabetic nephropathy. *FASEB J.* 22, 4126–4135. doi: 10.1096/fj.08-112326
- Wei, M., Li, Z., Xiao, L., and Yang, Z. (2015). Effects of ROS-relative NF-kappaB signaling on high glucose-induced TLR4 and MCP-1 expression in podocyte injury. *Mol. Immunol.* 68, 261–271. doi: 10.1016/j.molimm.2015.09.002
- Wonnacott, A., Bowen, T., and Fraser, D. J. (2017). MicroRNAs as biomarkers in chronic kidney disease. *Curr. Opin. Nephrol. Hypertens.* 26, 460–466. doi: 10.1097/MNH.0000000000000356
- Wu, H., Liu, Y., Shu, X. O., and Cai, Q. (2016). MiR-374a suppresses lung adenocarcinoma cell proliferation and invasion by targeting TGFA gene expression. *Carcinogenesis* 37, 567–575. doi: 10.1093/carcin/bgw038
- Xu, X., Wang, W., Su, N., Zhu, X., Yao, J., Gao, W., et al. (2015). miR-374a promotes cell proliferation, migration and invasion by targeting SRCIN1 in gastric cancer. *FEBS Lett.* 589, 407–413. doi: 10.1016/j.febslet.2014.12.027
- Yang, X., Wang, Y., and Gao, G. (2016). High glucose induces rat mesangial cells proliferation and MCP-1 expression via ROS-mediated activation of NF-kappaB pathway, which is inhibited by eleutheroside E. *J. Recept. Signal Transduct. Res.* 36, 152–157. doi: 10.3109/10799893.2015.1061002
- Yheskel, M., and Patel, V. (2017). Therapeutic microRNAs in polycystic kidney disease. *Curr. Opin. Nephrol. Hypertens.* 26, 282–289. doi: 10.1097/MNH.0000000000000333
- Zanchi, C., Macconi, D., Trionfini, P., Tomasoni, S., Rottoli, D., Locatelli, M., et al. (2017). MicroRNA-184 is a downstream effector of albuminuria driving renal fibrosis in rats with diabetic nephropathy. *Diabetologia* 60, 1114–1125. doi: 10.1007/s00125-017-4248-9
- Zhao, B., Li, H., Liu, J., Han, P., Zhang, C., Bai, H., et al. (2016). MicroRNA-23b Targets Ras GTPase-Activating Protein SH3 Domain-Binding Protein 2 to Alleviate Fibrosis and Albuminuria in Diabetic Nephropathy. *J. Am. Soc. Nephrol.* 27, 2597–2608. doi: 10.1681/ASN.2015030300
- Zhao, Y., Chen, S. J., Wang, J. C., Niu, H. X., Jia, Q. Q., Chen, X. W., et al. (2015). Sesquiterpene lactones inhibit advanced oxidation protein product-induced MCP-1 expression in podocytes via an IKK/NF-kappaB-dependent mechanism. *Oxid. Med. Cell. Longev.* 2015, 934058. doi: 10.1155/2015/934058
- Zheng, Z., and Zheng, F. (2016). Immune Cells and Inflammation in Diabetic Nephropathy. *J. Diabetes Res.* 2016, 1841690. doi: 10.1155/2016/1841690
- Zhu, S., Pan, W., Song, X., Liu, Y., Shao, X., Tang, Y., et al. (2012). The microRNA miR-23b suppresses IL-17-associated autoimmune inflammation by targeting TAB2, TAB3 and IKK-alpha. *Nat. Med.* 18, 1077–1086. doi: 10.1038/nm.2815
- Zununi, V. S., Poursadegh, Z. A., Ghanbarian, H., Ghojzadeh, M., Samadi, N., and Ardalan, M. (2017). Upregulated expression of circulating micrornas in kidney transplant recipients with interstitial fibrosis and tubular atrophy. *Iran. J. Kidney Dis.* 11, 309–318.

**Conflict of Interest Statement:** The authors declare that the research was conducted in the absence of any commercial or financial relationships that could be construed as a potential conflict of interest.

Copyright © 2018 Yang, Guo, Dong, Sheng, Wang, Yu, Wang and Tang. This is an open-access article distributed under the terms of the Creative Commons Attribution License (CC BY). The use, distribution or reproduction in other forums is permitted, provided the original author(s) and the copyright owner(s) are credited and that the original publication in this journal is cited, in accordance with accepted academic practice. No use, distribution or reproduction is permitted which does not comply with these terms.



# P311, Friend, or Foe of Tissue Fibrosis?

Leslie Stradiot, Inge Mannaerts and Leo A. van Grunsven\*

Liver Cell Biology Lab, Vrije Universiteit Brussel, Brussels, Belgium

P311 was first identified by the group of Studler et al. (1993) in the developing brain. In healthy, but mainly in pathological tissues, P311 is implicated in cell migration and proliferation. Furthermore, evidence in models of tissue fibrosis points to the colocalization with and the stimulation of transforming growth factor  $\beta$ 1 by P311. This review provides a comprehensive overview on P311 and discusses its potential as an anti-fibrotic target.

**Keywords:** P311, fibrosis, proliferation, migration, TGF $\beta$ 1

## OPEN ACCESS

### Edited by:

Cecilia Battistelli,  
Università degli Studi di Roma La  
Sapienza, Italy

### Reviewed by:

Martina Schmidt,  
University of Groningen, Netherlands  
Gaoping Luo,  
Third Military Medical University,  
China

### \*Correspondence:

Leo A. van Grunsven  
Leo.van.Grunsven@vub.ac.be

### Specialty section:

This article was submitted to  
Experimental Pharmacology  
and Drug Discovery,  
a section of the journal  
Frontiers in Pharmacology

**Received:** 27 July 2018

**Accepted:** 24 September 2018

**Published:** 12 October 2018

### Citation:

Stradiot L, Mannaerts I and  
van Grunsven LA (2018) P311,  
Friend, or Foe of Tissue Fibrosis?  
Front. Pharmacol. 9:1151.  
doi: 10.3389/fphar.2018.01151

## INTRODUCTION

Neuronal protein 3.1 (P311) is a small intracellular protein from an unknown family, whose transcript was first identified by Studler et al. (1993) in a differential screening comparing striatal cells from two different stages of brain development. P311 knockout mice have learning and memory deficiency and a disturbed pain affection (Sun et al., 2008; Taylor et al., 2008). During the past years, light has been shed on the broader expression pattern of P311 and its function in both health and pathology. P311 has proven to be a multifunctional protein with important implications in development, disease, and regeneration. For this review, we explore P311 functions and discuss possible implications of P311 in the development of tissue fibrosis by highlighting its role in tissue regeneration, cell migration, and its interaction with the pro-fibrotic cytokines transforming growth factor  $\beta$ 1 and 2 (TGF $\beta$ 1 and 2).

## GENERAL CONCEPTS IN TISSUE FIBROSIS

Tissue fibrosis can be defined as the hardening of epithelial tissues due to accumulation of secreted collagens. Initially it starts as a wound healing response, but upon repeated insults, the scarring increases and becomes pathogenic (Friedman et al., 2013). Under normal conditions, wound healing undergoes three phases; an inflammatory, a proliferative, and a regenerative phase. These phases are well characterized for liver fibrosis (Figure 1), while lung and kidney present a similar fibrotic process (Friedman et al., 2013).

### Inflammatory Phase

Upon tissue injury, we can distinguish different origins of pro-fibrogenic stimuli. Damaged endothelium and epithelium as well as activated platelets will secrete pro-fibrogenic and pro-inflammatory cytokines. Furthermore, they also attract extra mesenchymal cells, inter-organ and organ resident cells to the site of injury by secreting chemokines (Dranoff et al., 2004; Armulik et al., 2005; Darby et al., 2014).



## Proliferative Phase

Due to the inflammatory environment, fibroblasts will activate and differentiate into myofibroblasts. These will proliferate, gain tensile forces, and will secrete chemokines to attract other fibroblasts. Myofibroblasts at the site of injury will secrete a massive amount of matrix proteins, replacing the fibrin matrix with a dense collagen-rich one (Darby et al., 2014; Simone et al., 2015).

## Regeneration Phase

Once the insult is ceased, damage and inflammation is diminished and collagens will be degraded, mainly by matrix metalloproteinases. This will allow re-epithelialization. Most of the myofibroblasts present undergo apoptosis during healing or revert to an inactive phenotype as was shown in the liver (Desmouliere et al., 1995; Kisseleva et al., 2012; Darby et al., 2014).

When the injury is chronic, the first two phases are continuously repeated and the matrix resolution and epithelial restoration do not occur. The fibrotic site will expand, the organ tissue will continue to harden, leading to cellular dysfunction and eventually organ failure (**Figure 1**). This pathological process has been described in several organs, but is most intensely studied in liver, kidney, and lung. Hepatic stellate cells, renal mesangial cells, and resident lung fibroblasts, respectively, are the organ-specific resident cells that transdifferentiate to myofibroblasts and contribute to the scarring (Ardaillou et al., 1999; Friedman, 2008; Barkauskas and Noble, 2014). During the proliferative phase, activation of these cells is triggered by different pathways; damaged epithelial cells will stimulate fibroblast activation either by their released nucleotides or by expressing integrins, which will then mechanically activate TGF $\beta$ 1 that is transiently stored in the extracellular matrix (Munger et al., 1999; Dranoff et al., 2004; Zhan et al., 2006; Giacomini et al., 2012). Platelets present at the site of injury will recruit fibroblasts as well as inflammatory cells, which secrete pro-fibrogenic cytokines like tumor necrosis factor  $\alpha$ , interleukin (IL) 1 $\beta$ , IL13, and IL17 (Friedman et al., 2013; Darby et al., 2014). Upon activation, the myofibroblasts themselves will secrete chemokines, cytokines, as well as oxygen radicals, leading again to increased stress, immune response, and myofibroblast activation (Friedman et al., 2013). Once fibrosis is initiated, it is a self-stimulating system; matrix-stored TGF $\beta$ 1 is activated by the epithelial cells, this active TGF $\beta$ 1 in turn activates fibroblasts, which will then recruit and activate even more fibroblasts, which will produce TGF $\beta$ 1 and so on (Ignatz and Massague, 1987; Wang et al., 1996; Giacomini et al., 2012). In parallel, more myofibroblasts means more collagen secretion and crosslinking, finally leading to stiffening of the extracellular matrix. A stiff matrix in turn stimulates proliferation, drives cells to activate, inhibits the production of matrix digestive enzymes, and facilitates the activation of TGF $\beta$ 1 in the matrix (Li et al., 2007; Liu et al., 2010; Olsen et al., 2011; Huang et al., 2012).

The organ resident stromal cells are important targets to attenuate fibrosis development. Interfering with their recruitment, proliferation, TGF $\beta$ 1 response, or collagen secretion already greatly delays or sometimes even stops

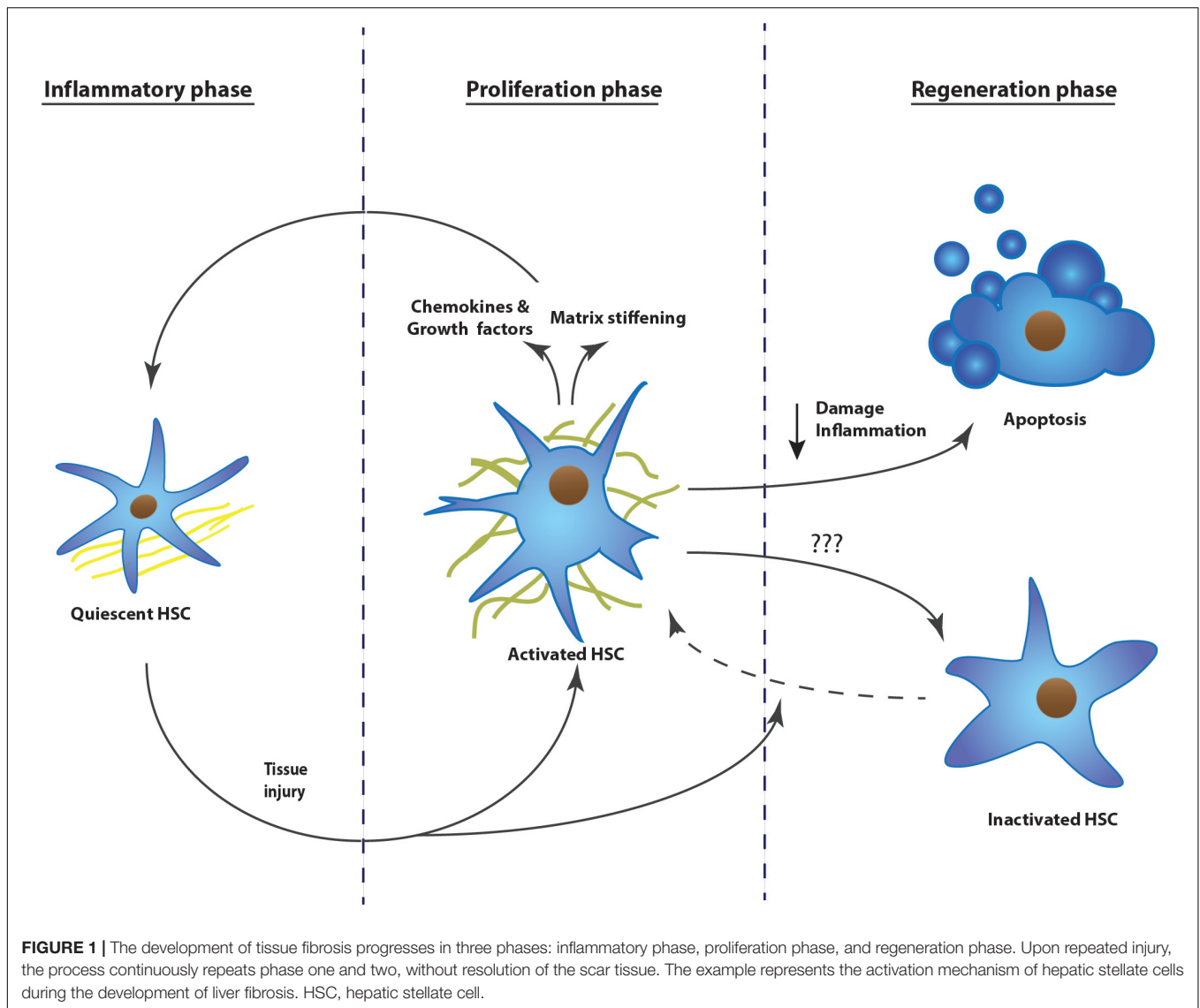
fibrosis progression in animal models of fibrosis (Munger et al., 1999; Liu et al., 2009a; Kuroda et al., 2015; Nayak et al., 2016). Unfortunately, these approaches have not yet evolved in clinically approved therapeutics (Schuppan and Kim, 2013; Schon et al., 2016). P311 is involved in several of these fibrosis stimulating pathways and might represent an interesting target for the development of anti-fibrotic drugs. We will discuss its involvement in cell migration, regeneration, and development in different tissues.

## THE BASICS OF P311

The first studies on P311 reported the transcript in the germinal zones of the brain at embryonic day 17, the transcript was observed in the striatum and the superficial cortical layers at E20, suggesting that the gene was expressed in cells from the second germinal migration wave. The expression persists during adulthood, where it is present in several brain regions with active postnatal neurogenesis like the cerebellum, hippocampus, and the olfactory bulb (Studler et al., 1993). P311 has been alternatively named pentylentetrazole 17, since it potentiates an inward calcium current upon pentylentetrazole administration in neurons, mimicking epileptic bursting (Kajiwara et al., 1995). The P311 open reading frame is located on chromosome 18 in mice, on chromosome 5 in humans, and has been highly conserved among mice, humans, rhesus monkeys, dogs, etc. This sequence is translated into an 8 kDa protein of 68 amino acids and contains a PEST domain responsible for the fast degradation by ubiquitin-dependent degradation as well as by an unknown metalloprotease, resulting in a half-life of approximately 5 min (Studler et al., 1993; Taylor et al., 2000). Research for P311 binding partners, using a predictor of naturally disordered regions analysis, suggested that P311 is an intrinsically disordered protein that needs an interaction partner to acquire a tertiary structure. Indeed, P311 was shown to interact with several cytoskeletal proteins such as Filamin A and non-muscle myosin heavy chain 9 (MYH9) and with eukaryotic translation initiation factor 3, subunit B (eIF3b), a component of the translation initiation complex (Yue et al., 2014).

## P311 IS EXPRESSED IN MIGRATING CELLS AND STIMULATES THE RAC1 PATHWAY

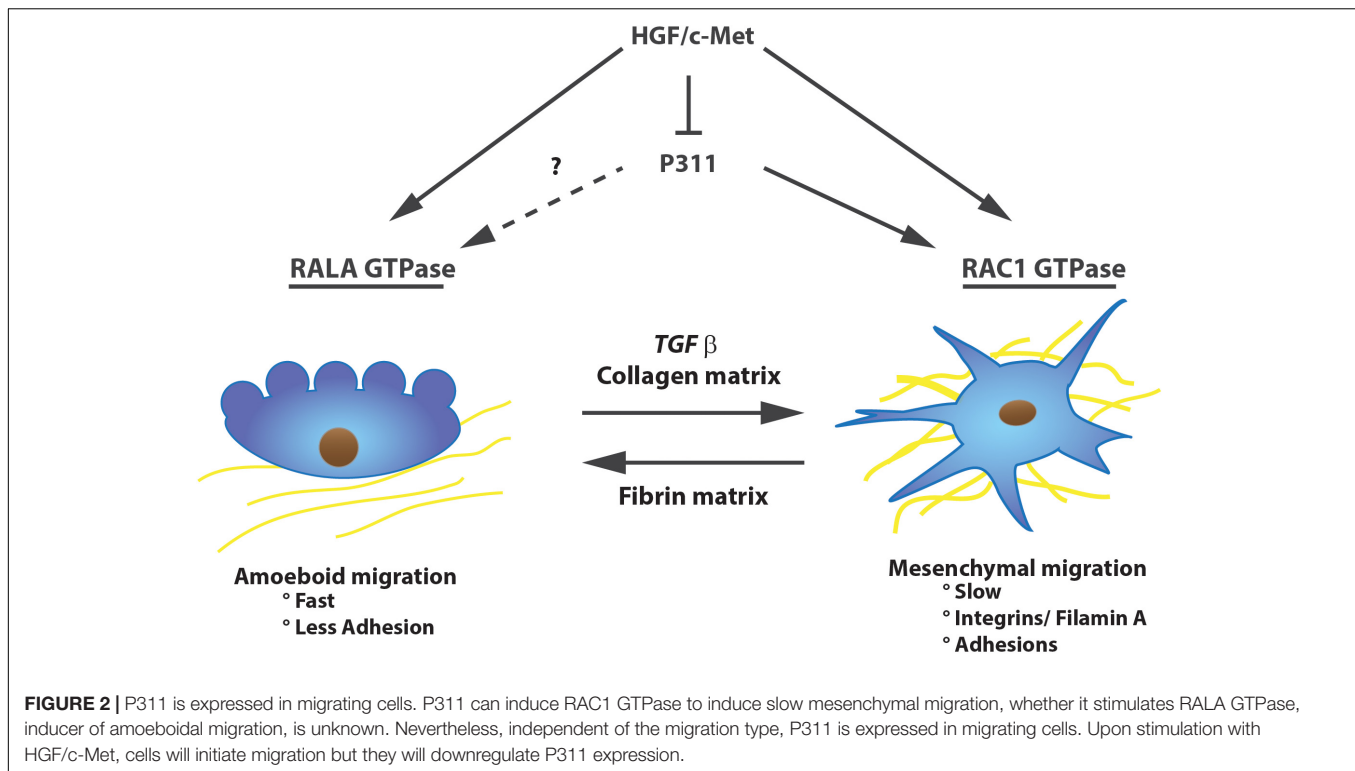
Fibroblast migration is a key event for organ development as well as fibrosis (Shimizu et al., 2001; Hattori et al., 2004; Scholten et al., 2011). P311 is described by different groups to play an important role during chemokine-induced cell migration (Studler et al., 1993; Mariani et al., 2001; McDonough et al., 2005; Guimaraes et al., 2015). The first study ever describing P311 already detected the mRNA in migrating cells in the developing brain (Studler et al., 1993). A study aiming at discovering mechanisms involved in invading glioma cells, determined that P311 is highly expressed in the invasive rim of human glioma tumors, when compared to P311 expression



in the tumor core (~threefold). Furthermore, knockdown of P311 in human glioma cells (SF767) reduced cell migration *in vitro*, while when cultured on glioma-derived extracellular membrane, glioma cells migrated at a higher rate and expressed higher P311 levels (Mariani et al., 2001). This correlation between P311 and cell migration was also shown during liver fibrosis. Upon liver injury, hepatic stellate cells activate, resulting in contractile and migrating hepatic stellate cells with increased P311 transcription (Guimaraes et al., 2015). When activated chronically, these cells deposit high levels of collagen, resulting in liver fibrosis and finally cirrhosis. Knocking down P311 expression in cultured primary hepatic stellate cells reduced chemokine-dependent cell migration (Guimaraes et al., 2015). Furthermore, immunohistochemical stainings demonstrated that the P311 protein was present in nuclei as well as at leading edges of migrating hepatic stellate cells and human astrocytes (Taylor et al., 2000; Guimaraes et al., 2015). In hepatic stellate cells and glioma cells, less P311 expression also resulted in

less lamellipodia, most likely resulting in a reduced migration (Mariani et al., 2001; Guimaraes et al., 2015).

P311-stimulated migration is strongly dependent on the half-life of the protein, which is regulated by constitutive phosphorylation of a serine (Ser59, situated right next to the PEST domain) by protein kinase C  $\delta$ ,  $\epsilon$ , and  $\zeta$ , resulting in a short-lived P311 protein and no migration.  $\beta 1$  integrin signaling on the other hand stimulates its dephosphorylation and consequently cell migration. Upon plating U118 cells on a motility-activating substrate Ser59's phosphorylation is reduced, P311 is not degraded and indirectly stimulates ras-related C3 botulinum toxin substrate 1 (RAC1) GTPase activity (McDonough et al., 2005). Additionally, mice with RAC1-deficient fibroblasts have impaired cutaneous wound healing and the fibroblasts have a less activated phenotype (Liu et al., 2009b). RAC1 GTPase was also shown to be important for glioma cell migration and is highly expressed in cells performing mesenchymal migration (Shaw et al., 1997; Huang et al., 2014).

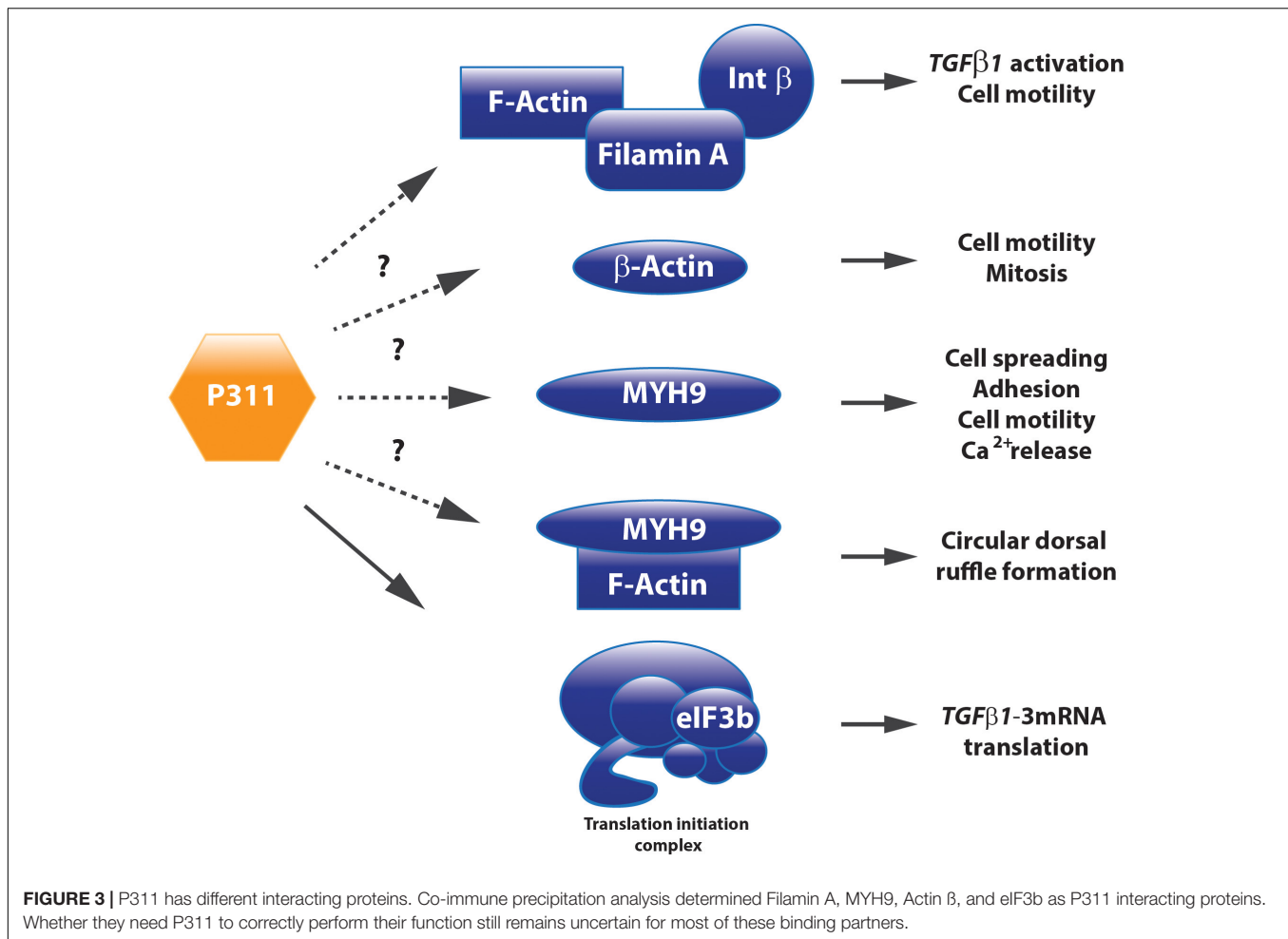


This type of migration acts “slow” and occurs with a lot of adhesions and integrin/filaminA interactions. On the other hand, amoeboid migration is faster and is characterized by less adhesions and mainly uses Ras-related protein A (RALA) and Ras homolog gene family, member A (RHOA) GTPases instead of RAC1 (**Figure 2**). P311 does not seem to be specific for one or the other migration mechanism. Fibroblasts overexpressing P311 can migrate in both fashions, depending on the culture dish coating or cytokine treatment, such as TGFβ1 (Shi et al., 2006; Huang et al., 2014). Correspondingly, human epidermal stem cells initiate P311 expression in response to skin damage to promote wound re-epithelialization. This was shown *in vitro* in human epidermal stem cells in which overexpression of P311 resulted in a faster migration through stimulation of RHOA and RAC1 activity while in P311 knockout mice skin wounds healed slower (Yao et al., 2017).

Filamin A, an interconnecting protein between F-actin and β1 integrin binding protein, was identified as a direct binding protein of P311 in glioma cells. Later on, this was confirmed in 3T3 cells overexpressing a Myc-tagged P311 protein. Co-immune precipitation and mass spectrometric analysis demonstrated that P311 interacts with cytoskeletal proteins MYH9, actin β, and filamin A (**Figure 3**). Filamin A was shown to interact with integrin β1, present in the cell membrane, to activate TGFβ1 and regulate cell motility (McDonough et al., 2005). Actin β is a fundamental cytoskeleton protein that is one of the driving forces for cell protrusions (Bunnell et al., 2011). MYH9 binds transiently to the cytoskeleton, by which it regulates cell spreading, adhesion, and migration (Huang et al., 2009; Liu et al., 2011; Casalou et al., 2014). One study on hepatic stellate cells demonstrated

that MYH9 enabled intracellular Ca<sup>2+</sup> release, a feature that was also described to P311 when administered to neuronal cells (Kajiwarra et al., 1995; Liu et al., 2011). Together with F-actin, MYH9 is also involved in the formation of circular dorsal ruffles upon PDGF-BB stimulation, which recycle integrins, remodel the cytoskeleton during migration, and their presence is enhanced by RAC1 (Casalou et al., 2014; **Figure 3**). Further research regarding the role of P311's interaction with these two proteins and the potential effect on circular dorsal ruffle formation still needs to be done (McDonough et al., 2005).

In contrast to the P311 overexpression migration studies, the group of Taylor et al. (2000) reported that P311 was decreased upon hepatocyte growth factor/scatter factor (HGF/SF) c-MET induced migration in a human leiomyosarcoma cell line (SK-LMS). The cells became metastatic and obtained increased tumorigenic capacities (Jeffers et al., 1996; Taylor et al., 2000). The fact that migration of these cells was driven by c-Met was not out of the ordinary, since it was already shown that both the mesenchymal and amoeboid migration pathways in carcinoma cells are stimulated by the c-Met pathway (Huang et al., 2014; **Figure 2**). While low P311 mRNA levels can be observed in glioma cell lines with a high expression of Met-HGF/SF, a tumor suppressive function for P311 was excluded since P311 overexpression in U118 glioma cells did not interfere with tumor growth *in vivo*. This suggested that diminished P311 expression is the result of a more transformed and tumorigenic phenotype. A similar observation was made for terminally differentiated human cortical neuronal cells (HCN-1A and HCN-2) where nerve growth factor exposure decreased P311 expression (Taylor et al., 2000).



During fibrosis, organ resident cells transform into myofibroblasts and accumulate at the site of injury due to chemokines. Interfering with P311 expression or function and thus with the migration potential of these myofibroblasts could be an opportunity to dampen scar formation. However, one needs to consider whether this would not lead to an accumulation of “triggered or activated” myofibroblast far from the injury site which might not be able to contribute to the resolution of the fibrosis once the injury subsides.

### P311 STIMULATES REGENERATION AND DIFFERENTIATION TOWARD A MYOGENIC PHENOTYPE

Tissue development and regeneration, at least in brain, muscle, and lung, can be influenced by P311 expression (Studler et al., 1993; Fujitani et al., 2004; Siller-Lopez et al., 2004; Ooi et al., 2006). The differentiation of a human neuroblastoma cell line (RTBM1), induced by retinoic acid, was accompanied by an increased P311 expression and neurite outgrowth (Ueda, 2001). This is not surprising, since these probing extensions migrate toward the neighboring cells using lamellipodia and filopodia,

mediated by the RAC1 pathway (Alberts et al., 2008). Upon neuron axotomy in adult rats, P311 is transiently upregulated between day 3 and day 21 post-surgery (Fujitani et al., 2004). Overexpressing P311 in undifferentiated PC12 cells (rat adrenal gland) or differentiated dorsal root ganglions induced neurite outgrowth, due to the induction of cyclin-dependent kinase inhibitor  $p21^{waf1}$ . During neuronal differentiation  $p21^{waf1}$  is up-regulated to prevent cells from entering the cell cycle (Billon et al., 1996; van Grunsven et al., 1996) and can block Rho kinase activity leading to neurite outgrowth (Erhardt and Pittman, 1998; Olson et al., 1998; Yamashita et al., 1999; Tanaka et al., 2002; Fujitani et al., 2004; Tanaka et al., 2004; **Figure 4**). Moreover, facial neurons that were transfected *in vivo* with P311 cDNA regenerated almost three times as fast as non-transfected facial neurons. This could suggest that P311 can interfere with Rho signaling by inducing  $p21^{waf1}$  expression through a thus far unknown mechanism (Fujitani et al., 2004). During human and mouse lung morphogenesis, P311 expression peaks during the saccular and alveolar formation. Smokers who develop emphysema express less P311 compared to smokers without emphysema. Mouse pups treated with dexamethasone, an inhibitor of alveolization, showed a decreased P311 expression when compared to the saline-treated littermates (Zhao et al.,



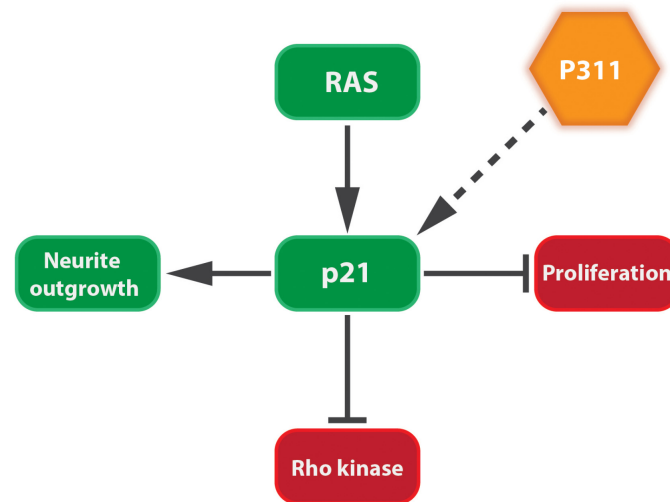


**FIGURE 4 |** P311 induces the expression of p21<sup>Waf1</sup>. p21<sup>Waf1</sup> stimulates neurite outgrowth by blocking cell proliferation and Rho kinase. This is stimulated by both Ras signaling and P311, although it is not yet known if the latter goes directly or indirectly.

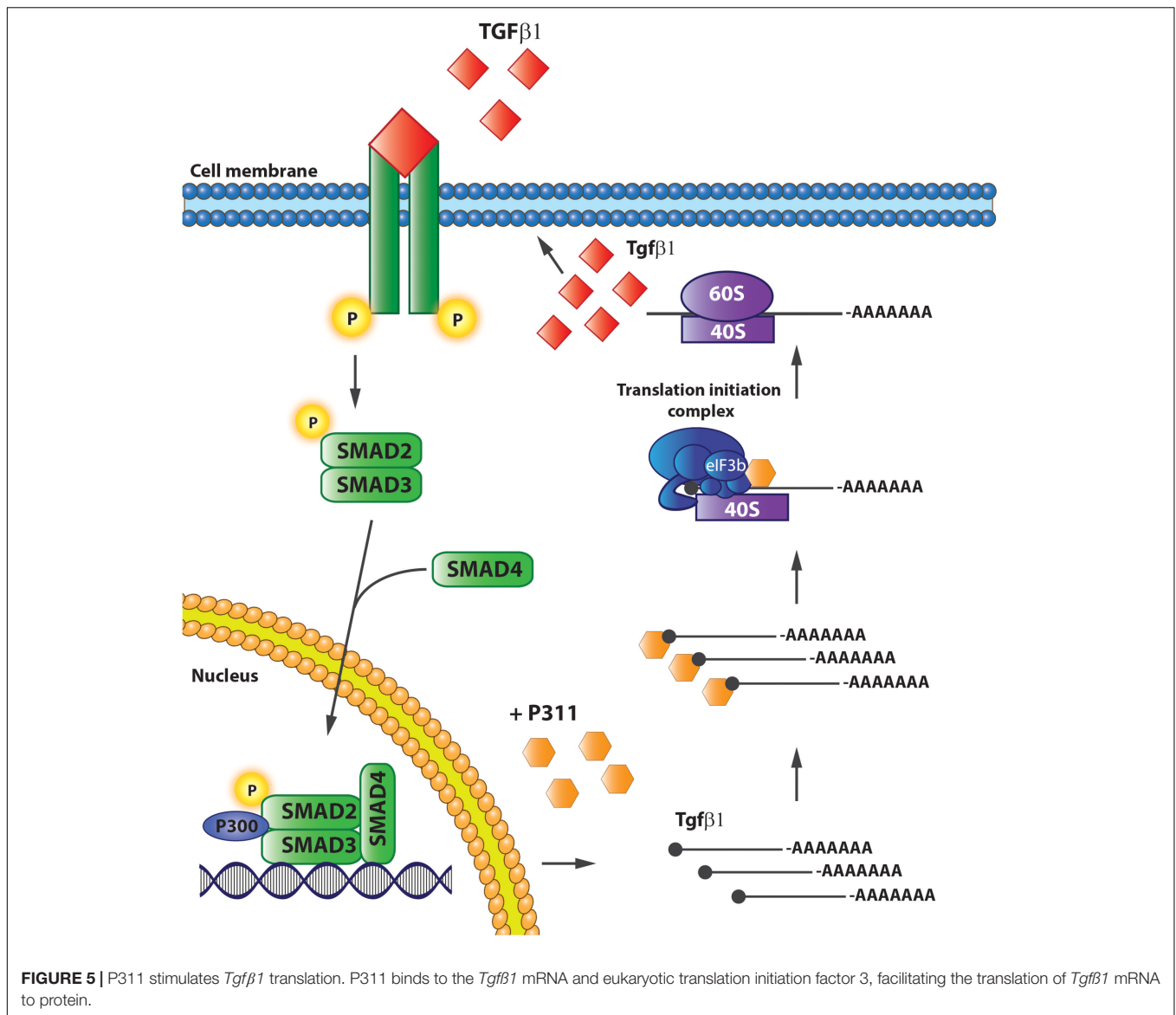
2006). Together this suggests that P311 seems to be involved in the alveolar repair upon injury.

In muscular tissue, P311 expression increases during embryonic pig development and stays active postnatally (Ooi et al., 2006). The opposite was demonstrated for muscle atrophy by two independent studies, one on rats and one on piglets, both looking for molecular patterns that occur during muscle atrophy. Muscle wasting due to skeletal muscle atrophy resulted in a decreased P311 expression, together with other muscle growth stimulating genes, and an increase in E3 ubiquitin ligase enzyme (MAFbx) (Lecker et al., 2004; Ooi et al., 2006). An artificial induction of P311 expression in fibroblasts (3T3 and C3H10) and undifferentiated muscle cell lines (C2C12) on the other hand, induces the expression of muscle-specific transcription factors like myogenic differentiation 1, serum responsive factor (SRF), and myosin heavy chain 4, but less of smooth or skeletal muscle-specific genes. The proliferation rate of these cells increased, but differentiation toward myotubes was attenuated. Myogenic factor 5 (Myf5) was downregulated in all studies, which can be explained by the fact that cell proliferation inhibits Myf5 (Lindon et al., 1998; Pan et al., 2002; Ooi et al., 2006). One of the most important genes that was upregulated is SRF, which interacts with its cofactor myosin light chain kinase 1 to bind to the alpha-smooth muscle actin ( $\alpha$ -SMA) promoter in response to matrix stiffness and regulates the expression of other pro-fibrotic genes after TGF $\beta$ 1 stimulation (Hirschi et al., 2002; Huang et al., 2012). Furthermore, it was shown that SRF has many target genes involved in cytoskeletal organization, migration, and cell proliferation, suggesting that this might be one of P311's key targets (Soulez et al., 1996; Schrott et al., 2002; Miano et al., 2007; Nolte et al., 2013). Similar to cortical neuron differentiation, when terminal differentiation was induced in C2C12 cells by the broad spectrum inducer of muscle differentiation calcineurin, P311 expression was reduced and accompanied by less cell proliferation (Ooi et al., 2006; Bassel-Duby and Olson, 2003).

A correlation between P311 levels and cell proliferation is also described in hepatic stellate cells, invasive glioma cells, and sensory epithelia from the inner ear. Knocking down P311 in hepatic stellate cells reduced cell proliferation *in vitro*. In glioma cells on the other hand, overexpression of anti-tumorigenic gene, melanoma antigen family D1 (DLXIN-1), resulted in less proliferation due to less matrix metalloproteinases (MMP)2 and 9 activity and through direct interaction with P311, DLXIN-1 blocks P311's invasive function. Finally, P311 is more expressed in regenerating sensory hair cells compared to hair cells that do not renew (Hawkins et al., 2006; Reddy et al., 2011; Guimaraes et al., 2015).

## THE P311–TGF $\beta$ 1 PARADOX

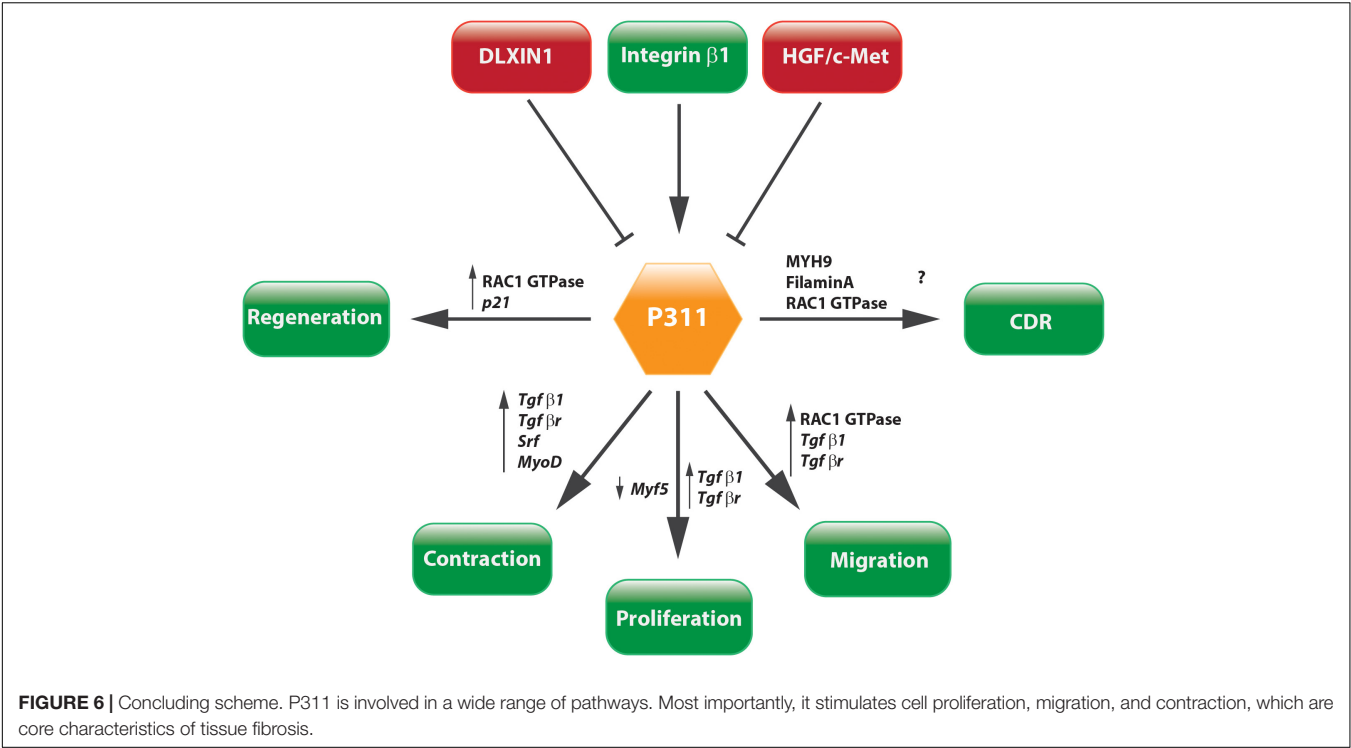
The TGF $\beta$ 1 pathway is one of the main pathways involved in tissue fibrosis. TGF $\beta$ 1 is a pro-fibrogenic agent, whose precursor [TGF $\beta$  bound to a latency-associated protein (LAP)] is stored in the matrix and its activated by proteolytic cleavage by MMP-2, MMP-9, or thrombospondin-1 or mechanical cleavage by integrins, upon tissue damage (Leask and Abraham, 2004; Liu et al., 2009a). Active TGF $\beta$ 1 accumulates and stimulates an epithelial-to-mesenchymal transition (EMT)-like conversion, and the conversion of fibroblasts and mesenchymal cells into myofibroblasts (Leask and Abraham, 2004; Desmouliere et al., 2005; Breitkopf et al., 2006; Bae et al., 2012). Upon stimulation, TGF $\beta$ 1 binds to the heteromeric TGF $\beta$ 1 receptor followed by signaling to TGF $\beta$  receptor I kinase, which phosphorylates the receptor-activated SMAD family members, SMAD2 and 3, intracellularly. Phosphorylated SMAD2/3 binds to SMAD4, after which the complex translocates to the nucleus, where the complex binds to p300 and stimulates the transcription of collagen and *Acta2*, as well as other factors involved in cell proliferation and differentiation of mesenchymal cells (Heldin et al., 1997;



Leask and Abraham, 2004; Breitkopf et al., 2006; Bae et al., 2012). Apart from its role in migration and proliferation, P311 has been strongly associated with the TGFβ1 pathway.

The mechanisms by which P311 can control the TGFβ1 pathway are numerous and depending on the experimental setup it can be stimulatory or inhibitory. P311-overexpressing 3T3 cells, which do not express endogenous P311, can differentiate into myofibroblasts but have inactive TGFβ proteins. In these cells P311 binds to LAP, rendering TGFβ1 and 2 inactive and preventing auto-induction (Piek et al., 2001; Pan et al., 2002; Paliwal et al., 2004). Consequently, these cells express less TGFβ1 and β2, collagen 1, and MMP 2 and 9, suggesting that P311 might be part of an intrinsic anti-fibrotic mechanism in myofibroblasts (Pan et al., 2002). In a renal tubular epithelial cell line (NRK-52E) P311 can inhibit EMT. TGFβ1 treatment stimulates proliferation and can induce EMT in these cells, accompanied with a downregulation of E-cadherin and an α-SMA upregulation.

These effects can be blocked by overexpression of P311 (Qi et al., 2015). These data indicate that overexpression of P311 can reverse or prevent EMT of renal tubular cells and 3T3 fibroblasts *in vitro* (Pan et al., 2002; Paliwal et al., 2004). On the other hand, several studies demonstrate that P311 stimulates TGFβ1 and 2 expression in vascular and lung smooth muscle cells (Badri et al., 2013; Yue et al., 2014). P311 null mice suffer from vascular hypotension, due to a shortage in TGFβ1 and β2 proteins and the absence of P311 in vascular smooth muscle cells results in less Rho A activity and consequently less contractility (Loirand and Pacaud, 2010). In these P311 null mice there is a striking discrepancy between TGFβ protein levels and mRNA levels, i.e., high *Tgfβ1/2* mRNA levels but low protein levels, suggesting that P311 is involved in the translation of *Tgfβ1/2*. Mice overexpressing P311 on the other hand are hypertensive. This was confirmed in samples from normo- and hypertensive patients. P311, and consequently TGFβ protein levels, are highly



expressed in tissues of hypertensive patients when compared to healthy ones (Badri et al., 2013).

P311 also appears to be involved in the formation of hypertrophic scar, which is the result of an imbalanced wound healing and is a fibrosis-like process (Singer and Clark, 1999). P311 is upregulated and co-expressed with  $\alpha$ -SMA, collagen 1, and TGF $\beta$ 1 in the scar tissue, while there is no expression detected in healthy skin. P311 overexpression in healthy skin induces the expression of TGF $\beta$ 1 and increases cell proliferation, while interfering with P311 in fibroblasts derived from scar tissue reduces TGF $\beta$ 1 expression and cell contractility (Tan et al., 2010). In P311 knockout mice, scars from excision wounds showed reduced TGF $\beta$ 1-3 protein levels, less collagen deposition, and consequently reduced tensile strength and scar stiffness (Cheng et al., 2017). Increased P311 expression can also be detected in tubular epithelial cells from patients with chronic kidney disease, colocalized and correlated with TGF $\beta$ 1, while healthy kidney tissue does not express either P311 or TGF $\beta$ 1 (Wang et al., 2010; Yao et al., 2015). The latter observation is confirmed *in vivo* in mice after an unilateral ureteral obstruction, where P311 protein seems to be colocalized with  $\alpha$ -SMA and TGF $\beta$ 1 in acidophilic degeneration regions. Unilateral ureteral obstruction in P311 null mice results in lower levels of collagen type 1 and  $\alpha$ -SMA, a reduced expression of TGF $\beta$  receptor 1 and 2 (TGF $\beta$ R1 and 2), and reduced phosphorylation of SMAD2/3. As indicated in earlier reports, *Tgf $\beta$ 1* mRNA levels in these mice did not differ between the wild type and P311 null mice, but they present reduced TGF $\beta$ 1 protein when P311 was absent (Yao et al., 2015).

Finally, Yue et al. (2014) gave conclusive evidence that P311 is indeed involved in *Tgf $\beta$ 1* translation by showing that it

**TABLE 1 |** Available data on the role of P311 in kidney, liver, and lung.

Organ	Kidney	Liver	Lung
Healthy tissue	<ul style="list-style-type: none"><li>• Low overall P311 expression human (Wang et al., 2010; Yao et al., 2015)</li></ul>	<ul style="list-style-type: none"><li>• Low overall P311 expression mouse (Guimaraes et al., 2015)</li></ul>	No data available
<i>In vivo</i> studies	<ul style="list-style-type: none"><li>• Tubular epithelial cells from injured kidneys express more P311 (Wang et al., 2010; Yao et al., 2015)</li><li>• Absence of P311 reduces TGF<math>\beta</math>1 and 2, <math>\alpha</math>SMA and collagens production upon injury human (Wang et al., 2010; Yao et al., 2015) and mouse (Yao et al., 2015)</li></ul>	<ul style="list-style-type: none"><li>• Hepatic stellate cells express more P311 upon liver injury mouse (Guimaraes et al., 2015)</li></ul>	<ul style="list-style-type: none"><li>• P311 is important for alveolar development</li><li>• P311 expression is associated with a lower risk for emphysema development (Zhao et al., 2006)</li></ul>
<i>In vitro</i> studies	<ul style="list-style-type: none"><li>• In a NRK-52E cell line P311 expression prevents EMT induced by TGF<math>\beta</math>1 (Qi et al., 2015)</li></ul>	<ul style="list-style-type: none"><li>• In primary hepatic stellate cells P311 knockdown hampers cell migration and reduces cell proliferation (Guimaraes et al., 2015)</li></ul>	<ul style="list-style-type: none"><li>• In a human lung smooth muscle cell line P311 stimulates TGF<math>\beta</math>1-3 translation (Yue et al., 2014)</li></ul>

interacts directly with eukaryotic translation initiation factor 3, subunit B (eIF3b), and a protein of the translation initiation complex. In addition, P311 forms a complex with the 5'UTRs of *Tgfb1*, 2, and 3 by which it recruits *Tgfb* mRNA and stimulates its translation (Yue et al., 2014). 3T3 fibroblasts without P311 do translate *Tgfb1*, but an exogenous expression of P311 can increase the levels of total and active TGFβ1 proteins, which is accompanied with increased mRNA levels due to auto-induction (Figure 5). Finally, they also showed that the interaction between P311 and eIF3b occurs on the P311–eIF3b binding motif, which is a highly conserved sequence among different eukaryotes (Yue et al., 2014). These results were confirmed in a study on skin re-epithelialization, where they indicate P311 as a driver of epidermal to mesenchymal transition upon skin damage. Epidermal stem cells expressing exogenous P311 had increased active and LAP-bound TGFβ1 protein levels, increased expression of *TgfbR1* and 2 mRNA, and increased SMAD2/3 phosphorylation, while gaining mesenchymal features. The P311-induced transition was blocked when TGFβRI/II kinases were inhibited. Furthermore, in these cells P311-enhanced methylation of the *Tgfb* promotor and an increased 5' and 3' UTR luciferase activity was observed, indicating that P311 stimulates *Tgfb* mRNA transcription (Li et al., 2016).

**TABLE 2 |** Overview of non-viral delivery systems and targeting molecules that are being used for the delivery of compounds and siRNAs to fibrotic organs.

Non-viral delivery systems		
System	Targeted organ	Reference
Lipid-based carriers (including liposomes, niosomes, lipid modified NP, etc.)	Liver, lung, and skin	Togami et al., 2015; Lyon et al., 2017; Blueschke et al., 2018
Gold particles	Liver and skin	Das et al., 2010
Silica particles	Liver and skin	Chang et al., 2005; Das et al., 2010; Morry et al., 2015
Ultrasound microbubbles	Kidney and liver	Zhang et al., 2013; Li et al., 2018
Targeting molecules		
Targeting molecule	Membrane target	Reference
Vitamin A	Retinol binding protein	Sato et al., 2008; Ishiwatari et al., 2013; Otsuka et al., 2017
RGD	Collagen type 4 receptor	Du et al., 2007; Chai et al., 2012
PDGF	PDGF receptor	Li et al., 2012
tbFGF	FGF receptor	Togami et al., 2015
Synaptophysin antibody	Synaptophysin	Luli et al., 2016
M6PHSA	Mannose-6-phosphate/insulin-like growth factor receptor	van Beuge et al., 2013

NP, nanoparticles; RGD, Arg-Gly-Asp peptide; PDGF, platelet-derived growth factor; tbFGF, truncated basic fibroblast growth factor; M6PHSA, mannose-6-phosphate coupled to human serum albumin.

Although contradictory results exist, it seems that there is a clear correlation between P311 and modulation of TGFβ1 protein levels and its signaling pathways; *in vivo* data indicates that P311 stimulates the TGFβ1 pathway, this was confirmed in cultured primary cells and cell lines (Tan et al., 2010; Wang et al., 2010; Badri et al., 2013; Yue et al., 2014; Yao et al., 2015) but contradicted in two cell lines (Pan et al., 2002; Paliwal et al., 2004; Qi et al., 2015). Nevertheless, some plausible mechanisms have been suggested to explain the observed *in vivo* events, indicating that P311 is an upstream regulator of the TGFβ1 pathway (Yue et al., 2014; Li et al., 2016).

## P311 AS A THERAPEUTIC TARGET?

Currently, different strategies are being applied in clinics/clinical trials to treat tissue fibrosis; anti-fibrotic, anti-inflammatory, anti-oxidant therapies, or combinations of the previous (Schuppan and Kim, 2013; Huang et al., 2015; Schon et al., 2016; Wang et al., 2016). Blocking the TGFβ1 pathway with, for example, fresolimumab or lysyl oxidase ligand 2 antibodies, or stimulating the cells with peroxisome proliferator-activated receptor γ agonists like pioglitazone, are both anti-fibrotic strategies (Rice et al., 2015; Wang et al., 2016). Interferon γ and Ribavirin on the other hand are administered to reduce inflammation (Fernandez et al., 2006), while vitamin E and anthocyanin are two anti-oxidation compounds (Sanyal et al., 2010; Wang et al., 2016). These compounds work well to reduce fibrosis, but are, however, hampered by unwanted side effects (Schon et al., 2016). Targets with a wide range of effects like TGFβ1 or interferon inhibition are supposed to be very efficient to reduce fibrosis, but since they are not tissue-specific, they come with systemic complications. Subjects suffer from mild adverse side effects like anemia, depression, rash, fever, myalgia, internal bleeding, and sometimes even major side effects like worsening of the fibrosis or developing cutaneous neoplasms (Fernandez et al., 2006; Lacouture et al., 2015; Rice et al., 2015). A therapeutic target involved specifically in fibrosis development is needed, preferably combined with a precise delivery method (Gandhi, 2017).

The question whether P311 is an interesting therapeutic target to be considered for anti-fibrotic therapy still remains unanswered, but circumstantial evidence indicates it might be a good candidate. Tissue fibrosis is mainly characterized by proliferative and contractile resident myofibroblasts and myofibroblast-like cells (Friedman et al., 2013; Darby et al., 2014). A process in which TGFβ1 is a master regulator that initiates a self-sustaining loop of attracting and activating myofibroblasts (Ignatz and Massague, 1987; Munger et al., 1999; Li et al., 2007; Giacomini et al., 2012). Studies provided evidence that P311 plays a role in different processes that are initiated during fibrosis development and stimulates the translation of *Tgfb1* mRNA (Figures 5, 6). Moreover, in P311 null mice, the TGFβ1 pathway is clearly less active, which results in hypotensive mice and reduces kidney fibrosis (Badri et al., 2013; Yao et al., 2015). With regard to organs like liver and lung, there is not yet much known regarding the interplay of P311 and TGFβ1 pathways (Table 1). It was demonstrated that P311 could induce a myogenic phenotype



in fibroblasts and stimulate its migration (Taylor et al., 2000; Pan et al., 2002; McDonough et al., 2005; Shi et al., 2006; Guimaraes et al., 2015; **Figure 6**). Finally, P311 might have a role in integrin  $\beta 1$  recycling, since P311 interacts with Filamin A and MYH9, while the former is an interconnecting protein between F-actin and integrin  $\beta 1$ , the latter is responsible for integrin  $\beta 1$  recycling with F-actin, which is stimulated by the RAC1 pathway (McDonough et al., 2005; Huang et al., 2009; Liu et al., 2011; Casalou et al., 2014; Yue et al., 2014; **Figures 3, 6**). Silencing P311 *in vivo* or interference with P311 functionality might hamper the fibrogenic process and could allow the tissue to enter the regeneration phase.

The safety of P311 inhibition can be estimated as relatively high, since P311-deficient mice do not present a detrimental phenotype, indicating that development and homeostasis of the body might not be influenced by P311 inhibition. However, since P311 stimulates cell migration, proliferation, and regeneration it indicates that untargeted delivery of siRNA or a compound that could block P311 function *in vivo* might randomly interfere with crucial processes for tissue repair. This can be deduced from studies that showed that patients with less P311 have a decreased alveolar repair after emphysema (Zhao et al., 2006). Therefore, a specific delivery of a P311 siRNA or inhibitory compound to resident myofibroblastic cells in the fibrotic organs would be essential. Local delivery of compounds or siRNA, either free or in nanocomplexes like liposomes, is not always straightforward. While hydrogels and aerosols can achieve this for the treatment of scars or lung fibrosis, respectively (Ivanova et al., 2013; Manosroi et al., 2013; Gumel et al., 2015; Sun, 2017), targeting myofibroblasts in the liver or kidney requires targeted nanomedicine. This can be achieved by using targeted viral vectors (Reetz et al., 2013; Cooney et al., 2018), but over the last decennia a wide array of non-viral delivery systems has been developed for both the delivery of siRNAs and compounds (**Table 2**). For example, delivery of siRNA loaded in targeted liposomes, as already been shown for hepatic and pancreatic fibrosis (Sato et al., 2008; Davies et al., 2014), or an ultrasound microbubble delivery of shRNA to kidneys (Li

et al., 2018). Such a specific inhibition of P311 in resident myofibroblasts might interfere with the fibrotic cascade by decreasing cell migration and proliferation and would interfere with the increased TGF $\beta 1$  protein levels. Due to this, the accumulation of myofibroblasts at the site of injury might be attenuated and the tissue would be able to initiate resolution of the extracellular matrix.

## CONCLUSION

A large body of evidence suggests that P311 is necessary for correct TGF $\beta 1$  production and its inhibition might result in a less myofibroblastic phenotype, decreased TGF $\beta 1$  protein expression and collagen deposition. Importantly, few studies have explored the *in vivo* effects of P311 modulation and its consequence to fibrosis (Yao et al., 2015). Thus, the potential of P311 as an anti-fibrotic target has still to be investigated in other organs, such as lung, liver, and skin, all of which have a high propensity to develop fibrosis. Nevertheless, the possibility of combining specific delivery targeting (i.e., targeted liposomes) and P311 inhibition may prove to be an efficient and safe treatment due to the distinct expression and role of this protein in fibrosis development.

## AUTHOR CONTRIBUTIONS

LS and LvG conceived the work and provided the layout for it. LS and IM drafted the work. LvG critically revised the text and figures and approved the final manuscript for publication.

## FUNDING

This work has been funded by the Vrije Universiteit Brussel and by the Instituut voor Innovatie door Wetenschap en Technologie (IWT/SB 121416).

## REFERENCES

- Alberts, B., Johnson, A., Lewis, J., Raff, M., Roberts, K., and Walter, P. (2008). "Neural development," in *Molecular biology of the cell*, eds M. Anderson, and S. Granum (New York, NY: Garland Science), 1383–1397.
- Ardaillou, R., Chansel, D., Chatziantoniou, C., and Dussaule, J. C. (1999). Mesangial AT1 receptors: expression, signaling, and regulation. *J. Am. Soc. Nephrol.* 10(Suppl. 11), S40–S46.
- Armulik, A., Abramsson, A., and Betsholtz, C. (2005). Endothelial/pericyte interactions. *Circ. Res.* 97, 512–523. doi: 10.1161/01.RES.0000182903.16652.d7
- Badri, K. R., Yue, M., Carretero, O. A., Aramgam, S. L., Cao, J., Sharkady, S., et al. (2013). Blood pressure homeostasis is maintained by a P311-TGF-beta axis. *J. Clin. Invest.* 123, 4502–4512. doi: 10.1172/JCI69884
- Bae, E., Kim, S. J., Hong, S., Liu, F., and Ooshima, A. (2012). Smad3 linker phosphorylation attenuates Smad3 transcriptional activity and TGF-beta1/Smad3-induced epithelial-mesenchymal transition in renal epithelial cells. *Biochem. Biophys. Res. Commun.* 427, 593–599. doi: 10.1016/j.bbrc.2012.09.103
- Barkauskas, C. E., and Noble, P. W. (2014). Cellular mechanisms of tissue fibrosis. 7. New insights into the cellular mechanisms of pulmonary fibrosis. *Am. J. Physiol. Cell Physiol.* 306, C987–C996. doi: 10.1152/ajpcell.00321.2013
- Bassel-Duby, R., and Olson, E. N. (2003). Role of calcineurin in striated muscle: development, adaptation, and disease. *Biochem. Biophys. Res. Commun.* 311, 1133–1141. doi: 10.1016/j.bbrc.2003.09.020
- Billon, N., van Grunsven, L. A., and Rudkin, B. B. (1996). The CDK inhibitor p21WAF1/Cip1 is induced through a p300-dependent mechanism during NGF-mediated neuronal differentiation of PC12 cells. *Oncogene* 13, 2047–2054.
- Blueschke, G., Boico, A., Negussie, A. H., Yarmolenko, P., Wood, B. J., Spasojevic, I., et al. (2018). Enhanced drug delivery to the skin using liposomes. *Plast. Reconstr. Surg. Glob. Open* 6:e1739. doi: 10.1097/GOX.0000000000001739
- Breitkopf, K., Godoy, P., Ciucan, L., Singer, M. V., and Dooley, S. (2006). TGF-beta/Smad signaling in the injured liver. *Z. Gastroenterol.* 44, 57–66. doi: 10.1055/s-2005-858989
- Bunnell, T. M., Burbach, B. J., Shimizu, Y., and Ervasti, J. M. (2011). Beta-Actin specifically controls cell growth, migration, and the G-actin pool. *Mol. Biol. Cell* 22, 4047–4058. doi: 10.1091/mbc.e11-06-0582
- Casalou, C., Seixas, C., Portelinha, A., Pintado, P., Barros, M., Ramalho, J. S., et al. (2014). Arl13b and the non-muscle myosin heavy chain IIA are required for

- circular dorsal ruffle formation and cell migration. *J. Cell Sci.* 127, 2709–2722. doi: 10.1042/jcs.143446
- Chai, N. L., Fu, Q., Shi, H., Cai, C. H., Wan, J., Xu, S. P., et al. (2012). Oxymatrine liposome attenuates hepatic fibrosis via targeting hepatic stellate cells. *World J. Gastroenterol.* 18, 4199–4206. doi: 10.3748/wjg.v18.i31.4199
- Chang, M. L., Yeh, C. T., Chang, P. Y., and Chen, J. C. (2005). Comparison of murine cirrhosis models induced by hepatotoxin administration and common bile duct ligation. *World J. Gastroenterol.* 11, 4167–4172. doi: 10.3748/wjg.v11.i27.4167
- Cheng, T., Yue, M., Aslam, M. N., Wang, X., Shekhawat, G., Varani, J., et al. (2017). Neuronal protein 3.1 deficiency leads to reduced cutaneous scar collagen deposition and tensile strength due to impaired transforming growth factor-beta1 to -beta3 translation. *Am. J. Pathol.* 187, 292–303. doi: 10.1016/j.ajpath.2016.10.004
- Cooney, A. L., Singh, B. K., Loza, L. M., Thornell, I. M., Hippee, C. E., Powers, L. S., et al. (2018). Widespread airway distribution and short-term phenotypic correction of cystic fibrosis pigs following aerosol delivery of piggyBac/adenovirus. *Nucleic Acids Res.* doi: 10.1093/nar/gky773 [Epub ahead of print].
- Darby, I. A., Laverdet, B., Bonte, F., and Desmouliere, A. (2014). Fibroblasts and myofibroblasts in wound healing. *Clin. Cosmet. Investig. Dermatol.* 7, 301–311.
- Das, A., Mukherjee, P., Singla, S. K., Guturu, P., Frost, M. C., Mukhopadhyay, D., et al. (2010). Fabrication and characterization of an inorganic gold and silica nanoparticle mediated drug delivery system for nitric oxide. *Nanotechnology* 21:305102. doi: 10.1088/0957-4484/21/30/305102
- Davies, L. A., Nunez-Alonso, G. A., McLachlan, G., Hyde, S. C., and Gill, D. R. (2014). Aerosol delivery of DNA/liposomes to the lung for cystic fibrosis gene therapy. *Hum. Gene Ther. Clin. Dev.* 25, 97–107. doi: 10.1089/humc.2014.019
- Desmouliere, A., Chaponnier, C., and Gabbiani, G. (2005). Tissue repair, contraction, and the myofibroblast. *Wound Rep. Regen.* 13, 7–12. doi: 10.1111/j.1067-1927.2005.130102.x
- Desmouliere, A., Redard, M., Darby, I., and Gabbiani, G. (1995). Apoptosis mediates the decrease in cellularity during the transition between granulation tissue and scar. *Am. J. Pathol.* 146, 56–66.
- Dranoff, J. A., Ogawa, M., Gaca, M. D., Sevigny, J., Robson, S. C., et al. (2004). Expression of P2Y nucleotide receptors and ectonucleotidases in quiescent and activated rat hepatic stellate cells. *Am. J. Physiol. Gastrointest. Liver Physiol.* 287, G417–G424. doi: 10.1152/ajpgi.00294.2003
- Du, S. L., Pan, H., Lu, W. Y., Wang, J., Wu, J., and Wang, J. Y. (2007). Cyclic Arg-Gly-Asp peptide-labeled liposomes for targeting drug therapy of hepatic fibrosis in rats. *J. Pharmacol. Exp. Ther.* 322, 560–568. doi: 10.1124/jpet.107.122481
- Erhardt, J. A., and Pittman, R. N. (1998). Ectopic p21(WAF1) expression induces differentiation-specific cell cycle changes in PC12 cells characteristic of nerve growth factor treatment. *J. Biol. Chem.* 273, 23517–23523. doi: 10.1074/jbc.273.36.23517
- Fernandez, I., Meneu, J. C., Colina, F., Garcia, I., Munoz, R., Castellano, G., et al. (2006). Clinical and histological efficacy of pegylated interferon and ribavirin therapy of recurrent hepatitis C after liver transplantation. *Liver Transpl.* 12, 1805–1812. doi: 10.1002/lt.20883
- Friedman, S. L. (2008). Hepatic stellate cells: protean, multifunctional, and enigmatic cells of the liver. *Physiol. Rev.* 88, 125–172. doi: 10.1152/physrev.00013.2007
- Friedman, S. L., Sheppard, D., Duffield, J. S., and Violette, S. (2013). Therapy for fibrotic diseases: nearing the starting line. *Sci. Transl. Med.* 5:167sr1. doi: 10.1126/scitranslmed.3004700
- Fujitani, M., Yamagishi, S., Che, Y. H., Hata, K., Kubo, T., Ino, H., et al. (2004). P311 accelerates nerve regeneration of the axotomized facial nerve. *J. Neurochem.* 91, 737–744. doi: 10.1111/j.1471-4159.2004.02738.x
- Gandhi, C. R. (2017). Hepatic stellate cell activation and pro-fibrogenic signals. *J. Hepatol.* 67, 1104–1105. doi: 10.1016/j.jhep.2017.06.001
- Giacomini, M. M., Travis, M. A., Kudo, M., and Sheppard, D. (2012). Epithelial cells utilize cortical actin/myosin to activate latent TGF-beta through integrin alpha(v)beta(6)-dependent physical force. *Exp. Cell Res.* 318, 716–722. doi: 10.1016/j.yexcr.2012.01.020
- Guimaraes, E. L., Stradiot, L., Mannaerts, I., Schroyen, B., and van Grunsven, L. A. (2015). P311 modulates hepatic stellate cells migration. *Liver Int.* 35, 1253–1264. doi: 10.1111/liv.12691
- Gumel, A. M., Razaif-Mazinah, M. R., Anis, S. N., and Annuar, M. S. (2015). Poly (3-hydroxyalkanoates)-co-(6-hydroxyhexanoate) hydrogel promotes angiogenesis and collagen deposition during cutaneous wound healing in rats. *Biomed. Mater.* 10:045001. doi: 10.1088/1748-6041/10/4/045001
- Hattori, T., Shimokawa, H., Higashi, M., Hiroki, J., Mukai, Y., Tsutsui, H., et al. (2004). Long-term inhibition of Rho-kinase suppresses left ventricular remodeling after myocardial infarction in mice. *Circulation* 109, 2234–2239. doi: 10.1161/01.CIR.0000127939.16111.58
- Hawkins, R. D., Helms, C. A., Winston, J. B., Warchol, M. E., and Lovett, M. (2006). Applying genomics to the avian inner ear: development of subtractive cDNA resources for exploring sensory function and hair cell regeneration. *Genomics* 87, 801–808. doi: 10.1016/j.ygeno.2005.12.014
- Heldin, C. H., Miyazono, K., and ten Dijke, P. (1997). TGF-beta signalling from cell membrane to nucleus through SMAD proteins. *Nature* 390, 465–471. doi: 10.1038/37284
- Hirschi, K. K., Lai, L., Belaguli, N. S., Dean, D. A., Schwartz, R. J., and Zimmer, W. E. (2002). Transforming growth factor-beta induction of smooth muscle cell phenotype requires transcriptional and post-transcriptional control of serum response factor. *J. Biol. Chem.* 277, 6287–6295. doi: 10.1074/jbc.M106649200
- Huang, B., Lu, M., Jolly, M. K., Tsarfaty, I., Onuchic, J., and Ben-Jacob, E. (2014). The three-way switch operation of Rac1/RhoA GTPase-based circuit controlling amoeboid-hybrid-mesenchymal transition. *Sci. Rep.* 4:6449. doi: 10.1038/srep06449
- Huang, H., Dai, H. P., Kang, J., Chen, B. Y., Sun, T. Y., and Xu, Z. J. (2015). Double-blind randomized trial of pirfenidone in chinese idiopathic pulmonary fibrosis patients. *Medicine* 94:e1600. doi: 10.1097/MD.0000000000001600
- Huang, X., Yang, N., Fiore, V. F., Barker, T. H., Sun, Y., Morris, S. W., et al. (2012). Matrix stiffness-induced myofibroblast differentiation is mediated by intrinsic mechanotransduction. *Am. J. Respir. Cell Mol. Biol.* 47, 340–348. doi: 10.1165/rcmb.2012-0050OC
- Huang, Y., Arora, P., McCulloch, C. A., and Vogel, W. F. (2009). The collagen receptor DDR1 regulates cell spreading and motility by associating with myosin IIA. *J. Cell Sci.* 122, 1637–1646. doi: 10.1242/jcs.046219
- Ignatz, R. A., and Massague, J. (1987). Cell adhesion protein receptors as targets for transforming growth factor-beta action. *Cell* 51, 189–197. doi: 10.1016/0092-8674(87)90146-2
- Ishiwatari, H., Sato, Y., Murase, K., Yoneda, A., Fujita, R., Nishita, H., et al. (2013). Treatment of pancreatic fibrosis with siRNA against a collagen-specific chaperone in vitamin A-coupled liposomes. *Gut* 62, 1328–1339. doi: 10.1136/gutjnl-2011-301746
- Ivanova, V., Garbuzenko, O. B., Reuhl, K. R., Reimer, D. C., Pozharov, V. P., and Minko, T. (2013). Inhalation treatment of pulmonary fibrosis by liposomal prostaglandin E2. *Eur. J. Pharm. Biopharm.* 84, 335–344. doi: 10.1016/j.ejpb.2012.11.023
- Jeffers, M., Rong, S., and Vande Woude, G. F. (1996). Enhanced tumorigenicity and invasion-metastasis by hepatocyte growth factor/scatter factor-met signalling in human cells concomitant with induction of the urokinase proteolysis network. *Mol. Cell. Biol.* 16, 1115–1125. doi: 10.1128/MCB.16.3.1115
- Kajiwara, K., Sugaya, E., Kimura, M., Katsuki, M., Nagasawa, H., Yuyama, N., et al. (1995). Cloning and characterization of pentylentetrazol-related cDNA, PTZ-17. *Brain Res.* 671, 170–174. doi: 10.1016/0006-8993(94)01308-5
- Kisseleva, T., Cong, M., Paik, Y., Scholten, D., Jiang, C., Benner, C., et al. (2012). Myofibroblasts revert to an inactive phenotype during regression of liver fibrosis. *Proc. Natl. Acad. Sci. U.S.A.* 109, 9448–9453. doi: 10.1073/pnas.1201840109
- Kuroda, S., Tashiro, H., Kimura, Y., Hirata, K., Tsutada, M., Mikuriya, Y., et al. (2015). Rho-kinase inhibitor targeting the liver prevents ischemia/reperfusion injury in the steatotic liver without major systemic adversity in rats. *Liver Transpl.* 21, 123–131. doi: 10.1002/lt.24020
- Lacouture, M. E., Morris, J. C., Lawrence, D. P., Tan, A. R., Olencki, T. E., Shapiro, G. I., et al. (2015). Cutaneous keratoacanthomas/squamous cell carcinomas associated with neutralization of transforming growth factor beta by the monoclonal antibody fresolimumab (GC1008). *Cancer Immunol. Immunother.* 64, 437–446. doi: 10.1007/s00262-015-1653-0
- Leask, A., and Abraham, D. J. (2004). TGF-beta signaling and the fibrotic response. *FASEB J.* 18, 816–827. doi: 10.1096/fj.03-1273rev

- Lecker, S. H., Jagoe, R. T., Gilbert, A., Gomes, M., Baracos, V., Bailey, J., et al. (2004). Multiple types of skeletal muscle atrophy involve a common program of changes in gene expression. *FASEB J.* 18, 39–51. doi: 10.1096/fj.03-0610com
- Li, F., Li, Q. H., Wang, J. Y., Zhan, C. Y., Xie, C., and Lu, W. Y. (2012). Effects of interferon-gamma liposomes targeted to platelet-derived growth factor receptor-beta on hepatic fibrosis in rats. *J. Control. Release* 159, 261–270. doi: 10.1016/j.jconrel.2011.12.023
- Li, H., Cai, H., Deng, J., Tu, X., Sun, Y., Huang, Z., et al. (2018). TGF-beta-mediated upregulation of Sox9 in fibroblast promotes renal fibrosis. *Biochim. Biophys. Acta* 1864, 520–532. doi: 10.1016/j.bbdis.2017.11.011
- Li, H., Yao, Z., He, W., Gao, H., Bai, Y., Yang, S., et al. (2016). P311 induces the transdifferentiation of epidermal stem cells to myofibroblast-like cells by stimulating transforming growth factor beta1 expression. *Stem cell Res. Ther.* 7:175. doi: 10.1186/s13287-016-0421-1
- Li, Z., Dranoff, J. A., Chan, E. P., Uemura, M., Sevigny, J., and Wells, R. G. (2007). Transforming growth factor-beta and substrate stiffness regulate portal fibroblast activation in culture. *Hepatology* 46, 1246–1256. doi: 10.1002/hep.21792
- Lindon, C., Montarras, D., and Pinset, C. (1998). Cell cycle-regulated expression of the muscle determination factor Myf5 in proliferating myoblasts. *J. Cell Biol.* 140, 111–118. doi: 10.1083/jcb.140.1.111
- Liu, F., Mih, J. D., Shea, B. S., Kho, A. T., Sharif, A. S., Tager, A. M., et al. (2010). Feedback amplification of fibrosis through matrix stiffening and COX-2 suppression. *J. Cell Biol.* 190, 693–706. doi: 10.1083/jcb.201004082
- Liu, S., Kapoor, M., Denton, C. P., Abraham, D. J., and Leask, A. (2009a). Loss of beta1 integrin in mouse fibroblasts results in resistance to skin scleroderma in a mouse model. *Arthritis Rheum.* 60, 2817–2821. doi: 10.1002/art.24801
- Liu, S., Kapoor, M., and Leask, A. (2009b). Rac1 expression by fibroblasts is required for tissue repair in vivo. *Am. J. Pathol.* 174, 1847–1856. doi: 10.2353/ajpath.2009.080779
- Liu, Z., Van Rossen, E., Timmermans, J. P., Geerts, A., van Grunsven, L. A., and Reynaert, H. (2011). Distinct roles for non-muscle myosin II isoforms in mouse hepatic stellate cells. *J. Hepatol.* 54, 132–141. doi: 10.1016/j.jhep.2010.06.020
- Loirand, G., and Pacaud, P. (2010). The role of Rho protein signaling in hypertension. *Nat. Rev. Cardiol.* 7, 637–647. doi: 10.1038/nrcardio.2010.136
- Luli, S., Di Paolo, D., Perri, P., Brignole, C., Hill, S. J., Brown, H., et al. (2016). A new fluorescence-based optical imaging method to non-invasively monitor hepatic myofibroblasts in vivo. *J. Hepatol.* 65, 75–83. doi: 10.1016/j.jhep.2016.03.021
- Lyon, P. C., Griffiths, L. F., Lee, J., Chung, D., Carlisle, R., Wu, F., et al. (2017). Clinical trial protocol for TARDOX: a phase I study to investigate the feasibility of targeted release of lyso-thermosensitive liposomal doxorubicin (ThermoDox(R)) using focused ultrasound in patients with liver tumours. *J. Ther. Ultrasound* 5:28. doi: 10.1186/s40349-017-0104-0
- Manosroi, A., Chankhampan, C., Manosroi, W., and Manosroi, J. (2013). Transdermal absorption enhancement of papain loaded in elastic niosomes incorporated in gel for scar treatment. *Eur. J. Pharm. Sci.* 48, 474–483. doi: 10.1016/j.ejps.2012.12.010
- Mariani, L., McDonough, W. S., Hoelzinger, D. B., Beaudry, C., Kaczmarek, E., Coons, S. W., et al. (2001). Identification and validation of P311 as a glioblastoma invasion gene using laser capture microdissection. *Cancer Res.* 61, 4190–4196.
- McDonough, W. S., Tran, N. L., and Berens, M. E. (2005). Regulation of glioma cell migration by serine-phosphorylated P311. *Neoplasia* 7, 862–872. doi: 10.1593/neo.05190
- Miano, J. M., Long, X., and Fujiwara, K. (2007). Serum response factor: master regulator of the actin cytoskeleton and contractile apparatus. *Am. J. Physiol. Cell Physiol.* 292, C70–C81. doi: 10.1152/ajpcell.00386.2006
- Morry, J., Ngamcherdtrakul, W., Gu, S., Goodyear, S. M., Castro, D. J., Reda, M. M., et al. (2015). Dermal delivery of HSP47 siRNA with NOX4-modulating mesoporous silica-based nanoparticles for treating fibrosis. *Biomaterials* 66, 41–52. doi: 10.1016/j.biomaterials.2015.07.005
- Munger, J. S., Huang, X., Kawakatsu, H., Griffiths, M. J., Dalton, S. L., Wu, J., et al. (1999). The integrin alpha v beta 6 binds and activates latent TGF beta 1: a mechanism for regulating pulmonary inflammation and fibrosis. *Cell* 96, 319–328. doi: 10.1016/S0092-8674(00)80545-0
- Nayak, B. K., Shanmugasundaram, K., Friedrichs, W. E., Cavaglieri, R. C., Patel, M., Barnes, J., et al. (2016). HIF-1 mediates renal fibrosis in OVE26 type 1 diabetic mice. *Diabetes Metab. Res. Rev.* 65, 1387–1397.
- Nolte, A., Aufderklamm, S., Scheu, K., Walker, T., Konig, O., Bottcher, M., et al. (2013). Small interfering RNA transfection against serum response factor mediates growth inhibition of benign prostatic hyperplasia fibroblasts. *Nucleic Acid Ther.* 23, 62–70. doi: 10.1089/nat.2012.0392
- Olsen, A. L., Bloomer, S. A., Chan, E. P., Gaca, M. D., Georges, P. C., Sackey, B., et al. (2011). Hepatic stellate cells require a stiff environment for myofibroblastic differentiation. *Am. J. Physiol. Gastrointest. Liver Physiol.* 301, G110–G118. doi: 10.1152/ajpgi.00412.2010
- Olson, M. F., Paterson, H. F., and Marshall, C. J. (1998). Signals from Ras and Rho GTPases interact to regulate expression of p21Waf1/Cip1. *Nature* 394, 295–299. doi: 10.1038/28425
- Ooi, P. T., da Costa, N., Edgar, J., and Chang, K. C. (2006). Porcine congenital splayleg is characterised by muscle fibre atrophy associated with relative rise in MAFbx and fall in P311 expression. *BMC Vet. Res.* 2:23. doi: 10.1186/1746-6148-2-23
- Otsuka, M., Shiratori, M., Chiba, H., Kuronuma, K., Sato, Y., Niitsu, Y., et al. (2017). Treatment of pulmonary fibrosis with siRNA against a collagen-specific chaperone HSP47 in vitamin A-coupled liposomes. *Exp. Lung Res.* 43, 271–282. doi: 10.1080/01902148.2017.1354946
- Paliwal, S., Shi, J., Dhru, U., Zhou, Y., and Schuger, L. (2004). P311 binds to the latency associated protein and downregulates the expression of TGF-beta1 and TGF-beta2. *Biochem. Biophys. Res. Commun.* 315, 1104–1109. doi: 10.1016/j.bbrc.2004.01.171
- Pan, D., Zhe, X., Jakkaraju, S., Taylor, G. A., and Schuger, L. (2002). P311 induces a TGF-beta1-independent, nonfibrogenic myofibroblast phenotype. *J. Clin. Invest.* 110, 1349–1358. doi: 10.1172/JCI0215614
- Piek, E., Ju, W. J., Heyer, J., Escalante-Alcalde, D., Stewart, C. L., Weinstein, M., et al. (2001). Functional characterization of transforming growth factor beta signaling in Smad2- and Smad3-deficient fibroblasts. *J. Biol. Chem.* 276, 19945–19953. doi: 10.1074/jbc.M102382200
- Qi, F., Cai, P., Liu, X., Peng, M., and Si, G. (2015). Adenovirus-mediated P311 inhibits TGF-beta1-induced epithelial-mesenchymal transition in NRK-52E cells via TGF-beta1-Smad-ILK pathway. *Biosci. Trends* 9, 299–306. doi: 10.5582/bst.2015.01129
- Reddy, E. M., Chettiar, S. T., Kaur, N., Ganeshkumar, R., Shepal, V., Shanbhag, N. C., et al. (2011). Dlxin-1, a member of MAGE family, inhibits cell proliferation, invasion and tumorigenicity of glioma stem cells. *Cancer Gene Ther.* 18, 206–218. doi: 10.1038/cgt.2010.71
- Reetz, J., Genz, B., Meier, C., Kowtharapu, B. S., Timm, F., Vollmar, B., et al. (2013). Development of adenoviral delivery systems to target hepatic stellate cells in vivo. *PLoS One* 8:e67091. doi: 10.1371/journal.pone.0067091
- Rice, L. M., Padilla, C. M., McLaughlin, S. R., Mathes, A., Ziemek, J., Goummih, S., et al. (2015). Fresolimumab treatment decreases biomarkers and improves clinical symptoms in systemic sclerosis patients. *J. Clin. Invest.* 125, 2795–2807. doi: 10.1172/JCI77958
- Sanyal, A. J., Chalasani, N., Kowdley, K. V., McCullough, A., Diehl, A. M., Bass, N. M., et al. (2010). Pioglitazone, vitamin E, or placebo for nonalcoholic steatohepatitis. *N. Engl. J. Med.* 362, 1675–1685. doi: 10.1056/NEJMoa0907929
- Sato, Y., Murase, K., Kato, J., Kobune, M., Sato, T., Kawano, Y., et al. (2008). Resolution of liver cirrhosis using vitamin A-coupled liposomes to deliver siRNA against a collagen-specific chaperone. *Nat. Biotechnol.* 26, 431–442. doi: 10.1038/nbt1396
- Scholten, D., Reichart, D., Paik, Y. H., Lindert, J., Bhattacharya, J., Glass, C. K., et al. (2011). Migration of fibrocytes in fibrogenic liver injury. *Am. J. Pathol.* 179, 189–198. doi: 10.1016/j.ajpath.2011.03.049
- Schon, H. T., Bartneck, M., Borkham-Kamphorst, E., Nattermann, J., Lammers, T., Tacke, F., et al. (2016). Pharmacological intervention in hepatic stellate cell activation and hepatic fibrosis. *Front. Pharmacol.* 7:33. doi: 10.3389/fphar.2016.00033
- Schratt, G., Philippar, U., Berger, J., Schwarz, H., Heidenreich, O., and Nordheim, A. (2002). Serum response factor is crucial for actin cytoskeletal organization and focal adhesion assembly in embryonic stem cells. *J. Cell Biol.* 156, 737–750. doi: 10.1083/jcb.200106008
- Schuppan, D., and Kim, Y. O. (2013). Evolving therapies for liver fibrosis. *J. Clin. Invest.* 123, 1887–1901. doi: 10.1172/JCI66028
- Shaw, L. M., Rabinovitz, I., Wang, H. H., Toker, A., and Mercurio, A. M. (1997). Activation of phosphoinositide 3-OH kinase by the alpha6beta4 integrin



- promotes carcinoma invasion. *Cell* 91, 949–960. doi: 10.1016/S0092-8674(00)80486-9
- Shi, J., Badri, K. R., Choudhury, R., and Schuger, L. (2006). P311-induced myofibroblasts exhibit amoeboid-like migration through RALA activation. *Exp. Cell Res.* 312, 3432–3442. doi: 10.1016/j.yexcr.2006.07.016
- Shimizu, Y., Dobashi, K., Iizuka, K., Horie, T., Suzuki, K., Tukagoshi, H., et al. (2001). Contribution of small GTPase Rho and its target protein rock in a murine model of lung fibrosis. *Am. J. Respir. Crit. Care Med.* 163, 210–217. doi: 10.1164/ajrcrm.163.1.2001089
- Siller-Lopez, F., Sandoval, A., Salgado, S., Salazar, A., Bueno, M., Garcia, J., et al. (2004). Treatment with human metalloproteinase-8 gene delivery ameliorates experimental rat liver cirrhosis. *Gastroenterology* 126, 1122–1133; discussion 949. doi: 10.1053/j.gastro.2003.12.045
- Simone, T. M., Longmate, W. M., Law, B. K., and Higgins, P. J. (2015). Targeted inhibition of PAI-1 activity impairs epithelial migration and wound closure following cutaneous injury. *Adv. Wound Care* 4, 321–328. doi: 10.1089/wound.2014.0611
- Singer, A. J., and Clark, R. A. (1999). Cutaneous wound healing. *N. Engl. J. Med.* 341, 738–746. doi: 10.1056/NEJM199909023411006
- Soulez, M., Rouviere, C. G., Chafey, P., Hentzen, D., Vandromme, M., Lautredou, N., et al. (1996). Growth and differentiation of C2 myogenic cells are dependent on serum response factor. *Mol. Cell. Biol.* 16, 6065–6074. doi: 10.1128/MCB.16.11.6065
- Studler, J. M., Glowinski, J., and Levi-Strauss, M. (1993). An abundant mRNA of the embryonic brain persists at a high level in cerebellum, hippocampus and olfactory bulb during adulthood. *Eur. J. Neurosci.* 5, 614–623. doi: 10.1111/j.1460-9568.1993.tb00527.x
- Sun, G. (2017). Pro-regenerative hydrogel restores scarless skin during Cutaneous wound healing. *Adv. Healthc. Mater.* 6:1700659 doi: 10.1002/adhm.201700659
- Sun, Y. G., Gao, Y. J., Zhao, Z. Q., Huang, B., Yin, J., Taylor, G. A., et al. (2008). Involvement of P311 in the affective, but not in the sensory component of pain. *Mol. Pain* 4:23. doi: 10.1186/1744-8069-4-23
- Tan, J., Peng, X., Luo, G., Ma, B., Cao, C., He, W., et al. (2010). Investigating the role of P311 in the hypertrophic scar. *PLoS One* 5:e9995. doi: 10.1371/journal.pone.0009995
- Tanaka, H., Yamashita, T., Asada, M., Mizutani, S., Yoshikawa, H., and Tohyama, M. (2002). Cytoplasmic p21(Cip1/WAF1) regulates neurite remodeling by inhibiting Rho-kinase activity. *J. Cell Biol.* 158, 321–329. doi: 10.1083/jcb.200202071
- Tanaka, H., Yamashita, T., Yachi, K., Fujiwara, T., Yoshikawa, H., and Tohyama, M. (2004). Cytoplasmic p21(Cip1/WAF1) enhances axonal regeneration and functional recovery after spinal cord injury in rats. *Neuroscience* 127, 155–164. doi: 10.1016/j.neuroscience.2004.05.010
- Taylor, G. A., Hudson, E., Resau, J. H., and Vande Woude, G. F. (2000). Regulation of P311 expression by Met-hepatocyte growth factor/scatter factor and the ubiquitin/proteasome system. *J. Biol. Chem.* 275, 4215–4219. doi: 10.1074/jbc.275.6.4215
- Taylor, G. A., Rodriguez, R. M., Greene, R. I., Daniell, X., Henry, S. C., Crooks, K. R., et al. (2008). Behavioral characterization of P311 knockout mice. *Genes Brain Behav.* 7, 786–795. doi: 10.1111/j.1601-183X.2008.00420.x
- Togami, K., Miyao, A., Miyakoshi, K., Kanehira, Y., Tada, H., and Chono, S. (2015). Efficient delivery to human lung fibroblasts (WI-38) of pirfenidone incorporated into liposomes modified with truncated basic fibroblast growth factor and its inhibitory effect on collagen synthesis in idiopathic pulmonary fibrosis. *Biol. Pharm. Bull.* 38, 270–276. doi: 10.1248/bpb.b14-00659
- Ueda, K. (2001). Detection of the retinoic acid-regulated genes in a RTBM1 neuroblastoma cell line using cDNA microarray. *Kurume Med. J.* 48, 159–164. doi: 10.2739/kurumedj.48.159
- van Beuge, M. M., Prakash, J., Lacombe, M., Post, E., Reker-Smit, C., Beljaars, L., et al. (2013). Enhanced effectivity of an ALK5-inhibitor after cell-specific delivery to hepatic stellate cells in mice with liver injury. *PLoS One* 8:e56442. doi: 10.1371/journal.pone.0056442
- van Grunsven, L. A., Billon, N., Savatier, P., Thomas, A., Urdiales, J. L., and Rudkin, B. B. (1996). Effect of nerve growth factor on the expression of cell cycle regulatory proteins in PC12 cells: dissection of the neurotrophic response from the anti-mitogenic response. *Oncogene* 12, 1347–1356.
- Wang, A., Yokosaki, Y., Ferrando, R., Balmes, J., and Sheppard, D. (1996). Differential regulation of airway epithelial integrins by growth factors. *Am. J. Respir. Cell Mol. Biol.* 15, 664–672. doi: 10.1165/ajrcmb.15.5.8918373
- Wang, F., Xie, X., Fan, J., Wang, L., Guo, D., Yang, L., et al. (2010). Expression of P311, a transforming growth factor beta latency-associated protein-binding protein, in human kidneys with IgA nephropathy. *Int. Urol. Nephrol.* 42, 811–819. doi: 10.1007/s11255-009-9681-3
- Wang, P., Koyama, Y., Liu, X., Xu, J., Ma, H. Y., Liang, S., et al. (2016). Promising therapy candidates for liver fibrosis. *Front. Physiol.* 7:47. doi: 10.3389/fphys.2016.00047
- Yamashita, T., Tucker, K. L., and Barde, Y. A. (1999). Neurotrophin binding to the p75 receptor modulates Rho activity and axonal outgrowth. *Neuron* 24, 585–593. doi: 10.1016/S0896-6273(00)81114-9
- Yao, Z., Li, H., He, W., Yang, S., Zhang, X., Zhan, R., et al. (2017). P311 accelerates skin wound reepithelialization by promoting epidermal stem cell migration through RhoA and Rac1 activation. *Stem Cells Dev.* 26, 451–460. doi: 10.1089/scd.2016.0249
- Yao, Z., Yang, S., He, W., Li, L., Xu, R., Zhang, X., et al. (2015). P311 promotes renal fibrosis via TGFbeta1/Smad signaling. *Sci. Rep.* 5:17032. doi: 10.1038/srep17032
- Yue, M. M., Lv, K., Meredith, S. C., Martindale, J. L., Gorospe, M., and Schuger, L. (2014). Novel RNA-binding protein P311 binds eukaryotic translation initiation factor 3 subunit b (eIF3b) to promote translation of transforming growth factor beta1-3 (TGF-beta1-3). *J. Biol. Chem.* 289, 33971–33983. doi: 10.1074/jbc.M114.609495
- Zhan, S. S., Jiang, J. X., Wu, J., Halsted, C., Friedman, S. L., Zern, M. A., et al. (2006). Phagocytosis of apoptotic bodies by hepatic stellate cells induces NADPH oxidase and is associated with liver fibrosis in vivo. *Hepatology* 43, 435–443. doi: 10.1002/hep.21093
- Zhang, S. H., Wen, K. M., Wu, W., Li, W. Y., and Zhao, J. N. (2013). Efficacy of HGF carried by ultrasound microbubble-cationic nano-liposomes complex for treating hepatic fibrosis in a bile duct ligation rat model, and its relationship with the diffusion-weighted MRI parameters. *Clin. Res. Hepatol. Gastroenterol.* 37, 602–607. doi: 10.1016/j.clinre.2013.05.011
- Zhao, L., Leung, J. K., Yamamoto, H., Goswami, S., Kheradmand, F., and Vu, T. H. (2006). Identification of P311 as a potential gene regulating alveolar generation. *Am. J. Respir. Cell Mol. Biol.* 35, 48–54. doi: 10.1165/rcmb.2005-0475OC

**Conflict of Interest Statement:** The authors declare that the research was conducted in the absence of any commercial or financial relationships that could be construed as a potential conflict of interest.

Copyright © 2018 Stradiot, Mannaerts and van Grunsven. This is an open-access article distributed under the terms of the Creative Commons Attribution License (CC BY). The use, distribution or reproduction in other forums is permitted, provided the original author(s) and the copyright owner(s) are credited and that the original publication in this journal is cited, in accordance with accepted academic practice. No use, distribution or reproduction is permitted which does not comply with these terms.





# Gremlin Regulates Tubular Epithelial to Mesenchymal Transition via VEGFR2: Potential Role in Renal Fibrosis

**Laura Marquez-Exposito<sup>1,2†</sup>, Carolina Lavoz<sup>3†</sup>, Raul R. Rodrigues-Diez<sup>2,4\*</sup>, Sandra Rayego-Mateos<sup>2,5</sup>, Macarena Orejudo<sup>1,2</sup>, Elena Cantero-Navarro<sup>1,2</sup>, Alberto Ortiz<sup>2,6</sup>, Jesús Egido<sup>6,7</sup>, Rafael Selgas<sup>2,4</sup>, Sergio Mezzano<sup>3</sup> and Marta Ruiz-Ortega<sup>1,2</sup>**

<sup>1</sup> Cellular Biology in Renal Diseases Laboratory, IIS-Fundación Jiménez Díaz, Universidad Autónoma de Madrid, Madrid, Spain, <sup>2</sup> Red de Investigación Renal, Madrid, Spain, <sup>3</sup> Division of Nephrology, School of Medicine, Universidad Austral, Valdivia, Chile, <sup>4</sup> Laboratory of Nephrology, Fundación para la Investigación Biomédica del Hospital Universitario la Paz, Universidad Autónoma de Madrid, Madrid, Spain, <sup>5</sup> Vascular and Renal Translational Research Group, Institut de Recerca Biomédica de Lleida, Lleida, Spain, <sup>6</sup> Division of Nephrology and Hypertension, IIS-Fundación Jiménez Díaz, Universidad Autónoma de Madrid, Madrid, Spain, <sup>7</sup> Spanish Biomedical Research Centre in Diabetes and Associated Metabolic Disorders, Madrid, Spain

## OPEN ACCESS

### Edited by:

Pilar Sandoval,  
Centro de Biología Molecular Severo  
Ochoa (CSIC-UAM), Spain

### Reviewed by:

Federica Finetti,  
Università degli Studi di Siena, Italy  
Nune Markosyan,  
University of Pennsylvania,  
United States

### \*Correspondence:

Raul R. Rodrigues-Diez  
rrodriguez@fjd.es

<sup>†</sup> These authors have contributed  
equally to this work as first authors

### Specialty section:

This article was submitted to  
Inflammation Pharmacology,  
a section of the journal  
Frontiers in Pharmacology

**Received:** 30 July 2018

**Accepted:** 28 September 2018

**Published:** 17 October 2018

### Citation:

Marquez-Exposito L, Lavoz C,  
Rodrigues-Diez RR,  
Rayego-Mateos S, Orejudo M,  
Cantero-Navarro E, Ortiz A, Egido J,  
Selgas R, Mezzano S and  
Ruiz-Ortega M (2018) Gremlin  
Regulates Tubular Epithelial  
to Mesenchymal Transition via  
VEGFR2: Potential Role in Renal  
Fibrosis. *Front. Pharmacol.* 9:1195.  
doi: 10.3389/fphar.2018.01195

Chronic kidney disease (CKD) is emerging as an important health problem due to the increase number of CKD patients and the absence of an effective curative treatment. Gremlin has been proposed as a novel therapeutic target for renal inflammatory diseases, acting via Vascular Endothelial Growth Factor Receptor-2 (VEGFR2). Although many evidences suggest that Gremlin could regulate renal fibrosis, the receptor involved has not been yet clarified. Gremlin, as other TGF- $\beta$  superfamily members, regulates tubular epithelial to mesenchymal transition (EMT) and, therefore, could contribute to renal fibrosis. In cultured tubular epithelial cells Gremlin binding to VEGFR2 is linked to proinflammatory responses. Now, we have found out that in these cells VEGFR2 is also involved in the profibrotic actions of Gremlin. VEGFR2 blockade by a pharmacological kinase inhibitor or gene silencing diminished Gremlin-mediated gene upregulation of profibrotic factors and restored changes in EMT-related genes. Moreover, VEGFR2 inhibition blocked EMT phenotypic changes and dampened the rate of wound healing in response to Gremlin. The role of VEGFR2 in experimental fibrosis was evaluated in experimental unilateral ureteral obstruction. VEGFR2 inhibition diminished the upregulation of profibrotic genes and EMT changes, as well as the accumulation of extracellular matrix proteins, such as fibronectin and collagens in the obstructed kidneys. Notch pathway activation participates in renal damage progression by regulating cell growth/proliferation, regeneration and inflammation. In cultured tubular epithelial cells, Notch inhibition markedly downregulated Gremlin-induced EMT changes and wound healing speed. These results show that Gremlin regulates the EMT process via VEGFR2 and Notch pathway activation, suggesting that the Gremlin/VEGFR2 axis could be a potential therapeutic target for CKD.

**Keywords:** gremlin, VEGFR2, notch, EMT, tubular cells, fibrosis, renal

## INTRODUCTION

Chronic kidney disease (CKD) is a devastating disease that affects 5–7% of the worldwide population and is a strong forecaster of end-stage renal disease, cardiovascular morbidity, and mortality (Sanchez-Niño et al., 2017). The elevated incidence of obesity, diabetes and aging will greatly increase the number of CKD patients in a near future. Regardless of the underlying etiology, most renal diseases progress to permanent loss of kidney function caused by progressive and irreversible nephron loss and reduced regenerative capacity. CKD progression is characterized by sustained inflammation (Anders, 2014) and excessive accumulation of extracellular matrix (ECM) in the kidney, leading to tubulointerstitial fibrosis that is associated to renal function loss and end stage renal disease (Cortinovis et al., 2016). The current therapeutic armamentarium for CKD only slows disease progression, and novel therapeutic strategies are needed. Intensive research has focused on finding novel potential therapeutic targets for CKD, based on different approaches from anti-inflammatory treatments to novel epigenetic drugs (Duffield, 2014; Ruiz-Andres et al., 2016; Liu et al., 2018). A current hypothesis is that the re-emergence of developmental programs could participate in the pathogenesis of CKD and, therefore, their blockade could exert protective effects (Roxburgh et al., 2006). Among developmental genes, Gremlin has a potential relevance as a therapeutic target (Lappin et al., 2002; Mezzano et al., 2018).

Gremlin is a member of the DAN family of secreted Bone Morphogenetic Proteins (BMPs) antagonists, contains a cysteine-rich region and a cysteine knot motif responsible for BMP binding, whose structure is shared by members of the transforming growth factor beta (TGF- $\beta$ ) superfamily (Topol et al., 2000; Mezzano et al., 2018). Earlier studies demonstrate an important role of Gremlin in development, including nephrogenesis, acting as a BMP antagonist (Merino et al., 1999; Khokha et al., 2003; Michos et al., 2004). More recently, Gremlin has been suggested as an important promoter of fibrosis in different pathological conditions including renal, liver, lung, and myocardial diseases (Dolan et al., 2005; Carvajal et al., 2008; Mueller et al., 2013; Brazil, 2015; Erdmann et al., 2015; Mezzano et al., 2018). Moreover, *in vitro* studies have demonstrated direct effects of Gremlin in the regulation of profibrotic-related events (Zode et al., 2009; Li et al., 2012; Rodrigues-Diez et al., 2012; Huang et al., 2013). However, the potential Gremlin receptor involved in fibrotic processes has not been fully defined.

Renal fibrosis is a major hallmark of CKD, and finding an anti-fibrotic therapy is an unmet need. During the past decade, the origin of myofibroblasts, the primary source of ECM in scar tissue formation, has been intensively investigated. Current data strongly suggest that in the kidney these myofibroblasts may arise from a number of sources such as activation of tissue fibroblasts, migration of circulating mesenchymal progenitors or cell transitions, such as epithelial-to-mesenchymal transition (EMT) or endothelial-to-mesenchymal transition (EndoMT) (Zeisberg and Neilson, 2009; Duffield, 2014; Lovisa et al., 2015; Liu et al., 2018). Interestingly Gremlin can induce EMT of tubular epithelial cells and cancer cells (Li et al., 2012;

Rodrigues-Diez et al., 2012; Rodrigues-Diez et al., 2014), and can activate other renal cells, including fibroblasts and mesangial cells to increase the production of ECM proteins, such as collagens (Rodrigues-Diez et al., 2012; Huang et al., 2013). However, the receptor involved in Gremlin-induced fibrosis and EMT has not been found out yet. Some studies suggest that Gremlin regulates fibrosis by its BMP antagonist activity (Mylärniemi et al., 2008; Staloch et al., 2015), whereas many other studies have observed cellular actions of Gremlin independently of BMP antagonism (Mezzano et al., 2018). Recently, the vascular endothelial growth factor receptor 2 (VEGFR2) has been described as a Gremlin receptor in endothelial and tubular epithelial cells, showing some differences to canonical ligands in binding affinity and downstream responses (Mitola et al., 2010; Corsini et al., 2014; Lavoze et al., 2015; Mezzano et al., 2018). We have recently described that Gremlin activates VEGFR2 signaling pathway in the murine kidney, mainly on tubular epithelial cells, and this is linked to the induction of an acute inflammatory response (Lavoze et al., 2015). Interestingly, activation of VEGFR2 signaling and re-expression of Gremlin in tubular epithelial cells has been observed in several human nephropathies (Lavoze et al., 2015), suggesting that the Gremlin/VEGFR2 axis could be involved in CKD progression.

Notch signaling is an evolutionarily conserved pathway involved in cell fate control during development, stem cell self-renewal and postnatal tissue differentiation (Siebel and Lendahl, 2017). This pathway is one of the most relevant mechanisms regulating EMT in many cell types, including carcinogenesis (Takebe et al., 2015). Levels of some Notch pathway components have been proposed as biomarkers of renal disease progression in human CKD and many preclinical studies have suggested that Notch inhibition could be a therapeutic option for renal diseases, by modulating, cell proliferation, inflammation and EMT (Bielez et al., 2010; Murea et al., 2010; Sharma et al., 2011; Marquez-Exposito et al., 2018). We have previously described that Gremlin activates Notch signaling in the kidney leading into an acute inflammatory responses (Lavoze et al., 2018), however, the role of this pathway in Gremlin-induced EMT remains unstudied.

According to this background, we have investigated the potential role of VEGFR2 in the regulation of Gremlin-induced EMT in cultured tubular epithelial cells, and its role in renal fibrosis, testing the effects of VEGFR2 blockade in experimental renal fibrosis.

## MATERIALS AND METHODS

### Ethics Statement

All animal procedures were performed according to the guidelines of animal research in the European Community and with prior approval by the Ethics Committee of the Health Research of the IIS-Fundación Jiménez Díaz.

### Experimental Model of Renal Fibrosis

The model of unilateral ureteral obstruction (UUO) was performed in male C57BL/6 mice under isoflurane-induced

anesthesia. The left ureter was ligated with silk (5/0) at two locations and cut between ligatures to prevent urinary tract infection (obstructed kidney), as described (Lavoz et al., 2015) and mice were studied after 5 days. To examine the VEGFR2 pathway, some animals were treated daily with the VEGFR2 kinase inhibitor SU5416 (i.p.; 0.1 mg per day, Vichem, Budapest, Hungary). To study the Notch pathway, some animals were treated daily with the Notch inhibitor DAPT (a  $\gamma$ -secretase inhibitor; i.p.; 0.1 mg per day, Calbiochem). Both treatments were started 1 day before UO surgery ( $n = 8$  mice per group). At the time of sacrifice, animals were anesthetized with 5 mg/kg xylazine (Rompun, Bayer AG) and 35 mg/kg ketamine (Ketolar, Pfizer) and the kidneys were perfused *in situ* with cold saline before removal. A piece of the kidney (2/3) was fixed, embedded in paraffin, and used for immunohistochemistry, and the rest was snap-frozen in liquid nitrogen for renal cortex RNA and protein studies. In both models, studies compared the contralateral and obstructed kidney in each mouse. In addition, a control group of sham-operated mice showed the same results as contralateral kidneys (data not shown).

Paraffin-embedded kidney sections were stained using standard histology procedures. Immunostaining was carried out in 3  $\mu$ m thick tissue sections. Renal fibrosis was evaluated by Sirius Red staining. Samples were mounted in non-aqueous medium DPX new (Merck-Millipore) and examined by a Nikon Eclipse E400 microscope. For quantification, the percentage stained area out of the total area was calculated in five randomly chosen fields ( $\times 200$  magnification) using Image-Pro Plus software (Media Cybernetics, Washington) and results were expressed as fold-change over control.

## Cell Culture Studies

Human renal proximal tubular epithelial cells (HK2 cell line, ATCC CRL-2190) were grown in RPMI 1640 medium with 10% heat-inactivated fetal bovine serum (FBS), 2 mM glutamine, 100 U/ml penicillin, 100  $\mu$ g/ml streptomycin, 5  $\mu$ g/ml Insulin Transferrin Selenium (ITS) and 36 ng/ml hydrocortisone in 5% CO<sub>2</sub> at 37°C. All the *in vitro* studies were done in HK2 cell line (limitation of the study). At confluence, cells were growth-arrested in serum-free medium for 24 h before the experiments. Cells were cultured in six-well plates and stimulated with vehicle or recombinant human Gremlin (PeproTech, 10 ng/mL) for 24 (gene expression) or 48 h (protein levels) in serum-free medium. In some experiments, cells were preincubated for 1 h with VEGFR2 kinase inhibitor SU5416 (5  $\mu$ M; Vichem, Budapest, Hungary), or DAPT (30 nM, Calbiochem). DMSO, used as solvent, as well as SU5416 and DAPT alone had no effect on cell viability, gene and protein expression (data not shown). Cells were used for protein or RNA studies. Fibronectin was measured in supernatants (cell-conditioned media) and in total protein extract (cell-associated fraction).

## Cell Transfection and Gene Silencing

Gene silencing in cultured cells was performed using either a predesigned siRNA corresponding to the human KDR/VEGFR2 cDNA sequence (s7822; Ambion) or a non-specific control siRNA

(Ambion). Subconfluent HK2 cells were transfected for 24 h with Lipofectamine<sup>TM</sup> RNAiMAX Reagent (Invitrogen) according to the manufacturer's guidelines. Then, cells were incubated in serum-free medium for 24 h before the experiments. Some cells were stimulated with Gremlin or vehicle for different time intervals.

## Wound Healing

For wound healing assays, a single scrape wound was made with a p20 pipette tip on a monolayer of cultured HK2 cells, and two pictures per well were taken at this time point ( $t = 0$ ) using an inverted microscope (Leica DMI3000 B). Wounded cells were preincubated 1 h with treatments (SU5416: 5  $\mu$ M or DAPT: 30 nM) and later stimulated with Gremlin (10 ng/mL) or TGF- $\beta$ 1 (1 ng/mL). Seventy-two hours later two pictures were taken again in the same point as at  $t = 0$  and the gap area was measured using the Image-Pro Plus software (Media Cybernetics, Washington). Data are expressed as mean percentage of wound healing  $\pm$  SEM.

## Protein Studies

Proteins were obtained from cells or mouse kidneys using lysis buffer (50 mmol/l Tris-HCl, 150 mol/l NaCl, 2 mmol/l EDTA, 2 mmol/l EGTA, 0.2% Triton X-100, 0.3% IGEPAL, 10  $\mu$ l/ml proteinase inhibitor cocktail, 0.2 mmol/l PMSF, and 0.2 mmol/l orthovanadate). Protein levels were quantified using a Pierce<sup>TM</sup> BCA protein assay kit (Thermo Scientific, Rockford, IL, United States). For Western blotting, cell protein extracts (20–25  $\mu$ g/lane) or cell supernatants (25–30  $\mu$ l/lane) were separated on 6–12% polyacrylamide-SDS gels under reducing conditions. Samples were then transferred onto PVDF membranes (Bio-Rad, Spain), blocked with TBS/5% non-fat milk/0.05% Tween-20, and incubated overnight at 4°C with the corresponding primary antibodies. After washing, membranes were incubated with the appropriate HRP (horseradish peroxidase)-conjugated secondary antibody (Amersham Biosciences) and developed using an ECL kit (Amersham Biosciences). The quality of proteins and efficacy of protein transfer were evaluated by Red Ponceau staining (data not shown). The loading control for soluble proteins (cell supernatants) was Red Ponceau staining and the albumin band (67 kDa) was used for quantification of the loading control. Digital chemiluminescence images were taken by LAS 4000 (GEHealthcare) and quantified by Quantity One<sup>®</sup> software. The following primary antibodies were employed [dilution]:  $\alpha$ -smooth muscle actin ( $\alpha$ -SMA) ([1:1000], Sigma), E-cadherin ([1:500], CST), Fibronectin ([1:5000]; BD Pharmingen), panCytokeratin ([1:500], Sigma), Vimentin (E-5) ([1:1000]; Santa Cruz, sc-373717),  $\alpha$ -tubulin ([1:5000]; Sigma) and GAPDH ([1:5000]; Chemicon International).

## Immunofluorescence Staining of EMT Markers

To determine EMT changes, specific EMT markers were assessed by immunofluorescence in control and Gremlin-stimulated cells for 72 h. Cells were fixed with 4% PFA, permeabilized with triton X-100 (0.2%), blocked with 4% BSA in PBS and incubated



with the following primary antibodies [dilution]: Vimentin ([1:200], Santa Cruz, sc-373717), panCytokeratin (C11) ([1:200]; Santa Cruz, sc-8018) and  $\alpha$ -SMA ([1:200], Sigma). Secondary antibodies were Alexa Fluor®-488 conjugated antibody ([1/200] A21206, Invitrogen) and Alexa Fluor®-633 conjugated antibody ([1/200]; A21206, Invitrogen). Nuclei were stained with 1  $\mu$ g/ml DAPI (Sigma-Aldrich) as control of equal cell density. Absence of primary antibody was used as negative control. Samples were mounted in ProLong™ Gold Antifade Reagent (Invitrogen by Thermo Fisher Scientific) and examined by a Leica TCS SP5 confocal microscope.

## Gene Expression Studies

RNA from cells or renal tissue (pulverized in a metallic chamber) was isolated with TriPure reagent (Roche). cDNA was synthesized by a High Capacity cDNA Archive kit (Applied Biosystems) using 2  $\mu$ g of total RNA primed with random hexamer primers following the manufacturer's instructions. Next, quantitative gene expression analysis was performed by real-time PCR on an AB7500 fast real-time PCR system (Applied Biosystems) using fluorogenic TaqMan MGB probes and primers designed by Assay-on-Demand™ gene expression products. Human assays IDs were: *E-CADHERIN* (CDH1), Hs01023895\_m1; *TFG- $\beta$  1* (TGFB1), Hs00998133\_m1; *CTGF*, Hs00170014\_m1, *FIBRONECTIN*, Hs00401006\_m1, and *VIMENTIN*: Hs00185584\_m1. Mouse assays IDs were: *fibronectin* (Fn1), Mm01256744\_m1; *type I collagen* (Col1a2), Mm00483888\_m1; *tgf- $\beta$ 1* (tgfb1), Mm01178820\_m1; *pai-1* (Serpine), Mm00435858\_m1. Data were normalized to human *GAPDH* Hs02786624\_g1, or mouse *gapdh*: Mm99999915\_g1. The mRNA copy numbers were calculated for each sample by the instrument software using Ct value ("arithmetic fit point analysis for the lightcycler"). Results were expressed in copy numbers, calculated relative to unstimulated cells after normalization against GAPDH.

## Statistical Analysis

Results throughout the text are expressed as mean  $\pm$  SEM of fold increase over control. Differences between groups were assessed by Student t (cells) and Mann-Whitney (mice) tests. Statistical significance was assumed when a null hypothesis could be rejected at  $p < 0.05$ . Statistical analysis was performed using the SPSS statistical software, version 16.0, Chicago, IL, United States.

## RESULTS

### Gremlin via VEGFR2 Regulates the Expression of Many Genes Involved in Fibrosis in Cultured Tubular Epithelial Cells

Gremlin binds to VEGFR2 present in tubular epithelial cells *in vivo* and *in vitro* (Lavozy et al., 2015). Previous studies in cultured tubular epithelial cells have shown Gremlin regulates several profibrotic factors and ECM components (Li et al., 2012; Rodrigues-Diez et al., 2012, 2014), however, the role of VEGFR2

in these processes had not been investigated. Preincubation of cultured human tubular epithelial cells (HK2 cell line) with the pharmacological VEGFR2 kinase inhibitor SU5416 diminished Gremlin-mediated gene upregulation of profibrotic factors, including TGF- $\beta$ 1 and CTGF, and ECM components, such as fibronectin, evaluated by real time PCR (**Figure 1A**). Moreover, Gremlin-induced production of soluble fibronectin was blocked by treatment with the VEGFR2 kinase inhibitor, as determined by western blot (**Figure 1B**). Cell-associated fibronectin showed the same tendency but not statistical differences were found (**Figure 1C**).

The involvement of VEGFR2 on profibrotic gene regulation was further evaluated by gene silencing. HK2 cells were transfected with a siRNA against VEGFR2 or its corresponding scrambled control siRNA, and then stimulated with Gremlin for 24 h. In VEGFR2-silenced cells, Gremlin did not increase the gene expression of profibrotic factors and ECM related proteins, whereas in untransfected cells or in cells transfected with a control siRNA, Gremlin increased all those genes (**Figure 1D**).

### Gremlin Induces EMT in Cultured Tubular Epithelial Cells via VEGFR2 Signaling Activation

An early study observed that during the transdifferentiation of tubular epithelial cells to fibroblasts, one of the most upregulated genes was Gremlin (Murphy et al., 2002). Latter, we described that Gremlin, both by stimulation with a recombinant Gremlin protein or by transfection with a Gremlin expression vector, could induce EMT in cultured human tubular epithelial cells (Rodrigues-Diez et al., 2012, 2014). Now, we have investigated whether VEGFR2 behaves as a Gremlin receptor involved in EMT regulation. EMT is initiated by the disruption of intercellular junctions resulting in a loss of their apical-basolateral polarity, and the acquisition of a front-back polarity. In HK2 cells, stimulation with Gremlin (10 ng/ml) decreased the expression of proteins that keep basolateral polarity, such as the epithelial marker Cytokeratin, as shown by confocal microscopy, that was restored in cells pretreated with the VEGFR2 inhibitor SU5416 (**Figure 2A**). EMT was also characterized by *de novo* synthesis of mesenchymal markers, such as  $\alpha$ -SMA and vimentin (Zeisberg and Neilson, 2009). Gremlin induced vimentin expression associated to a change in cell phenotype from the typical cobblestone pattern of an epithelial monolayer to myofibroblast morphology, which was prevented by SU5416 (**Figure 2A**). Changes in EMT-related proteins were also confirmed by western blot. Gremlin decreased the protein levels of Cytokeratin and E-cadherin, essential proteins for the structural integrity of the renal epithelium, and increased vimentin and  $\alpha$ -SMA levels, which were prevented by VEGFR2 inhibition in the case of e-cadherin,  $\alpha$ -SMA and Vimentin (**Figure 2B**). To further demonstrate the role of VEGFR2 in the regulation of Gremlin-induced EMT process, gene-silencing experiments were done. The evaluation of changes in the representative marker of activated myofibroblasts  $\alpha$ -SMA by confocal microscopy clearly showed that stimulation with Gremlin in VEGFR2 gene silenced cells, was not able to induce the phenotype



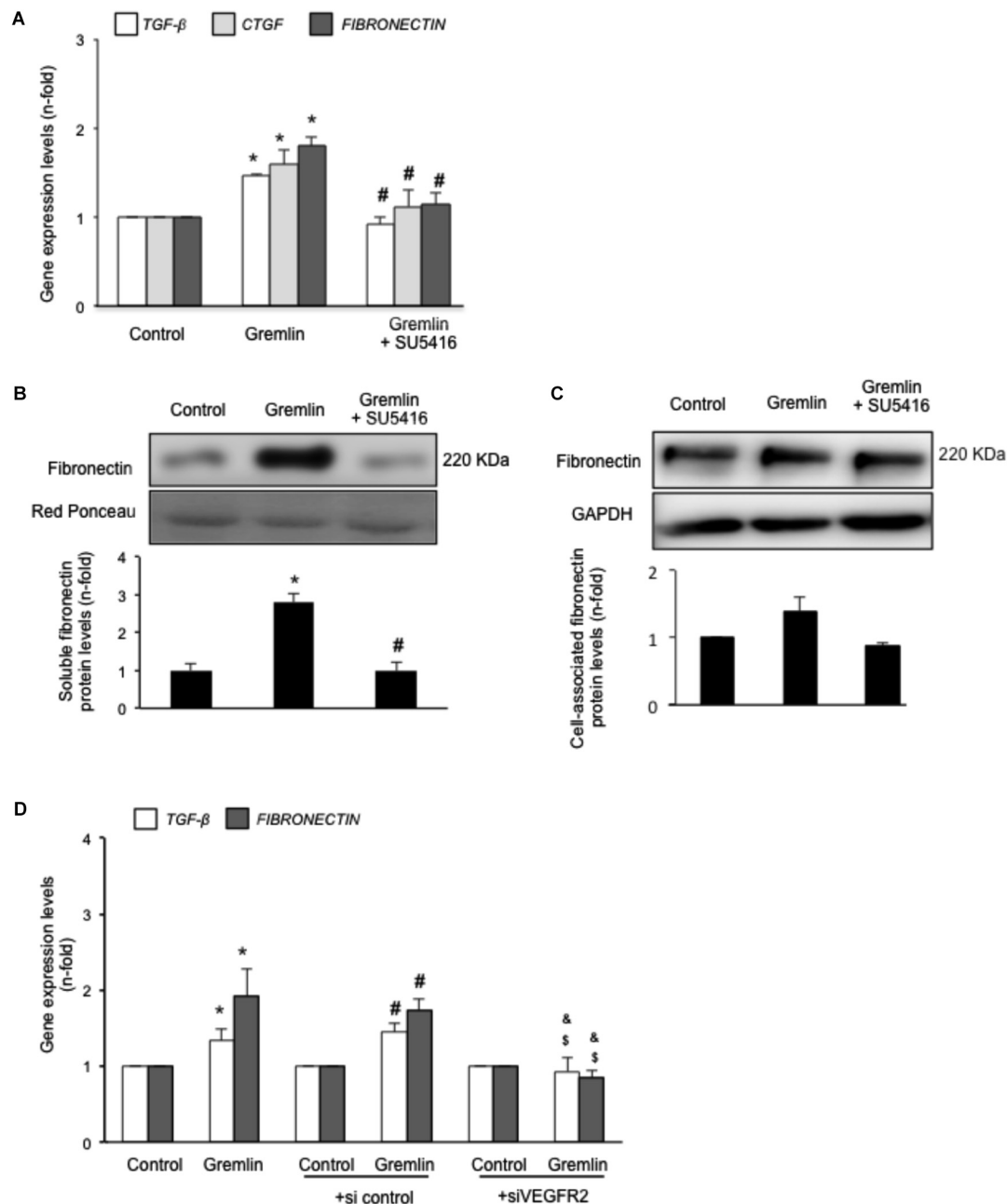


**FIGURE 1 |** Gremlin via VEGFR2 regulates profibrotic factors and ECM components in cultured human tubular epithelial cells. Cells (HK2 cell line) were preincubated with the VEGFR2 kinase inhibitor SU5416 (5  $\mu$ M) or vehicle before stimulation with Gremlin (10 ng/ml). **(A)** Gene expression was evaluated 24 h after Gremlin stimulation. Total cell RNA was isolated to assess mRNA levels of TGF- $\beta$ , CTGF, and FIBRONECTIN by quantitative real-time PCR. **(B)** Effect of VEGFR2 blockade on Gremlin-induced ECM protein production was evaluated by quantifying soluble fibronectin levels by western blot, after 48 h of incubation. Figures show a representative experiment of soluble **(B)** and cell associated **(C)** Fibronectin (upper panel) and quantification (lower panel). Results are expressed as mean  $\pm$  SEM of six independent experiments. \* $p$  < 0.05 vs. control, # $p$  < 0.05 vs. Gremlin. **(D)** VEGFR2 gene silencing blocked Gremlin-induced gene upregulation of matrix-related factors. HK2 cells were transfected with a siRNA against VEGFR2 or siRNA scrambled as described in Materials and Methods. Then, cells were stimulated or not with 10 ng/mL Gremlin for 24 h. Data are expressed as mean  $\pm$  SEM of five independent experiments. \* $p$  < 0.05 vs. control untransfected; # $p$  < 0.05 vs. untreated control siRNA-transfected cells; & $p$  < 0.05 vs. Gremlin-treated control siRNA-transfected cells; & $p$  < 0.05 vs. Gremlin-treated untransfected cells.

changes and there was lower staining intensity compared to Gremlin-treated control siRNA transfected cells (Figure 3A). Additionally, SU5416 pretreatment or VEGFR2 gene silencing

also modulated Gremlin-induced changes at the gene expression level, as observed for E-Cadherin and vimentin mRNA levels (Figures 2C, 3B).

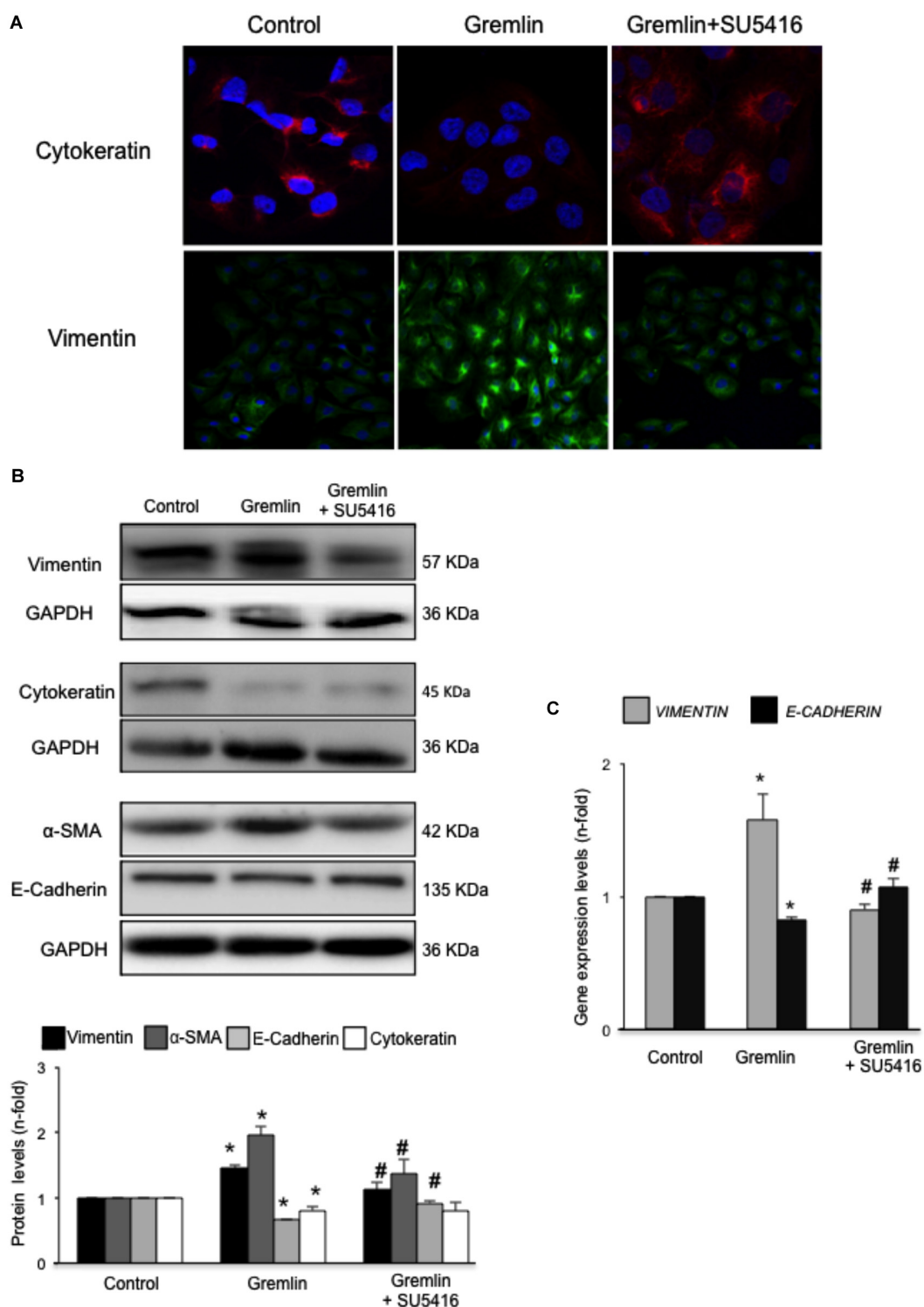


**FIGURE 2 |** Gremlin via VEGFR2 induces EMT in tubular epithelial cells. **(A)** Cells (HK2 cell line) were preincubated with the VEGFR2 kinase inhibitor SU5416 (5  $\mu$ M) or vehicle before stimulation with Gremlin (10 ng/ml) for 72 h. By confocal microscopy changes in epithelial phenotype and EMT-markers were evaluated. Vimentin is shown in green and Cytokeratin in red. Figure shows a representative experiment of two done by confocal microscopy. **(B)** Changes in EMT-related markers were quantified by western blot Gremlin diminished the levels of the epithelial markers E-Cadherin and Cytokeratin and increased the expression of mesenchymal markers,  $\alpha$ -SMA and vimentin. All these changes were prevented by VEGFR2 inhibition. **(C)** Gene expression was evaluated 24 h after Gremlin stimulation. Total cell RNA was isolated to assess mRNA levels of VIMENTIN, and E-CADHERIN by quantitative real-time PCR. Figure shows mean  $\pm$  SEM of six independent experiments. \* $p$  < 0.05 vs. control; # $p$  < 0.05 vs. Gremlin.

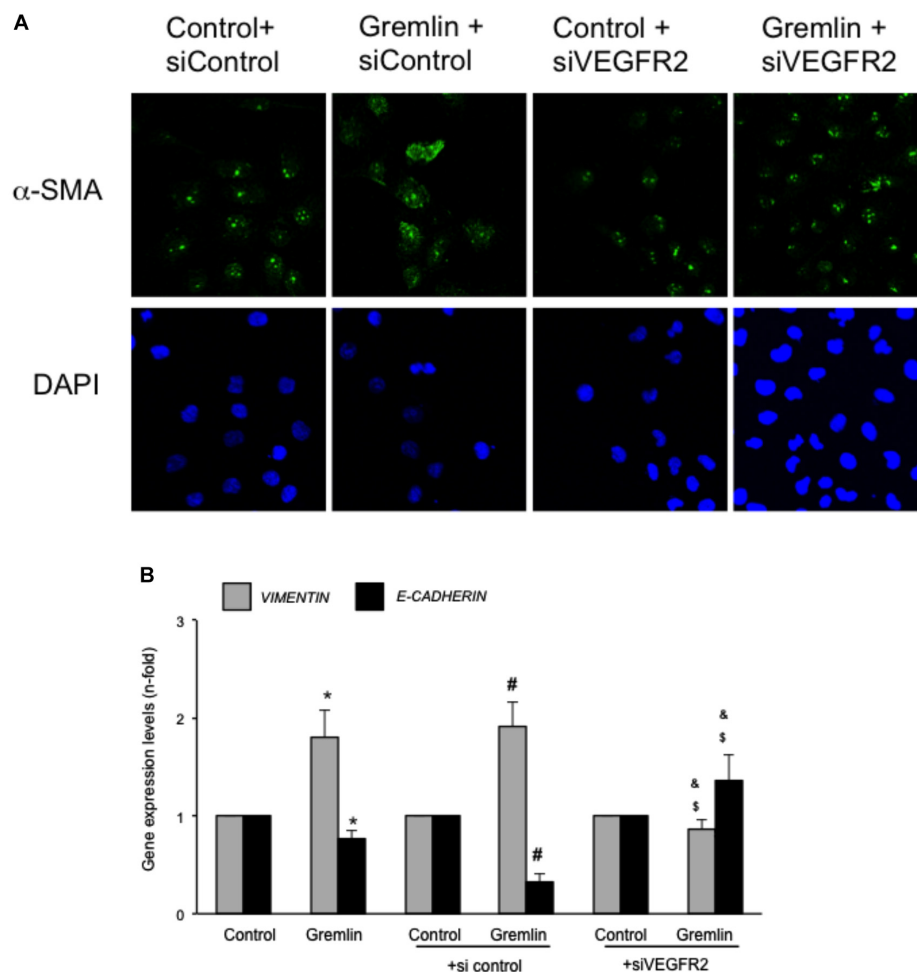


**FIGURE 3 |** VEGFR2 gene silencing blocked Gremlin-induced EMT related changes in tubular epithelial cells. Sub-confluent HK2 cells were transfected with a siRNA against VEGFR2 or siRNA scrambled during 48 h. Then, cells were stimulated or not with 10 ng/mL Gremlin for 72 h. **(A)** Changes in the representative marker of activated myofibroblasts  $\alpha$ -SMA was evaluated by confocal microscopy. To see cell density the nuclear marker DAPI was used. Figure shows a representative experiment of two done by confocal microscopy. **(B)** Gene expression was evaluated in silenced cells 24 h after Gremlin stimulation. Total cell RNA was isolated to assess mRNA levels of VIMENTIN, and E-CADHERIN by quantitative real-time PCR. Data are expressed as mean  $\pm$  SEM of five independent experiments. \* $p < 0.05$  vs. control untransfected; # $p < 0.05$  vs. untreated control siRNA-transfected cells; & $p < 0.05$  vs. Gremlin-treated control siRNA-transfected cells; & $p < 0.05$  vs. Gremlin-treated untransfected cells.

## Gremlin via VEGFR2 Modulates Wound Healing in Cultured Tubular Epithelial Cells

Wound healing assays showed that Gremlin (10 ng/ml) increased the speed of epithelial cells invading the scar region compared to untreated cells, evaluated after 72 h (**Figure 4**). This response was similar to that observed in response to TGF- $\beta$ 1 stimulation (10 ng/ml), used as a positive control. The VEGFR2 kinase inhibitor SU5416 significantly diminished the percentage of wound healing induced by Gremlin (**Figure 4**).

## VEGFR2 Blockade Inhibits Experimental Renal Fibrosis

Gremlin administration in the murine kidney induces an acute inflammatory response, however, there was no

increased ECM deposition in the kidney (Lavoz et al., 2018). Therefore, to evaluate the potential *in vivo* effects of Gremlin on renal fibrosis the UUO model was employed. This model is characterized by tubulo-interstitial fibrosis, observed as early as 5 days followed renal injury (Ucero et al., 2014). Moreover, in obstructed kidneys, Gremlin is increased and is associated to VEGFR2 activation (Lavoz et al., 2015). VEGFR2 kinase inhibition in obstructed kidneys prevented the increase in the expression of profibrotic (TGF- $\beta$ 1 and PAI-1) and matrix-related (fibronectin and type I collagen) genes that was observed in untreated obstructed kidneys (**Figure 5A**) and prevented the increase in Fibronectin protein (**Figure 5B**). The effect of VEGFR2 inhibition on renal fibrosis was further evaluated by Sirius red staining (**Figure 5D**). This technique disclosed a clear diminution of collagen deposition in mice treated with

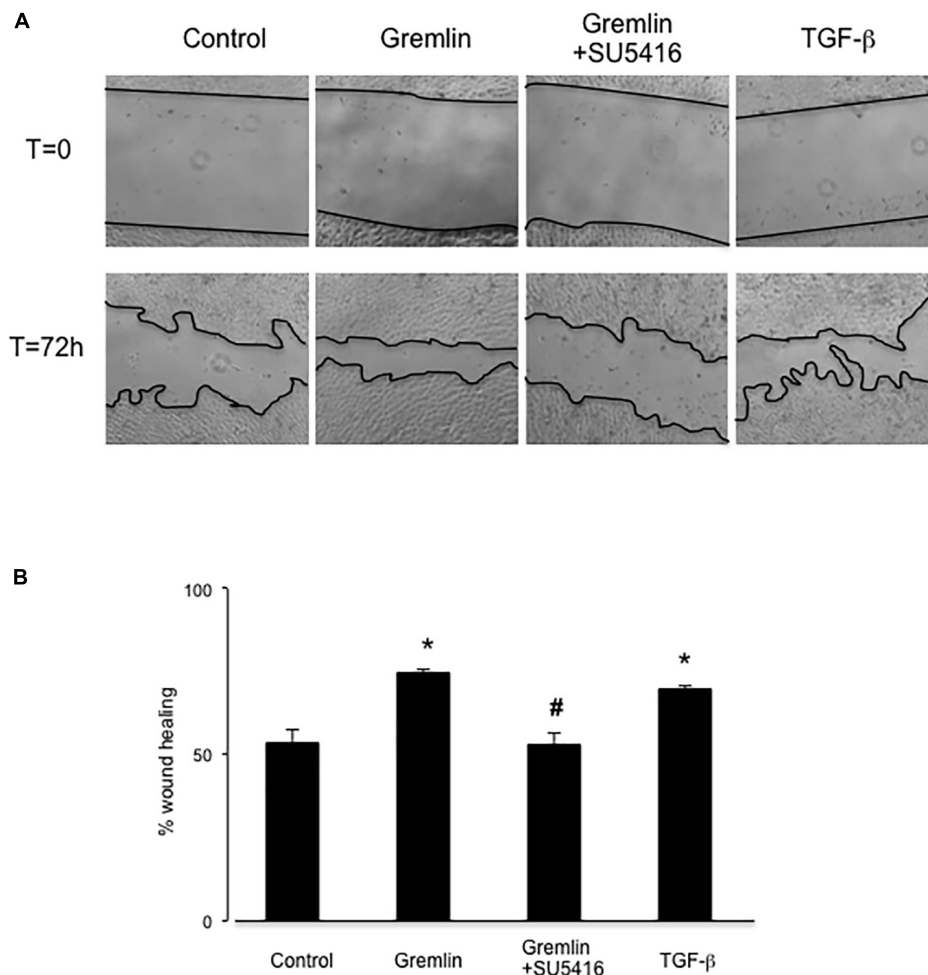


**FIGURE 4 |** Gremlin via VEGFR2 regulates cells migration and proliferation in wound healing experiments. A monolayer of epithelial cells (HK2 cell line) was used as starting point. A single scrape wound was made in all cells and then they were stimulated with Gremlin (10 ng/ml) in the presence or absence of VEGFR2 kinase inhibitor SU5416 (5  $\mu$ M, preincubated 1 h before). After 72 h, cells were evaluated under inverted microscopy. **(A)** Representative images of wound healing experiments and **(B)** their quantification. Results are expressed as mean  $\pm$  SEM of four independent experiments, done by duplicate. \* $p$  < 0.05 vs. control; # $p$  < 0.05 vs. Gremlin.

VEGFR2 inhibition as compared to untreated obstructed kidneys (**Figure 5C**). These data show that inhibition of VEGFR2 signaling ameliorates renal fibrosis and suggest that blockade of Gremlin/VEGFR2 could be responsible for downregulation of profibrotic events in injured kidneys.

### Blockade of Notch Pathway Activation Inhibited Experimental Renal Fibrosis

In some experimental models, Notch blockade ameliorates renal damage, mainly by inhibiting fibroblast proliferation and therefore, decreasing fibrosis (Bielez et al., 2010; Marquez-Exposito et al., 2018). Treatment of obstructed mice with the  $\gamma$ -secretase inhibitor DAPT, an inhibitor of Notch activation, prevented the increase in renal profibrotic gene expression (**Figure 5A**), fibronectin levels (**Figure 5B**), and collagen deposition (**Figures 5C,D**)

to levels similar to contralateral kidneys. These data confirms and extend previous observations (Bielez et al., 2010).

### Notch Pathway Activation Is Involved in Gremlin-Induced EMT

Finally, we further investigated whether the Notch pathway could be directly involved in Gremlin profibrotic responses. Preincubation with the  $\gamma$ -secretase inhibitor DAPT diminished Gremlin-induced changes in profibrotic gene expression and ECM components (**Figure 6**). Changes caused by Gremlin in the cell morphology and in EMT-related genes and proteins levels were prevented by DAPT (**Figure 7**). Moreover, the effects of Gremlin on wound healing speed were also inhibited by DAPT (**Figure 8**). DAPT alone did not show effect on wound healing when compared to control (Pazos et al., 2017).



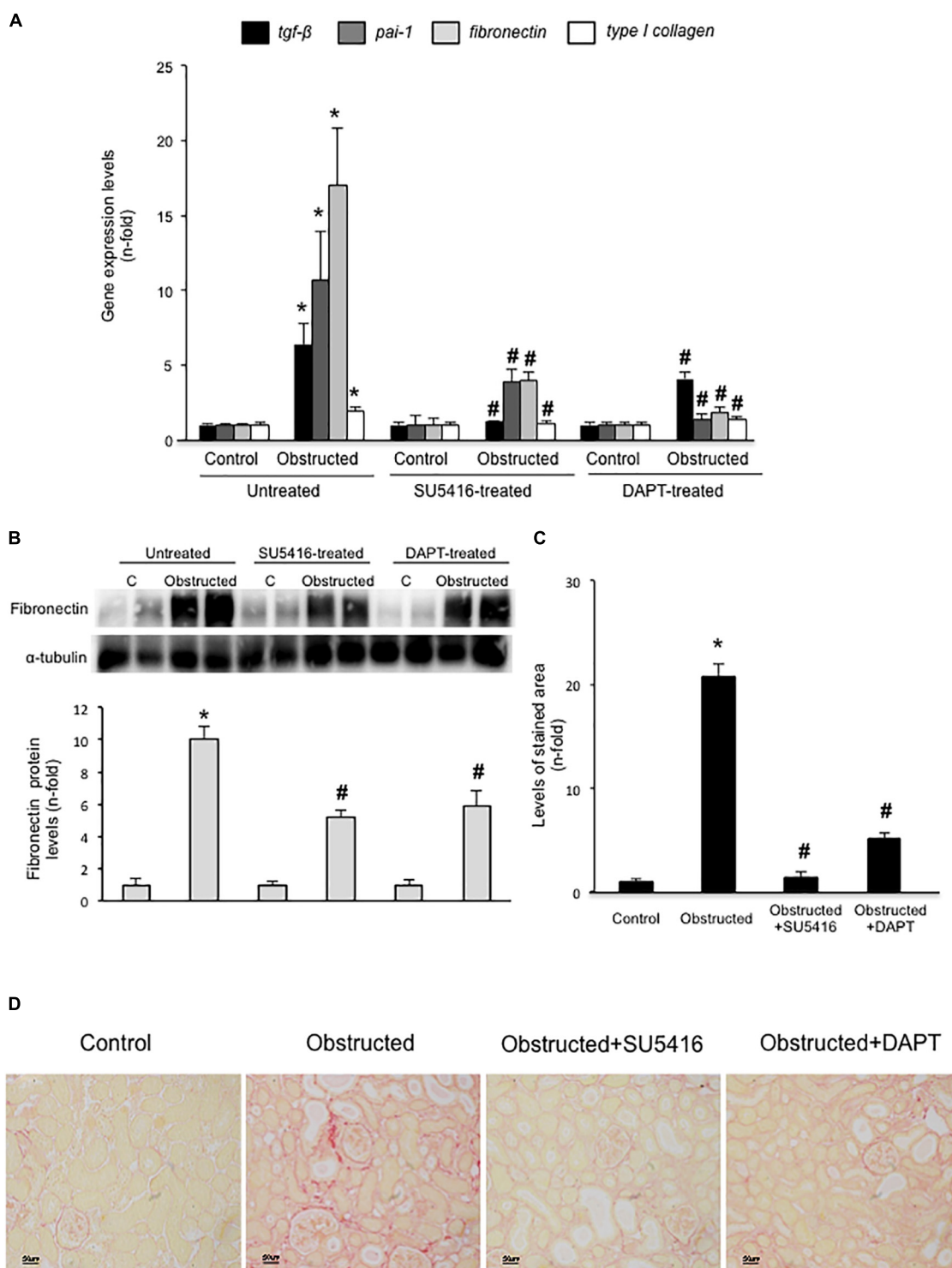


**FIGURE 5 |** VEGFR2 kinase inhibition ameliorates experimental renal fibrosis in the model of unilateral ureteral obstruction. Mice were treated with SU5416 (i.p.; 0.1 mg per day) starting 24 h before UUO surgery and were studied after 5 days. To evaluate the role of the Notch pathway, some mice were also treated with the Notch inhibitor DAPT (i.p.; 0.1 mg per day). **(A)** RNA was obtained from total renal extracts and *tgf- $\beta$ 1*, *pai-1*, *fibronectin*, and *type I collagen* mRNA levels were determined by RT-qPCR. **(B)** Fibronectin protein levels were evaluated in total renal extracts by Western blotting. Levels of  $\alpha$ -tubulin were used as a loading control. Figure shows several representative mice from each group and the quantification of the Western blot data. **(C,D)** Collagen deposition was evaluated in paraffin-embedded sections by Sirius Red staining, quantification assessed the stained area as a proportion of total area. **(D)** Figures show a representative mouse from each group. Magnification 200 $\times$ , and **(C)** the quantification. Data are expressed as mean  $\pm$  SEM of 6–8 animals per group. \* $p < 0.05$  vs. control; # $p < 0.05$  vs. UUO 5 days.

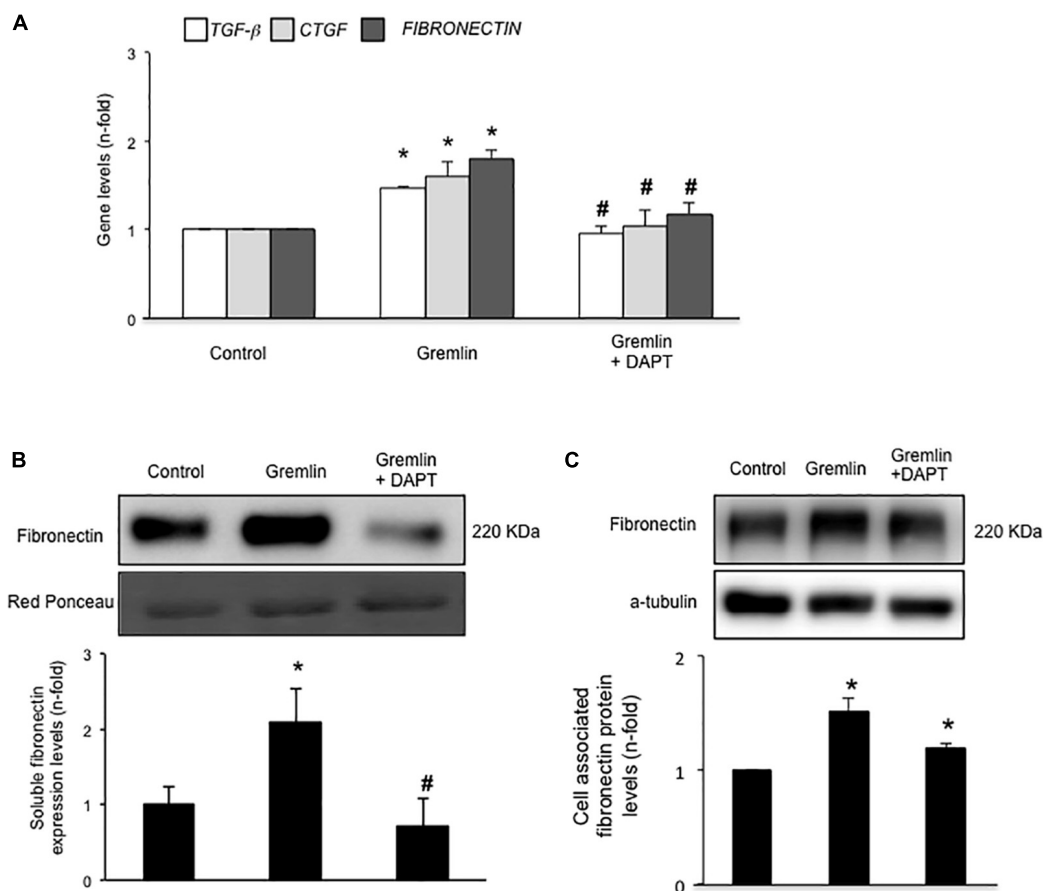


**FIGURE 6 |** Gremlin via Notch pathway regulates profibrotic factors and ECM components in cultured human tubular epithelial cells. Cells (HK2 cell line) were preincubated with DAPT (30 nM) before stimulation with Gremlin (10 ng/ml). **(A)** Gene expression levels were evaluated 24 h after Gremlin stimulation. Total cell RNA was isolated to assess mRNA levels by RT-qPCR. Fibronectin levels were evaluated after 48 h in cell supernatants **(B)** and in total protein extracts **(C)**. A representative western blot experiment is shown in upper panel and quantification in the lower panel. \* $p < 0.05$  vs. control, # $p < 0.05$  vs. Gremlin.

## DISCUSSION

In this paper we have described that in cultured tubular epithelial cells, VEGFR2 is the receptor involved in the regulation of the EMT program and of profibrotic-related genes in response to Gremlin. In human progressive CKD, Gremlin upregulation was associated to activation of VEGFR2 signaling, mainly in tubular epithelial cells (Lavoz et al., 2015). Moreover, Gremlin overexpression was found in areas of increased ECM deposition (Dolan et al., 2005; Mezzano et al., 2018), suggesting that this factor can participate in renal fibrosis. Our *in vivo* studies show anti-fibrotic effects of VEGFR2 inhibition in experimental kidney fibrosis, suggesting that the Gremlin/VEGFR2 axis could be a potential therapeutic target in renal disease.

In the kidney, Gremlin binds to VEGFR2 in tubular epithelial cells activating this receptor and subsequent downstream signaling pathways linked to regulation of renal inflammation (Lavoz et al., 2015, 2018). Now, our *in vitro* data in cultured tubular epithelial cells show that Gremlin via VEGFR2 activation regulates several gene programs to control profibrotic, ECM and EMT related factors. In other cell types Gremlin actions are also

mediated by VEGFR2. In endothelial cells, Gremlin binds to VEGFR2 and activates this pathway regulating cell proliferation, migration, and angiogenesis (Shibuya and Claesson-Welsh, 2006; Mitola et al., 2010; Corsini et al., 2014). In skin keratinocytes and fibroblasts, Gremlin via VEGFR2 activates NF-E2-related factor 2 (NERF2) signaling and cell growth (Ji et al., 2016), and in retinal epithelial cells via mTOR regulates proliferation and migration (Liu et al., 2017). However, the receptor involved in Gremlin responses in other renal cells had not been investigated. In this sense, podocytes seem not to express VEGFR2 (Li et al., 2013). Our *in vitro* data suggest that VEGFR2 could be the receptor involved in Gremlin-mediated fibrotic responses in the kidney, but future research is needed in other kidney cell types beyond tubular cells.

Epithelial to mesenchymal transition is a cell reprogramming process in which epithelial cells acquire a mesenchymal phenotype. The contribution of tubular EMT to renal fibrosis is a matter of intense debate (LeBleu et al., 2013; Duffield, 2014; Lovisa et al., 2015; Liu et al., 2018). EMT is characterized by the loss of the epithelial properties of tubular epithelial cells, including permeability and polarity, which may result in

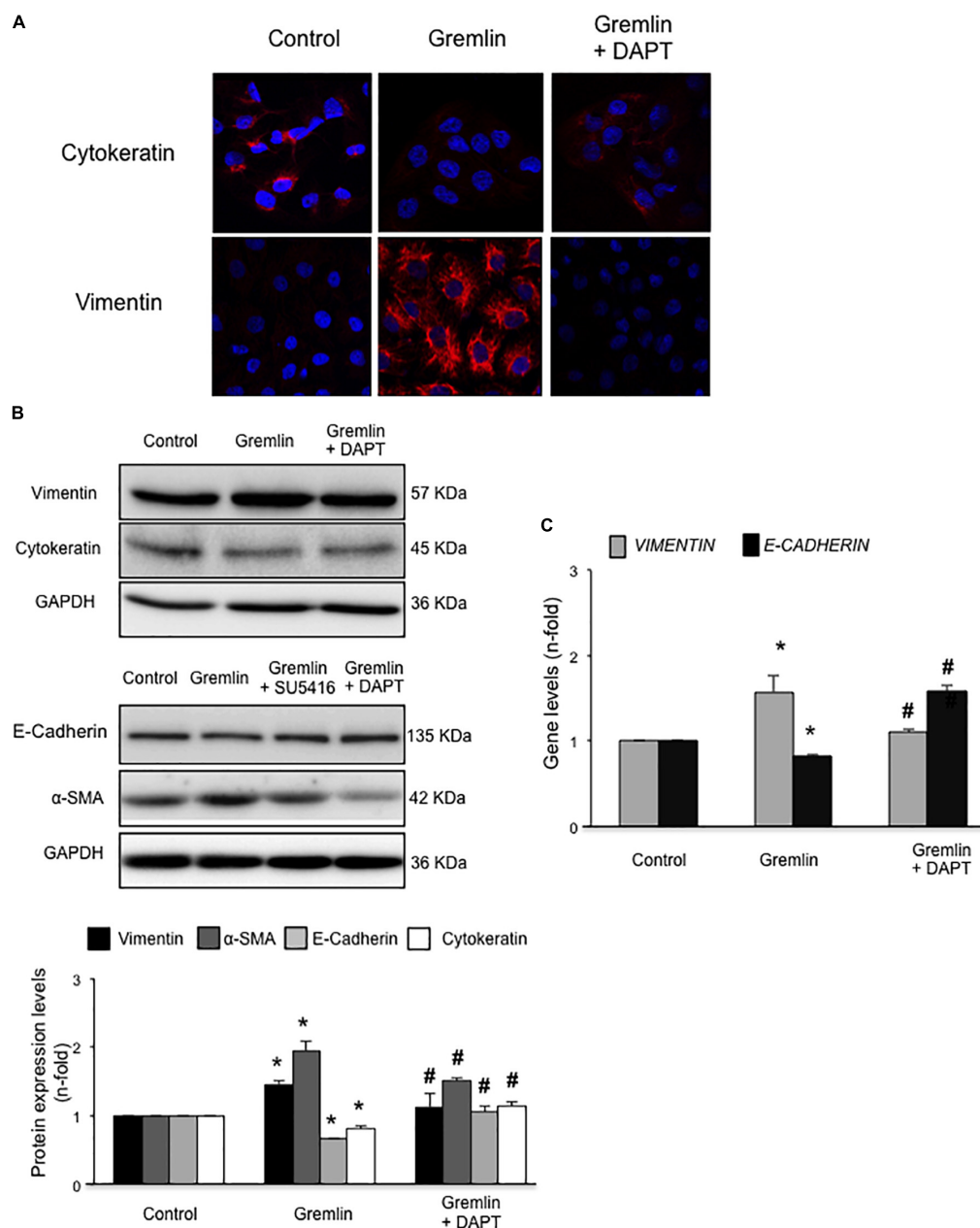
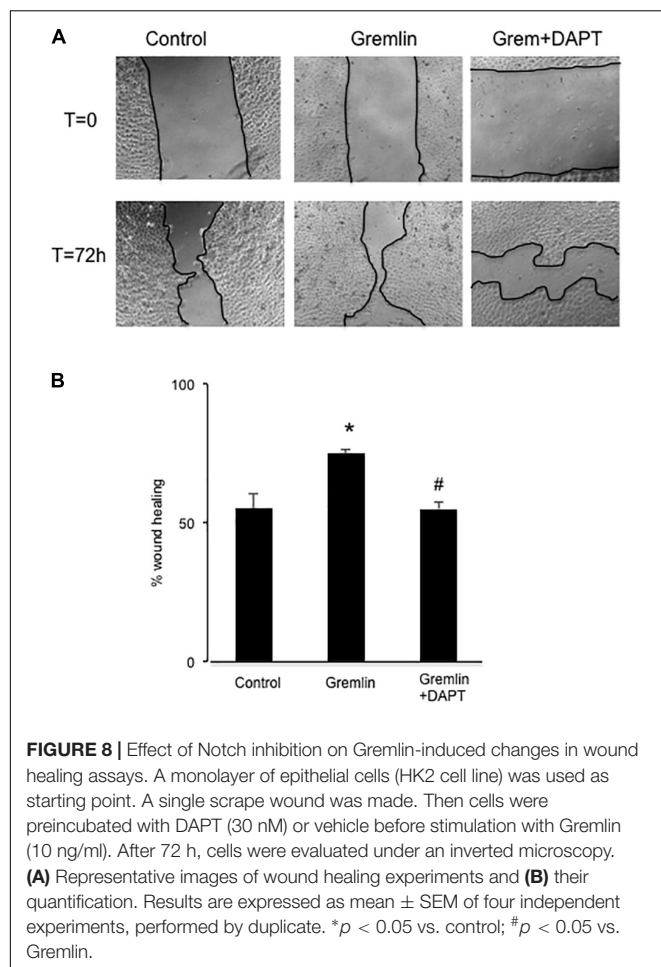


**FIGURE 7 |** Gremlin via Notch pathway induces EMT in cultured human tubular epithelial cells. Cells (HK2 cell line) were preincubated with DAPT (30 nM) before stimulation with Gremlin (10 ng/ml). Changes in EMT-related markers were assessed by confocal microscopy (**A**) or western blot (**B**). Please, note that the pictures of e-cadherin, α-sma and their corresponding loading control (GAPDH) are the same images as shown in the Figure 2B but, in this case, Gremlin + DAPT point is included in the fourth lane. Results are expressed as mean ± SEM of five independent experiments. All changes induced by Gremlin were prevented by Notch inhibition. Figure (**A**) shows a representative experiment out of two performed by confocal microscopy and (**B**) shows representative images of western blot and quantification. (**C**) Gene expression levels were evaluated 24 h after Gremlin stimulation. Total cell RNA was isolated to assess mRNA levels by RT-qPCR. Data are expressed as mean ± SEM of six independent experiments. \* $p < 0.05$  vs. control; # $p < 0.05$  vs. Gremlin.

decreased viability and contribute to renal injury (Duffield, 2014; Lovisa et al., 2015; Liu et al., 2018). Although in experimental and human CKD the number of myofibroblasts of tubular origin could be scarce, and it is not relevant to the total increase in collagen deposition, partial EMT is an initial step in renal damage and an important potential therapeutic target.

In cultured tubular epithelial cells, we have found that VEGFR2 blockade, by the pharmacological inhibitor SU5416 or by gene silencing, inhibited the EMT program induced by Gremlin. Therefore, Gremlin/VEGFR2 blockade could exert protective effects in renal injury by restoring or preventing the loss of epithelial integrity.



Epithelial to mesenchymal transition also participates in wound healing, malignant transformation and embryogenesis. In our study, we show that VEGFR2 is involved in Gremlin-induced wound healing in tubular epithelial cells. Gremlin induces EMT changes in other cell types, including airway epithelial cells (McCormack et al., 2013). In cancer cell lines, Gremlin besides EMT, also causes cell migration, invasion, and proliferation through BMP and VEGFR2-independent mechanisms (Kim et al., 2012; Yin et al., 2017; Mezzano et al., 2018). Future studies are needed to define the receptor involved in Gremlin-induced EMT in proliferative disorders.

Earliest studies showed that Gremlin could acts as a BMPs antagonist, mainly involved in embryogenesis, including kidney development (Merino et al., 1999; Khokha et al., 2003; Michos et al., 2004). However, the role of Gremlin as BMPs antagonists in other physiological and pathological conditions is controversial. Gremlin-induced inflammatory responses are BMP-independent, as described in endothelial and tubular epithelial cells, and are linked to activation of several transcription factors, NF- $\kappa$ B and Notch-1 (Corsini et al., 2014; Lavozy et al., 2015, 2018). Gremlin affinity for BMPs can vary between cells and pathological conditions, explaining the divergent results published. In isolated pancreatic stellate

cells Gremlin acting as a BMP antagonist abolished BMP2's suppression effects on TGF- $\beta$ -induced collagen expression, by its binding to BMP2 and subsequent blockade of Smad1/5 phosphorylation, and therefore inhibiting BMP2 anti-fibrotic effects (Staloch et al., 2015). BMP7 have proven to be capable of reversing renal fibrosis in mice, EMT and *in vitro* profibrotic effects of TGF- $\beta$  and Gremlin (Zeisberg et al., 2003; Weiskirchen and Meurer, 2013). In this regard, there is a complex relationship between BMPs and TGF- $\beta$  signaling in the regulation of homeostasis and tissue fibrosis. Novel data indicate that Gremlin is another important player in this context. In cultured renal cells Gremlin is a downstream mediator of TGF- $\beta$  profibrotic responses, including EMT of tubular epithelial cells (Rodrigues-Diez et al., 2012). *In vitro* Gremlin activates TGF- $\beta$ /Smad pathway in tubular epithelial cells and in podocytes (Li et al., 2013; Rodrigues-Diez et al., 2014). Additionally, TGF- $\beta$  blockade inhibited Gremlin-induced EMT (Rodrigues-Diez et al., 2014). All these data show a close interrelation between TGF- $\beta$  and Gremlin, acting both as profibrotic factors.

Many experimental evidences suggest that Gremlin could be an important promoter of fibrosis in different pathologies, including liver fibrosis, lung diseases (particularly pulmonary hypertension and idiopathic pulmonary fibrosis), myocardial fibrosis, and chronic pancreatitis (Khokha et al., 2003; Mueller et al., 2013; Brazil, 2015; Mezzano et al., 2018). In several human renal diseases, Gremlin was found overexpressed, mainly in areas of tubulointerstitial fibrosis (Murphy et al., 2002; Dolan et al., 2005; Carvajal et al., 2008), suggesting that Gremlin could be involved in the fibrotic process during CKD. Several studies have demonstrated a direct fibrogenic effect of Gremlin in renal cells. In mesangial cells, Gremlin increased cell proliferation and ECM accumulation via ERK (Huang et al., 2013) and in renal fibroblasts Gremlin increased ECM production (Rodrigues-Diez et al., 2012). Accordingly, we have recently observed that in a model of Gremlin-induced renal damage there was an upregulation of fibrotic related genes, including TGF- $\beta$ 1, which were blocked by VEGFR2 kinase inhibition (Lavozy et al., 2018). However, no renal fibrosis was observed. Now, we have found out that experimental renal fibrosis was prevented by VEGFR2 blockade. In the UUO model, treatment with a VEGFR2 kinase inhibitor significantly prevented the renal overexpression of profibrotic factors and accumulation of key ECM proteins such as collagen. Interestingly, blocking VEGFR2 by circulating soluble receptor ectodomains, diminished fibrosis and capillary rarefaction in UUO (Lin et al., 2011). In that study, VEGFR2 blockade also blocked pericyte PDGFR $\beta$  activation, and pericyte differentiation and proliferation (Lin et al., 2011), thus blocking another source of scar-producing myofibroblasts. Unfortunately, that study did not assess Gremlin levels nor the role of Gremlin/VEGFR2 responses on endothelial cells. In mice, Gremlin blockade diminished ECM accumulation, as observed in streptozotocin-induced diabetes in knockout mice heterozygous for Grem1 (Roxburgh et al., 2009) and by Gremlin gene silencing (Zhang et al., 2010). Moreover, transgenic mice overexpressing Grem-1 specifically in tubular cells presented increased susceptibility



to renal damage, induced by streptozotocin or folic acid administration (Droguett et al., 2014; Marchant et al., 2015). Accordingly, specific deletion of Grem-1 in tubular cells diminished renal fibrosis in folic acid-induced damage in mice (Church et al., 2017). These data show that inhibition of VEGFR2 signaling ameliorates renal fibrosis and suggest that Gremlin/VEGFR2 blockade could be responsible of the downregulation of profibrotic events, suggesting a novel anti-fibrotic therapy for CKD.

Activation of the Notch pathway participates in renal damage progression, but the precise mechanisms are not fully elucidated (Marquez-Exposito et al., 2018). In some experimental models of renal damage, including acute kidney injury models, such as folic acid administration in mice, Notch blockade by pharmacological inhibitors or soluble Notch ligands ameliorates renal damage, mainly by inhibiting fibroblast proliferation and therefore decreasing fibrosis (Bielez et al., 2010; Murea et al., 2010; Sharma et al., 2011; Marquez-Exposito et al., 2018). More recently, anti-inflammatory properties of Notch inhibition have been described in experimental renal damage (Lavozy et al., 2018). In a previous study in the UUO model, authors demonstrated that a  $\gamma$ -secretase inhibitor downregulated gene expression of fibronectin and type I Collagen (Bielez et al., 2010). Here, we have extended these data at the protein level showing that DAPT prevented the increase of profibrotic factors, including TGF- $\beta$ 1, and the renal accumulation of collagen and fibronectin in a UUO model. Notch is involved in EMT in carcinogenesis (Takebe et al., 2015; De Francesco et al., 2018). In cultured tubular epithelial cells, we found that DAPT diminished Gremlin-induced EMT changes, confirming the role of the Notch pathway in EMT regulation.

Chronic progressive kidney fibrosis remains an unresolved challenge. Irrespective of the underlying cause, CKD is linked to the development of tubulo-interstitial fibrosis. Our data show that blockade of Gremlin-mediated VEGFR2/Notch activation ameliorates fibrotic events and EMT processes, suggesting that Gremlin might be a fibrosis driver through VEGFR2 and Notch pathway, and a possible therapeutic target.

## REFERENCES

- Anders, H. J. (2014). Immune system modulation of kidney regeneration-mechanisms and implications. *Nat. Rev. Nephrol.* 10, 347–358. doi: 10.1038/nrneph.2014.68
- Bielez, B., Sirin, Y., Si, H., Niranjana, T., Gruenwald, A., Ahn, S., et al. (2010). Epithelial Notch signaling regulates interstitial fibrosis development in the kidneys of mice and humans. *J. Clin. Invest.* 120, 4040–4054. doi: 10.1172/JCI43025
- Brazil, D. P. (2015). Gremlin1 and chronic pancreatitis: a new clinical target and biomarker? *J. Mol. Med.* 93, 1057–1060. doi: 10.1007/s00109-015-1335-6
- Carvajal, G., Droguett, A., Burgos, M. E., Aros, C., Ardiles, L., Flores, C., et al. (2008). Gremlin: a novel mediator of epithelial mesenchymal transition and fibrosis in chronic allograft nephropathy. *Transplant. Proc.* 40, 734–739. doi: 10.1016/j.transproceed.2008.02.064
- Church, R. H., Ali, I., Tate, M., Lavin, D., Krishnakumar, A., Kok, H. M., et al. (2017). Gremlin1 plays a key role in kidney development and renal fibrosis. *Am. J. Physiol. Renal Physiol.* 312, F1141–F1157. doi: 10.1152/ajprenal.00344.2016
- Corsini, M., Moroni, E., Ravelli, C., Andrés, G., Grillo, E., Ali, I. H., et al. (2014). Cyclic adenosine monophosphate response element-binding protein mediates

## AUTHOR CONTRIBUTIONS

LM-E and CL contributed to the design of the experiments, acquisition, analysis, and interpretation of all data, and drafted the manuscript. RR-D contributed to design of the experiments, analysis and interpretation of data, and drafted the manuscript. SR-M, MO, and EC-N participated in the development of mouse models and analysis of data. AO, SM, RS, and JE contributed to the critical review of the manuscript and the financial support of the work. MR-O contributed to the design of the experiments, analysis and interpretation of the all data, draft of the manuscript, and financial support of the experiments. All authors have reviewed the manuscript and approved the final version.

## FUNDING

This work was supported by grants from the Instituto de Salud Carlos III (ISCIII) and Fondos FEDER European Union (PI16/02057, PI17/00119, PI17/01495, and Red de Investigación Renal REDINREN: RD16/0009), Sociedad Española de Nefrología, “NOVELREN-CM: Enfermedad renal crónica: nuevas Estrategias para la prevención, Diagnóstico y tratamiento”; B2017/BMD-3751, B2017/BMD-3686 CIFRA2-CM, PAI 82140017, and FONDECYT 1160465 (Chile) and Bayer HealthCare AG (Grants4Targets initiative, Berlin, Germany).

## ACKNOWLEDGMENTS

Part of the data were included in the Thesis of CL (Lavozy, 2014) presented at the UAM. We want to thank M<sup>a</sup> Mar Gonzalez Garcia-Parreño for her technical help with confocal microscopy and Laura Santos for her help in the experimental models and immunohistochemical techniques.

- the proangiogenic or proinflammatory activity of gremlin. *Arterioscler. Thromb. Vasc. Biol.* 34, 136–145. doi: 10.1161/ATVBAHA.113.302517
- Cortinovis, M., Ruggerenti, P., and Remuzzi, G. (2016). Progression, remission and regression of chronic renal diseases. *Nephron* 134, 20–24. doi: 10.1159/000445844
- De Francesco, E. M., Maggolini, M., and Musti, A. M. (2018). Crosstalk between Notch, HIF-1 $\alpha$  and GPER in Breast Cancer EMT. *Int. J. Mol. Sci.* 19:2011. doi: 10.3390/ijms19072011
- Dolan, V., Murphy, M., Sadler, D., Lappin, D., Doran, P., Godson, C., et al. (2005). Expression of gremlin, a bone morphogenetic protein antagonist, in human diabetic nephropathy. *Am. J. Kidney Dis.* 45, 1034–1039. doi: 10.1053/j.ajkd.2005.03.014
- Droguett, A., Krall, P., Burgos, M. E., Valderrama, G., Carpio, D., Ardiles, L., et al. (2014). Tubular overexpression of gremlin induces renal damage susceptibility in mice. *PLoS One* 9:e101879. doi: 10.1371/journal.pone.0101879
- Duffield, J. S. (2014). Cellular and molecular mechanisms in kidney fibrosis. *J. Clin. Invest.* 124, 2299–2306. doi: 10.1172/JCI72267
- Erdmann, R., Ozden, C., Weidmann, J., and Schultze, A. (2015). Targeting the Gremlin-VEGFR2 axis - a promising strategy for multiple diseases? *J. Pathol.* 236, 403–406. doi: 10.1002/path.4544

- Huang, H., Huang, H., Li, Y., Liu, M., Shi, Y., Chi, Y., et al. (2013). Gremlin induces cell proliferation and extra cellular matrix accumulation in mouse mesangial cells exposed to high glucose via the ERK1/2 pathway. *BMC Nephrol.* 14:33. doi: 10.1186/1471-2369-14-33
- Ji, C., Huang, J. W., Xu, Q. Y., Zhang, J., Lin, M. T., Tu, Y., et al. (2016). Gremlin inhibits UV-induced skin cell damages via activating VEGFR2-Nrf2 signaling. *Oncotarget* 7, 84748–84757. doi: 10.18632/oncotarget.12454
- Khokha, M. K., Hsu, D., Brunet, L. J., Dionne, M. S., and Harland, R. M. (2003). Gremlin is the BMP antagonist required for maintenance of Shh and Fgf signals during limb patterning. *Nat. Genet.* 34, 303–307. doi: 10.1038/ng1178
- Kim, M., Yoon, S., Lee, S., Ha, S. A., Kim, H. K., Kim, J. W., et al. (2012). Gremlin-1 induces BMP-independent tumor cell proliferation, migration, and invasion. *PLoS One* 7:e35100. doi: 10.1371/journal.pone.0035100
- Lappin, D. W., McMahon, R., Murphy, M., and Brady, H. R. (2002). Gremlin: an example of the re-emergence of developmental programmes in diabetic nephropathy. *Nephrol. Dial Transplant.* 17(Suppl. 9), 65–67.
- Lavoz, C. (2014). *Gremlin, un Nuevo Mediador en la Progresión de la Enfermedad Renal*. Master's thesis, Universidad Autónoma de Madrid, Madrid.
- Lavoz, C., Alique, M., Rodrigues-Diez, R., Pato, J., Keri, G., Mezzano, S., et al. (2015). Gremlin regulates renal inflammation via the vascular endothelial growth factor receptor 2 pathway. *J. Pathol.* 236, 407–420. doi: 10.1002/path.4537
- Lavoz, C., Poveda, J., Marquez-Exposito, L., Rayego-Mateos, S., Rodrigues-Diez, R. R., Ortiz, A., et al. (2018). Gremlin activates the Notch pathway linked to renal inflammation. *Clin. Sci.* 132, 1097–1115. doi: 10.1042/CS20171553
- LeBleu, V. S., Taduri, G., O'Connell, J., Teng, Y., Cooke, V. G., Woda, C., et al. (2013). Origin and function of myofibroblasts in kidney fibrosis. *Nat. Med.* 19, 1047–1053. doi: 10.1038/nm.3218
- Li, G., Li, Y., Liu, S., Shi, Y., Chi, Y., Liu, G., et al. (2013). Gremlin aggravates hyperglycemia-induced podocyte injury by a TGF $\beta$ /smad dependent signaling pathway. *J. Cell. Biochem.* 114, 2101–2113. doi: 10.1002/jcb.24559
- Li, Y., Wang, Z., Wang, S., Zhao, J., Zhang, J., and Huang, Y. (2012). Gremlin-mediated decrease in bone morphogenetic protein signaling promotes aristolochic acid-induced epithelial-to-mesenchymal transition (EMT) in HK-2 cells. *Toxicology* 297, 68–75. doi: 10.1016/j.tox.2012.04.004
- Lin, S. L., Chang, F. C., Schrimpf, C., Chen, Y. T., Wu, C. F., Wu, V. C., et al. (2011). Targeting endothelium-pericyte cross talk by inhibiting VEGF receptor signaling attenuates kidney microvascular rarefaction and fibrosis. *Am. J. Pathol.* 178, 911–923. doi: 10.1016/j.ajpath.2010.10.012
- Liu, B. C., Tang, T. T., Lv, L. L., and Lan, H. Y. (2018). Renal tubule injury: a driving force toward chronic kidney disease. *Kidney Int.* 93, 568–579. doi: 10.1016/j.kint.2017.09.033
- Liu, Y., Chen, Z., Cheng, H., Chen, J., and Qian, J. (2017). Gremlin promotes retinal pigmentation epithelial (RPE) cell proliferation, migration and VEGF production via activating VEGFR2-Akt-mTORC2 signaling. *Oncotarget* 8, 979–987. doi: 10.18632/oncotarget.13518
- Lovisa, S., LeBleu, V. S., Tampe, B., Sugimoto, H., Vадnagara, K., Carstens, J. L., et al. (2015). Epithelial-to-mesenchymal transition induces cell cycle arrest and parenchymal damage in renal fibrosis. *Nat. Med.* 21, 998–1009. doi: 10.1038/nm.3902
- Marchant, V., Droguett, A., Valderrama, G., Burgos, M. E., Carpio, D., Kerr, B., et al. (2015). Tubular overexpression of Gremlin in transgenic mice aggravates renal damage in diabetic nephropathy. *Am. J. Physiol. Renal Physiol.* 309, F559–F568. doi: 10.1152/ajprenal.00023.2015
- Marquez-Exposito, L., Cantero-Navarro, E., Lavoz, C., Fierro-Fernández, M., Poveda, J., Rayego-Mateos, S., et al. (2018). Could Notch signaling pathway be a potential therapeutic option in renal diseases? *Nefrologia* doi: 10.1016/j.nefro.2017.11.027 [Epub ahead of print].
- McCormack, N., Molloy, E. L., and O'Dea, S. (2013). Bone morphogenetic proteins enhance an epithelial-mesenchymal transition in normal airway epithelial cells during restitution of a disrupted epithelium. *Respir. Res.* 14:36. doi: 10.1186/1465-9921-14-36
- Merino, R., Rodriguez-Leon, J., Macias, D., Gañan, Y., Economides, A. N., and Hurler, J. M. (1999). The BMP antagonist Gremlin regulates outgrowth, chondrogenesis and programmed cell death in the developing limb. *Development* 126, 5515–5522.
- Mezzano, S., Droguett, A., Lavoz, C., Krall, P., Egido, J., and Ruiz-Ortega, M. (2018). Gremlin and renal diseases: ready to jump the fence to clinical utility? *Nephrol. Dial Transplant.* 33, 735–741. doi: 10.1093/ndt/gfx194
- Michos, O., Panman, L., Vintersten, K., Beier, K., Zeller, R., and Zuniga, A. (2004). Gremlin-mediated BMP antagonism induces the epithelial-mesenchymal feedback signaling controlling metanephric kidney and limb organogenesis. *Development* 131, 3401–3410. doi: 10.1242/dev.01251
- Mitola, S., Ravelli, C., Moroni, E., Salvi, V., Leali, D., Ballmer-Hofer, K., et al. (2010). Gremlin is a novel agonist of the major proangiogenic receptor VEGFR2. *Blood* 116, 3677–3680. doi: 10.1182/blood-2010-06-291930
- Mueller, K. A., Tavlaki, E., Schneider, M., Jorbenadze, R., Geisler, T., Kandolf, R., et al. (2013). Gremlin-1 identifies fibrosis and predicts adverse outcome in patients with heart failure undergoing endomyocardial biopsy. *J. Card Fail.* 19, 678–684. doi: 10.1016/j.cardfail.2013.09.001
- Murea, M., Park, J. K., Sharma, S., Kato, H., Gruenwald, A., Niranjan, T., et al. (2010). Expression of Notch pathway proteins correlates with albuminuria, glomerulosclerosis, and renal function. *Kidney Int.* 78, 514–522. doi: 10.1038/ki.2010.172
- Murphy, M., McMahon, R., Lappin, D. W., and Brady, H. R. (2002). Gremlins: is this what renal fibrogenesis has come to? *Exp. Nephrol.* 10, 241–244. doi: 10.1159/000063698
- Myllärniemi, M., Lindholm, P., Ryynänen, M. J., Kliment, C. R., Salmenkivi, K., Keski-Oja, J., et al. (2008). Gremlin-mediated decrease in bone morphogenetic protein signaling promotes pulmonary fibrosis. *Am. J. Respir. Crit. Care Med.* 177, 321–329. doi: 10.1164/rccm.200706-945OC
- Pazos, M. C., Abramovich, D., Bechis, A., Accialini, P., Parborell, F., Tesone, M., et al. (2017). Gamma secretase inhibitor impairs epithelial-to-mesenchymal transition induced by TGF- $\beta$  in ovarian tumor cell lines. *Mol. Cell. Endocrinol.* 15, 125–137. doi: 10.1016/j.mce.2016.11.025
- Rodrigues-Diez, R., Lavoz, C., Carvajal, G., Rayego-Mateos, S., Rodrigues Diez, R. R., Ortiz, A., et al. (2012). Gremlin is a downstream profibrotic mediator of transforming growth factor-beta in cultured renal cells. *Nephron Exp. Nephrol.* 122, 62–74. doi: 10.1159/000346575
- Rodrigues-Diez, R., Rodrigues-Diez, R. R., Lavoz, C., Carvajal, G., Droguett, A., Garcia-Redondo, A. B., et al. (2014). Gremlin activates the Smad pathway linked to epithelial mesenchymal transdifferentiation in cultured tubular epithelial cells. *Biomed. Res. Int.* 2014:802841. doi: 10.1155/2014/802841
- Roxburgh, S. A., Kattla, J. J., Curran, S. P., O'Meara, Y. M., Pollock, C. A., Goldschmeding, R., et al. (2009). Allelic depletion of grem1 attenuates diabetic kidney disease. *Diabetes* 58, 1641–1650. doi: 10.2337/db08-1365
- Roxburgh, S. A., Murphy, M., Pollock, C. A., and Brazil, D. P. (2006). Recapitulation of embryological programmes in renal fibrosis—the importance of epithelial cell plasticity and developmental genes. *Nephron Physiol.* 103, 139–148. doi: 10.1159/000092453
- Ruiz-Andres, O., Sanchez-Niño, M. D., Moreno, J. A., Ruiz-Ortega, M., Ramos, A. M., Sanz, A. B., et al. (2016). Downregulation of kidney protective factors by inflammation: role of transcription factors and epigenetic mechanisms. *Am. J. Physiol. Renal Physiol.* 311, F1329–F1340. doi: 10.1152/ajprenal.00487.2016
- Sanchez-Niño, M. D., Sanz, A. B., Ramos, A. M., Ruiz-Ortega, M., and Ortiz, A. (2017). Translational science in chronic kidney disease. *Clin. Sci.* 131, 1617–1629. doi: 10.1042/CS20160395
- Sharma, S., Sirin, Y., and Susztak, K. (2011). The story of Notch and chronic kidney disease. *Curr. Opin. Nephrol. Hypertens.* 20, 56–61. doi: 10.1097/MNH.0b013e3283414c88
- Shibuya, M., and Claesson-Welsh, L. (2006). Signal transduction by VEGF receptors in regulation of angiogenesis and lymphangiogenesis. *Exp. Cell Res.* 312, 549–560. doi: 10.1016/j.yexcr.2005.11.012
- Siebel, C., and Lendahl, U. (2017). Notch signaling in development tissue homeostasis, and disease. *Physiol. Rev.* 97, 1235–1294. doi: 10.1152/physrev.00005.2017
- Staloch, D., Gao, X., Liu, K., Xu, M., Feng, X., Aronson, J. F., et al. (2015). Gremlin is a key pro-fibrogenic factor in chronic pancreatitis. *J. Mol. Med.* 93, 1085–1093. doi: 10.1007/s00109-015-1308-9
- Takebe, N., Miele, L., Harris, P. J., Jeong, W., Bando, H., Kahn, M., et al. (2015). Targeting Notch, Hedgehog, and Wnt pathways in cancer stem cells: clinical update. *Nat. Rev. Clin. Oncol.* 12, 445–464. doi: 10.1038/nrclinonc.2015.61

- Topol, L. Z., Bardot, B., Zhang, Q., Resau, J., Huillard, E., Marx, M., et al. (2000). Biosynthesis, post-translation modification, and functional characterization of Drm/Gremlin. *J. Biol. Chem.* 275, 8785–8793. doi: 10.1074/jbc.275.12.8785
- Ucero, A. C., Benito-Martin, A., Izquierdo, M. C., Sanchez-Niño, M. D., Sanz, A. B., Ramos, A. M., et al. (2014). Unilateral ureteral obstruction: beyond obstruction. *Int. Urol. Nephrol.* 46, 765–776. doi: 10.1007/s11255-013-0520-1
- Weiskirchen, R., and Meurer, S. K. (2013). BMP-7 counteracting TGF-beta1 activities in organ fibrosis. *Front. Biosci.* 18, 1407–1434. doi: 10.2741/4189
- Yin, M., Tissari, M., Tamminen, J., Ylivinkka, I., Rönty, M., von Nandelstadh, P., et al. (2017). Gremlin-1 is a key regulator of the invasive cell phenotype in mesothelioma. *Oncotarget* 8, 98280–98297. doi: 10.18632/oncotarget.21550
- Zeisberg, M., Hanai, J., Sugimoto, H., Mammoto, T., Charytan, D., Strutz, F., et al. (2003). BMP-7 counteracts TGF-beta1-induced epithelial-to-mesenchymal transition and reverses chronic renal injury. *Nat. Med.* 9, 964–968. doi: 10.1038/nm888
- Zeisberg, M., and Neilson, E. G. (2009). Biomarkers for epithelial-mesenchymal transitions. *J. Clin. Invest.* 119, 1429–1437. doi: 10.1172/JCI36183
- Zhang, Q., Shi, Y., Wada, J., Malakauskas, S. M., Liu, M., Ren, Y., et al. (2010). In vivo delivery of Gremlin siRNA plasmid reveals therapeutic potential against diabetic nephropathy by recovering bone morphogenetic protein-7. *PLoS One* 5:e11709. doi: 10.1371/journal.pone.0011709
- Zode, G. S., Clark, A. F., and Wordinger, R. J. (2009). Bone morphogenetic protein 4 inhibits TGF-beta2 stimulation of extracellular matrix proteins in optic nerve head cells: role of gremlin in ECM modulation. *Glia* 57, 755–766. doi: 10.1002/glia.20803

**Conflict of Interest Statement:** The authors declare that the research was conducted in the absence of any commercial or financial relationships that could be construed as a potential conflict of interest.

Copyright © 2018 Marquez-Exposito, Lavo, Rodrigues-Diez, Rayego-Mateos, Orejudo, Cantero-Navarro, Ortiz, Egido, Selgas, Mezzano and Ruiz-Ortega. This is an open-access article distributed under the terms of the Creative Commons Attribution License (CC BY). The use, distribution or reproduction in other forums is permitted, provided the original author(s) and the copyright owner(s) are credited and that the original publication in this journal is cited, in accordance with accepted academic practice. No use, distribution or reproduction is permitted which does not comply with these terms.



# Low Expression of miR-466f-3p Sustains Epithelial to Mesenchymal Transition in Sonic Hedgehog Medulloblastoma Stem Cells Through Vegfa-Nrp2 Signaling Pathway

**Zein Mersini Besharat<sup>1†</sup>, Claudia Sabato<sup>2,3†</sup>, Agnese Po<sup>2\*†</sup>, Francesca Gianno<sup>4</sup>, Luana Abballe<sup>1</sup>, Maddalena Napolitano<sup>2</sup>, Evelina Miele<sup>5</sup>, Felice Giangaspero<sup>4,6</sup>, Alessandra Vacca<sup>1</sup>, Giuseppina Catanzaro<sup>1†</sup> and Elisabetta Ferretti<sup>1,6†</sup>**

## OPEN ACCESS

### Edited by:

Raffaele Strippoli,  
Università degli Studi di Roma  
La Sapienza, Italy

### Reviewed by:

Barbara Stecca,  
Istituto per lo Studio e la Prevenzione  
Oncologica (ISPO), Italy  
Federica Finetti,  
Università degli Studi di Siena, Italy

### \*Correspondence:

Agnese Po  
agnese.po@uniroma1.it

<sup>†</sup> These authors have contributed  
equally to this work

### Specialty section:

This article was submitted to  
Inflammation Pharmacology,  
a section of the journal  
Frontiers in Pharmacology

**Received:** 31 July 2018

**Accepted:** 18 October 2018

**Published:** 12 November 2018

### Citation:

Besharat ZM, Sabato C, Po A,  
Gianno F, Abballe L, Napolitano M,  
Miele E, Giangaspero F, Vacca A,  
Catanzaro G and Ferretti E (2018)  
Low Expression of miR-466f-3p  
Sustains Epithelial to Mesenchymal  
Transition in Sonic Hedgehog  
Medulloblastoma Stem Cells Through  
Vegfa-Nrp2 Signaling Pathway.  
Front. Pharmacol. 9:1281.  
doi: 10.3389/fphar.2018.01281

<sup>1</sup> Department of Experimental Medicine, Sapienza University, Rome, Italy, <sup>2</sup> Department of Molecular Medicine, Sapienza University, Rome, Italy, <sup>3</sup> Center for Life NanoScience@Sapienza, Istituto Italiano di Tecnologia, Rome, Italy, <sup>4</sup> Department of Radiological, Oncological and Pathological Science, Sapienza University, Rome, Italy, <sup>5</sup> Department of Hematology/Oncology and Stem Cell Transplantation, Bambino Gesù Children's Hospital, Istituto di Ricovero e Cura a Carattere Scientifico, Rome, Italy, <sup>6</sup> IRCCS Neuromed, Isernia, Italy

High-throughput analysis has improved the knowledge of medulloblastoma (MB), the leading cause of cancer related death in children, allowing a better comprehension of the key molecular pathways in MB pathogenesis. However, despite these advances, 30% of patients still die from the disease and survivors face severe long-term side effects. Cancer stem cells (CSCs) represent a subset of cells that not only drive tumorigenesis, but are also one of the main determinants of chemoresistance. Epithelial mesenchymal transition (EMT) is a hallmark of cancer and up to now few data is available in MB. To give insight into the role of the EMT process in maintaining the mesenchymal phenotype of CSCs, we analyzed the expression of EMT related transcripts and microRNAs in these cells. We firstly isolated CSCs from Sonic Hedgehog (SHH) MB derived from Ptch1 heterozygous mice and compared their expression level of EMT-related transcripts and microRNAs with cerebellar NSCs. We identified two molecules linked to SHH and EMT, Vegfa and its receptor Nrp2, over-expressed in SHH MB CSCs. Inhibition of Vegfa showed impairment of cell proliferation and self-renewal ability of CSCs concurrent with an increase of the expression of the EMT gene, E-cadherin, and a decrease of the EMT marker, Vimentin. Moreover, among deregulated microRNAs, we identified miR-466f-3p, a validated inhibitor of both Vegfa and Nrp2. These results allowed us to describe a new EMT molecular network, involving the down-regulation of miR-466f-3p together with the concordant up-regulation of Vegfa and Nrp2, that sustains the mesenchymal phenotype of SHH MB CSCs.

**Keywords:** medulloblastoma, sonic hedgehog medulloblastoma cancer stem cells, epithelial to mesenchymal transition, vegfa, Nrp2, miR-466f-3p



## INTRODUCTION

Medulloblastoma (MB) is the most common malignant brain tumor of the pediatric age and a leading cause of cancer related morbidity and mortality (Northcott et al., 2012). Despite the fact that multimodal aggressive therapy has improved MB outcome, 30% of patients still die of disease and about 40% face tumor recurrence. Moreover, survivors frequently develop long-term severe side effects (Wang et al., 2018). In recent years, high-throughput studies have been conducted to better understand MB biology and key signaling pathways that could be addressed to reach a better management of MB patients. These studies allowed the recent WHO 2016 subgrouping of MB (Louis et al., 2016), identifying five subgroups: WNT activated, SHH activated P53 wild-type, SHH activated P53 mutant, non-WNT/non-SHH Group 3, non-WNT/non-SHH Group 4 (Louis et al., 2016) and more recently 12 molecular subtypes (Cavalli et al., 2017; Northcott et al., 2017). In this context, SHH subgroups account for about 30% of cases (Cavalli et al., 2017) and they are the most common MB subtypes in infants and adults (Kool et al., 2012).

Cancer stem cells (CSCs) have been described in MB (Lee et al., 2005; Po et al., 2010; Manoranjan et al., 2013; Mastronuzzi et al., 2014). CSCs may arise from the malignant transformation of neural stem cells (NSCs) and represent a reservoir for cancer maintenance and progression (Northcott et al., 2012). We isolated CSCs from *Ptch* heterozygous mice, a model of the SHH MB subgroup (Goodrich et al., 1997; Po et al., 2010; Wu et al., 2011; Ronci et al., 2015), and performed transcriptome analysis of both SHH MB CSCs and NSCs isolated from postnatal murine cerebellum for comparison. Among the identified transcripts that characterize SHH MB CSCs, genes involved in the epithelial-mesenchymal transition (EMT) were highly represented and some of them resulted significantly differentially expressed between SHH MB CSCs and NSCs. EMT is characterized by the loss of epithelial characteristics and the acquisition of mesenchymal properties and previous studies linked a shift toward mesenchymal properties to metastatic progression and acquisition of stemness features (Taube et al., 2010). Among deregulated markers of EMT in SHH MB CSCs, we focused on *Vegfa* and *Nrp2* that have been described as pivotal players in tumorigenesis and in maintaining stemness and proliferation (Prud'homme and Glinka, 2012; Fantozzi et al., 2014). We show that both *Vegfa* and *Nrp2* correlate with stemness features in SHH MB CSCs and that *Vegfa* inhibition determines an increase in the expression of the epithelial marker E-cadherin, a reduction of the mesenchymal marker Vimentin and an impairment of self-renewal. Moreover, since accumulating evidence indicate a crucial role of microRNAs in the regulation of a variety of biological processes, including EMT (Markopoulos et al., 2017), we also focused our attention on the microRNAs differentially expressed between NSCs and SHH MB CSCs and involved in EMT identifying an epigenetic circuitry that sustains the mesenchymal phenotype of SHH MB CSCs.

## MATERIALS AND METHODS

Unless otherwise indicated, media and supplements were purchased from Gibco/Invitrogen (Carlsbad, CA) and chemicals from Sigma-Aldrich (St. Louis, MO). Animal experiments were approved by local ethic authorities and conducted in accordance with Italian Governing Law (D.lgs 26/2014; Prot. no. 03/2013).

### Cell Culture, Treatments, Proliferation and Oncosphere-Forming Assays

SHH MB CSCs were derived from spontaneous tumours arisen in *Ptch1* + /− mice and maintained as previously described (Po et al., 2010). To induce differentiation, cells were plated on D-poly-lysine coated supports and treated for 48 h with 2 μM retinoic acid (Ronci et al., 2015). BrdU incorporation was used to evaluate SHH MB CSCs proliferation before (CSC) and after differentiation (CSC-diff) (Miele et al., 2017a). Pharmacological inhibition of *Vegfa* was induced by treating SHH MB CSC cells for 72 h with 10, 20, 40 and 60 ng/ml anti-*Vegf* (MAB 293, R&D Systems). Synthetic miR-466f-3p (4464066, Thermo Fisher Scientific) or negative control (miRIDIAN CN-001000-01; Dharmacon) were used as previously described (Catanzaro et al., 2018). Cell proliferation was evaluated by trypan blue exclusion assay (Catanzaro et al., 2018). Oncosphere-forming assay of SHH MB CSC was performed as previously described (Po et al., 2010). Unpaired *t*-test of three independent experiments was performed using GraphPad Prism Software version 6.0 (CA, United States), *p*-values < 0.05 were considered statistically significant.

### RNA Extraction, miRNA and mRNA Sequencing

Three biological replicates of SHH MB CSCs were subjected to miRNA-sequencing or mRNA sequencing, quality control, mapping, quantification and differential expression analysis was performed between SHH MB CSCs and NSCs (Besharat et al., 2018; Po et al., 2018).

### Immunofluorescence

Immunofluorescence studies were performed according to standard procedures (Catanzaro et al., 2011) using the following primary antibodies: anti-*Vegfa* Clone VG1 (05-1117, Millipore), anti-*Nrp2* H-300 (sc-5542), anti-Nanog (8600S, Cell Signaling), anti-NeuN (MAB377, Millipore).

### Immunochemical Analysis

Western blotting was performed as previously described (Miele et al., 2017b) using the following primary antibodies: anti-E-cadherin (610181, BD Biosciences), anti-Vimentin (92547, Abcam), anti-*Vegfa* Clone VG1 (05-1117, Millipore), anti-*Nrp2* (ab 185710, Abcam), anti-β-actin I-19 (sc-1616, Santa Cruz).

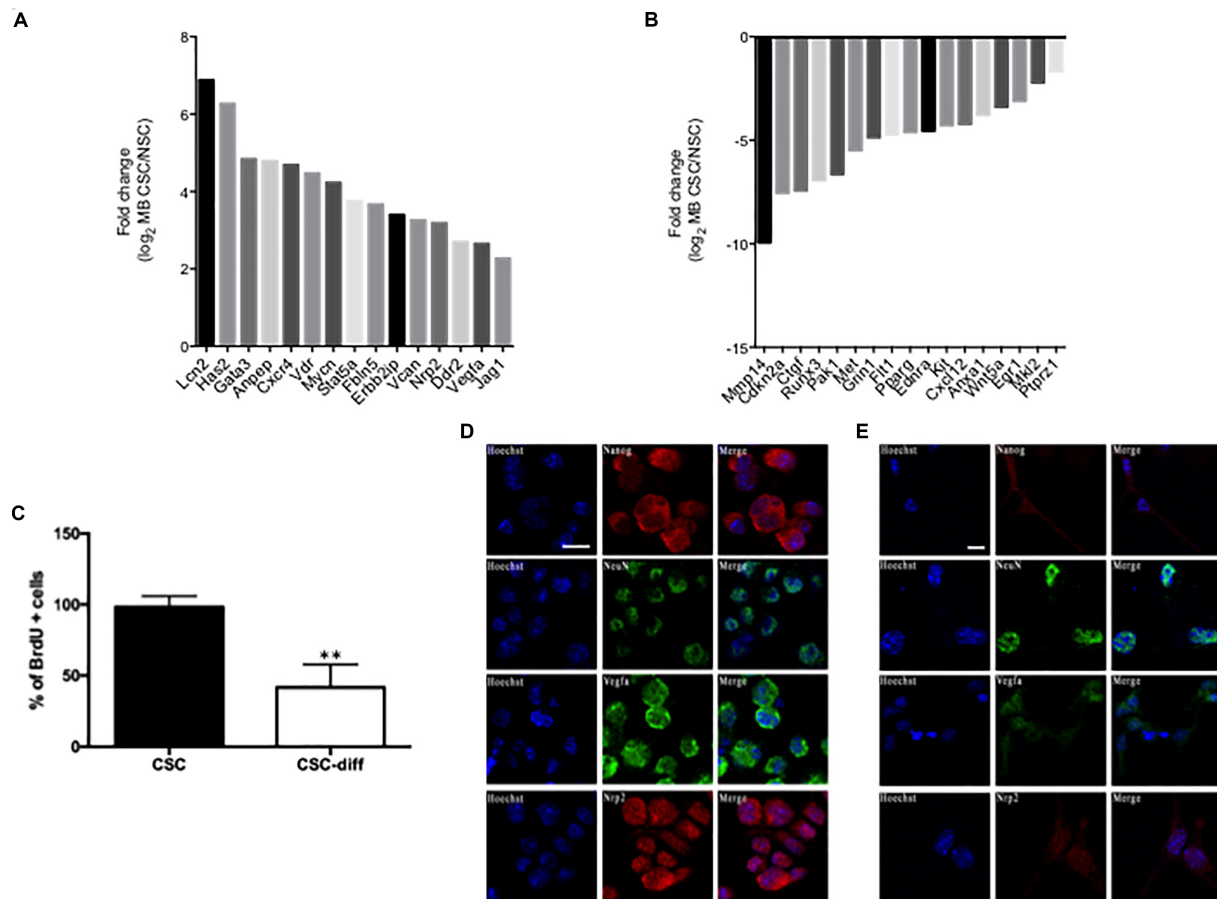


**FIGURE 1 |** EMT-related characterization of SHH MB CSC. **(A,B)** Statistically significant up-regulated **(A)** and down-regulated **(B)** EMT-related genes in SHH MB CSC vs. NSC. **(C)** Bromodeoxyuridine (BrdU) uptake in SHH MB CSC before (CSC) and after differentiation (CSC-diff). \*\* indicates  $p < 0.01$  vs. CSC-diff. **(D,E)** Immunofluorescence staining of the stemness marker Nanog and the neuronal marker NeuN, and of the EMT-related markers, Vegfa and Nrp2, in SHH MB CSC before **(D)** and after 48 h differentiation with 2  $\mu$ M RA **(E)**. SHH MB CSCs express higher levels of Vegfa and Nrp2 than SHH MB CSC-diff. The differentiated status of SHH MB CSC was confirmed by the down-regulation of Nanog and the up-regulation of NeuN in SHH MB CSC after 48 h of differentiation. Bars, 10  $\mu$ m.

## RESULTS

### EMT Related Transcripts Characterize SHH MB CSC

We recently conducted small RNA and transcriptome sequencing on SHH MB CSCs and NSCs (Besharat et al., 2018; Po et al., 2018). In this study, we focused on the EMT related RNAs that characterize SHH MB CSCs compared to NSCs, querying the differentially expressed transcripts listed in the EMT gene database dbEMT (Zhao et al., 2015). Deregulated transcripts are shown in **Figure 1**, specifically, 17 mRNA resulted down-regulated and 15 up-regulated in SHH MB CSCs when compared with NSCs (**Figures 1A,B**). Since we were interested in the mechanisms that could regulate EMT in SHH MB CSCs, we used qPCR to validate the up-regulated transcripts (data not shown). Among them, we focused on Nrp2 and Vegfa, whose role in maintaining stemness and proliferation in lung cancer stem cells we recently demonstrated (Po et al., 2017). To investigate whether they correlate with stemness features in the context of SHH MB,

the protein expression of Vegfa and Nrp2 in SHH MB CSCs was evaluated before (CSC) and after differentiation (CSC-diff). Differentiated cells are characterized by a lower proliferative rate, as shown by the reduction in BrdU incorporation (**Figure 1C**), and less aggressive behavior in comparison with SHH MB CSCs (Morelli et al., 2012). We observed a reduction in the protein level of Vegfa and Nrp2 in SHH MB CSC after 48h of Retinoic Acid (RA)-induced differentiation (**Figures 1D,E**). The differentiated status of SHH MB CSCs was confirmed by the decrease of the stemness marker Nanog and the increase of the neuronal marker NeuN (Preusser et al., 2006) after differentiation (**Figure 1E**).

### EMT-Related Circuitry Activation in SHH MB CSCs

To unravel the role of Vegfa in SHH MB CSCs, we performed pharmacological modulation by using a blocking antibody. We focused on Vegfa since it acts as a ligand for Nrp2, therefore its inhibition likely determines an inhibition of the Nrp2-mediated signaling. After 72h, Vegfa inhibition induced an impairment

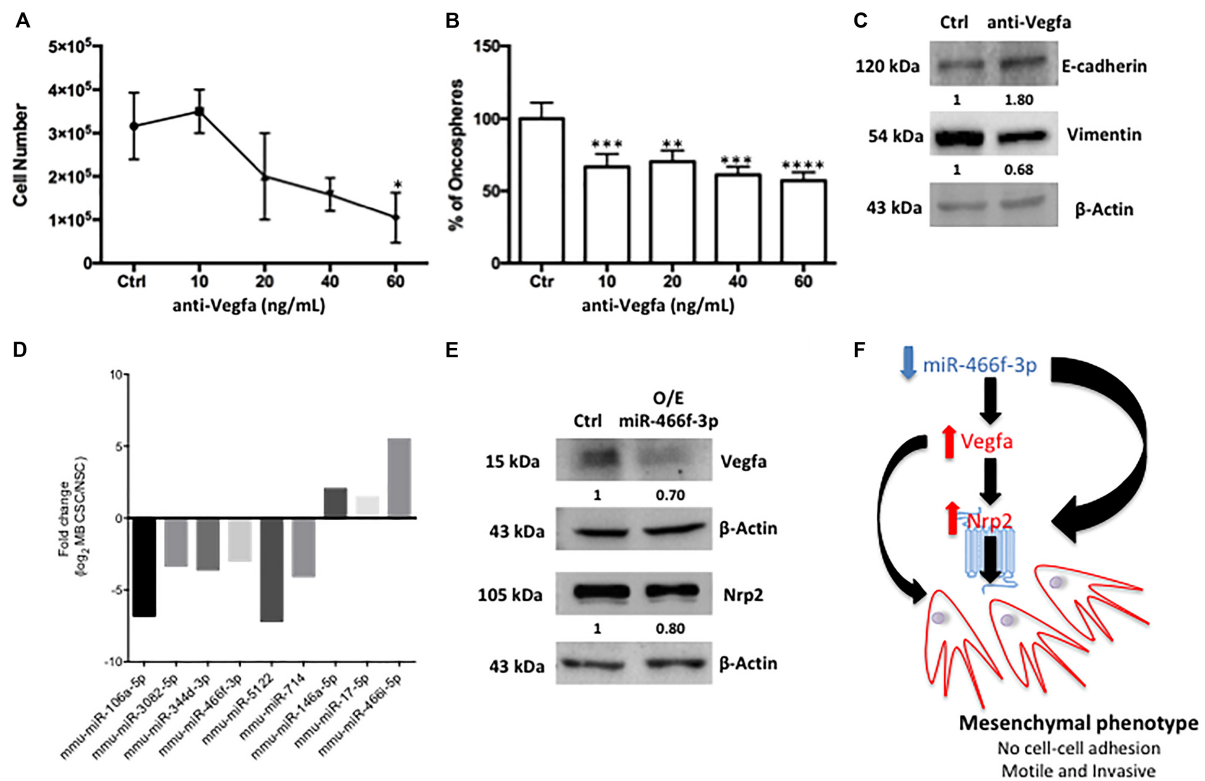


**FIGURE 2 |** Pharmacologic inhibition of Vegfa signaling and EMT-related microRNA/mRNA network in SHH MB CSC. **(A–C)** After 72 h of Vegfa inhibition cell proliferation **(A)** and self-renewal **(B)** were impaired. Western blot analysis was performed with the more effective anti-Vegfa concentration (60 ng/mL) and showed an increase in the expression of the epithelial marker E-cadherin and a reduction in the level of the mesenchymal marker Vimentin in respect to untreated SHH MB CSC (Ctrl) **(C)**. \* indicates  $p < 0.05$ , \*\* $p < 0.01$ , \*\*\* $p < 0.001$ , and \*\*\*\* $p < 0.0001$  vs. Ctrl **(D)** Statistically significant deregulated EMT-related microRNAs in SHH MB CSC vs. NSC that target the previously identified deregulated transcripts. **(E)** Western blot analysis was performed after over-expression of 20 nM of miR-466f-3p for 48 h and demonstrated a reduction of Vegfa and Nrp2 expression in respect to untreated SHH MB CSCs (Ctrl) **(F)** The miR-466f-3p/Vegfa/Nrp2 circuitry sustaining the mesenchymal phenotype of SHH MB CSC.

of both cell proliferation (**Figure 2A**) and clonogenic ability (**Figure 2B**) of SHH MB CSCs. Concordantly, we observed an increase in the epithelial marker E-cadherin and a reduction in the mesenchymal marker Vimentin (**Figure 2C**), indicating that Vegfa is involved in the induction of EMT in SHH MB CSCs. Subsequently, we investigated an EMT-related network involving both mRNAs and microRNAs that could characterize SHH MB CSCs. With this aim, we compared the miRnome of SHH MB CSC and NSC (Besharat et al., 2018) focusing on the differentially expressed microRNAs that target the previously identified deregulated transcripts (**Figures 1A,B**) as reported in miRTarBase (Chou et al., 2017). Specifically, we observed six down-regulated and three up-regulated microRNAs in SHH MB CSCs (**Figure 2D**), that we validated by using qPCR (data not shown). Among them, miR-106a targeted only Vegfa, while miR-3082 and miR-5122 targeted only Nrp2. Interestingly, miR-466f-3p targeted both Vegfa and Nrp2. To confirm the regulation of Vegfa and Nrp2 by miR-466f-3p in SHH MB CSCs, we overexpressed this microRNA obtaining a reduction of Vegfa and Nrp2 levels (**Figure 2E**). These results indicate the existence of a functional circuitry between these molecules (**Figure 2F**) involved in the induction of EMT in SHH MB CSCs.

## DISCUSSION

MB is the most frequent malignant childhood brain tumor and CSCs have been an important focus for researchers. On the basis of the cancer stem cell hypothesis, CSCs represent a subset of cells within the tumor with the ability to proliferate and maintain tumor growth (Manorajan et al., 2013). CSCs have been identified in all MB subtypes and are responsible for therapeutic resistance and invasion (Kumar et al., 2017). The cellular origin and stage of differentiation are of pivotal importance in determining the tumor phenotype in MB (Lin et al., 2016). Specifically, in SHH MB the deregulated SHH signaling works as a potent mitogen to induce the proliferation of the granule neuron precursors, where a specific deletion of *Ptch1* or *Smo* activation determines MB in mouse models (Schüller et al., 2008). Some reports described the importance of EMT in increasing the migratory and invasive abilities of MB cells (Asuthkar et al., 2011; Gupta et al., 2011; Singh et al., 2016; Ferrucci et al., 2018; Gao et al., 2018), however, no report has addressed the EMT phenomenon in MB CSCs. Since CSCs represent interesting candidates to determine MB migration and invasion, we examined the role of EMT in CSCs belonging

to a SHH MB model, derived from specific transgenic mice haploinsufficient for *Ptch1* (*Ptch1* + /-).

Firstly, we evaluated the expression of EMT-related genes in SHH MB CSC in comparison with NSC cells derived from postnatal cerebellum, where medulloblastoma arises.

Among the 15 up-regulated EMT-related transcripts we focused on *Vegfa*, which is one of the main mammalian HH target genes (Kumar et al., 2017), and *Nrp2*, a transmembrane protein required for HH signal transduction (Gephart et al., 2013). *Vegfa* has been described in solid cancers as a crucial determinant of the increase in tumorigenicity of cells that undergo EMT, both inducing angiogenetic (Fantozzi et al., 2014) and non-angiogenetic events (Gonzalez-Moreno et al., 2010). Moreover, *Vegfa* has been demonstrated to increase the tumor-initiating stem cell population, to induce EMT and metastasis (Kim et al., 2017), suggesting a strong link between CSC and EMT. On this basis, we inhibited *Vegfa* and evaluated the proliferative and self-renewal ability of CSCs and the modulation of two critical markers of the EMT process. *Vegfa* inhibition induced a reduction in cell growth and clonogenic ability of CSCs and an up-regulation of the cell adhesion molecule E-cadherin, paralleled by a down-regulation of the mesenchymal marker, Vimentin. These results indicate that *Vegfa* is involved both in maintaining the stem cells niche and in promoting cancer invasion and metastasis by controlling the EMT program. Also *Nrp2* is involved in EMT and has been reported as up-regulated both in hepatocellular carcinoma and in lung cancer cells after EMT induction by TGF- $\beta$ 1 (Nasarre et al., 2013; Wittmann et al., 2015). *Nrp2* inhibition in a cellular mouse model of SHH MB decreased tumor growth both *in vitro* and *in vivo* and the consequent mortality (Gephart et al., 2013). Since the importance of microRNAs has been well documented in cancers and we were interested in the identification of possible networks connecting *Vegfa* and/or *Nrp2* with the EMT phenomenon in SHH MB

CSC, we extended the analysis to the EMT related microRNAs deregulated between SHH MB CSC and NSC. Interestingly we identified a microRNA, miR-466f-3p, that targeted both *Vegfa* and *Nrp2*. Knowledge about this microRNA is scarce and scant. In 2011 Zheng demonstrated that the miR-466 group is contained in the intron of *Sfmbt2* (Zheng et al., 2011), while in 2012 Hunsberger et al. showed an increase in miR-466f expression in a rat model of middle cerebral artery occlusion (Hunsberger et al., 2012). The low level of miR-466f-3p in SHH MB CSCs is involved in the more mesenchymal phenotype of these cells in respect to NSCs. In fact the down-regulation of miR-466f-3p is related with an increase of the *Nrp2* level or of its ligand, *Vegfa*, with a consequent increase in *Nrp2* activation. In both cases the final result sustains the mesenchymal phenotype of SHH MB CSCs. In summary, our study provides novel evidence of an epigenetic mechanism that sustains EMT related genes in SHH MB CSC, however, future investigations and additional studies are needed to better clarify the role of the miR-466f-3p/*Vegfa*/*Nrp2* circuitry.

## AUTHOR CONTRIBUTIONS

ZB, CS, FGianno, EM, and LA performed the experiments and analysis. FGiannaspero, AV, and MN contributed reagents and analytical tools. GC and AP conceived and designed the research. GC and EF wrote the paper. EF supervised the project. All authors contributed to the final version of the manuscript.

## FUNDING

This work was supported by Sapienza University Research Grants 2016 and 2017, Agenzia Spaziale Italiana (ASI), Istituto Italiano di Tecnologia (IIT), and Ricerca Corrente to EM.

## REFERENCES

- Asuthkar, S., Nalla, A. K., Gondi, C. S., Dinh, D. H., Gujrati, M., Mohanam, S., et al. (2011). Gadd45a sensitizes medulloblastoma cells to irradiation and suppresses MMP-9-mediated EMT. *Neuro Oncol.* 13, 1059–1073. doi: 10.1093/neuonc/nor109
- Besharat, Z. M., Abballe, L., Cicconardi, F., Bhutkar, A., Grassi, L., Le Pera, L., et al. (2018). Foxm1 controls a pro-stemness microRNA network in neural stem cells. *Sci. Rep.* 8:3523. doi: 10.1038/s41598-018-21876-y
- Catanzaro, G., Battista, N., Rossi, G., Di Tommaso, M., Pucci, M., Pirazzi, V., et al. (2011). Effect of capacitation on the endocannabinoid system of mouse sperm. *Mol. Cell. Endocrinol.* 343, 88–92. doi: 10.1016/j.mce.2011.01.022
- Catanzaro, G., Besharat, Z. M., Miele, E., Chiacchiarini, M., Po, A., Carai, A., et al. (2018). The miR-139-5p regulates proliferation of supratentorial paediatric low-grade gliomas by targeting the PI3K/AKT/mTORC1 signalling. *Neuropathol. Appl. Neurobiol.* doi: 10.1111/nan.12479 [Epub ahead of print].
- Cavalli, F. M., Remke, M., Rampasek, L., Peacock, J., Shih, D. J., Luu, B., et al. (2017). Intertumoral heterogeneity within medulloblastoma subgroups. *Cancer Cell* 31, 737–754.e6. doi: 10.1016/j.ccell.2017.05.005
- Chou, C.-H., Shrestha, S., Yang, C.-D., Chang, N.-W., Lin, Y.-L., Liao, K.-W., et al. (2017). miRTarBase update 2018: a resource for experimentally validated microRNA-target interactions. *Nucleic Acids Res.* 46, D296–D302. doi: 10.1093/nar/gkx1067
- Fantozzi, A., Gruber, D. C., Pisarsky, L., Heck, C., Kunita, A., Yilmaz, M., et al. (2014). VEGF-mediated angiogenesis links EMT-induced cancer stemness to tumor initiation. *Cancer Res.* 74, 1566–1575. doi: 10.1158/0008-5472.CAN-13-1641
- Ferrucci, V., De Antonellis, P., Pennino, F. P., Asadzadeh, F., Virgilio, A., Montanaro, D., et al. (2018). Metastatic group 3 medulloblastoma is driven by PRUNE1 targeting NME1-TGF- $\beta$ -OTX2-SNAIL via PTEN inhibition. *Brain* 141, 1300–1319. doi: 10.1093/brain/awy039
- Gao, R., Lv, G., Zhang, C., Wang, X., and Chen, L. (2018). TRIM59 induces epithelial-to-mesenchymal transition and promotes migration and invasion by PI3K/AKT signaling pathway in medulloblastoma. *Oncol. Lett.* 15, 8253–8260. doi: 10.3892/ol.2018.8432
- Gephart, M. G. H., Su, Y. S., Bandara, S., Tsai, F.-C., Hong, J., Conley, N., et al. (2013). Neuropilin-2 contributes to tumorigenicity in a mouse model of Hedgehog pathway medulloblastoma. *J. Neurooncol.* 115, 161–168. doi: 10.1007/s11060-013-1216-1
- Gonzalez-Moreno, O., Lecanda, J., Green, J. E., Segura, V., Catena, R., Serrano, D., et al. (2010). VEGF elicits epithelial-mesenchymal transition (EMT) in prostate intraepithelial neoplasia (PIN)-like cells via an autocrine loop. *Exp. Cell Res.* 316, 554–567. doi: 10.1016/j.yexcr.2009.11.020
- Goodrich, L. V., Milenković, L., Higgins, K. M., and Scott, M. P. (1997). Altered neural cell fates and medulloblastoma in mouse patched mutants. *Science* 277, 1109–1113. doi: 10.1126/science.277.5329.1109
- Gupta, R., Chetty, C., Bhoopathi, P., Lakka, S., Mohanam, S., Rao, J. S., et al. (2011). Downregulation of uPA/uPAR inhibits intermittent hypoxia-induced epithelial-mesenchymal transition (EMT) in DAOY and D283 medulloblastoma cells. *Int. J. Oncol.* 38, 733–744. doi: 10.3892/ijo.2010.883



- Hunsberger, J. G., Fessler, E. B., Wang, Z., Elkahoul, A. G., and Chuang, D.-M. (2012). Post-insult valproic acid-regulated microRNAs: potential targets for cerebral ischemia. *Am. J. Transl. Res.* 4, 316–332.
- Kim, L. C., Cook, R. S., and Chen, J. (2017). mTORC1 and mTORC2 in cancer and the tumor microenvironment. *Oncogene* 36, 2191–2201. doi: 10.1038/ncr.2016.363
- Kool, M., Korshunov, A., Remke, M., Jones, D., Schlanstein, M., Northcott, P., et al. (2012). Molecular subgroups of medulloblastoma: an international meta-analysis of transcriptome, genetic aberrations, and clinical data of WNT, SHH, Group 3, and Group 4 medulloblastomas. *Acta Neuropathol.* 123, 473–484. doi: 10.1007/s00401-012-0958-8
- Kumar, V., Kumar, V., McGuire, T., Coulter, D. W., Sharp, J. G., and Mahato, R. I. (2017). Challenges and recent advances in medulloblastoma therapy. *Trends Pharmacol. Sci.* 38, 1061–1084. doi: 10.1016/j.tips.2017.09.002
- Lee, A., Kessler, J. D., Read, T.-A., Kaiser, C., Corbeil, D., Huttner, W. B., et al. (2005). Isolation of neural stem cells from the postnatal cerebellum. *Nat. Neurosci.* 8, 723–729. doi: 10.1038/nn1473
- Lin, C. Y., Erkek, S., Tong, Y., Yin, L., Federation, A. J., Zapotka, M., et al. (2016). Active medulloblastoma enhancers reveal subgroup-specific cellular origins. *Nature* 530, 57–62. doi: 10.1038/nature16546
- Louis, D. N., Perry, A., Reifenberger, G., Von Deimling, A., Figarella-Branger, D., Cavenee, W. K., et al. (2016). The 2016 World Health Organization classification of tumors of the central nervous system: a summary. *Acta Neuropathol.* 131, 803–820. doi: 10.1007/s00401-016-1545-1
- Manoranjan, B., Wang, X., Hallett, R. M., Venugopal, C., Mack, S. C., McFarlane, N., et al. (2013). FoxG1 interacts with Bmi1 to regulate self-renewal and tumorigenicity of medulloblastoma stem cells. *Stem Cells* 31, 1266–1277. doi: 10.1002/stem.1401
- Markopoulos, G. S., Roupakia, E., Tokamani, M., Chavdoula, E., Hatziaepostolou, M., Polyarchou, C., et al. (2017). A step-by-step microRNA guide to cancer development and metastasis. *Cell. Oncol.* 40, 303–339. doi: 10.1007/s13402-017-0341-9
- Mastronuzzi, A., Miele, E., Po, A., Antonelli, M., Buttarelli, F. R., Colafati, G. S., et al. (2014). Large cell anaplastic medulloblastoma metastatic to the scalp: tumor and derived stem-like cells features. *BMC Cancer* 14:262. doi: 10.1186/1471-2407-14-262
- Miele, E., Po, A., Begalli, F., Antonucci, L., Mastronuzzi, A., Marras, C. E., et al. (2017a).  $\beta$ -arrestin1-mediated acetylation of Gli1 regulates Hedgehog/Gli signaling and modulates self-renewal of SHH medulloblastoma cancer stem cells. *BMC Cancer* 17:488. doi: 10.1186/s12885-017-3477-0
- Miele, E., Valente, S., Alfano, V., Silvano, M., Mellini, P., Borovika, D., et al. (2017b). The histone methyltransferase EZH2 as a druggable target in SHH medulloblastoma cancer stem cells. *Oncotarget* 8, 68557–68570. doi: 10.18632/oncotarget.19782
- Morelli, M. B., Nabissi, M., Amantini, C., Farfariello, V., Ricci-Vitiani, L., Di Martino, S., et al. (2012). The transient receptor potential vanilloid-2 cation channel impairs glioblastoma stem-like cell proliferation and promotes differentiation. *Int. J. Cancer* 131, E1067–E1077. doi: 10.1002/ijc.27588
- Nasarre, P., Gemmill, R., Pitoron, V., Roche, J., Lu, X., Barón, A., et al. (2013). Neuropilin-2 is upregulated in lung cancer cells during TGF- $\beta$ 1-induced epithelial-mesenchymal transition. *Cancer Res.* 73, 7111–7121. doi: 10.1158/0008-5472.CAN-13-1755
- Northcott, P. A., Buchhalter, I., Morrissy, A. S., Hovestadt, V., Weischenfeldt, J., Ehrenberger, T., et al. (2017). The whole-genome landscape of medulloblastoma subtypes. *Nature* 547, 311–317. doi: 10.1038/nature22973
- Northcott, P. A., Korshunov, A., Pfister, S. M., and Taylor, M. D. (2012). The clinical implications of medulloblastoma subgroups. *Nat. Rev. Neurol.* 8, 340–351. doi: 10.1038/nrneurol.2012.78
- Po, A., Abballe, L., Sabato, C., Gianno, F., Chiacchiarini, M., Catanzaro, G., et al. (2018). Sonic hedgehog medulloblastoma cancer stem cells miRNome and transcriptome highlight novel functional networks. *Int. J. Mol. Sci.* 19:E2326. doi: 10.3390/ijms19082326
- Po, A., Ferretti, E., Miele, E., De Smaele, E., Paganelli, A., Canettieri, G., et al. (2010). Hedgehog controls neural stem cells through p53-independent regulation of Nanog. *EMBO J.* 29, 2646–2658. doi: 10.1038/emboj.2010.131
- Po, A., Silvano, M., Miele, E., Capalbo, C., Eramo, A., Salvat, I. V., et al. (2017). Noncanonical Gli1 signaling promotes stemness features and in vivo growth in lung adenocarcinoma. *Oncogene* 36, 4641–4652. doi: 10.1038/ncr.2017.91
- Preusser, M., Laggner, U., Haberler, C., Heinzl, H., Budka, H., and Hainfellner, J. (2006). Comparative analysis of NeuN immunoreactivity in primary brain tumours: conclusions for rational use in diagnostic histopathology. *Histopathology* 48, 438–444. doi: 10.1111/j.1365-2559.2006.02359.x
- Prud'homme, G. J., and Glinka, Y. (2012). Neuropilins are multifunctional coreceptors involved in tumor initiation, growth, metastasis and immunity. *Oncotarget* 3, 921–939. doi: 10.18632/oncotarget.626
- Ronci, M., Catanzaro, G., Pieroni, L., Po, A., Besharat, Z. M., Greco, V., et al. (2015). Proteomic analysis of human sonic hedgehog (SHH) medulloblastoma stem-like cells. *Mol. Biosyst.* 11, 1603–1611. doi: 10.1039/c5mb00034c
- Schüller, U., Heine, V. M., Mao, J., Kho, A. T., Dillon, A. K., Han, Y.-G., et al. (2008). Acquisition of granule neuron precursor identity is a critical determinant of progenitor cell competence to form Shh-induced medulloblastoma. *Cancer Cell* 14, 123–134. doi: 10.1016/j.ccr.2008.07.005
- Singh, S., Howell, D., Trivedi, N., Kessler, K., Ong, T., Rosmaninho, P., et al. (2016). Zeb1 controls neuron differentiation and germinal zone exit by a mesenchymal-epithelial-like transition. *elife* 5:e12717. doi: 10.7554/eLife.12717
- Taube, J. H., Herschkowitz, J. I., Komurov, K., Zhou, A. Y., Gupta, S., Yang, J., et al. (2010). Core epithelial-to-mesenchymal transition interactome gene-expression signature is associated with claudin-low and metaplastic breast cancer subtypes. *Proc. Natl. Acad. Sci. U.S.A.* 107, 15449–15454. doi: 10.1073/pnas.1004900107
- Wang, J., Garancher, A., Ramaswamy, V., and Wechsler-Reya, R. J. (2018). Medulloblastoma: from molecular subgroups to molecular targeted therapies. *Annu. Rev. Neurosci.* 41, 207–232. doi: 10.1146/annurev-neuro-070815-013838
- Wittmann, P., Grubinger, M., Gröger, C., Huber, H., Sieghart, W., Peck-Radosavljevic, M., et al. (2015). Neuropilin-2 induced by transforming growth factor- $\beta$  augments migration of hepatocellular carcinoma cells. *BMC Cancer* 15:909. doi: 10.1186/s12885-015-1919-0
- Wu, X., Northcott, P. A., Croul, S., and Taylor, M. D. (2011). Mouse models of medulloblastoma. *Chin. J. Cancer* 30, 442–449. doi: 10.5732/cjc.011.10040
- Zhao, M., Kong, L., Liu, Y., and Qu, H. (2015). dbEMT: an epithelial-mesenchymal transition associated gene resource. *Sci. Rep.* 5:11459. doi: 10.1038/srep11459
- Zheng, G. X., Ravi, A., Gould, G. M., Burge, C. B., and Sharp, P. A. (2011). Genome-wide impact of a recently expanded microRNA cluster in mouse. *Proc. Natl. Acad. Sci. U.S.A.* 108, 15804–15809. doi: 10.1073/pnas.1112772108

**Conflict of Interest Statement:** The authors declare that the research was conducted in the absence of any commercial or financial relationships that could be construed as a potential conflict of interest.

The handling editor declared a shared affiliation, though no other collaboration, with several of the authors EM, AP at the time of the review.

Copyright © 2018 Besharat, Sabato, Po, Gianno, Abballe, Napolitano, Miele, Giangaspero, Vacca, Catanzaro and Ferretti. This is an open-access article distributed under the terms of the Creative Commons Attribution License (CC BY). The use, distribution or reproduction in other forums is permitted, provided the original author(s) and the copyright owner(s) are credited and that the original publication in this journal is cited, in accordance with accepted academic practice. No use, distribution or reproduction is permitted which does not comply with these terms.



# Glutamyl-Prolyl-tRNA Synthetase Regulates Epithelial Expression of Mesenchymal Markers and Extracellular Matrix Proteins: Implications for Idiopathic Pulmonary Fibrosis

Dae-Geun Song<sup>1,2</sup>, Doyeun Kim<sup>3</sup>, Jae Woo Jung<sup>4</sup>, Seo Hee Nam<sup>1</sup>, Ji Eon Kim<sup>1</sup>, Hye-Jin Kim<sup>1</sup>, Jong Hyun Kim<sup>3</sup>, Cheol-Ho Pan<sup>2</sup>, Sunghoon Kim<sup>3</sup> and Jung Weon Lee<sup>1,3\*</sup>

## OPEN ACCESS

### Edited by:

Marc Diederich,  
Seoul National University, South Korea

### Reviewed by:

Suresh Kumar Kalangi,  
Indrashil University, India  
Carole L. Wilson,  
Medical University of South Carolina,  
United States

### \*Correspondence:

Jung Weon Lee  
jwl@snu.ac.kr

### Specialty section:

This article was submitted to  
Inflammation Pharmacology,  
a section of the journal  
Frontiers in Pharmacology

**Received:** 02 August 2018

**Accepted:** 30 October 2018

**Published:** 20 November 2018

### Citation:

Song D-G, Kim D, Jung JW, Nam SH,  
Kim JE, Kim H-J, Kim JH, Pan C-H,  
Kim S and Lee JW (2018)  
Glutamyl-Prolyl-tRNA Synthetase  
Regulates Epithelial Expression of  
Mesenchymal Markers and  
Extracellular Matrix Proteins:  
Implications for Idiopathic Pulmonary  
Fibrosis. *Front. Pharmacol.* 9:1337.  
doi: 10.3389/fphar.2018.01337

<sup>1</sup> Department of Pharmacy, Research Institute of Pharmaceutical Sciences, College of Pharmacy, Seoul National University, Seoul, South Korea, <sup>2</sup> Systems Biotechnology Research Center, Korea Institute of Science and Technology (KIST), Gangneung-si, South Korea, <sup>3</sup> Medicinal Bioconvergence Research Center, Seoul National University, Seoul, South Korea, <sup>4</sup> Interdisciplinary Program in Genetic Engineering, Seoul National University, Seoul, South Korea

Idiopathic pulmonary fibrosis (IPF), a chronic disease of unknown cause, is characterized by abnormal accumulation of extracellular matrix (ECM) in fibrotic foci in the lung. Previous studies have shown that the transforming growth factor  $\beta$ 1 (TGF $\beta$ 1) and signal transducers and activators of transcription (STAT) pathways play roles in IPF pathogenesis. Glutamyl-prolyl-tRNA-synthetase (EPRS) has been identified as a target for anti-fibrosis therapy, but the link between EPRS and TGF $\beta$ 1-mediated IPF pathogenesis remains unknown. Here, we studied the role of EPRS in the development of fibrotic phenotypes in A549 alveolar epithelial cells and bleomycin-treated animal models. We found that EPRS knockdown inhibited the TGF $\beta$ 1-mediated upregulation of fibronectin and collagen I and the mesenchymal proteins  $\alpha$ -smooth muscle actin ( $\alpha$ -SMA) and snail 1. TGF $\beta$ 1-mediated transcription of collagen I- $\alpha$ 1 and laminin  $\gamma$ 2 in A549 cells was also down-regulated by EPRS suppression, indicating that EPRS is required for ECM protein transcriptions. Activation of STAT signaling in TGF $\beta$ 1-induced ECM expression was dependent on EPRS. TGF $\beta$ 1 treatment resulted in EPRS-dependent *in vitro* formation of a multi-protein complex consisting of the TGF $\beta$ 1 receptor, EPRS, Janus tyrosine kinases (JAKs), and STATs. *In vivo* lung tissue from bleomycin-treated mice showed EPRS-dependent STAT6 phosphorylation and ECM production. Our results suggest that epithelial EPRS regulates the expression of mesenchymal markers and ECM proteins via the TGF $\beta$ 1/STAT signaling pathway. Therefore, epithelial EPRS can be used as a potential target to develop anti-IPF treatments.

**Keywords:** idiopathic pulmonary fibrosis, bleomycin fibrotic animal model, extracellular matrix, prolyl-tRNA-synthetase, signal transduction, STAT6

## INTRODUCTION

Idiopathic pulmonary fibrosis (IPF) is a chronic, progressive, fatal, fibrotic interstitial lung disease of unknown cause (Zhou et al., 2017; Bai et al., 2018; Lederer and Martinez, 2018; Milara et al., 2018). Typical clinical symptoms include dyspnoea, decreased exercise capacity, and dry cough; most patients survive for 2.5–5 years after diagnosis (Raghu et al., 2015). Idiopathic pulmonary fibrosis (IPF) is characterized by the excessive accumulation of extracellular matrix (ECM) components, which correlates with the proliferation and activation of fibroblasts, myofibroblasts, and abnormal lung epithelial cells (Wolters et al., 2014). Although the origins and activation of invasive lung myofibroblasts remain unclear, some potential causes include activation of lung resident fibroblasts, recruitment of circulating fibrocytes, and blood mesenchymal precursors; and mesenchymal transformation of alveolar type II epithelial cells, endothelial cells, pericytes, and/or mesothelial cells (Bagnato and Harari, 2015).

Current pharmacologic treatments for IPF include two U.S. Food & Drug Administration-approved drugs (nintedanib and pirfenidone) that improve symptoms but do not cure the disease (Lederer and Martinez, 2018). Given the limited treatment options, it is urgent to investigate the mechanisms of IPF pathogenesis (Milara et al., 2018).

Transforming growth factor  $\beta$ 1 (TGF $\beta$ 1) is a multifunctional cytokine that regulates immune responses during homeostasis and inflammation (Luzina et al., 2015). During IPF pathogenesis, TGF $\beta$ 1 activates lung fibroblasts and promotes epithelial mesenchymal transformations (EMT) of various cell types, such as alveolar type II cells (Ghosh et al., 2013; Milara et al., 2018). Disrupting TGF $\beta$ 1-mediated signaling will be important to develop effective anti-fibrogenesis drugs.

Prolyl-tRNA synthetase (PRS) catalyzes the attachment of proline to transfer RNA (tRNA) during translation. Halofuginone (HF), a plant alkaloid isolated from *Dichroa febrifuga* (Keller et al., 2012), is an anti-fibrotic agent that blocks PRS catalytic activity. HF inhibits mRNA levels of collagens, *COL1A1* (with 19% proline/total residues) and *COL1A2*, but this effect is reversed by exogenous proline (Keller et al., 2012). HF also blocks non-translational functions of PRS, such as inhibiting synthesis of fibronectin 1 (with 7.9% proline/total residues), an ECM protein that is not proline-rich. HF-mediated inhibition of PRS leads to the accumulation of naked tRNA molecules, which activates the amino-acid response (AAR) pathway to inhibit the synthesis of ECM proteins. Such HF-mediated inhibition of PRS and ECM expression are overcome by exogenous proline treatment, indicating that PRS can be involved in ECM translation via proline charging of prolyl-tRNA (Keller et al., 2012). However, it may still be likely that roles of PRS in ECM expression involve non-translational processes, since variable ECMs can be composed with different levels of proline.

**Abbreviations:**  $\alpha$ -SMA,  $\alpha$ -smooth muscle actin; AAR, amino acid starvation response; ECM, extracellular matrix; EPRS, glutamyl-prolyl-tRNA-synthetase; ERS, glutamyl-tRNA-synthetase; JAKs, Janus kinases; PRS, prolyl-tRNA-synthetase; STAT, Signal transducer and activator of transcription.

Studies have demonstrated a role for the Janus kinase (JAK)-signal transducer and activator of transcription (STAT) pathway in IPF. STAT3 is activated in the lungs of patients with IPF (Pechkovsky et al., 2012; Prele et al., 2012; Pedroza et al., 2016). TGF $\beta$  receptor 1 (TGF $\beta$ R1) forms a protein complex with JAK1 that activates STAT3 via SMAD3 mediation (Tang et al., 2017). STAT3 is essential for activation of the *COL1A2* enhancer (Papaioannou et al., 2018). A link between STAT3/STAT6 and IPF has also been reported (Nikola et al., 2017; Milara et al., 2018). However, the role of EPRS in TGF $\beta$ 1/STAT signaling-induced IPF pathogenesis remains.

Here, we studied the functional role of EPRS in TGF $\beta$ 1-mediated fibrosis. We found that EPRS activated TGF $\beta$ 1-induced ECM protein expression both *in vitro* and *in vivo*. TGF $\beta$ 1 treatment resulted in the formation of a multi-protein complex consisting of TGF $\beta$ R1, EPRS, JAKs, and STATs in alveolar type II epithelial cells. EPRS-dependent STAT6 phosphorylation correlated with ECM production in the lungs of bleomycin-treated mice. Our results suggested that epithelial EPRS regulates TGF $\beta$ /STAT signaling to induce expression of mesenchymal markers and ECM proteins during IPF development.

## MATERIALS AND METHODS

### Reagents and Plasmids

All cytokines and growth factors including TGF $\beta$ 1 were purchased from Peprotech (Rocky Hill, NJ, United States). Hydroxyproline assay kits, and CCL<sub>4</sub> were purchased from Sigma-Aldrich (St. Louis, MO, United States). Bleomycin and target specific pooled siRNAs siSTAT3 and siSTAT6 were purchased from Santa Cruz Biotechnology (Santa Cruz, CA, United States). EPRS in pEXPR-103-Strep vector (IBA Lifesciences, Göttingen, Germany) were gifts from Dr. Myung Hee Kim at the Korea Research Institute of Bioscience and Biotechnology (KRIBB, Daejeon, Korea). EPRS (1–1440 amino acids) consists of ERS (1–687 amino acids) and PRS (935–1,440 amino acids) linked via non-catalytic WHEP repeat domains (688–934 amino acids) (Ray and Fox, 2014). The PRS domain of EPRS was cloned into pEXPR-103-Strep vector (IBA Lifesciences). pRc/CMV-WT STAT3 was previously described (Choi et al., 2009) and pCMV-STAT6-IRES-Neo was a gift from Axel Nohturfft (Addgene plasmid # 35482). Adenovirus expressing SMAD2 or SMAD3 were described previously (Lee et al., 2005).

### Cell Culture

A549 lung adenocarcinoma cells were purchased from the Korean Cell Line Bank (KCLB, Seoul, Korea) and cultured in RPMI (SH30027.01, Hyclone, South Logan, UT, United States). Media were supplemented with 10% fetal bovine serum (FBS, GenDEPOT, Barker, TX, United States) and 1% penicillin/streptomycin (GenDEPOT) and cells were grown at 37°C in 5% CO<sub>2</sub>. The SMARTvector shEPRS doxycycline-inducible knockdown cell line was established by treating lentiviral particles (EPRS mCMV-turboGFP V2IHSMCG\_687815, 687823, Dharmacon, Lafayette, CO, United States). Positive clones were enriched by treatment of

**TABLE 1** | Antibodies and their dilution ratio used in this study.

Name	Company	Catalog	WB dil.	IHC dil.
EPRS	Neomics	NMS-01-0004	1:5,000	1:200
Fibronectin	DAKO	A0245	1:5,000	1:200
Collagen I	Acris	R1038X	1:1,000	1:200
$\beta$ -actin	Abcam	AB133626	1:1,000	–
pY <sup>641</sup> STAT6	Abcam	AB28829	1:1,000	1:100
STAT6	Cell signaling technology	#9362	1:1,000	–
pY <sup>705</sup> STAT3	Abcam	AB76315	1:1,000	–
pY <sup>705</sup> STAT3	Cell signaling technology	#9145	–	1:200
STAT3	Santa cruz biotechnology	SC-482	1:1,000	–
pS <sup>465/467</sup> SMAD2	Cell signaling technology	#3108	1:1,000	1:100
SMAD2	Cell signaling technology	#5339	1:1,000	–
pS <sup>423/425</sup> SMAD3	Cell signaling technology	#9520	1:1,000	–
SMAD3	Cell signaling technology	#9523	1:1,000	–
TGF $\beta$ 1-Receptor	Santa cruz biotechnology	SC-399	1:500	–
JAK1	Cell signaling technology	#3344	1:1,000	–
JAK2	Millipore	04-001	1:1,000	–
STAT1	Santa cruz biotechnology	SC-346	1:1,000	–
STAT5	Santa cruz biotechnology	SC-835	1:1,000	–
KRS	Neomics	NMS-01-0005	1:2,000	–
ERKs	Cell signaling technology	#9102	1:1,000	–
Anti-Strep	IBA life sciences	2-1509-001	1:2,500	–
$\alpha$ -SMA	Sigma	A2547	–	1:200
Snail 1	Cell signaling technology	#3895	1:1,000	–
Laminin $\gamma$ 2	Santa cruz biotechnology	SC-28330	–	1:200
Laminins	Abcam	AB11575	1:1,000	–

2  $\mu$ g/ml puromycin (GenDEPOT) and maintained in complete media supplemented with 1  $\mu$ g/ml puromycin. siRNAs or cDNA plasmids were transiently transfected using Lipofectamine RNAiMAX or Lipofectamine 3000, respectively, following the manufacturer's instructions (Thermo Fisher Scientific, Waltham, MA, United States).

## Western Blot Analysis

Subconfluent cells or animal tissues were harvested for whole cell or tissue extracts using RIPA buffer. Proteins in the lysates were separated in Tris-Glycine SDS-polyacrylamide gels at concentrations ranging from 8 to 12%, and transferred to nitrocellulose membranes (Thermo Fisher Scientific). Target-specific antibodies used in this study are summarized in **Table 1** (Supplementary Data Sheet 1).

## qRT-PCR

Total RNAs from animal tissues or cells were isolated using Qiazol Reagent (Qiagen, Hilden, Germany), and their cDNAs were synthesized using amfiRivert Platinum cDNA synthesis master mix (GenDEPOT) according to the manufacturer's instructions. Quantitative real time PCR (q-PCR) samples were prepared with LaboPass™ EvaGreen Q Master (Cosmo Genetech, Seoul, Korea) prior to analysis in a CFX Connect™ Real-Time PCR machine (Bio-Rad, Hercules, CA, United States).

mRNA levels were normalized against GAPDH and CFX Maestro™ software (Sunnyvale, CA, United States) was used to analyse the data. Primers were purchased from Cosmo Genetech (Seoul, Korea). The primer sequences are shown in **Table 2**.

## Co-immunoprecipitation

Whole-cell lysates were prepared using immunoprecipitation lysis buffer (40 mM HEPES pH7.4, 150 mM NaCl, 1 mM EDTA, 0.5% Triton X-100, and protease inhibitors) and precipitated with Pierce High-Capacity Streptavidin Agarose beads (Thermo Fisher Scientific) overnight at 4°C. Precipitates were washed three times with ice-cold lysis buffer, three times with immunoprecipitation wash buffer (40 mM HEPES pH 7.4, 500 mM NaCl, 1 mM EDTA, 0.5% Triton X-100, and protease inhibitors), and then boiled in 2  $\times$  SDS-PAGE sample buffer before immunoblotting.

## Luciferase Assay

To analyze promoter activity, *LAMC2* (laminin  $\gamma$ 2) promoters (encoding regions of –1871 to +388) and *COL1A1* (collagen I  $\alpha$ 1) promoters (encoding regions of –2865 to +89) were amplified by PCR and cloned into the pGL3-basic vector. A549 cells were seeded in 48 well plates and the next day the plasmids were transfected using Lipofectamine 3000 transfection reagent (Thermo Fisher Scientific).  $\beta$ -Gal was co-transfected to allow normalization. One day after transfection, TGF $\beta$ 1 (2 ng/ml) was added to the culture media. After 24 h, luciferase activity was measured according to the manufacturer's instructions using a luciferase reporter assay kit (Promega, Madison, WI, United States) with a luminometer (DE/Centro LB960, Berthold Technologies, Oak Ridge, TN, United States).

## Animal Experiments

Wildtype (WT) *EPRS*<sup>+/+</sup> ( $n = 4$  for vehicle and  $n = 9$  for bleomycin) and *EPRS*<sup>-/+</sup> hetero-knockout ( $n = 5$  for vehicle and  $n = 7$  for bleomycin) C57BL/6 mice were housed in a specific pathogen-free room with controlled temperature and humidity. Mouse protocol and animal experiments were approved by the Institutional Animal Care and Use Committee (IACUC) of Seoul National University (SNU-161201-1-3). For the lung fibrosis model, bleomycin (Santa Cruz Biotechnology) was dissolved in sterilized saline and intratracheal instillation was performed through surgically exposed trachea as a single dose of 1 mg/kg in 100  $\mu$ l solution per animal. Mice were sacrificed 4 weeks post-intratracheal instillation. Lung tissue samples were snap frozen in liquid nitrogen for western blot, qPCR, and hydroxyproline analysis, or fixed in 4% formaldehyde in PBS for histological analysis.

## Immunohistochemistry and Staining

Paraffin blocks and sections (6- $\mu$ m thickness) of lung tissues were prepared by Abion Inc. (Seoul, Korea) for immunohistochemistry analysis. Primary antibodies and their dilution ratios are listed in **Table 1**. Vectastain ABC-HRP kit (Vector Laboratories, Burlingame, CA, United States) were used to visualize the stained samples. Mayer's hematoxylin (Sigma-Aldrich) was used for counter-staining the nuclei.



**TABLE 2 |** qRT-PCR primers used in this study.

Gene name	Forward	Reverse	Size (bp)
Human EPRS	AGGAAAGACCAACACCTTCTC	CTCCTTGAACAGCCACTCTATT	87
Human collagen1A1	CAGACTGGCAACCTCAAGAA	CAGTGACGCTGTAGGTGAAG	97
Human DDIT3	GAGATGGCAGCTGAGTCATT	TTTCCAGGAGGTGAAACATAGG	134
Human collagen4A1	CGGGCCCTAAAGGAGATAAAG	GAACCTGGAACCCAGGAAT	115
Human fibronectin	CCACAGTGGAGTATGTGGTTAG	CAGTCCTTTAGGGCGATCAAT	104
Human laminin $\gamma$ 2	CTCAGGAGGCCACAAGATTAG	TGAGAGGGCTTGTTTGAATAG	101
Mouse collagen 1A1	AGACCTGTGTGTTCCCTACT	GAATCCATCGGTGATGCTCTC	113
Mouse fibronectin	TCTGTCTACCTCAGACTAC	GTCTACTCCACCGAACACAA	96
Mouse laminin $\gamma$ 2	TGGAGTTTGACACGGATAAGG	GAGTGTGTCTTGGATGGTAACT	104

## Statistics

Statistical analyses were performed using Prism software version 6.0 (GraphPad, La Jolla, CA, United States). Two-way analysis of variance (ANOVA) in group analysis or Student's *t*-tests were performed to determine statistical significance. A value of  $p < 0.05$  was considered significant.

## RESULTS

### EPRS Expression Regulated ECM Production in A549 Alveolar Type II Cells Upon TGF $\beta$ 1 Stimulation

We studied the regulatory effect of EPRS on the expression of different ECM proteins by introducing doxycycline-inducible EPRS knockdown vectors into the A549 alveolar type II cell line. Expression of ECM proteins such as collagen I, fibronectin, and laminin  $\gamma$ 2 were tested by immunoblotting EPRS-knockdown and control A549 cells. All the ECM proteins showed increased expression in control cells treated with TGF $\beta$ 1 and this effect was abolished in EPRS-knockdown cells (**Figure 1A**). Expression levels of mesenchymal proteins including  $\alpha$ -smooth muscle actin ( $\alpha$ -SMA) and snail 1 were also dependent on TGF $\beta$ 1 treatment and/or EPRS expression (**Figure 1A**). Since EPRS protein consists of two glutamyl-tRNA-synthetase (ERS) and prolyl-tRNA-synthetase (PRS), it would be reasonable to see whether PRS alone could achieve these effects. Overexpression of PRS enhanced TGF $\beta$ 1-induced ECM protein expression (**Figure 1B**). However, overexpression of ERS alone did not increase TGF $\beta$ 1-mediated ECM protein expression (**Figure 1C**), indicating that the PRS component of EPRS regulates ECM protein expression. TGF $\beta$ 1 treatment also increased mRNA levels of *COL1A1*, *COL4A1*, *FN1*, and *LAMC2* in control cells, while EPRS suppression inhibited this effect (**Figure 1D**). Our results suggest that EPRS positively regulated TGF $\beta$ 1-induced expression of ECM proteins. A previous report (Keller et al., 2012) stated that EPRS suppression increases mRNA levels of DNA damage-inducible transcript 3 (*DDIT3*, also known as *CHOP*) to indicate an activation of AAR pathway that supports for tRNA charging processes. However, we found that *DDIT3* mRNA levels were

unaffected by TGF $\beta$ 1 treatment, indicating that TGF $\beta$ 1-induced regulation of ECM protein expression involves alternative mechanism(s) in addition to the role in tRNA charging (**Figure 1D**).

### Regulation of TGF $\beta$ 1-Induced ECM Protein Synthesis by EPRS Occurred via STAT Activation

To investigate potential signaling molecules or pathways involved in EPRS-mediated regulation of ECM protein synthesis following TGF $\beta$ 1-treatment, we studied the dependency of STAT3 and STAT6, known mediators of IPF (Nikola et al., 2017; Milara et al., 2018), on EPRS expression. We found that TGF $\beta$ 1 promoted the phosphorylation of STAT3 at Tyr705 (pY<sup>705</sup>STAT3) and STAT6 at Tyr641 (pY<sup>641</sup>STAT6), and these effects were abolished by EPRS suppression (**Figure 2A**). EPRS overexpression increased pY<sup>705</sup>STAT3 and pY<sup>641</sup>STAT6 levels upon TGF $\beta$ 1 treatment in A549 cells (**Figure 2B**). Our results suggest that EPRS and TGF $\beta$ 1 signaling regulate STAT3 and STAT6 phosphorylation. We studied the role of EPRS in STAT-mediated expression of ECM proteins. Overexpression of STAT6 indicate greater increases in basal and TGF $\beta$ 1-induced levels of  $\alpha$ -SMA, snail 1, fibronectin, and collagen I in EPRS-positive A549 cells compared with EPRS-knockdown cells (**Figure 2C**). However, basal and TGF $\beta$ 1-induced expression levels of fibronectin and collagen I were decreased when STAT6 levels were suppressed (**Figure 2D**). A similar EPRS-dependent regulation pattern of fibronectin and collagen I was observed when STAT3 was modulated (**Figures 2E,F**). We also tested the transcriptional activities of *COL1A1* and *LAMC2* promoters in A549 cells lacking STAT3 or STAT6. *COL1A1* or *LAMC2* promoters containing STAT-responsive consensus sequences showed increased transcriptional activity in A549 cells treated with TGF $\beta$ 1. However, EPRS suppression reduced these effects (**Figure 2G**). Suppression of STAT3 or STAT6 abolished the increased transcriptional activity of *COL1A1* or *LAMC2* in EPRS-positive A549 cells but not EPRS-suppressed cells (**Figure 2G**). Together, our results suggested that EPRS regulates ECM protein expression via STAT3 or STAT6 signaling induced by TGF $\beta$ 1.

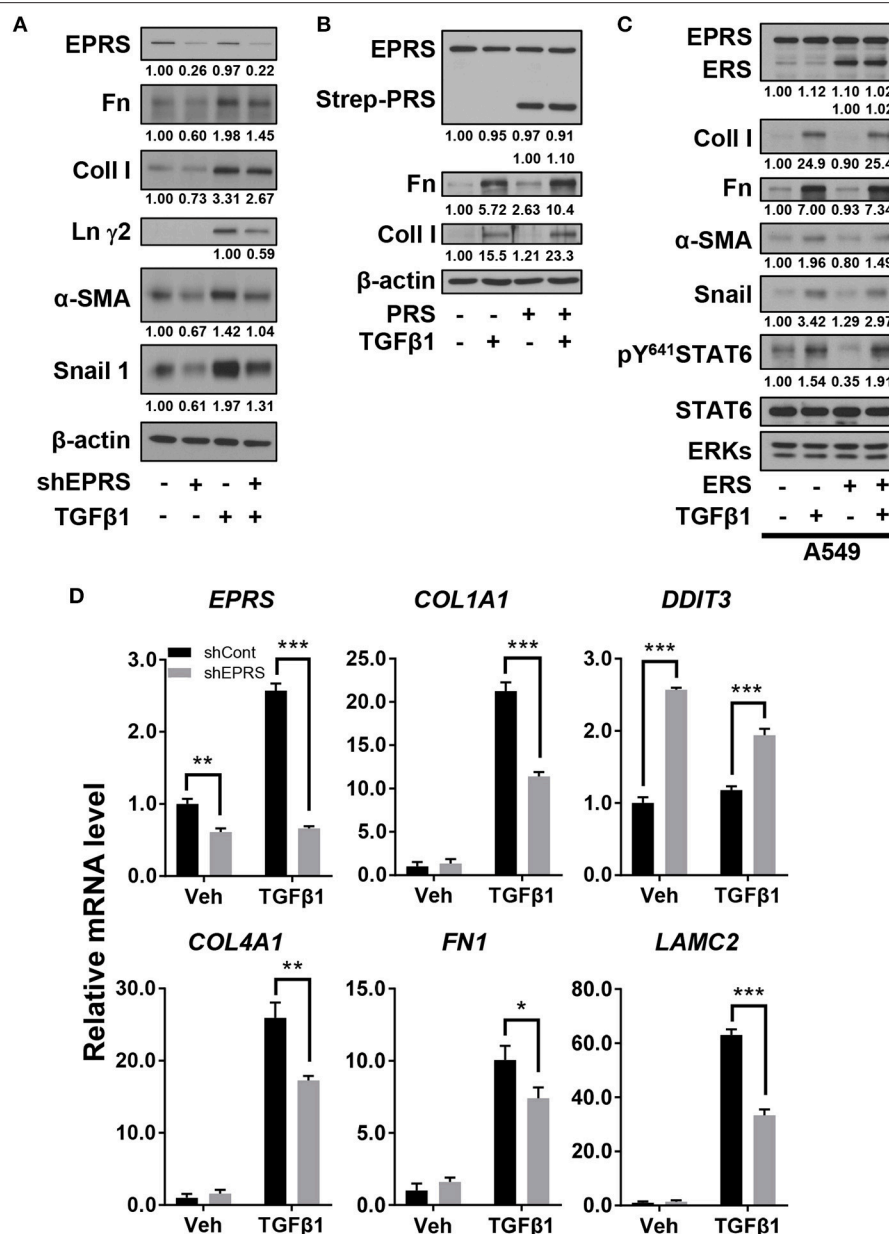


**FIGURE 1 |** EPRS expression regulated ECM protein production in A549 alveolar type II cells treated with TGF $\beta$ 1. **(A,B)** A549-control (-) or shEPRS doxycycline-inducible knockdown (+) A549 cell line or control A549 cells transiently transfected with PRS expression vector (pEXPR-103-Strep-PRS) were treated without or with TGF $\beta$ 1 (2 ng/ml) for 24 h, and harvested for immunoblottings for the indicated molecules. **(C)** A549 cells were transfected without or with ERS expression plasmid for 24 h and then treated without or with TGF $\beta$ 1 (2 ng/ml) for 24 h before lysate preparation and immunoblotting. **(D)** Subconfluent control (shCont) or shEPRS-A549 cells were treated with TGF $\beta$ 1 (2 ng/ml) for 24 h, before qRT-PCR analysis. Data are presented at mean  $\pm$  standard deviation (SD). \*, \*\*, and \*\*\* indicate significance at  $p < 0.05$ , 0.01, and 0.001, respectively (calculated by Student's  $t$ -tests). Data shown represent three independent experiments.

## TGF $\beta$ 1-Mediated SMAD3 Phosphorylation Upregulated Phosphorylation of STAT6 Depending on EPRS Expression

We investigated the role of the TGF $\beta$ 1-mediated SMAD signaling in EPRS-dependent ECM protein expression and STAT3/6 activity. TGF $\beta$ 1-mediated SMAD2 and SMAD3 phosphorylation was partially inhibited by EPRS

suppression (Figure 3A). However, EPRS overexpression did not affect the levels of phosphorylated SMAD2 or SMAD3, which might have already been saturated by TGF $\beta$ 1 treatment (Figure 3B). TGF $\beta$ 1-induced levels of pY<sup>641</sup>STAT6 were increased by overexpression of SMAD3 but not SMAD2. EPRS suppression abolished that effect (Figures 3C,D).

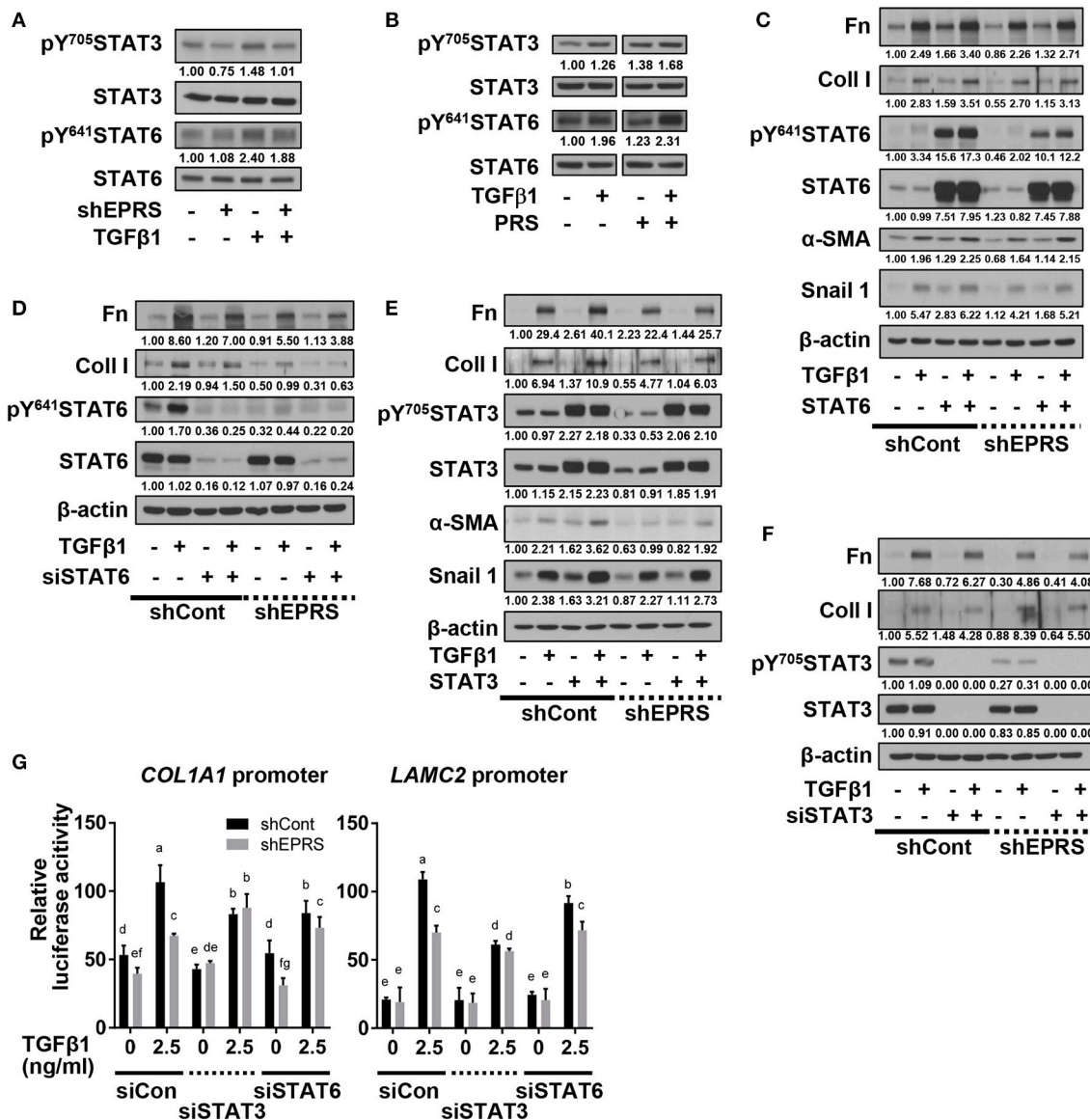
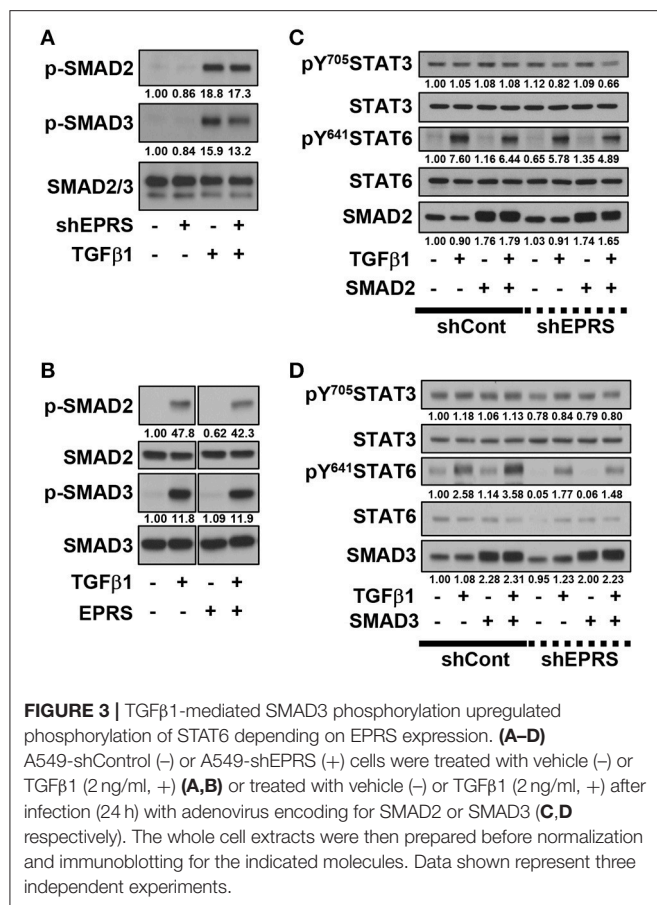


**FIGURE 2 |** Regulation of TGFβ1-induced ECM protein synthesis by EPRS occurred via STAT activation. **(A–G)** A549 cells stably infected with control (–) or shEPRS virus (A549-shEPRS) or control A549 cells transiently transfected with different expression vectors or siRNAs as indicated were treated without (–) or with TGFβ1 (2 ng/ml, +) for 24 h, before whole cell extracts preparation and immunoblotting for the indicated molecules. **(G)** A549 cells transfected with *COL1A1* or *LAMC2* promoter-luciferase constructs with STATs-consensus responsive sequences (*Col1a1*-2.9 and *Lamc2*-2.3 kb constructs with upstream promoter regions up to –2.9 and –2.3 kb, respectively) together with either siRNA against control sequence (siCon), STAT3 (siSTAT3), or STAT6 (siSTAT6) were treated with TGFβ1 (0 or 2.5 ng/ml) for 24 h, prior to luciferase reporter analysis. Data are presented as mean ± SD. Different letters indicate statistical significance at  $p < 0.05$  according to one-way ANOVA. Data shown are from three isolated experiments.

## EPRS-Mediated Signaling in TGFβ1-Treated Cells Involved the Formation of a Multi-Protein Complex Consisting of STAT6 and TGFβ1R

We then tested for potential protein-protein interactions between TGFβ1 signaling and EPRS that regulate STAT6 phosphorylation. A549 cells containing Streptavidin-tagged EPRS (Strep-EPRS) were treated with or without TGFβ1, prior to precipitation

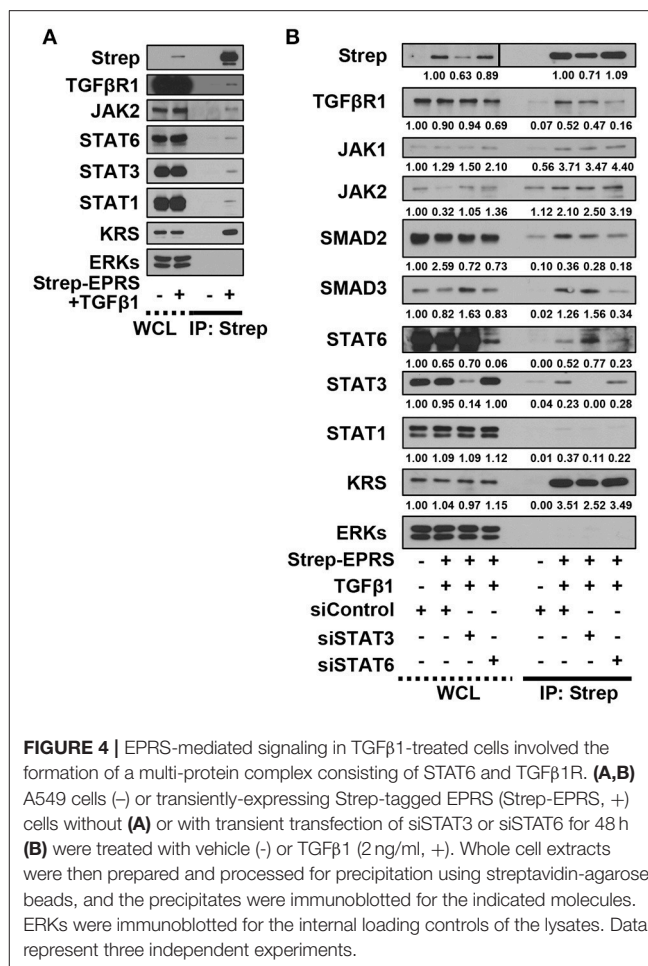
of whole-cell extracts using streptavidin agarose beads for immunoblotting assays. Lysyl-tRNA synthetase (KRS), which forms a multi-aminoacyl-tRNA synthetase complex (MSC) with EPRS (Park et al., 2008), was used as a positive control. In TGFβ1-treated cells, Strep-EPRS transiently precipitated with TGFβ1R1, JAKs, and STATs, which included STAT6 (**Figure 4A**). We tested the effect of STAT3 or STAT6 suppression on multi-protein interactions. STAT6 expression was required for the EPRS-mediated multi-protein complex formation (**Figure 4B**).



Specifically, EPRS interaction with TGFβ1R and SMAD2/3 required STAT6 but not STAT3. Interestingly, STAT3 suppression resulted in increased binding of STAT6 to the EPRS/TGFβ1R-containing protein complex (**Figure 4B**). Interactions between EPRS and JAKs were independent of STAT3 and STAT6 (**Figure 4B**). Our results suggest that STAT6 is critical for the formation of the multi-protein complex for TGFβ1-induced signaling of ECM protein expression. STAT3 and STAT6 may be involved in parallel signaling pathways to regulate this process.

### Lung Tissues From Bleomycin-Treated Mice Showed EPRS-Dependent STAT6 Phosphorylation and ECM Protein Production *in vivo*

To investigate the physiological roles of EPRS in pulmonary fibrosis *in vivo*, WT (*Eprs*<sup>+/+</sup>) and *Eprs*<sup>-/-</sup> hetero-knockout (KO) mice were treated with bleomycin to induce lung fibrosis by intratracheal instillation before analysis, since homozygous *Eprs*<sup>-/-</sup> is embryonic lethal. Bleomycin-treated WT *Eprs*<sup>+/+</sup> mice showed the highest increase in expression of ECM proteins, such as fibronectin, collagen I, and laminins, compared with bleomycin-treated *Eprs*<sup>-/-</sup> hetero-KO mice and untreated WT mice (**Figure 5A**). Levels of pY<sup>705</sup>STAT3 and pY<sup>641</sup>STAT6 were also elevated in bleomycin-treated *Eprs*<sup>+/+</sup> mice, compared with



*Eprs*<sup>-/+</sup> hetero-KO mice (**Figure 5A**). Our results suggest that STAT6 activation is part of EPRS-dependent signaling for ECM protein expression *in vivo*. We observed a slight upregulation in EPRS expression in bleomycin-treated WT *Eprs*<sup>+/+</sup> mice, compared with other groups, indicating that EPRS might function as a pro-fibrotic molecule.

Hydroxyproline assays to measure collagen I levels in lung extracts showed that bleomycin-treated *Eprs*<sup>+/+</sup> mice had higher levels compared with bleomycin-treated *Eprs*<sup>-/+</sup> mice (**Figure 5B**). In addition to *IL8*, which is used to characterize IPF (Carre et al., 1991), *Col1a1*, *Fn1*, and *Lamc2* mRNA levels were also upregulated by bleomycin treatment in *Eprs*<sup>+/+</sup> lungs but not *Eprs*<sup>-/+</sup> hetero-KO lungs (**Figure 5C**).

Lung immunohistochemistry revealed more patchy fibrosis and fibroblastic foci in bleomycin-treated *Eprs*<sup>+/+</sup> mice compared with *Eprs*<sup>-/+</sup> mice (**Figure 5D**). Bleomycin treatment also led to marked increases in collagen I, fibronectin, and laminin γ2 synthesis in *Eprs*<sup>+/+</sup> mice compared with *Eprs*<sup>-/+</sup> mice. Levels of phospho-SMAD2, pY<sup>705</sup>STAT3, and pY<sup>641</sup>STAT6, which showed intense nuclear staining, were diminished in *Eprs*<sup>-/+</sup> mice (**Figure 5D**). The myofibroblasts marker α-SMA was positive in fibroblastic foci of bleomycin-treated mice lungs.



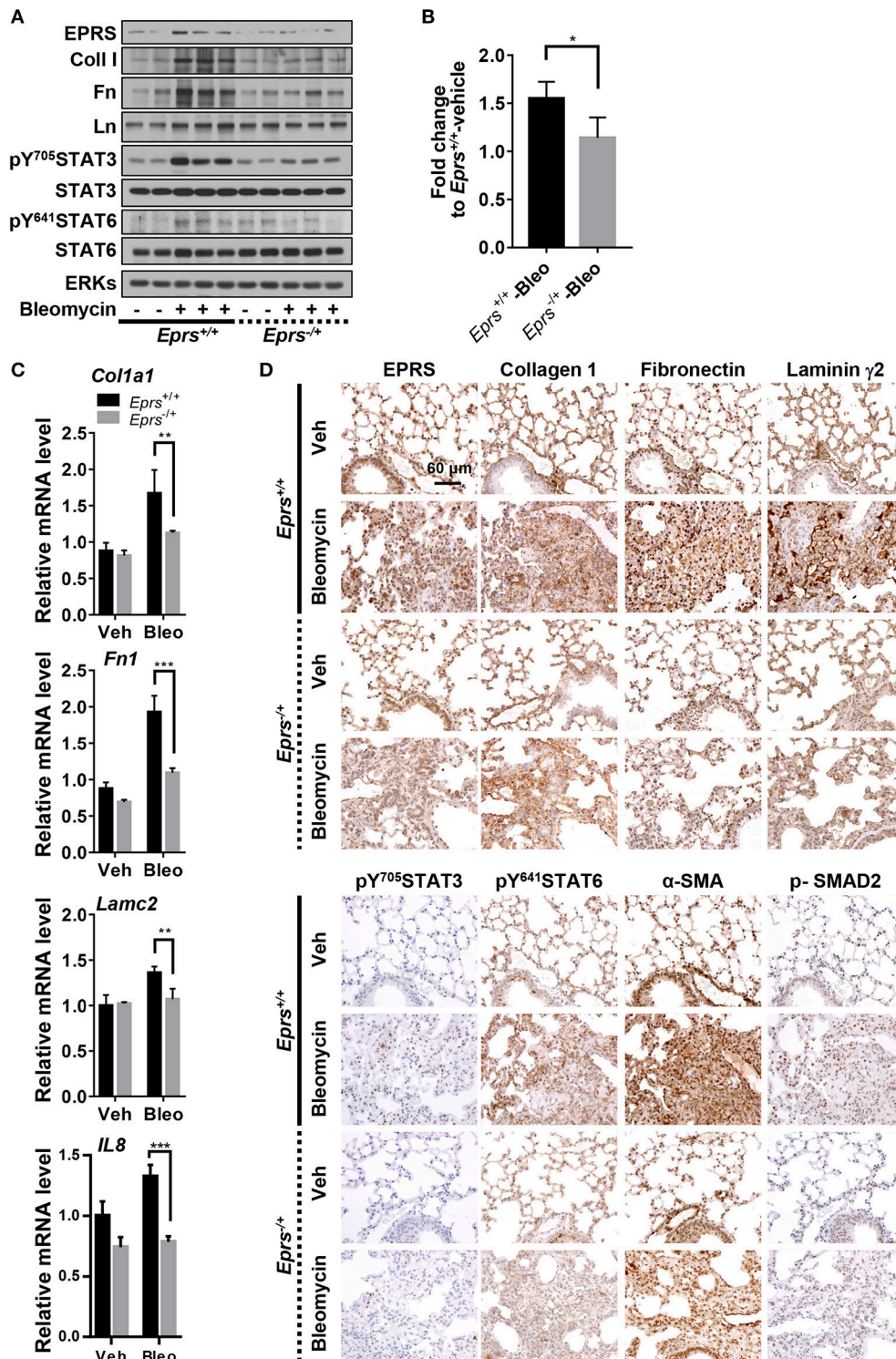


**FIGURE 5 |** Lung tissues from bleomycin-treated mice showed EPRS-dependent STAT6 phosphorylation and ECM protein production *in vivo*. **(A–D)** Wildtype (WT, *Eprs*<sup>+/+</sup>) and *Eprs*<sup>+/-</sup> hetero-knockout (KO) C57BL/6 mice were intratracheally treated once with vehicle ( $n = 4$  for WT and  $n = 5$  for *Eprs*<sup>+/-</sup> hetero-KO) or bleomycin (1 mg/kg in PBS,  $n = 9$  for WT and  $n = 7$  for *Eprs*<sup>+/-</sup> hetero-KO). After 28 days, mice were sacrificed, and lung tissues were collected for analyses. Lung tissue extracts were prepared and processed for immunoblots for the indicated molecules **(A)**, hydroxyproline assays **(B)**, and qRT-PCR for the indicated mRNAs **(C)**. Data are presented at mean  $\pm$  SD. \*, \*\*, and \*\*\* indicate significance at  $p < 0.05$ , 0.01, and 0.001, respectively (calculated by Student's *t*-tests). **(D)** The lung tissues were processed for immunohistochemistry, before image capturing at 40 x. Data represent three different experiments.

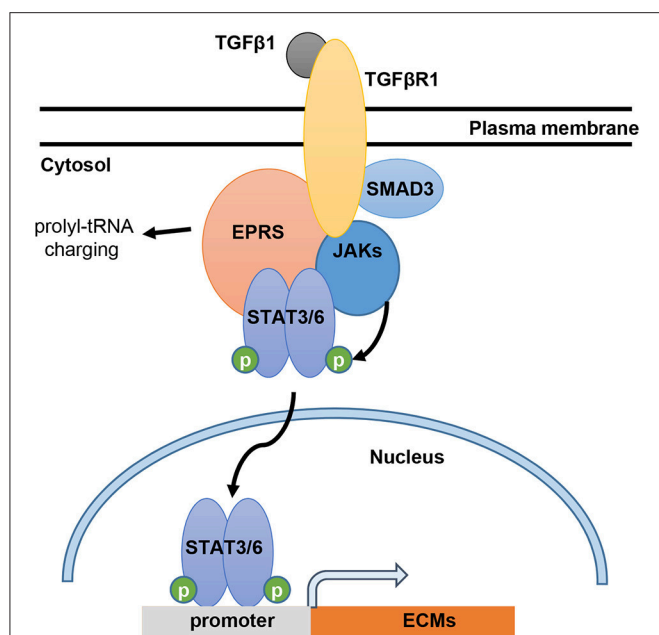


**FIGURE 6 |** Working model for EPRS-dependent signaling during TGFβ1-mediated expression of ECMs. TGFβ1 binding to TGFβR1 can stimulate formation of a signaling complex consisting of TGFβR1, SMAD3, JAKs, STAT3/6 and EPRS for active JAKs-mediated STAT3/6 phosphorylation. Phosphorylated STAT3/6 can enter the nucleus for transcriptional induction of ECM genes, such as collagen α1 (*COLA1*), laminin γ2 (*LAMC2*), and fibronectin 1 (*FN1*).

These results suggest that the bleomycin-mediated fibrotic phenotypes in animal lungs are dependent on EPRS expression.

## DISCUSSION

In this study, we showed that EPRS regulates the TGFβ1-mediated expression of ECM proteins such as collagen I and fibronectin. Our *in vitro* and *in vivo* analyses demonstrated that the signal for ECM protein synthesis might be transduced via a multi-protein signaling complex composed of TGFβR1, SMAD3, JAKs, and STAT6. EPRS may have functions independent of translational tRNA charging that serve as a signaling molecule for TGFβ1-induced ECM protein synthesis and mesenchymal marker expression, presumably leading to fibrotic phenotypes (Figure 6). Therefore, EPRS is a promising target for anti-IPF therapy.

The binding target of the anti-fibrotic agent, HF, first revealed the link between EPRS and fibrosis (Keller et al., 2012). HF competitively inhibits PRS, which activates the AAR pathway because of naked-tRNA accumulation. HF-mediated inhibition of PRS also cause decreased ECM expression, which is overcome by exogenous proline treatment, indicating that PRS can be involved in ECM translation via tRNA charging with proline (Keller et al., 2012). However, it cannot be ruled out that PRS play roles in ECM expression at non-translational processes, since variable ECMs can be composed

with different levels of proline. Additionally, this previous study had not shown EPRS regulation of TGFβ1-induced ECM protein synthesis. Moreover, although a previous study showed a fibrotic role of EPRS in a lung fibroblast IMR90 cell line, here we found that alveolar type II epithelial cells may lead to the formation of fibrotic foci in IPF under the influence of TGFβ1. TGFβ1 is a master regulator of fibrosis that induces epithelial to mesenchymal transition (EMT) and analyzing its role in EPRS-mediated ECM regulation is critical for developing IPF treatments.

Idiopathic pulmonary fibrosis (IPF) (Lederer and Martinez, 2018) is currently managed with nintedanib and pirfenidone. These drugs slow down the rate of forced vital capacity decline by ~50% over 1-year period (Lederer and Martinez, 2018) but do not completely cure the disease. The anti-fibrotic reagent, HF, causes significant side effects including severe gastrointestinal lesions and hemorrhage (Jiang et al., 2005). Novel and safe treatment methods for IPF are therefore needed. Recent studies have begun uncovering the mechanisms of IPF pathogenesis. STAT6-mediated signaling is important for the development of carbon nanotube-induced fibrotic lung disease (Nikola et al., 2017). The JAK2/STAT3 pathway is activated in IPF, and treatment with JSI-124 (a dual inhibitor of JAK2/STAT3) decreases collagen deposition during lung fibrosis (Milara et al., 2018). In the present study, we used *in vitro* and *in vivo* models to reveal a novel relationship between EPRS and STAT6 and their participation in IPF.

In studying TGFβ1-induced activation of the STAT signaling cascade for ECM protein synthesis, we found that EPRS was an upstream regulator of STAT3/6 activation. TGFβ1-induced SMAD3 activation was important for activating STAT6, which was critical for formation of the multi-protein complex of TGFβR1, EPRS, JAKs, and STAT3/6. Both STAT3 and STAT6 appear to act downstream of TGFβ1 stimulation, possibly in parallel signaling pathways. However, STAT3 suppression led to higher levels of STAT6 in the multi-protein complex, indicating that STAT6 was more important than STAT3 for TGFβ1-induced, EPRS-mediated ECM protein synthesis. Previous studies have shown that EPRS forms complexes with other proteins. EPRS translocates to the cell surface to bind to TGFβR1. Phosphorylation of EPRS at Ser999 causes it to dissociate from the MSC and translocate to the membrane where it interacts with the fatty-acid transporter, FATP1, upon insulin stimulation of adipocytes (Arif et al., 2017). TGFβ1 treatment induces TGFβR1-JAK1 and STAT3-SMAD3 to form a protein complex (Tang et al., 2017). These studies validate our results regarding the EPRS-containing multi-protein complex. We also found that suppression of STAT6 but not of STAT3 abolished the formation of a complex between EPRS, TGFβR1, and SMAD2/3. Our findings suggest that EPRS is a novel component of the TGFβR1-JAKs-STATs multi-protein signaling complex that mediates ECM synthesis.

Our *in vivo* animal studies showed that EPRS protein levels were slightly upregulated in bleomycin-treated WT *Eprs*<sup>+/+</sup> mice

compared with *Eprs*<sup>-/+</sup> KO mice. However, EPRS mRNA levels were upregulated 2.5-fold in TGFβ1-treated A549 cells compared with control cells, although EPRS protein levels were unchanged (Figure 1C). These differences in EPRS mRNA and protein levels might be the result of variable treatment times between the *in vitro* and *in vivo* experiments (1 vs. 28 days). Because IPF is a chronic disease, EPRS might be upregulated during the development of fibrosis, as seen in our *in vivo* experimental model.

In conclusion, our study showed that EPRS might be a signaling molecule underlying TGFβ1-induced ECM protein synthesis and is a promising potential target for the treatment of IPF.

## AUTHOR CONTRIBUTIONS

D-GS performed most experiments and wrote the 1st version of manuscript. DK: helped with animal study, JHK and SK helped with experimental reagents. JWJ, SHN, JEK, and H-JK helped with imaging experiments or with reagents. C-HP, SK, and JWL discussed the data and JWL wrote the manuscript.

## REFERENCES

- Arif, A., Terenzi, F., Potdar, A. A., Jia, J., Sacks, J., China, A., et al. (2017). EPRS is a critical mTORC1-S6K1 effector that influences adiposity in mice. *Nature* 542, 357–361. doi: 10.1038/nature21380
- Bagnato, G., and Harari, S. (2015). Cellular interactions in the pathogenesis of interstitial lung diseases. *Eur. Respir. Rev.* 24, 102–114. doi: 10.1183/09059180.00003214
- Bai, Y., Li, J., Zhao, P., Li, Y., Li, M., Feng, S., et al. (2018). A Chinese herbal formula Ameliorates pulmonary fibrosis by inhibiting oxidative stress via upregulating Nrf2. *Front. Pharmacol.* 9:628. doi: 10.3389/fphar.2018.00628
- Carre, P. C., Mortenson, R. L., King, T. E. Jr., Noble, P. W., Sable, C. L., and Riches, D. W. (1991). Increased expression of the interleukin-8 gene by alveolar macrophages in idiopathic pulmonary fibrosis. A potential mechanism for the recruitment and activation of neutrophils in lung fibrosis. *J. Clin. Invest.* 88, 1802–1810. doi: 10.1172/JCI115501
- Choi, S., Lee, S.-A., Kwak, T. K., Kim, H. J., Lee, M. J., Ye, S.-K., et al. (2009). Cooperation between integrin α5 and tetraspan TM4SF5 regulates VEGF-mediated angiogenic activity. *Blood* 113, 1845–1855. doi: 10.1182/blood-2008-05-160671
- Ghosh, A. K., Quaggin, S. E., and Vaughan, D. E. (2013). Molecular basis of organ fibrosis: potential therapeutic approaches. *Exp. Biol. Med.* 238, 461–481. doi: 10.1177/1535370213489441
- Jiang, S., Zeng, Q., Gettayacamin, M., Tungtaeng, A., Wannaying, S., Lim, A., et al. (2005). Antimalarial activities and therapeutic properties of febrifugine analogs. *Antimicrob. Agents Chemother.* 49, 1169–1176. doi: 10.1128/AAC.49.3.1169-1176.2005
- Keller, T. L., Zocco, D., Sundrud, M. S., Hendrick, M., Edenius, M., Yum, J., et al. (2012). Halofuginone and other febrifugine derivatives inhibit prolyl-tRNA synthetase. *Nat. Chem. Biol.* 8, 311–317. doi: 10.1038/nchembio.790
- Lederer, D. J., and Martinez, F. J. (2018). Idiopathic pulmonary fibrosis. *N. Engl. J. Med.* 378, 1811–1823. doi: 10.1056/NEJMra1705751
- Lee, M.-S., Kim, T. Y., Kim, Y.-B., Lee, S.-Y., Ko, S.-G., Jong, H.-S., et al. (2005). The signaling network of transforming growth factor β1, protein kinase Cδ, and integrin underlies the spreading and invasiveness of gastric carcinoma cells. *Mol. Cell. Biol.* 25, 6921–6936. doi: 10.1128/MCB.25.16.6921-6936.2005

## FUNDING

This work was supported by the Korea Institute of Science and Technology Gangneung Institute intramural research grant (2Z05310) to C-HP and D-GS and Basic Science Research Program through the National Research Foundation of Korea (NRF) funded by the Ministry of Science, ICT & Future Planning (NRF-2018M3A9C8020027 and NRF-2017R1A2B3005015), the Tumor Microenvironment GCRC (2011-0030001), and the Medicinal Bioconvergence Research Center (NRF-2013M3A6A4044019) to JWL.

## ACKNOWLEDGMENTS

We appreciate kind gifts from Dr. Myung Hee Kim (KRIBB) for EPRS constructs.

## SUPPLEMENTARY MATERIAL

The Supplementary Material for this article can be found online at: <https://www.frontiersin.org/articles/10.3389/fphar.2018.01337/full#supplementary-material>

- Luzina, I. G., Todd, N. W., Sundararajan, S., and Atamas, S. P. (2015). The cytokines of pulmonary fibrosis: much learned, much more to learn. *Cytokine* 74, 88–100. doi: 10.1016/j.cyt.2014.11.008
- Milara, J., Hernandez, G., Ballester, B., Morell, A., Roger, I., Montero, P., et al. (2018). The JAK2 pathway is activated in idiopathic pulmonary fibrosis. *Respir. Res.* 19:24. doi: 10.1186/s12931-018-0728-9
- Nikola, J., Banville, A., Goodwin, L. R., Wu, D., Williams, A., Yauk, C. L., et al. (2017). Stat-6 signaling pathway and not Interleukin-1 mediates multi-walled carbon nanotube-induced lung fibrosis in mice: insights from an adverse outcome pathway framework. *Part. Fibre Toxicol.* 14:37. doi: 10.1186/s12989-017-0218-0
- Papaioannou, I., Xu, S., Denton, C. P., Abraham, D. J., and Ponticos, M. (2018). STAT3 controls COL1A2 enhancer activation cooperatively with JunB, regulates type I collagen synthesis post-transcriptionally, and is essential for lung myofibroblast differentiation. *Mol. Biol. Cell* 29, 84–95. doi: 10.1091/mbc.E17-06-0342
- Park, S. G., Schimmel, P., and Kim, S. (2008). Aminoacyl tRNA synthetases and their connections to disease. *Proc. Natl. Acad. Sci. U.S.A.* 105, 11043–11049. doi: 10.1073/pnas.0802862105
- Pechkovsky, D. V., Prele, C. M., Wong, J., Hogaboam, C. M., Mcanulty, R. J., Laurent, G. J., et al. (2012). STAT3-mediated signaling dysregulates lung fibroblast-myofibroblast activation and differentiation in UIP/IPF. *Am. J. Pathol.* 180, 1398–1412. doi: 10.1016/j.ajpath.2011.12.022
- Pedroza, M., Le, T. T., Lewis, K., Karmouty-Quintana, H., To, S., George, A. T., et al. (2016). STAT-3 contributes to pulmonary fibrosis through epithelial injury and fibroblast-myofibroblast differentiation. *FASEB J.* 30, 129–140. doi: 10.1096/fj.15-273953
- Prele, C. M., Yao, E., O'donoghue, R. J., Mutsaers, S. E., and Knight, D. A. (2012). STAT3: a central mediator of pulmonary fibrosis? *Proc. Am. Thorac. Soc.* 9, 177–182. doi: 10.1513/pats.201201-007AW
- Raghu, G., Rochwerf, B., Zhang, Y., Garcia, C. A., Azuma, A., Behr, J., et al. (2015). An official ATS/ERS/JRS/ALAT clinical practice guideline: treatment of idiopathic pulmonary fibrosis. an update of the 2011 clinical practice guideline. *Am. J. Respir. Crit. Care Med.* 192:e3–19. doi: 10.1164/rccm.201506-1063ST
- Ray, P. S., and Fox, P. L. (2014). Origin and evolution of glutamyl-prolyl tRNA synthetase WHEP domains reveal evolutionary relationships within Holozoa. *PLoS ONE* 9:e98493. doi: 10.1371/journal.pone.0098493

- Tang, L. Y., Heller, M., Meng, Z., Yu, L. R., Tang, Y., Zhou, M., et al. (2017). Transforming Growth Factor- $\beta$  (TGF- $\beta$ ) directly activates the JAK1-STAT3 axis to induce hepatic fibrosis in coordination with the SMAD pathway. *J. Biol. Chem.* 292, 4302–4312. doi: 10.1074/jbc.M116.773085
- Wolters, P. J., Collard, H. R., and Jones, K. D. (2014). Pathogenesis of idiopathic pulmonary fibrosis. *Annu. Rev. Pathol.* 9, 157–179. doi: 10.1146/annurev-pathol-012513-104706
- Zhou, X. M., Wang, G. L., Wang, X. B., Liu, L., Zhang, Q., Yin, Y., et al. (2017). GHK Peptide Inhibits Bleomycin-Induced Pulmonary Fibrosis in Mice by Suppressing TGF $\beta$ 1/Smad-Mediated Epithelial-to-Mesenchymal Transition. *Front. Pharmacol.* 8:904. doi: 10.3389/fphar.2017.00904

**Conflict of Interest Statement:** The authors declare that the research was conducted in the absence of any commercial or financial relationships that could be construed as a potential conflict of interest.

The handling editor declared a shared department with several of the authors (D-GS, DK, JWJ, SHN, JEK, H-JK, JHK, SK and JWL) at time of review.

Copyright © 2018 Song, Kim, Jung, Nam, Kim, Kim, Kim, Pan, Kim and Lee. This is an open-access article distributed under the terms of the Creative Commons Attribution License (CC BY). The use, distribution or reproduction in other forums is permitted, provided the original author(s) and the copyright owner(s) are credited and that the original publication in this journal is cited, in accordance with accepted academic practice. No use, distribution or reproduction is permitted which does not comply with these terms.





# Dual Tumor Suppressor and Tumor Promoter Action of Sirtuins in Determining Malignant Phenotype

Vincenzo Carafa, Lucia Altucci and Angela Nebbioso\*

Dipartimento di Medicina di Precisione, Università degli Studi della Campania Luigi Vanvitelli, Naples, Italy

## OPEN ACCESS

### Edited by:

Sergio Valente,  
Sapienza Università di Roma, Italy

### Reviewed by:

Satish Ramalingam,  
SRM Institute of Science  
and Technology, India  
Elisabetta Ferretti,  
Sapienza Università di Roma, Italy

### \*Correspondence:

Angela Nebbioso  
angela.nebbioso@unicampania.it

### Specialty section:

This article was submitted to  
Inflammation Pharmacology,  
a section of the journal  
Frontiers in Pharmacology

**Received:** 30 July 2018

**Accepted:** 14 January 2019

**Published:** 30 January 2019

### Citation:

Carafa V, Altucci L and  
Nebbioso A (2019) Dual Tumor  
Suppressor and Tumor Promoter  
Action of Sirtuins in Determining  
Malignant Phenotype.  
Front. Pharmacol. 10:38.  
doi: 10.3389/fphar.2019.00038

Sirtuins (SIRT), class III histone deacetylases, are differentially expressed in several human cancers, where they display both oncogenic and tumor-suppressive properties depending on cellular context and experimental conditions. SIRT are involved in many important biological processes and play a critical role in cancer initiation, promotion, and progression. A growing body of evidence indicates the involvement of SIRT in regulating three important tumor processes: epithelial-to-mesenchymal transition (EMT), invasion, and metastasis. Many SIRT are responsible for cellular metabolic reprogramming and drug resistance by inactivating cell death pathways and promoting uncontrolled proliferation. In this review, we summarize current knowledge on the role of SIRT in cancer and discuss their puzzling dual function as tumor suppressors and tumor promoters, important for the future development of novel tailored SIRT-based cancer therapies.

**Keywords:** Sirtuins, epigenetics, cancer, EMT, cancer therapy

## INTRODUCTION

Cancer is a leading cause of death worldwide, accounting for 8.8 million deaths in 2015, as recently reported by the World Health Organization. It is becoming increasingly evident that epigenetic alterations due to defects in chromatin modifiers and remodelers contribute to carcinogenesis (Nebbioso et al., 2018). The biological capabilities acquired by cells during malignant transformation were identified and denoted as the six “hallmarks of cancer”: sustaining proliferative signaling, evading growth suppressors, resisting cell death, enabling replicative immortality, inducing angiogenesis, and activating invasion and metastasis (Hanahan and Weinberg, 2000, 2011). In cell invasion and metastasis, alterations in cell-cell adhesions and cell shape are early processes responsible for the acquisition of invasive capabilities by a malignant cell. Epithelial-to-mesenchymal transition (EMT) is a dynamic and reversible transdifferentiation process that transforms an epithelial cell into a mesenchymal cell, endowing it with the ability to invade, escape apoptosis, and disseminate (Lamouille et al., 2014).

Epithelial-to-mesenchymal transition is classified into three different types: (i) type 1, which generates mesenchymal cells that undergo further differentiation into epithelial cells, and has a role in embryogenesis and organogenesis; (ii) type 2, which is involved in tissue repair after trauma and injury, and normally generates fibroblasts; (iii) type 3, which occurs in cancer progression and metastasis. EMT is activated by a number of transcriptional factors (TFs) and epigenetic regulators, including Sirtuins (SIRT), members of the class III histone deacetylase family.

Several studies describe a correlation between cellular glucose metabolism and tumorigenesis, as in order to sustain energetic demands due to increased cell proliferation, cancer cells need to readjust their cellular metabolism (Sebastian and Mostoslavsky, 2015). Reprogramming of energy metabolism was recently introduced into the list of cancer hallmarks, increasing the complexity of the disease (Hanahan and Weinberg, 2011). Adjustments of energy metabolism sustain the rapid and uncontrolled growth and proliferation of cancer cells. While normal cells commonly switch from aerobic to anaerobic status by changing their glucose metabolism, cancer cells display elevated glycolysis and glutaminolysis, with an increase in and accumulation of glycolytic intermediates, as fuel for macromolecular synthesis leading to growth in tumor mass (Jeong and Haigis, 2015). Despite efforts to gain a greater insight into how this reprogramming can affect cancer development, its function remains unclear and controversial (Liberti and Locasale, 2016). Emerging evidence highlights a crucial role for SIRT6 in this process (Bosch-Presegue and Vaquero, 2011; Chalkiadaki and Guarente, 2015; O'Callaghan and Vassilopoulos, 2017). Growing awareness of the pivotal role of epigenetic alterations in initiation, promotion, and progression of human cancers has led to a better understanding of the role of these epi-enzymes in driving human disease. Here, we summarize recent advances in our knowledge of the role of SIRT6 in carcinogenesis. We also discuss their dual role as tumor promoters and tumor suppressors in cancer, including their involvement in EMT and energy metabolism programs.

## SIRTUIN FAMILY

Mammalian SIRT6s include seven proteins (SIRT1-7) with deacetylase activity belonging to the class III histone deacetylase family. SIRT6s share homology with the yeast deacetylase Sir2, and have different sequences and lengths in both their N- and C-terminal domains (Carafa et al., 2012). Expressed from bacteria to humans (Vaquero, 2009), SIRT6s target histone and non-histone proteins. Although their best-characterized enzymatic activity is NAD<sup>+</sup>-dependent lysine deacetylation, SIRT6s also catalyze other reactions, below discussed (Table 1).

Localization of SIRT6s is restricted to three different subcellular compartments: cytoplasm, nucleus, and mitochondria. SIRT1, SIRT6, and SIRT7 are principally localized in the nucleus, SIRT2 in the cytosol, and SIRT3, SIRT4, and SIRT5 in the mitochondria. Different studies report the ability of some SIRT6s to re-localize under different conditions (e.g., cell cycle phase, tissue type, developmental stage, stress condition, and metabolic status), suggesting the important role of their localization in regulating specific pathways (McGuinness et al., 2011). Specifically, SIRT1, SIRT2, and SIRT7 are often found in both the nucleus and cytoplasm (Michishita et al., 2005).

Sirtuins modulate different pivotal cellular pathways such as DNA repair, transcriptional regulation, metabolism, aging, and senescence. As these biological processes are involved in cancer initiation and progression, interest in SIRT6s as targets in cancer research has increased. Interestingly, in terms of

energy metabolic reprogramming, emerging evidence shows the complex association of two metabolism-associated TFs, MYC and hypoxia inducible factor-1 (HIF-1), with some SIRT6s (Zwaans and Lombard, 2014; Figure 1).

It is well documented that SIRT6s act as tumor suppressors or tumor promoters (oncogenes) by modulating cell proliferation, differentiation, and death. Their different biological function in cancer depends on cell context and experimental conditions. Although the dual role of SIRT6s is crucial in cancer biology, it remains a highly debated and controversial topic. Whether SIRT6s act as tumor suppressors or promoters depends on (i) their different expression levels in tumors; (ii) their effect on cell cycle, cell growth, and cell death; (iii) their action on specific proto-oncogene and oncosuppressor proteins (Deng, 2009).

## SIRTUIN REACTIONS

The most known and well-studied enzymatic reaction catalyzed by SIRT6s is NAD<sup>+</sup>-dependent deacetylation, but others have been reported (Table 1). Deacetylation reaction begins with amide cleavage from NAD<sup>+</sup> with the formation of nicotinamide and an intermediate of reaction, O-ADP-ribose. This intermediate is necessary for the deacetylation process by which SIRT6s catalyze the transfer of one acetyl group from a lysine to O-ADP-ribose moiety to form O-acetyl-ADP-ribose and the deacetylated lysine product. This reaction consumes a mole equivalent of NAD<sup>+</sup> per acetyl group removed and is controlled by the cellular [NAD]/[NADH] ratio (Sauve, 2010; Shi et al., 2013).

Although SIRT6 enzymes are known primarily as protein deacetylases, among the seven mammalian SIRT6s only SIRT1, SIRT2, and SIRT3 possess a robust deacetylase activity. Other SIRT6s (SIRT4, SIRT5, SIRT6, and SIRT7) exhibit a weak or no detectable deacetylation activity.

SIRT4 and SIRT6 display another well-described and well-studied enzymatic reaction, ADP-ribosyltransferase activity, by which they transfer a single ADP-ribosyl group from NAD<sup>+</sup> to proteins (Sauve, 2010). Mechanistically, ADP-ribosylation and deacetylation reactions are similar because they cleave NAD<sup>+</sup>, thereby releasing nicotinamide. By ADP-ribosylation, SIRT4 and SIRT6 regulate the activity of glutamate dehydrogenase and PARP, respectively (Haigis et al., 2006; Pan et al., 2011).

It was recently reported that some SIRT6s are able to catalyze other enzymatic reactions by removing different acyl groups. The first SIRT6 found to have a novel enzymatic activity was SIRT5, which exhibits weak physiological deacetylation but efficient demalonylation and desuccinylation activities. SIRT5 preferentially deacylates negatively charged carboxylate acyl groups by removing carboxylacyl-lysine. Studies performed on the crystal structure of SIRT5 confirmed that it is an NAD-dependent demalonylase and desuccinylase (Du et al., 2011). Its demalonylase or desuccinylase activity is much greater than its deacetylase activity. The best known acyl-CoA molecules with a carboxylate group are malonyl-CoA, made from acetyl-CoA by acetyl-CoA carboxylase and succinyl-CoA, an intermediate of the Krebs cycle. The preference for negatively charged acyl

**TABLE 1** | Classification of SIRT6 including localization, enzymatic activity, targets, and involvement in cancer.

Sirtuin	Principal cellular localization	Biochemical activity	Histone targets	Protein targets	Association with cancer	
					Up-regulation	Down-regulation
SIRT1	Nucleus	Deacetylase	H1-K26Ac H3-K9Ac H4-K16Ac H4-K20me H3-K9me3	FOXO family members, KU70, P53, GATA4-5, MYC, HIF-1 $\alpha$ , MLH1, RB, P73, STAT3	Prostate, breast, lung, colon, ovarian, gastric, lymphoblastic leukemia, chronic lymphocytic leukemia, diffuse large B-cell leukemia, chronic myeloid leukemia, melanoma	Glioma, bladder, prostate, ovarian, triple negative breast cancer
SIRT2	Cytoplasm	Deacetylase	H3-K18Ac H3-K56Ac H4-K16Ac	MYC, HIF-1 $\alpha$ , $\alpha$ -tubulin, KRAS, CDH, CDC20, PEPCK, FOXO1, FOXO3, P53	Leukemia, neuroblastoma, hepatocellular carcinoma, pancreatic, breast	Glioma, neck squamous cell carcinoma, breast, prostate, esophageal, ovarian, breast melanoma
SIRT3	Mitochondria	Deacetylase		SOD2, IDH2, FOXO3a, KU70, P53, HIF-1 $\alpha$	Colon, gastric, oral squamous, esophageal, renal, bladder, melanoma	Colon, breast, gastric, leukemia
SIRT4	Mitochondria	ADP-ribosylase		E-cadherin, MLYCD	Colorectal, Burkitt lymphoma	Bladder, breast, colon stomach, ovarian, thyroid
SIRT5	Mitochondria	Deacetylase desuccinylase deglutarylase demalonylase		CSP1 SOD1	Non-small cell lung, colorectal	Lung
SIRT6	Nucleus	Deacetylase ADP-ribosylase deacetylase demylristoylase depalmitoylase	H3-K9Ac H3-K56Ac H3-K18Ac	PARP1, FOXO3a, NRF1, MYC, HIF-1 $\alpha$	Lung, prostate, melanoma, non-melanoma skin cancer	Pancreatic, breast, colon, hepatocellular carcinoma
SIRT7	Nucleus	Deacetylase desuccinylase	H3-K18Ac	HIF-1 $\alpha$ , P53	Ovarian, colorectal, thyroid, prostate, breast, osteosarcoma, hepatocellular carcinoma	

groups can be explained by the presence of two amino acid residues, Tyr102 and Arg105, in the active site, which are well conserved in most SIRT6s (Yang et al., 2015). Another activity described for SIRT5 is glutarylation, which involves the removal of glutaryl-CoA, a metabolite of amino acid metabolism, structurally similar to succinyl-CoA and malonyl-CoA (Tan et al., 2014).

The discovery of these novel enzymatic properties of this class of proteins suggested that all SIRT6s with a weak deacetylase activity may preferentially act on other acyl lysine modifications (Carafa et al., 2016). This observation led to the discovery of the defatty-acylation activity of SIRT6. Similar to PfSir2A, the *Plasmodium falciparum* SIRT, SIRT6 is able to efficiently hydrolyze different long-chain fatty acyl groups such as acetyl, malonyl, succinyl, butyryl, myristoyl, and palmitoyl several hundred-fold more efficiently than hydrolyzing acetyl groups. Through these reactions, SIRT6s are able to regulate several key cellular processes (Jiang et al., 2013; Zhang et al., 2017b).

## ROLE OF SIRTUINS IN EMT

The principal property of invasive cancer is tumor metastasis, resulting from the activation of EMT. This transdifferentiation process changes a polarized epithelial cell into a mesenchymal

cell, which is able to migrate away from the epithelium in which it originated due to its increased migratory and invasive capacities. EMT is a reversible process caused by widespread epigenetic reprogramming of gene expression. Its counterpart is mesenchymal-to-epithelial transition (MET; Lamouille et al., 2014). Regardless of differences in tissue and signaling context, EMT is activated by EMT-TFs and epigenetic regulators controlling expression of proteins involved in cell polarity, cell–cell adhesion, cytoskeleton architecture, and extracellular matrix degradation. In addition, the maintenance of a stable mesenchymal phenotype depends on the level of histone acetylation and DNA methylation regulating the interconversion of heterochromatin into euchromatin, and vice versa. A growing body of evidence points to SIRT6s as key epigenetic modulators of EMT activation and maintenance. However, SIRT6s also display a contradictory role in EMT regulation, either promoting or suppressing this process (Palmirotta et al., 2016; O'Callaghan and Vassilopoulos, 2017; Sun et al., 2018), although the activation or repression of different cellular pathways in which they are involved depend on cellular context, stage of cancer, tissue of origin, and microenvironment. The best-characterized event occurring in EMT is loss of the fundamental cell–cell adhesion protein E-cadherin. E-cadherin loss correlates with poor prognosis, lower survival, and high rate of metastasis (Sun et al., 2018).

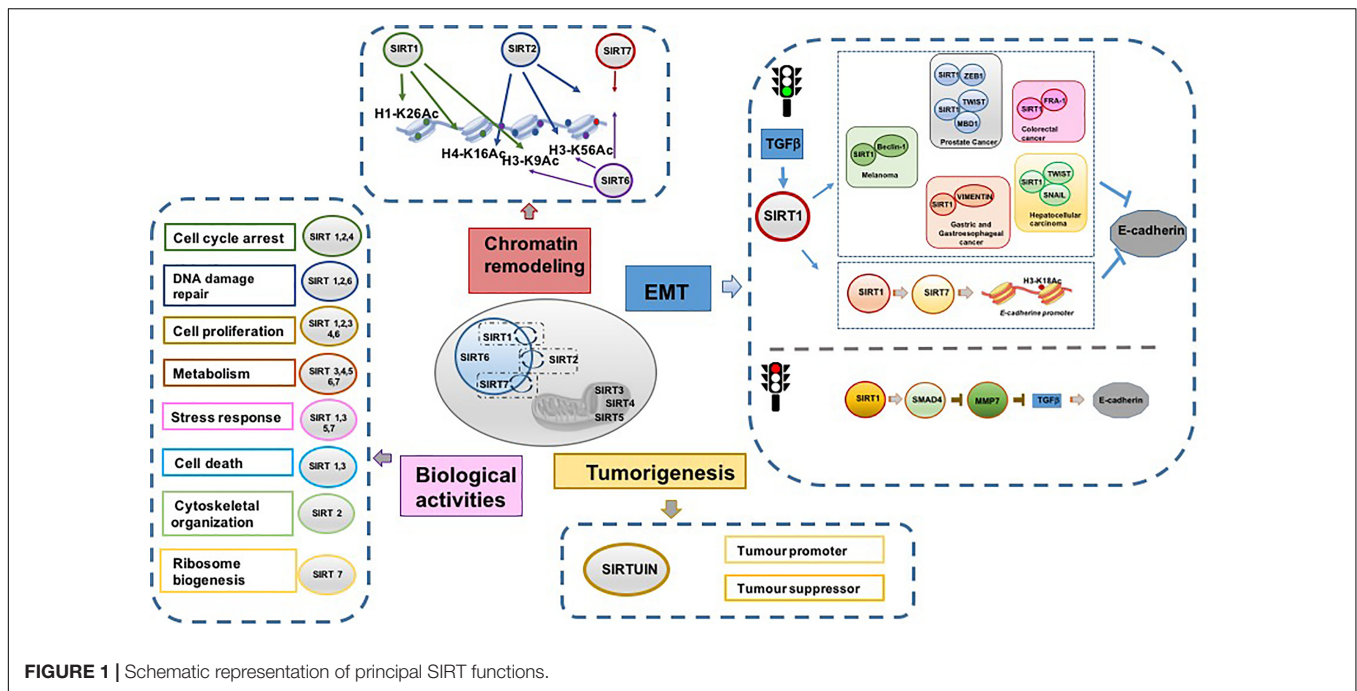


**FIGURE 1 |** Schematic representation of principal SIRT functions.

The positive regulation of EMT is mediated by TGF- $\beta$ . TGF- $\beta$  upregulates SIRT1, which in turn determines downregulation or degradation of E-cadherin by interacting with other TFs, promoting resistance to cell death, and cancer cell migration and invasion (Palmirotta et al., 2016). Several recent studies demonstrated that SIRT1 is involved in EMT activation by inactivating E-cadherin expression. miR-217 and SIRT1 play a key role in regulating EMT in chronic pancreatitis and pancreatic cancer (Deng et al., 2014). In particular, TGF- $\beta$ 1 was shown to induce EMT by downregulating miR-217 and upregulating SIRT1, leading to degradation of E-cadherin. miR-217 was shown to function as a tumor suppressor in pancreatic ductal adenocarcinoma by targeting KRAS (Zhao et al., 2010), and is downregulated and associated with poor survival in clear cell renal cell carcinoma (Li et al., 2013) and in gastric cancer (Chen et al., 2015).

SIRT1 regulates EMT in prostate cancer cells by interacting with the EMT-TF ZEB1 (Byles et al., 2012). Specifically, ZEB1 recruits SIRT1 to the *E-cadherin* promoter, leading to its gene suppression by deacetylating histone H3 and decreasing RNA polII binding. In addition, methyl-CpG binding domain protein 1 (MBD1) has an important function in pancreatic cancer, where it is upregulated and correlates with lymph node metastasis and poor survival (Xu et al., 2013). Mechanistically, MBD1 is associated with TWIST and SIRT1, via the TWIST-MBD1-SIRT1 complex on E-cadherin, which results in reduced E-cadherin transcription activity and induction of EMT. Significantly, targeting MBD1 reverses the EMT phenotype of pancreatic cancer and restores sensitivity to chemotherapy. SIRT1 is upregulated in the majority of hepatocellular carcinomas (HCCs) and enhances the invasive and metastatic potential of HCC by activating EMT markers, such as SNAIL, TWIST, and

VIMENTIN, and inhibiting E-cadherin. SIRT1 expression is correlated with an unfavorable prognosis in patients with HCC (Hao et al., 2014; Serrano-Gomez et al., 2016), suggesting a potential therapeutic use for selective SIRT1-targeting drugs.

In gastric cancer metastasis, SIRT1-mediated downregulation of miR-204 inactivates LKB1, promoting cell invasion. Overexpression of miR-204 and knock-down of SIRT1 induce an MET phenotype by increasing E-cadherin and decreasing VIMENTIN levels, and inhibit gastric cancer metastasis (Zhang et al., 2013). The promotion of gastric cancer cell metastasis mediated by miR-204 downregulation suggests that this miR acts as a tumor suppressor and may represent a potential target in gastric cancer therapy (Zhang et al., 2013; Shrestha et al., 2017). Additional studies suggest miR-204 as useful target in treatment of glioblastoma (Song et al., 2016) and breast cancer (Shen et al., 2017).

In melanoma, SIRT1 was reported to promote EMT by downregulation of E-cadherin and its degradation via autophagy, due to deacetylation of BECLIN-1 (Sun et al., 2018). In colorectal cancer, EMT is activated by SIRT1 and the EMT-TF FRA-1 (Cheng et al., 2016).

In 2015, SIRT7 was identified as an important regulator of metastasis. SIRT7 is recruited by SIRT1 on the *E-cadherin* promoter, triggering deacetylation of histone H3-K18Ac with consequent transcriptional repression of downstream targets (Malik et al., 2015). The maintenance of malignant properties was also found to be a consequence of deacetylation of H3-K18Ac by SIRT7 (Barber et al., 2012). Consistent with these findings, SIRT7 overexpression promotes the development and progression of human colorectal cancer (Yu et al., 2014).

As tumor suppressors, SIRT1s are also reported as negative modulators of EMT. SIRT1 overexpression in breast cancer cells



reduces EMT in nude mice, while SIRT1 repression increases EMT (Simic et al., 2013). The repressive role of SIRT1 in EMT was also described in kidney tubular epithelial cells overexpressing SIRT1, which maintained the epithelial phenotype after TGF- $\beta$  treatment (Simic et al., 2013). Conversely, silencing of SIRT1 increased EMT, as confirmed by E-cadherin decrease. Significantly, this function of SIRT1 was also observed in fibrosis following kidney injury. This effect was found mitigated in murine kidney tubular epithelial cells overexpressing SIRT1, and increased in SIRT1 knock-down cells. The absence of SIRT1 leads to hyperactivation of TGF- $\beta$  and hyperacetylation of SMAD4, which in turn increases the expression of its target MMP7. Higher levels of MMP7 result in degradation of E-cadherin, thereby releasing  $\beta$ -catenin which then translocates to the nucleus, determining a mesenchymal phenotype (Simic et al., 2013).

The effect of SIRT1 on MMP7 expression via deacetylation of SMAD4 was also found in oral squamous cell carcinoma (OSCC) (Chen et al., 2014). The overexpression of SIRT1 or its activation by resveratrol, a SIRT activator, inhibits the migration, invasion, and metastasis of OSCC cells, with an increase in E-cadherin expression and decrease in mesenchymal markers. This repressive effect is due to the hypoacetylation of SMAD4 followed by inhibition of TGF- $\beta$  signaling and MMP7 repression (Chen et al., 2014). Resveratrol was also found to play an inhibitory role in EMT in renal injury and fibrosis both *in vitro* and *in vivo*. Resveratrol-mediated SIRT1 upregulation attenuated renal injury and fibrosis by inhibiting TGF- $\beta$  pathway via MMP7 through deacetylation of SMAD4 (Xiao et al., 2016).

Evidence of SIRT1 repressive action in EMT via inhibition of cell migration was also described in lung and ovarian cancer cells (Sun et al., 2013a,b). Specifically, SIRT1 activation by resveratrol hampers cancer metastasis *in vitro* and *in vivo* by blocking EMT.

Hypoxia inhibits SIRT1 expression by promoting its transcriptional repressor hypermethylated in cancer-1 (HIC1) binding on the SIRT1 proximal promoter in a SUMOylation-dependent manner, preventing binding with the transcriptional activator SP1. Disrupting SUMOylation by targeting either UBC9 or PIASy, the E2 and E3 small ubiquitin-like modifier (SUMO)-conjugating enzymes restored SIRT1 expression and promoted an epithelial-like phenotype of cancer cells, thereby arresting metastasis (Sun et al., 2013b). Decreased SIRT1 levels combined with elevated PIASy expression is implicated in more invasive types of cancers. SIRT1 suppresses hypoxia-induced EMT in nasal polyp formation (Lee et al., 2016). This repressive role is due to deacetylation of hypoxia-inducible factor 1  $\alpha$  (HIF-1 $\alpha$ ). Tissue-specific SIRT1 knock-down restores polyp formation in transgenic mice.

Other SIRTs are known to play a role in EMT. In non-malignant cells, SIRT2 was found to inhibit WNT signaling by direct binding to  $\beta$ -catenin. This interaction increases upon oxidative stress induced by ionizing radiation, inhibiting the expression of WNT target genes. An increase in MMP9 and a decrease in E-cadherin promoting cellular migration and invasion were observed in SIRT2-null cells (Nguyen et al., 2014).

The repressive role of SIRT3 and SIRT4 in EMT is associated with their ability to reprogram the energy metabolism. Specifically, it was demonstrated that the reciprocal interplay

between cancer-associated fibroblasts (CAFs) and prostate cancer cells results in a mutual metabolic reprogramming (Fiaschi et al., 2012). Upon contact, both cell types undergo metabolic reprogramming, with CAFs and prostate cancer cells shifting toward a more glycolic and more aerobic metabolism, respectively. This process is controlled by HIF-1 $\alpha$ , which drives redox- and SIRT3-dependent stabilization of HIF-1 $\alpha$  in normoxic conditions. Lactate extruded from CAFs shuttles back to prostate cancer cells, which gradually became independent of glucose consumption while developing dependence on lactate upload to drive anabolic pathways and therefore cell growth. SIRT4 overexpression was shown to block proliferation, migration, and invasion of colon cancer cells via inhibition of glutamine metabolism (Miyao et al., 2015). Specifically, repression of glutamine metabolism drives the upregulation of E-cadherin expression and inhibits cell motility. Further, a decrease in SIRT4 expression is closely associated with the progression and recurrence of colorectal cancer.

SIRT7 overexpression inhibits EMT in OSCC, where SIRT7 expression correlates inversely with patient survival. Overexpression of SIRT7 strongly decreased OSCC migration and invasion, increased E-cadherin and downregulated VIMENTIN and MMP7 protein levels by deacetylating SMAD4, a key regulator of EMT (Levy and Hill, 2005; Ioannou et al., 2018; Li et al., 2018). In contrast with other studies (Barber et al., 2012; Yu et al., 2014; Malik et al., 2015), this report provides evidence of a new role for SIRT7 in tumor metastasis. In agreement, an association was found between SIRT7, breast cancer, and lung metastasis (Tang et al., 2017). Resveratrol treatment inhibits breast cancer and lung metastasis, and increases survival by activating SIRT7. A plausible explanation of this controversial function of SIRT7 in tumorigenesis could be derived from its dynamic regulation during tumor development, where high SIRT7 levels may initially contribute to oncogenic transformation and tumor growth (Aljada et al., 2015), while inhibit migration and invasion at later stages of cancer progression (Tang et al., 2017).

## SIRTIINS AND CANCER

Sirtuins are predominantly located in either nucleus (SIRT1, SIRT6, SIRT7), cytoplasm (SIRT2), or mitochondria (SIRT3, SIRT4, SIRT5).

### Nuclear Sirtuins SIRT1

SIRT1 is the proto member of the SIRT family, and is the best known and most studied. SIRT1 is located primarily in the nucleus, is able to deacetylate histone and non-histone proteins, and is involved in several biological processes. SIRT1 regulates histone deacetylation and methylation through deacetylation of lysine 26 on histone H1 (H1-K26Ac), lysine 9 on histone H3 (H3-K9Ac), and lysine 16 on histone H4 (H4-K16Ac). It also deacetylates several non-histone proteins involved in cell cycle regulation, cell death induction, and metabolism, such as FOXO family members and KU70. In addition, SIRT1 affects

histone methylation levels via production of mono-methylated histone H4 in lysine 20 (H4-K20me1) and tri-methylated histone H3 in lysine 9 (H3-K9me3) (Zhang and Kraus, 2010; **Table 1**).

Elevated expression of SIRT1 was observed in several cancer cell lines, and is generally associated with poor prognosis and overall survival (Wang et al., 2017). SIRT1 interacts with P53, triggering its deacetylation in Lys382 residue, and determines a block of all P53-dependent pathways, leading to uncontrolled cell cycle and inactivation of the apoptotic process (Vaziri et al., 2001). Chemo-resistance is a phenomenon observed in tumors overexpressing SIRT1, determining hyper proliferation and survival of cancer cells.

SIRT1 plays a dual role in tumorigenesis. An increasing number of studies report that SIRT1 has a function in metastasis and invasiveness in several cancers. The deacetylation of many proteins involved in tumor suppressor processes or DNA damage repair, and the inactivation of specific pathways support the role of SIRT1 as a tumor promoter. SIRT1 is involved in the initiation, promotion, and progression of several malignant tumors including prostate cancer (Jung-Hynes et al., 2009), breast cancer (Jin et al., 2018), lung cancer (Han et al., 2013), leukemia (Chen and Bhatia, 2013), colon cancer (Lin and Fang, 2013), melanoma (Ohanna et al., 2014), and ovarian and gastric cancer (Han et al., 2013; Shuang et al., 2015). *In vitro* experiments demonstrate that the inhibition of SIRT1 by treatment with small molecule SIRT1 inhibitors determines a significant decrease in cell growth, proliferation and viability (Wilking et al., 2014).

In gastric tumors, high expression levels of SIRT1 are associated with malignant status and poor survival. Studies of the molecular mechanisms responsible for gastric cancer progression highlight SIRT1 association with STAT3 (Nie et al., 2009; Zhang et al., 2017a). SIRT1 deacetylates STAT3, suppressing its inhibitory effect on gluconeogenesis. This interaction leads to an acceleration of the malignant process by activating proteins involved in cell survival, downregulating tumor suppressor genes, and conferring drug resistance.

SIRT1 expression is found increased in hematopoietic malignancies such as T-cell acute lymphoblastic leukemia, chronic lymphocytic leukemia, diffuse large B-cell leukemia, and chronic myeloid leukemia (CML) (Jang et al., 2008; Wang et al., 2011; Kozako et al., 2012). Specifically, several studies demonstrated the importance of the interaction between SIRT1 and onco-fusion proteins driving these pathologies. In CML, the onco-fusion protein BCR-ABL, generated by STAT5-mediated SIRT1 activation, plays a crucial role in malignant transformation and development of hematopoietic progenitor cells. SIRT1 promotes cell survival and cancer progression by deacetylating multiple substrates including FOXO1, P53, and KU70 (Yuan et al., 2012). Inhibition of SIRT1 might therefore selectively reduce survival and growth of CML stem cells and increase their responsiveness to clinical treatment with tyrosine kinase inhibitors. In acute myeloid leukemia, patients harboring the chromosomal translocation t(8;21)(q22;q22), AML1-ETO fusion protein binds the promoter region of *SIRT1* gene and is responsible for its activation and overexpression (Zhou et al., 2017).

SIRT1 also acts as a tumor suppressor via direct interaction with and consequent repression of other oncogenes, such as c-MYC (Yuan et al., 2009). In addition, a variety of human cancers including glioma, bladder, prostate, and ovarian cancer display decreased levels of SIRT1 (Wilking and Ahmad, 2015). Surprisingly, some studies report an opposing role for SIRT1 in the same tumor types. High protein and mRNA expression levels of SIRT1 in hormone receptor-positive and HER2 breast cancer subtypes demonstrate its oncogenic role (Rifai et al., 2017). In contrast, SIRT1 acts as a tumor suppressor in triple negative breast cancer cells, where it determines a block of cancer proliferation and cell growth (Yi et al., 2013). Conflicting findings were also reported in human prostate cancer cell lines, where SIRT1 pharmacological inhibition induces cell death, and reduces tumor growth and chemo-resistance (Long et al., 2014). Conversely, recent studies with SIRT1<sup>-/-</sup> mice showed increased survival (Di Sante et al., 2015). This opposite behavior may be explained by the different role of SIRT1 in examined species (human vs murine), but requires further investigation.

## SIRT6

SIRT6 shows low deacetylation and ADP-ribosylation activities. In addition, it was recently found to exhibit deacylase activity by removing myristoyl and palmitoyl groups (long-chain fatty acyl groups) from lysine residues (Feldman et al., 2013). SIRT6 is mainly located in the nucleus, where it binds and deacetylates chromatin, nucleosomes, and many TFs. It is also present in the endoplasmic reticulum, where it regulates tumor necrosis factor  $\alpha$  by removing myristoyl groups from lysines 19 and 20, leading to its secretion from macrophages (Jiang et al., 2013). SIRT6 deacetylates lysine 9 on histone H3 (H3-K9Ac) and lysine 56 on histone H3 (H3-K56Ac) (Michishita et al., 2008; Michishita et al., 2009). Lysine 18 on histone H3 (H3-K18Ac) was recently identified as a new substrate of SIRT6 (Tasselli et al., 2016).

The principal function of SIRT6 is the control of cellular homeostasis by regulating DNA-damage repair, telomere maintenance, and metabolism. SIRT6 involvement in the DNA-damage repair pathway is principally due to its ADP-ribosyltransferase activity on poly-ADP-ribose-polymerase under stress conditions (Mao et al., 2011). The action of SIRT6 is strictly correlated to that of SIRT1. Upon nutritional stress, SIRT1 regulates SIRT6 by forming a complex with other proteins involved in metabolism regulation, such as FOXO3a and NRF1. Like SIRT1, SIRT6 is also able to reduce the transcription of MYC and HIF-1 in cancer cells by reprogramming glucose metabolism (Palmirotta et al., 2016).

Similarly, SIRT6 involvement in tumorigenesis is tissue-context specific, and displays both functions of tumor promoter and tumor suppressor (Qu et al., 2017). SIRT6 tumor suppressor activity is documented in pancreatic cancer (Kugel et al., 2016), breast cancer, colon cancer (Ioris et al., 2017), and HCCs (Zhang and Qin, 2014). In these tumors, expression levels of SIRT6 are decreased and aerobic glycolysis pathways are blocked. In other cancer types, such as lung cancer (Desantis et al., 2018), prostate cancer (Bai et al., 2016), melanoma, and non-melanoma skin cancer (Garcia-Peterson et al., 2017), SIRT6 is upregulated both

at mRNA and protein level, and acts as an oncogene responsible for cancer cell proliferation.

### SIRT7

SIRT7 is the last deacetylase discovered and is therefore the least well characterized. SIRT7 deacetylates lysine 18 on histone H3 (H3-K18Ac) as well as non-histone proteins. Recent studies reported that SIRT7 also exhibits desuccinylase activity, acting after a genomic insult on lysine 122 of histone H3 (Li et al., 2016). SIRT7 has a role in the control of ribosomal RNA expression (Zhang et al., 2016). It is localized in the nucleus, where it participates in the activation of RNA polI (Wei et al., 2017). SIRT7 is involved in seven cellular pathways regulating metabolism control, genome stability, aging, stress response, transcription, ribosome biogenesis, and tumorigenesis (Blank and Grummt, 2017). SIRT7 has an oncogenic role in tumorigenesis, activating cancer proliferation via deacetylation of specific promoters of different tumor suppressor genes. SIRT7 is a biomarker for aggressive and metastatic tumors with poor clinical outcome, and its overexpression correlates with advanced tumor stage. SIRT7 was found overexpressed and upregulated in several tumors, including ovarian cancer (Wang et al., 2015), colorectal cancer, osteosarcoma (Wei et al., 2017), prostate cancer (Haider et al., 2017), breast cancer (Geng et al., 2015), and HCC (Kim et al., 2013). SIRT7 knock-down determines a reduction in tumor invasiveness and progression, and an induction of apoptotic pathways.

The oncogenic properties of SIRT7 may be due to its interaction with P53, a secondary effect observed after upregulation of rRNA synthesis, determining rapid tumor growth (Ford et al., 2006; Blank and Grummt, 2017).

## Cytoplasmic Sirtuins

### SIRT2

SIRT2 is mainly localized in the cytoplasm, but translocates rapidly to the nucleus during G2/M cell cycle transition. In the nucleus, SIRT2 binds chromatin and deacetylates histone and non-histone proteins, controlling cell cycle progression. SIRT2 deacetylates lysine 18 on histone H3 (H3-K18Ac), lysine 56 on histone H3 (H3-K56Ac) and lysine 16 on histone H4 (H4-K16Ac) (Table 1). The different cellular localization of SIRT2 is responsible for different biological downstream effects causing many pathologies including cancer. SIRT2 is involved in regulation of mitotic processes, cell motility, differentiation, oxidative metabolism, and cell death (Inoue et al., 2007a). It plays a fundamental role in cytoskeletal organization by deacetylating  $\alpha$ -tubulin. In tumorigenesis, SIRT2 shows both tumor suppressor and oncogenic activities. Its tumor suppressor action is the result of the deacetylation of many proteins involved in important biological pathways such as cell proliferation, cell integrity, and DNA damage (Huang et al., 2017). In addition, SIRT2 acts as a checkpoint and prevents chromatin condensation and hyperploid cell formation through its ability to regulate mitotic integrity. In several cancer cell lines, including glioma (Inoue et al., 2007b), neck squamous cell carcinoma (Lai et al., 2013), non-small cell lung cancer (Grbesa et al., 2015), breast cancer (McGlynn et al., 2014), prostate cancer (Kim et al.,

2011), and HCC (Chen et al., 2013), SIRT2 gene is found downregulated or deleted. Recent evidence highlights the role of SIRT2 in serous ovarian carcinoma, where its reduced expression is responsible for cancer progression, promoting cell migration, invasion, lymph node metastasis, and peritoneal dissemination (Du et al., 2017). In breast cancer progression, SIRT2 function depends on the grade and classification of the tumor. Specifically, in moderately differentiated grade 2 breast tumors, SIRT2 expression is very low and G2/M phase transition is deregulated, correlating with poor prognosis. In this scenario, SIRT2 exerts a tumor suppressor function. Conversely, in poorly differentiated breast cancers, such as grade 3 breast tumors, SIRT2 expression levels are high and are responsible for further dysregulation of cell cycle progression and DNA repair processes. This correlates with a more aggressive tumor, shorter time to relapse and death, highlighting the oncogenic role of SIRT2 (McGlynn et al., 2014). Tumors with high levels of SIRT2 were found resistant and refractory to chemotherapy. In leukemia, neuroblastoma, HCC, and pancreatic cancer, SIRT2 gene is upregulated and is responsible for vascular invasion, cell proliferation, and tumor growth. SIRT2 induces myeloid differentiation and deacetylates KRAS, increasing the tumorigenesis process, in association with nicotinamide phosphoribosyltransferase and HDAC6, respectively (Yang et al., 2013). A feedback interaction is also described between SIRT2 and N-MYC in neuroblastoma cells, and with c-MYC in pancreatic cancer cells (Liu et al., 2013). The activity of SIRT2 enhances N-MYC and c-MYC protein stability, promoting cancer cell proliferation.

## Mitochondrial Sirtuins

SIRT3, SIRT4, and SIRT5 are known as mitochondrial SIRTs (mtSIRTs) and are involved in the regulation of many biological and physiological processes such as cell cycle, cell viability, stress response, energy homeostasis, and metabolism (Lombard et al., 2011). mtSIRTs are critical regulators of metabolic functions, and act as checkpoints for mitochondrial membrane integrity by inhibiting the translocation of the pro-apoptotic protein BAX. mtSIRTs can also regulate cell survival and death by controlling metabolic state of cells. Since tumorigenesis involves several alterations in cellular and mitochondrial energy metabolism (Parihar et al., 2015), the role of mtSIRTs in tumor initiation is crucial. Several studies reported that alterations of mitochondrial metabolism lead to an increase in reactive species of oxygen (ROS) production, a key event in both aging and cancer. At low levels, ROS act as second messengers, stimulating cell proliferation and aggressive phenotype, preventing apoptosis, and promoting tumorigenesis (Murphy, 2013; Sullivan and Chandel, 2014).

### SIRT3

SIRT3 is the best-characterized mtSIRT. It is principally located in mitochondria, where under stress conditions it translocates into the mitochondrial matrix, and after a proteolytic process is activated (Onyango et al., 2002; Table 1). Although some studies describe its possible localization in the nucleus, its function in



this compartment is not yet clarified. Nuclear SIRT3 is reported to be a possible regulator of gene expression after cellular stress (Iwahara et al., 2012). SIRT3 controls the acetylation status of different proteins regulating mitochondrial metabolism, oxidative stress, and ROS production, thereby preventing apoptosis, growth arrest, and senescence, and promoting cancer cell proliferation (Park et al., 2011). Cell stress causes damage to mitochondria, leading to a reduction in SIRT3 activity, correlating with a decrease in deacetylation and NAD/NADH ratio and growth arrest (Hershberger et al., 2017). Several studies describe a crucial role for SIRT3 in cancer development and progression. In different types of cancers including colon, gastric, renal, oral squamous, and esophageal cancer and melanoma, SIRT3 expression is upregulated (Finley and Haigis, 2012; Liu et al., 2014), determining an alteration of many important biological processes and correlating with high tumor grade, positive lymph node status, and poor prognosis. In bladder carcinoma, SIRT3 promotes proliferation by abrogating the anti-proliferative activity of P53 in mitochondria (Li et al., 2010). In cervical cancer, its interaction with KU70 alters the DNA repair pathway. SIRT3 was also reported to have a dual function in tumorigenesis, due to its deacetylation activity of mitochondrial proteins such as SOD2, IDH2, and FOXO3a, and inhibition of mitochondrial ROS production and cancer cell proliferation (Torrens-Mas et al., 2017). The treatment of two different leukemia cell lines with a natural flavonoid, kaempferol, increases the expression and mitochondrial localization of SIRT3, resulting in AKT pathway inactivation as well as cytochrome c release and apoptotic cell activation (Marfe et al., 2009). In human breast and gastric cancer, downregulation of SIRT3 correlates with upregulation of HIF-1 $\alpha$  and cell proliferation arrest (Finley et al., 2011; Yang et al., 2014).

### SIRT4

SIRT4 is principally involved in genome stability and metabolism. Unlike other SIRTs, SIRT4 does not have nicotinamide adenine dinucleotide-dependent deacetylase activity, but does display ADP-ribosylase activity (Table 1). SIRT4 also negatively regulates mitochondrial glutamine metabolism by inhibiting glutamate dehydrogenase activity (Haigis et al., 2006). SIRT4-associated function on glutamine metabolism contributes to the control of cell cycle progression and proliferation, and is important for genomic integrity in response to DNA damage (Jeong et al., 2013). SIRT4 exerts tumor suppressor activity, arresting cell cycle and inhibiting invasion, proliferation, and cell migration. Although few studies have analyzed the role of SIRT4 in tumorigenesis to date, low expression of SIRT4 is reported in many cancers such as bladder, breast, colon, stomach, ovarian, and thyroid cancer, and correlates with a worse prognosis (Jeong et al., 2013; Huang and Zhu, 2018). SIRT4 loss leads to both increased glutamine-dependent proliferation and stress-induced genomic instability, resulting in tumorigenic phenotype. In colorectal cancer, SIRT4 overexpression was shown to suppress malignancy by blocking cancer cell proliferation via association with E-cadherin (Miyo et al., 2015). In breast cancer, loss of SIRT4 correlates with short time to

metastasis development (Shi et al., 2016). In Burkitt lymphoma, SIRT4 is able to block MYC-driven lymphomagenesis by inhibiting mitochondrial glutamine metabolism (Jeong et al., 2014).

### SIRT5

To date, only one physiological substrate for SIRT5 has been identified, carbamoyl-phosphate synthetase 1, an enzyme that plays an important role in urea cycle (Kumar and Lombard, 2015). Other enzymatic activities for SIRT5 such as desuccinylation, glutarylation, and demalonylation were recently characterized (Du et al., 2011; Table 1). Although the role of SIRT5 in tumorigenesis is not yet well characterized, it is likely related to its desuccinylation activity and to induction of the antioxidant enzyme SOD1 involved in ROS production. SIRT5 is overexpressed in human non-small cell lung cancer, and its role was recently investigated in colorectal cancer (Lu et al., 2014). High expression of SIRT5 is a predictor of poor survival, facilitating cancer cell growth and drug resistance. Accordingly, SIRT5 knock-down makes lung cancer cells more sensitive to chemotherapy (Wang et al., 2018).

## SIRTUIN MODULATORS IN CANCER

A growing body of evidence in recent years suggests that SIRT deregulation is involved in human carcinogenesis, placing these enzymes at the center of extensive pharmacological investigations such as drug target studies (Blum et al., 2011). SIRT activity can be modulated by several molecules, and high-throughput and *in silico* screenings have identified a number of small SIRT inhibitor (SIRTi) and activator compounds. In terms of their potential application in cancer treatment, the most promising data have been generated from the use of SIRTi rather than activators.

### Sirtuin Inhibitors

Besides nicotinamide, a few SIRTi displaying therapeutic potential in several human diseases have been developed (Carafa et al., 2012, 2018). To date, little is known about their specific anticancer action. SIRTi are grouped according to their pharmacophore type:  $\beta$ -naphthol, indole, urea and thiourea derivatives, and miscellaneous.

Sirtinol is a  $\beta$ -naphthol derivative identified by a high-throughput phenotypic screen in cells (Grozing et al., 2001) which exerts anticancer activity via p53 acetylation (Vaziri et al., 2001; Peck et al., 2010) and senescence-like growth arrest (Ota et al., 2006). Sirtinol treatment is also able to increase cancer cell sensitivity to camptothecin and cisplatin (Kojima et al., 2008; Jin et al., 2010). Splitomicin is another  $\beta$ -naphthol derivative identified by a cell-based screen for Sir2p inhibitors (Bedalov et al., 2001), but has a weak action on human SIRTs. In contrast, splitomicin analogs have shown activity against SIRT1 and SIRT2 as well as antiproliferative properties in cancer cells (Neugebauer et al., 2008; Freitag et al., 2011). Cambinol is the most stable and effective  $\beta$ -naphthol derivative. It inhibits SIRT1, SIRT2, and, weakly, SIRT5



(Heltweg et al., 2006). Cambinol displays antitumor activity *in vitro* and in a Burkitt lymphoma mouse xenograft model by hyperacetylating tubulin, p53 and BCL6 (Heltweg et al., 2006). Salermide is able to induce a strong anticancer effect by reactivating proapoptotic genes through SIRT1-mediated K16H4 deacetylation (Lara et al., 2009). Its derivatives show broad-spectrum anticancer properties (Rotili et al., 2012). EX-527, the most well-described indole derivative, was identified by high-throughput screening against human SIRT1 (Napper et al., 2005). This inhibitor acts after the release of nicotinamide from the SIRT1 enzyme and prevents the release of deacetylated peptide and O-acetyl-ADP-ribose, products of the SIRT reaction. Thanks to its chemical properties (low molecular weight, cell permeability, oral bioavailability, and metabolic stability), EX-527 has been used to study the biology of SIRT1 and to explore therapeutic applications for SIRT1 inhibitors. This SIRT1-selective inhibitor showed a strong antiproliferative effect in pancreatic cancer cells and enhanced sensitivity of cancer cells to gemcitabine treatment through increased apoptosis (Zhang et al., 2014; Oon et al., 2015). Suramin is a polyanionic urea derivative used for treatment of trypanosomiasis (Voogd et al., 1993) and is also a potent anticancer agent that acts by inhibiting cell proliferation and angiogenesis (Stein et al., 1989; Li et al., 2015). However, its neurologic toxicity has limited its use in the clinic. Suramin analogs have been synthesized, and show a more potent antiangiogenic action (Meyers et al., 2000). In addition, in non-toxic doses, suramin potentiates the *in vitro* and *in vivo* activity of chemotherapeutics (Song et al., 2000; Zhang et al., 2001; Villalona-Calero et al., 2008), accounting for its use in several completed phase 1/2 clinical trials involving patients with solid tumors. Tenovins, SIRT1/2 inhibitors, are thiourea derivatives identified as a class of small molecules able to activate p53 and decrease tumor growth (Lain et al., 2008). Their water soluble analog is Tenovin 6, a promising agent for treating uveal melanoma (Dai et al., 2016). MC2494, a new pan-SIRTi, was recently found to display promising anticancer activity via acetylated RIP1/caspase-8-mediated apoptosis. MC2494 displays tumor-selective potential *in vitro*, in leukemic blasts *ex vivo*, and *in vivo* in both xenograft and allograft cancer models (Carafa et al., 2018).

## Sirtuin Activators

High-throughput screening identified small molecule SIRT-activating compounds (STACs). Resveratrol and other polyphenols were the first STACS to be discovered (Howitz et al., 2003), followed by an increasing number of molecules of doubtful activity (Baur and Sinclair, 2006). Other phenolic STACs include butein, piceatannol, isoliquiritigenin, fisetin, and quercetin (Link et al., 2010). Although several efforts have focused on better understanding the effects of resveratrol in cancer (Baur and Sinclair, 2006), many aspects remain unclear and controversial (Hubbard and Sinclair, 2014). In 1997, a report described the ability of resveratrol to inhibit development of preneoplastic lesions in carcinogen-treated mouse mammary glands in culture and tumorigenesis in a mouse skin cancer model (Jang et al., 1997). Subsequent

studies showed that the anticancer activity of resveratrol was mediated at least in part by SIRT1 (Boily et al., 2009). Resveratrol reduces the proliferation of different cancers (Aggarwal et al., 2004; Firestein et al., 2008). Conversely, resveratrol fails to do so in breast cancer (Bove et al., 2002) and in multiple myeloma (Popat et al., 2013). This contrasting anticancer effect of resveratrol may be due to different doses used and its bioavailability in different tissues (Baur and Sinclair, 2006) as well as to its pharmacokinetic properties (Boocock et al., 2007). Recently, major efforts have focused on non-polyphenolic SIRT1 activators, including new second-generation (SRT2183, SRT1460, and SRT1720) and third-generation (STAC-5, STAC-9, and STAC-10) small molecules. Again, their anticancer effects remain elusive. SRT1720 was reported to induce cell death in breast cancer (Lahusen and Deng, 2015) and in multiple myeloma cells (Chauhan et al., 2011), but also to promote tumor cell migration and lung metastasis of breast cancer (Suzuki et al., 2012).

## CONCLUSION

Sirtuins are known to be involved in several biological processes, and play a critical role in contributing to the hallmarks of cancer. The dual role of SIRT in tumor initiation, promotion, and progression may depend on their tissue- and cancer-specific expression as well as experimental conditions. A better characterization of each SIRT will enhance our understanding of their specific role in altered cancer signaling pathways. Targeting these epigenetic modulators may sensitize malignant cells to anticancer treatment, increasing the cytotoxic effect of chemotherapeutics and reducing tumor cell proliferation. Depending on their specific function as tumor promoters or tumor suppressors, a greater insight into SIRT modulators may open the way toward tailored medicine either inhibiting or activating SIRT action in a tumor-specific manner. The effects of SIRT on cell energy metabolism that contribute to determining cellular microenvironment both in normal and pathological conditions add another layer of complexity to our understanding of their dual function. Further studies are required to shed light on this intricate role of SIRT in different cancers and cell types in order to clarify in which conditions a specific SIRT functions as a tumor promoter or suppressor. Although several SIRT modulators, mainly inhibitors, were developed and tested *in vitro* (Carafa et al., 2012), few have been investigated *in vivo*. To date, only one phase 2/3 clinical trial (recruiting) is currently studying the combinatorial effect of the SIRTi nicotinamide in modulating SIRT activity in non-small cell lung carcinoma (NCT02416739).

The discovery of novel SIRT-selective modulators will help elucidate the role of individual SIRT in cancer development and unveil other downstream target genes in cancers involving SIRT regulation.

Given the opposing role of SIRT in cancer, it is crucial that future investigations focus on the undesired potential of SIRT (and their modulators) to act against one cancer while promoting

the genesis of other tumor types. Advanced technologies, such as the discovery of selective biomarkers for individual cancer types, the development of effective precision cancer therapies, and targeted delivery systems, will help address this concern and drive future clinical practice toward non-invasive, personalized, and controllable therapies.

## AUTHOR CONTRIBUTIONS

VC, LA, and AN substantially contributed to the redaction of the manuscript and gave the final approval of the manuscript.

## REFERENCES

- Aggarwal, B. B., Bhardwaj, A., Aggarwal, R. S., Seeram, N. P., Shishodia, S., and Takada, Y. (2004). Role of resveratrol in prevention and therapy of cancer: preclinical and clinical studies. *Anticancer Res.* 24, 2783–2840.
- Aljada, A., Saleh, A. M., Alkathiri, M., Shamsa, H. B., Al-Bawab, A., and Nasr, A. (2015). Altered sirtuin 7 expression is associated with early stage breast cancer. *Breast Cancer* 9, 3–8. doi: 10.4137/BCBCR.S23156
- Bai, L., Lin, G., Sun, L., Liu, Y., Huang, X., Cao, C., et al. (2016). Upregulation of SIRT6 predicts poor prognosis and promotes metastasis of non-small cell lung cancer via the ERK1/2/MMP9 pathway. *Oncotarget* 7, 40377–40386. doi: 10.18632/oncotarget.9750
- Barber, M. F., Michishita-Kioi, E., Xi, Y., Tasselli, L., Kioi, M., Moqtaderi, Z., et al. (2012). SIRT7 links H3K18 deacetylation to maintenance of oncogenic transformation. *Nature* 487, 114–118. doi: 10.1038/nature11043
- Baur, J. A., and Sinclair, D. A. (2006). Therapeutic potential of resveratrol: the in vivo evidence. *Nat. Rev. Drug Discov.* 5, 493–506. doi: 10.1038/nrd2060
- Bedalov, A., Gatabont, T., Irvine, W. P., Gottschling, D. E., and Simon, J. A. (2001). Identification of a small molecule inhibitor of Sir2p. *Proc. Natl. Acad. Sci. U.S.A.* 98, 15113–15118. doi: 10.1073/pnas.261574398
- Blank, M. F., and Grummt, I. (2017). The seven faces of SIRT7. *Transcription* 8, 67–74. doi: 10.1080/21541264.2016.1276658
- Blum, C. A., Ellis, J. L., Loh, C., Ng, P. Y., Perni, R. B., and Stein, R. L. (2011). SIRT1 modulation as a novel approach to the treatment of diseases of aging. *J. Med. Chem.* 54, 417–432. doi: 10.1021/jm100861p
- Boily, G., He, X. H., Pearce, B., Jardine, K., and McBurney, M. W. (2009). SirT1-null mice develop tumors at normal rates but are poorly protected by resveratrol. *Oncogene* 28, 2882–2893. doi: 10.1038/onc.2009.147
- Boocock, D. J., Faust, G. E., Patel, K. R., Schinas, A. M., Brown, V. A., Ducharme, M. P., et al. (2007). Phase I dose escalation pharmacokinetic study in healthy volunteers of resveratrol, a potential cancer chemopreventive agent. *Cancer Epidemiol. Biomarkers Prev.* 16, 1246–1252. doi: 10.1158/1055-9965.EPI-07-0022
- Bosch-Presegue, L., and Vaquero, A. (2011). The dual role of sirtuins in cancer. *Genes Cancer* 2, 648–662. doi: 10.1177/1947601911417862
- Bove, K., Lincoln, D. W., and Tsan, M. F. (2002). Effect of resveratrol on growth of 4T1 breast cancer cells in vitro and in vivo. *Biochem. Biophys. Res. Commun.* 291, 1001–1005. doi: 10.1006/bbrc.2002.6554
- Byles, V., Zhu, L., Lovaas, J. D., Chmielewski, L. K., Wang, J., Faller, D. V., et al. (2012). SIRT1 induces EMT by cooperating with EMT transcription factors and enhances prostate cancer cell migration and metastasis. *Oncogene* 31, 4619–4629. doi: 10.1038/onc.2011.612
- Carafa, V., Nebbioso, A., and Altucci, L. (2012). Sirtuins and disease: the road ahead. *Front. Pharmacol.* 3:4. doi: 10.3389/fphar.2012.00004
- Carafa, V., Nebbioso, A., Cuomo, F., Rotili, D., Cobellis, G., Bontempo, P., et al. (2018). RIP1-HAT1-SIRT complex identification and targeting in treatment and prevention of cancer. *Clin. Cancer Res.* 24, 2886–2900. doi: 10.1158/1078-0432.CCR-17-3081
- Carafa, V., Rotili, D., Forgione, M., Cuomo, F., Serretiello, E., Hailu, G. S., et al. (2016). Sirtuin functions and modulation: from chemistry to the clinic. *Clin. Epigenetics* 8:61. doi: 10.1186/s13148-016-0224-3
- ## FUNDING
- This work was supported by EU Blueprint project (282510), the VALERE: Vanvitelli per la Ricerca Program, the Italian Flagship Project EPIGEN, PRIN-20152TE5PK, the Italian Association for Cancer Research (AIRC-17217) and Regione Campania project iCURE (ID 29229).
- ## ACKNOWLEDGMENTS
- The authors would like to thank C. Fisher for language editing.
- Chalkiadaki, A., and Guarente, L. (2015). The multifaceted functions of sirtuins in cancer. *Nat. Rev. Cancer* 15, 608–624. doi: 10.1038/nrc3985
- Chauhan, D., Bandi, M., Singh, A. V., Ray, A., Raje, N., Richardson, P., et al. (2011). Preclinical evaluation of a novel SIRT1 modulator SRT1720 in multiple myeloma cells. *Br. J. Haematol.* 155, 588–598. doi: 10.1111/j.1365-2141.2011.08888.x
- Chen, D. L., Zhang, D. S., Lu, Y. X., Chen, L. Z., Zeng, Z. L., He, M. M., et al. (2015). microRNA-217 inhibits tumor progression and metastasis by downregulating EZH2 and predicts favorable prognosis in gastric cancer. *Oncotarget* 6, 10868–10879. doi: 10.18632/oncotarget.3451
- Chen, I. C., Chiang, W. F., Huang, H. H., Chen, P. F., Shen, Y. Y., and Chiang, H. C. (2014). Role of SIRT1 in regulation of epithelial-to-mesenchymal transition in oral squamous cell carcinoma metastasis. *Mol. Cancer* 13:254. doi: 10.1186/1476-4598-13-254
- Chen, J., Chan, A. W., To, K. F., Chen, W., Zhang, Z., Ren, J., et al. (2013). SIRT2 overexpression in hepatocellular carcinoma mediates epithelial to mesenchymal transition by protein kinase B/glycogen synthase kinase-3beta/beta-catenin signaling. *Hepatology* 57, 2287–2298. doi: 10.1002/hep.26278
- Chen, W., and Bhatia, R. (2013). Roles of SIRT1 in leukemogenesis. *Curr. Opin. Hematol.* 20, 308–313. doi: 10.1097/MOH.0b013e328360ab64
- Cheng, F., Su, L., Yao, C., Liu, L., Shen, J., Liu, C., et al. (2016). SIRT1 promotes epithelial-mesenchymal transition and metastasis in colorectal cancer by regulating Fra-1 expression. *Cancer Lett.* 375, 274–283. doi: 10.1016/j.canlet.2016.03.010
- Dai, W., Zhou, J., Jin, B., and Pan, J. (2016). Class III-specific HDAC inhibitor Tenovin-6 induces apoptosis, suppresses migration and eliminates cancer stem cells in uveal melanoma. *Sci. Rep.* 6:22622. doi: 10.1038/srep22622
- Deng, C. X. (2009). SIRT1, is it a tumor promoter or tumor suppressor? *Int. J. Biol. Sci.* 5, 147–152.
- Deng, S., Zhu, S., Wang, B., Li, X., Liu, Y., Qin, Q., et al. (2014). Chronic pancreatitis and pancreatic cancer demonstrate active epithelial-mesenchymal transition profile, regulated by miR-217-SIRT1 pathway. *Cancer Lett.* 355, 184–191. doi: 10.1016/j.canlet.2014.08.007
- Desantis, V., Lamanuzzi, A., and Vacca, A. (2018). The role of SIRT6 in tumors. *Haematologica* 103, 1–4. doi: 10.3324/haematol.2017.182675
- Di Sante, G., Pestell, T. G., Casimiro, M. C., Bisetto, S., Powell, M. J., Lisanti, M. P., et al. (2015). Loss of Sirt1 promotes prostatic intraepithelial neoplasia, reduces mitophagy, and delays PARK2 translocation to mitochondria. *Am. J. Pathol.* 185, 266–279. doi: 10.1016/j.ajpath.2014.09.014
- Du, J., Zhou, Y., Su, X., Yu, J. J., Khan, S., Jiang, H., et al. (2011). Sirt5 is a NAD-dependent protein lysine demalonylase and desuccinylase. *Science* 334, 806–809. doi: 10.1126/science.1207861
- Du, Y., Wu, J., Zhang, H., Li, S., and Sun, H. (2017). Reduced expression of SIRT2 in serous ovarian carcinoma promotes cell proliferation through disinhibition of CDK4 expression. *Mol. Med. Rep.* 15, 1638–1646. doi: 10.3892/mmr.2017.6183
- Feldman, J. L., Baeza, J., and Denu, J. M. (2013). Activation of the protein deacetylase SIRT6 by long-chain fatty acids and widespread deacetylation by mammalian sirtuins. *J. Biol. Chem.* 288, 31350–31356. doi: 10.1074/jbc.C113.511261
- Fiaschi, T., Marini, A., Giannoni, E., Taddei, M. L., Gandellini, P., De Donatis, A., et al. (2012). Reciprocal metabolic reprogramming through lactate shuttle

- coordinately influences tumor-stroma interplay. *Cancer Res.* 72, 5130–5140. doi: 10.1158/0008-5472.CAN-12-1949
- Finley, L. W., Carracedo, A., Lee, J., Souza, A., Egia, A., Zhang, J., et al. (2011). SIRT3 opposes reprogramming of cancer cell metabolism through HIF1 $\alpha$  destabilization. *Cancer Cell* 19, 416–428. doi: 10.1016/j.ccr.2011.02.014
- Finley, L. W., and Haigis, M. C. (2012). Metabolic regulation by SIRT3: implications for tumorigenesis. *Trends Mol. Med.* 18, 516–523. doi: 10.1016/j.molmed.2012.05.004
- Firestein, R., Blander, G., Michan, S., Oberdoerffer, P., Ogino, S., Campbell, J., et al. (2008). The SIRT1 deacetylase suppresses intestinal tumorigenesis and colon cancer growth. *PLoS One* 3:e2020. doi: 10.1371/journal.pone.0002020
- Ford, E., Voit, R., Liszt, G., Magin, C., Grummt, I., and Guarente, L. (2006). Mammalian Sir2 homolog SIRT7 is an activator of RNA polymerase I transcription. *Genes Dev.* 20, 1075–1080. doi: 10.1101/gad.1399706
- Freitag, M., Schemies, J., Larsen, T., El Gaghlab, K., Schulz, F., Rumpf, T., et al. (2011). Synthesis and biological activity of splitomicin analogs targeted at human NAD(+)-dependent histone deacetylases (sirtuins). *Bioorg. Med. Chem.* 19, 3669–3677. doi: 10.1016/j.bmc.2011.01.026
- Garcia-Peterson, L. M., Ndiaye, M. A., Singh, C. K., Chhabra, G., Huang, W., and Ahmad, N. (2017). SIRT6 histone deacetylase functions as a potential oncogene in human melanoma. *Genes Cancer* 8, 701–712. doi: 10.18632/genesandcancer.153
- Geng, Q., Peng, H., Chen, F., Luo, R., and Li, R. (2015). High expression of sirt7 served as a predictor of adverse outcome in breast cancer. *Int. J. Clin. Exp. Pathol.* 8, 1938–1945.
- Grbesa, I., Pajares, M. J., Martinez-Terroba, E., Agorreta, J., Mikecin, A. M., Larrayoz, M., et al. (2015). Expression of sirtuin 1 and 2 is associated with poor prognosis in non-small cell lung cancer patients. *PLoS One* 10:e0124670. doi: 10.1371/journal.pone.0124670
- Grozinger, C. M., Chao, E. D., Blackwell, H. E., Moazed, D., and Schreiber, S. L. (2001). Identification of a class of small molecule inhibitors of the sirtuin family of NAD-dependent deacetylases by phenotypic screening. *J. Biol. Chem.* 276, 38837–38843. doi: 10.1074/jbc.M106779200
- Haider, R., Massa, F., Kaminski, L., Clavel, S., Djabari, Z., Robert, G., et al. (2017). Sirtuin 7: a new marker of aggressiveness in prostate cancer. *Oncotarget* 8, 77309–77316. doi: 10.18632/oncotarget.20468
- Haigis, M. C., Mostoslavsky, R., Haigis, K. M., Fahie, K., Christodoulou, D. C., Murphy, A. J., et al. (2006). SIRT4 inhibits glutamate dehydrogenase and opposes the effects of calorie restriction in pancreatic beta cells. *Cell* 126, 941–954. doi: 10.1016/j.cell.2006.06.057
- Han, L., Liang, X. H., Chen, L. X., Bao, S. M., and Yan, Z. Q. (2013). SIRT1 is highly expressed in brain metastasis tissues of non-small cell lung cancer (NSCLC) and in positive regulation of NSCLC cell migration. *Int. J. Clin. Exp. Pathol.* 6, 2357–2365.
- Hanahan, D., and Weinberg, R. A. (2000). The hallmarks of cancer. *Cell* 100, 57–70. doi: 10.1016/S0092-8674(00)81683-9
- Hanahan, D., and Weinberg, R. A. (2011). Hallmarks of cancer: the next generation. *Cell* 144, 646–674. doi: 10.1016/j.cell.2011.02.013
- Hao, C., Zhu, P. X., Yang, X., Han, Z. P., Jiang, J. H., Zong, C., et al. (2014). Overexpression of SIRT1 promotes metastasis through epithelial-mesenchymal transition in hepatocellular carcinoma. *BMC Cancer* 14:978. doi: 10.1186/1471-2407-14-978
- Heltweg, B., Gattbonton, T., Schuler, A. D., Posakony, J., Li, H., Goehle, S., et al. (2006). Antitumor activity of a small-molecule inhibitor of human silent information regulator 2 enzymes. *Cancer Res.* 66, 4368–4377. doi: 10.1158/0008-5472.CAN-05-3617
- Hershberger, K. A., Martin, A. S., and Hirschey, M. D. (2017). Role of NAD(+) and mitochondrial sirtuins in cardiac and renal diseases. *Nat. Rev. Nephrol.* 13, 213–225. doi: 10.1038/nrneph.2017.5
- Howitz, K. T., Bitterman, K. J., Cohen, H. Y., Lamming, D. W., Lavu, S., Wood, J. G., et al. (2003). Small molecule activators of sirtuins extend *Saccharomyces cerevisiae* lifespan. *Nature* 425, 191–196. doi: 10.1038/nature01960
- Huang, G., and Zhu, G. (2018). Sirtuin-4 (SIRT4), a therapeutic target with oncogenic and tumor-suppressive activity in cancer. *Onco Targets Ther.* 11, 3395–3400. doi: 10.2147/OTT.S157724
- Huang, S., Zhao, Z., Tang, D., Zhou, Q., Li, Y., Zhou, L., et al. (2017). Downregulation of SIRT2 inhibits invasion of hepatocellular carcinoma by inhibiting energy metabolism. *Transl. Oncol.* 10, 917–927. doi: 10.1016/j.tranon.2017.09.006
- Hubbard, B. P., and Sinclair, D. A. (2014). Small molecule SIRT1 activators for the treatment of aging and age-related diseases. *Trends Pharmacol. Sci.* 35, 146–154. doi: 10.1016/j.tips.2013.12.004
- Inoue, T., Hiratsuka, M., Osaki, M., and Oshimura, M. (2007a). The molecular biology of mammalian SIRT proteins: sirt2 in cell cycle regulation. *Cell Cycle* 6, 1011–1018. doi: 10.4161/cc.6.9.4219
- Inoue, T., Hiratsuka, M., Osaki, M., Yamada, H., Kishimoto, I., Yamaguchi, S., et al. (2007b). SIRT2, a tubulin deacetylase, acts to block the entry to chromosome condensation in response to mitotic stress. *Oncogene* 26, 945–957. doi: 10.1038/sj.onc.1209857
- Ioannou, M., Kouvaras, E., Papamichali, R., Samara, M., Chiotoglou, I., and Koukoulis, G. (2018). Smad4 and epithelial-mesenchymal transition proteins in colorectal carcinoma: an immunohistochemical study. *J. Mol. Histol.* 49, 235–244. doi: 10.1007/s10735-018-9763-6
- Ioris, R. M., Galie, M., Ramadori, G., Anderson, J. G., Charollais, A., Konstantinidou, G., et al. (2017). SIRT6 suppresses cancer stem-like capacity in tumors with pi3k activation independently of its deacetylase activity. *Cell Rep.* 18, 1858–1868. doi: 10.1016/j.celrep.2017.01.065
- Iwahara, T., Bonasio, R., Narendra, V., and Reinberg, D. (2012). SIRT3 functions in the nucleus in the control of stress-related gene expression. *Mol. Cell. Biol.* 32, 5022–5034. doi: 10.1128/MCB.00822-12
- Jang, K. Y., Hwang, S. H., Kwon, K. S., Kim, K. R., Choi, H. N., Lee, N. R., et al. (2008). SIRT1 expression is associated with poor prognosis of diffuse large B-cell lymphoma. *Am. J. Surg. Pathol.* 32, 1523–1531. doi: 10.1097/PAS.0b013e31816b6478
- Jang, M., Cai, L., Udeani, G. O., Slowing, K. V., Thomas, C. F., Beecher, C. W., et al. (1997). Cancer chemopreventive activity of resveratrol, a natural product derived from grapes. *Science* 275, 218–220. doi: 10.1126/science.275.5297.218
- Jeong, S. M., and Haigis, M. C. (2015). Sirtuins in cancer: a balancing act between genome stability and metabolism. *Mol. Cells* 38, 750–758. doi: 10.14348/molcells.2015.0167
- Jeong, S. M., Lee, A., Lee, J., and Haigis, M. C. (2014). SIRT4 protein suppresses tumor formation in genetic models of Myc-induced B cell lymphoma. *J. Biol. Chem.* 289, 4135–4144. doi: 10.1074/jbc.M113.525949
- Jeong, S. M., Xiao, C., Finley, L. W., Lahusen, T., Souza, A. L., Pierce, K., et al. (2013). SIRT4 has tumor-suppressive activity and regulates the cellular metabolic response to DNA damage by inhibiting mitochondrial glutamine metabolism. *Cancer Cell* 23, 450–463. doi: 10.1016/j.ccr.2013.02.024
- Jiang, H., Khan, S., Wang, Y., Charron, G., He, B., Sebastian, C., et al. (2013). SIRT6 regulates TNF- $\alpha$  secretion through hydrolysis of long-chain fatty acyl lysine. *Nature* 496, 110–113. doi: 10.1038/nature12038
- Jin, K. L., Park, J. Y., Noh, E. J., Hoe, K. L., Lee, J. H., Kim, J. H., et al. (2010). The effect of combined treatment with cisplatin and histone deacetylase inhibitors on HeLa cells. *J. Gynecol. Oncol.* 21, 262–268. doi: 10.3802/jgo.2010.21.4.262
- Jin, X., Wei, Y., Xu, F., Zhao, M., Dai, K., Shen, R., et al. (2018). SIRT1 promotes formation of breast cancer through modulating akt activity. *J. Cancer* 9, 2012–2023. doi: 10.7150/jca.24275
- Jung-Hynes, B., Nihal, M., Zhong, W., and Ahmad, N. (2009). Role of sirtuin histone deacetylase SIRT1 in prostate cancer. a target for prostate cancer management via its inhibition? *J. Biol. Chem.* 284, 3823–3832. doi: 10.1074/jbc.M807869200
- Kim, H. S., Vassilopoulos, A., Wang, R. H., Lahusen, T., Xiao, Z., Xu, X., et al. (2011). SIRT2 maintains genome integrity and suppresses tumorigenesis through regulating APC/C activity. *Cancer Cell* 20, 487–499. doi: 10.1016/j.ccr.2011.09.004
- Kim, J. K., Noh, J. H., Jung, K. H., Eun, J. W., Bae, H. J., Kim, M. G., et al. (2013). Sirtuin7 oncogenic potential in human hepatocellular carcinoma and its regulation by the tumor suppressors MiR-125a-5p and MiR-125b. *Hepatology* 57, 1055–1067. doi: 10.1002/hep.26101
- Kojima, K., Ohhashi, R., Fujita, Y., Hamada, N., Akao, Y., Nozawa, Y., et al. (2008). A role for SIRT1 in cell growth and chemoresistance in prostate cancer PC3 and DU145 cells. *Biochem. Biophys. Res. Commun.* 373, 423–428. doi: 10.1016/j.bbrc.2008.06.045
- Kozako, T., Aikawa, A., Shoji, T., Fujimoto, T., Yoshimitsu, M., Shirasawa, S., et al. (2012). High expression of the longevity gene product SIRT1 and apoptosis



- induction by sirtinol in adult T-cell leukemia cells. *Int. J. Cancer* 131, 2044–2055. doi: 10.1002/ijc.27481
- Kugel, S., Sebastian, C., Fitamant, J., Ross, K. N., Saha, S. K., Jain, E., et al. (2016). SIRT6 suppresses pancreatic cancer through control of lin28b. *Cell* 165, 1401–1415. doi: 10.1016/j.cell.2016.04.033
- Kumar, S., and Lombard, D. B. (2015). Mitochondrial sirtuins and their relationships with metabolic disease and cancer. *Antioxid. Redox Signal.* 22, 1060–1077. doi: 10.1089/ars.2014.6213
- Lahusen, T. J., and Deng, C. X. (2015). SIRT1720 induces lysosomal-dependent cell death of breast cancer cells. *Mol. Cancer Ther.* 14, 183–192. doi: 10.1158/1535-7163.MCT-14-0584
- Lai, C. C., Lin, P. M., Lin, S. F., Hsu, C. H., Lin, H. C., Hu, M. L., et al. (2013). Altered expression of SIRT gene family in head and neck squamous cell carcinoma. *Tumour Biol.* 34, 1847–1854. doi: 10.1007/s13277-013-0726-y
- Lain, S., Hollick, J. J., Campbell, J., Staples, O. D., Higgins, M., Aoubala, M., et al. (2008). Discovery, in vivo activity, and mechanism of action of a small-molecule p53 activator. *Cancer Cell* 13, 454–463. doi: 10.1016/j.ccr.2008.03.004
- Lamouille, S., Xu, J., and Derynck, R. (2014). Molecular mechanisms of epithelial-mesenchymal transition. *Nat. Rev. Mol. Cell Biol.* 15, 178–196. doi: 10.1038/nrm3758
- Lara, E., Mai, A., Calvanese, V., Altucci, L., Lopez-Nieva, P., Martinez-Chantar, M. L., et al. (2009). Salermide, a Sirtuin inhibitor with a strong cancer-specific proapoptotic effect. *Oncogene* 28, 781–791. doi: 10.1038/onc.2008.436
- Lee, M., Kim, D. W., Yoon, H., So, D., Khalmuratova, R., Rhee, C. S., et al. (2016). Sirtuin 1 attenuates nasal polypogenesis by suppressing epithelial-to-mesenchymal transition. *J. Allergy Clin. Immunol.* 137, 87.e7–98.e7. doi: 10.1016/j.jaci.2015.07.026
- Levy, L., and Hill, C. S. (2005). Smad4 dependency defines two classes of transforming growth factor  $\beta$  (TGF- $\beta$ ) target genes and distinguishes TGF- $\beta$ -induced epithelial-mesenchymal transition from its antiproliferative and migratory responses. *Mol. Cell Biol.* 25, 8108–8125. doi: 10.1128/MCB.25.18.8108-8125.2005
- Li, H., Li, H., Qu, H., Zhao, M., Yuan, B., Cao, M., et al. (2015). Suramin inhibits cell proliferation in ovarian and cervical cancer by downregulating heparanase expression. *Cancer Cell Int.* 15:52. doi: 10.1186/s12935-015-0196-y
- Li, H., Zhao, J., Zhang, J. W., Huang, Q. Y., Huang, J. Z., Chi, L. S., et al. (2013). MicroRNA-217, down-regulated in clear cell renal cell carcinoma and associated with lower survival, suppresses cell proliferation and migration. *Neoplasma* 60, 511–515. doi: 10.4149/neo\_2013\_066
- Li, L., Shi, L., Yang, S., Yan, R., Zhang, D., Yang, J., et al. (2016). SIRT7 is a histone desuccinylase that functionally links to chromatin compaction and genome stability. *Nat. Commun.* 7:12235. doi: 10.1038/ncomms12235
- Li, S., Banck, M., Mujtaba, S., Zhou, M. M., Sugrue, M. M., and Walsh, M. J. (2010). p53-induced growth arrest is regulated by the mitochondrial SirT3 deacetylase. *PLoS One* 5:e10486. doi: 10.1371/journal.pone.0010486
- Li, W., Zhu, D., and Qin, S. (2018). SIRT7 suppresses the epithelial-to-mesenchymal transition in oral squamous cell carcinoma metastasis by promoting SMAD4 deacetylation. *J. Exp. Clin. Cancer Res.* 37:148. doi: 10.1186/s13046-018-0819-y
- Liberti, M. V., and Locasale, J. W. (2016). The warburg effect: how does it benefit cancer cells? *Trends Biochem. Sci.* 41, 211–218. doi: 10.1016/j.tibs.2015.12.001
- Lin, Z., and Fang, D. (2013). The roles of SIRT1 in cancer. *Genes Cancer* 4, 97–104. doi: 10.1177/1947601912475079
- Link, A., Balaguer, F., and Goel, A. (2010). Cancer chemoprevention by dietary polyphenols: promising role for epigenetics. *Biochem. Pharmacol.* 80, 1771–1792. doi: 10.1016/j.bcp.2010.06.036
- Liu, C., Huang, Z., Jiang, H., and Shi, F. (2014). The sirtuin 3 expression profile is associated with pathological and clinical outcomes in colon cancer patients. *Biomed. Res. Int.* 2014:871263. doi: 10.1155/2014/871263
- Liu, P. Y., Xu, N., Malyukova, A., Scarlett, C. J., Sun, Y. T., Zhang, X. D., et al. (2013). The histone deacetylase SIRT2 stabilizes myc oncoproteins. *Cell Death Differ.* 20, 503–514. doi: 10.1038/cdd.2012.147
- Lombard, D. B., Tishkoff, D. X., and Bao, J. (2011). Mitochondrial sirtuins in the regulation of mitochondrial activity and metabolic adaptation. *Handb. Exp. Pharmacol.* 206, 163–188. doi: 10.1007/978-3-642-21631-2\_8
- Long, Q., Xu, J., Osunkoya, A. O., Sannigrahi, S., Johnson, B. A., Zhou, W., et al. (2014). Global transcriptome analysis of formalin-fixed prostate cancer specimens identifies biomarkers of disease recurrence. *Cancer Res.* 74, 3228–3237. doi: 10.1158/0008-5472.CAN-13-2699
- Lu, W., Zuo, Y., Feng, Y., and Zhang, M. (2014). SIRT5 facilitates cancer cell growth and drug resistance in non-small cell lung cancer. *Tumour Biol.* 35, 10699–10705. doi: 10.1007/s13277-014-2372-4
- Malik, S., Villanova, L., Tanaka, S., Aonuma, M., Roy, N., Berber, E., et al. (2015). SIRT7 inactivation reverses metastatic phenotypes in epithelial and mesenchymal tumors. *Sci. Rep.* 5:9841. doi: 10.1038/srep09841
- Mao, Z., Hine, C., Tian, X., Van Meter, M., Au, M., Vaidya, A., et al. (2011). SIRT6 promotes DNA repair under stress by activating PARP1. *Science* 332, 1443–1446. doi: 10.1126/science.1202723
- Marfe, G., Tafani, M., Indelicato, M., Sinibaldi-Salimei, P., Reali, V., Pucci, B., et al. (2009). Kaempferol induces apoptosis in two different cell lines via akt inactivation, bax and SIRT3 activation, and mitochondrial dysfunction. *J. Cell Biochem.* 106, 643–650. doi: 10.1002/jcb.22044
- McGlynn, L. M., Zino, S., MacDonald, A. I., Curle, J., Reilly, J. E., Mohammed, Z. M., et al. (2014). SIRT2: tumour suppressor or tumour promoter in operable breast cancer? *Eur. J. Cancer* 50, 290–301. doi: 10.1016/j.ejca.2013.10.005
- McGuinness, D., McGuinness, D. H., McCaul, J. A., and Shiels, P. G. (2011). Sirtuins, bioageing, and cancer. *J. Aging Res.* 2011:235754. doi: 10.4061/2011/235754
- Meyers, M. O., Gagliardi, A. R., Flattmann, G. J., Su, J. L., Wang, Y. Z., and Woltering, E. A. (2000). Suramin analogs inhibit human angiogenesis in vitro. *J. Surg. Res.* 91, 130–134. doi: 10.1006/jsre.2000.5920
- Michishita, E., McCord, R. A., Berber, E., Kioi, M., Padilla-Nash, H., Damian, M., et al. (2008). SIRT6 is a histone H3 lysine 9 deacetylase that modulates telomeric chromatin. *Nature* 452, 492–496. doi: 10.1038/nature06736
- Michishita, E., McCord, R. A., Boxer, L. D., Barber, M. F., Hong, T., Gozani, O., et al. (2009). Cell cycle-dependent deacetylation of telomeric histone H3 lysine K56 by human SIRT6. *Cell Cycle* 8, 2664–2666. doi: 10.4161/cc.8.16.9367
- Michishita, E., Park, J. Y., Burnes, J. M., Barrett, J. C., and Horikawa, I. (2005). Evolutionarily conserved and nonconserved cellular localizations and functions of human SIRT proteins. *Mol. Biol. Cell* 16, 4623–4635. doi: 10.1091/mbc.e05-01-0033
- Miyo, M., Yamamoto, H., Konno, M., Colvin, H., Nishida, N., Koseki, J., et al. (2015). Tumour-suppressive function of SIRT4 in human colorectal cancer. *Br. J. Cancer* 113, 492–499. doi: 10.1038/bjc.2015.226
- Murphy, M. P. (2013). Mitochondrial dysfunction indirectly elevates ROS production by the endoplasmic reticulum. *Cell Metab.* 18, 145–146. doi: 10.1016/j.cmet.2013.07.006
- Napper, A. D., Hixon, J., McDonagh, T., Keavey, K., Pons, J. F., Barker, J., et al. (2005). Discovery of indoles as potent and selective inhibitors of the deacetylase SIRT1. *J. Med. Chem.* 48, 8045–8054. doi: 10.1021/jm050522v
- Nebbio, A., Tambaro, F. P., Dell'Aversana, C., and Altucci, L. (2018). Cancer epigenetics: moving forward. *PLoS Genet.* 14:e1007362. doi: 10.1371/journal.pgen.1007362
- Neugebauer, R. C., Uchichowska, U., Meier, R., Hruby, H., Valkov, V., Verdin, E., et al. (2008). Structure-activity studies on splitomicin derivatives as sirtuin inhibitors and computational prediction of binding mode. *J. Med. Chem.* 51, 1203–1213. doi: 10.1021/jm700972e
- Nguyen, P., Lee, S., Loran-Leins, D., Trepel, J., and Smart, D. K. (2014). SIRT2 interacts with beta-catenin to inhibit wnt signaling output in response to radiation-induced stress. *Mol. Cancer Res.* 12, 1244–1253. doi: 10.1158/1541-7786.MCR-14-0223-T
- Nie, Y., Erion, D. M., Yuan, Z., Dietrich, M., Shulman, G. I., Horvath, T. L., et al. (2009). STAT3 inhibition of gluconeogenesis is downregulated by SirT1. *Nat. Cell Biol.* 11, 492–500. doi: 10.1038/ncb1857
- O'Callaghan, C., and Vassilopoulos, A. (2017). Sirtuins at the crossroads of stemness, aging, and cancer. *Aging Cell* 16, 1208–1218. doi: 10.1111/acel.12685
- Ohanna, M., Bonet, C., Bille, K., Allegra, M., Davidson, I., Bahadoran, P., et al. (2014). SIRT1 promotes proliferation and inhibits the senescence-like phenotype in human melanoma cells. *Oncotarget* 5, 2085–2095. doi: 10.18632/oncotarget.1791
- Onyango, P., Celic, I., McCaffery, J. M., Boeke, J. D., and Feinberg, A. P. (2002). SIRT3, a human SIR2 homologue, is an NAD-dependent deacetylase localized to mitochondria. *Proc. Natl. Acad. Sci. U.S.A.* 99, 13653–13658. doi: 10.1073/pnas.222538099



- Oon, C. E., Strell, C., Yeong, K. Y., Ostman, A., and Prakash, J. (2015). SIRT1 inhibition in pancreatic cancer models: contrasting effects in vitro and in vivo. *Eur. J. Pharmacol.* 757, 59–67. doi: 10.1016/j.ejphar.2015.03.064
- Ota, H., Tokunaga, E., Chang, K., Hikasa, M., Iijima, K., Eto, M., et al. (2006). Sirt1 inhibitor, Sirtinol, induces senescence-like growth arrest with attenuated Ras-MAPK signaling in human cancer cells. *Oncogene* 25, 176–185. doi: 10.1038/sj.onc.1209049
- Palmirotta, R., Cives, M., Della-Morte, D., Capuani, B., Lauro, D., Guadagni, F., et al. (2016). Sirtuins and cancer: role in the epithelial-mesenchymal transition. *Oxid. Med. Cell Longev.* 2016:3031459. doi: 10.1155/2016/3031459
- Pan, P. W., Feldman, J. L., Devries, M. K., Dong, A., Edwards, A. M., and Denu, J. M. (2011). Structure and biochemical functions of SIRT6. *J. Biol. Chem.* 286, 14575–14587. doi: 10.1074/jbc.M111.218990
- Parihar, P., Solanki, I., Mansuri, M. L., and Parihar, M. S. (2015). Mitochondrial sirtuins: emerging roles in metabolic regulations, energy homeostasis and diseases. *Exp. Gerontol.* 61, 130–141. doi: 10.1016/j.exger.2014.12.004
- Park, S. H., Ozden, O., Jiang, H., Cha, Y. I., Pennington, J. D., Aykin-Burns, N., et al. (2011). Sirt3, mitochondrial ros, ageing, and carcinogenesis. *Int. J. Mol. Sci.* 12, 6226–6239. doi: 10.3390/ijms12096226
- Peck, B., Chen, C. Y., Ho, K. K., Di Fruscia, P., Myatt, S. S., Coombes, R. C., et al. (2010). SIRT inhibitors induce cell death and p53 acetylation through targeting both SIRT1 and SIRT2. *Mol. Cancer Ther.* 9, 844–855. doi: 10.1158/1535-7163.MCT-09-0971
- Popat, R., Plesner, T., Davies, F., Cook, G., Cook, M., Elliott, P., et al. (2013). A phase 2 study of SRT501 (resveratrol) with bortezomib for patients with relapsed and/or refractory multiple myeloma. *Br. J. Haematol.* 160, 714–717. doi: 10.1111/bjh.12154
- Qu, N., Hu, J. Q., Liu, L., Zhang, T. T., Sun, G. H., Shi, R. L., et al. (2017). SIRT6 is upregulated and associated with cancer aggressiveness in papillary thyroid cancer via BRAF/ERK/Mcl1 pathway. *Int. J. Oncol.* 50, 1683–1692. doi: 10.3892/ijo.2017.3951
- Rifai, K., Judes, G., Idrissou, M., Daures, M., Bignon, Y. J., Penault-Llorca, F., et al. (2017). Dual SIRT1 expression patterns strongly suggests its bivalent role in human breast cancer. *Oncotarget* 8, 110922–110930. doi: 10.18632/oncotarget.23006
- Rotili, D., Tarantino, D., Nebbioso, A., Paolini, C., Huidobro, C., Lara, E., et al. (2012). Discovery of salermide-related sirtuin inhibitors: binding mode studies and antiproliferative effects in cancer cells including cancer stem cells. *J. Med. Chem.* 55, 10937–10947. doi: 10.1021/jm3011614
- Sauve, A. A. (2010). Sirtuin chemical mechanisms. *Biochim. Biophys. Acta* 1804, 1591–1603. doi: 10.1016/j.bbapap.2010.01.021
- Sebastian, C., and Mostoslavsky, R. (2015). The role of mammalian sirtuins in cancer metabolism. *Semin. Cell Dev. Biol.* 43, 33–42. doi: 10.1016/j.semdb.2015.07.008
- Serrano-Gomez, S. J., Maziveyi, M., and Alahari, S. K. (2016). Regulation of epithelial-mesenchymal transition through epigenetic and post-translational modifications. *Mol. Cancer* 15:18. doi: 10.1186/s12943-016-0502-x
- Shen, S. Q., Huang, L. S., Xiao, X. L., Zhu, X. F., Xiong, D. D., Cao, X. M., et al. (2017). miR-204 regulates the biological behavior of breast cancer MCF-7 cells by directly targeting FOXA1. *Oncol. Rep.* 38, 368–376. doi: 10.3892/or.2017.5644
- Shi, Q., Liu, T., Zhang, X., Geng, J., He, X., Nu, M., et al. (2016). Decreased sirtuin 4 expression is associated with poor prognosis in patients with invasive breast cancer. *Oncol. Lett.* 12, 2606–2612. doi: 10.3892/ol.2016.5021
- Shi, Y., Zhou, Y., Wang, S., and Zhang, Y. (2013). Sirtuin deacetylation mechanism and catalytic role of the dynamic cofactor binding loop. *J. Phys. Chem. Lett.* 4, 491–495. doi: 10.1021/jz302015s
- Shrestha, S., Yang, C. D., Hong, H. C., Chou, C. H., Tai, C. S., Chiew, M. Y., et al. (2017). Integrated microRNA-mRNA analysis reveals miR-204 inhibits cell proliferation in gastric cancer by targeting CKS1B, CXCL1 and GPRC5A. *Int. J. Mol. Sci.* 19, E87. doi: 10.3390/ijms19010087
- Shuang, T., Wang, M., Zhou, Y., and Shi, C. (2015). Over-expression of Sirt1 contributes to chemoresistance and indicates poor prognosis in serous epithelial ovarian cancer (EOC). *Med. Oncol.* 32:260. doi: 10.1007/s12032-015-0706-8
- Simic, P., Williams, E. O., Bell, E. L., Gong, J. J., Bonkowski, M., and Guarente, L. (2013). SIRT1 suppresses the epithelial-to-mesenchymal transition in cancer metastasis and organ fibrosis. *Cell Rep.* 3, 1175–1186. doi: 10.1016/j.celrep.2013.03.019
- Song, S., Fajol, A., Tu, X., Ren, B., and Shi, S. (2016). miR-204 suppresses the development and progression of human glioblastoma by targeting ATF2. *Oncotarget* 7, 70058–70065. doi: 10.18632/oncotarget.11732
- Song, S., Wientjes, M. G., Gan, Y., and Au, J. L. (2000). Fibroblast growth factors: an epigenetic mechanism of broad spectrum resistance to anticancer drugs. *Proc. Natl. Acad. Sci. U.S.A.* 97, 8658–8663. doi: 10.1073/pnas.140210697
- Stein, C. A., LaRocca, R. V., Thomas, R., McAtee, N., and Myers, C. E. (1989). Suramin: an anticancer drug with a unique mechanism of action. *J. Clin. Oncol.* 7, 499–508. doi: 10.1200/JCO.1989.7.4.499
- Sullivan, L. B., and Chandel, N. S. (2014). Mitochondrial reactive oxygen species and cancer. *Cancer Metab.* 2:17. doi: 10.1186/2049-3002-2-17
- Sun, L., Li, H., Chen, J., Dehennaut, V., Zhao, Y., Yang, Y., et al. (2013a). A Sumoylation-dependent pathway regulates SIRT1 transcription and lung cancer metastasis. *J. Natl. Cancer Inst.* 105, 887–898. doi: 10.1093/jnci/djt118
- Sun, L., Li, H., Chen, J., Iwasaki, Y., Kubota, T., Matsuoka, M., et al. (2013b). PIASy mediates hypoxia-induced SIRT1 transcriptional repression and epithelial-to-mesenchymal transition in ovarian cancer cells. *J. Cell Sci.* 126(Pt 17), 3939–3947. doi: 10.1242/jcs.127381
- Sun, T., Jiao, L., Wang, Y., Yu, Y., and Ming, L. (2018). SIRT1 induces epithelial-mesenchymal transition by promoting autophagic degradation of E-cadherin in melanoma cells. *Cell Death Dis.* 9:136. doi: 10.1038/s41419-017-0167-4
- Suzuki, K., Hayashi, R., Ichikawa, T., Imanishi, S., Yamada, T., Inomata, M., et al. (2012). SIRT1720, a SIRT1 activator, promotes tumor cell migration, and lung metastasis of breast cancer in mice. *Oncol. Rep.* 27, 1726–1732. doi: 10.3892/or.2012.1750
- Tan, M., Peng, C., Anderson, K. A., Chhoy, P., Xie, Z., Dai, L., et al. (2014). Lysine glutarylation is a protein posttranslational modification regulated by SIRT5. *Cell Metab.* 19, 605–617. doi: 10.1016/j.cmet.2014.03.014
- Tang, X., Shi, L., Xie, N., Liu, Z., Qian, M., Meng, F., et al. (2017). SIRT7 antagonizes TGF-beta signaling and inhibits breast cancer metastasis. *Nat. Commun.* 8:318. doi: 10.1038/s41467-017-00396-9
- Tasselli, L., Xi, Y., Zheng, W., Tennen, R. I., Odrowaz, Z., Simeoni, F., et al. (2016). SIRT6 deacetylates H3K18ac at pericentric chromatin to prevent mitotic errors and cellular senescence. *Nat. Struct. Mol. Biol.* 23, 434–440. doi: 10.1038/nsmb.3202
- Torrens-Mas, M., Oliver, J., Roca, P., and Sastre-Serra, J. (2017). SIRT3: oncogene and tumor suppressor in cancer. *Cancers* 9:90. doi: 10.3390/cancers9070090
- Vaquero, A. (2009). The conserved role of sirtuins in chromatin regulation. *Int. J. Dev. Biol.* 53, 303–322. doi: 10.1387/ijdb.082675av
- Vaziri, H., Dessain, S. K., Ng Eaton, E., Imai, S. I., Frye, R. A., Pandita, T. K., et al. (2001). hSIR2(SIRT1) functions as an NAD-dependent p53 deacetylase. *Cell* 107, 149–159. doi: 10.1016/S0092-8674(01)00527-X
- Villalona-Calero, M. A., Otterson, G. A., Wientjes, M. G., Weber, F., Bekaii-Saab, T., Young, D., et al. (2008). Noncytotoxic suramin as a chemosensitizer in patients with advanced non-small-cell lung cancer: a phase II study. *Ann. Oncol.* 19, 1903–1909. doi: 10.1093/annonc/mdn412
- Voogd, T. E., Vansterkenburg, E. L., Wilting, J., and Janssen, L. H. (1993). Recent research on the biological activity of suramin. *Pharmacol. Rev.* 45, 177–203.
- Wang, C., Yang, W., Dong, F., Guo, Y., Tan, J., Ruan, S., et al. (2017). The prognostic role of Sirt1 expression in solid malignancies: a meta-analysis. *Oncotarget* 8, 66343–66351. doi: 10.18632/oncotarget.18494
- Wang, H. L., Lu, R. Q., Xie, S. H., Zheng, H., Wen, X. M., Gao, X., et al. (2015). SIRT7 exhibits oncogenic potential in human ovarian cancer cells. *Asian Pac. J. Cancer Prev.* 16, 3573–3577. doi: 10.7314/APJCP.2015.16.8.3573
- Wang, J. C., Kafeel, M. I., Avezbakiyev, B., Chen, C., Sun, Y., Rathnasabapathy, C., et al. (2011). Histone deacetylase in chronic lymphocytic leukemia. *Oncology* 81, 325–329. doi: 10.1159/000334577
- Wang, Y. Q., Wang, H. L., Xu, J., Tan, J., Fu, L. N., Wang, J. L., et al. (2018). Sirtuin5 contributes to colorectal carcinogenesis by enhancing glutaminolysis in a deglutarylation-dependent manner. *Nat. Commun.* 9:545. doi: 10.1038/s41467-018-02951-4
- Wei, W., Jing, Z. X., Ke, Z., and Yi, P. (2017). Sirtuin 7 plays an oncogenic role in human osteosarcoma via downregulating CDC4 expression. *Am. J. Cancer Res.* 7, 1788–1803.
- Wilking, M. J., and Ahmad, N. (2015). The role of SIRT1 in cancer: the saga continues. *Am. J. Pathol.* 185, 26–28. doi: 10.1016/j.ajpath.2014.10.002
- Wilking, M. J., Singh, C., Nihal, M., Zhong, W., and Ahmad, N. (2014). SIRT1 deacetylase is overexpressed in human melanoma and its small molecule

- inhibition imparts anti-proliferative response via p53 activation. *Arch. Biochem. Biophys.* 563, 94–100. doi: 10.1016/j.abb.2014.04.001
- Xiao, Z., Chen, C., Meng, T., Zhang, W., and Zhou, Q. (2016). Resveratrol attenuates renal injury and fibrosis by inhibiting transforming growth factor-beta pathway on matrix metalloproteinase 7. *Exp. Biol. Med.* 241, 140–146. doi: 10.1177/1535370215598401
- Xu, J., Zhu, W., Xu, W., Yao, W., Zhang, B., Xu, Y., et al. (2013). Up-regulation of MBD1 promotes pancreatic cancer cell epithelial-mesenchymal transition and invasion by epigenetic down-regulation of E-cadherin. *Curr. Mol. Med.* 13, 387–400.
- Yang, B., Fu, X., Shao, L., Ding, Y., and Zeng, D. (2014). Aberrant expression of SIRT3 is conversely correlated with the progression and prognosis of human gastric cancer. *Biochem. Biophys. Res. Commun.* 443, 156–160. doi: 10.1016/j.bbrc.2013.11.068
- Yang, M. H., Laurent, G., Bause, A. S., Spang, R., German, N., Haigis, M. C., et al. (2013). HDAC6 and SIRT2 regulate the acetylation state and oncogenic activity of mutant K-RAS. *Mol. Cancer Res.* 11, 1072–1077. doi: 10.1158/1541-7786.MCR-13-0040-T
- Yang, X., Liu, B., Zhu, W., and Luo, J. (2015). SIRT5, functions in cellular metabolism with a multiple enzymatic activities. *Sci. China Life Sci.* 58, 912–914. doi: 10.1007/s11427-015-4902-8
- Yi, Y. W., Kang, H. J., Kim, H. J., Kong, Y., Brown, M. L., and Bae, I. (2013). Targeting mutant p53 by a SIRT1 activator YK-3-237 inhibits the proliferation of triple-negative breast cancer cells. *Oncotarget* 4, 984–994. doi: 10.18632/oncotarget.1070
- Yu, H., Ye, W., Wu, J., Meng, X., Liu, R. Y., Ying, X., et al. (2014). Overexpression of sirt7 exhibits oncogenic property and serves as a prognostic factor in colorectal cancer. *Clin. Cancer Res.* 20, 3434–3445. doi: 10.1158/1078-0432.CCR-13-2952
- Yuan, H., Wang, Z., Li, L., Zhang, H., Modi, H., Horne, D., et al. (2012). Activation of stress response gene SIRT1 by BCR-ABL promotes leukemogenesis. *Blood* 119, 1904–1914. doi: 10.1182/blood-2011-06-361691
- Yuan, J., Minter-Dykhouse, K., and Lou, Z. (2009). A c-Myc-SIRT1 feedback loop regulates cell growth and transformation. *J. Cell Biol.* 185, 203–211. doi: 10.1083/jcb.200809167
- Zhang, J. G., Hong, D. F., Zhang, C. W., Sun, X. D., Wang, Z. F., Shi, Y., et al. (2014). Sirtuin 1 facilitates chemoresistance of pancreatic cancer cells by regulating adaptive response to chemotherapy-induced stress. *Cancer Sci.* 105, 445–454. doi: 10.1111/cas.12364
- Zhang, L., Wang, X., and Chen, P. (2013). MiR-204 down regulates SIRT1 and reverts SIRT1-induced epithelial-mesenchymal transition, anoikis resistance and invasion in gastric cancer cells. *BMC Cancer* 13:290. doi: 10.1186/1471-2407-13-290
- Zhang, P. Y., Li, G., Deng, Z. J., Liu, L. Y., Chen, L., Tang, J. Z., et al. (2016). Dicer interacts with SIRT7 and regulates H3K18 deacetylation in response to DNA damaging agents. *Nucleic Acids Res.* 44, 3629–3642. doi: 10.1093/nar/gkv1504
- Zhang, S., Huang, S., Deng, C., Cao, Y., Yang, J., Chen, G., et al. (2017a). Co-ordinated overexpression of SIRT1 and STAT3 is associated with poor survival outcome in gastric cancer patients. *Oncotarget* 8, 18848–18860. doi: 10.18632/oncotarget.14473
- Zhang, X., Spiegelman, N. A., Nelson, O. D., Jing, H., and Lin, H. (2017b). SIRT6 regulates Ras-related protein R-Ras2 by lysine defatty-acylation. *eLife* 6:e25158. doi: 10.7554/eLife.25158
- Zhang, T., and Kraus, W. L. (2010). SIRT1-dependent regulation of chromatin and transcription: linking NAD(+) metabolism and signaling to the control of cellular functions. *Biochim. Biophys. Acta* 1804, 1666–1675. doi: 10.1016/j.bbapap.2009.10.022
- Zhang, Y., Song, S., Yang, F., Au, J. L., and Wientjes, M. G. (2001). Nontoxic doses of suramin enhance activity of doxorubicin in prostate tumors. *J. Pharmacol. Exp. Ther.* 299, 426–433.
- Zhang, Z. G., and Qin, C. Y. (2014). Sirt6 suppresses hepatocellular carcinoma cell growth via inhibiting the extracellular signal-regulated kinase signaling pathway. *Mol. Med. Rep.* 9, 882–888. doi: 10.3892/mmr.2013.1879
- Zhao, W. G., Yu, S. N., Lu, Z. H., Ma, Y. H., Gu, Y. M., and Chen, J. (2010). The miR-217 microRNA functions as a potential tumor suppressor in pancreatic ductal adenocarcinoma by targeting KRAS. *Carcinogenesis* 31, 1726–1733. doi: 10.1093/carcin/bgq160
- Zhou, L., Wang, Q., Chen, X., Fu, L., Zhang, X., Wang, L., et al. (2017). AML1-ETO promotes SIRT1 expression to enhance leukemogenesis of t(8;21) acute myeloid leukemia. *Exp. Hematol.* 46, 62–69. doi: 10.1016/j.exphem.2016.09.013
- Zwaans, B. M., and Lombard, D. B. (2014). Interplay between sirtuins, MYC and hypoxia-inducible factor in cancer-associated metabolic reprogramming. *Dis. Model. Mech.* 7, 1023–1032. doi: 10.1242/dmm.016287

**Conflict of Interest Statement:** The authors declare that the research was conducted in the absence of any commercial or financial relationships that could be construed as a potential conflict of interest.

Copyright © 2019 Carafa, Altucci and Nebbioso. This is an open-access article distributed under the terms of the Creative Commons Attribution License (CC BY). The use, distribution or reproduction in other forums is permitted, provided the original author(s) and the copyright owner(s) are credited and that the original publication in this journal is cited, in accordance with accepted academic practice. No use, distribution or reproduction is permitted which does not comply with these terms.



# Estrogens Modulate Somatostatin Receptors Expression and Synergize With the Somatostatin Analog Pasireotide in Prostate Cells

Valentina Rossi<sup>1†</sup>, Erika Di Zazzo<sup>1†</sup>, Giovanni Galasso<sup>1</sup>, Caterina De Rosa<sup>1</sup>,  
Ciro Abbondanza<sup>1</sup>, Antonio A. Sinisi<sup>2</sup>, Lucia Altucci<sup>1</sup>, Antimo Migliaccio<sup>1</sup> and  
Gabriella Castoria<sup>1\*</sup>

<sup>1</sup> Dipartimento di Medicina di Precisione, Università degli Studi della Campania "Luigi Vanvitelli", Naples, Italy, <sup>2</sup> Dipartimento di Scienze Mediche, Chirurgiche, Neurologiche, Metaboliche e dell'Invecchiamento, Università degli Studi della Campania "Luigi Vanvitelli", Naples, Italy

## OPEN ACCESS

### Edited by:

Sergio Valente,  
Sapienza Università di Roma, Italy

### Reviewed by:

Elisabetta Ferretti,  
Sapienza Università di Roma, Italy  
Daniela Triscioglio,  
Istituto di Biologia e Patologia  
Molecolari (IBPM), Consiglio  
Nazionale delle Ricerche (CNR), Italy

### \*Correspondence:

Gabriella Castoria  
gabriella.castoria@unicampania.it

<sup>†</sup>These authors have contributed  
equally to this work

### Specialty section:

This article was submitted to  
Experimental Pharmacology  
and Drug Discovery,  
a section of the journal  
Frontiers in Pharmacology

**Received:** 26 September 2018

**Accepted:** 11 January 2019

**Published:** 15 February 2019

### Citation:

Rossi V, Di Zazzo E, Galasso G,  
De Rosa C, Abbondanza C, Sinisi AA,  
Altucci L, Migliaccio A and Castoria G  
(2019) Estrogens Modulate  
Somatostatin Receptors Expression  
and Synergize With the Somatostatin  
Analog Pasireotide in Prostate Cells.  
Front. Pharmacol. 10:28.  
doi: 10.3389/fphar.2019.00028

Prostate cancer (PC) is one of the most frequently diagnosed cancers and a leading cause of cancer-related deaths in Western society. Current PC therapies prevalently target the functions of androgen receptor (AR) and may only be effective within short time periods, beyond which the majority of PC patients progress to castration-resistant PC (CRPC) and metastatic disease. The role of estradiol/estradiol receptor (ER) axis in prostate transformation and PC progression is well established. Further, considerable efforts have been made to investigate the mechanism by which somatostatin (SST) and somatostatin receptors (SSTRs) influence PC growth and progression. A number of therapeutic strategies, such as the combination of SST analogs with other drugs, show, indeed, strong promise. However, the effect of the combined treatment of SST analogs and estradiol on proliferation, epithelial mesenchyme transition (EMT) and migration of normal- and cancer-derived prostate cells has not been investigated so far. We now report that estradiol plays anti-proliferative and pro-apoptotic effect in non-transformed EPN prostate cells, which express both ER $\alpha$  and ER $\beta$ . A weak apoptotic effect is observed in transformed CPEC cells that only express low levels of ER $\beta$ . Estradiol increases, mainly through ER $\alpha$  activation, the expression of SSTRs in EPN, but not CPEC cells. As such, the hormone enhances the anti-proliferative effect of the SST analog, pasireotide in EPN, but not CPEC cells. Estradiol does not induce EMT and the motility of EPN cells, while it promotes EMT and migration of CPEC cells. Addition of pasireotide does not significantly modify these responses. Altogether, our results suggest that pasireotide may be used, alone or in combination with other drugs, to limit the growth of prostate proliferative diseases, provided that both ER isoforms ( $\alpha$  and  $\beta$ ) are present. Further investigations are needed to better define the cross talk between estrogens and SSTRs as well as its role in PC.

**Keywords:** prostate cancer, estrogens, somatostatin analogs, somatostatin receptors, apoptosis, EMT, migration

**Abbreviations:** ADT, androgen deprivation therapy; AR, androgen receptor; BC, breast cancer; CRPC, castrate resistant prostate cancer; EMT, epithelial mesenchymal transition; ER, estrogen receptor; PC, prostate cancer; PSA, prostate specific antigen; SST, somatostatin; SSTR, somatostatin receptor.

## INTRODUCTION

Prostate cancer represents the most common type of cancer among males in Western society and it is commonly considered a “hormone-dependent cancer”. Sex steroids, mainly the androgens, control, indeed, its initiation and progression. PC is initially an androgen-dependent disease and the ADT still represents the major pharmacological option at this tumor stage (reviewed in Ryan and Tindall, 2011). ADT, however, frequently fails, and the disease progresses to an androgen-independent state, also known as CRPC. At this stage, current therapies scantily improve patient's survival. New pharmacological approaches are, therefore, needed to limit or inhibit PC growth and spreading (reviewed in Castoria et al., 2017).

Estrogens are involved in PC etiology and progression. Epidemiologic and clinical evidence links the sustained exposure to estrogens with increased risk of developing PC. Nevertheless, the mechanism by which estrogens induce prostate cancerogenesis and foster PC progression has not been fully identified (reviewed in Di Zazzo et al., 2016). As it occurs in BC (Huang et al., 2007) and benign prostatic hyperplasia (Shao et al., 2014), estrogens might control EMT, thereby leading to PC invasiveness and metastasis.

ERs,  $\alpha$  or  $\beta$ , mediate the estrogen effects in target cells and normal human prostate expresses both ER isoforms. It is generally accepted that ER $\alpha$  mediates the adverse effects (i.e., proliferation and inflammation) induced by estrogens, while ER $\beta$  mediates the protective and anti-apoptotic estrogen effects in PC. However, the concept that ER  $\alpha$  and  $\beta$  mutually antagonize their action in PC is debated, since cellular responses might depend on the cross talk between the two receptors occurring at transcriptional (Madak-Erdogan et al., 2013; Karamouzis et al., 2016) or non-transcriptional (Rossi et al., 2009) level. Furthermore, the ratio between the two ER isoforms, the fluctuations in ligand concentration, the presence of endogenous inhibitors and the availability of transcriptional co-regulators might differently modulate the ER $\alpha$ - or  $\beta$ -mediated responses in target cells (Warner et al., 2017). Conflicting findings on the role of ER $\alpha$  or  $\beta$  in PC continue to emerge (Di Zazzo et al., 2018). High ER $\beta$  protein levels are associated, for instance, with EMT in PC cells and a worse prognosis in PC patients (Nanni et al., 2009). In contrast, specific activation of ER $\beta$  seems to maintain an epithelial phenotype and repress PC cell invasiveness (Mak et al., 2010). It seems clear that additional studies are needed to disclose these discrepancies as well as the exact role of ER $\alpha$  or  $\beta$  in EMT and PC progression (reviewed in Montanari et al., 2017).

The regulatory neuropeptide, SST induces the growth arrest and apoptosis in neuroendocrine and inflammatory cells (Patel, 1999). By acting on both pituitary hormone release and prostate gland, SST exerts a pro-apoptotic effect in prostate cells. Moreover, SST analogs exhibit a potent anticancer activity in cultured cells as well as *in vivo* models. As such, therapeutic strategies, based on the combination of SST analogs with other antineoplastic drugs, appear very promising.

Somatostatin action is mediated by five specific high-affinity G-protein coupled receptors SSTR1-5, which belong to the seven-trans-membrane segment receptor superfamily and are expressed

in a wide variety of solid tumors, including PC (Møller et al., 2003; Msaouel et al., 2009). All of the five SSTRs can be detected in the prostate epithelial cells or PC tissues. SSTR-2 is expressed in normal prostate tissue and in a subset of highly invasive PC, while SSTR-1 and SSTR-5 are prevalently expressed in PC (Sinisi et al., 1997; Halmos et al., 2000; Lattanzio et al., 2013). Therefore, SSTRs represent a target for PC therapies, although the mechanism of their action as well as their cross talk with steroid receptors is still unclear. Estrogens up-regulate SSTR expression in BC cells as well as in goldfish pituitary and cerebral tissues (Djordjijevic et al., 1998; Kimura et al., 2001; Canosa et al., 2003). However, the effect of the combined treatment of SST analogs and estradiol on proliferation, EMT and migration of normal and PC cells has not been investigated so far.

In the present study we have used two *in vitro* cultured cell models, the prostate epithelial EPN cell line, which expresses AR and both the ER isoforms ( $\alpha$  and  $\beta$ ) and a PC-derived cell line, CPEC, which expresses low levels of both ER $\beta$  and AR, but lacks ER $\alpha$  (Sinisi et al., 2002; Rossi et al., 2009 and present paper). In these cell lines, we have compared the effects of estradiol and pasireotide, alone or in combination, on SSTR1, SSTR2, SSTR3 and SSTR5 expression at both mRNA and protein levels. At last, we have assessed the effect of these treatments on cell viability, EMT and migration by analyzing cell cycle, apoptosis as well as EMT markers and cell motility in the aforementioned models.

## MATERIALS AND METHODS

### Cell Culture and Chemicals

Cell media and supplements were supplied by Invitrogen. EPN and CPEC cell lines were derived from epithelial normal prostate tissue or PC, respectively. Isolation and characterization of both cell lines has been previously described (Sinisi et al., 2002; Pasquali et al., 2006; Rossi et al., 2009). Cells were maintained at 37°C in humidified 5% CO<sub>2</sub> atmosphere and cultured in Nutrient Ham's F12, supplemented with 3% fetal calf serum (FCS) and antibiotics. Cells (at 70% confluence) were cultured for 5 days in phenol red-free Minimum Essential Medium, containing antibiotics and 1% charcoal-treated FCS, to remove steroids and minimize serum effect. The culture medium was changed every day. Cells were left untreated or treated for the indicated times with estradiol (Sigma-Aldrich; at 20 nM final concentration), in the absence or presence of pasireotide (Novartis; at 0,1  $\mu$ M final concentration), before harvesting. Parallel cells were treated with vehicle or pasireotide alone, as a control. When indicated, the cells were treated with the ER $\beta$  agonist, DPN (Tocris; at 3 nM final concentration) or the ER $\alpha$  agonist, PPT (Tocris; at 3 nM final concentration). Human BC-derived cells MCF-7 cells and PC-derived LNCaP cells were from Cell Bank Interlab Cell Line Collection (ICLC, Genova, Italy). Cells were maintained at 37°C in humidified 5% CO<sub>2</sub> atmosphere. MCF-7 cells were cultured in DMEM supplemented with glutamine (2 mM), penicillin (100 U/ml), streptomycin (100 U/ml), insulin (6 ng/ml), hydrocortisone (3.75 ng/ml) and 5% FBS. LNCaP cells were cultured in RPMI-1640 supplemented with 10% FBS, glutamine (2 mM), penicillin



(100 U/ml), streptomycin (100 U/ml), sodium pyruvate (1 mM) and non-essential amino acids (10 mM). Media and supplements were from Gibco. The cell lines employed throughout the paper were routinely monitored for Mycoplasma contamination, expression of steroid receptors and steroid responsiveness, as reported (Castoria et al., 2014).

## RNA Isolation and Semi-Quantitative Reverse-Transcription PCR (RT-PCR) Analysis

At the indicated times, total RNA (1 µg) was extracted from EPN and CPEC cells and then purified, using TRIzol Reagent (Sigma-Aldrich) as reported (Porcile et al., 2014). RNA samples were eluted in 50 µl of water treated with diethyl-pyrocabonate and stored at  $-80^{\circ}\text{C}$ . The quality of RNA was assessed by gel electrophoresis in denaturing conditions and evaluation of 260/280 nm and 260/230 nm absorbance ratios. RNA samples with absorbance ratio 260/280 nm lower than 1.9 or with absorbance ratio 260/230 lower than 2.2 were discarded. RNA samples were then treated with 40U of RNase-free DNase-I (Boehringer Mannheim) for 45 min at  $37^{\circ}\text{C}$ . To exclude the presence of genomic DNA, PCR amplification was performed on RNA samples not reverse-transcribed, too. MMLV-Reverse Transcriptase and random primers (Bio-Rad Laboratories) were used to reverse-transcribe total RNA. cDNAs amplification was performed by RT-PCR with specific primers set for Bcl-2, GAPDH (Pasquali et al., 2006; Rossi et al., 2009, 2011), c-Myc (Gazzerro et al., 2006), SSTR1, SSTR2, SSTR3 and SSTR5 (Pasquali et al., 2008) transcripts, using JF buffer (30 mM Tris base, 8 mM HEPES base, 20 mM K glutamate, 60 mM  $\text{NH}_4$  acetate, 2 mM DTT, 8% glycerol, 1.5 mM  $\text{MgCl}_2$ , 0.2 mM dNTPs). RT-PCR analysis was done as previously described (Abbondanza et al., 2012). Calibration curve for RT-PCR analysis was obtained by serial dilutions of cDNA, which were analyzed to verify the linearity of the PCR reaction. Data obtained by RT-PCR fell within the linearity range. cDNAs were amplified in triplicate and reaction was done using a thermal cycler (Eppendorf). Amplified products were analyzed by electrophoresis, using 2% agarose gel. Gel images were acquired by the Gel DOC XR System platform (Bio-Rad Laboratories).

## Cell Cycle Analysis

Growing EPN and CPEC cells at 70% confluence were made quiescent and then left unstimulated or stimulated for the indicated times with estradiol (20 nM), in the absence or presence of pasireotide (0.1 µM). When indicated, pasireotide (0.1 µM) was used alone, as control. Cells were harvested in PBS containing 5 mM EDTA. Cell pellets were washed twice with PBS and then centrifuged at 1,200 rpm. Permeabilization was performed by incubating  $10^6$  cells in 0.5 ml of flow cytometry analysis (FACS) permeabilizing solution, which contains RNases and propidium iodide (Beckton Dickinson). Incubation was done for 2 h at  $4^{\circ}\text{C}$  in the dark. Flow cytometry data were collected using a FACScalibur instrument and analyzed by CELL QUEST software (Beckton Dickinson).

## Epithelial Mesenchyme Transition (EMT) Analysis, BrdU Incorporation, Scratch Wound Migration Analysis and Contrast-Phase Microscopy

Growing EPN or CPEC cells were plated ( $4 \times 10^4$  cells) in culture multiwell plates (6 plates). After 24 h, the cells were made quiescent and then left unstimulated or stimulated for 48 h with 20 nM estradiol, in the absence or presence of the indicated compounds. Pasireotide was used at 0.1 µM. Cell lysates were then prepared, as below described. Parallel multiwell plates were used for wound scratch analysis, which was done as reported (Castoria et al., 2011). Briefly, cells at 90% confluence were made quiescent and then scratch wounded with sterile pipette tip. They were left untreated or treated for 48 h with estradiol (20 nM), in the absence or presence of pasireotide (0.1 µM). Parallel cells were left untreated or treated with pasireotide alone (0.1 µM) or the ERβ agonist DPN (3 nM) or the ERα agonist PPT (3 nM). Cytosine arabinoside (Sigma; at 20 µM final concentration) was included in the cell medium to avoid cell proliferation. The proliferation rate of cells was monitored by BrdU incorporation analysis in immunofluorescence microscopy (Pagano et al., 2004), using a DMBL Leica (Leica) fluorescent microscope equipped with HCX PL Apo 63x oil objective. Morphological changes and wound scratch analysis were analyzed by contrast-phase microscopy using a DMIRB (Leica) microscope, equipped with X-Plan 10x or HCX PL Fluotar 40x or 63x objectives. Images were acquired using a Leica DFC 450C digital camera and processed using Leica Suite software, as reported (Di Donato et al., 2015a, 2018). Images are representative of 3 different experiments. When indicated, the wound gap was calculated using Image J software and expressed as % of the decrease in the wound area.

## Lysates, Antibodies and Western Blot

Epithelial mesenchyme transition markers were analyzed by Western blot technique. Briefly, unstimulated or stimulated cells were harvested in PBS containing 5 mM EDTA. Cell pellets were washed twice by centrifugation with PBS at 1,200 rpm and lysate proteins were prepared as reported (Castoria et al., 2011). SDS-PAGE and Western blot analysis were done according to the same report. Mouse monoclonal anti-cytokeratin (C11; Santa Cruz) and rabbit polyclonal anti-vimentin (H-84; Santa Cruz) antibodies were used to detect cytokeratin and vimentin, respectively. The mouse monoclonal anti E-cadherin (clone HECD-1; Abcam) antibody was used to detect E-cadherin. Unless otherwise stated, lysate preparation, SDS-PAGE and Western blot analysis (WB) were done as described elsewhere (Donini et al., 2012). A new panel of monoclonal antibodies to human SSTRs (MoAb Y/SSTR1, MoAb Y/SSTR2, MoAb Y/SSTR3, MoAb Y/SSTR5) was used for the primary immunoreaction. Antibodies were raised against a peptide sequence of SST-binding domains endowed within the extracellular loop of the SSTRs. Antibody specificity was assessed by Western blot analysis of proteins extracted from normal pancreas tissue (Supplementary Figure S1). ERα and ERβ were detected as described (Castoria et al., 2014), using the rabbit polyclonal anti-ERα antibody (543; Santa Cruz) or the

rabbit polyclonal anti-ER $\beta$  antibody (UBI). c-Myc was revealed as reported (Castoria et al., 2004), using the anti-c-Myc mouse monoclonal antibody (clone 9E10; Zymed Laboratories). Bcl-2 was detected as reported (Perillo et al., 2000), using the mouse monoclonal anti Bcl-2 antibody (clone Bcl-2-100; ThermoFisher). Caspase-3 activation was detected using the rabbit polyclonal anti-cleaved caspase-3 antibody (Millipore). Tubulin was detected using mouse monoclonal anti-tubulin antibody (Sigma-Aldrich). Immunoreactive proteins were revealed using the ECL system (GE Healthcare). When indicated, densitometry analysis was done by Image J software (ImageJ, U. S. National Institutes of Health, Bethesda, MD, United States<sup>1</sup>), using the “Gel Plot” plug-in.

## Statistical Analysis

Statistical analysis was performed by using ANOVA for multiple comparisons and paired *t*-test to compare individual cell responses to treatment. *P* < 0.05 values were considered significant.

## RESULTS

### Estradiol Effect on SSTRs in EPN and CPEC Cells

To assess the effects of estradiol on SSTRs expression, we used EPN, which express ER $\alpha$  and ER $\beta$  and CPEC, which only express low levels of ER $\beta$  (Supplementary Figure S2 and Rossi et al., 2011). The cells were left untreated or treated with estradiol (20 nM) for 24 h. Figure 1A and inset show that estradiol treatment of EPN cells resulted in a significant increase in SSTR1, 2 and 5 mRNA, as compared to untreated cells. Hormone treatment did not affect SSTR3 gene expression. In contrast, estradiol treatment of CPEC cells significantly reduced SSTR1 and 2 mRNAs. A negligible hormonal effect was observed on SSTR3 and SSTR5 gene expression (Figure 1B and inset). The Western blot analysis and densitometry quantification of bands show that estradiol treatment increased the expression of SSTR1, 2 and 5 in EPN cells (Figure 1C and inset). A weak, but significant reduction of SSTR1 and SSTR2 protein levels was detectable in CPEC cells, in the absence of significant changes in SSTR3 protein levels (Figure 1C and inset). The observation that estradiol down-regulates SSTR5 protein levels (Figure 1C and inset) in the absence of significant changes in gene expression might be due to post-translational modification and degradation of SSTR5 induced by the hormone. SSTRs undergo, indeed, phosphorylation at different sites with the subsequent degradation (Csaba et al., 2012) and estradiol activates multiple kinases in target cells (Migliaccio et al., 2007a,b; Castoria et al., 2008).

To further evaluate the role of hormone regulation in SSTR expression, we challenged quiescent EPN cells with estradiol, or PPT and DPN ligands, which specifically bind ER $\alpha$  or ER $\beta$ , respectively. The Western blot analysis in Figure 1C (lower section) shows that the increase in expression of SSTR1, 2 and 5 is mainly due to ER $\alpha$  activation by PPT ligand in EPN cells.

The down regulation of these receptors in CPEC cells, which only express ER $\beta$ , is very likely caused by ER $\beta$  activation. We did not use siRNA approach, since a cross talk between ER $\alpha$  and ER $\beta$  regulates the expression of each other in PC cells (Pisolato et al., 2016).

In sum, experiments in the Figure 1 shows that estradiol up-regulation of SSTR1, SSTR2 and SSTR5 occurs mainly through ER $\alpha$  activation in EPN cells. The absence ER $\alpha$  is likely responsible for estradiol-induced down-regulation of SSTR1, SSTR2 and SSTR5 in CPEC cells.

### Effect of Estradiol and Pasireotide in EPN and CPEC Cells: Studies on Cell Cycle Progression and Caspase-3 Activation

A 24- and 48-h response of propidium-iodide incorporation analysis was then performed to test the role of estradiol in EPN and CPEC cell proliferation. The FACS analysis in Figure 2A shows that 24 and 48 h treatment of EPN cells with estradiol induced in both conditions a significant increase of pre-G1 apoptotic cells associated with a persistently elevated number of cells in G0/G1 phases and a low amount of cells in S-phase. In contrast, estradiol treatment of CPEC cells did not significantly affect the number of apoptotic cells, with cells persistently arrested in G0/G1 phase (Figure 2B).

Twenty-four h treatment of EPN (Figure 3A) and CPEC (Figure 3B) cells with 0,1  $\mu$ M of the SSTR-specific agonist, pasireotide, significantly increased the number of apoptotic cells. Co-treatment with estradiol reinforced the pro-apoptotic effect of pasireotide in EPN cells, with a reduction in the number of cells in S-phase (Figure 3A). In contrast, co-treatment of CPEC cells with estradiol and pasireotide (0,1  $\mu$ M) did not enhance the number of apoptotic cells (Figure 3B). By prolonging the time of treatment (48 h) and by increasing the concentration of pasireotide (1  $\mu$ M), we did not observe any further increase in the number of apoptotic cells (not shown). The strong stability of pasireotide, together with its high affinity for all SSTRs (reviewed in Feelders et al., 2013) might be responsible for its efficacy in inducing the apoptotic response at very low concentration (0,1  $\mu$ M) and within a relatively short time frame (24h). Lastly, the Western blot analysis of activated caspase-3 in Figure 3C confirmed the data obtained by FACS analysis of EPN and CPEC cells.

In sum, Figures 2, 3 show that EPN cells challenged with estradiol undergo a robust apoptotic response, while CPEC cells remain arrested in G0/G1. Pasireotide induces apoptotic death in both EPN and CPEC cells, and the simultaneous treatment with estradiol enhances the pasireotide effect only in EPN cells.

### Effect of Estradiol and Pasireotide in EPN and CPEC Cells: Regulation of Bcl-2 and Myc Gene Expression and Protein Levels

To evaluate the putative intracellular targets responsible for the observed effects of estradiol and pasireotide on cell cycle, we analyzed by semi-quantitative RT-PCR the Bcl-2 gene

<sup>1</sup><http://imagej.nih.gov/ij/>

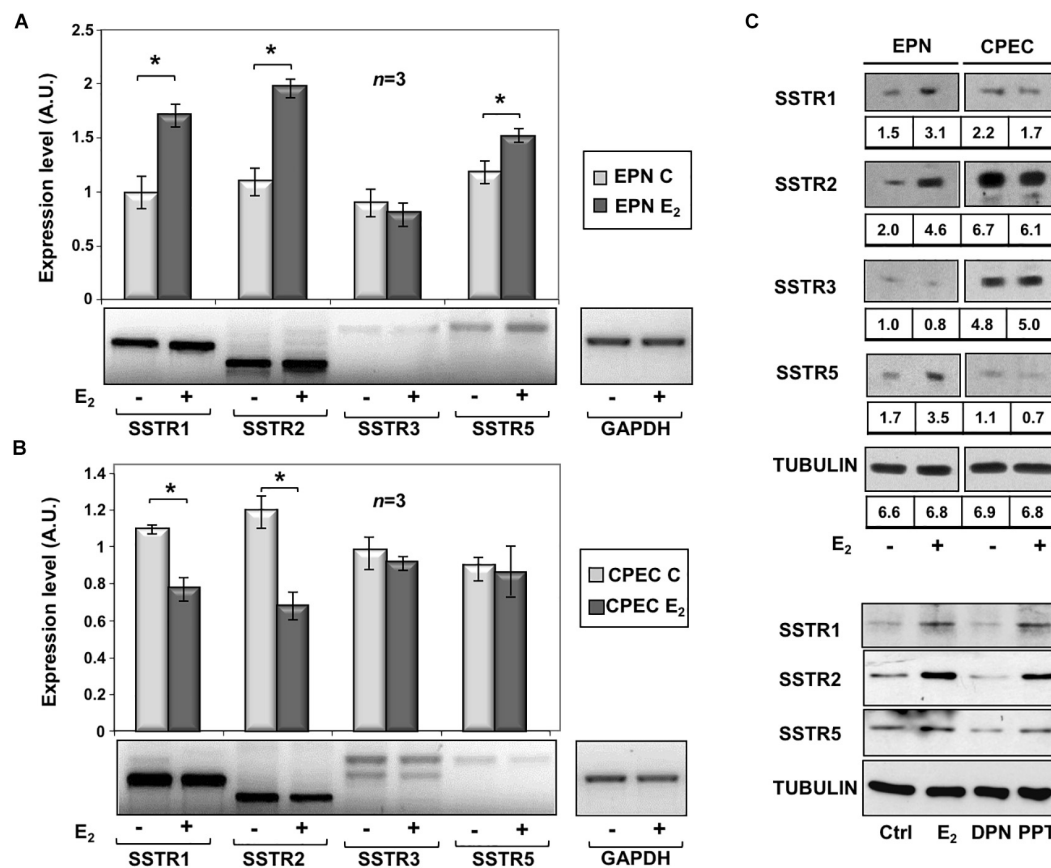


**FIGURE 1 |** Effect of estradiol on SSTRs mRNA and protein expression levels. RT-PCR analysis of SSTR1, 2, 3 and 5 mRNA levels in EPN (A) or CPEC (B) cells untreated or treated for 24h with 20 nM estradiol (E<sub>2</sub>) was done. In panel (A,B), densitometry analysis of agarose gel electrophoresis is shown. The expression level is indicated as fold changes over the basal conditions (A.U.). Histograms represent the averages ( $\pm$  standard error) from 3 independent experiments, normalized for the expression of the control housekeeping gene GAPDH (\*indicates  $p < 0.05$  for each gene versus its untreated control). Means and SEMs are shown.  $n$  represents the number of experiments. \* $p < 0.05$ . Insets are representative from one experiment in A or B. In panel (C, upper section), the Western blot analysis of lysate proteins from EPN and CPEC cell lines untreated or treated with estradiol (20 nM; E<sub>2</sub>) for 48 h was done. Lysate proteins (1 mg/ml) were resolved by SDS-PAGE, transferred to PVDF membrane and probed with anti-SSTRs or anti-tubulin antibodies. Inset in panel (C), densitometry analysis of SSTRs was done in two different experiments using the NIH/Image J software. Results were expressed as relative change over the basal level of each SSTR isoform. In panel (C, lower section), the Western blot analysis of lysate proteins from EPN cells untreated or treated with estradiol (20 nM; E<sub>2</sub>) or PPT (3 nM) or DPN (3 nM) for 48 h was done. Lysate proteins (2 mg/ml) were resolved by SDS-PAGE, transferred to nitrocellulose membrane and probed with the antibodies against the indicated proteins. In panel (C, upper and lower sections), the Western blot analysis of tubulin is shown, as loading control.

expression in both EPN and CPEC cells treated with estradiol and pasireotide, alone or in combination. Estradiol induced a down-regulation of Bcl-2 gene expression in EPN cells and pasireotide co-treatment enhanced this effect (left panel in **Figure 4A**). In contrast, estradiol induced an increase in Bcl-2 mRNA, and simultaneous treatment with pasireotide enhanced such effect in CPEC cells (right panel in **Figure 4A**).

We next analyzed c-Myc gene expression levels. Twenty-nM estradiol induced a down-regulation of c-Myc mRNA in EPN cells and co-treatment with pasireotide reinforced the estradiol effect (left panel in **Figure 4B**). Estradiol, alone or in combination with pasireotide, induced a weak, but significant increase of c-Myc mRNA in CPEC cells (right panel in **Figure 4B**). Similar findings were observed by Western blot analysis for Bcl-2 and c-Myc protein levels (**Figure 4C**), although the synergic effect of estradiol and pasireotide was more evident by gene

expression analysis. The slight difference we observe might be due to modification of Bcl-2 and c-Myc occurring at post-translational level.

These findings indicate that estradiol and pasireotide have a synergic effect in decreasing Bcl-2 and c-Myc gene expression in EPN cells, while they increase such responses in CPEC cells.

## Effect of Estradiol and Pasireotide on EMT and Migration of EPN and CPEC Cells

Conflicting findings on the role of ER $\alpha$  or  $\beta$  in EMT of prostate cells and PC progression have been reported (Montanari et al., 2017). We then investigated by Western blot analysis the effect of estradiol, or pasireotide or combination of both in EMT of EPN cells (**Figure 5A**). Quiescent cells were left unchallenged

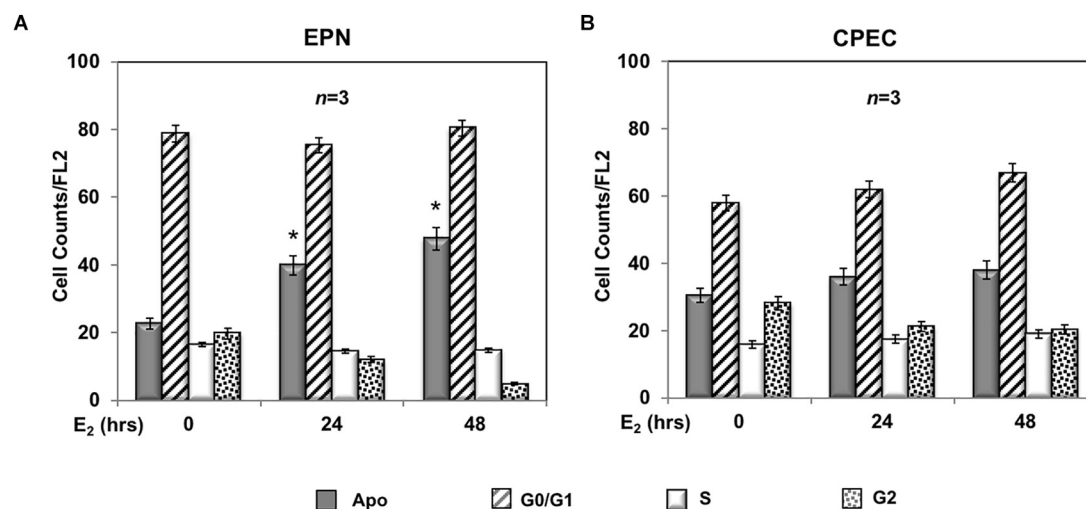


**FIGURE 2 |** Effect of estradiol on cell cycle. Flow cytometry analysis of propidium iodide-labeled EPN (A) or CPEC (B) cells was done, as described in Methods. Quiescent cells were left under basal conditions or treated with estradiol (20 nM; E<sub>2</sub>) for the indicated times. Histograms represent the % counts/FL2 areas of labeled cells in the different cell cycle phases after 24 or 48 h of hormonal treatment. Means and SEMs are shown. *n* represents the number of experiments. \**p* < 0,05 for each experimental point vs. the corresponding untreated control.

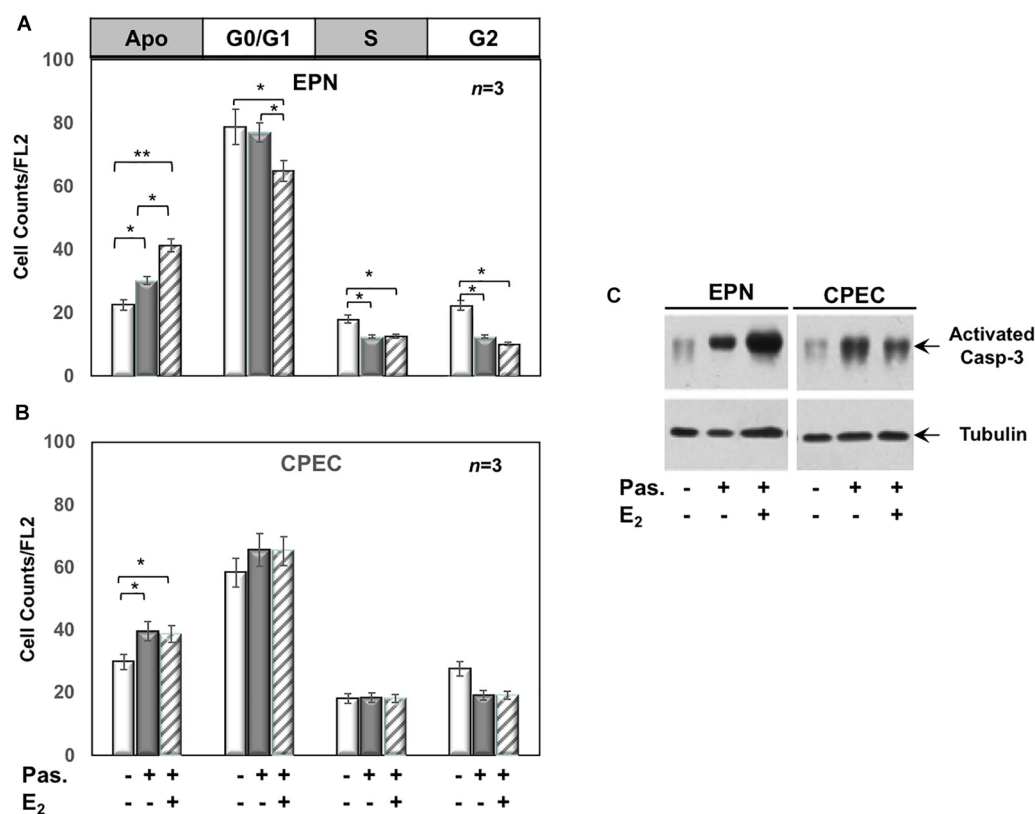
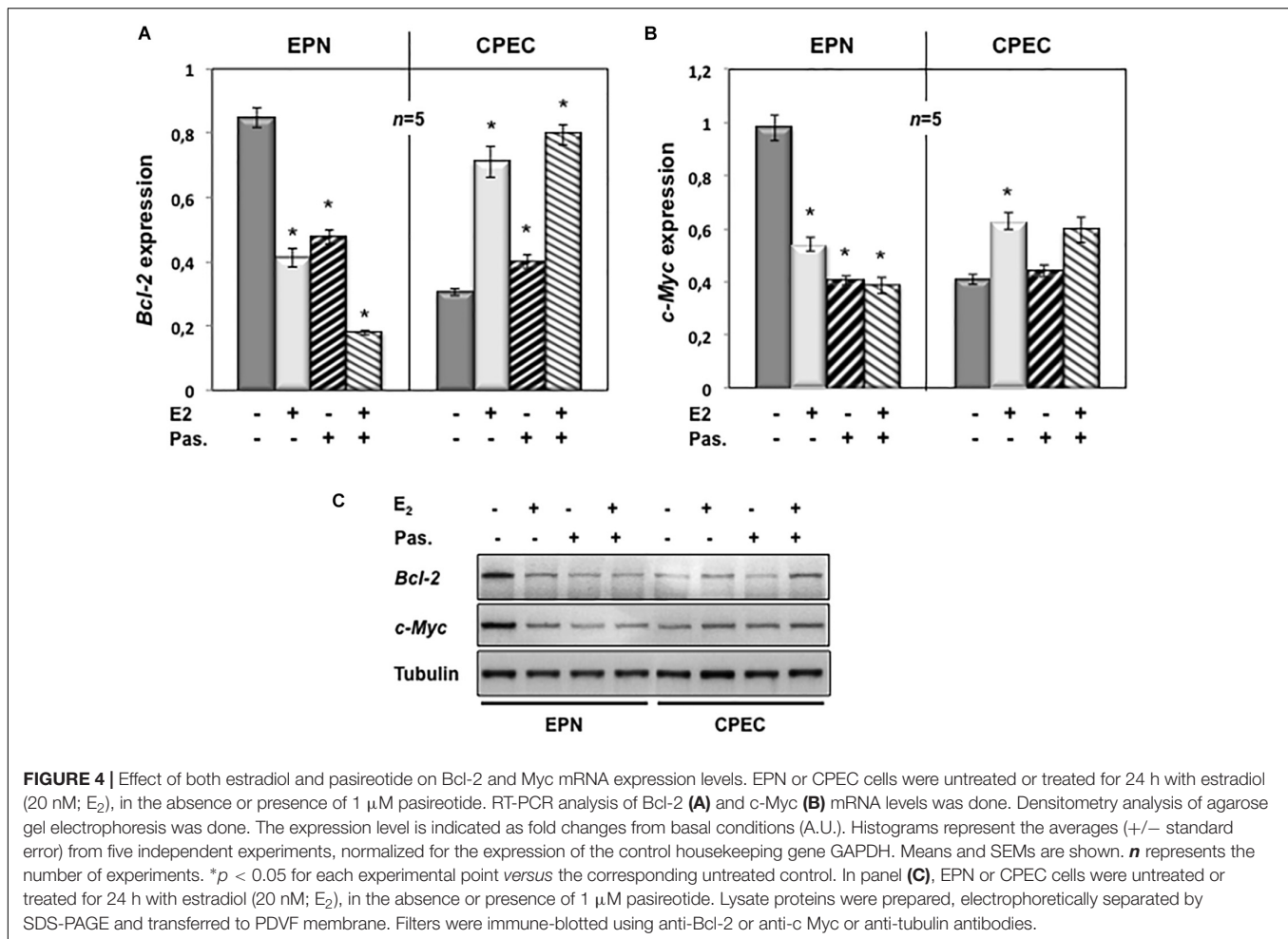


**FIGURE 3 |** Effect of both estradiol and pasireotide on cell cycle. Flow cytometry analysis of propidium iodide-labelled EPN (A) or CPEC (B) was done, as described in Methods. In panel (A,B), quiescent cells were left under untreated or treated for 24 h with 0,1  $\mu$ M pasireotide, in the absence or presence of 20 nM estradiol. Histograms in panel (A,B) represent the % counts/FL2 areas of labeled cells in the different cell cycle phases after the indicated treatments. Means and SEMs are shown. *n* represents the number of experiments. \**p* < 0,05; \*\**p* < 0,01. In panel (C), quiescent EPN (left section) or CPEC (right section) cells were left untreated or treated for 24 h with 0,1  $\mu$ M pasireotide, in the absence or presence of 20 nM estradiol. Lysate proteins were separated by SDS-PAGE, transferred to PDVF membrane and filters were then analyzed by Western blot, using the anti-activated caspase 3 or anti-tubulin antibodies.





or challenged for 48h with the indicated stimuli and lysate proteins were analyzed for expression of vimentin, E-cadherin and cytokeratins. Regardless of stimuli, the Western blots in **Figure 5A** shows that no significant changes in vimentin and E-cadherin levels were observed in EPN cells. Estradiol or pasireotide slightly increased the cytokeratin levels. Noticeably, estradiol up-regulates cytokeratin levels in BC cells (Courtts et al., 1996; Spencer et al., 1998), and pasireotide may impact cytokeratin levels through activation of signaling networks (Loschke et al., 2015). Under the same experimental conditions, estradiol treatment did not induce significant morphological changes in EPN cells (**Figure 5B**), and similar findings were observed in cells stimulated with pasireotide, alone or in combination with estradiol (not shown). We then evaluated cell migration by the wound scratch analysis in EPN cells. At 48h treatment, neither estradiol, nor pasireotide, nor combination of both affected cell migration in wound scratch assay. Notably, challenging of cells with PPT and DPN, which specifically activate ER $\alpha$  or  $\beta$ , did not modify the migratory capacity of EPN cells (**Figure 5C**).

This set of experiments shows that, irrespective of pasireotide presence, estradiol treatment does not promote EMT and migration of EPN cells. In the same experimental

conditions, hormonal stimulation of EPN cells activates the apoptotic machinery, and pasireotide enhances this response (see **Figures 2, 3**).

Quiescent CPEC cells were then used. The cells were left untreated or treated for 48 h with the indicated compounds and lysates were analyzed for expression of vimentin, E-cadherin and cytokeratin. The Western blot in **Figure 6A** shows that estradiol remarkably up-regulated the vimentin level in CPEC cells. Combination of both, estradiol and pasireotide did not significantly modify such an increase. Up-regulation of vimentin was also observed in pasireotide-stimulated cells. Simultaneously, estradiol decreased E-cadherin and cytokeratin levels. Similar findings were observed by combining both estradiol and pasireotide. A slight decrease in E-cadherin was also observed in cells treated with pasireotide, alone. CPEC cells were then analyzed for morphological changes. The cells appeared elongated and less adherent upon 48h estradiol treatment (**Figure 6B**). Notably, a simultaneous significant increase in motility was observed upon estradiol challenging of quiescent CPEC cells, as the wound gap was significantly reduced, in the absence of cell proliferation (**Figures 6C,D** and legend). Addition of pasireotide did not further increase the estradiol-induced effect on cell motility. Although able to

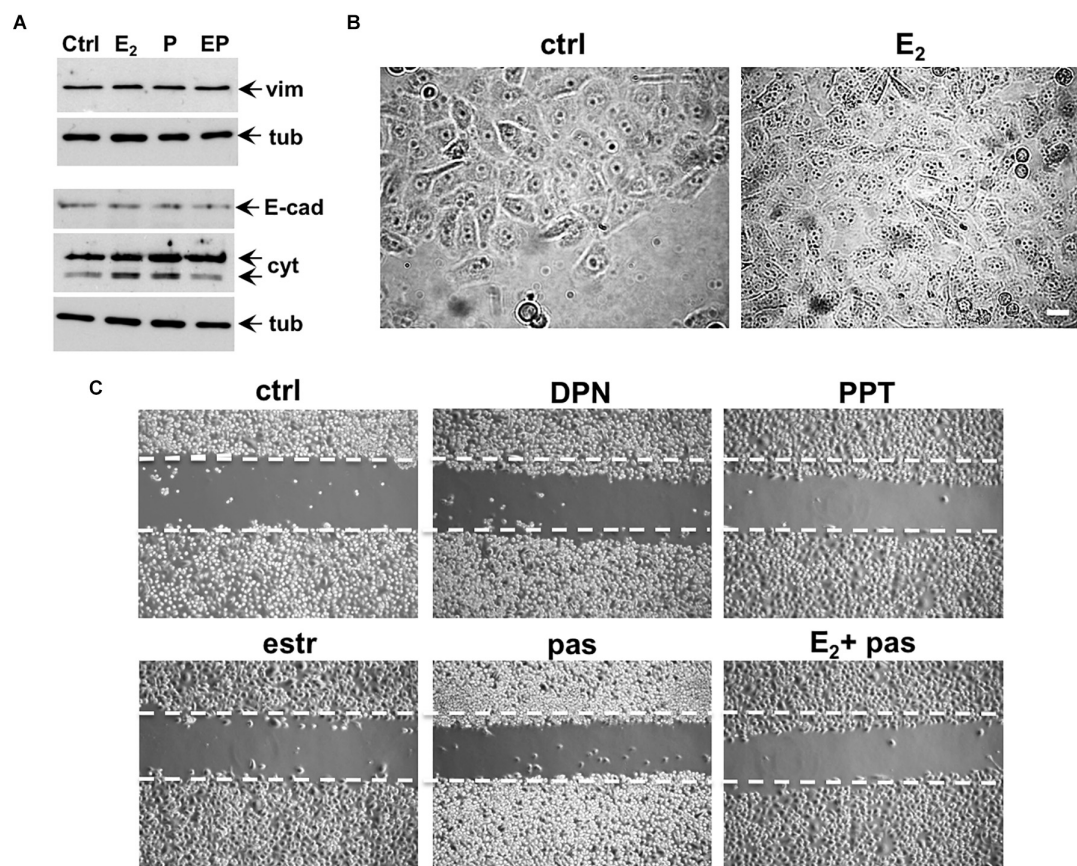


**FIGURE 5 |** Effect of estradiol and pasireotide on EMT, morphology and motility of EPN cells. Quiescent EPN cells were untreated or treated for 48 h with the indicated compounds. Estradiol was used at 20 nM, pasireotide at 0.1  $\mu$ M, PPT and DPN both at 3 nM. In panel (A), lysate proteins (2 mg/ml) were prepared, separated by SDS-PAGE and transferred to nitrocellulose membrane. Filters were immune-blotted using the antibodies against the indicated proteins. The blots are representative of two different experiments. In panel (B), the cells were analyzed for morphological changes using contrast-phase microscopy. Bar, 10  $\mu$ M. In panel (C), the cells were wounded and then left unstimulated or stimulated with the indicated compounds. Cytosine arabinoside (20  $\mu$ M) was added to the cell medium to avoid cell proliferation. Contrast-phase images in panel (B,C) are representative of 3 different experiments.

induce an increase in vimentin levels and a slight decrease in E-cadherin (Figure 6A), pasireotide did not significantly modify the migratory capacity of CPEC cells, when used alone (Figures 6C,D). Acquisition of a mesenchymal cell state, indeed, is not a prerequisite of a migratory phenotype *in vitro* and *in vivo* (Schaeffer et al., 2014) and pasireotide might be unable, in our experimental conditions, to activate the signaling networks (e.g., Rho family GTPases, paxillin/focal adhesion kinase signaling module) required for cell locomotion (Devreotes and Horwitz, 2015). Notably, stimulation of CPEC cells with the ER $\beta$  agonist, DNP strongly reduced the wound gap, indicating that specific activation of ER $\beta$ , the only ER isoform expressed in CPEC cells, is responsible for the migratory phenotype here observed (Figures 6C,D).

Collectively, the data in 6 show that by activating ER $\beta$ , estradiol promotes EMT and motility in CPEC cells. Addition of pasireotide, or pasireotide alone does not significantly modify these effects. Here again, hormonal stimulation of CPEC cells scanty activates the apoptotic machinery, and pasireotide does not enhance this response (see Figures 2, 3).

In sum, findings in Figures 5, 6 are consistent with the concept that cells undergoing EMT become resistant to the apoptotic effect (Thiery, 2002).

## DISCUSSION

In this study, we have used the prostate epithelial EPN cell line and the PC-derived epithelial CPEC cells. In both cell lines we have assessed the responsiveness to estradiol and the SST analog, pasireotide. Estradiol increases the expression of SSTR1, SSTR2 and SSTR5 at mRNA and protein levels in EPN cells, while hormone treatment reduces the SSTR1 and SSTR2 mRNA and SSTR1, SSTR2 and SSTR5 protein levels in CPEC cells. Our study for the first time reports the regulation of SSTRs by estradiol in prostate cell lines. Estradiol up-regulation of SSTR1, 2 and 5 depends on ER $\alpha$ , since EPN cells express both ER $\alpha$  and  $\beta$ , while CPEC cells only express low amounts of ER $\beta$  (Rossi et al., 2011 and Supplementary Figure S2). Experiments with the specific ER $\alpha$  ligand, PPT further support this concept. However, it cannot

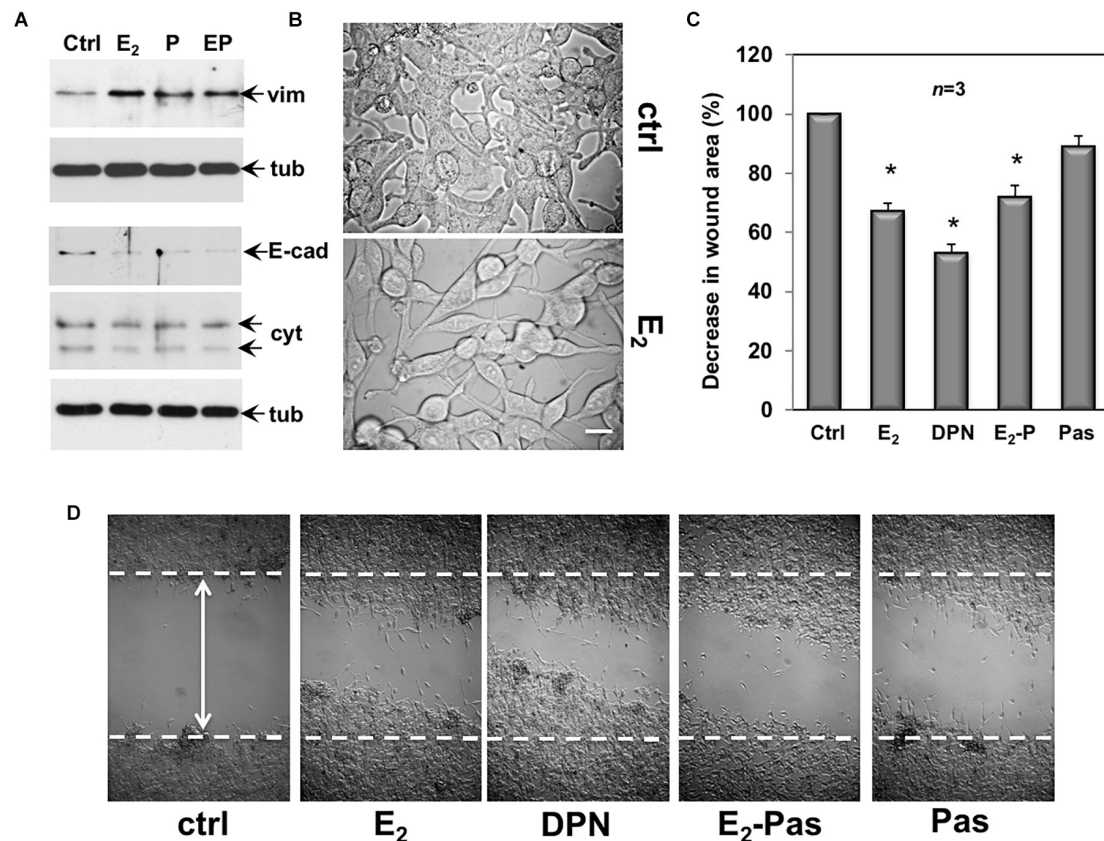


**FIGURE 6 |** Effect of estradiol and pasireotide on EMT, morphology and motility of CPEC cells. Quiescent CPEC cells were untreated or treated for 48 h with the indicated compounds. Estradiol was used at 20 nM, pasireotide at 0,1  $\mu$ M and DPN at 3 nM. In panel (A), lysate proteins (2 mg/ml) were prepared, separated by SDS-PAGE and transferred to nitrocellulose membrane. Filters were immune-blotted using the antibodies against the indicated proteins. The blots are representative of two different experiments. In panel (B), the cells were analyzed for morphological changes using contrast-phase microscopy. Bar, 10  $\mu$ M. In panel (C), the cells were wounded (the arrow indicates the wound length) and then left unstimulated or stimulated with the indicated compounds. Cytosine arabinoside (20  $\mu$ M) was added to the cell medium to avoid cell proliferation. The wound gap from three different experiments was calculated using Image J software and expressed as % of the decrease in wound area. Means and SEM are shown. *n* represents the number of experiments. \**p* < 0.05 for each experimental point versus the corresponding untreated control. Contrast-phase images in panel (D) are representative of 3 different experiments. In panel (C,D), quiescent cells on coverslips were left unstimulated or stimulated for 24 h with estradiol (20 nM), or DPN (3 nM), or pasireotide (0,1  $\mu$ M) or a combination of estradiol plus pasireotide. After *in vivo* pulse with BrdU (100  $\mu$ M; Sigma), the DNA synthesis was analyzed by IF as reported in Methods and calculated by the formula: percentage of BrdU-positive cells = (No. of BrdU-positive cells/No. of total cells)  $\times$  100. In unstimulated cells, the BrdU incorporation was observed in less than 14% of total cells. Neither estradiol, nor DPN, nor pasireotide, nor combination of estradiol and pasireotide increased the BrdU incorporation, which was detected in 18, 16, 15, and 17% of total cells, respectively.

be excluded the possibility that the balance between the two ER isoforms regulates SSTR levels in EPN cells. In CPEC cells, estradiol down-regulates SSTR1, 2 and 5 likely because of the absence of ER $\alpha$ .

The expression pattern of SSTRs correlates with different biological responses elicited by estradiol. Hormone treatment induces a robust apoptotic response in EPN, but not in CPEC cells, suggesting that up-regulation of SSTR1, 2 and 5 by estradiol is involved in the apoptotic machinery. The finding that estradiol triggers cell death in EPN, but not in CPEC cells, also suggests that the balance between ER $\alpha$  and  $\beta$  expression plays a role in estradiol-induced apoptosis. Loss of this balance, which occurs in CPEC cells, enables cell cycle arrest. The SST analog, pasireotide exerts at very low concentration (0,1  $\mu$ M) a significant apoptotic effect in both cell lines. The effect is stronger in CPEC cells, as compared with EPN cells, likely because CPEC cells show a

more the robust expression of SSTR3, which mainly mediates the SST-induced cytotoxic effect (War et al., 2011). However, other mechanisms (e.g., regulation of PI3-K- or MAPK- or the protein tyrosine phosphatase-dependent pathways or the p27<sup>Kip1</sup> cell cycle inhibitor) might be involved in CPEC cells. Estradiol reinforces the apoptotic effect by pasireotide only in EPN cells. This finding might be due to the estradiol-induced increases in SSTR2 expression and the consequent apoptotic effect. However, co-expression of both ER $\alpha$  and  $\beta$  might sensitize the EPN cells toward cell death and estradiol activation of both the ER isoforms might be permissive in the apoptotic response.

We observe a down-regulation of Bcl-2 and c-Myc mRNA levels upon estradiol or pasireotide treatment of EPN cells. Combination of estradiol plus pasireotide further increases the Bcl-2 and c-Myc down-regulation. Thus, the apoptotic effect



induced by estradiol is mediated by down-regulation of both Bcl-2 and Myc. These findings are consistent with results previously obtained in estradiol-treated EPN cells (Rossi et al., 2011). It has been reported that estradiol up-regulates the Bcl-2 gene in estrogen responsive BC cells (Perillo et al., 2000, 2008). The down regulation of Bcl-2 we observe in EPN cells suggests that estradiol regulation of Bcl-2 depends on cell-context and/or ER $\alpha$ / $\beta$  ratio. In sum, by increasing the expression levels of SSTRs, estradiol synergizes with pasireotide in prostate cells expressing both ER isoforms. In CPEC cells, which only express low ER $\beta$  levels, such regulation is lost and estradiol-treated cells result prevalently arrested in G0/G1. Simultaneously, a significant increase in Bcl-2 level is detected, with a weak elevation in Myc levels, suggesting the involvement of Bcl-2 in estradiol-mediated survival of CPEC cells. It cannot be excluded, however, that a faint elevation in c-Myc levels might amplify pre-existing transcriptional programs (McMahon, 2014).

Conflicting findings on the role of ER $\alpha$  or  $\beta$  in EMT and migration of prostate tissues and PC continue to emerge. Irrespective of pasireotide presence, we did not observe significant morphological changes in estradiol-treated EPN cells. They did not undergo EMT and migration. Noticeably, estradiol induces EMT in prostate benign hyperplasia (Shi et al., 2017). However, the different experimental conditions (2 and 3D conditions), the ratio between ER $\alpha$  and ER $\beta$  might explain these discrepancies. In contrast, estradiol challenging of transformed CPEC cells promotes EMT and enables migration. These effects are mediated by ER $\beta$ , as CPEC cells only express ER $\beta$  and the DPN specific ligand exerts an impressive effect in our migration assay. Overall, our findings are consistent with the concept that apoptosis and motility are mutually exclusive and that migrating cells usually activate survival mechanisms as they move (Hood and Cheresch, 2002). Thus, EPN cells undergo apoptosis, while CPEC cells easily migrate on hormonal stimulation.

The findings we observe call for additional comments. SST analogs, such as octreotide, lanreotide and pasireotide, have been used in PC-derived cells (Lattanzio et al., 2013). Pasireotide, a new synthetic SST analog active on SST1-3 and SST5 (Weckbecker et al., 2003), induces apoptosis in malignant PC-derived cells and potentiates the antineoplastic effects of prednisone and docetaxel in phase I clinical trial (Lo Nigro et al., 2008; Erten et al., 2009; Thakur et al., 2018). Lanreotide, in combination with dexamethasone and ADT, induces a decrease in PSA level and improves the bone pain in PC patients (Mitsogiannis et al., 2009). Relevant to the findings here reported, combination of SST analogs with ethinyl estradiol restores clinical responses (Di Silverio and Sciarra, 2003) and decreases PSA levels in CRPC patients (Mitsogiannis et al., 2009). Thus CRPC patients benefit from combination of ethinylestradiol and SST analogs in terms of both clinical responses and symptomatic relief. Our findings strongly suggest that combination of SST analogs with estradiol might be efficacious in PC, provided it expresses both the ER isoforms. It cannot be excluded, however, that such combinatorial therapy may act in PC patients by targeting not only PC cells, but also the tumor microenvironment, which confers invasiveness, protection from apoptosis and therapy escape (reviewed in Di Donato et al.,

2015b). Somatostatin analogs neutralize, indeed, the protective effect elicited by survival signals derived by neuroendocrine prostate cells (Hejna et al., 2002), which often surround PC epithelial cells. On the other, estrogens might exert a direct cytotoxic effect on epithelial PC cells, provided they express both the ER isoforms. Further experiments in 3D models of PC are needed to disclose this concern.

In conclusion, our findings for the first time reports that estradiol controls SSTRs in normal and PC cells. By up-regulating SSTRs, estradiol fosters the anti-proliferative effect of pasireotide in EPN but not CPEC cells. Consistent with these results, estradiol does not promote EMT and motility in EPN cells, while it induces EMT and migration in CPEC cells. In addition to offering valuable hints into the identification of hormonal biomarkers in PC specimens, this study provides new insights in the management of PC, which still remains a challenge for clinicians.

## AUTHOR CONTRIBUTIONS

VR, LA, and CA contributed to concept and design of study. VR, EDZ, GG, and CDR performed the experiments. VR developed monoclonal antibody panel. EDZ and GG contributed to analysis and representation of data. AS, LA, and CA revised the final draft of the manuscript. GC and AM contributed to writing of the manuscript.

## FUNDING

This study has been funded by Italian Ministry of University and Scientific Research (P.R.I.N. 2015B7M39T\_003 to GC, PRIN20152TE5PK\_003 to LA, and PRIN 2010NFEB9L to AS), P.O.R-Regione Calabria (Progetto “Razionale” to AM and LA), BLUEPRINT (282510), the Italian Flagship Project EPIGEN, the Italian Association for Cancer Research (AIRC-17217), and VALERE (Vanvitelli per la Ricerca).

## SUPPLEMENTARY MATERIAL

The Supplementary Material for this article can be found online at: <https://www.frontiersin.org/articles/10.3389/fphar.2019.00028/full#supplementary-material>

**FIGURE S1 |** Western blot analysis of protein extracted from normal pancreas with anti-SSTRs monoclonal antibodies (MAbs). Lysate proteins were extracted from normal pancreas and electrophoretically separated as described in Methods. Proteins were then transferred to PVDF membrane and immunoblotted with antibodies against SSTRs receptors (–). Control blots (+) were obtained using anti-SSTRs MAb pre-adsorbed with immune-reactive specific peptide.

**FIGURE S2 |** Western blot analysis of EPN or CPEC lysate proteins with anti-ER ( $\alpha$  or  $\beta$ ) antibodies. The Western blot analysis of lysate proteins from EPN and CPEC cell lines was done. Proteins from cell lysates (1 mg/ml) were resolved by SDS–PAGE, transferred to nitrocellulose membrane and then probed with anti-ER $\alpha$  or  $\beta$  antibodies, as described in Methods. Lysate proteins from ER $\alpha$ -positive MCF-7 or ER $\alpha$ -negative LNCaP cells were analyzed in parallel, as control. The Western blot analysis with anti-tubulin antibody was also done as loading control.



## REFERENCES

- Abbondanza, C., De Rosa, C., D'Arcangelo, A., Pacifico, M., Spizuoco, C., Piluso, G., et al. (2012). Identification of a functional estrogen-responsive enhancer element in the promoter 2 of PRDM2 gene in breast cancer cell lines. *J. Cell. Physiol.* 227, 964–975. doi: 10.1002/jcp.22803
- Canosa, L. F., Lin, X., and Peter, R. E. (2003). Effects of sex steroid hormones on the expression of somatostatin receptors sst1 and sst5 in goldfish pituitary and forebrain. *Neuroendocrinology* 78, 81–89. doi: 10.1159/000071963
- Castoria, G., Auricchio, F., and Migliaccio, A. (2017). Extranuclear partners of androgen receptor: at the crossroads of proliferation, migration, and neurogenesis. *FASEB J.* 4, 1289–1300. doi: 10.1096/fj.201601047R
- Castoria, G., D'Amato, L., Ciociola, A., Giovannelli, P., Giraldi, T., Sepe, L., et al. (2011). Androgen-induced cell migration: role of androgen receptor/filamin A association. *PLoS One* 6:e17218. doi: 10.1371/journal.pone.0017218
- Castoria, G., Giovannelli, P., Di Donato, M., Ciociola, A., Hayashi, R., Bernal, F., et al. (2014). Role of non-genomic androgen signalling in suppressing proliferation of fibroblasts and fibrosarcoma cells. *Cell Death Dis.* 5:e1548. doi: 10.1038/cddis.2014.497
- Castoria, G., Migliaccio, A., D'Amato, L., Di Stasio, R., Ciociola, A., Lombardi, M., et al. (2008). Integrating signals between cAMP and MAPK pathways in breast cancer. *Front. Biosci.* 13:1318–1327. doi: 10.2741/2764
- Castoria, G., Migliaccio, A., Di Domenico, M., Lombardi, M., de Falco, A., Varricchio, L., et al. (2004). Role of atypical protein kinase C in estradiol-triggered G1/S progression of MCF-7 cells. *Mol. Cell. Biol.* 17, 7643–7653. doi: 10.1128/MCB.24.17.7643-7653.2004
- Coutts, A. S., Davie, J. R., Dotzlaw, H., and Murphy, L. C. (1996). Estrogen regulation of nuclear matrix-intermediate filament proteins in human breast cancer cells. *J. Cell. Biochem.* 63, 174–184. doi: 10.1002/(SICI)1097-4644(19961101)63:2<174::AID-JCB5>3.0.CO;2-V
- Csaba, Z., Peineau, S., and Dournaud, P. (2012). Molecular mechanisms of somatostatin receptor trafficking. *J. Mol. Endocrinol.* 48, R1–R12. doi: 10.1530/JME-11-0121
- Devreotes, P., and Horwitz, A. R. (2015). Signaling networks that regulate cell migration. *Cold Spring Harb. Perspect. Biol.* 7:a005959. doi: 10.1101/cshperspect.a005959
- Di Donato, M., Bilancio, A., D'Amato, L., Claudiani, P., Oliviero, M. A., Barone, M. V., et al. (2015a). Cross-talk between androgen receptor/filamin A and TrkA regulates neurite outgrowth in PC12 cells. *Mol. Biol. Cell* 26, 2858–2872. doi: 10.1091/mbc.E14-09-1352
- Di Donato, M., Giovannelli, P., Cerner, G., Di Santi, A., Marino, I., Bilancio, A., et al. (2015b). Non-genomic androgen action regulates proliferative/migratory signaling in stromal cells. *Front. Endocrinol.* 5:225. doi: 10.3389/fendo.2014.00225
- Di Donato, M., Cerner, G., Auricchio, F., Migliaccio, A., and Castoria, G. (2018). Cross-talk between androgen receptor and nerve growth factor receptor in prostate cancer cells: implications for a new therapeutic approach. *Cell Death Discov.* 4:5. doi: 10.1038/s41420-017-0024-3
- Di Silverio, F., and Sciarra, A. (2003). Combination therapy of ethinylestradiol and somatostatin analogue reintroduces objective clinical responses and decreases chromogranin a in patients with androgen ablation refractory prostate cancer. *J. Urol.* 170, 1812–1816. doi: 10.1097/01.ju.0000092480.71873.26
- Di Zazzo, E., Galasso, G., Giovannelli, P., Di Donato, M., and Castoria, G. (2018). Estrogens and their receptors in prostate cancer: therapeutic implications. *Front. Oncol.* 8:2. doi: 10.3389/fonc.2018.00002
- Di Zazzo, E., Galasso, G., Giovannelli, P., Di Donato, M., Di Santi, A., Cerner, G., et al. (2016). Prostate cancer stem cells: the role of androgen and estrogen receptors. *Oncotarget* 7, 193–208. doi: 10.18632/oncotarget.6220
- Djordjijevic, D., Zhang, J., Priam, M., Viollet, C., Gourdji, D., Kordon, C., et al. (1998). Effect of 17beta-estradiol on somatostatin receptor expression and inhibitory effects on growth hormone and prolactin release in rat pituitary cell cultures. *Endocrinology* 139, 2272–2277. doi: 10.1210/endo.139.5.5990
- Donini, C. F., Di Zazzo, E., Zuchegna, C., Di Domenico, M., D'Inzeo, S., Nicolussi, A., et al. (2012). The p85 $\alpha$  regulatory subunit of PI3K mediates cAMP-PKA and retinoic acid biological effects on MCF7 cell growth and migration. *Int. J. Oncol.* 40, 1627–1635.
- Erten, C., Karaca, B., Kucukzeybek, Y., Gorumlu, G., Cengiz, E., Gul, M. K., et al. (2009). Regulation of growth factors in hormone- and drug-resistant prostate cancer cells by synergistic combination of docetaxel and octreotide. *BJU Int.* 104, 107–114. doi: 10.1111/j.1464-410X.2009.08340.x
- Fielders, R. A., de Herder, W. W., Neggers, S. J., van der Lely, A. J., and Hofland, L. J. (2013). Pasireotide, a multi-somatostatin receptor ligand with potential efficacy for treatment of pituitary and neuroendocrine tumors. *Drugs Today (Barc)* 49, 89–103. doi: 10.1358/dot.2013.49.2.1915142
- Gazzerro, P., Abbondanza, C., D'Arcangelo, A., Rossi, M., Medici, N., Monchamont, B., et al. (2006). Modulation of RIZ gene expression is associated to estradiol control of MCF-7 breast cancer cell proliferation. *Exp. Cell Res.* 312, 340–349.
- Halmos, G., Schally, A. V., Sun, B., Davis, R., Bostwick, D. G., and Plonowski, A. (2000). High expression of somatostatin receptors and messenger ribonucleic acid for its receptor subtypes in organ-confined and locally advanced human prostate cancers. *J. Clin. Endocrinol. Metab.* 85, 2564–2571.
- Hejna, M., Schmidinger, M., and Raderer, M. (2002). The clinical role of somatostatin analogues as antineoplastic agents: much ado about nothing? *Ann. Oncol.* 13, 653–668. doi: 10.1093/annonc/mdf142
- Hood, J. D., and Cheresch, D. A. (2002). Role of integrins in cell invasion and migration. *Nat. Rev. Cancer* 2, 91–100. doi: 10.1038/nrc727
- Huang, Y., Fernandez, S. V., Goodwin, S., Russo, P. A., Russo, I. H., Sutter, T. R., et al. (2007). Epithelial to mesenchymal transition in human breast epithelial cells transformed by 17beta-estradiol. *Cancer Res.* 67, 11147–11157. doi: 10.1158/0008-5472.CAN-07-1371
- Karamouz, M. V., Papavassiliou, K. A., Adamopoulos, C., and Papavassiliou, A. G. (2016). Targeting androgen/estrogen receptors crosstalk in cancer. *Trends Cancer* 2, 35–48. doi: 10.1016/j.trecan.2015.12.001
- Kimura, N., Tomizawa, S., Arai, K. N., Osamura, R. Y., and Kimura, N. (2001). Characterization of 5'-flanking region of rat somatostatin receptor sst2 gene: transcriptional regulatory elements and activation by Pitx1 and estrogen. *Endocrinology* 142, 1427–1441. doi: 10.1210/endo.142.4.8098
- Lattanzio, L., Tonissi, F., Monteverde, M., Milano, G., Merlano, M. C., and Lo Nigro, C. (2013). Differential molecular mechanism of docetaxel-octreotide combined treatment according to the docetaxel-resistance status in PC3 prostate cancer cells. *Anticancer Drugs* 24, 120–130. doi: 10.1097/CAD.0b013e328358d1dc
- Lo Nigro, C., Maffi, M., Fischel, J. L., Formento, P., Milano, G., and Merlano, M. (2008). The combination of docetaxel and the somatostatin analogue lanreotide on androgen-independent docetaxel-resistant prostate cancer: experimental data. *BJU Int.* 102, 622–627. doi: 10.1111/j.1464-410X.2008.07706.x
- Loschke, F., Seltmann, K., Bouameur, J. E., and Magin, T. M. (2015). Regulation of keratin network organization. *Curr. Opin. Cell Biol.* 32, 56–64. doi: 10.1016/j.ceb.2014.12.006
- Madak-Erdogan, Z., Charn, T. H., Jiang, Y., Liu, E. T., Katzenellenbogen, J. A., and Katzenellenbogen, B. S. (2013). Integrative genomics of gene and metabolic regulation by estrogen receptors  $\alpha$  and  $\beta$ , and their coregulators. *Mol. Syst. Biol.* 9:676. doi: 10.1038/msb.2013.28
- Mak, P., Leav, I., Pursell, B., Bae, D., Yang, X., Taglienti, C. A., et al. (2010). ER $\beta$  impedes prostate cancer EMT by destabilizing HIF-1 $\alpha$  and inhibiting vegf-mediated snail nuclear localization: implications for gleason grading. *Cancer Cell* 17, 319–332. doi: 10.1016/j.ccr.2010.02.030
- McMahon, S. B. (2014). MYC and the control of apoptosis. *Cold Spring Harb. Perspect. Med.* 4, a014407. doi: 10.1101/cshperspect.a014407
- Migliaccio, A., Castoria, G., and Auricchio, F. (2007a). Src-dependent signalling pathway regulation by sex-steroid hormones: therapeutic implications. *Int. J. Biochem. Cell Biol.* 39, 1343–1348. doi: 10.1016/j.biocel.2006.12.009
- Migliaccio, A., Varricchio, L., De Falco, A., Castoria, G., Arra, C., Yamaguchi, H., et al. (2007b). Inhibition of the SH3 domain-mediated binding of Src to the androgen receptor and its effect on tumor growth. *Oncogene* 26, 6619–6629. doi: 10.1038/sj.onc.1210487
- Mitsogiannis, I. C., Skolarikos, A., and Deliveliotis, C. (2009). Somatostatin analog lanreotide in the treatment of castration-resistant prostate cancer (CRPC). *Expert. Opin. Pharmacother.* 10, 493–501. doi: 10.1517/14656560802694689
- Møller, L. N., Stidsen, C. E., Hartmann, B., and Holst, J. J. (2003). Somatostatin receptors. *Biochim. Biophys. Acta* 1616, 1–84. doi: 10.1016/S0005-2736(03)00235-9
- Montanari, M., Rossetti, S., Cavaliere, C., D'Aniello, C., Malzone, M. G., Vanacore, D., et al. (2017). Epithelial-mesenchymal transition in prostate

- cancer: an overview. *Oncotarget* 8, 35376–35389. doi: 10.18632/oncotarget.15686
- Msaouel, P., Galanis, E., and Koutsilieris, M. (2009). Somatostatin and somatostatin receptors: implications for neoplastic growth and cancer biology. *Expert Opin. Investig. Drugs* 18, 1297–1316. doi: 10.1517/13543780903176399
- Nanni, S., Benvenuti, V., Grasselli, A., Priolo, C., Aiello, A., Mattiussi, S., et al. (2009). Endothelial NOS, estrogen receptor beta, and HIFs cooperate in the activation of a prognostic transcriptional pattern in aggressive human prostate cancer. *J. Clin. Invest.* 119, 1093–1108. doi: 10.1172/JCI35079
- Pagano, M., Naviglio, S., Spina, A., Chiosi, E., Castoria, G., Romano, M., et al. (2004). Differentiation of H9c2 cardiomyoblasts: the role of adenylate cyclase system. *J. Cell. Physiol.* 198, 408–416. doi: 10.1002/jcp.10420
- Pasquali, D., Rossi, V., Conzo, G., Pannone, G., Bufo, P., De Bellis, A., et al. (2008). Effects of somatostatin analog SOM230 on cell proliferation, apoptosis, and catecholamine levels in cultured pheochromocytoma cells. *J. Mol. Endocrinol.* 40, 263–271. doi: 10.1677/JME-08-0012
- Pasquali, D., Rossi, V., Staibano, S., De Rosa, G., Chieffi, P., Prezioso, D., et al. (2006). The endocrine-gland-derived vascular endothelial growth factor (EG-VEGF)/prokineticin 1 and 2 and receptor expression in human prostate: up-regulation of EG-VEGF/prokineticin 1 with malignancy. *Endocrinology* 147, 4245–4251. doi: 10.1210/en.2006-0614
- Patel, Y. C. (1999). Somatostatin and its receptor family. *Front. Neuroendocrinol.* 20:157–198. doi: 10.1006/frne.1999.0183
- Perillo, B., Ombra, M. N., Berton, A., Cuozzo, C., Sacchetti, S., Sasso, A., et al. (2008). DNA oxidation as triggered by H3K9me2 demethylation drives estrogen-induced gene expression. *Science* 319, 202–206. doi: 10.1126/science.1147674
- Perillo, B., Sasso, A., Abbondanza, C., and Palumbo, G. (2000). 17beta-estradiol inhibits apoptosis in MCF-7 cells, inducing bcl-2 expression via two estrogen-responsive elements present in the coding sequence. *Mol. Cell. Biol.* 20, 2890–2901. doi: 10.1128/MCB.20.8.2890-2901.2000
- Pisolato, R., Lombardi, A. P., Vicente, C. M., Lucas, T. F., Lazari, M. F., and Porto, C. S. (2016). Expression and regulation of the estrogen receptors in PC-3 human prostate cancer cells. *Steroids* 107, 74–86. doi: 10.1016/j.steroids.2015.12.021
- Porcile, C., Di Zazzo, E., Monaco, M. L., D'Angelo, G., Passarella, D., Russo, C., et al. (2014). Adiponectin as novel regulator of cell proliferation in human glioblastoma. *J. Cell. Physiol.* 229, 1444–1454. doi: 10.1002/jcp.24582
- Rossi, V., Bellastella, G., De Rosa, C., Abbondanza, C., Visconti, D., Maione, L., et al. (2011). Raloxifene induces cell death and inhibits proliferation through multiple signaling pathways in prostate cancer cells expressing different levels of estrogen receptor  $\alpha$  and  $\beta$ . *J. Cell. Physiol.* 226, 1334–1339. doi: 10.1002/jcp.22461
- Rossi, V., Staibano, S., Abbondanza, C., Pasquali, D., De Rosa, C., Mascolo, M., et al. (2009). Expression of RIZ1 protein (Retinoblastoma-interacting zinc-finger protein 1) in prostate cancer epithelial cells changes with cancer grade progression and is modulated in vitro by DHT and E2. *J. Cell. Physiol.* 221, 771–777. doi: 10.1002/jcp.21920
- Ryan, C. J., and Tindall, D. J. (2011). Androgen receptor rediscovered: the new biology and targeting the androgen receptor therapeutically. *J. Clin. Oncol.* 29, 3651–3658. doi: 10.1200/JCO.2011.35.2005
- Schaeffer, D., Jason, A., Somarelli, G. H., Palmer, G. M., and Garcia-Blanco, M. A. (2014). Cellular migration and invasion uncoupled: increased migration is not an inexorable consequence of epithelial-to-mesenchymal transition. *Mol. Cell. Biol.* 34, 3486–3499. doi: 10.1128/MCB.00694-14
- Shao, R., Shi, J., Liu, H., Shi, X., Du, X., Klocker, H., et al. (2014). Epithelial-to-mesenchymal transition and estrogen receptor alpha mediated epithelial dedifferentiation mark the development of benign prostatic hyperplasia. *Prostate* 74, 970–982. doi: 10.1002/pros.22814
- Shi, X., Peng, Y., Du, X., Liu, H., Klocker, H., Lin, Q., et al. (2017). Estradiol promotes epithelial-to-mesenchymal transition in human benign prostatic epithelial cells. *Prostate* 77, 1424–1437. doi: 10.1002/pros.23404
- Sinisi, A. A., Bellastella, A., Prezioso, D., Nicchio, M. R., Lotti, T., Salvatore, M., et al. (1997). Different expression patterns of somatostatin receptor subtypes in cultured epithelial cells from human normal prostate and prostate cancer. *J. Clin. Endocrinol. Metab.* 82, 2566–2569. doi: 10.1210/jc.82.8.2566
- Sinisi, A. A., Chieffi, P., Pasquali, D., Kisslinger, A., Staibano, S., Bellastella, A., et al. (2002). EPN: a novel epithelial cell line derived from human prostate tissue. *In Vitro Cell Dev. Biol. Anim.* 38, 165–172. doi: 10.1290/1071-2690(2002)038<0165:EANECL>2.0.CO;2
- Spencer, V. A., Coutts, A. S., Samuel, S. K., Murphy, L. C., and Davie, J. R. (1998). Estrogen regulates the association of intermediate filament proteins with nuclear DNA in human breast cancer cells. *J. Biol. Chem.* 273, 29093–29097. doi: 10.1074/jbc.273.44.29093
- Thakur, M. K., Heilbrun, L., Dobson, K., Boerner, J., Stark, K., Li, J., et al. (2018). Phase I trial of the combination of docetaxel, prednisone, and pasireotide in metastatic castrate-resistant prostate cancer. *Clin. Genitourin. Cancer* 695:e703. doi: 10.1016/j.clgc.2018.01.019
- Thiery, J. P. (2002). Epithelial-mesenchymal transitions in tumour progression. *Nat. Rev. Cancer* 2, 442–454. doi: 10.1038/nrc822
- War, S. A., Somvanshi, R. K., and Kumar, U. (2011). Somatostatin receptor-3 mediated intracellular signaling and apoptosis is regulated by its cytoplasmic terminal. *Biochim. Biophys. Acta* 1813, 390–402. doi: 10.1016/j.bbamcr.2010.12.015
- Warner, M., Huang, B., and Gustafsson, J. A. (2017). Estrogen receptor  $\beta$  as a pharmaceutical target. *Trends Pharmacol. Sci.* 38, 92–99. doi: 10.1016/j.tips.2016.10.006
- Weckbecker, G., Lewis, I., Albert, R., Schmid, H. A., Hoyer, D., and Bruns, C. (2003). Opportunities in somatostatin research: biological, chemical and therapeutic aspects. *Nat. Rev. Drug Discov.* 2, 999–1017. doi: 10.1038/nrd1255

**Conflict of Interest Statement:** The authors declare that the research was conducted in the absence of any commercial or financial relationships that could be construed as a potential conflict of interest.

Copyright © 2019 Rossi, Di Zazzo, Galasso, De Rosa, Abbondanza, Sinisi, Altucci, Migliaccio and Castoria. This is an open-access article distributed under the terms of the Creative Commons Attribution License (CC BY). The use, distribution or reproduction in other forums is permitted, provided the original author(s) and the copyright owner(s) are credited and that the original publication in this journal is cited, in accordance with accepted academic practice. No use, distribution or reproduction is permitted which does not comply with these terms.



# Wedelolactone Attenuates Pulmonary Fibrosis Partly Through Activating AMPK and Regulating Raf-MAPKs Signaling Pathway

Jin-yu Yang<sup>1</sup>, Li-jun Tao<sup>1†</sup>, Bei Liu<sup>1</sup>, Xin-yi You<sup>1</sup>, Chao-feng Zhang<sup>1\*</sup>, Hai-feng Xie<sup>2</sup> and Ren-shi Li<sup>1\*</sup>

<sup>1</sup> State Key Laboratory of Natural Medicines, School of Traditional Chinese Medicine, China Pharmaceutical University, Nanjing, China, <sup>2</sup> Chengdu Biopurify Phytochemicals Ltd., Chengdu, China

## OPEN ACCESS

### Edited by:

Cecilia Battistelli,  
Sapienza University of Rome, Italy

### Reviewed by:

Longshuang Huang,  
University of Illinois at Chicago,  
United States  
Xia Wang,  
Shanghai Chest Hospital, Shanghai  
Jiao Tong University, China

### \*Correspondence:

Chao-feng Zhang  
zhangchao-feng@cpu.edu.cn  
Ren-shi Li  
li-renshi@cpu.edu.cn;  
Li-renshi@hotmail.com

<sup>†</sup>Co-first author

### Specialty section:

This article was submitted to  
Experimental Pharmacology  
and Drug Discovery,  
a section of the journal  
Frontiers in Pharmacology

**Received:** 30 October 2018

**Accepted:** 08 February 2019

**Published:** 05 March 2019

### Citation:

Yang J-y, Tao L-j, Liu B, You X-y,  
Zhang C-f, Xie H-f and Li R-s (2019)  
Wedelolactone Attenuates Pulmonary  
Fibrosis Partly Through Activating  
AMPK and Regulating Raf-MAPKs  
Signaling Pathway.  
Front. Pharmacol. 10:151.  
doi: 10.3389/fphar.2019.00151

Pulmonary fibrosis is common in a variety of inflammatory lung diseases, there is currently no effective clinical drug treatment. It has been reported that the ethanol extract of *Eclipta prostrata* L. can improve the lung collagen deposition and fibrosis pathology induced by bleomycin (BLM) in mice. In the present study, we studied whether wedelolactone (WEL), a major coumarin ingredient of *E. prostrata*, provided protection against BLM-induced pulmonary fibrosis. ICR or C57/BL6 strain mice were treated with BLM to establish lung fibrosis model. WEL (2 or 10 mg/kg) was given daily via intragastric administration for 2 weeks starting at 7-day after intratracheal instillation. WEL at 10 mg/kg significantly reduced BLM-induced inflammatory cells infiltration, pro-inflammatory factors expression, and collagen deposition in lung tissues. Additionally, treatment with WEL also impaired BLM-induced increases in fibrotic marker expression (collagen I and  $\alpha$ -SMA) and decrease in an anti-fibrotic marker (E-cadherin). Treatment with WEL significantly prevented BLM-induced increase in TGF- $\beta$ 1 and Smad2/3 phosphorylation in the lungs. WEL administration (10 mg/kg) also significantly promoted AMPK activation compared to model group in BLM-treated mice. Further investigation indicated that activation of AMPK by WEL can suppressed the transdifferentiation of primary lung fibroblasts and the epithelial mesenchymal transition (EMT) of alveolar epithelial cells, the inhibitive effects of WEL was significantly blocked by an AMPK inhibitor (compound C) *in vitro*. Together, these results suggest that activation of AMPK by WEL followed by reduction in TGF $\beta$ 1/Raf-MAPK signaling pathways may have a therapeutic potential in pulmonary fibrosis.

**Keywords:** *Eclipta prostrata*, wedelolactone, pulmonary fibrosis, AMPK, bleomycin

**Abbreviations:**  $\alpha$ -SMA,  $\alpha$ -smooth muscle actin; AMPK, adenosine 5'-monophosphate (AMP)-activated protein kinase; BLM, bleomycin; BSA, bovine serum albumin; COL1, collagen I; DAB, diaminobenzidine; ECL, enhanced chemiluminescence; ECM, extracellular matrix; EMT, epithelial mesenchymal transition; ERK, extracellular signal-regulated kinase; HYP, hydroxyproline; JNK, c-JUN N-terminal kinase; MAPK, mitogen-activated protein kinase; TGF- $\beta$ 1, transforming growth factor- $\beta$ 1; WEL, wedelolactone.

## INTRODUCTION

*Eclipta prostrata* L. is widely used to treat respiratory diseases such as diphtheria, pertussis, tuberculosis in the traditional medicine of China (Roy et al., 2008; Deng and Fang, 2012), which exhibits hepatoprotective (Tabassum and Agrawal, 2004; Manvar et al., 2012), anti-tumor (Liu et al., 2012) and other biological activities (Tewtrakul et al., 2011; Jaiswal et al., 2012). In Brazil, extracts of *E. prostrata* are also used to treat asthma (Chichioco-Hernandez and Paguigan, 2010; Sharma et al., 2012; Jahan et al., 2014). It has been reported that the methanol extract of this plant significantly attenuated experimental pulmonary fibrosis in mice (You et al., 2015). Although it has been found that WEL, a main component of *E. prostrata*, can improve bronchial epithelial cell injury (Ding et al., 2015) and fibrosis process of activated hepatic stellate cells (Xia et al., 2013), its effects on pulmonary function, collagen deposition and epithelial-mesenchymal transition remain to be researched.

Pulmonary fibrosis is a chronic inflammatory interstitial lung disease. Recently, several tyrosine kinase receptors, such as nintedanib (BIBF 1120), has been approved for treatment of PF (Myllärniemi and Kaarteenaho, 2015), but its potential side effects are still unknown. Recently, researchers have identified the close relationship between AMPK activation and lung fibrogenesis (Sato et al., 2016; Rangarajan et al., 2018). The administration of WEL can attenuate hepatic steatosis in mice by activating AMPK (Zhao Y. et al., 2015), but the therapeutic effect of WEL on pulmonary fibrosis is not sure. The processes of normal lung repair after injury include epithelial cell migration, proliferation and differentiation, lung fibroblast migration, and transformation of lung fibroblast into myofibroblasts (Selman and Pardo, 2001). The fibrotic response is driven by abnormally activated alveolar epithelial cells resulting in epithelial to mesenchyme transition (EMT) and formation of myofibroblast foci secreting amounts of ECM (Ley et al., 2011; Wynn, 2011).

Suppressing the activation of fibroblasts can ameliorate pulmonary fibrogenesis (Postlethwaite et al., 2004). TGF- $\beta$ 1 is the main cytokine in pulmonary fibrosis pathogenesis, which regulates fibroblasts proliferation and differentiation leading to ECM over-production (Sime et al., 1997; Khalil et al., 2001). BLM (an anti-neoplastic agent) causes alveolar cell damage, inflammatory response, EMT and subsequent ECM deposition to induce lung injury and pulmonary fibrosis *in vivo* (Gong et al., 2005). In the present study, the administration of WEL effectively attenuated BLM-induced pulmonary fibrosis process in mice by activating AMPK to negatively regulate collagen production and transformation of lung fibroblast into myofibroblasts.

## MATERIALS AND METHODS

### Chemicals and Reagents

Wedelolactone (Pubchem CID: 5281813, purity above 99%) was prepared by Mr. Haifeng Xie in Chengdu Biopurify Phytochemical Ltd. (Chengdu, China). Prednisone acetate

(PNS, Pubchem CID: 91438) was purchased from Zhejiang Xianju Pharmaceutical Co., Ltd. (Xianju, China). Bleomycin hydrochloride (BLM) was purchased from Nippon Kayaku (Tokyo, Japan). Compound C (Pubchem CID: 11524144), an AMPK inhibitor, was purchased from Shanghai Chembest Research Laboratories Limited (Shanghai, China). Recombinant TGF- $\beta$ 1 was purchased from PeproTech (Rocky Hill, NJ, United States). 3-(4,5-dimethylthiazol-2-yl)-2,5-diphenyl tetrazolium bromide (MTT) was purchased from Biosharp (Anhui, China).

Hydroxyproline assay kit was purchased from Beyotime Biotechnology (Jiangsu, China). Antibodies against ERK (#4695), phospho-ERK (#4370), JNK (#9258), phospho-JNK (#9255), p38 (#8690), phospho-p38 (#4511), AMPK (#2531), phospho-AMPK (#2532) and TGF- $\beta$  (#3711) were all purchased from Cell Signal Technology Inc. (Danvers, MA, United States). Antibodies against COL1 (WL0088), Raf1 (WL00553), and Vimentin (WL01960) were all obtained from Wanleibio (Shenyang, China). Antibodies against  $\alpha$ -SMA (ab32575) was obtained from Abcam (Cambridge, United Kingdom). Antibodies against E-cadherin (BS72286) was obtained from Bioworld Technology Inc. (Dublin, OH, United States). HRP-conjugated secondary antibody was purchased from Bioworld Technology Inc. (Dublin, OH, United States).

### Cell Culture

Primary lung fibroblasts (PLFs) were derived from 6 to 8 weeks old male C57/BL6 mice. The lungs were cleaned in phosphate-buffered saline (PBS), minced into 1–2 mm<sup>3</sup> sections and digested with trypsin for 30 min at 37°C. The cell suspensions obtained after digestion were plated into sterile cell culture bottle containing 5–6 mL of Dulbecco's modified Eagle's complete medium (DMEM, GIBCO, Grand Island, NY, United States) and incubated at 37°C. These cells were detached with 0.25% trypsinization and seeded in 6-well plates ( $1 \times 10^5$  cells per well). The cells were pretreated with either compound C (50  $\mu$ M) or solvent (DMSO) for 1.5 h and then incubated with/without TGF- $\beta$ 1 (10 ng/ml), WEL (10  $\mu$ M) or solvents (PBS or DMSO) for 48 h. Then, these cells were subjected to the following analysis. In cell experiments, solutions of chemicals were prepared in DMSO, and diluted in FBS-free medium, the concentrations of DMSO is less than 0.05%.

The human type II alveolar epithelial cell MLE-12 were purchased from Saiqi BioTech Co., Ltd. (Shanghai, China) and maintained in DMEM/F12 (KeyGen BioTech Co., Ltd., Jiangsu, China) supplemented with 10% FBS (Hyclone, Thermo, South America), penicillin (100 U/mL) and streptomycin (100  $\mu$ g/mL) at 37°C, with 95% humidity and 5% carbon dioxide. The cells were pretreated with either compound C (50  $\mu$ M) or solvent for 1.5 h and then incubated with/without TGF- $\beta$ 1 (10 ng/ml), WEL (10  $\mu$ M) or solvents for 48 h. Then, these cells were subjected to the following analysis.

### Cell Viability Assay

$5 \times 10^4$  cells were seeded in 96 well plates and incubated in DMEM or DMEN/F12 containing 10% FBS for 24 h. The cells were pretreated with either compound C (50  $\mu$ M) or solvent



(DMSO) for 1.5 h and subsequently incubated with/without TGF- $\beta$ 1 (10 ng/ml), WEL (10  $\mu$ M) or solvent for 48 h, then MTT solvent (5 mg/ml) was added and incubated for 4 h at 37°C. The optical density was measured at 490 nm with 630 nm as reference wavelength.

## Animals

Male C57/BL6 mice (6–8 weeks old, weighing between 18 and 20 g) and male ICR mice (6–8 weeks old, weighing between 22 and 25 g) were supplied from Qinglongshan Standard Animal Propagation Center in Nanjing. The care and use of animals was performed in accordance with the General Recommendation and Provisions of the Chinese Experimental Animals Administration Legislation. All experiments were approved by the Institutional Ethical Committee of China Pharmaceutical University, Nanjing. Animals were housed in a climate-controlled room temperature at  $22 \pm 2^\circ\text{C}$  and  $50 \pm 10\%$  humidity with a 12 h light/dark cycle. Additionally, the animals were given free drinking water and conventional rodent chow.

## Mouse Model of BLM-Induced Pulmonary Fibrosis

The BLM-induced experimental pulmonary fibrosis model was described as our previous study (You et al., 2015). In brief, mice were divided into groups after 1 week of acclimation. Each group of mice was anesthetized with intraperitoneal injection of chloral hydrate solution (4%, 10 ml/kg) before intratracheal instillation, respectively, of BLM (5 mg/kg). Mice receiving an instillation of equivoluminal vehicle (0.9% sterilized saline solution) served as controls. Preliminary experimental were investigated in male ICR mice. We divide mice into five groups: normal group, BLM group, BLM and prednisone (PNS, positive drug), BLM and large dose of WEL (WEL-H, 10 mg/kg) as well as BLM and small dose of BLM groups (WEL-L, 2 mg/kg) at random. One week later after BLM administration, two doses of WEL (2 mg/kg or 10 mg/kg) and prednisone acetate (PNS, 6 mg/kg, positive drug) were orally administered to mice for 7 or 21 consecutive days, the control and the BLM groups were given the equivoluminal vehicle (0.9% sterilized saline). On the day 14 and day 28 after BLM instillation. After blood collection, each group's mice were sacrificed randomly by excessive intraperitoneal injection of chloral hydrate. Lungs were excised for pulmonary coefficient measurement (lung weight/body weight; mg/g) (Turgut et al., 2016). The left lower lobes were fixed in 10% formalin for the examination of histopathology, and the other lung tissue samples were stored at  $-80^\circ\text{C}$ .

Formal experiments were investigated in male C57/BL6 mice, 1 week later after BLM administration, WEL (10 mg/kg/day) were orally administered to mice for 14 consecutive days. On the day 21, mice were euthanized by excessive intraperitoneal injection of chloral hydrate. Lung tissues were excised for pulmonary index measurement (lung weight/body weight; mg/g). The left lower lobes were fixed in 10% formalin for the examination of histopathology, and the other lung tissue samples were stored at  $-80^\circ\text{C}$ .

## Cytokine Assays in Bleomycin-Induced PF Model in ICR Mice

IL-1 $\beta$ , TNF- $\alpha$ , and TGF- $\beta$  levels in lung tissues were measured with ELISA kits according to the instructions recommended by the manufactures (BioLegend, Inc., San Diego, CA, United States), and the optical density (OD) of the microplate was read at 450 nm.

## Histological Analysis

The lung tissues fixed with 10% formalin were embedded in paraffin for histological examination and stained with hematoxylin–eosin (HE) or Masson's trichrome, then evaluated under a light microscopy conducted by experienced pathologists, who were blinded for groups. The results were scored in accordance with the previously reported method, and the score numbers (0–3) were, respectively, corresponded to the grades of –, +, ++, and +++ (Szapiel et al., 1979).

## Hydroxyproline Assay

Collagen deposition was determined by measuring the total HYP content, which was measured by a HYP assay kit according to the provided manufacturer's protocol. In brief, lungs were hydrolyzed at  $100^\circ\text{C}$  for 40 min and mixed every 10 min. After neutralization with hydrochloric acid, the hydrolyzation products were diluted with distilled water, and assessed at 550 nm and expressed as  $\mu\text{g}/\text{mg}$  (You et al., 2015).

## Western Blot Analysis

The levels of Col I,  $\alpha$ -SMA, TGF- $\beta$ 1, p-Smad2/3, p-AMPK, Raf1, MAPKs, Vimentin and E-cadherin were detected by Western blotting. Total proteins extracted from lung homogenate or cell lysate were lysed in ice-cold RIPA lysis buffer containing 1:100 dilution of phenylmethanesulfonyl fluoride (PMSF, Beyotime). Total protein concentrations were determined by BCA Protein Assay Kit (Beyotime). After boiling for 10 min, equal amounts of the protein (50  $\mu\text{g}/\text{lane}$ ) were separated by SDS-PAGE and transferred to PVDF membrane (Millipore, Billerica, MA, United States) that were probed with primary antibodies overnight at  $4^\circ\text{C}$  and HRP-labeled secondary antibodies at  $25^\circ\text{C}$  for 2 h and visualized using super ECL detection reagent (Beyotime).

## Preparation of RNA and RT-PCR Analysis

Total RNA from cultured cells and lung samples were isolated and one-step real-time RT-PCR and real-time PCR performed using SYBR Green PCR Reagents (TaKaRa, China), the StepOne™ Real-Time PCR (Life Technologies, United States), and the Opticon DNA Engine (MJ Research Inc., South San Francisco, CA, United States). Total RNA was extracted from the treated cells or lung tissues using Trizol reagent (Invitrogen Life Technologies, United States), reverse-transcribed to complementary DNA (cDNA) using the TransScript first-Strand cDNA Synthesis kit (TOYOBO, Japan), and stored at  $-80^\circ\text{C}$  until reverse transcription. The relative gene expression was quantified by Q-PCR using SYBR® Premix Ex Taq™ (TaKaRa, China) in StepOne™ Real-Time PCR (Life Technologies,

United States). In each reaction, 0.5 µg of total RNA was reverse transcribed before the following PCR conditions: 94°C for 2 min followed by 40 cycles at 94°C for 15 s, 58°C for 30 s, 72°C for 30 s, with final extension at 72°C for 10 min. Primers and amplicon sizes were shown in **Table 1**. The relative amount of mRNA was calculated using the comparative Ct ( $\Delta$ Ct) method compared with  $\beta$ -actin and expressed as the mean  $\pm$  SD.

## Statistical Analysis

Data were presented as mean  $\pm$  SD from at least three independent experiments. One-way analysis of variance (ANOVA) was used for performing differences among different groups followed by the Student–Newman–Keuls test (GraphPad Prism Software 5.0, GraphPad Software Inc., San Diego, CA, United States). Values of  $p < 0.05$  were considered statistically significant.

## RESULTS

### WEL Protects Against Bleomycin-Induced Pulmonary Fibrosis in ICR Mice

Bleomycin-induced PF model in mice is characterized by activated myofibroblasts (Bhattacharyya et al., 2013). In this model, 7–9 days is the switch point from lung inflammation to fibrotic phase (Chaudhary et al., 2006). In the present study, two doses of WEL-L (2 mg/kg) and WEL-H (10 mg/kg) were orally administered for 14 days, respectively, starting 7 days after BLM (5 mg/kg) administration. The high dose of WEL treatment (WEL-H, 10 mg/kg) markedly attenuated BLM-induced the weight loss and the increasing pulmonary index as well as HYP content in lungs (**Figures 1E,F**). Moreover, the levels of pro-inflammatory cytokines, IL-1 $\beta$ , TNF- $\alpha$ , and TGF- $\beta$ 1, in lung tissues were elevated at day 14 from different groups, but greatly reduced after WEL treatment at the dose of 10 mg/kg

(**Figure 1F**), indicating an inhibitive effect of WEL in BLM-induced lung inflammation.

### WEL Protects Against Bleomycin-Induced Pathological Changes of Lungs in ICR Mice

The mice that received intratracheal instillations of BLM suffered serious lung damage and fibrosis, which manifested as weight loss, poor survival rate, collagen deposition in lung tissues. Histological analysis by HE and Masson's staining showed WEL group displayed slightly thickened alveolar walls, some inflammatory cells, and minimum deposition of collagen fibers at day 14 and day 28 compared to BLM alone group (**Figure 2**).

### WEL Protects Against Bleomycin-Induced Pulmonary Fibrosis in C57/BL6 Mice

In most studies, C57/BL6 mice are more susceptible to BLM-induced fibrosis (Lattaa et al., 2015). Then, C57/BL6 mice were also selected in the present study, and similar results were achieved in BLM-challenged PF model. The inflammation and fibrosis scores as well as HYP content in WEL groups were also significantly decreased compared to BLM alone group (**Figures 3E–G**). In addition, the expression of  $\alpha$ -SMA (a hallmark of myofibroblasts) and Col I as well as its mRNA levels were also dramatically reduced in WEL-treated mice compared to BLM group (**Figures 3H,I**). Taken together, these results further confirmed that WEL could effectively ameliorated BLM-induced inflammation infiltration and fibrosis degree of lung tissues.

### WEL Down-Regulates TGF- $\beta$ /Smad Signaling Pathway and Promotes the Activation of AMPK in Bleomycin-Induced PF in C57/BL6 Mice

Growth factor TGF- $\beta$ 1 has been widely detected in idiopathic pulmonary fibrosis, which activates fibroblast proliferation and collagen production, and TGF- $\beta$ /Smad signaling pathway is the canonical signaling pathway during the fibrosis process (Pedram et al., 2010). As shown in **Figures 4A,B**, WEL treatment significantly decreased TGF- $\beta$ 1 over-expression and its mRNA levels as well as the phosphorylated Smad2/3 level in lungs compared to BLM alone group (**Figure 4C**). Additionally, WEL administration notably activated AMPK in lungs compared to BLM alone group (**Figure 4D**), suggesting that there is a close relationship between the activation AMPK by WEL treatment and its anti-fibrotic effects.

### WEL Prevents ECM Accumulation by Activating AMPK in PLFs Exposed to TGF- $\beta$ 1

Following lung injury, PLFs transform into myofibroblast-like cells and are the major source of ECM accumulation in the fibrotic lungs with  $\alpha$ -SMA overexpression (Todd et al., 2012). In the current study, primary mouse lung fibroblasts (PLFs) were treated with TGF- $\beta$ 1 to induce fibrosis-related protein

**TABLE 1** | Sequences of primers used for real-time quantitative PCR.

Gene	Forward primer (5'–3')	Reverse primer (5'–3')	Product size (bp)
M- $\alpha$ -SMA	CCA CGA AAC CAC CTA TAA CAG C	GGA AGG TAG ACA GCG AAG CC	236
M-Collagen I	CTG ACT GGA AGA GCG GAG AG	CGG CTG AGT AGG GAA CAC AC	116
M-TGF- $\beta$ 1	AGA GCC CTG GAT ACC AAC TAT TG	TGC GAC CCA CGT AGT AGA CG	286
M-Vimentin	TCC ACA CGC ACC TAC AGT CT	CCG AGG ACC GGG TCA CAT A	124
M-E-cadherin	CAG GTC TCC TCA TGG CTT TGC	CTT CCG AAA AGA AGG CTG TCC	175
M- $\beta$ -actin	CTG AGA GGG AAA TCG TGC GT	CCA CAG GAT TCC ATA CCC AAG A	208
H- $\alpha$ -SMA	CTG TTC CAG CCA TCC TTC AT	TCA TGA TGC TGT TGT AGG TGG T	70
H-GAPDH	CAT CTT CTT TTG CGT CGC CA	TTA AAA GCA GCC CTG GTG ACC	115

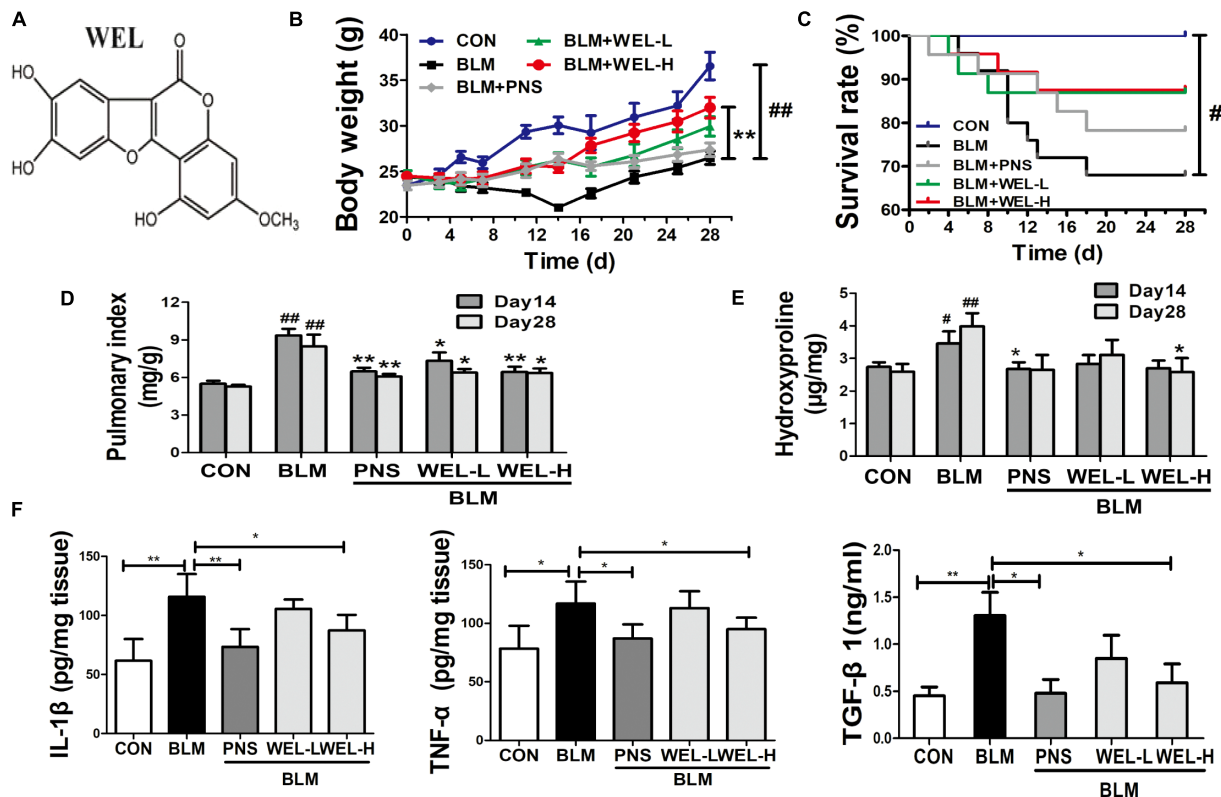


**FIGURE 1 |** WEL attenuated bleomycin (BLM)-induced pulmonary fibrosis in ICR mice. One week after 5 mg/kg bleomycin (BLM) treatment, mice were orally administered with two doses of WEL-L (2 mg/kg/day) and WEL-H (10 mg/kg/day) and prednisone (PNS, 6 mg/kg) once a day for 7 or 21 days. **(A)** The chemical structure of WEL, changes of body weight **(B)**, survival rate **(C)**, and pulmonary index **(D)** were shown in different groups. **(E)** The HYP contents in lung tissues were determined by an assay kit. **(F)** The levels of pro-inflammatory cytokines (IL-1 $\beta$ , TNF- $\alpha$ , and TGF- $\beta$ 1) in lung tissue from different groups at day 14 were detected by ELISA assay. Data are shown as mean  $\pm$  SD ( $n = 10$ ). # $p < 0.05$ , ## $p < 0.01$  vs. the control group; \* $p < 0.05$ , \*\* $p < 0.01$  vs. the BLM group.

expression. As shown in **Figure 5A**, WEL at the concentration of 0.1–100  $\mu$ M had no significant cytotoxicity to normal PFLs, but tend to weakly promote normal PFLs growths. Recent study reported that the activation of AMPK effectively alleviated inflammation-related fibrosis in lungs (Rangarajan et al., 2018).

Wedelolactone treatment (10  $\mu$ M) significantly inhibited  $\alpha$ -SMA overexpression ( $P < 0.01$ , **Figure 5B**), but the effect of WEL were significantly blocked by the inhibition of AMPK with compound C in TGF- $\beta$ -stimulated PLFs (**Figure 5E**). In addition, TGF- $\beta$ 1 acts the non-genomic functions in lung myofibroblast proliferation via regulating Raf1-MAPK (ERK, JNK and P38) signaling pathways (Flores-Delgado et al., 2001). We found that WEL also significantly suppressed TGF- $\beta$ -induced abnormal protein expressions of Raf1/MAPKs signaling pathways in PFLs (**Figure 5F**). Taken together, WEL treatment effectively suppressed the accumulation of ECM of activated lung fibroblasts partly by activating AMPK and its inflammation level.

## AMPK Activation by WEL Treatment Is Responsible for EMT Process

TGF- $\beta$ 1 level mediated the epithelial-mesenchymal transition (EMT) process of alveolar epithelial cells during pulmonary fibrosis (Kuiper et al., 1998). In the present study, protective

effects of WEL were obtained in TGF- $\beta$ -treated MLE-12 cell lines. We examined the effect of WEL on cell viability at 0.1–100  $\mu$ M for MLE-12 cells. WEL did not influence the cell growth at 0.1–10  $\mu$ M (**Figures 6A,B**). WEL treatment (10  $\mu$ M) significantly inhibited the TGF- $\beta$ 1-induced abnormal expressions and mRNA levels of EMT markers, such as  $\alpha$ -SMA, Vimentin, Col I and E-cadherin (**Figures 6C–J**) without influence on normal protein levels of MLE-12 cells (see **Supplementary Figures S1, S2**). However, the inhibition of WEL on EMT was significantly blocked by compound C (**Figures 6K,L**), suggesting that WEL could effectively ameliorated EMT of alveolar epithelial cells through activating AMPK. In addition, WEL also significantly inhibited Raf1-MAPKs signaling pathway in MLE-12 cells exposed to TGF- $\beta$ 1 (**Figure 6M** and **Supplementary Figure S1**). Taken together, WEL effectively suppressed EMT of alveolar epithelial cells partly through activating AMPK and its inflammation level.

## DISCUSSION

Wedelolactone is the major component in *Ecliptae Herba*. WEL is reported to inhibit topoisomerase II $\alpha$  and 5-lipoxygenase (Wagner and Fessler, 1986; Benes et al., 2011) hepatic stellate cells



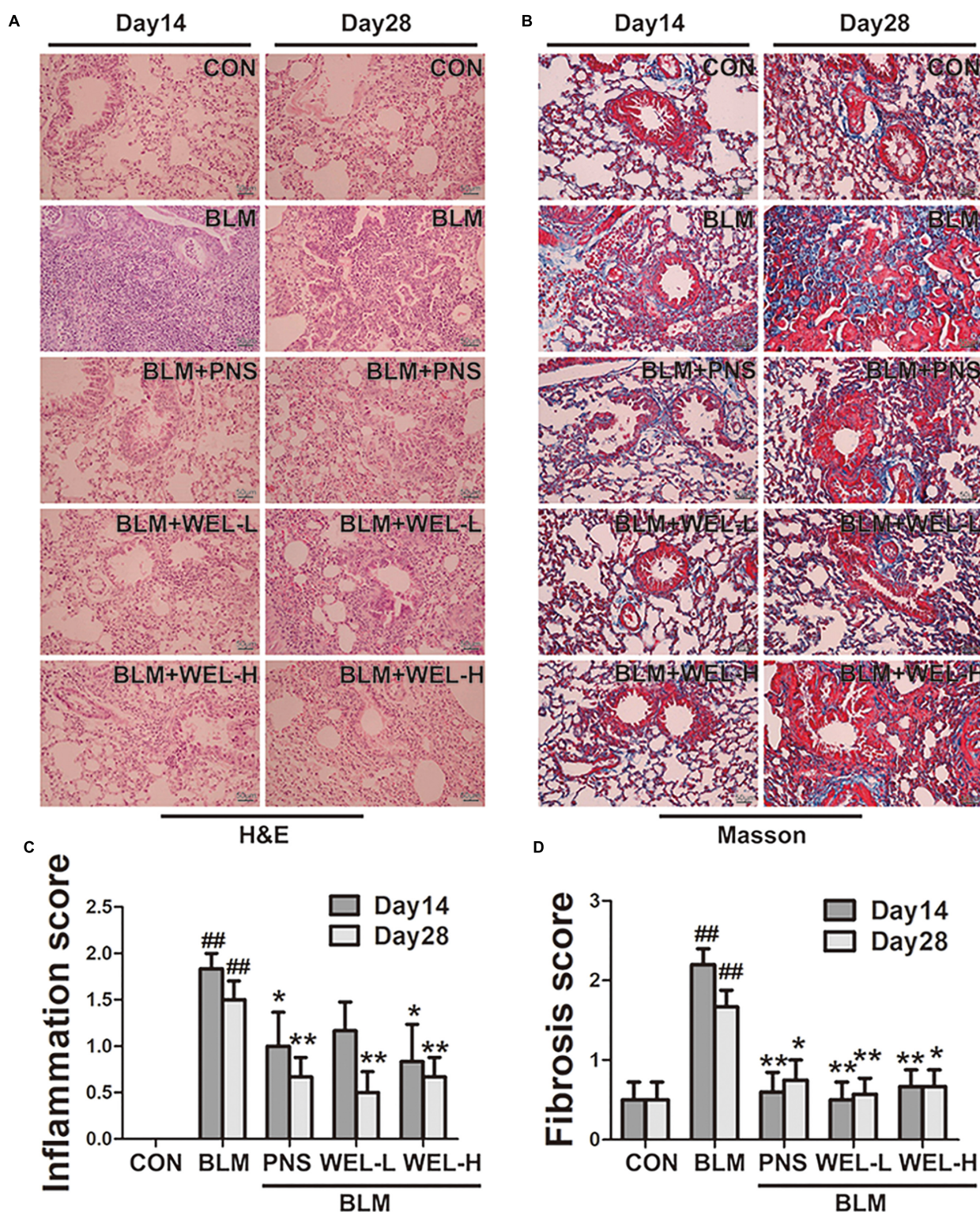


**FIGURE 2 |** WEL protects against bleomycin-induced pathological changes of lungs in ICR mice. One week after BLM treatment (5 mg/kg), mice were orally administered with WEL-L (2 mg/kg) or WEL-H (10 mg/kg) and prednisone (6 mg/kg, positive drug) once a day for 7 or 21 days. Representative pictures ( $\times 200$ ) of HE-stained (A) and Masson's trichrome-stained (B) lung sections from mice on day 14 or day 28 were shown. Bar = 100  $\mu$ m. The inflammation (C) and fibrosis (D) score numbers of 0–3, corresponding to the grades of –, +, ++, and +++, were evaluated by experienced pathologists in a blinded fashion. Data are presented as the mean  $\pm$  SD ( $n = 10$ ). <sup>##</sup> $p < 0.01$  vs. the control group; <sup>\*</sup> $p < 0.05$ , <sup>\*\*</sup> $p < 0.01$  vs. the BLM alone group.



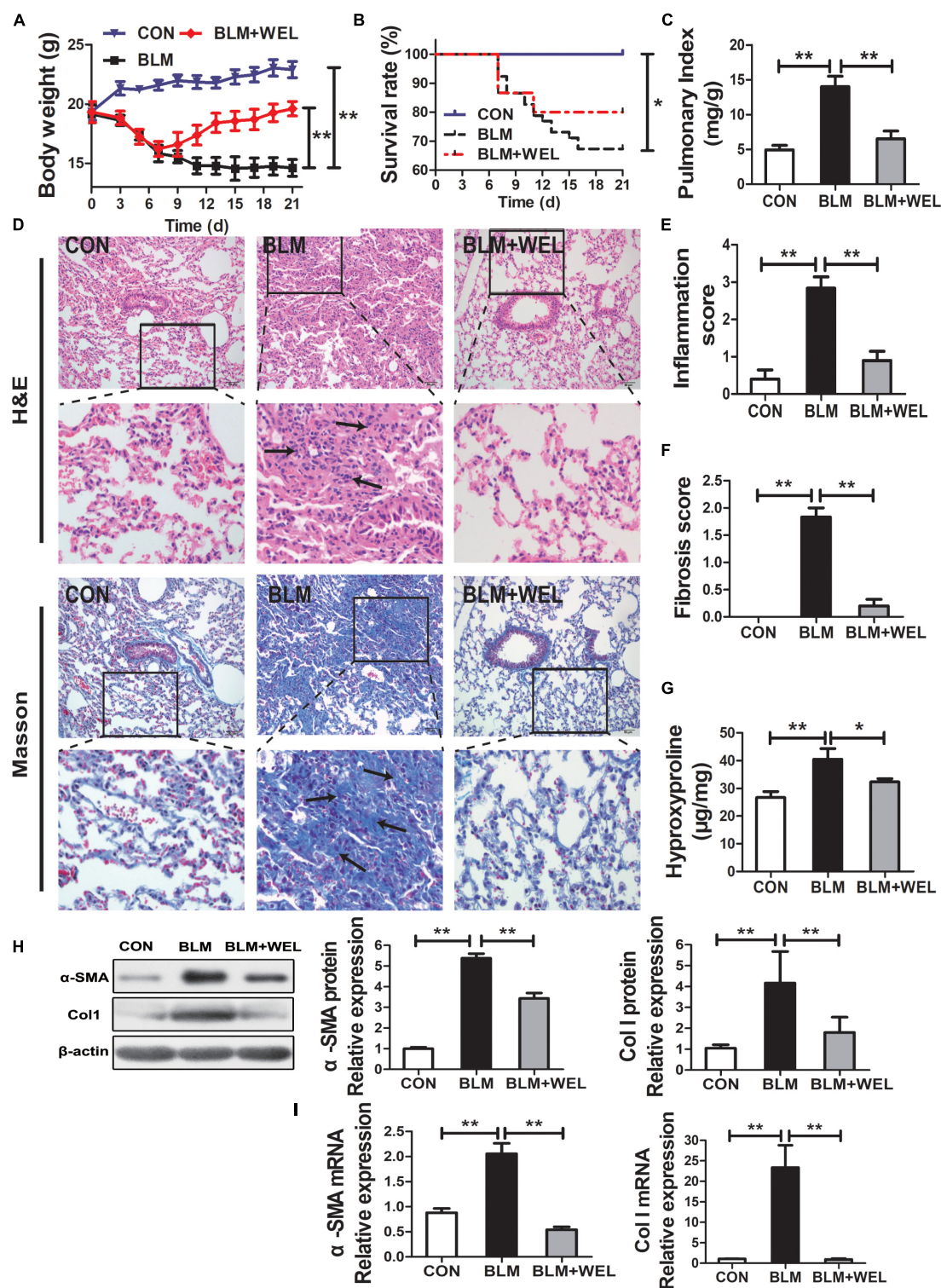


**FIGURE 3 |** WEL ameliorated bleomycin (BLM)-induced pulmonary fibrosis in C57/BL6 mice. One week after 5 mg/kg BLM treatment, mice were orally administered with WEL (10 mg/kg) once a day for 14 days. **(A)** Body weight, **(B)** survival rate, and **(C)** pulmonary index of BLM mice and BLM mice that received WEL were determined on day 21 ( $n = 6$ ). **(D)** Representative pictures ( $\times 200$ ) of HE-stained and Masson's trichrome-stained lung sections from mice on day 21 were shown. Bar = 100  $\mu\text{m}$ . The inflammation **(E)** and fibrosis **(F)** score numbers of 0–3, corresponding to the grades of –, +, ++, and +++, were evaluated by experienced pathologists in a blinded fashion. **(G)** HYP contents in lung tissues were determined by a assay kit. The protein expressions **(H)** of  $\alpha$ -SMA and collagen I (Col I) in lung tissues were determined by Western blotting. The mRNA levels **(I)** of  $\alpha$ -SMA and collagen I (Col I) in lung tissues were determined by PCR analysis. Data are presented as mean  $\pm$  SD ( $n = 9$ ). \* $p < 0.05$ , \*\* $p < 0.01$ .

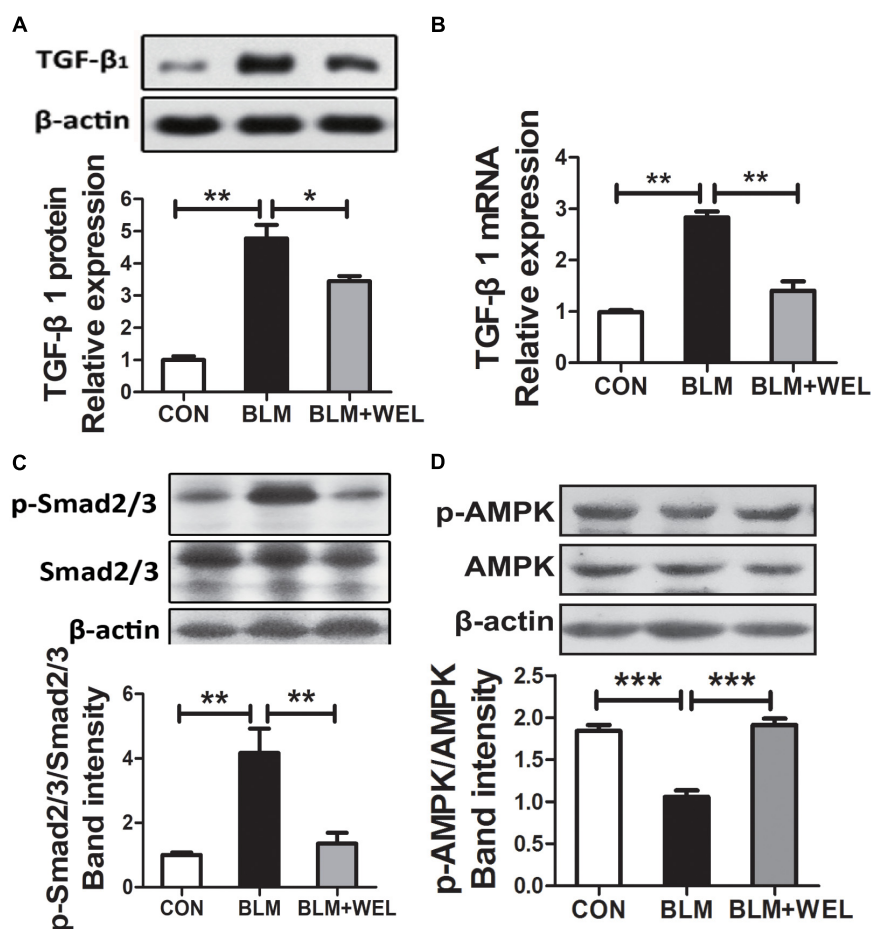


**FIGURE 4 |** WEL regulated TGF- $\beta$ /Smad signaling pathway and AMPK activation in lung tissue in bleomycin-induced PF in C57/BL6 mice. One week after 5 mg/kg BLM treatment, mice were orally administered with WEL (10 mg/kg) once a day for 14 days. The protein expression of TGF- $\beta$ 1 (**A**) and the phosphorylation levels of Smad2/3 (**C**) in lung tissues were determined by Western blotting. (**B**) The mRNA levels of TGF- $\beta$ 1 in lung tissues were determined by PCR analysis. (**D**) The protein phosphorylation levels of AMPK in lung tissues were determined by Western blotting. Data are presented as mean  $\pm$  SD ( $n = 9$ ). \* $p < 0.05$ , \*\* $p < 0.01$ , \*\*\* $p < 0.001$ .

activation (Xia et al., 2013), induce cell apoptosis (Sarveswaran et al., 2012), activate G protein (Deng and Fang, 2012), protect bronchial epithelial cell (Ding et al., 2015) and attenuate carbon tetrachloride-induced liver injury in mice (Ping et al., 2012). The content of WEL in *Ecliptae Herba* is not less than 0.04% (g/g) recorded in China Pharmacopoeia (2015 editions). Previous study has confirmed that the ethanol extract of *Ecliptae Herba* effectively can attenuated BLM-induced pulmonary fibrosis (PF) in mice (You et al., 2015), but the protective effects of WEL on PF is unclear.

Pulmonary fibrosis is a progressive, fatal fibrosis disease without clear etiology (Adamson and Bowden, 1974). It is associated with higher mortality, weight loss and histopathological damage (infiltration of inflammatory cells, collapse of alveolar spaces, thickened alveolar wall and so on) in BLM-induced PF model. The capacity to ameliorate PF is associated with decreasing excessive collagen deposition, and the content of HYP is an indicator of collagen metabolism in connective tissue diseases (Liang et al., 2011).

Previous trials to the PF treatment focused on inflammatory therapy, but researches indicate that the fibrosis process is driven by over-activated alveolar epithelial cells and fibroblasts (Daniels et al., 2004; Liang et al., 2011). During the process of EMT in lung fibrosis, epithelial cells disrupt their adhesion capacity due to the decrease in E-cadherin and the cytoskeleton rearrangement.

In the present study, the validity of WEL was investigated at the dosage of 2 mg/kg and 10 mg/kg, and WEL treatment at the dosage of 10 mg/kg showed significant protective effects on all kinds of clinical symptoms in BLM-induced lung fibrosis in ICR and C57/BL6 mice. Treatment with WEL at 10 mg/kg significantly reduced BLM-induced the collagen deposition in lung tissues compared to the model group (Figures 1, 3). Additionally, treatment with WEL also significantly impaired BLM-induced increase in TGF- $\beta$ 1 expression and Smad2/3 phosphorylation in the lungs (Figure 4). TGF- $\beta$ /Smad is a canonical signaling pathway during fibrosis process which promotes myofibroblast differentiation

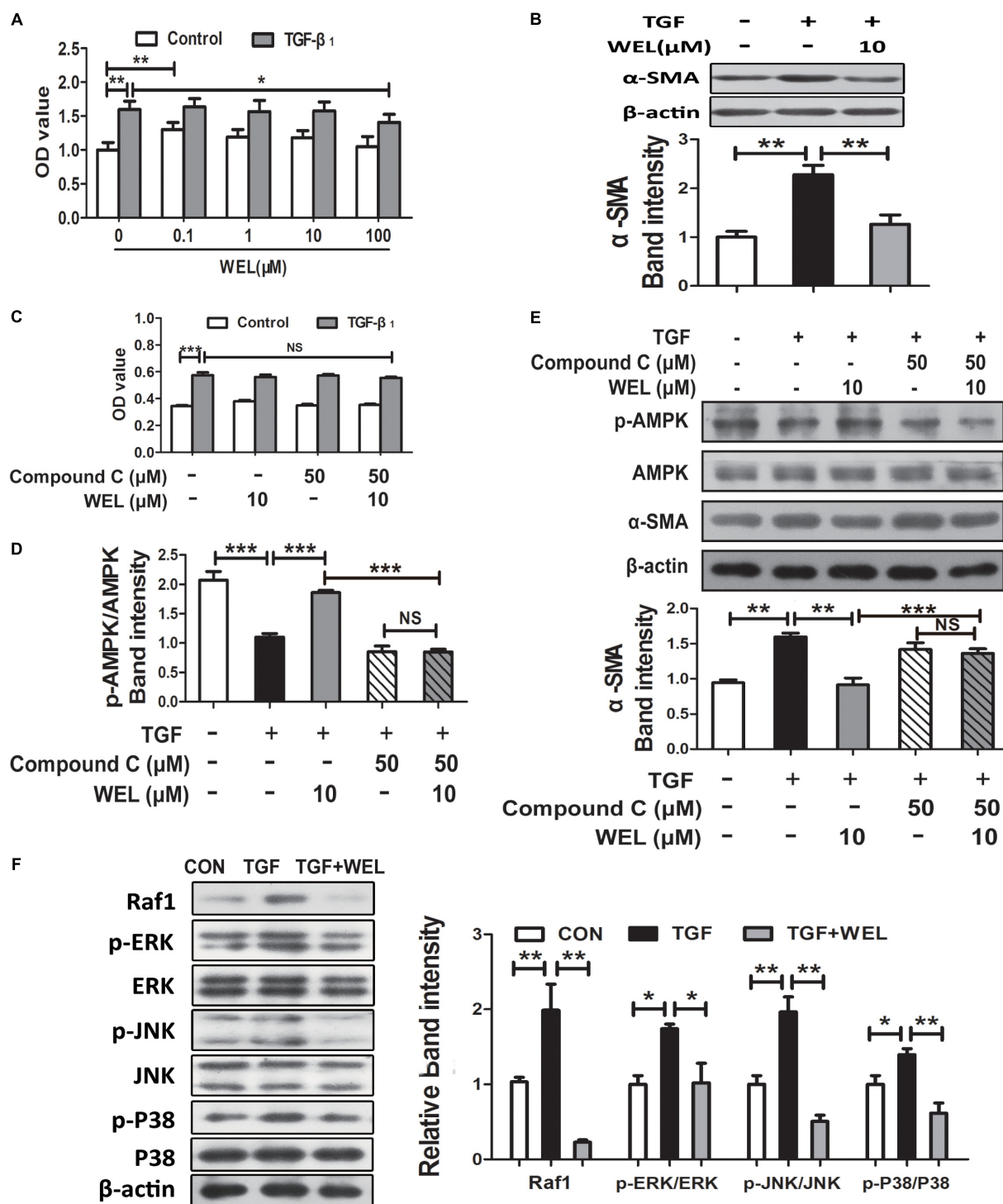


**FIGURE 5 |** WEL ameliorated TGF-β-induced myfibroblast differentiation partly through Raf1-MAPK signaling pathway and AMPK activation in primary mouse lung fibroblasts (PLFs). The cells were pretreated with compound C (50 μM) or solvent for 1.5 h and subsequently incubated with/without TGF-β<sub>1</sub> (10 ng/ml), WEL or solvent for 48 h. **(A)** The effect of WEL (0.1–100 μM) on PLFs proliferation cells were measured by the MTT assays. **(B)** The expression of α-SMA in PLFs treated with/without TGF-β<sub>1</sub> was detected by Western blotting. **(C)** The inhibition of WEL or compound C on PLFs proliferation cells were measured by the MTT assays. **(D)** Expression of p-AMPK/AMPK in PLFs treated with/without TGF-β<sub>1</sub> or compound C were determined by Western blotting. **(E)** The expression of α-SMA in PLFs treated with/without TGF-β<sub>1</sub> or compound C were determined by Western blotting. **(F)** Protein expressions of Raf1, JNK/p-JNK, p38/p-p38, and ERK1/2/p-ERK1/2 in PLFs treated with/without TGF-β<sub>1</sub> were detected by Western blotting. Data are presented as mean ± SD (n = 5). \*p < 0.05, \*\*p < 0.01, \*\*\*p < 0.001. NS, non-significant.

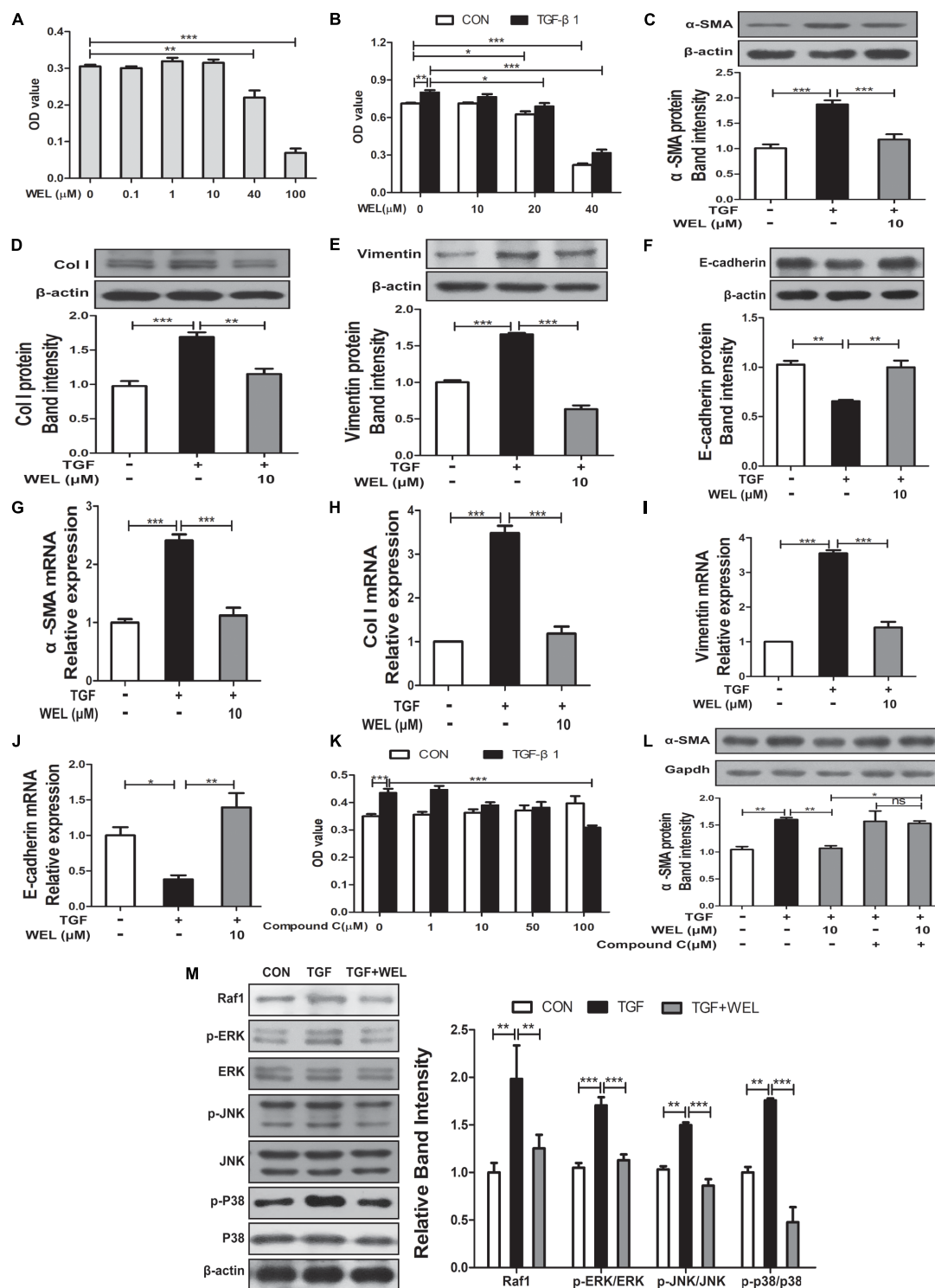


**FIGURE 6 |** Regulation of WEL on the EMT of alveolar epithelial cells partly and its inflammation in TGF-β1 mediated MLE-12 cells. The cells were pretreated with compound C (50 μM) or solvent for 1.5 h and subsequently incubated with/without TGF-β1 (TGF, 10 ng/ml), WEL or solvent for 48 h. **(A,B)** Effects of WEL (0.1–100 μM) on proliferation cells were measured by the MTT assays. **(C–J)** Protein expressions and mRNA levels of α-SMA, Vimentin, Col I, and E-cadherin in MLE-12 cells treated with/without TGF-β1 were detected by Western blotting and PCR analysis. **(K)** Effect of compound C (0.1–100 μM) on proliferation cells were measured by the MTT assays. **(L)** The expression of α-SMA in MLE-12 cells treated with/without TGF-β1 or compound C were determined by Western blotting analysis. **(M)** Protein expressions of Raf1, JNK/p-JNK, p38/p-p38, and ERK1/2/p-ERK1/2 in MLE-12 treated with/without TGF-β1 were detected by Western blotting analysis. Data are presented as mean ± SD (n = 5). \*p < 0.05, \*\*p < 0.01, \*\*\*p < 0.001. NS, non-significant.



and activates myofibroblasts to secrete excess amounts of ECM (King et al., 2011).

In present study, WEL treatment (10 mg/kg) significantly promoted the activation of AMPK in the lung tissues from BLM-treated mice (**Figure 4**). TGF- $\beta$ -induced myofibroblast differentiation and BLM-induced lung fibrosis in mice were effectively inhibited by metformin-mediated AMPK activation (Li et al., 2015; Sato et al., 2016). *In vitro*, WEL effectively inhibited not only the accumulation of ECM in pro-inflammatory cytokine TGF- $\beta$ -stimulated lung fibroblasts PLFs (**Figure 5**) but also the EMT of TGF- $\beta$ 1-mediated alveolar epithelial cells MLE-12 cells (**Figure 6**), however, these inhibition of WEL were significantly blocked by compound C (**Figures 5, 6**). AMPK activation is recognized to have potential beneficial effects on improving metabolic disorders and preventing organ dysfunction during fibrosis development (Zhao Y. et al., 2015), inhibiting AMPK activation by compound C (an AMPK inhibitor) could reverses metformin's protective effects on lung fibrosis (Liu et al., 2014). Recent research also showed that WEL could activated AMPK in liver tissues from rat steatosis (Zhao J. et al., 2015).

The AMPK activator inhibits not only fibrosis (Flores-Delgado et al., 2001; Gong et al., 2005; Zhang et al., 2010) but also inflammation status (Langenbach et al., 2007; Sarveswaran et al., 2012). Moreover, TGF- $\beta$ 1 acts the non-genomic functions by MAPK kinase pathway, and estrogen inhibits lung myofibroblast proliferation via Raf1-MAPK (p38, ERK, and JNK) signaling pathway (Flores-Delgado et al., 2001). In the present study, we found that WEL treatments significantly suppressed TGF- $\beta$ 1-mediated inflammation station in activated lung fibroblasts and alveolar epithelial cells through down-regulating the activation of Raf1 and phosphorylated MAPKs (ERK, JNK, and p38) (**Figures 5, 6**). Previous studies have shown that WEL acts as phytoestrogen inhibits breast cancer cells by regulating ER genomic and non-genomic signaling pathways (Nehybova et al., 2015). However, further investigation, for example, whether the regulation of Raf1-MAPKs by WEL is an AMPK-dependent response or estrogen-like effect, is needed in the future. More comprehensive studies are needed to illustrate the precise molecular mechanism and the full effects of WEL on pulmonary fibrosis.

## REFERENCES

- Adamson, I. Y., and Bowden, D. H. (1974). The pathogenesis of bleomycin-induced pulmonary fibrosis in mice. *Am. J. Pathol.* 77, 185–197.
- Benes, P., Knopfova, L., Trcka, F., Nemaierova, A., Pinheiro, D., Soucek, K., et al. (2011). Inhibition of topoisomerase II $\alpha$ : novel function of wedelolactone. *Cancer Lett.* 303, 29–38. doi: 10.1016/j.canlet.2011.01.002
- Bhattacharyya, S., Kelley, K., Melichian, D. S., Tamaki, Z., Fang, F., Su, Y. Y., et al. (2013). Toll-Like receptor 4 signaling augments transforming growth factor- $\beta$  responses: a novel mechanism for maintaining and amplifying fibrosis in scleroderma. *Am. J. Pathol.* 182, 192–205. doi: 10.1016/j.ajpath.2012.09.007
- Chaudhary, N. I., Schnapp, A., and Park, J. E. (2006). Pharmacologic differentiation of inflammation and fibrosis in the rat bleomycin model. *Am. J. Respir. Crit. Care Med.* 173, 769–776. doi: 10.1164/rccm.200505-717OC
- Chichioco-Hernandez, C. L., and Paguigan, N. D. (2010). Phytochemical profile of selected Philippine plants used to treat asthma. *Pharmacogn. J.* 2, 198–202. doi: 10.1016/S0975-3575(10)80092-6

## CONCLUSION

In conclusion, WEL can decrease the associated inflammation by attenuating Raf1-MAPKs signaling pathway to inhibiting inflammatory cytokines production, and increase the activation of AMPK in the BLM-induced pulmonary fibrosis models, preventing an increase in pro-fibrotic markers such as Col I and  $\alpha$ -SMA and attenuating a decreasing in anti-fibrotic marker such as E-cadherin. Mechanistic studies suggested that AMPK-mediated collagen suppression in particular is involved in WEL's anti-fibrotic mechanisms. Additional investigations are necessary to elucidate the full anti-fibrotic potential of WEL as an effective therapy for PF patients, including that produced during BLM treatment.

## AUTHOR CONTRIBUTIONS

J-yY, L-jT, BL, X-yY, and R-sL undertake main pharmacology experiments and help to Western blot analysis. H-fX has contributed to the preparation of WEL. C-fZ undertook the design of this project and did result analysis.

## ACKNOWLEDGMENTS

We would like to thank the Natural Science Foundation of China (81573553 and 81773982), Blue Project of Jiangsu Province and National Found for Fostering Talents of Basic Sciences (NFFTBS, J1030830) for financial supports. We also thank Xiao-Nan Ma and Ying-Jian Hou for technical support from Cellular and Molecular Biology Center of China Pharmaceutical University.

## SUPPLEMENTARY MATERIAL

The Supplementary Material for this article can be found online at: <https://www.frontiersin.org/articles/10.3389/fphar.2019.00151/full#supplementary-material>

- Daniels, C. E., Wilkes, M. C., Edens, M., Kottom, T. J., Murphy, S. J., Limper, A. H., et al. (2004). Imatinib mesylate inhibits the profibrogenic activity of TGF- $\beta$  and prevents bleomycin-mediated lung fibrosis. *J. Clin. Invest.* 114, 1308–1316. doi: 10.1172/JCI200419603
- Deng, H., and Fang, Y. (2012). Anti-inflammatory gallic acid and wedelolactone are G protein-coupled receptor-35 agonists. *Pharmacology* 89, 211–219. doi: 10.1159/000337184
- Ding, S., Hou, X., Yuan, J., Tan, X., Chen, J., and Yang, N. (2015). Wedelolactone protects human bronchial epithelial cell injury against cigarette smoke extract-induced oxidant stress and inflammation responses through Nrf2 pathway. *Int. Immunopharmacol.* 29, 648–655. doi: 10.1016/j.intimp.2015.09.015
- Flores-Delgado, G., Bringas, P., Buckley, S., Anderson, K. D., and Warburton, D. (2001). Nongenomic estrogen action in human lung myofibroblasts. *Biochem. Biophys. Res. Commun.* 283, 661–667. doi: 10.1006/bbrc.2001.4827
- Gong, L. K., Li, X. H., Wang, H., Zhang, L., Chen, F. P., and Cai, Y. (2005). Effect of Feitai on bleomycin-induced pulmonary fibrosis in rats. *J. Ethnopharmacol.* 96, 537–544. doi: 10.1016/j.jep.2004.09.046

- Jahan, R., Al-Nahain, A., Majumder, S., and Rahmatullah, M. (2014). Ethnopharmacological significance of *Eclipta alba* (L.) Hassk. (Asteraceae). *Int. Sch. Res. Notices* 2014:385969. doi: 10.1155/2014/385969
- Jaiswal, N., Bhatia, V., Srivastava, S. P., Srivastava, A. K., and Tamrakar, A. K. (2012). Antidiabetic effect of *Eclipta alba* associated with the inhibition of alpha-glucosidase and aldose reductase. *Nat. Prod. Res.* 26, 2363–2367. doi: 10.1080/14786419.2012.662648
- Khalil, N., Parekh, T. V., O'Connor, R., Antman, N., Kepron, W., Yehaulaeshet, T., et al. (2001). Regulation of the effects of TGF- $\beta$ 1 by activation of latent TGF- $\beta$ 1 and differential expression of TGF- $\beta$  receptors (T $\beta$ R-I and T $\beta$ R-II) in idiopathic pulmonary fibrosis. *Thorax* 56, 907–915. doi: 10.1136/thorax.56.12.907
- King, T. E. Jr., Pardo, A., and Selman, M. (2011). Idiopathic pulmonary fibrosis. *Lancet* 378, 1949–1961. doi: 10.1016/S0140-6736(11)60052-4
- Kuiper, G. G., Lemmen, J. G., Carlsson, B., Corton, J. C., Safe, S. H., Saag, P. T. V. D., et al. (1998). Interaction of estrogenic chemicals and phytoestrogens with estrogen receptor  $\beta$ . *Endocrinology* 139, 4252–4263. doi: 10.1210/endo.139.10.6216
- Langenbach, S. Y., Wheaton, B. J., Fernandes, D. J., Jones, C., Sutherland, T. E., Wraith, B. C., et al. (2007). Resistance of fibrogenic responses to glucocorticoid and 2-methoxyestradiol in bleomycin-induced lung fibrosis in mice. *Can. J. Physiol. Pharmacol.* 85, 727–738. doi: 10.1139/Y07-065
- Lattaa, V. D., Cecchetti, A., Rya, S. D., and Morales, M. A. (2015). Bleomycin in the setting of lung fibrosis induction: from biological mechanisms to counteractions. *Pharmacol. Res.* 97, 122–130. doi: 10.1016/j.phrs.2015.04.012
- Ley, B., Collard, H. R., and King, T. E. Jr. (2011). Clinical course and prediction of survival in idiopathic pulmonary fibrosis. *Am. J. Respir. Crit. Care Med.* 183, 431–440. doi: 10.1164/rccm.201006-0894CI
- Li, L., Huang, W., Li, K., Zhang, K., Lin, C., Han, R., et al. (2015). Metformin attenuates gefitinib-induced exacerbation of pulmonary fibrosis by inhibition of TGF- $\beta$  signaling pathway. *Oncotarget* 6, 43605–43619. doi: 10.18632/oncotarget.6186
- Liang, X., Tian, Q., Wei, Z., Liu, F., Chen, J., Zhao, Y., et al. (2011). Effect of Feining on bleomycin-induced pulmonary injuries in rats. *J. Ethnopharmacol.* 134, 971–976. doi: 10.1016/j.jep.2011.02.008
- Liu, W., Tan, X., Sun, H., Huang, H., Jin, P., Jia, X., et al. (2012). Protective effect and mechanism of *Ecliptae Herba* on cigarette smoke extract-induced cytotoxicity of NHBE cells. *Zhongguo Zhong Yao Za Zhi* 37, 2444–2447.
- Liu, Y., Tang, G., Li, Y., Wang, Y., Chen, X., Gu, X., et al. (2014). Metformin attenuates blood-brain barrier disruption in mice following middle cerebral artery occlusion. *J. Neuroinflammation* 11:177. doi: 10.1186/s12974-014-0177-4
- Manvar, D., Mishra, M., Kumar, S., and Pandey, V. N. (2012). Identification and evaluation of anti Hepatitis C virus phytochemicals from *Eclipta alba*. *J. Ethnopharmacol.* 144, 545–554. doi: 10.1016/j.jep.2012.09.036
- Mylärniemi, M., and Kaartenaho, R. (2015). Pharmacological treatment of idiopathic pulmonary fibrosis-preclinical and clinical studies of pirfenidone, nintedanib, and N-acetylcysteine. *Eur. Clin. Respir. J.* 2, 1–10. doi: 10.3402/ecrj.v2.26385
- Nehybova, T., Smarda, J., Daniel, L., Brezovsky, J., and Benes, P. (2015). Wedelolactone induces growth of breast cancer cells by stimulation of estrogen receptor signalling. *J. Steroid. Biochem. Mol. Biol.* 152, 76–83. doi: 10.1016/j.jsbmb.2015.04.019
- Pedram, A., Razandi, M., O'Mahony, F., Lubahn, D., and Levin, E. R. (2010). Estrogen receptor- $\beta$  prevents cardiac fibrosis. *Mol. Endocrinol.* 24, 2152–2165. doi: 10.1210/me.2010-0154
- Ping, P., Zhang, C. F., Xu, X. H., and Zhang, M. (2012). Effects of wedelolactone on mice's acute hepatic injury induced by carbon tetrachloride. *Chin. Wild Plant Resour.* 31, 41–43.
- Postlethwaite, A. E., Shigemitsu, H., and Kanangat, S. (2004). Cellular origins of fibroblasts: possible implications for organ fibrosis in systemic sclerosis. *Curr. Opin. Rheumatol.* 16, 733–738. doi: 10.1097/01.bor.0000139310.77347.9c
- Rangarajan, S., Bone, N. B., Zmijewska, A. A., Jiang, S., Park, D. W., Bernard, K., et al. (2018). Metformin reverses established lung fibrosis in a bleomycin model. *Nat. Med.* 24, 1121–1127. doi: 10.1038/s41591-018-0087-6
- Roy, R. K., Thakur, M., and Dixit, V. K. (2008). Hair growth promoting activity of *Eclipta alba* in male albino rats. *Arch. Dermatol. Res.* 300, 357–364. doi: 10.1007/s00403-008-0860-3
- Sarveswaran, S., Gautam, S. C., and Ghosh, J. (2012). Wedelolactone, a medicinal plant-derived coumestan, induces caspase-dependent apoptosis in prostate cancer cells via downregulation of PKC $\epsilon$  without inhibiting Akt. *Int. J. Oncol.* 41, 2191–2199. doi: 10.3892/ijo.2012.1664
- Sato, N., Takasaka, N., Yoshida, M., Tsubouchi, K., Minagawa, S., Araya, J., et al. (2016). Metformin attenuates lung fibrosis development via NOX4 suppression. *Respir. Res.* 17, 107–189. doi: 10.1186/s12931-016-0420-x
- Selman, M., and Pardo, A. (2001). Idiopathic pulmonary fibrosis: an epithelial/fibroblastic cross-talk disorder. *Respir. Res.* 3:3.
- Sharma, J., Gairola, S., Gaur, R. D., and Painuli, R. M. (2012). The treatment of jaundice with medicinal plants in indigenous communities of the Sub-Himalayan region of Uttarakhand. *India J. Ethnopharmacol.* 143, 262–291. doi: 10.1016/j.jep.2012.06.034
- Sime, P. J., Xing, Z., Graham, F. L., Csaky, K. G., and Gauldie, J. (1997). Adenovector-mediated gene transfer of active transforming growth factor- $\beta$ 1 induces prolonged severe fibrosis in rat lung. *J. Clin. Invest.* 100, 768–776. doi: 10.1172/JCI119590
- Szapiel, S. V., Elson, N. A., Fulmer, J. D., Hunninghake, G. W., and Crystal, R. G. (1979). Bleomycin-induced interstitial pulmonary disease in the nude, athymic mouse. *Am. Rev. Respir. Dis.* 120, 893–899.
- Tabassum, N., and Agrawal, S. S. (2004). Hepatoprotective activity of *Eclipta alba* Hassk. against paracetamol induced hepatocellular damage in mice. *JK Pract.* 11, 278–280.
- Tewtrakul, S., Subhadrakasul, S., Tansakul, P., Cheenpracha, S., and Karalai, C. (2011). Antiinflammatory constituents from *Eclipta prostrata* using RAW264.7 macrophage cells. *Phytother. Res.* 25, 1313–1316. doi: 10.1002/ptr.3383
- Todd, N. W., Luzina, I. G., and Atamas, S. P. (2012). Molecular and cellular mechanisms of pulmonary fibrosis. *Fibrog. Tissue Repair* 5:11. doi: 10.1186/1755-1536-5-11
- Turgut, N. H., Kara, H., Elagoz, S., Deveci, K., Gungor, H., and Arslanbas, E. (2016). The protective effect of naringin against bleomycin-induced pulmonary fibrosis in Wistar rats. *Pulm. Med.* 2016:7601393. doi: 10.1155/2016/7601393
- Wagner, H., and Fessler, B. (1986). In vitro 5-lipoxygenase inhibition by *Eclipta alba* extracts and the coumestan derivative wedelolactone. *Planta Med.* 52, 374–377. doi: 10.1055/s-2007-969189
- Wynn, T. A. (2011). Integrating mechanisms of pulmonary fibrosis. *J. Exp. Med.* 208, 1339–1350. doi: 10.1084/jem.20110551
- Xia, Y. Z., Chen, J., Cao, Y., Xu, C. S., Li, R. M., Pan, Y., et al. (2013). Wedelolactone exhibits anti-fibrotic effects on human hepatic stellate cell line LX-2. *Eur. J. Pharmacol.* 714, 105–111. doi: 10.1016/j.ejphar.2013.06.012
- You, X. Y., Xue, Q., Fang, Y., Liu, Q. Y., Zhang, C. F., Zhao, C., et al. (2015). Preventive effects of *Ecliptae Herba* extract and its component, ecliptasaponin A, on bleomycin-induced pulmonary fibrosis in mice. *J. Ethnopharmacol.* 175, 172–180. doi: 10.1016/j.jep.2015.08.034
- Zhang, C. F., Sun, Z. H., Zhang, D., and Zhang, M. (2010). Sulphur compounds from the aerial parts of *Eclipta prostrata*. *Biochem. Syst. Ecol.* 38, 1253–1256. doi: 10.1016/j.bse.2010.12.024
- Zhao, J., Miyamoto, S., You, Y. H., and Sharma, K. (2015). AMP-activated protein kinase (AMPK) activation inhibits nuclear translocation of Smad4 in mesangial cells and diabetic kidneys. *Am. J. Physiol. Renal Physiol.* 308, F1167–F1177. doi: 10.1152/ajprenal.00234.2014
- Zhao, Y., Peng, L., Yang, L., Xu, X., Li, W., Luo, X., et al. (2015). Wedelolactone regulates lipid metabolism and improves hepatic steatosis partly by AMPK activation and up-regulation of expression of PPAR $\alpha$ /LPL and LDLR. *PLoS One* 10:e0132720. doi: 10.1371/journal.pone.0132720

**Conflict of Interest Statement:** The authors declare that the research was conducted in the absence of any commercial or financial relationships that could be construed as a potential conflict of interest.

Copyright © 2019 Yang, Tao, Liu, You, Zhang, Xie and Li. This is an open-access article distributed under the terms of the Creative Commons Attribution License (CC BY). The use, distribution or reproduction in other forums is permitted, provided the original author(s) and the copyright owner(s) are credited and that the original publication in this journal is cited, in accordance with accepted academic practice. No use, distribution or reproduction is permitted which does not comply with these terms.



# Therapeutic Targeting of Fibrotic Epithelial-Mesenchymal Transition—An Outstanding Challenge

Attila Fintha<sup>1</sup>, Ákos Gasparics<sup>2</sup>, László Rosivall<sup>3</sup> and Attila Sebe<sup>3,4\*</sup>

<sup>1</sup>2nd Department of Pathology, Semmelweis University, Budapest, Hungary, <sup>2</sup>1st Department of Obstetrics and Gynecology, Semmelweis University, Budapest, Hungary, <sup>3</sup>Department of Pathophysiology, International Nephrology Research and Training Center, Semmelweis University, Budapest, Hungary, <sup>4</sup>Division of Medical Biotechnology, Paul Ehrlich Institute, Langen, Germany

## OPEN ACCESS

### Edited by:

Cecilia Battistelli,  
Sapienza University of Rome, Italy

### Reviewed by:

Olaf Grisk,  
University of Greifswald, Germany  
Erzsébet Bartolák-Suki,  
Boston University, United States

### \*Correspondence:

Attila Sebe  
attila.sebe@pei.de

### Specialty section:

This article was submitted to  
Translational Pharmacology,  
a section of the journal  
Frontiers in Pharmacology

**Received:** 30 November 2018

**Accepted:** 29 March 2019

**Published:** 18 April 2019

### Citation:

Fintha A, Gasparics Á, Rosivall L and Sebe A (2019) Therapeutic Targeting of Fibrotic Epithelial-Mesenchymal Transition—An Outstanding Challenge. *Front. Pharmacol.* 10:388. doi: 10.3389/fphar.2019.00388

Back in 1995, a landmark paper was published, which shaped the fibrosis literature for many years to come. During the characterization of a fibroblast-specific marker (FSP1) in the kidneys, an observation was made, which gave rise to the hypothesis that “fibroblasts in some cases arise from the local conversion of epithelium.” In the following years, epithelial-mesenchymal transition was in the spotlight of fibrosis research, especially in the kidney. However, the hypothesis came under scrutiny following some discouraging findings from lineage tracing experiments and clinical observations. In this review, we provide a timely overview of the current position of the epithelial-mesenchymal transition hypothesis in the context of fibrosis (with a certain focus on renal fibrosis) and highlight some of the potential hurdles and pitfalls preventing therapeutic breakthroughs targeting fibrotic epithelial-mesenchymal transition.

**Keywords:** epithelial to mesenchymal transition, fibrosis, myofibroblast, repair, chronic injury

## MYOFIBROBLASTS AND THEIR ROLE IN TISSUE FIBROSIS

In recent years, fibrotic disorders gradually earned a well-deserved spotlight as epidemiologic data revealed that nearly 45% of all deaths in the developed world are attributed to chronic fibroproliferative diseases (Wynn, 2007). Just listing fibrotic morbidity is impressive: pulmonary fibrosis, liver cirrhosis, progressive kidney disease, cardiovascular disease, atherosclerosis, and systemic sclerosis of connective tissues of the skin and internal organs. Alone, chronic kidney disease (CKD) accounts for a global and US prevalence of 13% (Thomas et al., 2008; Hill et al., 2016); irrespective of the pathological background and the initial cause, a progressive renal fibrosis is the key finding for CKDs. In addition to specific kidney diseases (chronic glomerulonephritis and polycystic kidney disease), conditions reaching epidemic levels globally such as diabetes or hypertension are the leading causes of CKD. Moreover, the link between wound healing, chronic fibrosis, and cancer progression is also recognized in the literature (Cox and Erler, 2014; Rybinski et al., 2014). Despite the enormous impact on human pathology, there are currently no approved, effective treatment strategies targeting fibrosis. Pirfenidone and nintedanib are the exception with the indication for idiopathic pulmonary fibrosis, however, the clinical experience with these drugs is inconclusive, and the long-term safety and efficacy of these medications is yet to be determined.

During their pathomechanism, most chronic diseases will eventually present excessive tissue scarring as a common feature. There is a well-known physiological process that resembles fibrosis—the wound healing process, which is fundamental for the replacement of damaged tissues following an acute injury. During wound healing following tissue injury, an inflammatory response is switched on where the activated macrophages and neutrophils clean up tissue debris and dead cells. An expansive expression of extracellular matrix components precedes a regeneration phase characterized by the restoration of blood vessels and normal tissue structures in conjunction with the elimination of the granulation tissue. Fibrosis is considered a dysregulated wound healing process, which occurs as a consequence of a chronic injury that persists for several weeks or months, or as a consequence of other chronic diseases. Such an uncontrolled wound healing process leads to the formation and accumulation of a permanent scar tissue, which progressively remodels and later destroys normal tissue architecture. The histological characteristics and regulatory mechanisms of fibrosis are similar across different organs (Wynn, 2007).

It has been shown that the main effector cell type responsible for the physiological accumulation of extracellular matrix in the granulation tissue and for the excess deposition of interstitial extracellular matrix under pathologic conditions is the myofibroblast (Roberts et al., 1997; Powell et al., 1999). Myofibroblasts are specialized fibroblast-like contractile cells exhibiting several ultrastructural features of smooth muscle cells. Myofibroblasts are spindle-shaped cells characterized by the presence of microfilament bundles (stress fibers) and  $\alpha$ -smooth muscle actin (SMA). Myofibroblasts have a surface characterized by prominent fibronectin fibrils and fibronexus junctions, and present abundant rough endoplasmic reticulum. SMA-expressing myofibroblasts and fibroblasts are distinct cellular entities, similar to smooth muscle cells, myofibroblasts are characterized by cytoplasmic bundles of contractile microfilaments (Desmouliere et al., 2003). Myofibroblasts are characterized by a higher proliferation rate, migration, cytokine expression, and enhanced interstitial matrix production (Guarino et al., 2009). Myofibroblasts synthesize a series of inflammatory and anti-inflammatory cytokines, chemokines, growth factors, inflammatory mediators, as well as extracellular matrix proteins and proteases. When classifying and characterizing myofibroblasts, vimentin, desmin, and SMA are the three filaments mostly used. There are three indispensable local events required to generate SMA-positive differentiated myofibroblasts: accumulation of the biologically active form of TGF- $\beta$ 1, the presence of specialized ECM proteins like the ED-A splice variant of fibronectin, and high cellular stress rendered by the mechanical properties of the ECM and cell remodeling activity (Eyden, 2001; Tomasek et al., 2002).

Under physiological conditions, large numbers of myofibroblasts accumulate at the sites of ongoing inflammation and repair. Besides matrix production, their role here is to effectively close wounds through their contraction (Hinz, 2010). Under such conditions, myofibroblasts act as repair cells, produce and organize extracellular matrix, and restore tissue integrity after injury. During normal wound healing, myofibroblasts

disappear following their apoptosis in parallel to the epithelialization stage of the repair (Gabbiani, 2003). However, in the context of pathological scarring, myofibroblasts create a collagen-rich stiff scar, which disrupts the architecture of tissues and alters the biochemical and biophysical microenvironment, resulting in a dysfunctional tissue. In the long term, deregulated activity of myofibroblasts impairs tissue function and leads to organ failure (Hinz, 2009).

## EPITHELIAL-MESENCHYMAL TRANSITION AS A SOURCE OF MYOFIBROBLASTS

The cellular origin of myofibroblasts was the focus of basic research for many years. The early view was that fibroblasts were responsible for producing interstitial extracellular matrix under physiological conditions. However, under pathologic conditions, these local fibroblasts proliferated and engaged in excessive fibrogenesis acquiring a highly activated phenotype characteristic of myofibroblasts. This idea was supported by findings indicating the presence of fibroblasts positive for proliferation markers at the periphery of the wound, which acquired additional smooth muscle characteristics during wound healing and progressive organ fibrosis (Grillo, 1963). In the kidneys, the leading role of tubulointerstitial fibrosis (TIF) during CKD was recognized when it was established that there is a strong correlation between tubulointerstitial fibrosis and the decrease of the glomerular filtration rate (Risdon et al., 1968). Here, too, interstitial fibroblasts were considered to be the main effector cells in renal fibrogenesis responsible for excessive matrix deposition. Later, the characterization of a novel fibroblast-specific marker, fibroblast-specific protein 1 (FSP1) led to the birth of a paradigm. When FSP1 expression was assessed, only a limited number of cells stained in normal renal parenchymal tissue. However, in kidneys with ongoing fibrosis caused by persistent inflammation, a high number of FSP1+ fibroblasts were found in the interstitial space, where collagen deposition occurred and in the tubular epithelium adjacent to the inflammation foci. This original observation led to the hypothesis that fibroblasts in some cases arise, as needed, from the local conversion of epithelium (Strutz et al., 1995). This conversion was later identified as an epithelial-mesenchymal transition (EMT). The phenomenon of EMT was already known in the literature as Elizabeth Hay described it as early as in 1968 following observations of cell migration in the primitive streak of chick embryos (Hay, 1968). Originally termed, epithelial-mesenchymal transformation or transdifferentiation, it was renamed as transition to reflect the transient and cyclical nature of this plasticity process during development: epithelial cells can undergo EMT and mesenchymal cells can undergo mesenchymal-epithelial transition (Thiery and Sleeman, 2006). As such, the term transition names a variant of transdifferentiation, and describes the mechanism of dispersing cells in vertebrate embryos during tissue differentiation, during fibroblast formation in injured tissues, or during the early steps of metastases in epithelial cancer (Kalluri and Neilson, 2003).



During EMT, epithelial cells lose the expression of characteristic markers (e.g., E-cadherin and zonula occludens protein-1) and undergo a rearrangement of cell contacts and cytoskeleton. As a consequence, cells lose their epithelial adhesive properties. Later, cells start expressing fibroblast-specific and mesenchymal proteins (e.g., FSP1 and plasminogen activator inhibitor-1), start to synthesize extracellular matrix (e.g., fibronectin), and ultimately differentiate into SMA-positive cells, acquiring the myofibroblast phenotype. In parallel to the disruption of the basal membrane cells acquire enhanced migration and invasion potential. The transition is sequentially orchestrated; cells undergo phenotypic changes according to a defined chronology: the epithelial program is switched off in parallel to the activation of the mesenchymal-fibrogenic program, followed by the activation of the myogenic program. Corresponding to a complete EMT, the process culminates with the appearance of myogenic properties characteristic of myofibroblasts (Yang and Liu, 2001; Gasparics and Sebe, 2018).

EMT was shown to play important roles during embryonic development, cancer progression, and fibrotic disorders of mature organs. EMT has been described in embryonic morphogenesis and organ formation. The role of EMT has been established in lung development and palate fusion (Kaarinen et al., 1995). EMT occurs during the development of endocardial cushions in the atrioventricular canal of the chicken heart (Romano and Runyan, 2000). EMT plays an important role in tumor progression and metastasis formation. During EMT, malignant cells lose their epithelial markers and become motile, EMT being linked to metastasis (Huber et al., 2004). “Fibrogenic” EMT has been shown to contribute to progressive fibrosis of the kidney (Yoshikawa et al., 2007), thyroid gland (Grande et al., 2002), lens (Stump et al., 2006), liver (Sicklick et al., 2006), lung (Kim et al., 2006), and in rheumatic diseases (Zvaifler, 2006).

## EPITHELIAL-MESENCHYMAL TRANSITION DURING RENAL FIBROSIS

In the kidney, tubular epithelial cells play an important role during fibrosis. Proteinuria, high glucose, growth factors, reactive oxygen species, and direct interaction with mononuclear cells are well-characterized stimuli that lead to pro-inflammatory reactions in tubular epithelial cells. The idea that the tubular cells may convert into fibrotic myofibroblasts gained wide acceptance after the original observation was published. In the context of T1E, EMT promotes the progression of the fibrotic disease by generating increased numbers of myofibroblasts, and in parallel, by causing a loss of epithelial cells leading to the destruction of renal tissue architecture. On a functional level, EMT means a loss of function (secretion and absorption), but also a gain of function (fibrogenesis) for the tubular epithelial cell (Quaggin and Kapus, 2011). In a transgenic mouse model of T1E, it was even shown that nearly 40% of fibroblasts may have originated from the tubular epithelium (Iwano et al., 2002). In obstructive nephropathy

induced by unilateral ureteral obstruction, Yang and Liu (2001) showed abundant cells co-expressing SMA and tubular markers, indicating a transition state between epithelia and mesenchyme. The clinical relevance of EMT has also been demonstrated in a study characterizing human kidney biopsies: EMT was observed in different renal diseases, independently of histological diagnosis. A strong correlation was found between the number of tubular epithelial cells presenting EMT features and serum creatinine (renal functional impairment). The number of tubular cells with EMT features also associated with the degree of interstitial damage (Rastaldi et al., 2002). Importantly, expression of tubular Snail, a key transcriptional regulator of EMT, was shown to repress the epithelial phenotype and has been observed in areas with significant collagen deposition in patients with renal fibrosis (Boutet et al., 2006). The EMT process during fibrosis is regulated by several cytokines and growth factors (Hay and Zuk, 1995), from which TGF- $\beta$ 1 is the most important regulator. Renal expression of TGF- $\beta$ 1 was shown to be elevated in human diabetic nephropathy (Yamamoto et al., 1993) and TGF- $\beta$ 1 was found to correlate with impaired renal function (Hellmich et al., 2000). Importantly, targeted disruption and inhibition of TGF- $\beta$ 1 signaling protected against renal tubulointerstitial fibrosis and epithelial-mesenchymal transition (Sato et al., 2003; Zeisberg et al., 2003). Even more compelling was the evidence for EMT when it was discovered that the highly similar process originating from endothelial cells, the endothelial-mesenchymal transition (Medici and Kalluri, 2012; Gasparics et al., 2016) contributes to cardiac fibrosis and to a large extent (around 40%) to the myofibroblast pool in renal fibrosis as well (Zeisberg et al., 2007a, 2008).

Following the initial observation that SMA expression occurred in the tubules of the fibrotic kidney, several studies did not find such evidence, questioning the validity of the hypothesis. The initial enthusiasm about the fibrotic EMT hypothesis in the kidney also faced criticism. After a line of confirmatory studies, there were also a series of negative results, where lineage tracing experiments yielded negative results, or simply tubular epithelial cells were found to be negative for EMT marker expression during renal fibrosis. In a model of progressive tubulointerstitial fibrosis in 5/6 nephrectomized rats, tubular epithelial cells were characterized by *de novo* expression of SMA 3 weeks after nephrectomy, in parallel with the disruption of the tubular basement membrane (TBM) (Ng et al., 1998). In human glomerulonephritis, there was a high significant correlation between tubular SMA expression and interstitial fibrosis, interstitial SMA(+) myofibroblast accumulation, deposition of collagen types I and III, tubular TGF- $\beta$ 1 expression, and renal dysfunction (Jinde et al., 2001). Others have found no evidence of tubular SMA expression in the context of renal fibrosis. In an accelerated model of angiotensin II-induced renal fibrosis, the staining of SMA-positive myofibroblasts dramatically increased in the peritubular interstitial spaces 48 h after induction of renal fibrosis with Habu venom plus angiotensin II, but tubular epithelial cells remained SMA-negative (Faulkner et al., 2005). Interestingly, in patients aged 4–44 months suffering congenital nephrotic syndrome of the Finnish type manifested by proteinuria, fibrosis, and inflammation, despite

the severe tubulointerstitial fibrosis, tubular epithelial cells did not show transition into myofibroblasts based on vimentin, SMA, collagen, or matrix metalloproteinases 2 and 9 (MMP-2 and -9) expression (Kuusniemi et al., 2005). In a tetracycline-controlled transgenic mouse model, overexpression of transforming growth factor (TGF)- $\beta$ 1 in renal tubules induced widespread peritubular fibrosis. Fibrotic tissue was characterizing the areas between intact tubules. Myofibroblasts were derived from local fibroblasts with no evidence for a transition of tubular cells into myofibroblasts, or for cells transgressing the tubular basement membrane (Koesters et al., 2010). Two lineage tracing experiments also contributed to questioning the validity of the EMT hypothesis. Humphreys and coworkers identified pericytes, but not tubular epithelial cells as the origin of myofibroblasts (Humphreys et al., 2010). In another study, Ksp-cadherin promoter was used to label all renal tubular cells with enhanced yellow fluorescence protein as a permanent marker. After UUO, these cells did not express markers of fibroblasts or myofibroblasts (Li et al., 2010). The conflicting and negative results lead to the conclusion that an EMT is not occurring during kidney fibrosis (Kriz et al., 2011). More recent cell fate tracing experiments evidenced that the myofibroblast pool originated to 50% from local resident fibroblasts, 35% through differentiation from bone marrow, 10% *via* EndMT and 5% *via* EMT (LeBleu et al., 2013).

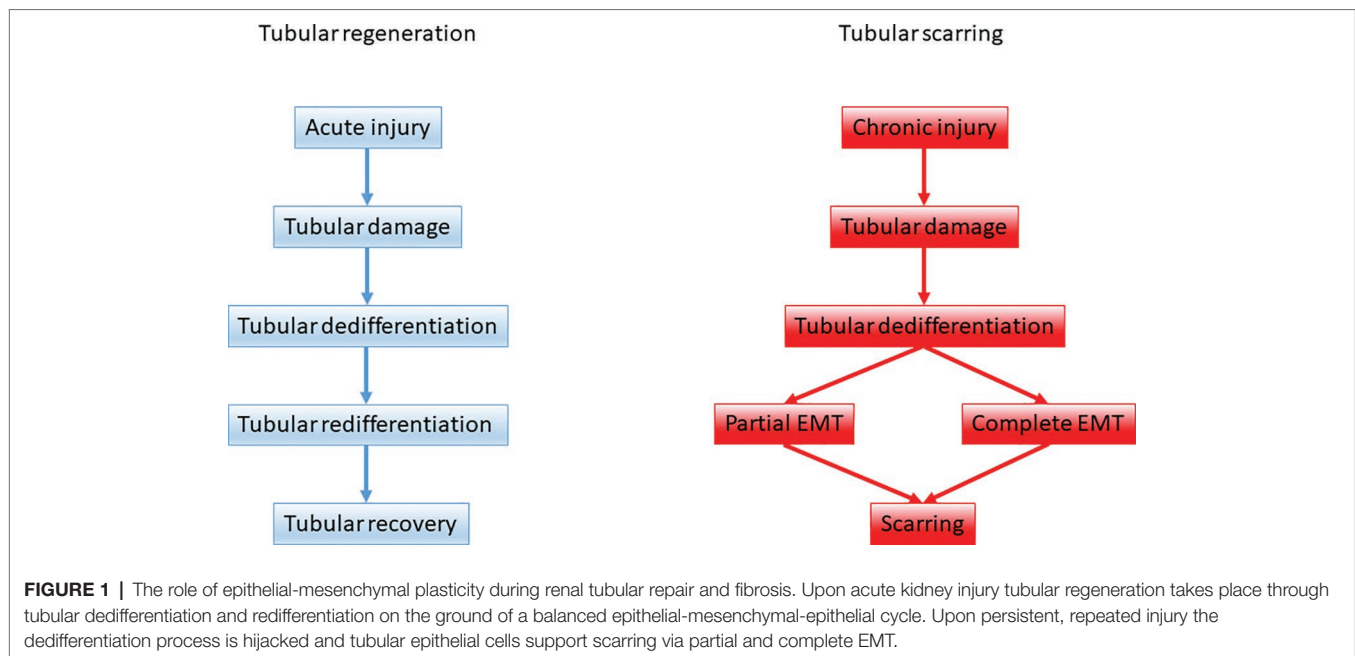
## THE CASE FOR EPITHELIAL-MESENCHYMAL TRANSITION AND EPITHELIAL-MESENCHYMAL PLASTICITY

The evidence for EMT is probably not as hazy as suggested by the publications mentioned above. The problems regarding the lineage tracing experiment could have been caused by technical issues widely discussed in the literature (Quaggin and Kapus, 2011). The lack of SMA expression in renal tubular cells during fibrosis could also be explained by a time factor: the fibrotic EMT is presumably a lengthy process in a chronic disease background, which is not entirely corresponding to the accelerated murine disease models, or the cell culture dish modeling, where EMT occurs within 3 days following TGF- $\beta$ 1 treatment (Sebe et al., 2008a). It could well be that by the time ex-tubular cells had undergone EMT, they would start expressing SMA and other definitive markers to the point, where the recognizable renal tissue architecture is long overtaken by a fibrotic mass. There are also some supporting data coming from a different aspect of kidney repair mechanisms.

Along SMA, vimentin expression is also considered to be a marker of EMT. It was shown that vimentin is expressed in injured tubular cells during tubular degeneration in chronic diseases and regeneration in acute tubular injury. Moreover, epithelial and mesenchymal markers could be simultaneously co-expressed (vimentin and keratin) in damaged and regenerating tubular epithelial cells after acute injury (Grone et al., 1987). A similar observation was done with

cytokeratin and SMA denoting an intermediate stage of phenotypic change (Jinde et al., 2001), where certain epithelial cells concomitantly express mesenchymal markers as well. This intermediate stage was later defined as a partial EMT, which could bring further meaning to experimental observations in this area: without directly contributing to the myofibroblast population, epithelial cells in this stage could relay signals to the interstitium to promote myofibroblast differentiation in other non-tubular cells, fibrogenesis, and inflammation (Grande et al., 2015; Lovisa et al., 2016). Partial EMT and chronic inflammation together create then a profibrotic milieu that enables collagen-production by various cell types involved in the fibrotic process.

The concept of partial EMT is an elegant solution to some of the problems, which arose in the field. This concept is probably in accordance with certain observations made in the context of cancer evolution. At some time point, it is plausible that epithelial cells express concomitantly epithelial and mesenchymal markers and recapitulate certain aspects of the EMT program, and which state would correspond to the recently termed epithelial-mesenchymal plasticity (EMP) phenomenon (Ye and Weinberg, 2015). The kidney is capable of certain regeneration following acute injury. Genetic fate-mapping techniques were used to show that the regeneration of outer medulla nephrons after ischemia/reperfusion injury is predominantly accomplished by surviving, less-injured tubular epithelial cells (Humphreys et al., 2008). Importantly, the same group evidenced that the outer medulla tubular cell proliferation after ischemic injury occurs by self-duplication of epithelial cells following epithelial dedifferentiation (Humphreys et al., 2011). Following acute injury, tubular epithelial cells recover their functionality following repair. During this dedifferentiation, step tubular epithelial cells undergo a plasticity process acquiring certain mesenchymal characteristics (characterized by vimentin expression) in parallel to a downgrade of the epithelial phenotype, resulting in a “hybrid” cellular phenotype (De Chiara and Crean, 2016). This means that the normal tubular repair and recovery following acute kidney injury undergoes a constant epithelial-mesenchymal-epithelial cycle characterized by epithelial dedifferentiation and re-differentiation that promotes renal healing (Ishibe and Cantley, 2008). Tissue fibrosis originates from a well-balanced protective repair response to tissue injury: fibrosis occurs when the responses to the initial injury become misbalanced and misdirected, and the response to the injury is no longer a self-limiting repair process. Dysregulation of this balanced process caused by repeated, ongoing cycles of tissue damage leads to a progression to chronic kidney disease (Schnaper, 2017). As such, during acute kidney injury, the dedifferentiation and proliferation of surviving proximal tubules is a central mechanism of repair and healing. However, continuous, chronic, and repeated injury induces a persistent dedifferentiation of the proximal tubule, which corresponds to the progressive kidney disease manifested in an epithelial-mesenchymal plasticity state characterized by attenuation of epithelial markers and expression of mesenchymal markers indicative of a partial EMT. As such, tissue fibrosis has a regenerative origin.



Thus, the identification of a “point of no return,” which characterizes the switch from a “benign” to progressive tubular dedifferentiation could have wide implications for antifibrotic therapies (Gewin, 2018). Importantly, tubular epithelial cells acquiring a partial EMT program suffer an arrest in the G2 phase of the cell cycle. This cell cycle arrest is TGF- $\beta$ 1, Snail and Twist1 dependent, and it limits the repair and regeneration potential of the cells (Lovisa et al., 2015). This growth-arrested cellular state corresponds to a failed re-differentiation in a dysregulated regeneration process and leads to a profibrotic tubular environment (Venkatachalam et al., 2015).

Throughout the years, evidence mounted for the multitude of cells from which myofibroblasts can originate. It is now clear that local interstitial fibroblasts, vascular pericytes, bone marrow-derived cells (fibrocytes), endothelial and epithelial cells can, to various degrees and through similarly regulated differentiation and dedifferentiation processes, undergo plasticity to give rise to the myofibroblast pool in the kidney (Grande and Lopez-Novoa, 2009). These data in corroboration with other, more recent cell fate tracing evidence give us a complex understanding of the role of EMT during renal fibrosis. There are probably three distinct paths whereby the EMT process is pivotally influencing tissue fibrosis and more specifically kidney fibrosis:

1. There is a balanced epithelial-mesenchymal-epithelial cycle characterizing renal tissue healing during acute kidney injuries. This cycle is marking the tubular dedifferentiation and re-differentiation steps during tubular regeneration.
2. Its dysregulation in the context of chronic renal diseases contributes to fibrogenesis, because EMT contributes to a certain extent to the expansion of the myofibroblast pool.
3. Snail-mediated EMT (partial EMT or epithelial plasticity state) represents a cellular regulatory mechanism, which

activates the non-epithelial compartment to promote myofibroblast differentiation and fibrogenesis and to sustain inflammation (Figure 1).

## ROLE OF FIBROTIC EPITHELIAL-MESENCHYMAL TRANSITION IN OTHER ORGANS

The data on the role of EMT during fibrosis was controversial in other organs as well, and lead to heated debates. Aggregates of proliferating fibroblasts and myofibroblasts characterize pulmonary fibrosis, which is the end stage of tissue responses to injury induced by toxic, autoimmune, and infectious insults (Chapman, 2011). Modeling lung fibrosis in cell fate tracking experiments revealed that vimentin-positive cells in injured lung were mostly of alveolar epithelial origin. This finding was indicative of the epithelial origin of mesenchymal cells during pulmonary fibrosis (Kim et al., 2006). Supportive of the EMT and partial EMT hypothesis, lung epithelial cells from patients suffering idiopathic pulmonary fibrosis were shown to co-express epithelial and mesenchymal markers (Willis et al., 2005; Kim et al., 2006). Later, lineage tracing experiments also confirmed the involvement of EMT in lung fibrosis, although to a lesser extent as in earlier studies (Tanjore et al., 2009). Importantly, significant nuclear  $\beta$ -catenin was detected in bronchiolar and alveolar epithelial cells in biopsies from patients with idiopathic pulmonary fibrosis, suggesting aberrant activation of Wnt/ $\beta$ -catenin signaling. It has been suggested that Wnt/ $\beta$ -catenin signaling would trigger divergent epithelial regeneration and EMT leading to fibrotic remodeling of the lung tissue (Chilosi et al., 2003). Still, the contribution of EMT to lung fibrosis remained controversial. Here as well, a general conclusion is that EMT may provide a direct source

of myofibroblasts, however, there is also evidence for the expression of mesenchymal markers in the context of epithelial injury and repair. This aspect, just as in the case of the kidney, makes therapeutic targeting of EMT very challenging and questions the potential therapeutic benefit (Kage and Borok, 2012).

In the liver, the scientific field showed a similar evolution. Liver cells of epithelial origin were suggested to be a relevant source of myofibroblasts. *In vitro* studies demonstrated that treatment of primary rat hepatocytes with TGF $\beta$  leads to the downregulation of epithelial markers, the upregulation of mesenchymal marker expression (SMA, collagen, FSP1), and an increase in the migratory potential of cells (Kaimori et al., 2007). Also, lineage tracing experiments evidenced the contribution of hepatocytes to liver myofibroblasts (Zeisberg et al., 2007b). Yet others found no *in vivo* evidence for hepatocytes acquiring a mesenchymal phenotype through EMT during liver fibrosis (Taura et al., 2010). Importantly, just as in the kidney, it was shown, that Snail deletion in hepatocytes attenuates liver fibrosis in adult transgenic mice, an observation also suggesting that hepatocyte-EMT may be involved in liver fibrosis (Rowe et al., 2011).

## THERAPEUTIC TARGETING OF EPITHELIAL-MESENCHYMAL TRANSITION AND FIBROSIS

Throughout the years, several strategies were developed to treat progressive organ fibrosis and EMT. Based on evidence accumulated through clinical and experimental studies, it became obvious that there are several aspects hampering the efficient targeting of this phenomenon.

The problems in the identification of EMT also have ramifications for therapy. First, there is a lack of specific markers to identify and evaluate EMT. The most commonly used markers are mesenchymal of origin and are not exclusively expressed by myofibroblasts: SMA, vimentin, FSP1, fibronectin, collagen I, N-cadherin, Snail, MMP-2, and MMP-9. The concept of epithelial-mesenchymal plasticity or partial EMT further blur the image: cells expressing both sets of epithelial and mesenchymal markers are also difficult to identify in the context of a highly dynamic process that EMT is, and this leads to the problem for therapy as well. Without any specific biomarkers, it is difficult to identify treatment rationales, disease progression, and follow-up. Specific biomarkers with value for treatment schemes need to be identified to precisely describe the different cellular entities and phenotypes arising during a complete or a partial EMT, during the epithelial-mesenchymal plasticity phenomenon. It has been suggested that vimentin and  $\beta$ -catenin tubular staining could be used for screening of early tubular injury in kidney-graft biopsies (Galichon and Hertig, 2011). Maybe not this particular combination (vimentin lacks specificity as a mesenchymal marker), but a combination of both epithelial and mesenchymal markers could shed some light on the complexity of EMT identification. Besides the cellular and mechanistic heterogeneity, patient and disease heterogeneity further complicate the task for the development of antifibrotic,

anti-EMT treatments. A more in-depth characterization of the EMT and fibrotic process in close consideration of normal tissue regeneration mechanisms is required to identify novel biomarkers that characterize different key stages, molecular tipping points that could be therapeutically targeted or could be used as accurate clinical endpoints for treatment schemes. The ideal biomarker in this setting would provide useful readouts on clinical efficacy and distinguish between patient strata depending on the response to the therapy.

Besides the biomarker conundrum, there are also other aspects of EMT, which could hamper developing therapeutic strategies. A potential EMT drug must have a broad specificity to cover all mechanisms leading to myofibroblast differentiation from all the different potential cellular sources, and it must have a specificity for the pathologic EMT phenomenon, not interfering with physiological forms of cellular plasticity (exemplified by normal wound healing). These might pose huge obstacles toward specific targeting of fibrotic EMT since the regulation of EMT is highly complex and EMT can be induced by a wide range of stimuli and mediators (Lamouille et al., 2014; Nieto et al., 2016). Among the signaling pathways involved in regulating EMT during renal fibrosis, three turned out to be essential in relaying upstream signals: TGF $\beta$ /Smad, Wnt/ $\beta$ -catenin, and integrin/ILK signaling. These pathways are interconnected and regulate further downstream pathways and transcription factors required for EMT (Liu, 2010).

TGF- $\beta$ 1 produced by inflammatory cells, fibroblasts, or epithelial cells is the main inducer of EMT. An important strategy was to target TGF- $\beta$  and achieve attenuation of EMT and fibrosis by inhibiting TGF- $\beta$ . There are now several clinical trials reported or still ongoing with the goal to test novel drugs targeting organ fibrosis. One recurring target of these trials is TGF- $\beta$  inhibition (Li et al., 2017a; Allinovi et al., 2018). Despite intensive research and developments, there are limited achievements coming from this direction. For example, pirfenidone is a drug already marketed with the indication for idiopathic pulmonary fibrosis. The clinical experience is however controversial (Levin and Beaulieu, 2011; Raghu and Thickett, 2013), despite data showing efficient inhibition of experimental fibrosis and EMT in various organs (Macias-Barragan et al., 2010; Li et al., 2017b). Pirfenidone has been assessed in diabetic nephropathy patients as well. The high rate of dropouts are concerning; it is also puzzling to see the lack of effect of the suggested maintenance dose (Sharma et al., 2011). Currently, there is only one therapy used as the standard of care in the case of renal fibrosis: ACE inhibitors have demonstrated protective renal effects and can ameliorate fibrosis (Brenner et al., 2001; Lewis et al., 2001). However, this treatment cannot completely suppress the progression of renal disease. Despite the fact that this effect is partly manifested by an inhibition of angiotensin II mediated expression of TGF- $\beta$ 1 (Kyuden et al., 2005; Peng et al., 2005), a recent clinical trial combining ACE inhibitors and TGF- $\beta$ 1-specific, humanized neutralizing monoclonal antibody had to be stopped early due to futility. This combination did not slow the progression of diabetic nephropathy and it seems that inhibition of TGF- $\beta$ 1 alone is not sufficient to induce further improvements in patient outcomes (Voelker et al., 2017).



Targeting TGF- $\beta$  may also interfere with physiological mechanisms, since TGF- $\beta$  is also involved in normal wound healing, immune regulation, and tumor suppression (Gabbiani, 2003; Bierie and Moses, 2006; Li et al., 2006). Influencing TGF- $\beta$  expression or systemic inhibition of TGF- $\beta$  may induce potential adverse effects. A more selective approach could be required to exploit the central role of TGF- $\beta$ 1 in the induction of EMT and fibrosis. One aspect of fibrosis is a systemic, but also a local overexpression of latent, inactive TGF- $\beta$ . TGF- $\beta$  can be locally activated, for example, by tissue stiffness (Hinz, 2009). This could mean a point of intervention, whereby reducing tissue stiffness could lead to less active TGF- $\beta$ . Such an approach would complement for strategies adjusting the level of TGF- $\beta$ 1 to a physiological one.

Another desirable alternative would be to target the principal downstream pro-fibrotic and EMT-inducing effectors of TGF- $\beta$ . The feasibility of such interventions has been shown: inactivating Snail1 in mice with established renal fibrosis improves organ morphology and function, significantly attenuating the disease (Grande et al., 2015). Nevertheless, caution has to be applied for such applications as well. In our earlier work, we identified the pivotal role of the myocardin-related transcription factors (MRTFs) during EMT, and this was later confirmed by other groups as well (Gasparics and Sebe, 2018). TGF- $\beta$ 1 and small GTPases regulate the function of MRTF during EMT of tubular epithelial cells (Fan et al., 2007; Sebe et al., 2008b, 2010). MRTFs are also influencing the expression of all major EMT markers and transcriptional regulators, and all three major EMT pathways delineated for renal fibrosis: TGF $\beta$ /Smad, Wnt/ $\beta$ -catenin, and integrin/ILK signaling (Gasparics and Sebe, 2018). There is even an endogenous mechanism inhibiting MRTF: by interfering with MRTF function SCAI inhibits EMT induced by TGF- $\beta$ 1 and angiotensin II (Fintha et al., 2013; Gasparics et al., 2018). Inhibition of MRTF was even shown to prevent lung fibrosis in two distinct murine models of fibrosis (Sisson et al., 2015). Yet these data are still not sufficient to indicate MRTF as a target for therapy in the context of organ fibrosis and EMT.

MRTFs are also important regulators of normal physiological processes. MRTF-B plays an essential role during smooth muscle differentiation (Oh et al., 2005), and RhoA-dependent smooth muscle cell-specific transcription is mediated by increased nuclear translocation of the MRTFs (Hinson et al., 2007). MRTF-A regulates capillary proliferation and pericyte recruitment while promoting neovascularization in ischemic hindlimb models (Hinkel et al., 2014). MRTF-A is a key regulator of mammary gland functions and is essential for the maintenance of lactation (Sun et al., 2006). MRTF-A is abundantly expressed in the newborn rat cortical and hippocampus neurons and in adult rat forebrain neurons. Its overexpression in the brain inhibited neuronal apoptosis (Cao et al., 2011). MRTF-dependent signaling is activated in response to skin injury, being an essential step mediating wound closure, wound healing and suppression of the inflammatory response (Velasquez et al., 2013). MRTFs are crucial in the hematopoietic system as well. MRTFs regulate hematopoietic stem cell progenitor cell homing into the bone marrow (Costello et al., 2015) and play a crucial role in

megakaryocyte maturation and platelet formation (Smith et al., 2012). MRTF-A regulates the normal function of lymphoid and myeloid lineage immune cells (Record et al., 2015). Therefore, the specificity requirement could not be fulfilled by systemic targeting of MRTFs or any other similar targets with wide implications for normal cellular functions. The requirement of exclusivity and specificity for targeting EMT and fibrosis are also mirrored by several clinical trials discontinued and prematurely stopped due to adverse events (Allinovi et al., 2018).

One strategy to relieve organ fibrosis could be the induction of apoptosis in the myofibroblasts. Such an approach would partly mimic physiological events occurring during wound healing, where myofibroblasts disappear by apoptosis when epithelialization occurs (Gabbiani, 2003). There are different approaches to induce myofibroblast apoptosis. It has been shown that bFGF can promote scarless wound healing upon the induction of apoptosis of myofibroblasts. This effect even seems to be specific for myofibroblast, but not fibroblasts (Abe et al., 2012). Also, pharmacologic disruption of mechanosensitive signaling with the ROCK inhibitor fasudil-induced myofibroblast apoptosis. Treatment with fasudil during the post-inflammatory fibrotic phase of lung injury protected mice from experimental lung fibrosis in an MRTF-dependent manner (Zhou et al., 2013). Nonetheless, irrespective of how successful such an approach will be in the future, the repair of the destroyed parenchymal tissue will not take place. This raises the question of whether fibrosis is reversible. Of course, due to its high regenerative potential, liver is not the best example here. Nevertheless, it was shown that by treating viral hepatitis organ function can be restored by resolution of hepatic fibrosis. Arresting the underlying injury, the viral infection, leads to a regression of cirrhosis often characterized by a return to normal liver structure and function (Chang et al., 2010; Ellis and Mann, 2012). It is the reversible nature of the epithelial-mesenchymal-epithelial transitions that makes such reversal of fibrosis possible. There were a number of *in vitro* studies showing that a reversal to the epithelial phenotype is possible in the context of fibrosis: the concept gained more acceptance once it was shown that the systemic administration of recombinant human BMP-7 in a mouse model of chronic renal injury lead to the repair of damaged renal tubular epithelial cells in conjunction with the reversal of the chronic renal injury (Zeisberg et al., 2003). The concept of reversal from the myofibroblast-mesenchymal state to an epithelial phenotype could also be potentially achieved by *in vivo* reprogramming, as recent evidence suggests. Transduction of four transcription factors that specify the skin-cell lineage enabled efficient and rapid *de novo* epithelialization from the surface of cutaneous ulcers in mice *via* the reprogramming and epithelial conversion of wound-resident mesenchymal cells (Kurita et al., 2018). Besides the “classical” methods developed to tackle EMT and tissue fibrosis with chemical compounds or monoclonal antibodies, the antifibrotic therapeutic toolbox may soon include some revolutionary methods worth further investigation. Recently a CRISPR/Cas9-based gene-specific demethylating technology was used to reactivate genes hypermethylated in kidney fibrosis. The reactivation of certain genes in UUO-challenged kidneys

led to a marked reduction of fibrosis (Xu et al., 2018). The specificity of the targeted genes in this particular study may be a matter of debate; nonetheless, the technology is very much appealing and could even allow organ specificity of application routes.

The conclusion of this review is on a dim note. We are farther away than ever from the therapeutic targeting of EMT during fibrosis. The whole EMT hypothesis and its role in fibrosis has been reconsidered in recent years, and its parallels to normal dedifferentiation-based healing mechanisms raise specificity concerns: an interference with overlapping mechanisms could lead to side effects manifested in a hampered physiological tissue healing processes in the same or other organs. Our understanding of acute injury repair has made significant process, yet we do not understand how this process gets derailed and turns detrimental in the context of progressive scarring. Also, a multitude of issues are hampering the identification

of specific signaling mechanisms and biomarkers which could be exploited for therapeutic purposes. A disentanglement of the different cellular plasticity events and substages in the process of partial EMT and EMP could provide further leads into identifying points of no return or tipping points qualifying as vulnerability spots delineating normal dedifferentiation processed from responses to chronic injury. All in all, more research needs to be carried out to further decipher and identify potential intervention targets, which would overcome many obstacles presented here.

## AUTHOR CONTRIBUTIONS

AF, ÁG, and AS drafted the manuscript. LR and AS edited and revised the manuscript. AS contributed to the conception and final approval of the manuscript.

## REFERENCES

- Abe, M., Yokoyama, Y., and Ishikawa, O. (2012). A possible mechanism of basic fibroblast growth factor-promoted scarless wound healing: the induction of myofibroblast apoptosis. *Eur. J. Dermatol.* 22, 46–53. doi: 10.1684/ejd.2011.1582
- Allinovi, M., De Chiara, L., Angelotti, M. L., Becherucci, F., and Romagnani, P. (2018). Anti-fibrotic treatments: a review of clinical evidence. *Matrix Biol.* 68–69, 333–354. doi: 10.1016/j.matbio.2018.02.017
- Bierie, B., and Moses, H. L. (2006). Tumour microenvironment: TGFbeta: the molecular Jekyll and Hyde of cancer. *Nat. Rev. Cancer* 6, 506–520. doi: 10.1038/nrc1926
- Boutet, A., De Frutos, C. A., Maxwell, P. H., Mayol, M. J., Romero, J., and Nieto, M. A. (2006). Snail activation disrupts tissue homeostasis and induces fibrosis in the adult kidney. *EMBO J.* 25, 5603–5613. doi: 10.1038/sj.emboj.7601421
- Brenner, B. M., Cooper, M. E., De Zeeuw, D., Keane, W. F., Mitch, W. E., Parving, H. H., et al. (2001). Effects of losartan on renal and cardiovascular outcomes in patients with type 2 diabetes and nephropathy. *N. Engl. J. Med.* 345, 861–869. doi: 10.1056/NEJMoa011161
- Cao, X. L., Hu, X. M., Hu, J. Q., and Zheng, W. X. (2011). Myocardin-related transcription factor-A promoting neuronal survival against apoptosis induced by hypoxia/ischemia. *Brain Res.* 1385, 263–274. doi: 10.1016/j.brainres.2011.02.016
- Chang, T. T., Liaw, Y. F., Wu, S. S., Schiff, E., Han, K. H., Lai, C. L., et al. (2010). Long-term entecavir therapy results in the reversal of fibrosis/cirrhosis and continued histological improvement in patients with chronic hepatitis B. *Hepatology* 52, 886–893. doi: 10.1002/hep.23785
- Chapman, H. A. (2011). Epithelial-mesenchymal interactions in pulmonary fibrosis. *Annu. Rev. Physiol.* 73, 413–435. doi: 10.1146/annurev-physiol-012110-142225
- Chilosi, M., Poletti, V., Zamo, A., Lestani, M., Montagna, L., Piccoli, P., et al. (2003). Aberrant Wnt/beta-catenin pathway activation in idiopathic pulmonary fibrosis. *Am. J. Pathol.* 162, 1495–1502. doi: 10.1016/S0002-9440(10)64282-4
- Costello, P., Sargent, M., Maurice, D., Esnault, C., Foster, K., Anjos-Afonso, F., et al. (2015). MRTF-SRF signaling is required for seeding of HSC/Ps in bone marrow during development. *Blood* 125, 1244–1255. doi: 10.1182/blood-2014-08-595603
- Cox, T. R., and Erler, J. T. (2014). Molecular pathways: connecting fibrosis and solid tumor metastasis. *Clin. Cancer Res.* 20, 3637–3643. doi: 10.1158/1078-0432.CCR-13-1059
- De Chiara, L., and Crean, J. (2016). Emerging transcriptional mechanisms in the regulation of epithelial to mesenchymal transition and cellular plasticity in the kidney. *J. Clin. Med.* 5:6. doi: 10.3390/jcm5010006
- Desmouliere, A., Darby, I. A., and Gabbiani, G. (2003). Normal and pathologic soft tissue remodeling: role of the myofibroblast, with special emphasis on liver and kidney fibrosis. *Lab. Invest.* 83, 1689–1707. doi: 10.1097/01.LAB.0000101911.53973.90
- Ellis, E. L., and Mann, D. A. (2012). Clinical evidence for the regression of liver fibrosis. *J. Hepatol.* 56, 1171–1180. doi: 10.1016/j.jhep.2011.09.024
- Eyden, B. (2001). The myofibroblast: an assessment of controversial issues and a definition useful in diagnosis and research. *Ultrastruct. Pathol.* 25, 39–50. doi: 10.1080/019131201300004672
- Fan, L., Sebe, A., Peterfi, Z., Masszi, A., Thirone, A. C., Rotstein, O. D., et al. (2007). Cell contact-dependent regulation of epithelial-myofibroblast transition via the rho-rho kinase-phospho-myosin pathway. *Mol. Biol. Cell* 18, 1083–1097. doi: 10.1091/mbc.e06-07-0602
- Faulkner, J. L., Szykalski, L. M., Springer, F., and Barnes, J. L. (2005). Origin of interstitial fibroblasts in an accelerated model of angiotensin II-induced renal fibrosis. *Am. J. Pathol.* 167, 1193–1205. doi: 10.1016/S0002-9440(10)61208-4
- Fintha, A., Gasparics, A., Fang, L., Erdei, Z., Hamar, P., Mozes, M. M., et al. (2013). Characterization and role of SCAI during renal fibrosis and epithelial-to-mesenchymal transition. *Am. J. Pathol.* 182, 388–400. doi: 10.1016/j.ajpath.2012.10.009
- Gabbiani, G. (2003). The myofibroblast in wound healing and fibrocontractive diseases. *J. Pathol.* 200, 500–503. doi: 10.1002/path.1427
- Galichon, P., and Hertig, A. (2011). Epithelial to mesenchymal transition as a biomarker in renal fibrosis: are we ready for the bedside? *Fibrogenesis Tissue Repair* 4:11. doi: 10.1186/1755-1536-4-11
- Gasparics, A., Kokeny, G., Fintha, A., Bencs, R., Mozes, M. M., Agoston, E. I., et al. (2018). Alterations in SCAI expression during cell plasticity, fibrosis and cancer. *Pathol. Oncol. Res.* 24, 641–651. doi: 10.1007/s12253-017-0293-4
- Gasparics, A., Rosivall, L., Krizbai, I. A., and Sebe, A. (2016). When the endothelium scores an own goal: endothelial cells actively augment metastatic extravasation through endothelial-mesenchymal transition. *Am. J. Physiol. Heart Circ. Physiol.* 310, H1055–H1063. doi: 10.1152/ajpheart.00042.2016
- Gasparics, A., and Sebe, A. (2018). MRTFs- master regulators of EMT. *Dev. Dyn.* 247, 396–404. doi: 10.1002/dvdy.24544
- Gewin, L. S. (2018). Renal fibrosis: primacy of the proximal tubule. *Matrix Biol.* 68–69, 248–262. doi: 10.1016/j.matbio.2018.02.006
- Grande, M., Franzen, A., Karlsson, J. O., Ericson, L. E., Heldin, N. E., and Nilsson, M. (2002). Transforming growth factor-beta and epidermal growth factor synergistically stimulate epithelial to mesenchymal transition (EMT) through a MEK-dependent mechanism in primary cultured pig thyrocytes. *J. Cell Sci.* 115, 4227–4236. doi: 10.1242/jcs.00091
- Grande, M. T., and Lopez-Novoa, J. M. (2009). Fibroblast activation and myofibroblast generation in obstructive nephropathy. *Nat. Rev. Nephrol.* 5, 319–328. doi: 10.1038/nrneph.2009.74
- Grande, M. T., Sanchez-Laorden, B., Lopez-Blau, C., De Frutos, C. A., Boutet, A., Arevalo, M., et al. (2015). Snail 1-induced partial epithelial-to-mesenchymal transition drives renal fibrosis in mice and can be targeted to reverse established disease. *Nat. Med.* 21, 989–997. doi: 10.1038/nm.3901

- Grillo, H. C. (1963). Origin of fibroblasts in wound healing. An autoradiographic study of inhibition of cellular proliferation by local x-irradiation. *Ann. Surg.* 157, 453–467.
- Grone, H. J., Weber, K., Grone, E., Helmchen, U., and Osborn, M. (1987). Coexpression of keratin and vimentin in damaged and regenerating tubular epithelia of the kidney. *Am. J. Pathol.* 129, 1–8.
- Guarino, M., Tosoni, A., and Nebuloni, M. (2009). Direct contribution of epithelium to organ fibrosis: epithelial-mesenchymal transition. *Hum. Pathol.* 40, 1365–1376. doi: 10.1016/j.humpath.2009.02.020
- Hay, E. D. (1968). "Organization and fine structure of epithelium and mesenchyme in the developing chick embryo" in *Proceedings of the 18th Hahnemann Symposium*. eds. R. Fleischmajer and R. E. Billingham (Baltimore: Williams & Wilkins), 31–55.
- Hay, E. D., and Zuk, A. (1995). Transformations between epithelium and mesenchyme: normal, pathological, and experimentally induced. *Am. J. Kidney Dis.* 26, 678–690. doi: 10.1016/0272-6386(95)90610-X
- Hellmich, B., Schellner, M., Schatz, H., and Pfeiffer, A. (2000). Activation of transforming growth factor-beta1 in diabetic kidney disease. *Metabolism* 49, 353–359. doi: 10.1016/S0026-0495(00)90264-6
- Hill, N. R., Fatoba, S. T., Oke, J. L., Hirst, J. A., O'Callaghan, C. A., Lasserson, D. S., et al. (2016). Global prevalence of chronic kidney disease - a systematic review and meta-analysis. *PLoS One* 11:e0158765. doi: 10.1371/journal.pone.0158765
- Hinkel, R., Trenkwalder, T., Petersen, B., Husada, W., Gesenhues, F., Lee, S., et al. (2014). MRTF-A controls vessel growth and maturation by increasing the expression of CCN1 and CCN2. *Nat. Commun.* 5:3970. doi: 10.1038/ncomms4970
- Hinson, J. S., Medlin, M. D., Lockman, K., Taylor, J. M., and Mack, C. P. (2007). Smooth muscle cell-specific transcription is regulated by nuclear localization of the myocardin-related transcription factors. *Am. J. Physiol. Heart Circ. Physiol.* 292, H1170–H1180. doi: 10.1152/ajpheart.00864.2006
- Hinz, B. (2009). Tissue stiffness, latent TGF-beta1 activation, and mechanical signal transduction: implications for the pathogenesis and treatment of fibrosis. *Curr. Rheumatol. Rep.* 11, 120–126. doi: 10.1007/s11926-009-0017-1
- Hinz, B. (2010). The myofibroblast: paradigm for a mechanically active cell. *J. Biomech.* 43, 146–155. doi: 10.1016/j.jbiomech.2009.09.020
- Huber, M. A., Azoitei, N., Baumann, B., Grunert, S., Sommer, A., Pehamberger, H., et al. (2004). NF-kappaB is essential for epithelial-mesenchymal transition and metastasis in a model of breast cancer progression. *J. Clin. Invest.* 114, 569–581. doi: 10.1172/JCI200421358
- Humphreys, B. D., Czerniak, S., Dirocco, D. P., Hasnain, W., Cheema, R., and Bonventre, J. V. (2011). Repair of injured proximal tubule does not involve specialized progenitors. *Proc. Natl. Acad. Sci. USA* 108, 9226–9231. doi: 10.1073/pnas.1100629108
- Humphreys, B. D., Lin, S. L., Kobayashi, A., Hudson, T. E., Nowlin, B. T., Bonventre, J. V., et al. (2010). Fate tracing reveals the pericyte and not epithelial origin of myofibroblasts in kidney fibrosis. *Am. J. Pathol.* 176, 85–97. doi: 10.2353/ajpath.2010.090517
- Humphreys, B. D., Valerius, M. T., Kobayashi, A., Mugford, J. W., Soeung, S., Duffield, J. S., et al. (2008). Intrinsic epithelial cells repair the kidney after injury. *Cell Stem Cell* 2, 284–291. doi: 10.1016/j.stem.2008.01.014
- Ishibe, S., and Cantley, L. G. (2008). Epithelial-mesenchymal-epithelial cycling in kidney repair. *Curr. Opin. Nephrol. Hypertens.* 17, 379–385. doi: 10.1097/MNH.0b013e3283046507
- Iwano, M., Plith, D., Danoff, T. M., Xue, C., Okada, H., and Neilson, E. G. (2002). Evidence that fibroblasts derive from epithelium during tissue fibrosis. *J. Clin. Invest.* 110, 341–350. doi: 10.1172/JCI0215518
- Jinde, K., Nikolic-Paterson, D. J., Huang, X. R., Sakai, H., Kurokawa, K., Atkins, R. C., et al. (2001). Tubular phenotypic change in progressive tubulointerstitial fibrosis in human glomerulonephritis. *Am. J. Kidney Dis.* 38, 761–769. doi: 10.1053/ajkd.2001.27693
- Kaartinen, V., Voncken, J. W., Shuler, C., Warburton, D., Bu, D., Heisterkamp, N., et al. (1995). Abnormal lung development and cleft palate in mice lacking TGF-beta 3 indicates defects of epithelial-mesenchymal interaction. *Nat. Genet.* 11, 415–421. doi: 10.1038/ng1295-415
- Kage, H., and Borok, Z. (2012). EMT and interstitial lung disease: a mysterious relationship. *Curr. Opin. Pulm. Med.* 18, 517–523. doi: 10.1097/MCP.0b013e3283283566721
- Kaimori, A., Potter, J., Kaimori, J. Y., Wang, C., Mezey, E., and Koteish, A. (2007). Transforming growth factor-beta1 induces an epithelial-to-mesenchymal transition state in mouse hepatocytes in vitro. *J. Biol. Chem.* 282, 22089–22101. doi: 10.1074/jbc.M700998200
- Kalluri, R., and Neilson, E. G. (2003). Epithelial-mesenchymal transition and its implications for fibrosis. *J. Clin. Invest.* 112, 1776–1784. doi: 10.1172/JCI200320530
- Kim, K. K., Kugler, M. C., Wolters, P. J., Robillard, L., Galvez, M. G., Brumwell, A. N., et al. (2006). Alveolar epithelial cell mesenchymal transition develops in vivo during pulmonary fibrosis and is regulated by the extracellular matrix. *Proc. Natl. Acad. Sci. USA* 103, 13180–13185. doi: 10.1073/pnas.0605669103
- Koesters, R., Kaissling, B., Lehir, M., Picard, N., Theilig, F., Gebhardt, R., et al. (2010). Tubular overexpression of transforming growth factor-beta1 induces autophagy and fibrosis but not mesenchymal transition of renal epithelial cells. *Am. J. Pathol.* 177, 632–643. doi: 10.2353/ajpath.2010.091012
- Kriz, W., Kaissling, B., and Le Hir, M. (2011). Epithelial-mesenchymal transition (EMT) in kidney fibrosis: fact or fantasy? *J. Clin. Invest.* 121, 468–474. doi: 10.1172/JCI44595
- Kurita, M., Araoka, T., Hishida, T., O'Keefe, D. D., Takahashi, Y., Sakamoto, A., et al. (2018). In vivo reprogramming of wound-resident cells generates skin epithelial tissue. *Nature* 561, 243–247. doi: 10.1038/s41586-018-0477-4
- Kuusniemi, A. M., Lapatto, R., Holmberg, C., Karikoski, R., Rapola, J., and Jalanko, H. (2005). Kidneys with heavy proteinuria show fibrosis, inflammation, and oxidative stress, but no tubular phenotypic change. *Kidney Int.* 68, 121–132. doi: 10.1111/j.1523-1755.2005.00386.x
- Kyuden, Y., Ito, T., Masaki, T., Yorioka, N., and Kohno, N. (2005). Tgf-beta1 induced by high glucose is controlled by angiotensin-converting enzyme inhibitor and angiotensin II receptor blocker on cultured human peritoneal mesothelial cells. *Perit. Dial. Int.* 25, 483–491.
- Lamouille, S., Xu, J., and Derynck, R. (2014). Molecular mechanisms of epithelial-mesenchymal transition. *Nat. Rev. Mol. Cell Biol.* 15, 178–196. doi: 10.1038/nrm3758
- LeBleu, V. S., Taduri, G., O'Connell, J., Teng, Y., Cooke, V. G., Woda, C., et al. (2013). Origin and function of myofibroblasts in kidney fibrosis. *Nat. Med.* 19, 1047–1053. doi: 10.1038/nm.3218
- Levin, A., and Beaulieu, M. C. (2011). Trials and tribulations of new agents, novel biomarkers, and retarding renal progression. *J. Am. Soc. Nephrol.* 22, 992–993. doi: 10.1681/ASN.2011040402
- Lewis, E. J., Hunsicker, L. G., Clarke, W. R., Berl, T., Pohl, M. A., Lewis, J. B., et al. (2001). Renoprotective effect of the angiotensin-receptor antagonist irbesartan in patients with nephropathy due to type 2 diabetes. *N. Engl. J. Med.* 345, 851–860. doi: 10.1056/NEJMoa011303
- Li, L., Zepeda-Orozco, D., Black, R., and Lin, F. (2010). Autophagy is a component of epithelial cell fate in obstructive uropathy. *Am. J. Pathol.* 176, 1767–1778. doi: 10.2353/ajpath.2010.090345
- Li, M. O., Wan, Y. Y., Sanjabi, S., Robertson, A. K., and Flavell, R. A. (2006). Transforming growth factor-beta regulation of immune responses. *Annu. Rev. Immunol.* 24, 99–146. doi: 10.1146/annurev.immunol.24.021605.090737
- Li, X., Zhu, L., Wang, B., Yuan, M., and Zhu, R. (2017a). Drugs and targets in fibrosis. *Front. Pharmacol.* 8:855. doi: 10.3389/fphar.2017.00855
- Li, Z., Liu, X., Wang, B., Nie, Y., Wen, J., Wang, Q., et al. (2017b). Pirfenidone suppresses MAPK signalling pathway to reverse epithelial-mesenchymal transition and renal fibrosis. *Nephrology* 22, 589–597. doi: 10.1111/nep.12831
- Liu, Y. (2010). New insights into epithelial-mesenchymal transition in kidney fibrosis. *J. Am. Soc. Nephrol.* 21, 212–222. doi: 10.1681/ASN.2008121226
- Lovisa, S., Lebleu, V. S., Tampe, B., Sugimoto, H., Vlodavets, K., Carstens, J. L., et al. (2015). Epithelial-to-mesenchymal transition induces cell cycle arrest and parenchymal damage in renal fibrosis. *Nat. Med.* 21, 998–1009. doi: 10.1038/nm.3902
- Lovisa, S., Zeisberg, M., and Kalluri, R. (2016). Partial epithelial-to-mesenchymal transition and other new mechanisms of kidney fibrosis. *Trends Endocrinol. Metab.* 27, 681–695. doi: 10.1016/j.tem.2016.06.004
- Macias-Barragan, J., Sandoval-Rodriguez, A., Navarro-Partida, J., and Armendariz-Borunda, J. (2010). The multifaceted role of pirfenidone and its novel targets. *Fibrogenesis Tissue Repair* 3:16. doi: 10.1186/1755-1536-3-16
- Medici, D., and Kalluri, R. (2012). Endothelial-mesenchymal transition and its contribution to the emergence of stem cell phenotype. *Semin. Cancer Biol.* 22, 379–384. doi: 10.1016/j.semcancer.2012.04.004
- Ng, Y. Y., Huang, T. P., Yang, W. C., Chen, Z. P., Yang, A. H., Mu, W., et al. (1998). Tubular epithelial-myofibroblast transdifferentiation in progressive tubulointerstitial fibrosis in 5/6 nephrectomized rats. *Kidney Int.* 54, 864–876. doi: 10.1046/j.1523-1755.1998.00076.x



- Nieto, M. A., Huang, R. Y., Jackson, R. A., and Thiery, J. P. (2016). Emt: 2016. *Cell* 166, 21–45. doi: 10.1016/j.cell.2016.06.028
- Oh, J., Richardson, J. A., and Olson, E. N. (2005). Requirement of myocardin-related transcription factor-B for remodeling of branchial arch arteries and smooth muscle differentiation. *Proc. Natl. Acad. Sci. USA* 102, 15122–15127. doi: 10.1073/pnas.0507346102
- Peng, H., Carretero, O. A., Vuljaj, N., Liao, T. D., Motivala, A., Peterson, E. L., et al. (2005). Angiotensin-converting enzyme inhibitors: a new mechanism of action. *Circulation* 112, 2436–2445. doi: 10.1161/CIRCULATIONAHA.104.528695
- Powell, D. W., Mifflin, R. C., Valentich, J. D., Crowe, S. E., Saada, J. I., and West, A. B. (1999). Myofibroblasts. I. Paracrine cells important in health and disease. *Am. J. Phys.* 277, C1–C9.
- Quaggin, S. E., and Kapus, A. (2011). Scar wars: mapping the fate of epithelial-mesenchymal-myofibroblast transition. *Kidney Int.* 80, 41–50. doi: 10.1038/ki.2011.77
- Raghu, G., and Thickett, D. R. (2013). Pirfenidone for IPF: pro/con debate; the 'con' viewpoint. *Thorax* 68, 605–608. doi: 10.1136/thoraxjnl-2011-201269
- Rastaldi, M. P., Ferrario, F., Giardino, L., Dell'antonio, G., Grillo, C., Grillo, P., et al. (2002). Epithelial-mesenchymal transition of tubular epithelial cells in human renal biopsies. *Kidney Int.* 62, 137–146. doi: 10.1046/j.1523-1755.2002.00430.x
- Record, J., Malinova, D., Zenner, H. L., Plagnol, V., Nowak, K., Syed, F., et al. (2015). Immunodeficiency and severe susceptibility to bacterial infection associated with a loss-of-function homozygous mutation of MKL1. *Blood* 126, 1527–1535. doi: 10.1182/blood-2014-12-611012
- Risdon, R. A., Sloper, J. C., and De Wardener, H. E. (1968). Relationship between renal function and histological changes found in renal-biopsy specimens from patients with persistent glomerular nephritis. *Lancet* 2, 363–366.
- Roberts, I. S., Burrows, C., Shanks, J. H., Venning, M., and McWilliam, L. J. (1997). Interstitial myofibroblasts: predictors of progression in membranous nephropathy. *J. Clin. Pathol.* 50, 123–127. doi: 10.1136/jcp.50.2.123
- Romano, L. A., and Runyan, R. B. (2000). Slug is an essential target of TGF $\beta$ 2 signaling in the developing chicken heart. *Dev. Biol.* 223, 91–102. doi: 10.1006/dbio.2000.9750
- Rowe, R. G., Lin, Y., Shimizu-Hirota, R., Hanada, S., Neilson, E. G., Greenson, J. K., et al. (2011). Hepatocyte-derived Snail1 propagates liver fibrosis progression. *Mol. Cell. Biol.* 31, 2392–2403. doi: 10.1128/MCB.01218-10
- Rybinski, B., Franco-Barraza, J., and Cukierman, E. (2014). The wound healing, chronic fibrosis, and cancer progression triad. *Physiol. Genomics* 46, 223–244. doi: 10.1152/physiolgenomics.00158.2013
- Sato, M., Muragaki, Y., Saika, S., Roberts, A. B., and Ooshima, A. (2003). Targeted disruption of TGF- $\beta$ 1/Smad3 signaling protects against renal tubulointerstitial fibrosis induced by unilateral ureteral obstruction. *J. Clin. Invest.* 112, 1486–1494. doi: 10.1172/JCI200319270
- Schnaper, H. W. (2017). The tubulointerstitial pathophysiology of progressive kidney disease. *Adv. Chronic Kidney Dis.* 24, 107–116. doi: 10.1053/j.ackd.2016.11.011
- Sebe, A., Erdei, Z., Varga, K., Bodor, C., Mucsi, I., and Rosivall, L. (2010). Cdc42 regulates myocardin-related transcription factor nuclear shuttling and alpha-smooth muscle actin promoter activity during renal tubular epithelial-mesenchymal transition. *Nephron Exp. Nephrol.* 114, e117–e125. doi: 10.1159/000265550
- Sebe, A., Leivonen, S. K., Fintha, A., Masszi, A., Rosivall, L., Kahari, V. M., et al. (2008a). Transforming growth factor-beta-induced alpha-smooth muscle cell actin expression in renal proximal tubular cells is regulated by p38 $\beta$  mitogen-activated protein kinase, extracellular signal-regulated protein kinase1.2 and the Smad signalling during epithelial-myofibroblast transdifferentiation. *Nephrol. Dial. Transplant.* 23, 1537–1545. doi: 10.1093/ndt/gfm789
- Sebe, A., Masszi, A., Zulus, M., Yeung, T., Speight, P., Rotstein, O. D., et al. (2008b). Rac, PAK and p38 regulate cell contact-dependent nuclear translocation of myocardin-related transcription factor. *FEBS Lett.* 582, 291–298. doi: 10.1016/j.febslet.2007.12.021
- Sharma, K., Ix, J. H., Mathew, A. V., Cho, M., Pflueger, A., Dunn, S. R., et al. (2011). Pirfenidone for diabetic nephropathy. *J. Am. Soc. Nephrol.* 22, 1144–1151. doi: 10.1681/ASN.2010101049
- Sicklick, J. K., Choi, S. S., Bustamante, M., McCall, S. J., Perez, E. H., Huang, J., et al. (2006). Evidence for epithelial-mesenchymal transitions in adult liver cells. *Am. J. Physiol. Gastrointest. Liver Physiol.* 291, G575–G583. doi: 10.1152/ajpgi.00102.2006
- Sisson, T. H., Ajayi, I. O., Subbotina, N., Dodi, A. E., Rodansky, E. S., Chibucos, L. N., et al. (2015). Inhibition of myocardin-related transcription factor/serum response factor signaling decreases lung fibrosis and promotes mesenchymal cell apoptosis. *Am. J. Pathol.* 185, 969–986. doi: 10.1016/j.ajpath.2014.12.005
- Smith, E. C., Thon, J. N., Devine, M. T., Lin, S., Schulz, V. P., Guo, Y., et al. (2012). MKL1 and MKL2 play redundant and crucial roles in megakaryocyte maturation and platelet formation. *Blood* 120, 2317–2329. doi: 10.1182/blood-2012-04-420828
- Strutz, F., Okada, H., Lo, C. W., Danoff, T., Carone, R. L., Tomaszewski, J. E., et al. (1995). Identification and characterization of a fibroblast marker: FSP1. *J. Cell Biol.* 130, 393–405. doi: 10.1083/jcb.130.2.393
- Stump, R. J., Lovicu, F. J., Ang, S. L., Pandey, S. K., and McAvoy, J. W. (2006). Lithium stabilizes the polarized lens epithelial phenotype and inhibits proliferation, migration, and epithelial mesenchymal transition. *J. Pathol.* 210, 249–257. doi: 10.1002/path.2049
- Sun, Y., Boyd, K., Xu, W., Ma, J., Jackson, C. W., Fu, A., et al. (2006). Acute myeloid leukemia-associated Mkl1 (Mrtf-a) is a key regulator of mammary gland function. *Mol. Cell. Biol.* 26, 5809–5826. doi: 10.1128/MCB.00024-06
- Tanjore, H., Xu, X. C., Polosukhin, V. V., Degryse, A. L., Li, B., Han, W., et al. (2009). Contribution of epithelial-derived fibroblasts to bleomycin-induced lung fibrosis. *Am. J. Respir. Crit. Care Med.* 180, 657–665. doi: 10.1164/rccm.200903-0322OC
- Taura, K., Miura, K., Iwaisako, K., Osterreicher, C. H., Kodama, Y., Penz-Osterreicher, M., et al. (2010). Hepatocytes do not undergo epithelial-mesenchymal transition in liver fibrosis in mice. *Hepatology* 51, 1027–1036. doi: 10.1002/hep.23368
- Thiery, J. P., and Sleeman, J. P. (2006). Complex networks orchestrate epithelial-mesenchymal transitions. *Nat. Rev. Mol. Cell Biol.* 7, 131–142. doi: 10.1038/nrm1835
- Thomas, R., Kalso, A., and Sedor, J. R. (2008). Chronic kidney disease and its complications. *Prim. Care* 35, 329–344. vii. doi: 10.1016/j.pop.2008.01.008
- Tomasek, J. J., Gabbiani, G., Hinz, B., Chaponnier, C., and Brown, R. A. (2002). Myofibroblasts and mechano-regulation of connective tissue remodelling. *Nat. Rev. Mol. Cell Biol.* 3, 349–363. doi: 10.1038/nrm809
- Velasquez, L. S., Sutherland, L. B., Liu, Z., Grinnell, F., Kamm, K. E., Schneider, J. W., et al. (2013). Activation of MRTF-A-dependent gene expression with a small molecule promotes myofibroblast differentiation and wound healing. *Proc. Natl. Acad. Sci. USA* 110, 16850–16855. doi: 10.1073/pnas.1316764110
- Venkatachalam, M. A., Weinberg, J. M., Kriz, W., and Bidani, A. K. (2015). Failed tubule recovery, AKI-CKD transition, and kidney disease progression. *J. Am. Soc. Nephrol.* 26, 1765–1776. doi: 10.1681/ASN.2015010006
- Voelker, J., Berg, P. H., Sheetz, M., Duffin, K., Shen, T., Moser, B., et al. (2017). Anti-TGF- $\beta$ 1 antibody therapy in patients with diabetic nephropathy. *J. Am. Soc. Nephrol.* 28, 953–962. doi: 10.1681/ASN.2015111230
- Willis, B. C., Liebler, J. M., Luby-Phelps, K., Nicholson, A. G., Crandall, E. D., Du Bois, R. M., et al. (2005). Induction of epithelial-mesenchymal transition in alveolar epithelial cells by transforming growth factor-beta1: potential role in idiopathic pulmonary fibrosis. *Am. J. Pathol.* 166, 1321–1332. doi: 10.1016/S0002-9440(10)62351-6
- Wynn, T. A. (2007). Common and unique mechanisms regulate fibrosis in various fibroproliferative diseases. *J. Clin. Invest.* 117, 524–529. doi: 10.1172/JCI31487
- Xu, X., Tan, X., Tampe, B., Wilhelmi, T., Hulshoff, M. S., Saito, S., et al. (2018). High-fidelity CRISPR/Cas9- based gene-specific hydroxymethylation rescues gene expression and attenuates renal fibrosis. *Nat. Commun.* 9:3509. doi: 10.1038/s41467-018-05766-5
- Yamamoto, T., Nakamura, T., Noble, N. A., Ruoslahti, E., and Border, W. A. (1993). Expression of transforming growth factor beta is elevated in human and experimental diabetic nephropathy. *Proc. Natl. Acad. Sci. USA* 90, 1814–1818.
- Yang, J., and Liu, Y. (2001). Dissection of key events in tubular epithelial to myofibroblast transition and its implications in renal interstitial fibrosis. *Am. J. Pathol.* 159, 1465–1475. doi: 10.1016/S0002-9440(10)62533-3
- Ye, X., and Weinberg, R. A. (2015). Epithelial-mesenchymal plasticity: a central regulator of cancer progression. *Trends Cell Biol.* 25, 675–686. doi: 10.1016/j.tcb.2015.07.012
- Yoshikawa, M., Hishikawa, K., Marumo, T., and Fujita, T. (2007). Inhibition of histone deacetylase activity suppresses epithelial-to-mesenchymal transition



- induced by TGF-beta1 in human renal epithelial cells. *J. Am. Soc. Nephrol.* 18, 58–65. doi: 10.1681/ASN.2005111187
- Zeisberg, M., Hanai, J., Sugimoto, H., Mammoto, T., Charytan, D., Strutz, F., et al. (2003). BMP-7 counteracts TGF-beta1-induced epithelial-to-mesenchymal transition and reverses chronic renal injury. *Nat. Med.* 9, 964–968. doi: 10.1038/nm888
- Zeisberg, E. M., Potenta, S. E., Sugimoto, H., Zeisberg, M., and Kalluri, R. (2008). Fibroblasts in kidney fibrosis emerge via endothelial-to-mesenchymal transition. *J. Am. Soc. Nephrol.* 19, 2282–2287. doi: 10.1681/ASN.2008050513
- Zeisberg, E. M., Tarnavski, O., Zeisberg, M., Dorfman, A. L., McMullen, J. R., Gustafsson, E., et al. (2007a). Endothelial-to-mesenchymal transition contributes to cardiac fibrosis. *Nat. Med.* 13, 952–961. doi: 10.1038/nm1613
- Zeisberg, M., Yang, C., Martino, M., Duncan, M. B., Rieder, F., Tanjore, H., et al. (2007b). Fibroblasts derive from hepatocytes in liver fibrosis via epithelial to mesenchymal transition. *J. Biol. Chem.* 282, 23337–23347. doi: 10.1074/jbc.M700194200
- Zhou, Y., Huang, X., Hecker, L., Kurundkar, D., Kurundkar, A., Liu, H., et al. (2013). Inhibition of mechanosensitive signaling in myofibroblasts ameliorates experimental pulmonary fibrosis. *J. Clin. Invest.* 123, 1096–1108. doi: 10.1172/JCI66700
- Zvaifler, N. J. (2006). Relevance of the stroma and epithelial-mesenchymal transition (EMT) for the rheumatic diseases. *Arthritis Res. Ther.* 8:210. doi: 10.1186/ar1963

**Conflict of Interest Statement:** The authors declare that the research was conducted in the absence of any commercial or financial relationships that could be construed as a potential conflict of interest.

Copyright © 2019 Fintha, Gasparics, Rosivall and Sebe. This is an open-access article distributed under the terms of the Creative Commons Attribution License (CC BY). The use, distribution or reproduction in other forums is permitted, provided the original author(s) and the copyright owner(s) are credited and that the original publication in this journal is cited, in accordance with accepted academic practice. No use, distribution or reproduction is permitted which does not comply with these terms.



# Natural Plants Compounds as Modulators of Epithelial-to-Mesenchymal Transition

Lorena Avila-Carrasco<sup>1\*</sup>, Pedro Majano<sup>2</sup>, José Antonio Sánchez-Tomé<sup>3,5</sup>, Rafael Selgas<sup>4,5</sup>, Manuel López-Cabrera<sup>5,6†</sup>, Abelardo Aguilera<sup>2,5†‡</sup> and Guadalupe González Mateo<sup>4,5,6†</sup>

<sup>1</sup> Therapeutic and Pharmacology Department, Health and Human Science Research, Academic Unit of Human Medicine and Health Sciences, Autonomous University of Zacatecas, Zacatecas, Mexico, <sup>2</sup> Molecular Biology Unit, Research Institute of University Hospital La Princesa (IP), Madrid, Spain, <sup>3</sup> Department and Nephrology, Research Institute of University Hospital La Princesa (IP), Madrid, Spain, <sup>4</sup> Research Institute of La Paz (IdiPAZ), University Hospital La Paz, Madrid, Spain, <sup>5</sup> Renal research network REDINREN, Madrid, Spain, <sup>6</sup> Molecular Biology Research Centre Severo Ochoa, Spanish Council for Scientific Research (CSIC), Madrid, Spain

## OPEN ACCESS

### Edited by:

Raffaele Strippoli,  
Sapienza University of Rome, Italy

### Reviewed by:

Marco Cordani,  
IMDEA Nanociencia, Spain  
Gautam Sethi,  
National University of Singapore,  
Singapore

### \*Correspondence:

Lorena Avila-Carrasco,  
laccoc\_@hotmail.com

<sup>†</sup>These authors have contributed  
equally to this work.

<sup>‡</sup>In memoriam.

### Specialty section:

This article was submitted to  
Inflammation Pharmacology,  
a section of the journal  
Frontiers in Pharmacology

**Received:** 10 March 2019

**Accepted:** 05 June 2019

**Published:** 30 July 2019

### Citation:

Avila-Carrasco L, Majano P,  
Sánchez-Tomé JA, Selgas R,  
López-Cabrera M, Aguilera A and  
González Mateo G (2019) Natural  
Plants Compounds as Modulators of  
Epithelial-to-Mesenchymal Transition.  
Front. Pharmacol. 10:715.  
doi: 10.3389/fphar.2019.00715

Epithelial-to-mesenchymal transition (EMT) is a self-regulated physiological process required for tissue repair that, in non-controlled conditions may lead to fibrosis, angiogenesis, loss of normal organ function or cancer. Although several molecular pathways involved in EMT regulation have been described, this process does not have any specific treatment. This article introduces a systematic review of effective natural plant compounds and their extract that modulates the pathological EMT or its deleterious effects, through acting on different cellular signal transduction pathways both *in vivo* and *in vitro*. Thereby, cryptotanshinone, resveratrol, oxymatrine, ligustrazine, osthole, codonolactone, betanin, tannic acid, gentiopicroside, curcumin, genistein, paeoniflorin, gambogic acid and *Cinnamomum cassia* extracts inhibit EMT acting on transforming growth factor- $\beta$  (TGF- $\beta$ )/Smads signaling pathways. Gedunin, carnosol, celastrol, black rice anthocyanins, *Duchesnea indica*, cordycepin and *Celastrus orbiculatus* extract downregulate vimentin, fibronectin and N-cadherin. Sulforaphane, luteolin, celastrol, curcumin, arctigenin inhibit  $\beta$ -catenin signaling pathways. Salvianolic acid-A and plumbagin block oxidative stress, while honokiol, gallic acid, piperlongumine, brusatol and paeoniflorin inhibit EMT transcription factors such as SNAIL, TWIST and ZEB. Plectranthoic acid, resveratrol, genistein, baicalin, polyphyllin I, cairicoside E, luteolin, berberine, nimbolide, curcumin, withaferin-A, jatrophone, ginsenoside-Rb1, honokiol, parthenolide, phoyunnanin-E, epicatechin-3-gallate, gigantol, eupatolide, baicalin and baicalein and nitidine chloride inhibit EMT acting on other signaling pathways (SIRT1, p38 MAPK, NFAT1, SMAD, IL-6, STAT3, AQP5, notch 1, PI3K/Akt, Wnt/ $\beta$ -catenin, NF- $\kappa$ B, FAK/AKT, Hh). Despite the huge amount of preclinical data regarding EMT modulation by the natural compounds of plant, clinical translation is poor. Additionally, this review highlights some relevant examples of clinical trials using natural plant compounds to modulate EMT and its deleterious effects. Overall, this opens up new therapeutic alternatives in cancer, inflammatory and fibrosing diseases through the control of EMT process.

**Keywords:** natural plants compounds, epithelial-to-mesenchymal transition (EMT), anti-fibrotic, anti-inflammatory, anti-oxidant agent

## INTRODUCTION

Epithelial-to-mesenchymal transition (EMT) is a tightly regulated physiological process implicated in tissue repair and in embryogenesis (Thiery et al., 2009). During EMT, epithelial cells undergo multiple morphologic, biochemical and genetic rearranges that gradually enable them to acquire a mesenchymal phenotype (Kalluri and Weinberg, 2009; Savagner, 2010; Kong et al., 2015).

We could consider two types of EMT, a physiological and a pathological EMT. The main characteristic of the physiological EMT is its ability to self-regulate, and it is related to embryonic development, organ formation, wound healing and tissue regeneration (Kalluri, 2009). In contrast, pathological EMT usually accompanies diseases and does not self-regulate. In this last case, EMT is an irreversible process and contributes to the failure of diseased organs (Thiery et al., 2009), which justifies the scientific investment into controlling such a process. Pathological EMT is present in many inflammatory and immunological diseases and leads to tissue fibrosis, angiogenesis, loss of organ function, cancer progression and metastasis (Corvol et al., 2009; Lee et al., 2006; Kalluri, 2009).

Although the involvement of EMT in some organ fibrosis, such as of the kidney, is controversial, more evidence about the role of pathological EMT has been reported in other organ fibrosis including that of the lung, the peritoneum and the heart, as well as in cancer progression (Yáñez-Mó et al., 2003; Rastaldi, 2006; Thiery et al., 2009; von Gise and Pu, 2012; Hertig et al., 2008).

EMT starts with the dissociation of intercellular junctions and the loss of microvilli and apical-basal polarity, followed by the acquirement of a front to back polarity and an increased migratory capacity. In the latest stages of EMT, the cell increases its capacity to degrade the basement membrane and to invade the fibrotic compact zone. Cells that have undergone a mesenchymal conversion possess increased capacity to synthesize extracellular matrix (ECM) components as well as a large number of pro-inflammatory, fibrotic and angiogenic factors, including vascular endothelial growth factor (VEGF), inducing angiogenesis (Boutet et al., 2006; Yoo et al., 2006; Lopez-Cabrera, 2014; Grande et al., 2015; Lovisa et al., 2015; Cho et al., 2017; Kida et al., 2007).

To control the pathological EMT, many drugs and molecular measures with variable results have been tested, but this therapeutic target remains a challenge for current medicine (Aguilera et al., 2005). Targeting EMT can be a really interesting weapon for the treatment of many fibroproliferative, cardiovascular and autoimmune diseases, and other pathologies such as cancer.

## Molecular Mechanisms Involved in EMT Regulation

Mechanistically, EMT is a complex, dynamic and progressive process that affects the cellular architecture and requires a deep molecular reprogramming with new biochemical instructions (Lopez-Cabrera, 2014). The EMT process results from an integration of diverse signals transduction pathways and multiple triggering factors, including inflammatory cytokines, advanced

glycation end products (AGEs), oxidative stress and hypoxia, transforming growth factor- $\beta$ 1 (TGF- $\beta$ 1)/Smads pathway, tyrosine kinase receptors, delta-like jagged Notch, caveolin (cav)-1, angiotensin receptor and integrins (Figure 1). A master molecule in the EMT induction appears to be TGF- $\beta$ , nonetheless the number of molecules and routes implicated in EMT is still growing (Lopez-Cabrera, 2014). The binding of the TGF- $\beta$ 1 to its "primary receptor" (receptor type II) permits the recruitment, trans-phosphorylation, and activation of the "signaling receptor" (receptor type I), also known as activin receptor-like kinase 5 (ALK5). Then, ALK5 is able to exert its activity to phosphorylate Smad2 and Smad3 (Masszi and Kapus, 2011). These receptor-activated Smads (R-Smads) form heterodimers with Smad4, a common mediator of the Smad pathways. These resulting Smad heterocomplexes are translocated into the nucleus, where they bind directly to DNA to regulate the transcription of target genes (Lopez-Cabrera, 2014). Another group of Smads, known as "inhibitory Smads" (e.g. Smad7), control TGF- $\beta$ 1-induced Smad signaling by preventing the phosphorylation and/or nuclear translocation of R-Smads and inducing receptor heterocomplex degradation (Lopez-Cabrera, 2014).

Among the R-Smads, Smad-3 appears to be the key mediator in TGF- $\beta$ -induced fibrosis and EMT (Zhou et al., 2010). In this context, it has been shown that the inhibition of Smad3 activation and nuclear translocation blocks EMT (Zhou et al., 2010) and tissue fibrosis (Sato et al., 2003). Translocated Smad-3 into the nucleus controls TGF- $\beta$ -responsive genes encoding integrin-linked kinase (ILK) (Massagué, 2000). The activation of ILK by  $\beta$ 1-integrins lead to protein kinase B (Akt) and glycogen synthase kinase-3 (GSK-3)-beta phosphorylation (Massagué and Wotton, 2000).

Phosphorylated-Akt activates nuclear factor- $\kappa$ B (NF- $\kappa$ B) (Tan et al., 2002), which induces the expression of Smad-7 (Bitzer et al., 2000) emphasizing the self-regulated nature of the whole EMT process (Figure 1). On the other hand, phosphorylated-GSK-3 $\beta$  is inactive, what subsequently stabilizes  $\beta$ -catenin, released from the adherens junction, and activator protein-1 (AP-1) (D'Amico et al., 2000). When stabilized,  $\beta$ -catenin per se may induce EMT (Kim et al., 2002a), while AP-1 activates matrix metalloproteinase (MMP)-9 expression inducing the invasion of the ECM (Troussard et al., 2000).

The Smad-dependent pathways are not the only ways by which TGF- $\beta$ 1 regulate the EMT process. Smad-independent pathways also participate in TGF- $\beta$ 1-induced EMT. These pathways can either potentiate or modulate the outcome of TGF- $\beta$ 1-induced Smad signaling (Lopez-Cabrera, 2014). A main Smad-independent signalling pathway activated by TGF- $\beta$ 1/receptor I interaction is the Ras homolog gene family member A (RhoA)/rho-associated, coiled-coil-containing protein kinase 1 (ROCK1) pathway. This route regulates cytoskeleton remodelling and cellular migration and invasion. RhoA also induces the expression of alpha smooth muscle actin ( $\alpha$ -SMA) in a ROCK-independent manner (Masszi et al., 2003).

TGF- $\beta$ 1 also activates the H-Ras/Raf/extracellular signal-regulated kinase (ERK) pathway, necessary for the induction of transcription factor SNAIL1 expression and of EMT (Peinado et al., 2003; Barberà et al., 2004; Huber et al., 2004), cooperating

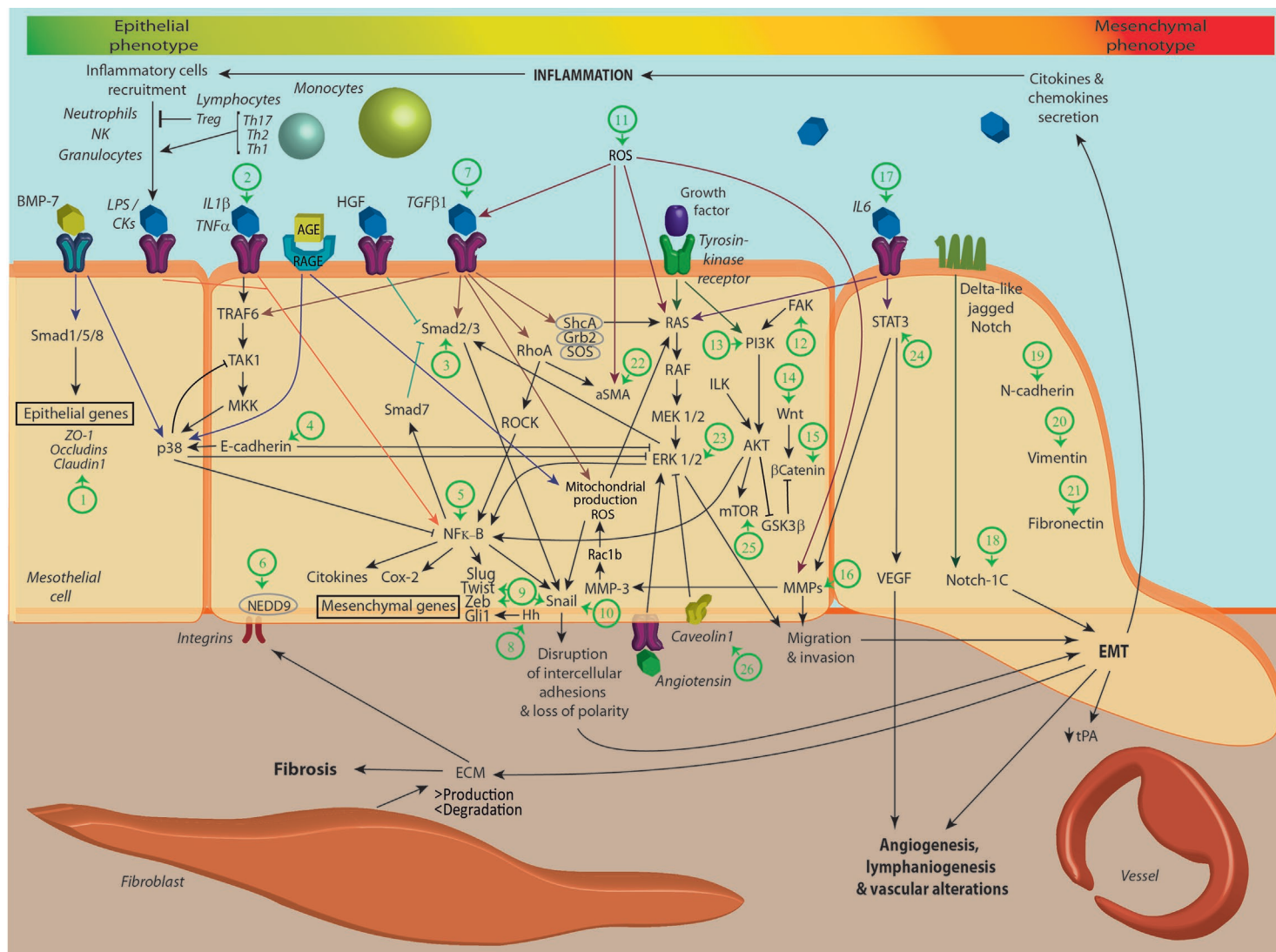


FIGURE 1 | Continued



**FIGURE 1 |** Key events during the development of epithelial-to-mesenchymal transition (EMT) and target pathways for therapeutic use of natural plant compounds (NPCs). The diagram shows key essential steps for the EMT course. Briefly, BMP7 and hepatocyte growth factor (HGF) are responsible for maintaining the cellular epithelial phenotype. Both molecules maintain E-cadherin and Smads1, 5, 7 and 8 expressions, and block Smads 2 and 3. On the other hand, inflammatory conditions triggered by exogenous or endogenous factors lead to a dysregulation of Th17/Treg equilibrium with IL6 synthesis that stimulates NFκB and induces EMT. Advanced glycation end products (AGEs) induce proteins structural crosslink, stimulate inflammatory response (monocytes), oxidative stress and finally upregulation of Snail, leading to EMT. These effects are mediated through specific receptors called RAGES. Reactive oxygen species (ROS) generate oxidation and stimulate TGF-β, αSMA, RAS/RAF/MEK/ERK cascade and matrix metalloproteinases (MMPs) upregulation initiating cell migration. TGF-β initiates the classic route of EMT induction overexpressing Snail, Slug, N-Cadherin, Smads 2 and 3 and downregulating E-Cadherin and Smads 1, 5, 7 and 8. TGF-β also stimulates RhoA/ROCK and finally NFκB. Growth factors also stimulate the RAS/RAF/MEK/ERK cascade and MMPs upregulation, again inducing cell migration and invasion. Likewise they stimulate the P13K/ integrin-linked kinase (ILK)/ protein kinase B (Akt) cascade and GSK3β is blocked. Inflammatory cytokines such as IL6 also stimulates signal transducer and activator of transcription 3 (STAT3), vascular endothelial growth factor (VEGF) and MMPs inducing migration, invasion and angiogenesis. Finally Notch-1C directly induces mesenchymal genes such as N-Cadherin. The numbers in green indicate where each NPC acts. Many of them have an effect on several molecules or pathways. Depending on the target route over which the corresponding NPC acts, we have defined the following groups (green numbers). Group 1 acts by increasing ZO-1 expression: (Plumbagin), Group 2 acts by decreasing IL-1β action: (Baicalin), Group 3 acts by blocking Smad 2/3 phosphorylation; Paeoniflorin, Eupatolide, Gallic acid, Caicoside E. Group 4 acts by up-regulating E-cadherin expression: α-solanine, Osthole, coumarin, *Cinnamomum cassia* extracts, Genistein, Withaferin A, Gedunin, *Celastrus orbiculatus* extract, Celastrol, Black rice anthocyanins, *Duchesnea* extracts, Cordycepin, Nitidine chloride, Phoyunnanin E, Epicatechin-3-gallate, Honokiol, Gallic acid, Piperlongumine, Brusatol, Berberine. Group 5 acts by inhibiting NFκ-β signaling: Honokiol, Parthenolide, Baicalin and baicalein Group 6 acts by inhibiting NEDD9/Rac1 signaling: Acid plectranthoic. Group 7 acts by blocking TGF-β-1 signaling: Cryptotanshinone, Resveratrol, Oximatrina, Ligustrazina, Osthole, coumarin, Codonolactone, Betanin, Tannic acid, *Cinnamomum cassia* extracts Caicoside E, Gentiopicroside, Genistein, Paeoniflorin, Gambogic acid, Arctigenin, Curcumin, Baicalin and baicalein, Baicalin and Caicoside-E. Group 8 acts by downregulating hedgehog (Hn) signaling: Resveratrol, *Sedum sarmentosum* Bunge and extract Nitidine chloride Group 9 acts by decreasing Twist and ZEB expression: Resveratrol, Paeoniflorin, Jatrophone, Gedunin, Nitidine chloride, Plumbagin, Honokiol, Phoyunnanin E, Gallic acid, Piperlongumine, Brusatol, Nimbolide, Baicalin and baicalein. Group 10 acts by downregulation Snail expression: Resveratrol, Osthole, coumarin, Paeoniflorin, Gedunin, Celastrol, Nitidine chloride, Plumbagin, Phoyunnanin E, Piperlongumine, Berberine and Nimbolide. Group 11 acts by Inhibit Nrf2-mediated oxidative stress signaling pathway: Betanin, Salvanolic-acid-A and Plumbagin. Group 12 acts by Suppressing focal adhesion kinase (FAK)/AKT signaling: Phoyunnanin, Epicatechin-3-gallate, Gigantol and Eupatolide. Group 13 acts by blocking P13K/Akt cascade: Berberine, Nimbolide, and Curcumin. Group 14 acts by blocking Wnt/β-catenin Wnt signaling: Withaferin A, Jatrophone, Ginsenoside-Rb1 and Withaferin-A. Group 15 acts by down-regulated β-Catenin expression: Celastrol, Sulforaphane, Arctigenin, Plumbagin, Curcumin and Luteolin. Group 16 acts by down-regulating MMPs expression: α-solanine, Resveratrol, *Cinnamomum cassia* extracts, Paeoniflorin and *Celastrus orbiculatus* extract. Group 17 acts by inhibiting IL-6 activity: Baicalin and Polyphyllin-I. Group 18 acts by blocking Notch-1 signaling: Gedunin, Nimbolide and Luteolin. Group 19 acts by down-regulating N-cadherin expression: Tannic acid, Paeoniflorin, Gedunin, *Celastrus orbiculatus* extract, Celastrol *Duchesnea indica*, Cordycepin, Nitidine chloride, Honokiol, Phoyunnanin E, Gigantol, Gallic acid, Berberine and Nimbolide. Group 20 acts by down-regulating Vimentin expression: α-solanine Tannic acid, *Cinnamomum cassia* extracts, Paeoniflorin, Withaferin A, Jatrophone, Gedunin, *Celastrus orbiculatus* extract, Celastrol Black rice anthocyanins, *Duchesnea indica*, Nitidine chloride, Plumbagin, Phoyunnanin E, Gigantol, Gallic acid, Berberine and Nimbolide. Group 21 acts by down-regulation Fibronectin expression: Tannic acid, *Cinnamomum cassia* extracts, Jatrophone, Withaferin A, Black rice anthocyanins, *Duchesnea indica*, Epicatechin-3-gallate, Gallic acid and Berberine. Group 22 acts by down-regulating α-SMA expression: Betanin, Celastrol and Salvanolic-acid-A. Group 23 acts by blocking extracellular signal-regulated kinase (ERK) signaling: Arctigenin, Gigantol, Eupatolide and Nimbolide. Group 24 acts by blocking STAT-3 signaling: Honokiol and Polyphyllin-I. Group 25 acts by blocking mammalian target of rapamycin (mTOR) signaling: Nimbolide. Group 26 acts by suppressing the cav-1 phosphorylation, stabilizing β-catenin: curcumin.

with fibroblast growth factor (FGF), a potent inducer of the mentioned route (Peinado et al., 2003). SNAIL1 regulates EMT by inhibiting E-cadherin (Cano et al., 2000; Poser et al., 2001) and by inducing growth arrest and survival, which confer advantage to migrating transdifferentiated cells (Vega et al., 2004).

The Notch signalling pathway is another EMT-activating route, able to induce SNAIL1 and SNAIL2 expression, down-regulating E-cadherin. The TGFβ/Smads classical pathway is able to cooperate with different signaling routes. The association of the tumor necrosis factor (TNF)-receptor associated factor 6 (TRAF6) with the TGFβ receptor heterocomplex activates TGFβ-activated kinase 1 (TAK1) and, as a result, p38 and c-Jun N-terminal kinase (JNK) (Thiery et al., 2009). Other stimuli such as advanced glycation endproducts AGEs are able to induce EMT by acting on specific cellular receptors (RAGE) (Chen et al., 2016b). Reactive oxygen species (ROS) can also directly activate TGF-β, the production of ECM, MMP and RAS (Thiery et al., 2009) (Figure 1). Finally, the activation of mammalian target of rapamycin (mTOR) induces inflammatory processes mediated by T helper 17 (Th17) cells, TH17, which in turn also triggers EMT (Liappas et al., 2015).

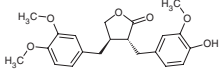
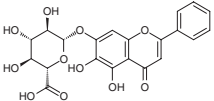
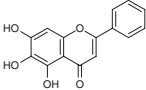
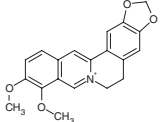
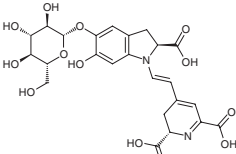
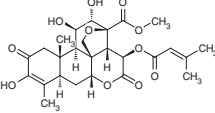
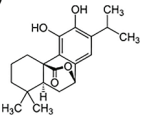
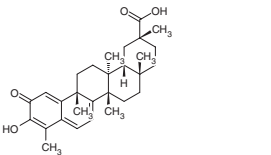
## Active Substances Derived from Plants Capable of Regulating EMT

Natural plant compounds (NPCs) have been used for many years as a source of therapeutic substances and a structural basis for drug elaboration. Unique architectures that can lead to novel therapeutic agents are provided by nature (Newman and Cragg, 2007; Song et al., 2014; Khan and Gurav, 2017).

NPCs are bioactive elements isolated from natural sources (plants) that can regulate the EMT through anti-inflammatory, anti-fibrotic or antioxidant mechanisms (Boldbaatar et al., 2017). Bioactive natural components are presented in this review which delves into their mechanisms of action against EMT (Table 1).

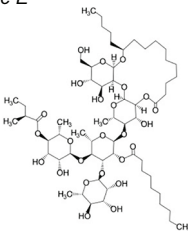
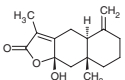
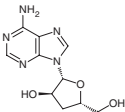
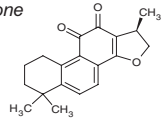
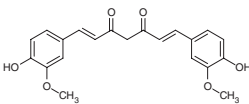
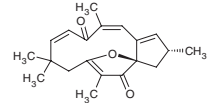
**Arctigenin (ARC).** It has been proposed as an anti-inflammatory and anti-cancer substance. In human lung cancer cells, ARC has been shown to inhibit TGF-β-induced phosphorylation, smad2/3 transcriptional activity, snail and N-cadherin expression, by contrast increasing the expression of E-cadherin in dose and time dependent manners. It blocks ERK-phosphorylation and β-catenin transcriptional activity. Through these mechanisms, ARC represses TGF-β-induced EMT (Xu et al., 2017).

**TABLE 1 |** Natural plants compounds able to modulate epithelial-to-mesenchymal transition (EMT).

Target	Scientific name of plant	Active compounds	EMT-related signaling pathways	Type of study	References
7,15,23	Asteraceae plants	<b>Arctigenin (ARC)</b> 	Represses TGF- $\beta$ -induced phosphorylation of ERK and transcriptional activity of $\beta$ -catenin	<i>In vitro</i>	Xu et al., 2017
2,7,5,9,17	<i>Scutellaria baicalensis</i> Georgi	<b>Baicalin and baicalein</b>  	Blocks TNF- $\alpha$ and IL-1 $\beta$ , reduce TGF- $\beta$ 1, TNF- $\alpha$ , IL-6 and increase IL-10 (anti-inflammatory cytokine). Downregulates Slug expression and block NF- $\kappa$ B pathway signaling.	<i>In vitro</i>	Chung et al., 2015; Zheng et al., 2016
4,10,13,19,20,21	<i>Berberis vulgaris</i> , <i>aristata</i> and <i>aquifolium</i>	<b>Berberine</b> 	Increases E-cadherin and decreases N-cadherin, vimentin, fibronectin and $\beta$ -catenin. Inhibits snail1, slug, and ZEB1. Blocks PI3K/AKT and RAR $\alpha$ /RAR $\beta$ .	<i>In vitro</i>	Kou et al., 2016
4,7,11,22	<i>Opuntia elatior</i> Mill.	<b>Betanin</b> 	Blocks TGF- $\beta$ signal pathway and modulates mRNA and protein expression of TGF- $\beta$ , type IV collagen, $\alpha$ -SMA and E-cadherin and regulates oxidative stress and TGF- $\beta$ pathway	<i>In vivo</i>	Sutariya and Brijesh, 2017
4,20,21	<i>Oryza sativa</i> L.	Black rice anthocyanins (BRACs). 9 anthocyanins have been detected in black rice (Hao et al., 2015)	Upregulates E-cadherin, and decreases fibronectin and vimentin expression	<i>In vivo</i> and <i>in vitro</i>	Sehitoglu et al., 2014; Hou, 2003; Zhou et al., 2017
4,9	<i>Bruceae fructus</i>	<b>Brusatol (BR)</b> 	Increases E-cadherin mRNA expression and decreases Twist expression	<i>In vitro</i>	Lu et al., 2017
2,7	Rosemary ( <i>Rosmarinus officinalis</i> L.)	<b>Carnosol (CAR)</b> 	Controls the TNF- $\alpha$ /TGF- $\beta$ -induced EMT and modulating the activation of miR-200c.	<i>In vitro</i>	Giacomelli et al., 2017
4,10,15,19,20,22	<i>Tripterygium wilfordii</i>	<b>Celastral (also named tripterine)</b> 	Upregulates E-cadherin and down-regulates N-cadherin, Vimentin and Snail Downregulates $\beta$ -catenin, N-cadherin, vimentin, $\alpha$ -SMA, FSP-1 and collagen expression and inhibits heat shock protein 90 signaling	<i>In vivo</i> and <i>in vitro</i> <i>In vivo</i> and <i>in vitro</i>	Lin et al., 2015 Divya et al., 2018

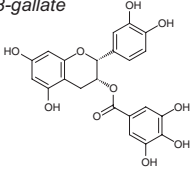
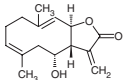
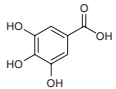
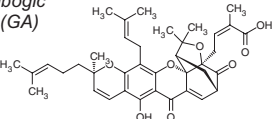
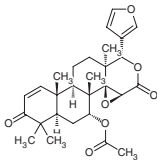
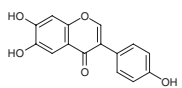
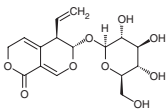
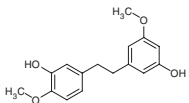
(Continued)

TABLE 1 | Continued

Target	Scientific name of plant	Active compounds	EMT-related signaling pathways	Type of study	References
3,7	<i>Ipomoea cairica</i>	<b>Cairicoside E (CE)</b> 	Down-regulates AQP5 expression and suppresses p-Smad2/3 induced by TGF- $\beta$ 1	<i>In vitro and in vivo</i>	Chen et al., 2017a
4,16,19,20	<i>Celastrus orbiculatus</i>	<b>Celastrus orbiculatus extract (COE)</b>  There are 11 compounds in the stems (Li et al., 2012a).	Reduces angiogenesis by targeting the VEGF protein Activates MAPK and inhibits Akt signaling pathways Inhibits Cofilin 1 signaling pathway, N-cadherin, vimentin, MMP-2 and MMP-9 protein expression and upregulates E-cadherin protein expression	<i>In vitro and in vivo</i>  <i>In vitro</i>  <i>in vitro</i>	Qian et al., 2012 Zhang et al., 2012a Wang et al., 2017b
4,7,16,20,21	<i>Cinnamomum cassia</i>	<b>Cinnamomum cassia extracts (CCE)</b> There are 15 compounds in the bark (Zhao et al., 2013)	Inhibits TGF- $\beta$ 1 by repressing MMP-2 and urokinase-type plasminogen activator also downregulating expression of vimentin and fibronectin and upregulating E-cadherin	<i>In vitro</i>	Lin et al., 2017
7	<i>Atractylodes lancea</i>	<b>Codonolactone (CLT)</b> 	Suppresses of TGF- $\beta$ signal pathway and Runx2 phosphorylation	<i>In vivo and in vitro</i>	Fu et al., 2016
4,19	<i>Cordyceps sinensis</i>	<b>Cordycepin (3'-deoxyadenosine)</b> 	Upregulates E-cadherin and downregulates N-cadherin protein expression	<i>in vitro</i>	Su et al., 2017
7	<i>Salvia miltiorrhiza</i>	<b>Cryptotanshinone (CTS)</b> 	Inhibits TGF- $\beta$ 1/ Smad3/integrin $\beta$ 1 signaling pathway	<i>In vivo and in vitro</i>	Li et al., 2015; Zhu et al., 2016; Jin et al., 2013; Ma et al., 2012; Ma et al., 2014; Wang et al., 2017c
7,13,15,26	<i>Curcuma longa</i>	<b>Curcumin (diferuloylmethane)</b> 	Blocks the PI3K/Akt/NF- $\kappa$ B signaling pathway Suppresses the cav-1 phosphorylation stabilizing $\beta$ -catenin Inhibits TGF- $\beta$ /Smad signaling	<i>In vitro</i> <i>In vivo and in vitro</i>  <i>In vivo and in vitro</i>	Li et al., 2018b Sun et al., 2014 Kong et al., 2015
9,14,20,21	<i>Jatropha isabelli</i> and <i>Jatropha gossypifolia</i>	<b>Jatrophone (JA).</b> 	Inhibits Wnt/ $\beta$ -catenin signaling and reduces mRNA expression levels for SLUG, fibronectin and vimentin.	<i>In vitro</i>	Fatima et al., 2017

(Continued)

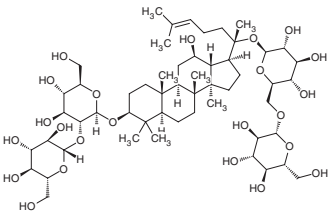
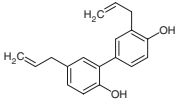
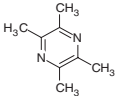
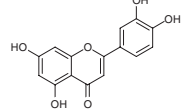
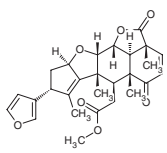
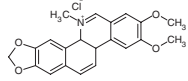
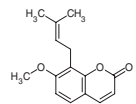
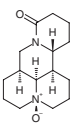
TABLE 1 | Continued

Target	Scientific name of plant	Active compounds	EMT-related signaling pathways	Type of study	References
4,19,20,21	<i>Duchesnea indica</i> and <i>Duchesnea chrysantha</i>	<i>Duchesnea</i> extracts. Involve a wide range of chemical compounds.	Downregulates N-cadherin, fibronectin and vimentin and upregulates E-cadherin expression. Exerts antioxidant action.	<i>In vivo</i> and <i>in vitro</i>	Chen et al., 2017c; Kim et al., 2002b; Kim et al., 2007; Hu et al., 2009; Hu et al., 2011
4,12,21	Green tea leaves	<b>Epicatechin-3-gallate (ECG)</b> 	Downregulates fibronectin expression, inhibits p-FAK and upregulates E-cadherin expression	<i>In vivo</i> and <i>in vitro</i>	Huang et al., 2016
3,12,23	<i>Inula britannica</i>	<b>Eupatolide</b> 	Suppresses TGF- $\beta$ 1-induced EMT via downregulation of Smad3 phosphorylation and decreasing the TGF- $\beta$ type 1 receptor.	<i>In vitro</i>	Lee et al., 2010a; Kim et al., 2013; Wrighton et al., 2009; Boldbaatar et al., 2017
3,4,9,19,20,21	<i>Polygonum minus</i>	<b>Gallic acid</b> 	Downregulates collagen types I, III, fibronectin, CTGF, N-cadherin, vimentin, SNAI1, TWIST1 expression, and Smad3 phosphorylation	<i>In vitro</i> and <i>in vivo</i>	Kee et al., 2014; Ryu et al., 2016; Jin et al., 2017
7	<i>Garcinia hanburyi</i> Hook.f.	<b>Gambogic acid (GA)</b> 	Suppresses TGF- $\beta$ 1/Smad3 pathway signaling and modulates VASH-2/VASH-1	<i>In vitro</i> and <i>in vivo</i>	Qu et al., 2016
4,9,10,18,19,20	<i>Azadirachta indica</i>	<b>Gedunin</b> 	Decreases expression of N-Cadherin, Slug, Snail, Vimentin, Notch 1 and 2, and Zeb while increases expression of E-cadherin.	<i>In vivo</i> and <i>in vitro</i> .	Subramani et al., 2017
7,4	Soybeans	<b>Genistein</b> 	Downregulates TGF- $\beta$ pathway signaling. Blocks Smad4-dependent and independent pathways signaling through p38 MAPK Downregulates the nuclear factor of activated T cells 1 (NFAT1)	<i>In vitro</i> <i>In vitro</i>	Kim et al., 2015 Han et al., 2012
7	<i>Gentiana</i>	<b>Gentiopicroside (GPS)</b> 	Downregulates the expression of TNF-alpha, IL1-b, TGF- $\beta$ 1 and CTGF	<i>In vivo</i> and <i>in vitro</i>	Chen et al., 2017b
12,19,20,23	<i>Dendrobium draconis</i>	<b>Gigantol</b> 	Downregulates N-cadherin, vimentin, and Slug, Inhibits AKT, ERK, and caveolin-1 (cav-1) signaling	<i>In vitro</i>	Unahabhokha et al., 2016

(Continued)

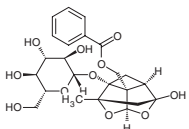
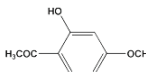
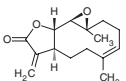
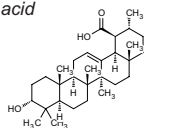
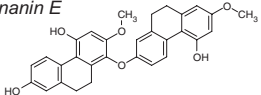
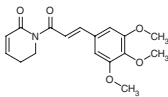
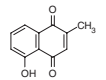
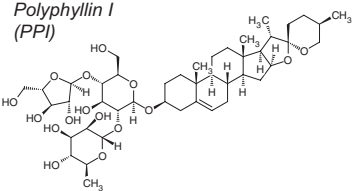
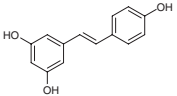


TABLE 1 | Continued

Target	Scientific name of plant	Active compounds	EMT-related signaling pathways	Type of study	References
14, 15	<i>Panax quinquefolius</i> and <i>notoginseng</i>	<b>Ginsenoside-Rb1</b> 	Inhibits Wnt/ $\beta$ -catenin signaling and EMT	<i>In vitro</i>	Deng et al., 2017
4, 5, 9, 19, 24	<i>Magnolia</i> spp. (officinalis, obovata, and grandiflora)	<b>Honokiol (HNK)</b> 	Downregulates Stat3 and Zeb1 expression. Upregulates E-cadherin. Downstream pathways of c-FLIP are NF- $\kappa$ B signaling and N-cadherin/snail signaling	<i>in vitro</i> and <i>in vivo</i>	Avtanski et al., 2014 Lv et al., 2016
7	<i>Ligusticum wallichii</i> Franchat.	<b>Ligustrazine (LIG)</b> 	Downregulates the TGF- $\beta$ 1-induced loss of cytokeratin-18 expression.	<i>In vivo</i>	Yuan et al., 2012
15, 18	Naturally found in several plant species including <i>Lonicera japonica</i> (Caprifoliaceae)	<b>Luteolin</b> 	Suppresses Notch1 signaling. Downregulates $\beta$ -catenin expression. Upregulates epithelial markers (E-cadherin and claudin) while downregulates mesenchymal markers (N-cadherin, vimentin, Snail and Slug).	<i>In vitro</i> <i>in vitro</i> and <i>in vivo</i>	Zang et al., 2017 Lin et al., 2017
9, 10, 13, 18, 19, 20, 23, 25	<i>Azadirachta indica</i>	<b>Nimbolide</b> 	Reduces PI3K/AKT/mTOR and ERK signaling and decreases Notch-2, N-cadherin, vimentin and Snail, Slug and Zeb expression	<i>In vitro</i>	Bodduluru et al., 2014; Hao et al., 2014; Subramani et al., 2016
4, 8, 9, 10, 19, 20	<i>Zanthoxylum nitidum</i>	<b>Nitidine chloride (NC)</b> 	Inhibits cellular migration and invasion. Downregulates Snail, Slug and Zeb1, decreases N-cadherin and Vimentin and increases E-cadherin expression	<i>In vitro</i>	Sun et al., 2014; Sun et al., 2016
4, 7, 10	<i>Cnidium monnieri</i>	<b>Osthole</b> 	Inhibits the TGF- $\beta$ /Akt/MAPK pathways signaling, reduces Snail-DNA-binding activity and induces E-cadherin expression	<i>In vivo</i> and <i>in vitro</i> .	Wen et al., 2015
7	<i>Sophora japonica</i>	<b>Oxymatrine (OM)</b> 	Blocks TGF- $\beta$ 1/Smad pathway signaling		Liu et al., 2012; Wu et al., 2008; Shi and Li, 2005; Chen et al., 2008; Shen et al., 2011; Fan et al., 2012; Liu et al., 2016

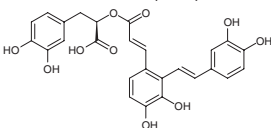
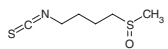
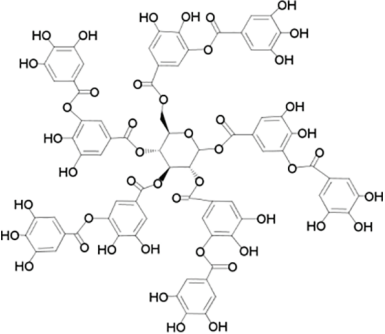
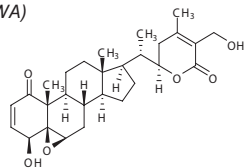
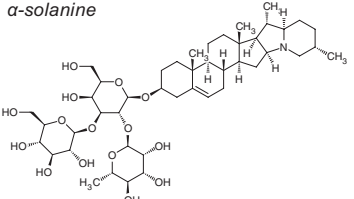
(Continued)

TABLE 1 | Continued

Target	Scientific name of plant	Active compounds	EMT-related signaling pathways	Type of study	References
3,7,9,10,16,19,20	<i>Paeonia lactiflora</i> Pallas	<b>Paeoniflorin (PF)</b> 	Downregulates TGF- $\beta$ 1 expression, maintains BMP-7 mRNA expression, and inhibits Smad2/3 activation Downregulates TGF $\beta$ , snail, N-cadherin, vimentin and MMP-2/-9 expressions Inhibits collagen-I synthesis and downregulates Snail and Slug expressions upregulating smad7	<i>In vivo</i> <i>In vivo and in vitro</i> <i>In vivo</i>	Zeng et al., 2013 Wang et al., 2018 Ji et al., 2016
16,15,11,5,4	<i>Paeonia suffruticosa</i> Andrews (Cortex Moutan)	<b>Paeonol</b> 	Decreased the expression levels of PCNA, $\beta$ -catenin, p53, and COX-2. Upregulated E-cadherin and MMP-2/-9, also eliminates ROS	<i>In vivo and in vitro</i>	Lu et al., 2018; Zhang et al., 2015; Lin et al., 2014; Chou, 2003
5	<i>Tanacetum parthenium</i>	<b>Parthenolide (PTL)</b> 	Blocks EMT via the NF- $\kappa$ B/Snail pathway	<i>In vitro and in vivo</i>	Hehner et al., 1999; Li et al., 2018a
6	<i>Ficus microcarpa</i>	<b>Plectranthoic acid (PA)</b> 	Inhibits NEDD9/Rac1 signaling	<i>In vitro</i>	Akhtar et al., 2018
4,9,10,12,19,20	<i>Dendrobium venustum</i>	<b>Phoyunnanin E</b> 	Suppresses FAK/AKT signals, decreases N-cadherin, vimentin, snail, and slug, and increases E-cadherin	<i>In vitro</i>	Petpiroon et al., 2017
4,9,10	<i>Piper longum</i>	<b>Piperlongumine (PL)</b> 	Downregulates the expression of Snail, Slug, $\beta$ -catenin, zeb1, N-Cadherin, Claudin-1, and ZO-1	<i>In vivo and in vitro</i>	Liu et al., 2017
1,9,10,11,15,20	Plumbaginaceae plants	<b>Plumbagin (PLB)</b> 	Inhibits Nrf2-mediated oxidative stress signaling pathway. Downregulates snail, slug, TCF-8/ZEB1, $\beta$ -catenin, and vimentin and upregulates claudin-1 and ZO-1 expression.	<i>In vitro</i>	Pan et al., 2015
17,24	<i>Polyphylla rhizomes</i>	<b>Polyphyllin I (PPI)</b> 	Blocks IL-6/STAT3 signaling pathway and stimulates epithelial marker expressions. Blocks EGF receptor tyrosine kinase inhibitors.	<i>In vitro</i>	Lou et al., 2017
7,9,10,8,16	Resveratrol (can be obtained from grapes, wine, mulberries and peanuts)	<b>Resveratrol (RSV; trans-3,5,4-trihydroxystilbene)</b> 	Suppresses TGF- $\beta$ 1-induced EMT, downregulates Snail and Slug expression, up-regulates E-cadherin and down-regulates fibronectin and vimentin Inhibits the Hedgehog signaling pathway Upregulates SIRT1 and inhibits Smad4 and MMP7 expression Suppresses MMP-2/-9 via MAPK and NF $\kappa$ B signals Represses EGF-induced ERK Downregulates Zeb-1, Slug and Snail.	<i>In vitro</i> <i>In vitro</i> <i>In vivo and in vitro</i> <i>In vitro</i> <i>In vitro</i> <i>In vitro</i>	Wang et al., 2013 Bai et al., 2014b; Gao et al., 2015 Xiao et al., 2016 Liu et al., 2010a; Yang et al., 2009 Vergara et al., 2011 Shankar et al., 2011

(Continued)

TABLE 1 | Continued

Target	Scientific name of plant	Active compounds	EMT-related signaling pathways	Type of study	References
11,22	<i>Salvia miltiorrhiza</i> Bunge	<b>Salvianolic acid A (SAA)</b> 	Downregulates $\alpha$ -SMA expression, suppresses oxidative stress. Inhibits the Nrf2/HO-1 pathway signaling	<i>In vivo</i> and <i>in vitro</i>	Chen et al., 2016a; Chen et al., 2017d
8	<i>Sedum sarmentosum</i> Bunge	<b>Sedum sarmentosum</b> Bunge (SSBE) extract	Downregulates the Hedgehog signaling activity.	<i>In vivo</i> and <i>in vitro</i>	Bai et al., 2014a; Bai et al., 2014b; Bai et al., 2017
15	Cruciferous plants "broccoli sprouts"	<b>Sulforaphane</b> 	Blocks miR-616-5p/GSK3 $\beta$ / $\beta$ -catenin pathway signaling	<i>In vivo</i> and <i>in vitro</i>	Wang et al., 2017a
7,19,20,21	Natural dietary polyphenolic compound	<b>Tannic acid (TA)</b> 	Reduces the TGF- $\beta$ 1-induced increase in TGF- $\beta$ receptors expression. Decreases expression of N-cadherin, type-1-collagen, fibronectin, and vimentin.	<i>In vitro</i>	Pattarayan et al., 2018
4, 14, 15	<i>Withania somnifera</i>	<b>Withaferin A (WA)</b> 	Witha-D partially inhibits EMT acting on Wnt/ $\beta$ -catenin signaling and recovering E-cadherin expression	<i>In vitro</i>	Chaurasiya et al., 2008; Sarkar et al., 2014
4, 16, 20	<i>Solanum nigrum</i> Linn.	<b><math>\alpha</math>-solanine</b> 	Reduces ERK and PI3K/Akt phosphorylation. Inhibits expression of MMP-2/-9, decreases vimentin, and increases E-cadherin.	<i>In vitro</i>	Shen et al., 2014

Chemical structures of the natural products included in this publication were obtained from scifinder and drawn with the program MarvinSketch.

**Baicalin and baicalein.** These molecules significantly decreased the TGF- $\beta$ 1-mediated EMT, by reducing the Slug expression and NF- $\kappa$ B signaling pathway in mammary epithelial cells. Likewise, both molecules decremented growth and cell migration capacities of human breast cancer cells (Chung et al., 2015). In the same way, *baicalin* also inhibited SMADs 2 and 3 phosphorylation and suppressed migration and invasion in pancreatic cancer cells (Zheng et al., 2016).

**Berberine.** It exhibits strong anti-cancer, anti-inflammatory, and anti-microbial effects (Tillhon et al., 2012). Kou et al. detected that berberine markedly upregulated E-cadherin and downregulated N-cadherin, fibronectin and vimentin expressions. Cadherin-bound  $\beta$ -catenin, which is required for cell adhesion, was also inhibited. The therapeutic spectrum of berberine also involved the downregulation of Snail, Slug and zinc finger E-box binding homeobox 1 (Zeb1) as well as the regulation of PI3K/Akt and retinoic acid receptor alpha and beta (RAR $\alpha$ /RAR $\beta$ ) signaling, acting on the proliferation capacity of various cancer cells (Liu et al., 2015; Kou et al., 2016).

**Betanin.** It presents powerful anti-oxidative and anti-inflammatory activities. Studies from Sutariya and Brijesh showed that betanin reduces streptozotocin (STZ) fibrosis induced in diabetic nephropathy model, by modulating EMT associated markers such as of TGF- $\beta$ , type IV collagen,  $\alpha$ -SMA and E-cadherin expression. Therefore, betanin can efficiently suppress renal fibrosis in diabetic nephropathy and may slow down the advancing to end-stage renal disease by regulating TGF- $\beta$  pathway (Sutariya and Brijesh, 2017).

**Black rice anthocyanins (BRACs).** These NPCs are extracted from the black rice, considered as a healthy food due to its effects on the liver and gastrointestinal tract (Kong et al., 2012). Anthocyanins happen to have potential beneficial effects such as antioxidant, anti-inflammatory, anti-cancerous and anti-metastatic effects (Hou, 2003; Sehitoglu et al., 2014). Zhou et al. observed that focal adhesion kinase (FAK) signaling pathway plays a function in the anti-metastatic properties of BRACs, decreasing the adhesion, migration and invasion of human HER-2-positive breast cancer cells *in vitro*. Likewise, these NPCs significantly modified the morphology of those cells from a mesenchymal to an epithelial phenotype. BRACs elevated the expression of E-cadherin and reduced the expression of fibronectin and vimentin (Zhou et al., 2017).

**Brusatol (BR).** This NPC strongly inhibits pancreatic tumor action *in vitro* (Zhao et al., 2011). Research suggests that BR could sensitize the current first-line chemotherapeutic agents to pancreatic cancer *via* inhibition of the EMT process. It has been proven that BR increased E-cadherin while decreasing vimentin protein expressions, and also reducing Twist mRNA expression (Lu et al., 2017).

**Carnosol (CAR)** is a naturally occurring phenolic diterpene located in several Mediterranean herbs and is a main component of rosemary (*Rosmarinus officinalis* L). It has been reported that the CAR anti-proliferative actions is preferentially directed towards cancer cells, as reported in both animal and *in vitro* models. Furthermore, CAR presented a favourable therapeutic option in glioblastoma cells (Johanson, 2011; Vergara et al., 2014; Giacomelli et al., 2016). CAR could interfere with the diverse

processes implicated in cancer resistance and aggressiveness, such as cancer stem cells (CSC) formation, proliferation and self-renewal. Fascinatingly, also diminished the influence of the cancer microenvironment by reducing the cytokine-induced EMT that underlies the possession of the mesenchymal phenotype. Likewise, CAR had the ability to reactivate the p53 functionality promoting CSC proliferation control and decreasing EMT was highlighted for the first time (Giacomelli et al., 2017).

It also possesses anti-cancer effects on several tumor types. It has shown to promote apoptotic cell death through p53 functional reactivation and to control the TNF- $\alpha$ /TGF- $\beta$ -induced EMT, counteracting the effects of the cytokine on EMT master regulator genes (Slug, Snail, Twist and ZEB1). It has also been demonstrated that CAR is able to modulate the activation of miR-200c, a key player in the EMT process. Finally, CAR increase the temozolomide anti-proliferative effects *in vitro* (Giacomelli et al., 2017).

**Cairicoside E (CE).** It has been published that this compound down-regulates the Aquaporin-5 (AQP5) expression and suppressed the EMT process in colon-rectal cancer cells. Research suggested that TGF- $\beta$ 1 increased the expression of AQP5 and activated the EMT by increasing the expressions of p-Smad2/3, while silence of AQP5 with CE blocked the levels of p-Smad2/3 (Chen et al., 2017a).

**Celastrol.** It is a pharmacologically active element that demonstrates significant therapeutic actions in chronic inflammatory, autoimmune, cancer, and neurodegenerative disorders (Allison et al., 2001; Dai et al., 2010; Ge et al., 2010; Venkatesha et al., 2011; Wong et al., 2012). Recently, Divya et al. suggested that celastrol decreased the N-cadherin, snail, slug, vimentin and  $\beta$ -catenin expression in a Bleomycin-induced lung fibrosis rat model. They, likewise, feature this anti-EMT effect to the inhibition of heat shock protein 90 inhibition (Divya et al., 2018). Other research established that celastrol suppresses inflammatory reactions, as well as regulates oncogenic proteins including  $\beta$ -catenin. Celastrol also decreases pro-inflammatory cytokines (TNF- $\alpha$ , IL-1 $\beta$  and IL-6) serum concentrations, down-regulates cyclooxygenase 2 (COX-2), inducible nitric oxide synthase (iNOS), N-cadherin, Vimentin and Snail expressions, inactivates NF- $\kappa$ B and upregulates E-cadherin (Lin et al., 2015).

**Celastrus orbiculatus Thunb extract (COE).** The extracts from the stems of this plant constitute 11 compounds (Li et al., 2012a). The ethyl acetate of COE constrains the proliferation, EMT (targeting VEGF, activating MAPK and inhibiting Akt signaling pathways), invasion and metastatic faculties of tumor cells (Qian et al., 2012; Zhang et al., 2012a). Moreover, COE is used in the antiinflammatory and analgesic handling of various diseases. In human gastric cancer AGS cells, it has been observed that Cofilin 1, Ncadherin, vimentin, MMP2 and MMP9 proteins expressions were significantly reduced by COE, whereas the Ecadherin expression was increased (Wang et al., 2017b).

**Cinnamomum cassia extracts (CCE).** Fifteen compounds were isolated from the bark extract of *C. cassia* growing in China (Zhao et al., 2013). These extracts were shown to diminish the TGF- $\beta$ 1-induced motility and invasive capacities of A549 and H1299 cells by inhibiting MMP-2 and urokinase-type plasminogen activator.



Moreover, they impaired cell adhesion associated with collagen production. CCE also down-regulated vimentin and fibronectin and upregulated E-cadherin expressions (Lin et al., 2017).

**Codonolactone (CLT).** It inhibited the expression of acquired EMT's mesenchymal markers such as N-cadherin and vimentin in a dose-dependent manner in *in vivo* and *in vitro* experiments in breast cancer. Likewise, it blocked the expression of transcription factors Snail, Slug, Twist-1 (TGF- $\beta$  signaling) and the Runx2 phosphorylation (Fu et al., 2016).

**Cordycepin.** Its properties have been evaluated on a human oral squamous cell carcinoma xenograft model, through its administration in a regular, low-dose upregulated E-cadherin and downregulated N-cadherin protein expressions, inhibiting EMT (Su et al., 2017).

**Cryptotanshinone (CTS).** It exhibits multiple pharmacological benefits, involving anti-cancer (Li et al., 2015; Zhu et al., 2016), anti-oxidative stress (Jin et al., 2013), and anti-cardiac fibrosis properties *via* downregulation of COX-2, NADPH oxidase 2 and 4 and MMP-2 (Ma et al., 2012; Ma et al., 2014). The antifibrotic mechanism proposed for CTS is the inhibition of Smad2 phosphorylation. Although it did not inhibit Smads 3 and 4 or mitogen-activated protein kinase (MAPK) signals, the ECM accumulation was importantly reduced in a renal fibrosis model (Wang et al., 2017c).

**Curcumin.** This NPC inhibit EMT in CoCl<sub>2</sub>-treated hepatocytes. This action might be due to its capacity to diminish TGF- $\beta$ -R1 expression in these cells. This effect suggests a disruption on the downstream signal transduction transmitted by SMADs pathway (Kong et al., 2015). Moreover, it was found that SMADs2 and 3 phosphorylation was inhibited by curcumin, pointing its powerful action blocking upstream the EMT pathway signaling. Another mechanism by which curcumin inhibits these pathways is by suppressing the cav-1 phosphorylation, stabilizing  $\beta$ -catenin (Sun et al., 2014). Recently, it has been published that curcumin inhibits the superoxide dismutase-induced invasion and migration of pancreatic cancer cells by inhibiting the PI3K/Akt/NF- $\kappa$ B signaling pathway (Li et al., 2018b). Curcumin was not related to toxicity including high dose administration, in human clinical trials (Gupta et al., 2013; Hewlings and Kalman, 2017).

**Jatrophone (JA).** This diterpene shows a broad assortment of biological actions, counting antitumoral, cytotoxic, anti-inflammatory, anti-malarial and fungicidal properties (Devappa et al., 2010). It has been demonstrated that JA reduces mRNA expression of Slug, fibronectin and vimentin, but not ZEB1, and also exhibits an anti-proliferative and anti-migratory effect acting on Wnt/ $\beta$ -catenin signaling in triple-negative breast cancer (Fatima et al., 2017).

**Duchesnea extracts.** *Duchesnea chrysantha* and *Duchesnea indica* belong to the *Rosaceae* family, and their extracts show a diversity of biological properties, involving anti-biotic, anti-oxidative, anti-inflammatory and some cytotoxic features (Kim et al., 2002b; Kim et al., 2007). These extracts involve a range of chemical compounds such as triterpenes, triterpene glycosides, flavonoid glycosides and sterols (Lee et al., 1994; Qiao et al., 2009). An *in vivo* research showed that tumor growth was importantly diminished in BALB/c nude mouse xenograft model

orally treated with *Duchesnea indica* extracts (DIE) (Chen et al., 2017c). In the same study, DIE also inhibited highly metastatic cells by reducing the secretions of MMP-2 and urokinase-type plasminogen activator (uPA) (Chen et al., 2017c). It was also able to decrease the cell adhesion capacity, down-regulate the N-cadherin, fibronectin, and vimentin and increase the E-cadherin expression (Kim et al., 2002b; Kim et al., 2007; Chen et al., 2017c). Another protective mechanism related with DIE is its antioxidant action which can also modulate the EMT (Hu et al., 2009; Hu et al., 2011).

**Epicatechin-3-gallate (ECG).** It elicits several anti-oxidant and anti-inflammatory activities and is one of the four types of catechins mainly detected in green tea, together with epicatechin, epigallocatechin and epigallocatechin-3-gallate (EGCG) (Chowdhury et al., 2016). In human lung cancer cells, ECG also reverts the TGF- $\beta$ 1-induced EMT by upregulating epithelial markers (E-cadherin) and downregulating mesenchymal markers (fibronectin). Moreover, it also phosphorylates FAK. Based on these facts, it has been recommended that ECG may be administered as an effective agent against TGF- $\beta$ 1-induced EMT (Huang et al., 2016).

**Eupatolide.** It shows anti-inflammatory, anti-proliferative and anti-migratory effects (Lee et al., 2010a; Kim et al., 2013). It has also been suggested that eupatolide might be employed as an inhibitor of the TGF- $\beta$ 1 signaling pathway to suppress EMT (Wrighton et al., 2009). Moreover, eupatolide suppress TGF- $\beta$ 1-induced EMT *via* downregulation of Smad3 phosphorylation and decreasing the TGF- $\beta$  type 1 receptor (Boldbaatar et al., 2017).

**Gallic acid.** *In vivo* experiments with this NPC diminished vascular calcification, cardiac hypertrophy, cardiac fibrosis and hypertension. Gallic acid also inhibited pathological changes in the lungs, such as pulmonary fibrosis (Kee et al., 2014; Ryu et al., 2016). Moreover, it reduced the expression of fibrosis-related genes, including collagen types I and III, fibronectin, connective tissue growth factor (CTGF), and Smad3. In a mouse model, Garlic acid blocked the of EMT-related genes expression, such as N-cadherin, vimentin, Snail, and TWIST1 (Jin et al., 2017).

**Gambogic acid (GA).** It has been proved *in vitro* that this compound reverses TGF- $\beta$ 1-mediated EMT and endothelial-mesenchymal transition (EndoMT) in human lung fibroblasts (HLF-1). It also prevents pulmonary fibrosis *in vivo* and attenuates the EMT by modulating the TGF $\beta$ 1/Smad3 pathway (Qu et al., 2016).

**Gedunin.** It has been shown to have potential anti-cancer activity (Kamath et al., 2009; Patwardhan et al., 2013; Hao et al., 2014). Recent research suggests that gedunin inhibits EMT by reducing the expression of the mesenchymal markers N-Cadherin, Slug, Snail, Vimentin, Notch 1 and 2, and Zeb whereas increasing the E-cadherin expression (Subramani et al., 2017).

**Genistein (GEN).** Soybeans and most soy products contain large amounts of isoflavones called soy phytoestrogens, and one of the most concentrated is the GEN (Lee et al., 2012). GEN is a phytoestrogen known for its chemopreventive effects in several types of cancers (Kim et al., 2015). It suppresses the EMT response induced by 17 $\beta$ -estradiol and two estrogens-like compounds,

bisphenol-A and nonylphenol. Thus, it reduces the protein expressions of vimentin, cathepsin D, and MMP-2, increases E-cadherin expression and downregulates TGF- $\beta$ . (Kim et al., 2015). In ovarian cancer derived cells, GEN inhibits the NF- $\kappa$ B and Akt signaling pathways, playing important roles in keeping the homeostatic balance between cell survival and apoptosis. It has been considered as a potential antiangiogenic, antioxidant and anticancer agent (Han et al., 2012; Dai et al., 2015).

**Gentiopicroside (GPS).** It has been proved that in bronchoalveolar cells isolated from fluids of lungs pulmonary fibrosis in a mouse model, GPS decreased the levels of proinflammatory cytokines, including TNF- $\alpha$  and IL-1 $\beta$ , and downregulated TGF- $\beta$ 1 and CTGF expression. *In vitro*, GPS inhibited the EMT of A549 cells stimulated by TGF- $\beta$ 1 to induce transdifferentiation at a dose-dependent manner (Chen et al., 2017b).

**Gigantol.** It has been described to have anti-proliferative, anti-apoptosis and anti-metastatic properties (Charoenrungruang et al., 2014; Klongkumnuankarn et al., 2015). Recent publications suggest that gigantol considerably reduces lung cancer cells' viability in a detached condition. It also shrinkages EMT biomarkers including N-cadherin, vimentin and Slug, leading to a meaningful suppression of AKT, ERK, and cav-1 survival pathways (Unahabhokha et al., 2016).

**Ginsenoside.** It has been registered in pharmacopeias for thousands of years due to its abundant content of saponins. One of the most extensively known saponins in the rhizome of ginseng is ginsenoside-Rb1 (Jia and Zhao 2009). *In vivo* studies mention that Rb1 showed cardioprotective, hepatoprotective and anti-inflammatory effects (Wang et al., 2008; Li et al., 2012b; Cheng et al., 2013; Hou et al., 2014). Likewise, it inhibits cell proliferation, angiogenesis and apoptosis stimulation (Zheng et al., 2013; Lee et al., 2016). A recent publication shows that ginsenoside-Rb1, especially its metabolite compound K, particularly sensitize cancer stem/tumor-initiating cells from ovarian cancer to chemotherapy through the inhibition of Wnt/ $\beta$ -catenin signaling and EMT (Deng et al., 2017).

**Honokiol (HNK).** It has been associated with anti-tumor and more recently anti-EMT effects (Fujita et al., 1973; Lee et al., 2005; Ahn et al., 2006; Sheu et al., 2008; Arora et al., 2011; Arora et al., 2012; Nagalingam et al., 2012). For instance, in breast cancer cells, Avtanski et al. demonstrated that HNK inhibited signal transducer and activator of transcription 3 (Stat3) phosphorylation and transactivation activity and Zeb1 expression, which plays a main role in EMT initiation. More than that, HNK induces an increase in E-cadherin (Avtanski et al., 2014). Additionally, it has been published that HNK inhibits EMT motility and migration by targeting cellular FLICE (FADD-like, IL-1 $\beta$ -converting enzyme)-inhibitory protein (c-FLIP), considered a master anti-apoptotic regulator in non-small-cell lung cancer (Lv et al., 2016).

**Isoviolanthin** extracted from the leaves of *Dendrobium officinale* inhibits transforming growth factor (TGF)- $\beta$ 1-induced EMT in hepatocellular carcinoma (HCC) cells, it is the most significant constituents responsible for the antimetastasis activity of *Dendrobium officinale*. Recent publications report that isoviolanthin targets the TGF- $\beta$ /Smad and PI3K/Akt/mTOR

pathways to repress TGF- $\beta$ 1-induced EMT phenotypes in HepG2 and Bel-7402 HCC cells. Furthermore, these results confirm that isoviolanthin could be a favorable natural compound with low toxicity for the treatment of metastatic HCC by affecting TGF- $\beta$ 1-induced EMT (Xing et al., 2018).

**Ligustrazine (LIG).** In a model of renal tubulointerstitial fibrosis, LIG showed pleiotropic effects acting at different levels of EMT induction. LIG decreased the mRNA expression of TGF- $\beta$ 1, CTGF, monocyte chemoattractant protein-1 (MCP-1) and osteopontin, and, subsequently cytokeratin-18 expression decreased. Mainly, this molecule increased the expression of the natural inhibitors of TGF- $\beta$ , hepatocyte growth factor (HGF) and bone morphogenetic protein (BMP)-7 (Yuan et al., 2012).

**Luteolin.** Many biological properties of luteolin, such as anti-inflammation, anti-allergy, antioxidant, anticancer and anti-microbial effects have been described (Chung et al., 2001; Chen et al., 2007; Lin et al., 2008). In breast cancer (*in vivo* and *in vitro*), epithelial markers such as E-cadherin and claudin were upregulated in response to luteolin while mesenchymal markers N-cadherin, vimentin, Snail and Slug were downregulated at dose-dependent manner. Researchers found that these positive effects of luteolin were extinguished by overexpression of  $\beta$ -catenin, indicating that downregulation of  $\beta$ -catenin expression may mediate the inhibitory effects of luteolin on EMT (Lin et al., 2017). Same results were found by Zang et al., who described that other pathways such as Notch1 were also blocked by Luteolin (Zang et al., 2017).

**Nimbolide.** Recent studies indicate that treatment with this agent reduces the expression of Notch-2, N-cadherin, vimentin and transcription factors (Snail, Slug and Zeb) in pancreatic cancer cell lines. Moreover, nimbolide treatment likewise increased the expression of E-cadherin. Additionally, the generation of ROS mediated by nimbolide reduces cell proliferation (via reduction of PI3K/AKT/mTOR and ERK signaling) and metastasis (via reduction of EMT, invasion, migration and colony forming abilities) through mitochondrial-mediated apoptosis but not through autophagy (Bodduluru et al., 2014; Hao et al., 2014; Subramani et al., 2016).

**Nitidine chloride (NC).** It has been shown to exert antimalarial (Bouquet et al., 2012), anti-inflammatory (Wang et al., 2012), anti-angiogenic (Chen et al., 2012), and anticancer effects (Fang et al., 2013). Likewise, NC inhibited the cellular migration and invasion through suppression of FAK-associated pathway in breast cancer metastasis (Sun et al., 2014). It has also been recently proposed that inactivation of Hedgehog signaling pathway by NC led to significantly decreased Smo and Gli expressions, targeting breast cancer metastasis. Thus, NC could be suitable for the prevention and treatment of breast cancer through dual-blocking EMT (Sun et al., 2016).

**Osthole.** It inhibits growth and metastasis in many types of cancer (Kao et al., 2012; Zhang et al., 2012b; Ding et al., 2014). It has also been proposed that osthole mediated the EMT by downregulating Snail and cell-invasive capability, suppressing the TGF- $\beta$ /Akt/MAPK pathway (Wen et al., 2015).

**Oxymatrine (OM).** Many studies have proved that OM shows an anti-fibrotic effect on liver, pulmonary, myocardial and skin scar tissue fibrosis through inhibition of the TGF- $\beta$ 1/

Smad signaling cascade (Shi and Li, 2005; Chen et al., 2008; Wu et al., 2008; Shen et al., 2011; Fan et al., 2012; Liu et al., 2012). Thus, Liu *et al.* demonstrated that OM inhibits the high glucose-induced renal tubular EMT, decreasing the degradation of SnoN mediated by a E3 ubiquitin ligase (Arkadia), and that promotes EMT amplifying TGF- $\beta$  signalling through Smad7 degradation (Liu et al., 2016).

**Paeoniflorin (PF).** Pharmacological reports have shown that it prevents pulmonary EMT inhibiting collagen type-I synthesis, downregulating Snail and Slug and up-regulating Smad7. These properties provide PF a protective action against cellular transdifferentiation in a lung bleomycin-induced fibrosis model in mice (Ji et al., 2016). It has also been demonstrated that PF down-regulates TGF- $\beta$ 1, maintains BMP-7 expression and inhibits Smad2/3 in a renal fibrosis model (Zeng et al., 2013). Likewise, PF blocks EMT in glioblastoma cells, and reduces TGF- $\beta$ , Snail, N-cadherin, Vimentin and MMP2/9 expression at doses depended manner (Wang et al., 2018).

**Paeonol.** It is an aspirin analogue extracted from numerous medicinal herbs including *Moutan Cortex*, *Cynanchi paniculati Radix et rhizome*, and *Paeoniae Radix rubra*. Paeonol was discovered to present comprehensive pharmacological activities, such as antioxidant, anti-inflammatory, anti-aging, and anti-cancer activities (Chou, 2003; Zhang et al., 2015). Another author reported that paeonol influenced antioxidative stress activity in endothelial cells by controlling the expressions of Sirt1. It has been described, too, that paeonol ameliorated colitis related colorectal cancer by suppressing cytokine-induced EMT and NF- $\kappa$ B activation (Lin et al., 2014). Likewise, suggested that paeonol inactivated ERK and TGF-beta1/Smad pathway leading to regulation of relevant EMT markers. These results suggest that paeonol might be developed as a potential agent used for oxidative stress injury and EMT in premalignant lesion (Yang et al., 2018).

**Parthenolide (PTL).** It has been conventionally used for the treatment of headaches and arthritis. Recent analyses suggest that PTL is a valuable antitumor and anti-inflammatory NPC, and it was evaluated in clinical studies for leukemia and neurological tumors (Ghantous et al., 2013). These effects of PTL in tumors and inflammatory diseases primarily happen *via* the inhibition of NF- $\kappa$ B signaling pathways (Hehner et al., 1999). Current studies have established that PTL inhibit pulmonary fibrosis increasing E-Cadherin and decreasing vimentin NF- $\kappa$ B and Snail expression in TGF- $\beta$ 1-treated primary lung epithelial cells (Li et al., 2018a).

**Plectranthoic acid (PA).** It induces cell cycle arrest and apoptosis in prostate cancer cells (Akhtar et al., 2016). Recent research demonstrates that PA-exposed cells exert considerably reduced cell migration capacity and a reversal of TGF- $\beta$  induced EMT, representing the potential effectiveness of PA against prostate cancer, throughout regulation of Rac1 signaling (Akhtar et al., 2018).

**Phoyunnanin-E.** Recent publications suggest that Phoyunnanin E decreased the E-cadherin to N-cadherin switch and reduced upregulation of mesenchymal markers such as vimentin and snail, as well as slug expression. Phoyunnanin-E has also been shown to inhibit migration and growth and promote EMT suppression, reduce migratory-associated integrins  $\alpha$ v and  $\beta$ 3, and suppress

FAK/AKT cascade, which subsequently suppressed downstream migratory proteins in lung cancer cells (Petpiroon et al., 2017).

**Piperlongumine (PL).** It has been identified as a powerful cytotoxic element highly selective to cancer cells (Raj et al., 2011; Bezerra et al., 2013; Liu et al., 2014; Zheng et al., 2016; Zhou et al., 2016). PL has also been demonstrated to accurately suppress bladder cancer development both *in vitro* and *in vivo*, *via* inhibition of EMT. Thereby, the expression of EMT-associated factors such as Slug,  $\beta$ -catenin, zeb1, N-Cadherin, Claudin-1, and zonula occludens-1 (ZO-1) were importantly decreased (Liu et al., 2017).

**Plumbagin (PLB).** It presents anti-inflammatory, anti-atherosclerotic, anti-bacterial, anti-fungal, and anti-cancer properties shown both *in vitro* and *in vivo* (Padhye et al., 2012). The anti-EMT effect of the PLB can be vinculated by its ability to adjust epithelial adherent junctions in human tongue squamous carcinoma cells. PLB also boosted the expression of E-cadherin and decreased of N-cadherin in these cells. Moreover, it reduced the expression of Snail, Slug, TCF-8/zeb1,  $\beta$ -catenin, and vimentin, whereas increased the expression of claudin-1 and ZO-1. Notably, PLB inhibited the translocation of nuclear factor erythroid 2-related factor (Nrf2) from cytosol to nucleus, causing an inhibition in the expression of downstream targets (Pan et al., 2015).

**Polyphyllin (PP) I.** It has been broadly investigated for its anti-inflammatory and anti-cancer activities. PPI exhibited inhibitory effect on various cancer types, involving hepatocarcinoma (Ong et al., 2008), non-small cell lung cancer (Kong et al., 2010), osteosarcoma (Chang et al., 2015), chronic myeloid leukemia (Wu et al., 2014), ovarian cancer (Gu et al., 2016) and glioma cells (Yu et al., 2014). Recent investigation described that PPI was capable to reverse EMT in osteosarcoma cells (Chang et al., 2015). Likewise, ZH-2, a compound derived from PP VII, exerts anti-chemoresistance properties through inhibiting EMT (He et al., 2016). In anacquired-erlotinib-resistant cell line, PPI inhibited IL-6/STAT3 signaling pathways and stimulates epithelial marker expression, reversing EMT. Significantly, PPI exhibited an inhibitory effect on epidermal growth factor (EGF) receptor tyrosine kinase inhibitors, which has a mutagenic and pro-EMT action in non-small cell lung cancer (Lou et al., 2017).

**Resveratrol (RSV).** RSV has been published to have many pharmacological activities, such as protection against coronary heart disease, anti-inflammatory properties, chemo-prevention of cancer, anti-oxidative and antiasthmatic effects (Frémont, 2000; Wallerath et al., 2002; Aggarwal et al., 2004; Bisht et al., 2010). It can be obtained from grapes, wine, mulberries and peanuts (Shakibaei et al., 2009). It also reduced renal injury and renal fibrosis by suppressing the inflammatory activity and by inhibiting lipid peroxidation (Chander and Chopra, 2005; De Jesus et al., 2007). The inhibitory effect of RSV on EMT has been demonstrated in prostate (Li et al., 2014), ovarian (Baribeau et al., 2014), breast (Tsai et al., 2013) and pancreatic cancer (Li et al., 2013). Recent papers show that RSV inhibits EMT in renal tubular cells by antagonizing the hedgehog signaling pathway (Bai et al., 2014b). Likewise, Gao *et al.* suggested that RSV prevents from cancer cell invasion and metastasis *in vitro* by inhibiting the hedgehog pathway and EMT (Gao et al., 2015). In this context, RSV downregulates the EMT-inducing transcription factor (including Zeb-1, Slug and Snail) to reduce migration and invasion in pancreatic cancer cells (Shankar



et al., 2011). EGF is a well-known EMT-inducer in human breast cancer cells (Ackland et al., 2003; Vergara et al., 2011). RSV blocks EGF-induced EMT by repressing EGF-induced ERK (Vergara et al., 2011). Furthermore, it is known that renal injury has a close relationship with the development of renal fibrosis and, during this process, tubular epithelial cells in the kidney undergo EMT *via* upregulating  $\beta$ -catenin/lymphoid enhancer-binding factor 1 (LEF1) signaling and MMP-7 (Liu, 2004; Shibata et al., 2009). A current study using RSV showed that this product attenuated renal injury and fibrosis through inhibition of EMT. Authors suggested that this inhibition was due to the fact that RSV up-regulated sirtuin 1 (SIRT1), which deacetylated Smad4 and inhibited the expression of MMP-7 (Xiao et al., 2016). Other findings also demonstrate that RSV modulates EMT by suppressing MMP-2 and MMP-9 *via* MAPK and NF- $\kappa$ B signals in lung cancer invasion and metastatic cells (Yang et al., 2009; Liu et al., 2010a). Moreover, RSV has been recently shown to limit EMT by controlling gene expression at post-transcriptional level (it favors the epithelial-type alternative splicing of pre-mRNAs that encode crucial factors in adhesion and migration, and enhances the expression of some RNA-Binding Proteins) (Moshiri et al., 2017). It also inhibits TGF- $\beta$ 1-induced EMT and suppresses lung cancer invasion and metastasis (Wang et al., 2013).

**Salvianolic acid A (SAA).** It exerts many pharmacological actions, such as myocardial protection, anti-thrombosis, anti-fibrosis, and the prevention of diabetes complications (Ho and Hong, 2011; Xu et al., 2014). Investigations have revealed that SAA treatment effectively decreased lung parenchymal injury and collagen deposition and diminished the apoptosis and lung fibrosis on a pulmonary arterial hypertension rat model. Furthermore, in pulmonary tissue, SAA treatment upregulated BMP type II receptor (BMPRII) expression and augmented the Smad1/5 phosphorylation. Both molecules showed an anti-EMT effect (Chen et al., 2016a). An anti-EndoMT capacity was also discovered in bleomycin-induced pulmonary fibrosis in mice, acting on Nrf2/HO-1 signaling pathway (Chen et al., 2017d).

**Sedum sarmentosum Bunge (SSBE).** Pharmacological reports have shown that SSBE has significant antiinflammatory, anti-tumor and anti-angiogenic effects (Oh et al., 2004; Morikawa et al., 2007; Ninomiya et al., 2007; Jung et al., 2008). Other authors demonstrated that SSBE has marked effects against renal fibrosis (Bai et al., 2014a; Bai et al., 2014b), down-regulating hedgehog signaling pathway (which promotes renal fibrogenesis fostering the formation of myofibroblasts from different cell types through an EMT process). SSBE also reduced the ECM accumulation and angiogenesis (Bai et al., 2017).

**Sulforaphane.** Numerous studies have observed the effects of *sulforaphane* in control of tumor generation or cancer progression, such as in lung, breast and prostate (Amjad et al., 2015; Atwell et al., 2015; Jiang et al., 2016), and also digestive system neoplasms (Jeon et al., 2011; Kim et al., 2015). Other authors demonstrated that reduced expression of the micro RNA miR-616-5p, transcriptionally induced by sulforaphane management, contributes to the suppression of EMT in non-small cell lung cancer and in lung cancer metastasis through the miR-616-5p/GSK3 $\beta$ / $\beta$ -catenin signaling pathway (Wang et al., 2017a).

**Tannic acid (TA).** This molecule acts upstairs in the EMT induction process, in lung epithelial cells. It reduces the expression of TGF- $\beta$  and N-cadherin and decreases the SMADs 2 and 3 phosphorylation and the production of ECM (fibronectin and vimentin). Moreover, cell proliferation in G0/G1 phase and the mitogenic activity of protein kinase (ERK1/2, JNK1/2, and p38) also decrease (Pattarayan et al., 2018).

**Withaferin-A (WA).** Pharmacological reports have shown anti-cancer effects in rodent experiments (Padmavathi et al., 2005; Garodia et al., 2007; Widodo et al., 2007). Withanolide-D (witha-D) is an active element of WA that partially inhibits EMT acting on Wnt/ $\beta$ -catenin signaling and recovering E-Cadherin expression in a human pancreatic tumour cell line (Chaurasiya et al., 2008; Sarkar et al., 2014).

**Alpha-Solanine.** This NPC presents pharmacological activities involving anti-proliferation, anti-apoptosis and anti-angiogenesis (Mohsenikia et al., 2013). Alpha-solanine also reduced ERK and PI3K/Akt phosphorylation. Likewise, this component also reduces the expression of MMP-2/9 and vimentin and induces the expression of E-cadherin (Shen et al., 2014).

## Potential Therapeutic Effects of Natural Plants Compounds

Currently, there is growing evidence for potential plant-derived compounds as inhibitors in several stages of tumorigenesis and inflammatory and fibrosis processes. In several clinical trials it has been demonstrated that NPCs have elicited anti-aging, anti-cancer and other health-enhancing effects. A key target of the effects of NPCs may be in suppressing oxidative stress and the induction of 5'AMP-activated Kinase (AMPK), or suppression of the WNT/ $\beta$ -catenin, PI3K/Akt/mTOR and RAS/MEK/ERK signaling pathways, among others, which results in cell death or prevents aging, diabetes, cardiovascular, cancer and other diseases (McCubrey et al., 2017).

One NPC is Berberine, which has been tested in a wide spectrum of clinical applications. Oral administration of berberine significantly reduced the familial adenomatous polyposis patients' polyp size along with the inhibition of cyclin D1 expression in polyp samples. These statements suggest that berberine inhibits colon tumour formation through inhibition of Wnt/ $\beta$ -catenin signalling and might be a favorable drug for the prevention of colon cancer (Zhang et al., 2013; Farooqi et al., 2019). Additionally, it has been described that Berberine shows an extensive array of pharmacological effects, being effective against gastroenteritis, abdominal pain and diarrhea, and having antimicrobial, antidiabetic and antiinflammatory properties (Imanshahidi and Hosseinzadeh, 2008; Kulkarni and Dhir, 2010; Vuddanda et al., 2010). Another beneficial effect of berberine has been reported on the treatment of type II diabetes (Yin et al., 2008). This natural compound has an explicit potential as a drug in a wide spectrum of already defined clinical purposes (Tillhon et al., 2012). Numerous pharmacological reports have suggested the cardiovascular effects of berberine and *B. vulgaris*, such as preventing ischemia induced ventricular tachyarrhythmia, improving cardiac contractility and lowering peripheral vascular resistance and blood pressure (Marin-Neto et al., 1988).



Likewise, RSV is being examined in many clinical trials, on age-related disease, cancer, cardiovascular problems, chronic renal insufficiency and other disorders (Boocock et al., 2007; Brown et al., 2010; la Porte et al., 2010; Howells et al., 2011; Popat et al., 2013).

Clinical trials show that RSV has been shown to activate sirtuins and such activation is able to explain most of the beneficial properties of the mediterranean diet (MD). While observational studies and meta-analysis have demonstrated an antiageing effect of MD accompanied by a reduced risk of age-related pathologies, such as cardiovascular, metabolic and neurodegenerative diseases, as well as cancer (Russo et al., 2014; Gliemann et al., 2016).

Other studies that involved healthy volunteers established that RSV synchronized the carcinogen metabolizing enzyme cytochrome P450 and phase II detoxification enzymes, which repressed carcinogen metabolism and subsequently prevented carcinogenesis (Chow et al., 2010).

In the same way, Curcumin is being evaluated in numerous clinical trials for various disorders such as acute kidney injury, neurodegenerative diseases, cancer cardiovascular abnormalities, psychiatric disorders, osteoarthritis, type 2 diabetes mellitus, ulcerative colitis, rheumatoid arthritis, lupus nephritis, multiple sclerosis and other health problems (Allegra et al., 2017; White and Lee, 2019; Yang et al., 2019). Its efficacy appears to be related to the induction of glutathione S-transferase enzymes, inhibition of prostaglandin E2 (PGE2) production, or the suppression of oxidative DNA adduct formation. Oral curcumin was administered to patients with advanced colorectal cancer refractory to standard chemotherapies to explore its pharmacodynamics in humans (Sharma et al., 2004). In this study, the authors concluded that administration of 0.5 to 3.6 g/day for up to 4 months is associated with mild diarrhea as its only toxicity, and that a dosis of 3.6 g/day generates detectable levels of parent compound and conjugates in plasma and urine, causing inhibition of PGE2 production in blood leukocytes measured *ex vivo*. They proposed that an oral dose of 3.6 g/day is suitable for evaluation in Phase II trials (Sharma et al., 2004). In fact, curcumin has been found to be safe when administered at doses up to 10 g/day. All of these studies suggest that curcumin has enormous potential in the prevention and therapy of cancer (Aggarwal et al., 2003). Another study showed that curcumin is not toxic to humans up to 8 g/day when taken orally for 3 months (Cheng et al., 2001).

Likewise, epigallocatechin-3-gallate (EGCG) have been studied in a wide range of illnesses related to excessive oxidative stress, involving cancers, cardiovascular diseases, metabolic syndromes, diabetes, cerebral ischemic stroke, lung diseases, and neurodegenerative disorders (Chowdhury et al., 2016). Recently, EGCG has been studied for management and prevention of various kidney diseases, which are usually associated with oxidative stress and inflammation (Bao and Peng, 2016; Kanlaya and Thongboonkerd, 2019).

Meanwhile, baicalin decreases blood lipids and inflammation in patients with coronary artery disease and rheumatoid arthritis, supporting its further clinical application (Hang et al., 2018). This NPC exhibits high clinical value, having anti-inflammatory, anti-arrhythmic and anti-hypertensive effects (Huang et al., 2005; Huang et al., 2006; Dinda et al., 2017).

The therapeutic usefulness and anti-inflammatory properties of celastrol have been studied in numerous inflammatory diseases,

involving rheumatoid arthritis, ankylosing spondylitis, systemic lupus erythematosus, inflammatory bowel disease, osteoarthritis, allergies, and skin inflammation (Cascão et al., 2017). Celastrol exhibits beneficial effects decreasing cardiovascular symptoms involving hypertension. Researchers investigated the treatment outcome against preeclampsia with a combined use of celastrol and nifedipine in clinical trials. A total of 626 patients with preeclampsia were enrolled, screened, and assigned randomly to groups receiving either nifedipine + placebo or nifedipine + celastrol orally. This study provides evidence for the potential role of celastrol serving as an effective and safe adjuvant to oral nifedipine against hypertension in patients with preeclampsia (Xiao et al., 2017). The therapeutic effects such as the anti-inflammatory, anticancer, and neuroprotective properties of celastrol can be mainly attributed to its capacity to inhibit NF- $\kappa$ B, a central player in inflammation, cancer and neurodegenerative diseases (Cascão et al., 2017).

Clinical investigation shows that gallic acid (GA) inhibits oxidative stress in diabetic patients. A small amount of GA prevents oxidative DNA injury and decreases markers which reflect inflammation and augmented risks of cancer and cardiovascular diseases (Ferk et al., 2018).

Clinical reports in asthma patients show that Genistein exerts antioxidant effects and could inhibit the pathway of NF- $\kappa$ B and TNF- $\alpha$  in these patients (Liu et al., 2010b).

It has been reported that Ginsenoside Rb1 (GS-Rb1) treatment was efficient in decreasing the extent of oxidative stress and inflammation in chronic kidney disease, whereas persistent deterioration was observed in the placebo group. Thus, extended treatments using GS-Rb1 may represent an interesting approach to slow the development of this disease at early stages (Xu et al., 2017).

## Limitations

Although NPCs are promising therapeutic agents, they need *in vivo* studies (animal models) mainly analyzing the specificity of their therapeutic action as well as toxic, mutagenic or side effects. Scientists must identify the components of each extract as well as the therapeutically active molecule/s. Moreover, previous prospective clinical trials are mandatory to recommend their use in clinical practice.

## CONCLUSION

EMT is a physiological and self-regulated process of tissue repair. However, pathologic EMT is characterized by its irreversibility and loss of self-regulation being a pathogenic part of many diseases. Thus, EMT is a therapeutic target with no established treatment yet. Natural products appear as therapeutic alternatives that need deep studies to be used in humans. Synergy and antagonism with other agents and interactions with prescription drugs should be studied in order to develop clinical trials.

The use of natural plant compounds versus standard drugs offers therapeutic advantages, such as the potential lower price and ease of being obtained, as they do not need to be artificially synthesized. Moreover, some of them are usually employed in the diet, like curcumin, although other routes of administration should be analyzed to calculate potential doses. Moreover, although many new drugs are made by synthetic chemistry and novel approaches

to drug discovery such as combinatorial chemistry and computer-based design have been developed, they cannot replace the role of plant compounds in drug discovery, serving as chemical templates for the design and synthesis of new therapeutical drugs.

The relevance of this study lies on the necessity of finding effective therapies against EMT, which is a process involved in many diseases.

## AUTHOR CONTRIBUTIONS

All the authors contributed to and approved the final manuscript.

## ACKNOWLEDGMENTS

This work was supported by grant SAF2013-47611R from the Ministerio de Economía y Competitividad and by grant S2010/

BMD-2321 (FIBROTEAM Consortium) from Comunidad Autónoma de Madrid to ML-C from Fondo de Investigaciones Sanitarias (FIS) and European Regional Development fund (FEDER), PI 15/00598 Instituto Carlos-III to AA. REDinREN is a group in which Spanish authors are involved, contributing to development of PD.

Thanks to the Academic Unit of Human Medicine and the Area of Health Sciences of the Autonomous University of Zacatecas, for their support in the Academic Stay in the Molecular Biology Unit at the University Hospital La Princesa, Madrid, Spain. We want to thank Cristobal de los Rios, Associate Researcher from Institute-Foundation Teófilo Hernando, Pharmacology and Therapeutics Department, Autonomous University of Madrid and Institute of Health Research from Hospital la Princesa, (Madrid, Spain), for providing us the chemical structures of the natural products included in this publication.

## REFERENCES

- Ackland, M. L., Newgreen, D. F., Fridman, M., Waltham, M. C., Arvanitis, A., Minichiello, J., et al. (2003). Epidermal growth factor-induced epitheliomesenchymal transition in human breast carcinoma cells. *Lab. Invest.* 83, 435–448. doi: 10.1097/01.LAB.0000059927.97515.FD
- Aggarwal, B. B., Bhardwaj, A., Aggarwal, R. S., Seeram, N. P., Shishodia, S., and Takada, Y. (2004). Role of resveratrol in prevention and therapy of cancer: preclinical and clinical studies. *Anticancer Res.* 24 (5A), 2783–2840.
- Aggarwal, B. B., Kumar, A., and Bharti A. C. (2003). Anticancer potential of curcumin: preclinical and clinical studies. *Anticancer Res.* 23 (1A), 363–98.
- Aguilera, A., Yáñez-Mo, M., Selgas, R., Sánchez-Madrid, F., and López-Cabrera, M. (2005). Epithelial to mesenchymal transition as a triggering factor of peritoneal membrane fibrosis and angiogenesis in peritoneal dialysis patients. *Curr. Opin. Invest. Drugs* 6 (3), 262–268.
- Ahn, K. S., Sethi, G., Shishodia, S., Sung, B., Arbiser, J. L., and Aggarwal, B. B. (2006). Honokiol potentiates apoptosis, suppresses osteoclastogenesis, and inhibits invasion through modulation of nuclear factor-kappaB activation pathway. *Mol. Cancer Res. MCR* 4, 621–633. doi: 10.1158/1541-7786.MCR-06-0076
- Akhtar, N., Syed, D. N., Khan, M. I., Adhami, V. M., Mirza, B., and Mukhtar, H. (2016). The pentacyclic triterpenoid, plectranthoic acid, a novel activator of AMPK induces apoptotic death in prostate cancer cells. *Oncotarget* 7, 3819. doi: 10.18632/oncotarget.6625
- Akhtar, N., Syed, D. N., Lall, R. K., Mirza, B., and Mukhtar, H. (2018). Targeting epithelial to mesenchymal transition in prostate cancer by a novel compound, plectranthoic acid, isolated from *Ficus microcarpa*. *Mol. Carcinog.* 57, 653–663. doi: 10.1002/mc.22790
- Allegra, A., Innaro, V., Russo, S., Gerace, D., Alonci, A., and Musolino, C. (2017). Anticancer activity of curcumin and its analogues: preclinical and clinical studies. *Cancer Invest.* 35 (1), 1–22. doi: 10.1080/07357907.2016.1247166
- Allison, A. C., Cacabelos, R., Lombardi, V. R., Alvarez, X. A., and Vigo, C. (2001). Celastrol, a potent antioxidant and anti-inflammatory drug, as a possible treatment for Alzheimer's disease. *Prog. Neuropsychopharmacol. Biol. Psychiatry* 25 (7), 1341–1357. doi: 10.1016/S0278-5846(01)00192-0
- Amjad, A. I., Parikh, R. A., Appleman, L. J., Hahm, E. R., Singh, K., and Singh, S. V. (2015). Broccoli-derived sulforaphane and chemoprevention of prostate cancer: from bench to bedside. *Curr. Pharmacol. Rep.* 1, 382–390. doi: 10.1007/s40495-015-0034-x
- Arora, S., Bhardwaj, A., Srivastava, S. K., Singh, S., McClellan, S., Wang, B., et al. (2011). Honokiol arrests cell cycle, induces apoptosis, and potentiates the cytotoxic effect of gemcitabine in human pancreatic cancer cells. *PLoS One* 6, e21573. doi: 10.1371/journal.pone.0021573
- Arora, S., Singh, S., Piazza, G. A., Contreras, C. M., Panyam, J., and Singh, A. P. (2012). Honokiol: a novel natural agent for cancer prevention and therapy. *Curr. Mol. Med.* 12, 1244–1252. doi: 10.2174/156652412803833508
- Atwell, L. L., Beaver, L. M., Shannon, J., Williams, D. E., Dashwood, R. H., and Ho, E. (2015). Epigenetic regulation by sulforaphane: opportunities for breast and prostate cancer chemoprevention. *Curr. Pharmacol. Rep.* 1 (2), 102–111. doi: 10.1007/s40495-014-0002-x
- Avtanski, D. B., Nagalingam, A., Bonner, M. Y., Arbiser, J. L., Saxena, N. K., and Sharma, D. (2014). Honokiol inhibits epithelial–mesenchymal transition in breast cancer cells by targeting signal transducer and activator of transcription 3/Zeb1/E-cadherin axis. *Mol. Oncol.* 8 (3), 565–580. doi: 10.1016/j.molonc.2014.01.004
- Bai, Y., Lu, H., Hu, L., Hong, D., Ding L and Chen, B. (2014a). Effect of sedum sarmentosum BUNGE extract on aristolochic acid-induced renal tubular epithelial cell injury. *J. Pharmacol. Sci.* 124, 445–456. doi: 10.1254/jphs.13216FP
- Bai, Y., Lu, H., Wu, C. Z., Liang, Y., Wang, S. L., Lin, C. C., et al. (2014b). Resveratrol inhibits epithelial-mesenchymal transition and renal fibrosis by antagonizing the hedgehog signaling pathway. *Biochem. Pharmacol.* 92, 484–493. doi: 10.1016/j.bcp.2014.09.002
- Bai, Y., Wu, C., Hong, W., Zhang, X., Liu, L., and Chen, B. (2017). Anti-fibrotic effect of Sedum sarmentosum Bunge extract in kidneys via the hedgehog signaling pathway. *Mol. Med. Rep.* 16 (1), 737–745. doi: 10.3892/mmr.2017.6628
- Bao, H., and Peng, A. (2016). The green tea polyphenol (-)-epigallocatechin-3-gallate and its beneficial roles in chronic kidney disease. *J. Transl. Int. Med.* 4, 99–103. doi: 10.1515/jtim-2016-0031
- Barberà, M. J., Puig, I., Domínguez, D., Julien-Grille, S., Guaita-Esteruelas, S., Peiró, S., et al. (2004). Regulation of snail transcription during epithelial to mesenchymal transition of tumor cells. *Oncogene* 23 (44), 7345–7354. doi: 10.1038/sj.onc.1207990
- Baribeau, S., Chaudhry, P., Parent, S., and Asselin, E. (2014). Resveratrol inhibits cisplatin-induced epithelial-to-mesenchymal transition in ovarian cancer cell lines. *PLoS One* 9, e86987. doi: 10.1371/journal.pone.0086987
- Bezerra, D. P., Pessoa, C., de Moraes, M. O., Saker-Neto, N., Silveira, E. R., and Costa-Lotufo, L. V. (2013). Overview of the therapeutic potential of piperlongumine (piperlongumine). *Eur. J. Pharm. Sci.* 48 (3), 453–463. doi: 10.1016/j.ejps.2012.12.003
- Bhadra, K., and Kumar, G. S. (2011). Therapeutic potential of nucleic acid-binding isoquinoline alkaloids: binding aspects and implications for drug design. *Med. Res. Rev.* 31, 821–862. doi: 10.1002/med.20202
- Bisht, K., Wagner, K. H., and Bulmer, A. C. (2010). Curcumin, resveratrol and flavonoids as anti-inflammatory, cyto- and DNA-protective dietary compounds. *Toxicology* 278, 88–100. doi: 10.1016/j.tox.2009.11.008
- Bitzer, M., von Gersdorff, G., Liang, D., Dominguez-Rosales, A., Beg, A. A., Rojkind, M., et al. (2000). A mechanism of suppression of TGF- $\beta$ /SMAD signaling by NF- $\kappa$ B/RelA. *Gene Dev.* 14 (2), 187–197.
- Boocock, D. J., Faust, G. E., Patel, K. R., Schinas, A. M., Brown, V. A., Ducharme, M. P., et al. (2007). Phase I dose escalation pharmacokinetic study in healthy volunteers of resveratrol, a potential cancer chemopreventive agent. *Cancer Epidemiol. Biomarkers Prev.* 16, 1246–1252. doi: 10.1158/1055-9965.EPI-07-0022

- Bodduluru, L. N., Kasala, E. R., Thota, N., Barua, C. C., and Sistla, R. (2014). Chemopreventive and therapeutic effects of nimbolide in cancer: the underlying mechanisms. *Toxicol. In Vitro* 28, 1026–1035. doi: 10.1016/j.tiv.2014.04.011
- Boldbaatar, A., Lee, S., Han, S., Jeong, A. L., Ka, H. I., Buyanravjikh, S., et al. (2017). Eupatolide inhibits the TGF- $\beta$ 1-induced migration of breast cancer cells via downregulation of SMAD3 phosphorylation and transcriptional repression of ALK5. *Oncol. Lett.* 14 (5), 6031–6039. doi: 10.3892/ol.2017.6957
- Bouquet, J., Rivaud, M., Chevalley, S., Deharo, E., Jullian, V., and Valentin, A. (2012). Biological activities of nitidine, a potential anti-malarial lead compound. *Malar. J.* 11, 67. doi: 10.1186/1475-2875-11-67
- Boutet, A., De Frutos, C. A., Maxwell, P. H., Mayol, M. J., Romero, J., and Nieto, M. A. (2006). Snail activation disrupts tissue homeostasis and induces fibrosis in the adult kidney. *EMBO J.* 25 (23), 5603–5613. doi: 10.1038/sj.emboj.7601421
- Brown, V. A., Patel, K. R., Viskaduraki, M., Crowell, J. A., Perloff, M., Booth, T. D., et al. (2010). Repeat dose study of the cancer chemopreventive agent resveratrol in healthy volunteers: safety, pharmacokinetics, and effect on the insulin-like growth factor axis. *Cancer Res.* 70 (22), 9003–9011. doi: 10.1158/0008-5472.CAN-10-2364
- Cano, A., Pérez-Moreno, M. A., Rodrigo, I., Locascio, A., Blanco, M. J., del Barrio, M. G., et al. (2000). The transcription factor snail controls epithelial-mesenchymal transitions by repressing E-cadherin expression. *Nat. Cell Biol.* 2, 76–83. doi: 10.1038/35000025
- Cascão, R., Fonseca, J. E., and Moita, L. F. (2017). Celastrol: a spectrum of treatment opportunities in chronic diseases. *Front. Med. (Lausanne)* 15 (4), 69. doi: 10.3389/fmed.2017.00069
- Chander, V., and Chopra, K. (2005). Role of nitric oxide in resveratrol-induced renal protective effects of ischemic preconditioning. *J. Vasc. Surg.* 42, 1198–1205. doi: 10.1016/j.jvs.2005.08.032
- Chang, C. C., Ling, X. H., Hsu, H. F., Wu, J. M., Wang, C. P., Yang, J. F., et al. (2016). Siegesbeckia orientalis extract inhibits TGF $\beta$ 1-induced migration and invasion of endometrial cancer cells. *Moléculas* 21, 8. doi: 10.3390/molecules21081021
- Chang, J., Wang, H., Wang, X., Zhao, Y., Zhao, D., Wang, C., et al. (2015). Molecular mechanisms of Polyphyllin I-induced apoptosis and reversal of the epithelial-mesenchymal transition in human osteosarcoma cells. *J. Ethnopharmacol.* 170, 117–127. doi: 10.1016/j.jep.2015.05.006
- Charoenrungruang, S., Chanvorachote, P., and Sritularak, B. (2014). Gigantol induced apoptosis in lung cancer cell through mitochondrial dependent pathway. *TJPS* 38 (2), 67–73. <http://www.thaiscience.info/journals/Article/TJPS/10963058.pdf>
- Chaurasiya, N. D., Uniyal, G. C., Lal, P., Misra, L., Sangwan, N. S., Tuli, R., et al. (2008). Analysis of withanolides in root and leaf of Withania somnifera by HPLC with photodiode array and evaporative light scattering detection. *Phytochem. Anal.* 19, 148–154. doi: 10.1002/pca.1029
- Chen, C., Ma, T., Zhang, C., Zhang, H., Bai, L., Kong, L., et al. (2017a). Down-regulation of aquaporin 5-mediated epithelial-mesenchymal transition and anti-metastatic effect by natural product Cairicoside E in colorectal cancer. *Mol. Carcinog.* 56 (12), 2692–2705. doi: 10.1002/mc.22712
- Chen, C., Wang, Y. Y., Wang, Y. X., Cheng, M. Q., Yin, J. B., Zhang, X., et al. (2017b). Gentiopicroside ameliorates bleomycin-induced pulmonary fibrosis in mice via inhibiting inflammatory and fibrotic process. *Biochem. Biophys. Res. Commun.* 495 (4), 2396–2403. doi: 10.1016/j.bbrc.2017.12.112
- Chen, P. N., Yang, S. F., Yu, C. C., Lin, C. Y., Huang, S. H., Chu, S. C., et al. (2017c). *Duchesnea indica* extract suppresses the migration of human lung adenocarcinoma cells by inhibiting epithelial-mesenchymal transition. *Environ. Toxicol.* 32 (8), 2053–2063. doi: 10.1002/tox.22420
- Chen, Y., Yuan, T., Zhang, H., Yan, Y., Wang, D., Fang, L., et al. (2017d). Activation of Nrf2 attenuates pulmonary vascular remodeling via inhibiting endothelial-to-mesenchymal transition: an insight from a plant polyphenol. *Int. J. Biol. Sci.* 13 (8), 1067–1081. doi: 10.7150/ijbs.20316
- Chen, C. Y., Peng, W. H., Tsai, K. D., and Hsu, S. L. (2007). Luteolin suppresses inflammation-associated gene expression by blocking NF- $\kappa$ B and AP-1 activation pathway in mouse alveolar macrophages. *Life Sci.* 81, 1602–1614. doi: 10.1016/j.lfs.2007.09.028
- Chen, J., Wang, J., Lin, L., He, L., Wu, Y., Zhang, L., et al. (2012). Inhibition of STAT3 signaling pathway by nitidine chloride suppressed the angiogenesis and growth of human gastric cancer. *Mol. Cancer Ther.* 11 (2), 277–287. doi: 10.1158/1535-7163.MCT-11-0648
- Chen, X., Sun, R., Hu, J., Mo, Z., Yang, Z., Liao, D., et al. (2008). Attenuation of Bleomycin-induced lung Fibrosis by oxymatrine is associated with regulation of fibroblast proliferation and collagen production in primary culture. *Basic Clin. Pharmacol. Toxicol.* 103 (3), 278–286. doi: 10.1111/j.1742-7843.2008.00287.x
- Chen, Y., Yuan, T., Zhang, H., Wang, D., Yan, Y., Niu, Z., et al. (2016a). Salvianolic acid A attenuates vascular remodeling in a pulmonary arterial hypertension rat model. *Acta Pharmacol. Sin.* 37 (6), 772–782. doi: 10.1038/aps.2016.22
- Chen, X. L., Bai, Y. J., Hu, Q. R., Lvzhen., Huang, and Li, X. X. (2016b). Advanced glycation end products induced the epithelial-mesenchymal transition in retinal pigment epithelial cells via ERK activation. *Int. J. Clin. Exp. Pathol.* 9 (4), 4891–4900. [www.ijcep.com/ISSN:1936-2625/IJCEP0024078](http://www.ijcep.com/ISSN:1936-2625/IJCEP0024078)
- Cheng, A. L., Hsu, C. H., Lin, J. K., Hsu, M. M., Ho, Y. F., Shen, T. S., et al. (2001). Phase I clinical trial of curcumin, a chemopreventive agent, in patients with high-risk or pre-malignant lesions. *Anticancer Res.* 21 (4B), 2895–2900.
- Cheng, W., Wu, D., Zuo, Q., Wang, Z., and Fan, W. (2013). Ginsenoside Rb1 prevents interleukin-1 beta induced inflammation and apoptosis in human articular chondrocytes. *Int. Orthop.* 37, 2065–2070. doi: 10.1007/s00264-013-1990-6
- Cho, H. S., Kim, J. H., Jang, H. N., Lee, T. W., Jung, M. H., Kim, T. H., et al. (2017). Alpha-lipoic acid ameliorates the epithelial-mesenchymal transition induced by unilateral ureteral obstruction in mice. *Sci. Rep.* 7, 46065. doi: 10.1038/srep46065
- Chou, T. C. (2003). Anti-inflammatory and analgesic effects of paeonol in carrageenan-evoked thermal hyperalgesia. *Br. J. Pharmacol.* 139 (6), 1146–1152. doi: 10.1038/sj.bjp.0705360
- Chow, H. H., Garland, L. L., Hsu, C. H., Vining, D. R., Chew, W. M., Miller, J. A., et al. (2010). Resveratrol modulates drug- and carcinogen-metabolizing enzymes in a healthy volunteer study. *Cancer Prev. Res. (Phila.)* 3 (9), 1168–75. doi: 10.1158/1940-6207.CAPR-09-0155
- Chowdhury, A., Sarkar, J., Chakraborti, T., Pramanik, P. K., and Chakraborti, S. (2016). Protective role of epigallocatechin-3-gallate in health and disease: a perspective. *Biomed. Pharmacother.* 78, 50–59. doi: 10.1016/j.biopha.2015.12.013
- Chung, H., Choi, H. S., Seo, E. K., Kang, D. H., and Oh, E. S. (2015). Baicalin and baicalein inhibit transforming growth factor-beta1-mediated epithelial-mesenchymal transition in human breast epithelial cells. *Biochem. Biophys. Res. Commun.* 458 (3), 707–713. doi: 10.1016/j.bbrc.2015.02.032
- Chung, J. G., Hsia, T. C., Kuo, H. M., Li, Y. C., Lee, Y. M., Lin, S. S., and Hung, C. F. (2001). Inhibitory actions of luteolin on the growth and arylamine N-acetyltransferase activity in strains of *Helicobacter pylori* from ulcer patients. *Toxicol. In Vitro* 15, 191–198. doi: 10.1016/S0887-2333(01)00015-7
- Corvol, H., Flamein, F., Epaul, R., Clement, A., and Guillot, L. (2009). Lung alveolar epithelium and interstitial lung disease. *Int. J. Biochem. Cell Biol.* 41 (8–9), 1643–1651. doi: 10.1016/j.biocel.2009.02.009
- D'Amico, M., Hult, J., Amanatullah, D. F., Zafonte, B. T., Albanese, C., Bouzahzah, B., et al. (2000). The integrin-linked kinase regulates the cyclin D1 gene through glycogen synthase kinase 3b and cAM-responsive element-binding protein-dependent pathways. *J. Biol. Chem.* 275, 32649–32657. doi: 10.1074/jbc.M000643200
- Dai, Y., Desano, J., Tang, W., Meng, X., Meng, Y., Burstein, E., et al. (2010). Natural proteasome inhibitor celastrol suppresses androgen-independent prostate cancer progression by modulating apoptotic proteins and NF- $\kappa$ B. *PLoS One* 5 (12), e14153. doi: 10.1371/journal.pone.0014153
- Dai, W., Wang, F., He, L., Lin, C., Wu, S., Chen, P., et al. (2015). Genistein inhibits hepatocellular carcinoma cell migration by reversing the epithelial-mesenchymal transition: partial mediation by the transcription factor NFAT1. *Mol. Carcinog.* 54 (4), 301–311. doi: 10.1002/mc.22100
- Deng, S., Wong, C. K. C., Lai, H. C., and Wong, A. S. T. (2017). Ginsenoside-Rb1 targets chemotherapy-resistant ovarian cancer stem cells via simultaneous inhibition of Wnt/ $\beta$ -catenin signaling and epithelial-to-mesenchymal transition. *Oncotarget* 8 (16), 25897–25914. doi: 10.18632/oncotarget.13071
- Devappa, R. K., Makkar, H. P., and Becker, K. (2010). Nutritional, biochemical, and pharmaceutical potential of proteins and peptides from jatropha: review. *J. Agric. Food Chem.* 58, 6543–6555. doi: 10.1021/jf100003z
- Dinda, B., Dinda, S., DasSharma, S., Banik, R., Chakraborty, A., and Dinda, M. (2017). Therapeutic potentials of baicalin and its aglycone, baicalein against inflammatory disorders. *Eur. J. Med. Chem.* 131, 68–80. doi: 10.1016/j.ejmech.2017.03.004
- Ding, Y., Lu, X., Hu, X., Ma, J., and Ding, H. (2014). Osthole inhibits proliferation and induces apoptosis in human osteosarcoma cells. *Int. J. Clin. Pharmacol. Ther.* 52, 112–117. doi: 10.5414/CP201923



- Divya, T., Velavan, B., and Sudhandiran, G. (2018). Regulation of transforming growth factor- $\beta$ /Smad-mediated epithelial-mesenchymal transition by celastrol provides protection against Bleomycin-induced pulmonary fibrosis. *Basic Clin. Pharmacol. Toxicol.* 123 (2), 122–129. doi: 10.1111/bcpt.12975
- Fan, D. L., Zhao, W. J., Wang, Y. X., Han, S. Y., and Guo, S. (2012). Oxymatrine inhibits collagen synthesis in keloid fibroblasts via inhibition of transforming growth factor- $\beta$ /Smad signaling pathway. *Int. J. Dermatol.* 51 (4), 463–472. doi: 10.1111/j.1365-4632.2011.05234.x
- Fang, Z., Tang, Y., Jiao, W., Xing, Z., Guo, Z., Wang, W., et al. (2013). Nitidine chloride inhibits renal cancer cell metastasis via suppressing AKT signaling pathway. *Food Chem. Toxicol.* 60, 246–251. doi: 10.1016/j.fct.2013.07.062
- Farooqi, A. A., Qureshi, M. Z., Khalid, S., Attar, R., Martinelli, C., Sabitaliyevich, U. Y., et al. (2019). Regulation of cell signaling pathways by Berberine in different cancers: searching for missing pieces of an incomplete jig-saw puzzle for an effective cancer therapy. *Cancers (Basel)*. 11 (4), E478. doi: 10.3390/cancers11040478
- Fatima, I., El-Ayachi, I., Taotao, L., Lillo, M. A., Krutilina, R., Seagroves, T. N., et al. (2017). The natural compound Jatrophone interferes with Wnt/ $\beta$ -catenin signaling and inhibits proliferation and EMT in human triple-negative breast cancer. *PLoS One* 12 (12), e0189864. doi: 10.1371/journal.pone.0189864
- Ferk, F., Kundi, M., Brath, H., Szekeres, T., Al-Serori, H., Mišić, M., et al. (2018). Gallic acid improves health-associated biochemical parameters and prevents oxidative damage of DNA in type 2 diabetes patients: results of a placebo-controlled pilot study. *Mol. Nutr. Food Res.* 62 (4), 1–30. doi: 10.1002/mnfr.201700482
- Frémont, L. (2000). Biological effects of resveratrol. *Life Sci.* 66 (8), 663–673. doi: 10.1016/S0024-3205(99)00410-5
- Fu, J., Ke, X., Tan, S., Liu, T., Wang, S., Ma, J., et al. (2016). The natural compound codonolactone attenuates TGF- $\beta$ 1-mediated epithelial-to-mesenchymal transition and motility of breast cancer cells. *Oncol. Rep.* 35 (1), 117–126. doi: 10.3892/or.2015.4394
- Fujita, M., Itokawa, H., and Sashida, Y. (1973). Studies on the components of *Magnolia obovata* Thunb. III. Occurrence of magnolol and honokiol in *M. obovata* and other allied plants. *Yakugaku Zasshi* 93, 429–434. doi: 10.1248/yakushi1947.93.4\_429
- Gao, Q., Yuan, Y., Gan, H. Z., and Peng, Q. (2015). Resveratrol inhibits the hedgehog signaling pathway and epithelial-mesenchymal transition and suppresses gastric cancer invasion and metastasis. *Oncol. Lett.* 9 (5), 2381–2387. doi: 10.3892/ol.2015.2988
- Garodia, P., Ichikawa, H., Malani, N., Sethi, G., and Aggarwal, B. B. (2007). From ancient medicine to modern medicine: ayurvedic concepts of health and their role in inflammation and cancer. *J. Soc. Integr. Oncol.* 5, 25–37. doi: 10.2310/7200.2006.029
- Ge, P., Ji, X., Ding, Y., Wang, X., Fu, S., Meng, F., et al. (2010). Celastrol causes apoptosis and cell cycle arrest in rat glioma cells. *Neurol. Res.* 32 (1), 94–100. doi: 10.1179/016164109X12518779082273
- Giacomelli, C., Natali, L., Trincavelli, M. L., Daniele, S., Bertoli, A., Flamini, G., et al. (2016). New insights into the anticancer activity of carnosol: p53 reactivation in the U87MG human glioblastoma cell line. *Int. J. Biochem. Cell. Biol.* 74, 95–108. doi: 10.1016/j.biocel.2016.02.019
- Giacomelli, C., Daniele, S., Natali, L., Iofrida, C., Flamini, G., Braca, A., et al. (2017). Carnosol controls the human glioblastoma stemness features through the epithelial-mesenchymal transition modulation and the induction of cancer stem cell apoptosis. *Sci. Rep.* 7 (1), 15174. doi: 10.1038/s41598-017-15360-2
- Ghantous, A., Sinjab, A., Herczeg, Z., and Darwiche, N. (2013). Parthenolide: from plant shoots to cancer roots. *Drug Discov. Today* 18 (17–18), 894–905. doi: 10.1016/j.drudis.2013.05.005
- Grande, M. T., Sanchez-Laorden, B., Lopez-Blau, C., De Frutos, C. A., Boutet, A., Arevalo, M., et al. (2015). Snail1-induced partial epithelial-to-mesenchymal transition drives renal fibrosis in mice and can be targeted to reverse established disease. *Nat. Med.* 21, 989–997. doi: 10.1038/nm.3901
- Gu, L., Feng, J., Zheng, Z., Xu, H., and Yu, W. (2016). Polyphyllin I inhibits the growth of ovarian cancer cells in nude mice. *Oncol. Lett.* 12, 4969–4974. doi: 10.3892/ol.2016.5348
- Gupta, S. C., Patchva, S., and Aggarwal, B. B. (2013). Therapeutic roles of curcumin: lessons learned from clinical trials. *AAPS J.* 15 (1), 195–218. doi: 10.1208/s12248-012-9432-8
- Gliemann, L., Nyberg, M., and Hellsten, Y. (2016). Effects of exercise training and resveratrol on vascular health in aging. *Free Radic. Biol. Med.* 98, 165–176. doi: 10.1016/j.freeradbiomed.2016.03.037
- Han, L., Zhang, H. W., Zhou, W. P., Chen, G. M., and Guo, K. J. (2012). The effects of genistein on transforming growth factor- $\beta$ 1-induced invasion and metastasis in human pancreatic cancer cell line Panc-1 in vitro. *Chin. Med. J. (Engl.)* 125 (11), 2032–2040.
- Hang, Y., Qin, X., Ren, T., and Cao, J. (2018). Baicalin reduces blood lipids and inflammation in patients with coronary artery disease and rheumatoid arthritis: a randomized, double-blind, placebo-controlled trial. *Lipids Health Dis.* 17 (1), 146. doi: 10.1186/s12944-018-0797-2
- Hao, F., Kumar, S., Yadav, N., and Chandra, D. (2014). Neem components as potential agents for cancer prevention and treatment. *Biochim. Biophys. Acta* 1846, 247–257. doi: 10.1016/j.bbcan.2014.07.002
- Hao, J., Zhu, H., Zhang, Z., Yang, S., and Li, H. (2015). Identification of anthocyanins in black rice (*Oryza sativa* L.) by UPLC/Q-TOF-MS and their in vitro and in vivo antioxidant activities. *J. Cereal Sci.* 64, 92–99. doi: 10.1016/j.jcs.2015.05.003
- He, D. X., Li, G. H., Gu, X. T., Zhang, L., Mao, A. Q., Wei, J., et al. (2016). A new agent developed by biotransformation of polyphyllin VII inhibits chemoresistance in breast cancer. *Oncotarget* 7, 31814–31824. doi: 10.18632/oncotarget.6674
- Hegner, S. P., Hofmann, T. G., Dröge, W., and Schmitz, M. L. (1999). The antiinflammatory sesquiterpene lactone parthenolide inhibits NF-kappa B by targeting the I kappa B kinase complex. *J. Immunol.* 163 (10), 5617–5623.
- Hertig, A., Anglicheau, D., Verine, J., Pallet, N., Touzot, M., Ancel, P. Y., et al. (2008). Early epithelial phenotypic changes predict graft fibrosis. *J. Am. Soc. Nephrol.* 19 (8), 1584–1591. doi: 10.1681/ASN.2007101160
- Hewlings, S. J., and Kalman, D. S. (2017). Curcumin: a review of its effects on human health. *Foods* 6 (10), 92. doi: 10.3390/foods6100092
- Howells, L. M., Berry, D. P., Elliott, P. J., Jacobson, E. W., Hoffmann, E., Hegarty, B., et al. (2011). Phase I randomized, double-blind pilot study of micronized resveratrol (SRT501) in patients with hepatic metastases—safety, pharmacokinetics, and pharmacodynamics. *Cancer Prev. Res. (Phila.)* 4 (9), 1419–25. doi: 10.1158/1940-6207.CAPR-11-0148
- Ho, J. H., and Hong, C. Y. (2011). Salvianolic acids: small compounds with multiple mechanisms for cardiovascular protection. *J. Biomed. Sci.* 18, 30. doi: 10.1186/1423-0127-18-30
- Hou, D. X. (2003). Potential mechanisms of cancer chemoprevention by anthocyanins. *Curr. Mol. Med.* 3, 149–159. doi: 10.2174/1566524033361555
- Hou, Y. L., Tsai, Y. H., Lin, Y. H., and Chao, J. C. (2014). Ginseng extract and ginsenoside Rb1 attenuate carbon tetrachloride-induced liver fibrosis in rats. *BMC Complement. Altern. Med.* 14, 415. doi: 10.1186/1472-6882-14-415
- Hu, W., Han, W., Huang, C., and Wang, M. H. (2011). Protective effect of the methanolic extract from *Duchesnea indica* against oxidative stress in vitro and in vivo. *Environ. Toxicol. Pharmacol.* 31 (1), 42–50. doi: 10.1016/j.etap.2010.09.004
- Hu, W., Shen, W., and Wang, M. H. (2009). Free radical scavenging activity and protective ability of methanolic extract from *Duchesnea indica* against protein oxidation and DNA damage. *J. Food Sci. Nutr.* 14, 77–282. doi: 10.3746/jfn.2009.14.4.277
- Huang, S. F., Horng, C. T., Hsieh, Y. S., Hsieh, Y. H., Chu, S. C., and Chen, P. N. (2016). Epicatechin-3-gallate reverses TGF- $\beta$ 1-induced epithelial-to-mesenchymal transition and inhibits cell invasion and protease activities in human lung cancer cells. *Food Chem. Toxicol.* 94, 1–10. doi: 10.1016/j.fct.2016.05.009
- Huang, W. H., Lee, A. R., and Yang, C. H. (2006). Antioxidative and anti-inflammatory activities of polyhydroxyflavonoids of *Scutellaria baicalensis* GEORGI. *Biosci. Biotechnol. Biochem.* 70 (10), 2371–2380.
- Huang, Y., Tsang, S. Y., Yao, X., and Chen, Z. Y. (2005). Biological properties of baicalin in cardiovascular system. *Curr. Drug Targets Cardiovasc. Haematol. Disord.* 5 (2), 177–184. doi: 10.2174/1568006043586206
- Hui, H., Tang, G., Go, V. L. (2009). Hypoglycemic herbs and their action mechanisms. *Chin Med.* 4, 11. doi: 10.1186/1749-8546-4-11
- Huber, M. A., Azoitei, N., Baumann, B., Grünert, S., Sommer, A., Pehamberger, H., et al. (2004). NF-kB is essential for epithelial-mesenchymal transition and metastasis in a model of breast cancer progression. *J. Clin. Invest.* 114, 569–581. doi: 10.1172/JCI200421358
- Imanshahidi, M., and Hosseinzadeh, H. (2008). Pharmacological and therapeutic effects of *Berberis vulgaris* and its active constituent, berberine. *Phytother. Res.* 22 (8), 999–1012. doi: 10.1002/ptr.2399
- Jeon, Y. K., Yoo, D. R., Jang, Y. H., Jang, S. Y., and Nam, M. J. (2011). Sulforaphane induces apoptosis in human hepatic cancer cells through inhibition of 6-phosphofructo-2-kinase/fructose-2,6-bisphosphatase 4, mediated by hypoxia



- inducible factor-1-dependent pathway. *Biochim. Biophys. Acta* 1814, 1340–1348. doi: 10.1016/j.bbapap.2011.05.015
- Ji, Q., Liu, X., Han, Z., Zhou, L., Sui, H., Yan, L., et al. (2015). Resveratrol suppresses epithelial-to-mesenchymal transition in colorectal cancer through TGF- $\beta$ /Smads signaling pathway mediated Snail/E-cadherin expression. *BMC Cancer* 15, 97. doi: 10.1186/s12885-015-1119-y
- Ji, Y., Dou, Y., Zhao, Q., Zhang, J., Yang, Y., Wang, T., et al. (2016). Paeoniflorin suppresses TGF- $\beta$  mediated epithelial mesenchymal transition in pulmonary fibrosis through a Smad- dependent pathway. *Acta Pharmacol. Sin.* 37 (6), 794–804. doi: 10.1038/aps.2016.36
- Jia, L., and Zhao, Y. (2009). Current evaluation of the millennium phyto medicine-ginseng (I): etymology, pharmacognosy, phytochemistry, market and regulations. *Curr. Med. Chem.* 16, 2475–2484. doi: 10.2174/092986709788682146
- Jiang, L. L., Zhou, S. J., Zhang, X. M., Chen, H. Q., and Liu, W. (2016). Sulforaphane suppresses in vitro and in vivo lung tumorigenesis through downregulation of HDAC activity. *Biomed. Pharmacother.* 78, 74–80. doi: 10.1016/j.biopha.2015.11.007
- Jin, H. J., Xie, X. L., Ye, J. M., and Li, C. G. (2013). TanshinoneIIA and cryptotanshinone protect against hypoxia-induced mitochondrial apoptosis in H9c2 cells. *PLoS One* 8 (1), e51720. doi: 10.1371/journal.pone.0051720
- Jin, L., Piao, Z. H., Sun, S., Liu, B., Ryu, Y., Choi, S. Y., et al. (2017). Gallic acid attenuates pulmonary fibrosis in a mouse model of transverse aortic contraction-induced heart failure. *Vascul. Pharmacol.* 99, 74–82. doi: 10.1016/j.vph.2017.10.007
- Jo, E., Park, S. J., Choi, Y. S., Jeon, W. K., and Kim, B. C. (2015). Kaempferol suppresses transforming growth factor- $\beta$ 1-induced epithelial-to-mesenchymal transition and migration of A549 lung cancer cells by inhibiting Akt1-mediated phosphorylation of Smad3 at Threonine-179. *Neoplasia* 17, 525–537. doi: 10.1016/j.neo.2015.06.004
- Johanson, J. J. (2011). Carnosol: a promising anti-cancer and inflammatory agent. *Cancer Lett.* 305 (1), 1–7. doi: 10.1016/j.canlet.2011.02.005
- Jung, H. J., Kang, H. J., Song, Y. S., Park, E. H., Kim, Y. M., and Lim, C. J. (2008). Anti-inflammatory, anti-angiogenic and anti-nociceptive activities of Sedum sarmentosum extract. *J. Ethnopharmacol.* 116, 138–143. doi: 10.1016/j.jep.2007.11.014
- Kalluri, R. (2009). EMT: when epithelial cells decide to become mesenchymal-like cells. *J. Clin. Invest.* 119 (6), 1417–1419. doi: 10.1172/JCI39675
- Kalluri, R., and Weinberg, R. A. (2009). The basics of epithelial-mesenchymal transition. *J. Clin. Invest.* 119, 1420–1428. doi: 10.1172/JCI39104
- Kamath, S. G., Chen, N., Xiong, Y., Wenham, R., Apte, S., Humphrey, M., et al. (2009). Gedunin, a novel natural substance, inhibits ovarian cancer cell proliferation. *Int. J. Gynecol. Cancer* 19, 1564–1569. doi: 10.1111/IGC.0b013e3181a83135
- Kanlaya, R., and Thongboonkerd, V. (2019). Protective effects of epigallocatechin-3-gallate from green tea in various kidney diseases. *Adv. Nutr.* 110 (1), 112–121. doi: 10.1093/advances/nmy077
- Kao, S. J., Su, J. L., Chen, C. K., Yu, M. C., Bai, K. J., Chang, J. H., et al. (2012). Osthole inhibits the invasive ability of human lung adenocarcinoma cells via suppression of NF-kappaB-mediated matrix metalloproteinase-9 expression. *Toxicol. Appl. Pharmacol.* 261, 105–115. doi: 10.1016/j.taap.2012.03.020
- Kee, H. J., Cho, S. N., Kim, G. R., Choi, S. Y., Ryu, Y., Kim, I. K., et al. (2014). Gallic acid inhibits vascular calcification through the blockade of BMP2-Smad1/5/8 signaling pathway. *Vasc. Pharmacol.* 63 (2), 71–78. doi: 10.1016/j.vph.2014.08.005
- Khan, A. L., Hussain, J., Hamayun, M., Gilani, S. A., Ahmad, S., Rehman, G., et al. (2010). Secondary metabolites from *Inula britannica* L. and their biological activities. *Molecules* 15 (3), 1562–1577. doi: 10.3390/molecules15031562
- Khan, T., and Gurav, P. (2017). PhytoNanotechnology: enhancing delivery of plant based anti-cancer drugs. *Front Pharmacol.* 8, 1002. doi: 10.3389/fphar.2017.01002
- Kida, Y., Asahina, K., Teraoka, H., Gitelman, I., and Sato, T. (2007). Twist relates to tubular epithelial-mesenchymal transition and interstitial fibrogenesis in the obstructed kidney. *J. Histochem. Cytochem.* 55 (7), 661–673. doi: 10.1369/jhc.6A7157.2007
- Kim, D. H., Sung, B., Kang, Y. J., Hwang, S. Y., Kim, M. J., Yoon, J. H., et al. (2015). Sulforaphane inhibits hypoxia-induced HIF-1 $\alpha$  and VEGF expression and migration of human colon cancer cells. *Int. J. Oncol.* 47, 2226–2232. doi: 10.3892/ijo.2015.3200
- Kim, K., Lu, Z., and Hay, E. D. (2002a). Direct evidence for a role of beta-catenin/LEF-1 signaling pathway in induction of EMT. *Cell Biol. Int.* 26, 463–476. doi: 10.1006/cbir.2002.0901
- Kim, I. G., Jung, I. L., Oh, T. J., Kim, K. C., and Shim, H. W. (2002b). Polysaccharide-enriched fraction isolated from *Duchesnea chrysanthi* protects against oxidative damage. *Biotechnol. Lett.* 24, 1299–1305. doi: 10.1023/A:1019812202099
- Kim, N., Hwangbo, C., Lee, S., and Lee, J. H. (2013). Eupatolide inhibits PDGF-induced proliferation and migration of aortic smooth muscle cells through ROS-dependent heme oxygenase-1 induction. *Phytother. Res.* 27, 1700–1707. doi: 10.1002/ptr.4924
- Kim, K. C., Kim, J. S., Son, J. K., and Kim, I. G. (2007). Enhanced induction of mitochondrial damage and apoptosis in human leukemia HL-60 cells by the *Ganoderma lucidum* and *Duchesnea chrysanthi* extracts. *Cancer Lett.* 246, 210–217. doi: 10.1016/j.canlet.2006.02.014
- Kim, Y. S., Choi, K. C., and Hwang, K. A. (2015). Genistein suppressed epithelial-mesenchymal transition and migration efficacies of BG-1 ovarian cancer cells activated by estrogenic chemicals via estrogen receptor pathway and downregulation of TGF-beta signaling pathway. *Phytomedicine* 22, 993–999. doi: 10.1016/j.phymed.2015.08.003
- Klongkumnuankarn, P., Busaranon, K., Chanvorachote, P., Sritularak, B., Jongbunprasert, V., and Likhitwitayawuid, K. (2015). Cytotoxic and Antimigratory activities of phenolic compounds from *dendrobium brymerianum*. *J. Evid. Based Complement. Altern Med.* 2015, 1–9. doi: 10.1155/2015/350410
- Kong, D., Zhang, F., Shao, J., Wu, L., Zhang, X., Chen, L., et al. (2015). Curcumin inhibits cobalt chloride-induced epithelial-to-mesenchymal transition associated with interference with TGF- $\beta$ /Smad signaling in hepatocytes. *Lab. Invest.* 95 (11), 1234–1245. doi: 10.1038/labinvest.2015.107
- Kong, M., Fan, J., Dong, A., Cheng, H., and Xu, R. (2010). Effects of polyphyllin I on growth inhibition of human non-small lung cancer cells and in xenograft. *Acta Biochim. Biophys. Sin.* 42, 827–833. doi: 10.1093/abbs/gmq091
- Kong, S., Kim, D. J., Oh, S. K., Choi, I. S., Jeong, H. S., and Lee, J. (2012). Black rice bran as an ingredient in noodles: chemical and functional evaluation. *J. Food Sci.* 77, C303–C307. doi: 10.1111/j.1750-3841.2011.02590.x
- Kou, Y., Li, L., Li, H., Tan, Y., Li, B., Wang, K., et al. (2016). Berberine suppressed epithelial mesenchymal transition through cross-talk regulation of PI3K/AKT and RAR $\alpha$ /RAR $\beta$  in melanoma cells. *Biochem. Biophys. Res. Commun.* 479 (2), 290–296. doi: 10.1016/j.bbrc.2016.09.061
- Kulkarni, S. K., and Dhir, A. (2010). Berberine: a plant alkaloid with therapeutic potential for central nervous system disorders. *Phytother. Res.* 24, 317–324. doi: 10.1002/ptr.2968
- la Porte, C., Voduc, N., Zhang, G., Seguin, I., Tardiff, D., Singhal, N., et al. (2010). Steady-State pharmacokinetics and tolerability of trans-resveratrol 2000 mg twice daily with food, quercetin and alcohol (ethanol) in healthy human subjects. *Clin. Pharmacokinet.* 49 (7), 449–454. doi: 10.2165/11531820-000000000-00000
- Lee, D. G., Jang, S. I., Kim, Y. R., Yang, K. E., Yoon, S. J., Lee, Z. W., et al. (2016). Anti-proliferative effects of ginsenosides extracted from mountain ginseng on lung cancer. *Chin. J. Integr. Med.* 22 (5), 344–352. doi: 10.1007/s11655-014-1789-8
- Lee, J., Hahm, E. R., Marcus, A. I., and Singh, S. V. (2013). Withaferin A inhibits experimental epithelial-mesenchymal transition in MCF-10A cells and suppresses vimentin protein level in vivo in breast tumors. *Mol. Carcinog.* 54 (6), 417–429. doi: 10.1002/mc.22110
- Lee, J., Hwangbo, C., Lee, J. J., Seo, J., and Lee, J. H. (2010a). The sesquiterpene lactone eupatolide sensitizes breast cancer cells to TRAIL through down-regulation of c-FLIP expression. *Oncol. Rep.* 23, 229–237. doi: 10.3892/or\_00000628
- Lee, J., Tae, N., Lee, J. J., Kim, T., and Lee, J. H. (2010b). Eupatolide inhibits lipopolysaccharide-induced COX-2 and iNOS expression in RAW264.7 cells by inducing proteasomal degradation of TRAF6. *Eur. J. Pharmacol.* 636, 173–180. doi: 10.1016/j.ejphar.2010.03.021
- Lee, J., Jung, E., Park, J., Jung, K., Lee, S., Hong, S., et al. (2005). Anti-inflammatory effects of magnolol and honokiol are mediated through inhibition of the downstream pathway of MEKK-1 in NF-kappaB activation signaling. *Planta Med.* 71, 338–343. doi: 10.1055/s-2005-864100
- Lee, J. M., Dedhar, S., Kalluri, R., and Thompson, E. W. (2006). The epithelial-mesenchymal transition: new insights in signaling, development, and disease. *J. Cell Biol.* 172 (7), 973–981.

- Lee, J. Y., Kim, H. S., and Song, Y. S. (2012). Genistein as a potential anticancer agent against ovarian cancer. *J. Tradit. Complement. Med.* 2 (2), 96–104. doi: 10.1016/S2225-4110(16)30082-7
- Lee, I. R., and Yang, M. Y. (1994). Phenolic compounds from *Duchesnea chrysanthra* and their cytotoxic activities in human cancer cell. *Arch. Pharm. Res.* 17, 476–479. doi: 10.1007/BF02979129
- Li, J., Chong, T., Wang, Z., Chen, H., Li, H., Cao, J., et al. (2014). A novel anti-cancer effect of resveratrol: reversal of epithelial-mesenchymal transition in prostate cancer cells. *Mol. Med. Rep.* 10, 1717–1724. doi: 10.3892/mmr.2014.2417
- Li, J., Yang, J., Lü, F., Qi, Y. T., Liu, Y. Q., Sun, Y., et al. (2012a). Chemical constituents from the stems of *Celastrus orbiculatus*. *Chin. J. Nat. Med.* 10 (4), 279–283. ISSN 1875-5364. doi: 10.3724/SPJ.1009.2012.00279
- Li, J., Shao, Z. H., Xie, J. T., Wang, C. Z., Ramachandran, S., Yin, J. J., et al. (2012b). The effects of ginsenoside Rb1 on JNK in oxidative injury in cardiomyocytes. *Arch. Pharm. Res.* 35, 1259–1267. doi: 10.1007/s12272-012-0717-3
- Li, W., Ma, J., Ma, Q., Li, B., Han, L., Liu, J., et al. (2013). Resveratrol inhibits the epithelial-mesenchymal transition of pancreatic cancer cells via suppression of the PI-3 K/Akt/NF- $\kappa$ B pathway. *Curr. Med. Chem.* 20, 4185–4194. doi: 10.2174/09298673113209990251
- Li, W., Saud, S. M., Young, M. R., Colburn, N. H., and Hua, B. (2015). Cryptotanshinone, a Stat3 inhibitor, suppresses colorectal cancer proliferation and growth in vitro. *Mol. Cell Biochem.* 406 (1–2), 63–73. doi: 10.1007/s11010-015-2424-0
- Li, X. H., Xiao, T., Yang, J. H., Qin, Y., Gao, J. J., Liu, H. J., et al. (2018a). Parthenolide attenuated bleomycin-induced pulmonary fibrosis via the NF- $\kappa$ B/Snail signaling pathway. *Respir. Res.* 19 (1), 111. doi: 10.1186/s12931-018-0806-z
- Li, W., Jiang, Z., Xiao, X., Wang, Z., Wu, Z., Ma, Q., et al. (2018b). Curcumin inhibits superoxide dismutase-induced epithelial-to-mesenchymal transition via the PI3K/Akt/NF- $\kappa$ B pathway in pancreatic cancer cells. *Int. J. Oncol.* 52, 1593–1602. doi: 10.3892/ijo.2018.4295
- Liappas, G., González-Mateo, G. T., Majano, P., Sánchez-Tomero, J. A., Ruiz-Ortega, M., Rodríguez Díez, R., et al. (2015). T helper 17/regulatory T Cell balance and experimental models of peritoneal dialysis-induced damage. *Biomed. Res. Int.* 2017, 6130208. doi: 10.1155/2017/6130208
- Lin, C. Y., Hsieh, Y. H., Yang, S. F., Chu, S. C., Chen, P. N., and Hsieh, Y. S. (2017). Cinnamomum cassia extracts reverses TGF- $\beta$ 1-induced epithelial-mesenchymal transition in human lung adenocarcinoma cells and suppresses tumor growth in vivo. *Environ. Toxicol.* 32 (7), 1878–1887. doi: 10.1002/tox.22410
- Lin, D., Kuang, G., Wan, J., Zhang, X., Li, H., Gong, X., et al. (2016). Luteolin suppresses the metastasis of triple-negative breast cancer by reversing epithelial-to-mesenchymal transition via downregulation of  $\beta$ -catenin expression. *Oncol. Rep.* 37 (2), 895–902. doi: 10.3892/or.2016.5311
- Lin, X., Yi, Z., Diaio, J., Shao, M., Zhao, L., Cai, H., et al. (2014). ShaoYao decoction ameliorates colitis-associated col-orectal cancer by downregulating proinflammatory cytokines and promoting epithelial-mesenchymal transition. *J. Transl. Med.* 12, 105. doi: 10.1186/1479-5876-12-105
- Lin, Y., Shi, R., Wang X and Shen, H. M. (2008). Luteolin, a flavonoid with potential for cancer prevention and therapy. *Curr. Cancer Drug Targets* 8, 634–646. doi: 10.2174/156800908786241050
- Lin, L., Sun, Y., Wang, D., Zheng, S., Zhang, J., and Zheng, C. (2015). Celastrol ameliorates ulcerative colitis-related colorectal cancer in mice via suppressing inflammatory responses and epithelial-mesenchymal transition. *Front. Pharmacol.* 6, 320. doi: 10.3389/fphar.2015.00320
- Liu, D., Qiu, X. Y., Wu, X., Hu, D. X., Li, C. Y., Yu, S. B., et al. (2017). Piperlongumine suppresses bladder cancer invasion via inhibiting epithelial mesenchymal transition and F-actin reorganization. *Biochem. Biophys. Res. Commun.* 494 (1–2), 165–172. doi: 10.1016/j.bbrc.2017.10.061
- Liu, L., Lu, W., Ma, Z., and Li, Z. (2012). Oxymatrine attenuates bleomycin-induced pulmonary fibrosis in mice via the inhibition of inducible nitric oxide synthase expression and the TGF- $\beta$ /Smad signaling pathway. *Int. J. Mol. Med.* 29 (5), 815–822. doi: 10.3892/ijmm.2012.923
- Liu, Q. R., Liu, J. M., Chen, Y., Xie, X. Q., Xiong, X. X., Qiu, X. Y., et al. (2014). Piperlongumine inhibits migration of glioblastoma cells via activation of ROS-dependent p38 and JNK signaling pathways. *Oxidative Med. Cell. Longev.* 2014, 653732. doi: 10.1155/2014/653732
- Liu, Y. (2004). Epithelial to mesenchymal transition in renal fibrogenesis: pathologic significance, molecular mechanism, and therapeutic intervention. *J. Am. Soc. Nephrol.* 15, 1–12. doi: 10.1097/01.ASN.0000106015.29070.E7
- Liu, C., Wang, Z., Song, Y., Wu, D., Zheng, X., Li P., et al. (2015). Effects of berberine on amelioration of hyperglycemia and oxidative stress in high glucose and high fat diet-induced diabetic hamsters in vivo. *Biomed. Res. Int.* 2015, 313808. doi: 10.1155/2015/313808
- Liu, L., Wang, Y., Yan, R., Li, S., Shi, M., Xiao, Y., et al. (2016). Oxymatrine inhibits renal tubular EMT induced by high glucose via upregulation of snoN and inhibition of TGF- $\beta$ 1/Smad signaling pathway. *PLoS One* 11 (3), e0151986. doi: 10.1371/journal.pone.0151986
- Liu, P. L., Tsai, J. R., Charles, A. L., Hwang, J. J., Chou, S. H., Ping, Y. H., et al. (2010a). Resveratrol inhibits human lung adenocarcinoma cell metastasis by suppressing heme oxygenase 1-mediated nuclear factor-kappaB pathway and subsequently downregulating expression of matrix metalloproteinases. *Mol. Nutr. Food Res.* 54 (Suppl. 2), S196–S204. doi: 10.1002/mnfr.200900550
- Liu, X. J., Zhao, J., and Gu, X. Y. (2010b). The effects of genistein and puerarin on the activation of nuclear factor-kappaB and the production of tumor necrosis factor-alpha in asthma patients. *Pharmazie* 65 (2), 127–131.
- Lopez-Cabrera, M. (2014). Mesenchymal conversion of mesothelial cells is a key event in the pathophysiology of the peritoneum during peritoneal dialysis. *Adv. Med.* 2014, 473134. doi: 10.1155/2014/473134
- Lou, W., Chen, Y., Zhu, K. Y., Deng, H., Wu, T., and Wang, J. (2017). Polyphyllin I Overcomes EMT-associated resistance to erlotinib in lung cancer cells via IL-6/STAT3 pathway inhibition. *Biol. Pharm. Bull.* 40 (8), 1306–1313. doi: 10.1248/bpb.b17-00271
- Lovisa, S., LeBleu, V. S., Tampe, B., Sugimoto, H., Vlodavsky, K., Carstens, J. L., et al. (2015). Epithelial-to-mesenchymal transition induces cell cycle arrest and parenchymal damage in renal fibrosis. *Nat. Med.* 21, 998–1009. doi: 10.1038/nm.3902
- Lu, Z., Lai, Z.-Q., Leung, A. W. N., Leung, P. S., Li, Z.-S., and Lin, Z.-X. (2017). Exploring brusatol as a new anti-pancreatic cancer adjuvant: biological evaluation and mechanistic studies. *Oncotarget* 8 (49), 84974–84985. doi: 10.18632/oncotarget.17761
- Lu, L., Qin, Y., Chen, C., and Guo, X. (2018). Beneficial effects exerted by paeonol in the management of atherosclerosis. *Oxid. Med. Cell Longev.* 2018, 1098617. doi: 10.1155/2018/1098617
- Lv, X. Q., Qiao, X. R., Su, L., and Chen, S. Z. (2016). Honokiol inhibits EMT-mediated motility and migration of human non-small cell lung cancer cells in vitro by targeting c-FLIP. *Acta Pharmacol. Sin.* 37 (12), 1574–1586. doi: 10.1038/aps.2016.81
- Ma, S., Yang, D., Wang, K., Tang, B., Li, D., and Yang, Y. (2012). Cryptotanshinone attenuates isoprenaline-induced cardiac fibrosis in mice associated with upregulation and activation of matrix metalloproteinase-2. *Mol. Med. Rep.* 6 (1), 145–150. doi: 10.3892/mmr.2012.866
- Ma, Y., Li, H., Yue, Z., Guo, J., Xu, S., Xu, J., et al. (2014). Cryptotanshinone attenuates cardiac fibrosis via downregulation of COX-2, NOX-2, and NOX-4. *J. Cardiovasc. Pharmacol.* 64 (1), 28–37. doi: 10.1097/FJC.0000000000000086
- Marín-Neto, J. A., Maciel, B. C., Secches, A. L., and Gallo, L. (1988). Cardiovascular effects of berberine in patients with severe congestive heart failure. *Clin. Cardiol.* 11, 253–260. doi: 10.1002/clc.4960110411
- Massagué, J., and Wotton, D. (2000). Transcriptional control by the TGF- $\beta$ /Smad signaling. *EMBO J.* 19, 1745–1754. doi: 10.1093/emboj/19.8.1745
- Massagué, J. (2000). How cells read TGF- $\beta$  signals. *Nat. Rev. Mol. Cell Biol.* 1, 169–178. doi: 10.1038/35043051
- Masszi, A., Di Ciano, C., Sirokmány, G., Arthur, W. T., Rotstein, O. D., Wang, J., et al. (2003). Central role for Rho in TGF- $\beta$ 1-induced  $\alpha$ -smooth muscle actin expression during epithelial-mesenchymal transition. *Am. J. Physiol. Renal Physiol.* 284, F911–F924. doi: 10.1152/ajprenal.00183.2002
- Masszi, A., and Kapus, A. (2011). Smad3: the role of Smad3 in epithelial-myofibroblast transition. *Cells Tissues Organs* 193, 41–52. doi: 10.1159/000320180
- McCubrey, J. A., Lertpiriyapong, K., Steelman, L. S., Abrams, S. L., Yang, L. V., Murata, et al. (2017). Effects of resveratrol, curcumin, berberine and other nutraceuticals on aging, cancer development, cancer stem cells and microRNAs. *Aging (Albany N. Y.)* 9, 1477–1536. doi: 10.18632/aging.101250
- Mohsenikia, M., Alizadeh, A. M., Khodayari, S., Khodayari, H., Kouhpayeh, S. A., Karimi, A., et al. (2013). The protective and therapeutic effects of alpha-solanine on mice breast cancer. *Eur. J. Pharmacol.* 718, 1–9. doi: 10.1016/j.ejphar.2013.09.015
- Morikawa, T., Zhang, Y., Nakamura, S., Matsuda, H., Muraoka, O., and Yoshikawa, M. (2007). Bioactive constituents from Chinese natural medicines. XXII. Absolute structures of new megastigmane glycosides, sedumosides E1, E2, E3, F1, F2

- and G, from *Sedum sarmentosum* (Crassulaceae). *Chem. Pharm. Bull.* 55, 435–441. doi: 10.1248/cpb.55.435
- Moshiri, A., Puppo, M., Rossi, M., Gherzi, R., and Briata, P. (2017). Resveratrol limits epithelial to mesenchymal transition through modulation of KHSRP/hnRNP1-dependent alternative splicing in mammary gland cells. *Biochim. Biophys. Acta Gene Regul. Mech.* 1860 (3), 291–298. doi: 10.1016/j.bbgrm.2017.01.001
- Nagalingam, A., Arbiser, J. L., Bonner, M. Y., Saxena, N. K., and Sharma D. (2012). Honokiol activates AMP-activated protein kinase in breast cancer cells via an LKB1-dependent pathway and inhibits breast carcinogenesis. *Breast Cancer Res.* 14 (1), R35.
- Newman, D. J., and Cragg, G. M. (2007). Natural products as sources of new drugs over the last 25 years. *J. Nat. Prod.* 70, 461–477. doi: 10.1021/np068054v
- Nieto, M. A., Huang, R. Y., Jackson, R. A., and Thiery, J. P. (2016). EMT: 2016. *Cell* 166, 21–45. doi: 10.1016/j.cell.2016.06.028
- Ninomiya, K., Morikawa, T., Zhang, Y., Nakamura, S., Matsuda, H., Muraoka, O., et al. (2007). Bioactive constituents from Chinese natural medicines. XXIII. Absolute structures of new megastigmane glycosides, sedumosides A(4), A(5), A(6), H, and I, and hepatoprotective megastigmanes from *Sedum sarmentosum*. *Chem. Pharm. Bull.* 55, 1185–1191. doi: 10.1248/cpb.55.1185
- Oh, H., Kang, D. G., Kwon, J. W., Kwon, T. O., Lee, S. Y., Lee, D. B., et al. (2004). Isolation of angiotensin converting enzyme (ACE) inhibitory flavonoids from *Sedum sarmentosum*. *Biol. Pharm. Bull.* 27, 2035–2037. doi: 10.1248/bpb.27.2035
- Ong, R. C., Lei, J., Lee, R. K., Cheung, J. Y., Fung, K. P., Lin, C., et al. (2008). Polyphyllin D induces mitochondrial fragmentation and acts directly on the mitochondria to induce apoptosis in drug-resistant HepG2 cells. *Cancer Lett.* 261, 158–164. doi: 10.1016/j.canlet.2007.11.005
- Padhye, S., Dandawate, P., Yusufi, M., Ahmad, A., and Sarkar, F. H. (2012). Perspectives on medicinal properties of plumbagin and its analogs. *Med. Res. Rev.* 32 (6), 1131–1158. doi: 10.1002/med.20235
- Padmavathi, B., Rath, P. C., Rao, A. R., and Singh, R. P. (2005). Roots of *Withania somnifera* inhibit forestomach and skin carcinogenesis in mice. *Evid. Based Complement. Alternat. Med.* 2, 99–105. doi: 10.1093/ecam/neh064
- Pan, S.-T., Qin, Y., Zhou, Z.-W., He, Z.-X., Zhang, X., Yang, T., et al. (2015). Plumbagin suppresses epithelial to mesenchymal transition and stemness via inhibiting Nrf2-mediated signaling pathway in human tongue squamous cell carcinoma cells. *Drug Des. Dev. Ther.* 9, 5511–5551. doi: 10.2147/DDDT.S89621
- Pattarayan, D., Sivanantham, A., Krishnaswami, V., Loganathan, L., Palanichamy, R., Natesan, S., et al. (2018). Tannic acid attenuates TGF- $\beta$ 1-induced epithelial-to-mesenchymal transition by effectively intervening TGF- $\beta$  signaling in lung epithelial cells. *J. Cell Physiol.* 233 (3), 2513–2525. doi: 10.1002/jcp.26127
- Patwardhan, C. A., Fauq, A., Peterson, L. B., Miller, C., Blagg, B. S., and Chadli, A. (2013). Gedunin inactivates the co-chaperone p23 protein causing cancer cell death by apoptosis. *J. Biol. Chem.* 288, 7313–7325. doi: 10.1074/jbc.M112.427328
- Peinado, H., Quintanilla, M., and Cano, A. (2003). Transforming growth factor  $\beta$ -1 induces snail transcription factor in epithelial cell lines. *J. Biol. Chem.* 278, 21113–21123. doi: 10.1074/jbc.M211304200
- Peng, C. H., Chyau, C. C., Wang, C. J., Lin, H. T., Huang, C. N., and Ker, Y. B. (2016). *Abelmoschus esculentus* fractions potentially inhibited the pathogenic targets associated with diabetic renal epithelial to mesenchymal transition. *Food Funct.* 7 (2), 728–740. doi: 10.1039/C5FO01214G
- Petpiroon, N., Sritularak, B., and Chanvorachote, P. (2017). Phoyunnanin E inhibits migration of non-small cell lung cancer cells via suppression of epithelial-to-mesenchymal transition and integrin  $\alpha$ v and integrin  $\beta$ 3. *BMC Complement. Altern. Med.* 17, 553. doi: 10.1186/s12906-017-2059-7
- Popat, R., Plesner, T., Davies, F., Cook, G., Cook, M., Elliott, P., et al. (2013). A phase 2 study of SRT501 (resveratrol) with bortezomib for patients with relapsed and/or refractory multiple myeloma. *Br. J. Haematol.* 160 (5), 714–717. doi: 10.1111/bjh.12154
- Poser, I., Dominguez, D., de Herreros, A. G., Varnai, A., Buettner, R., and Bosserhoff, A. K. (2001). Loss of E-cadherin expression in melanoma cells involves up-regulation of the transcriptional repressor snail. *J. Biol. Chem.* 276, 24661–24666. doi: 10.1074/jbc.M011224200
- Qian, Y. Y., Zhang, H., Hou, Y., Yuan, L., Li, G. Q., Guo, S. Y., et al. (2012). Celastrol orbiculatus extract inhibits tumor angiogenesis by targeting vascular endothelial growth factor signaling pathway and shows potent antitumor activity in hepatocarcinomas *in vitro* and *in vivo*. *Chin. J. Integr. Med.* 18, 752–760. doi: 10.1007/s11655-011-0819-7
- Qiao, W., Yao, Z., Zhang, W., and Duan, H. Q. (2009). Two new triterpenes from *Duchesnea indica*. *Chin. Chem. Lett.* 20, 572–575. doi: 10.1016/j.ccl.2008.12.052
- Qu, Y., Zhang, G., Ji, Y., Zhua, H., Lv, C., and Jiang, W. (2016). Protective role of gambogic acid in experimental pulmonary fibrosis *in vitro* and *in vivo*. *Phytomedicine* 23 (4), 350–358. doi: 10.1016/j.phymed.2016.01.011
- Raj, L., Ide, T., Gurkar, A. U., Foley, M., Schenone, M., Li, X., et al. (2011). Selective killing of cancer cells by a small molecule targeting the stress response to ROS. *Nature* 475, 231e234. doi: 10.1038/nature10167
- Rastaldi, M. P. (2006). Epithelial-mesenchymal transition and its implications for the development of renal tubulointerstitial fibrosis. *J. Nephrol.* 19 (4), 407–412.
- Russo, M. A., Sansone, L., Polletta, L., Runci, A., Rashid, M. M., De Santis, E., et al. (2014). Sirtuins and resveratrol-derived compounds: a model for understanding the beneficial effects of the Mediterranean diet. *Endocr. Metab. Immune Disord. Drug Targets* 14 (4), 300–308. Review. doi: 10.2174/1871530314666140709093305
- Ryu, Y., Jin, L., Kee, H. J., Piao, Z. H., Cho, J. Y., Kim, G. R., et al. (2016). Gallic acid prevents isoproterenol-induced cardiac hypertrophy and fibrosis through regulation of JNK2 signaling and Smad3 binding activity. *Sci. Rep.* 6, 34790. doi: 10.1038/srep34790
- Sarkar, S., Mandal, C., Sangwan, R., and Mandal, C. (2014). Coupling G2/M arrest to the Wnt/ $\beta$ -catenin pathway restrains pancreatic adenocarcinoma. *Endocr. Relat. Cancer* 21 (1), 113–125. doi: 10.1530/ERC-13-0315
- Sato, M., Muragaki, Y., Saika, S., Roberts, A. B., and Ooshima, A. (2003). Targeted disruption of TGF- $\beta$ 1/Smad3 signaling protects against renal tubulointerstitial fibrosis induced by unilateral ureteral obstruction. *J. Clin. Invest.* 112 (10), 1486–1494. doi: 10.1172/JCI200319270
- Savagner, P. (2010). The epithelial-mesenchymal transition (EMT) phenomenon. *Ann. Oncol.* 21 (Suppl 7), vii89–vii92. doi: 10.1093/annonc/mdq292
- Sehitoglu, M. H., Farooqi, A. A., Qureshi, M. Z., Butt, G., and Aras, A. (2014). Anthocyanins: targeting of signaling networks in cancer cells. *Asian Pac. J. Cancer Prev.* 15, 2379–2381. doi: 10.7314/APJCP.2014.15.5.2379
- Shakibaei, M., Harikumar, K. B., and Aggarwal, B. B. (2009). Resveratrol addition: to die or not to die. *Mol. Nutr. Food Res.* 53, 115–128. doi: 10.1002/mnfr.200800148
- Shankar, S., Nall, D., Tang, S. N., Meeker, D., Passarini, J., Sharma, J., et al. (2011). Resveratrol inhibits pancreatic cancer stem cell characteristics in human and KrasG12D transgenic mice by inhibiting pluripotency maintaining factors and epithelial-mesenchymal transition. *PLoS One* 316 (1), e16530. doi: 10.1371/journal.pone.0016530
- Sharma, R. A., Euden, S. A., Platten, S. L., Cooke, D. N., Shafayat, A., Hewitt, H. R., et al. (2004). Phase I clinical trial of oral curcumin: biomarkers of systemic activity and compliance. *Clin. Cancer Res.* 10, 6847–6854. doi: 10.1158/1078-0432.CCR-04-0744
- Shen, K. H., Liao, A. C., Hung, J. H., Lee, W. J., Hu, K. C., Lin, P. T., et al. (2014).  $\alpha$ -Solane inhibits invasion of human prostate cancer cell by suppressing epithelial-mesenchymal transition and MMPs expression. *Molecules* 1119 (8), 11896–11914. doi: 10.3390/molecules190811896
- Shen, X. C., Yang, Y. P., Xiao, T. T., Peng, J., and Liu, X. D. (2011). Protective effect of oxymatrine on myocardial fibrosis induced by acute myocardial infarction in rats involved in TGF- $\beta$ 1-Smad signal pathway. *J. Asian Nat. Prod. Res.* 13 (3), 215–224. doi: 10.1080/10286020.2010.550883
- Sheu, M. L., Chiang, C. K., Tsai, K. S., Ho, F. M., Weng, T. I., Wu, H. Y., et al. (2008). Inhibition of NADPH oxidase-related oxidative stress-triggered signaling by honokiol suppresses high glucose-induced human endothelial cell apoptosis. *Free Radic. Biol. Med.* 44, 2043–2050. doi: 10.1016/j.freeradbiomed.2008.03.014
- Shi, G. F., and Li, Q. (2005). Effects of oxymatrine on experimental hepatic fibrosis and its mechanism *in vivo*. *World J. Gastroenterol.* 11 (2), 268–271. doi: 10.3748/wjg.v11.i2.268
- Shibata, S., Marushima, H., Asakura, T., Matsuura, T., Eda, H., Aoki, K., et al. (2009). Three-dimensional culture using a radial flow bioreactor induces matrix metalloproteinase 7-mediated EMT-like process in tumor cells via TGF $\beta$ 1/Smad pathway. *Int. J. Oncol.* 34 (5), 1433–1448.
- Song, Y. H., Sun, H., Zhang, A., Yan, G., Han, Y., and Wang, X. (2014). Plant-derived natural products as leads to anti-cancer drugs. *J. Med. Plant Herb. Ther. Res.* 2, 6–15.



- Su, N.-W., Wu, S.-H., Chi, C.-W., Liu, C.-J., Tsai, T.-H., and Chen, Y.-J. (2017). Metronomic cordycepin therapy prolongs survival of oral cancer-bearing mice and inhibits epithelial-mesenchymal transition. *Molecules* 22, 629. doi: 10.3390/molecules22040629
- Subramani, R., Gonzalez, E., Arumugam, A., Nandy, S., Gonzalez, V., Medel, J., et al. (2016). Nimbolide inhibits pancreatic cancer growth and metastasis through ROS-mediated apoptosis and inhibition of epithelial-to-mesenchymal transition. *Sci. Rep.* 6, 19819. doi: 10.1038/srep19819
- Subramani, R., Gonzalez, E., Nandy, S. B., Arumugam, A., Camacho, F., Medel, J., et al. (2017). Gedunin inhibits pancreatic cancer by altering sonic hedgehog signaling pathway. *Oncotarget* 8 (7), 10891–10904. doi: 10.18632/oncotarget.8055
- Sun, L. N., Chen, Z. X., Liu, X. C., Liu, H. Y., Guan, G. J., and Liu, G. (2014). Curcumin ameliorates epithelial-to mesenchymal transition of podocytes in vivo and in vitro via regulating caveolin-1. *Biomed. Pharmacother.* 68 (8), 1079–1088. doi: 10.1016/j.biopha.2014.10.005
- Sun, M., Zhang, N., Wang, X., Cai, C., Cun, J., Li, Y., et al. (2014). Nitidine chloride induces apoptosis, cell cycle arrest, and synergistic cytotoxicity with doxorubicin in breast cancer cells. *Tumour Biol.* 35 (10), 10201–10212. doi: 10.1007/s13277-014-2327-9
- Sun, M., Zhang, N., Wang, X., Li, Y., Qi, W., Zhang, H., et al. (2016). Hedgehog pathway is involved in nitidine chloride induced inhibition of epithelial-mesenchymal transition and cancer stem cells-like properties in breast cancer cells. *Cell Biosci.* 6, 44. doi: 10.1186/s13578-016-0104-8
- Sutariya and Brijesh, S. (2017). Betanin, isolated from fruits of *Opuntia elatior* Mill attenuates renal fibrosis in diabetic rats through regulating oxidative stress and TGF- $\beta$  pathway. *J. Ethnopharmacol.* 198, 432–443. doi: 10.1016/j.jep.2016.12.048
- Tan, C., Mui, A., and Dedhar, S. (2002). Integrin-linked kinase regulate inducible nitric oxide synthase and cyclooxygenase-2 expression in an NF- $\kappa$ B-dependent manner. *J. Biol. Chem.* 277, 3109–3116. doi: 10.1074/jbc.M108673200
- Thiery, J. P., Acloque, H., Huang, R. Y., and Nieto, M. A. (2009). Epithelial-mesenchymal transitions in development and disease. *Cell* 139, 871–890. doi: 10.1016/j.cell.2009.11.007
- Tillhon, M., Guaman Ortiz, L. M., Lombardi, P., and Scovassi, A. I. (2012). Berberine: new perspectives for old remedies. *Biochem. Pharmacol.* 84, 1260–1267. doi: 10.1016/j.bcp.2012.07.018
- Troussard, A. A., Costello, P., Yoganathan, T. N., Kumagai, S., Roskelley, C. D., and Dedhar, S. (2000). The integrin linked kinase (ILK) induces an invasive phenotype via AP-1 transcription factor-dependent upregulation of matrix metalloproteinase 9 (MMP-9). *Oncogene* 16, 5444–5452. doi: 10.1038/sj.onc.1203928
- Tsai, J. H., Hsu, L. S., Lin, C. L., Hong, H. M., Pan, M. H., Way, T.-D., et al. (2013). 3,5,4'-Trimethoxystilbene, a natural methoxylated analog of resveratrol, inhibits breast cancer cell invasiveness by downregulation of PI3K/Akt and Wnt/beta-catenin signaling cascades and reversal of epithelial-mesenchymal transition. *Toxicol. Appl. Pharmacol.* 272, 746–756. doi: 10.1016/j.taap.2013.07.019
- Unahabhokha, T., Chanvorachote, P., and Pongrakhananon, V. (2016). The attenuation of epithelial to mesenchymal transition and induction of anoikis by gigantol in human lung cancer H460 cells. *Tumour Biol.* 37 (7), 8633–8641. doi: 10.1007/s13277-015-4717-z
- Vega, S., Morales, A. V., Ocaña, O. H., Valdés, F., Fabregat, I., and Nieto, M. A. (2004). Snail blocks the cell cycle and confers resistance to cell death. *Gene Dev.* 18, 1131–1143. doi: 10.1101/gad.294104
- Venkatesha, S. H., Yu, H., Rajaiiah, R., Tong, L., and Moudgil, K. D. (2011). Celastrol-derived celastrol suppresses autoimmune arthritis by modulating antigen-induced cellular and humoral effector responses. *J. Biol. Chem.* 286 (17), 15138–15146. doi: 10.1074/jbc.M111.226365
- Vergara, D., Valente, C. M., Tinelli, A., Siciliano, C., Lorusso, V., Acierno, R., et al. (2011). Resveratrol inhibits the epidermal growth factor-induced epithelial mesenchymal transition in MCF-7 cells. *Cancer Lett.* 310 (1), 1–8. doi: 10.1016/j.canlet.2011.04.009
- Vergara, D., et al. (2014). Antitumor activity of the dietary diterpene carnosol against a panel of human cancer cell lines. *Food Funct.* 5, 1261–1269. doi: 10.1039/c4fo00023d
- von Gise, A., and Pu, W. T. (2012). Endocardial and epicardial epithelial to mesenchymal transitions in heart development and disease. *Circ. Res.* 110 (12), 1628–1645. doi: 10.1161/CIRCRESAHA.111.259960
- Vuddanda, P. R., Chakraborty, S., and Singh, S. (2010). Berberine: a potential phytochemical with multispectrum therapeutic activities. *Expert Opin. Invest. Drugs* 19, 1297–1307. doi: 10.1517/13543784.2010.517745
- Wallerath, T., Deckert, G., Ternes, T., Anderson, H., Li, H., Witte, K., et al. (2002). Resveratrol, a polyphenolic phytoalexin present in red wine, enhances expression and activity of endothelial nitric oxide synthase. *Circulation* 106 (13), 1652–1658. doi: 10.1161/01.CIR.0000029925.18593.5C
- Wang, J., Qiao, L., Li, Y., and Yang, G. (2008). Ginsenoside Rb1 attenuates intestinal ischemia-reperfusion-induced liver injury by inhibiting NF- $\kappa$ B activation. *Exp. Mol. Med.* 40, 686–698. doi: 10.3858/emmm.2008.40.6.686
- Wang, Z., Jiang, W., Zhang, Z., Qian, M., and Du, B. (2012). Nitidine chloride inhibits LPS-induced inflammatory cytokines production via MAPK and NF- $\kappa$ B pathway in RAW 264.7 cells. *J. Ethnopharmacol.* 144 (1), 145–150. doi: 10.1016/j.jep.2012.08.041
- Wang, H., Zhang, H., Tang, L., Chen, H., Wu, C., Zhao, M., et al. (2013). Resveratrol inhibits TGF- $\beta$ 1-induced epithelial-to-mesenchymal transition and suppresses lung cancer invasion and metastasis. *Toxicologia* 303, 139–146. doi: 10.1016/j.tox.2012.09.017
- Wang, D., Zou, Y., Zhuang, X., Chen, S., Lin, Y., Li, W., et al. (2017a). Sulforaphane suppresses EMT and metastasis in human lung cancer through miR-616-5p-mediated GSK3 $\beta$ / $\beta$ -catenin signaling pathways. *Acta Pharmacol. Sin.* 38 (2), 241–251. doi: 10.1038/aps.2016.122
- Wang, H., Gu, H., Feng, J., Qian, Y., Yang, L., Jin, F., et al. (2017b). Celastrol orbiculatus extract suppresses the epithelial-mesenchymal transition by mediating cytoskeleton rearrangement via inhibition of the Cofilin 1 signaling pathway in human gastric cancer. *Oncol. Lett.* 14 (3), 2926–2932. doi: 10.3892/ol.2017.6470
- Wang, W., Zhou, P. H., Hu, W., Xu, C. G., Zhou, X. J., Liang, C. Z., et al. (2017c). Cryptotanshinone hinders renal fibrosis and epithelial transdifferentiation in obstructive nephropathy by inhibiting TGF  $\beta$ 1/Smad3/integrin  $\beta$ 1 signal. *Oncotarget* 9 (42), 26625–26637. doi: 10.18632/oncotarget.23803
- Wang, Z., Liu, Z., Yu, G., Nie, X., Jia, W., Liu, R., et al. (2018). Paeoniflorin inhibits migration and invasion of human glioblastoma cells via suppression transforming growth factor  $\beta$ -induced epithelial-mesenchymal transition. *Neurochem. Res.* 43 (3), 760–774. doi: 10.1007/s11064-018-2478-y
- Wen, Y. C., Lee, W. J., Tan, P., Yang, S. F., Hsiao, M., Lee, L. M., et al. (2015). By inhibiting snail signaling and miR-23a-3p, osthole suppresses the EMT-mediated metastatic ability in prostate cancer. *Oncotarget* 6 (25), 21120–21136. doi: 10.18632/oncotarget.4229
- Widodo, N., Kaur, K., Shrestha, B. G., Takagi, Y., Ishii, T., Wadhwa, R., et al. (2007). Selective killing of cancer cells by leaf extract of *Ashwagandha*: identification of a tumor-inhibitory factor and the first molecular insights to its effect. *Clin. Cancer Res.* 13, 2298–2306. doi: 10.1158/1078-0432.CCR-06-0948
- White, C. M., and Lee, J. Y. (2019). The impact of turmeric or its curcumin extract on nonalcoholic fatty liver disease: a systematic review of clinical trials. *Pharm. Pract. (Granada)* 17 (1), 1350. doi: 10.18549/PharmPract.2019.1.1350
- Wong, K. F., Yuan, Y., and Luk, J. M. (2012). Tripterygium wilfordii bioactive compounds as anticancer and anti-inflammatory agents. *Clin. Exp. Pharmacol. Physiol.* 39 (3), 311–320. doi: 10.1111/j.1440-1681.2011.05586.x
- Wrighton, K. H., Lin, X., and Feng, X. H. (2009). Phospho-control of TGF-beta superfamily signaling. *Cell Res.* 19, 8–20. doi: 10.1038/cr.2008.327
- Wu, L., Li, Q., and Liu, Y. (2014). Polyphyllin D induces apoptosis in K562/A02 cells through G2/M phase arrest. *J. Pharm. Pharmacol.* 66, 713–721. doi: 10.1111/jphp.12188
- Wu, X., Zeng, W. Z., Jiang, M. D., Qin, J. P., and Xu, H. (2008). Effect of Oxymatrine on the TGF beta-Smad signaling pathway in rats with CCl4-induced hepatic fibrosis. *World J. Gastroenterol.* 14 (13), 2100–2105. doi: 10.3748/wjg.14.2100
- Xiao, Z., Chen, C., Meng, T., Zhang, W., and Zhou, Q. (2016). Resveratrol attenuates renal injury and fibrosis by inhibiting transforming growth factor-beta pathway on matrix metalloproteinase 7. *Exp. Biol. Med.* 241, 140–146. doi: 10.1177/1535370215598401
- Xiao, S., Zhang, M., Liang, Y., and Wang, D. (2017). Celastrol synergizes with oral nifedipine to attenuate hypertension in preeclampsia: a randomized, placebo-controlled, and double blinded trial. *J. Am. Soc. Hypertens.* 11 (9), 598–603. doi: 10.1016/j.jash.2017.07.004
- Xing, S., Yu, W., Zhang, X., Luo, Y., Lei, Z., Huang, D., et al. (2018). Isoviolanthin extracted from *Dendrobium officinale* reverses TGF- $\beta$ 1-mediated epithelial-mesenchymal transition in hepatocellular carcinoma cells via deactivating the TGF- $\beta$ /Smad and PI3K/Akt/mTOR signaling pathways. *Int. J. Mol. Sci.* 19 (6), E1556. doi: 10.3390/ijms19061556



- Xu, T., Wu, X., Chen, Q., Zhu, S., Liu, Y., Pan, D., et al. (2014). The anti-apoptotic and cardioprotective effects of salvianolic acid a on rat cardiomyocytes following ischemia/reperfusion by DUSP-mediated regulation of the ERK1/2/JNK pathway. *PLoS One* 9 (7), e102292. doi: 10.1371/journal.pone.0102292
- Xu, Y., Lou, Z., and Lee, S. H. (2017). Arctigenin represses TGF- $\beta$ -induced epithelial mesenchymal transition in human lung cancer cells. *Biochem. Biophys. Res. Commun.* 493 (2), 934–939. doi: 10.1016/j.bbrc.2017.09.117
- Xu, Q., Zong, L., Chen, X., Jiang, Z., Nan, L., Li, J., et al. (2015). Resveratrol in the treatment of pancreatic cancer. *Ann. N. Y. Acad. Sci.* 1348, 10–19. doi: 10.1111/nyas.12837
- Xu, J., Y., Wang, J. H., and Xue, W. (2009). Clinical analysis of the preventive effect of Schisandra chinensis on anti-tuberculosis therapy induced liver injury. *J. Yichun College* 36 (6), 65–67.
- Yáñez-Mó, M., Lara-Pezzi, E., Selgas, R., Ramírez-Huesca, M., Domínguez-Jiménez, C., Jiménez-Heffernan, J. A., et al. (2003). Peritoneal dialysis and epithelial-to-mesenchymal transition of mesothelial cells. *N. Engl. J. Med.* 348 (5), 403–413.
- Yan, F., Zhang, G. H., Feng, M., Zhang, W., Zhang, J. N., Dong, W. Q., et al. (2015). Glucagon-like Peptide 1 protects against hyperglycemic-induced endothelial-to-mesenchymal transition and improves myocardial dysfunction by suppressing Poly(ADP-Ribose) polymerase 1 activity. *Mol. Med.* 21, 15–25. doi: 10.2119/molmed.2014.00259
- Yang, Y. T., Weng, C. J., Ho, C. T., and Yen, G. C. (2009). Resveratrol analog-3,5,4-trimethoxytrans-stilbene inhibits invasion of human lung adenocarcinoma cells by suppressing the MAPK pathway and decreasing matrix metalloproteinase-2 expression. *Mol. Nutr. Food Res.* 53, 407–416. doi: 10.1002/mnfr.200800123
- Yang, L., Xing, S., Wang, K., Yi, H., and Du, B. (2018). Paeonol attenuates aging MRC-5 cells and inhibits epithelial-mesenchymal transition of premalignant HaCaT cells induced by aging MRC-5 cell-conditioned medium. *Mol. Cell Biochem.* 439 (1–2), 117–129. doi: 10.1007/s11010-017-3141-7
- Yang, M., Akbar, U., and Mohan, C. (2019). Curcumin in autoimmune and rheumatic diseases. *Nutrients* 2, 11(5). doi: 10.3390/nu11051004
- Yin, J., Xing, H., and Ye, J. (2008). Efficacy of berberine in patients with type 2 diabetes mellitus. *Metabolism* 57 (5), 712–717. doi: 10.1016/j.metabol.2008.01.013
- Yoo, K. H., Thornhill, B. A., Forbes, M. S., Coleman, C. M., Marcinko, E. S., Liaw, L., et al. (2006). Osteopontin regulates renal apoptosis and interstitial fibrosis in neonatal chronic unilateral ureteral obstruction. *Kidney Int.* 70 (10), 1735–41. doi: 10.1038/sj.ki.5000357
- Yu, Q., Li, Q., Lu, P., and Chen, Q. (2014). Polyphyllin D induces apoptosis in U87 human glioma cells through the c-Jun NH2-terminal kinase pathway. *J. Med. Food* 17, 1036–1042. doi: 10.1089/jmf.2013.2957
- Yuan, T., Chen, Y., Zhang, H., Fang, L., and Du, G. (2017). Salvianolic acid A, a component of salvia miltiorrhiza, attenuates endothelial-mesenchymal transition of HPAECs induced by hypoxia. *Am. J. Chin. Med.* 45 (6), 1185–1200. doi: 10.1142/S0192415X17500653
- Yuan, X. P., Liu, L. S., Fu, Q., and Wang, C. X. (2012). Effects of ligustrazine on ureteral obstruction-induced renal tubulointerstitial fibrosis. *Phytother. Res.* 26 (5), 697–703. doi: 10.1002/ptr.3630
- Zang, M. D., Hu, L., Fan, Z. Y., Wang, H. X., Zhu, Z. L., Cao, S., et al. (2017). Luteolin suppresses gastric cancer progression by reversing epithelial-mesenchymal transition via suppression of the Notch signaling pathway. *J. Transl. Med.* 15 (1), 52. doi: 10.1186/s12967-017-1151-6
- Zeng, J., Dou, Y., Guo, J., Wu, X., and Dai, Y. (2013). Paeoniflorin de Paeonia lactiflora previene Fibrosis interstitial renal inducida por obstrucción ureteral unilateral en ratones. *Fitomedicina* 20 (8–9), 753–759. doi: 10.1016/j.phymed.2013.02.010
- Zhang, H., Qian, Y., Liu, Y., Li, G., Cui, P., Zhu, Y., et al. (2012a). Celastrus orbiculatus extract induces mitochondrial-mediated apoptosis in human hepatocellular carcinoma cells. *J. Tradit. Chin. Med.* 32, 621–626. doi: 10.1016/S0254-6272(13)60081-3
- Zhang, L., Jiang, G., Yao, F., He, Y., Liang, G., Zhang, Y., et al. (2012b). Growth inhibition and apoptosis induced by osthole, a natural coumarin, in hepatocellular carcinoma. *PLoS One* 7 (5), e37865. doi: 10.1371/journal.pone.0037865
- Zhang, J., Cao, H., Zhang, B., Cao, H., Xu, X., Ruan, H., et al. (2013). Berberine potentially attenuates intestinal polyps growth in ApcMin mice and familial adenomatous polyposis patients through inhibition of Wnt signalling. *J. Cell. Mol. Med.* 17 (11), 1484–1493. doi: 10.1111/jcmm.12119
- Zhang, L., Tao, L., Shi, T., Zhang, F., Sheng, X., Cao, Y., et al. (2015). Paeonol inhibits B16F10 melanoma metastasis *in vitro* and *in vivo* via disrupting proinflammatory cytokines-mediated NF- $\kappa$ B and STAT3 pathways. *IUBMB Life* 67, 778–788. doi: 10.1002/iub.1435
- Zhang, Z., Liu, T., Yu, M., Li, K., and Li, W. (2018). The plant alkaloid tetrandrine inhibits metastasis via autophagy-dependent Wnt/ $\beta$ -catenin and metastatic tumor antigen 1 signaling in human liver cancer cells. *J. Exp. Clin. Cancer Res.* 37, 7. doi: 10.1186/s13046-018-0678-6
- Zhao, M., Lau, S. T., Leung, P. S., Che, C. T., and Lin, Z. X. (2011). Seven quassinoids from Fructus Bruceae with cytotoxic effects on pancreatic adenocarcinoma cell lines. *Phytother. Res.* 25 (12), 1796–800. doi: 10.1002/ptr.3477
- Zhao, K., Yang, Y., Xue, P.-F., and Tu, P.-F. (2013). Chemical constituents from barks of *Cinnamomum cassia* growing in China. *Chin. Tradit. Herb. Drugs* 44, 2358–2363. doi: 10.7501/j.issn.0253-2670.2013.17.005
- Zheng, J., Son, D. J., Gu, S. M., Woo, J. R., Ham, Y. W., Lee, H. P., et al. (2016). Piperlongumine inhibits lung tumor growth via inhibition of nuclear factor kappa B signaling pathway. *Sci. Rep.* 6, 26357. doi: 10.1038/srep26357
- Zheng, Y., Nan, H., Hao, M., Song, C., Zhou, Y., and Gao, Y. (2013). Antiproliferative effects of protopanaxadiol ginsenosides on human colorectal cancer cells. *Biomed. Rep.* 1, 555–558. doi: 10.3892/br.2013.104
- Zhou, L. X., Liang, L., Zhang, L., Yang, N., Nagao, H., Wu, C., et al. (2016). MiR-27a-3p functions as an oncogene in gastric cancer by targeting BTG2. *Oncotarget* 7, 51943e51954. doi: 10.18632/oncotarget.10460
- Zhou, Y., Mao, H., Li, S., Cao, S., Li, Z., Zhuang, S., et al. (2010). HSP72 inhibits Smad3 activation and nuclear translocation in renal epithelial-to-mesenchymal transition. *J. Am. Soc. Nephrol.* 21, 598–609. doi: 10.1681/ASN.2009050552
- Zhou, J., Zhu, Y. F., Chen, X. Y., Han, B., Li, F., Chen, J. Y., et al. (2017). Black rice-derived anthocyanins inhibit HER-2-positive breast cancer epithelial-mesenchymal transition-mediated metastasis *in vitro* by suppressing FAK signaling. *Int. J. Mol. Med.* 40 (6), 1649–1656. doi: 10.3892/ijmm.2017.3183
- Zhu, Z., Zhao, Y., Li, J., Tao, L., Shi, P., Wei, Z., et al. (2016). Cryptotanshinone, a novel tumor angiogenesis inhibitor, destabilizes tumor necrosis factor- $\alpha$  mRNA via decreasing nuclear-cytoplasmic translocation of RNA-binding protein HuR. *Mol. Carcinog.* 55 (10), 1399–1410. doi: 10.1002/mc.22383

**Conflict of Interest Statement:** The authors declare that the research was conducted in the absence of any commercial or financial relationships that could be construed as a potential conflict of interest.

Copyright © 2019 Avila-Carrasco, Majano, Sánchez-Tomé, Selgas, López-Cabrera, Aguilera and González Mateo. This is an open-access article distributed under the terms of the Creative Commons Attribution License (CC BY). The use, distribution or reproduction in other forums is permitted, provided the original author(s) and the copyright owner(s) are credited and that the original publication in this journal is cited, in accordance with accepted academic practice. No use, distribution or reproduction is permitted which does not comply with these terms.



OPEN ACCESS

**Edited by:**

Annalisa Bruno,  
Università degli Studi G. d'Annunzio  
Chieti e Pescara, Italy

**Reviewed by:**

Syamantak Majumder,  
Birla Institute of Technology and  
Science, India  
Paul J. Higgins,  
Albany Medical College,  
United States  
William Dean Carlson,  
Massachusetts General Hospital  
and Harvard Medical School,  
United States

**\*Correspondence:**

Alessandra Marchetti  
alessandra.marchetti@uniroma1.it  
Marco Tripodi  
marco.tripodi@uniroma1.it

<sup>†</sup>These authors have contributed  
equally to this work

**Specialty section:**

This article was submitted to  
Inflammation Pharmacology,  
a section of the journal  
Frontiers in Pharmacology

**Received:** 05 April 2019

**Accepted:** 24 July 2019

**Published:** 30 August 2019

**Citation:**

Bisceglia F, Battistelli C, Noce V,  
Montaldo C, Zammataro A,  
Strippoli R, Tripodi M, Amicone L  
and Marchetti A (2019) TGF $\beta$   
Impairs HNF1 $\alpha$  Functional Activity in  
Epithelial-to-Mesenchymal Transition  
Interfering With the Recruitment of  
CBP/p300 Acetyltransferases.  
Front. Pharmacol. 10:942.  
doi: 10.3389/fphar.2019.00942

# TGF $\beta$ Impairs HNF1 $\alpha$ Functional Activity in Epithelial-to-Mesenchymal Transition Interfering With the Recruitment of CBP/p300 Acetyltransferases

**Francesca Bisceglia<sup>1†</sup>, Cecilia Battistelli<sup>1†</sup>, Valeria Noce<sup>1</sup>, Claudia Montaldo<sup>2</sup>, Agatino Zammataro<sup>1</sup>, Raffaele Strippoli<sup>1,2</sup>, Marco Tripodi<sup>1,2\*</sup>, Laura Amicone<sup>1</sup> and Alessandra Marchetti<sup>1\*</sup>**

<sup>1</sup> Istituto Pasteur Italia–Fondazione Cenci Bolognietti, Department of Molecular Medicine, Sapienza University of Rome, Rome, Italy, <sup>2</sup> National Institute for Infectious Diseases L. Spallanzani, IRCCS, Rome, Italy

The cytokine transforming growth factor  $\beta$  (TGF $\beta$ ) plays a crucial role in the induction of both epithelial-to-mesenchymal transition (EMT) program and fibro-cirrhotic process in the liver, where it contributes also to organ inflammation following several chronic injuries. All these pathological situations greatly increase the risk of hepatocellular carcinoma (HCC) and contribute to tumor progression. In particular, late-stage HCCs are characterized by constitutive activation of TGF $\beta$  pathway and by an EMT molecular signature leading to the acquisition of invasive and metastatic properties. In these pathological conditions, the cytokine has been shown to induce the transcriptional downregulation of HNF1 $\alpha$ , a master regulator of the epithelial/hepatocyte differentiation and of the EMT reverse process, the mesenchymal-to-epithelial transition (MET). Therefore, the restoration of HNF1 $\alpha$  expression/activity has been proposed as targeted therapeutic strategy for liver fibro-cirrhosis and late-stage HCCs. In this study, TGF $\beta$  is found to trigger an early functional inactivation of HNF1 $\alpha$  during EMT process that anticipates the effects of the transcriptional downregulation of its own gene. Mechanistically, the cytokine, while not affecting the HNF1 $\alpha$  DNA-binding capacity, impaired its ability to recruit CBP/p300 acetyltransferases on target gene promoters and, consequently, its transactivating function. The loss of HNF1 $\alpha$  capacity to bind to CBP/p300 and HNF1 $\alpha$  functional inactivation have been found to correlate with a change of its posttranslational modification profile. Collectively, the results obtained in this work unveil a new level of HNF1 $\alpha$  functional inactivation by TGF $\beta$  and contribute to shed light on the early events triggering EMT in hepatocytes. Moreover, these data suggest that the use of HNF1 $\alpha$  as anti-EMT tool in a TGF $\beta$ -containing microenvironment may require the design of new therapeutic strategies overcoming the TGF $\beta$ -induced HNF1 $\alpha$  inactivation.

**Keywords:** HNF1 $\alpha$ , TGF $\beta$ , CBP/p300, histone acetylation, EMT, fibrosis, HCC

## INTRODUCTION

Transforming growth factor  $\beta$  (TGF $\beta$ ) has emerged as a major microenvironmental factor playing a role in all phases of chronic liver diseases (Fabregat et al., 2016). This cytokine, in fact, is primarily involved in liver inflammation (by stimulating lymphocytes to produce inflammatory cytokines), in fibrosis (by activating the trans-differentiation of hepatic stellate cells to myofibroblasts and the subsequent production of large amount of extracellular matrix), and in the onset of hepatocellular carcinoma (HCC) that, in almost all the cases, develops on the described pathological tissue background (Amicone and Marchetti, 2018). Furthermore, once the tumor is established, the continuous production of TGF $\beta$  by both tumor and nontumor tissue, contributes to its growth and metastasization, mainly through the induction of epithelial-to-mesenchymal transition (EMT) in transformed hepatocytes (Zavadil and Bottinger, 2005). Accordingly, an unbalanced level of the cytokine in the tumor niche and high amount of the circulating cytokine have been shown to contribute to tumor progression and to a poor prognosis (Amicone et al., 2002; Lee et al., 2012).

TGF $\beta$  is a well-known inducer of EMT in several types of epithelial cells. In hepatocytes, the cytokine induces the trans-differentiation process through the upregulation of EMT/mesenchymal genes (Xu et al., 2009) and the strong transcriptional downregulation of master regulators of epithelial/hepatocyte differentiation, such as HNF4 $\alpha$  and HNF1 $\alpha$  (Marchetti et al., 2013).

In particular, TGF $\beta$  was shown to interfere with *HNF4 $\alpha$*  and *HNF1 $\alpha$*  gene expression in hepatocytes by upregulating the EMT master gene *Snail*, a transcriptional inhibitor that, in turn, induces HNF4 $\alpha$  and HNF1 $\alpha$  transcriptional repression through the direct binding to their promoters (Cicchini et al., 2006; Cozzolino et al., 2013; Battistelli et al., 2017).

HNF4 $\alpha$  and HNF1 $\alpha$  are well-known master regulators of hepatocyte differentiation, able to drive a complex epithelial/hepatocyte transcriptional program. Recently, it has been shown that, in fully differentiated hepatocytes, HNF4 $\alpha$  and HNF1 $\alpha$  are responsible not only for the maintenance of the epithelial program but also for a stable and continuous inhibition of the mesenchymal one, through the transcriptional repression of EMT/mesenchymal genes (Noce et al., in press; Santangelo et al., 2011). Furthermore, these proteins have been largely described as mesenchymal-to-epithelial transition (MET) master genes and tumor suppressors. HNF4 $\alpha$  and HNF1 $\alpha$  expression is lost during liver fibrosis and HCC progression (Lazarevich et al., 2004; Lazarevich et al., 2010; Willson et al., 2013; Ni et al., 2017), while their exogenous expression triggers growth arrest in hepatoma cell lines (Lazarevich et al., 2004; Pelletier et al., 2011) and induces hepatocyte differentiation in dedifferentiated cells (Santangelo et al., 2011). Most significantly, HNF4 $\alpha$  and HNF1 $\alpha$  delivery in animal models attenuates liver fibrosis (Yue et al., 2010; Song et al., 2016) and inhibits growth of xenograft tumors (Ning et al., 2010; Zeng et al., 2011).

For all these reasons, HNF4 $\alpha$  and HNF1 $\alpha$  have been proposed as therapeutic molecules for HCC (Marchetti et al., 2015).

However, recent data from our laboratory suggested that, in a TGF $\beta$ -containing environment, such as that in which HCC

develops, the restoration of HNF4 $\alpha$  function is not effective in suppressing the malignant behavior. We unveiled, in fact, a functional inactivation of HNF4 $\alpha$  by TGF $\beta$  due to specific posttranslational modifications (PTMs) on the protein that correlate with the early loss of target gene promoters binding capacity (Cozzolino et al., 2013).

Here, we show that also HNF1 $\alpha$  is subjected to a further level of TGF $\beta$ -induced downregulation, other than the transcriptional one. While TGF $\beta$  does not interfere with the HNF1 $\alpha$  ability to bind to DNA, it negatively impairs HNF1 $\alpha$  activity affecting its capacity to interact with CBP/p300 histone acetyltransferases. The loss of CBP/p300 recruitment on regulatory regions of HNF1 $\alpha$  target genes, with consequent loss of a main transcription activating chromatin modification, prevents the HNF1 $\alpha$  transcriptional function. Furthermore, we correlated the functional inactivation of HNF1 $\alpha$  protein to a change in its PTM profile.

Altogether, our results demonstrate a new level of control of HNF1 $\alpha$  by TGF $\beta$  that can represent the first event in triggering EMT process in hepatocyte and disclose a potential limitation to the use of an exogenous molecule as therapeutic MET inducer and tumor suppressor tool. However, and notably, the described mechanisms could allow the design of new therapeutic approaches aimed at overcoming the inactivating effect of the cytokine.

## MATERIALS AND METHODS

### Cell Cultures and Treatments

Nontumorigenic murine hepatocytes (Amicone et al., 1997) and their Ras-transformed counterpart (Cozzolino et al., 2013) were grown on collagen-I-coated dishes in RPMI-1640 medium supplemented with 10% fetal bovine serum (GIBCO® Life Technology, Monza, Italy), 50 ng/ml epidermal growth factor, 30 ng/ml insulin-like growth factor II (PeproTech Inc., Rocky Hill, NJ, USA), 10  $\mu$ g/ml insulin (Roche, Mannheim, Germany), and antibiotics. Where indicated, cells were treated with 4 ng/ml of TGF $\beta$ 1 (PeproTech Inc., Rocky Hill, NJ, USA) for the indicated time. As previously reported, cell lines utilized in this study undergo EMT following TGF $\beta$  treatment (Cozzolino et al., 2013; Grassi et al., 2015; De Santis Puzzonina et al., 2016; Battistelli et al., 2018).

HNF1 $\alpha$ -overexpressing cells were obtained by transient transfection with pLPCX-HNF1 $\alpha$ <sup>Myc</sup> (carrying the rat HNF1 $\alpha$  cDNA, Myc-tagged at the 5' end). Control cell lines were obtained by transfection with the empty vector. Nontumorigenic and Ras-transformed hepatocytes were transfected with Lipofectamine 2000 (Invitrogen, San Diego, CA) or FuGENE® HD Transfection Reagent (Promega Corporation, Madison, WI), respectively, according to the manufacturer's protocol, and collected 48 h after transfection.

### RNA Extraction, Reverse Transcription, and Quantitative Real-Time PCR

Total RNAs were extracted with Total RNA Mini Kit (Geneaid) according to manufacturer's protocol and reverse-transcribed

using PrimeScript RT Master Mix (Takara, Dalian, China). cDNA was amplified by qPCR using GoTaq qPCR Master Mix (Promega Corporation, Madison, WI) in BioRad-iQ-iCycler. Relative amounts, calculated with the  $2^{(-\Delta C_t)}$  method, were normalized with respect to the housekeeping gene RPL34 (60S ribosomal protein L34) or 18S rRNA. The sequence of primers utilized are listed in **Table 1**.

## SDS-PAGE and Western Blotting

Cells were lysed in radioimmunoprecipitation assay buffer containing freshly added cocktail protease inhibitors [complete, ethylenediaminetetraacetic acid (EDTA)-free protease inhibitor cocktail; Sigma-Aldrich, St. Louis, MO]. Western Blots were performed as previously described (Cuzzolino et al., 2013) using the following primary antibodies: rabbit polyclonal α-HNF1α (NBP1-33596, 1:1000; Novus Biologicals, USA), rabbit polyclonal α-CBP/p300 (451, 1:1000; Santa Cruz Biotechnology Inc., Santa Cruz, CA, USA), rabbit monoclonal α-cyclin-dependent kinase 4 (CD22, 1:1000; Santa Cruz Biotechnology Inc., Santa Cruz, CA, USA), and mouse monoclonal α-glyceraldehyde 3-phosphate dehydrogenase (MAB374, 1:1000; Millipore Corp., Bedford, MA, USA). Blots were then incubated with horseradish-peroxidase-conjugated species-specific secondary antibodies (Bio-Rad, Hercules, CA, USA), followed by enhanced chemiluminescence reaction (Bio-Rad Laboratories Inc., Hercules, CA, USA). Densitometric analyses were performed with ImageJ.

## Immunofluorescence Staining

For indirect immunofluorescence analysis, cells were fixed in 4% paraformaldehyde, permeabilized with 0.2% Triton-X100, and incubated with α-HNF1α antibody (NBP1-33596, 1:50; Novus Biologicals, USA), α-Myc-Tag antibody (9B11, 1:200; Cell Signaling Technologies Inc. Danvers, USA), and E-cadherin antibody (610182, 1:50; BD Biosciences). Alexa Fluor 488-conjugated and Alexa Fluor-594-conjugated secondary antibodies (1:400; Molecular Probes, Eugene, OR,

USA) were utilized. Nuclei were stained with 4',6-diamidino-2-phenylindole (DAPI; Calbiochem Merck, Darmstadt, Germany). Images were examined with a Nikon Eclipse microscope (Nikon Corporation, Tokyo, Japan) equipped with a charge-coupled device camera. Digital images were acquired by Nikon NIS elements software (Nikon Corporation, Tokyo, Japan) and processed with Adobe Photoshop 7 software (Adobe Systems, Mountain View, CA). The same enhanced color levels were applied for all channels.

## Chromatin Immunoprecipitation

Chromatin immunoprecipitation (ChIP) analysis was performed as previously reported (Cuzzolino et al., 2016; Battistelli et al., 2017) using 5 μg of the following antibodies for the immunoprecipitation: goat polyclonal α-HNF1α (C-19; Santa Cruz Biotechnology Inc., Santa Cruz, CA, USA), rabbit polyclonal α-CBP (451; Santa Cruz Biotechnology Inc., Santa Cruz, CA, USA), rabbit polyclonal α-acetyl H3 (06-599; Millipore Corp., Bedford, MA, USA), normal rabbit antiserum (Millipore Corp., Bedford, MA, USA), and normal goat IgG (AB-108-C; R&D Systems, Minneapolis, USA) were used as negative controls. Equal amounts of immunoprecipitated DNA and relative controls were used for qPCR analysis, performed in triplicate. The list of primers utilized is shown in **Table 2**. qPCR analysis of the immunoprecipitated samples and of the negative controls (IgG) were both normalized to total chromatin input. The promoter of *Neurogenin 1*, a gene not expressed in hepatocytes, was used as negative control.

## Electrophoretic Mobility Shift Assay

Cells were scraped in cold phosphate-buffered saline (PBS), lysed in 10 mM Hepes pH 7.9, 1.5 mM MgCl<sub>2</sub>, 10 mM KCl, 0.1% NP40, 0.1 mM EDTA, 0.5 mM dithiothreitol (DTT), standard protease and phosphatase inhibitors, and centrifuged to pellet the nuclei. Nuclear proteins were extracted in 20 mM Hepes pH 7.9, 20% glycerol, 0.42 M NaCl, 1.5 mM MgCl<sub>2</sub>, 0.2 mM EDTA, 0.1%

**TABLE 1** | List of mouse primers used for RT-qPCR experiments.

Gene	Forward primer	Reverse primer
<i>HNF4α</i>	5'-TCTTCTTTGATCCAGATGCC-3'	5'-GGTCGTTGATGTAATCCTCC-3'
<i>HNF1α</i>	5'-TATCATGGCCTCGCTACCTG-3'	5'-ACTCCCATGCTGTTGATGA-3'
<i>TTR</i>	5'-CCATGAATTCGCGGATGTGG-3'	5'-TCAATTCTGGGGTTGCTGA-3'
<i>Albumin</i>	5'-TTCTGCGCACGTTCTTGTA-3'	5'-GCAGCACTTTTCCAGAGTGG-3'
<i>18S</i>	5'-ACGACCCATTGCAACGTCTG-3'	5'-GCACGGCGACTACCATCG-3'
<i>RPL34</i>	5'-GGAGCCCCATCCAGACTC-3'	5'-CGCTGGATATGGCTTTCCTA-3'

**TABLE 2** | List of mouse primers used for qPCR in ChIP experiments.

Promoter	Forward primer	Reverse primer
<i>Albumin</i>	5'-AGGAACCAATGAAATGCGAGG-3'	5'-AGACGAAGAGGAGGAGGAGA-3'
<i>HNF4α</i>	5'-ACTTGGGCTCCATAGCAAGA-3'	5'-CAGGACAGGCACAGACAAGA-3'
<i>Neurog1</i>	5'-CCTCCCGCGAGCATAAATTA-3'	5'-GCGATCAGATCAGCTCCTGT-3'
<i>RPL30</i>	5'-TAAGGCAGGAAGATGGTGG-3'	5'-CAGTGTGCTCAAAATCTATCC-3'



NP40, 0.5 mM DTT, and standard protease inhibitors. Protein concentrations were determined with the Bio-Rad Protein Assay Dye Reagent (Bio-Rad Laboratories, Hercules, CA).

For nonradioactive electrophoretic mobility shift assay (EMSA), biotin end-labeled oligonucleotide probes were obtained with the Biotin 3' End DNA Labeling Kit (Thermo Fisher Scientific, Waltham, MA, USA), according to manufacturer's protocol. The sequences of oligonucleotides used are the followings: for the mouse HNF4 $\alpha$  promoter, 5'-CGGGGTGATTTAACCATTAACTCCTACCCCT-3' and 5'-AGGGGTAGGAGTTAATGGTTAATCACCCCG-3' (the HNF1 $\alpha$  binding site is underlined); for the mouse ApoC3 promoter, 5'-CAGCAGGTGACCTTTGCCCAGCTCAC-3' and 5'-GTGAGCTGGGCAAAGGTCACCTGCTG-3' (the HNF4 $\alpha$  binding site is underlined).

Gel shift assays were performed using LightShift Chemiluminescent EMSA Kit (Thermo Fisher Scientific, Waltham, MA, USA), according to the manufacturer's protocol. The binding reaction was prepared in a final volume of 20  $\mu$ l incubating 1 $\times$  binding buffer, 2.5% glycerol, 5 mM MgCl<sub>2</sub>, 50 ng/ $\mu$ l PolydI-dC, 0.05% NP-40, and 10  $\mu$ g of nuclear extracts (except for the free probe sample) for 10' at 4°C. Then, 25 fmol of the double-strand biotinylated probe were added and the reaction conducted for further 20' at RT. Where specified, a 100-fold excess of unlabeled annealed oligonucleotide or 5  $\mu$ g of the following antibodies were added to the binding reaction before addition of nuclear extracts: rabbit polyclonal  $\alpha$ -HNF1 $\alpha$  (H-140; Santa Cruz Biotechnology Inc., Santa Cruz, CA, USA) or rabbit polyclonal  $\alpha$ -HNF1 $\alpha$  (NBP1-33596; Novus Biologicals) and mouse monoclonal  $\alpha$ -tubulin (TU-02; Santa Cruz Biotechnology Inc., Santa Cruz, CA, USA). Samples were loaded on a 6% nondenaturing polyacrylamide gel in 0.5 $\times$  tris borate EDTA and transferred to a nylon membrane (Biodyne B Nylon Membrane, Thermo Fisher Scientific, Waltham, MA, USA). After cross-linking to the membrane at 120 mJ/cm<sup>2</sup> for 1' with UV Stratalinker 1800 (Stratagene, San Diego, CA, USA), biotin-labeled DNA was detected using Chemiluminescent Nucleic Acid Detection Module Kit (Thermo Fisher Scientific, Waltham, MA, USA).

## Co-immunoprecipitation

Cells were lysed in IP lysis buffer (150 mM NaCl, 50 mM Tris-HCl pH 7.5, 2 mM EDTA, 1% Triton-X100, 10% glycerol) supplemented with protease and phosphatase inhibitors. One milligram of cell lysates, after preclearing with protein A-Sepharose (GE Healthcare, Little Chalfont, Buckinghamshire, UK), was incubated with 5  $\mu$ g of goat polyclonal  $\alpha$ -HNF1 $\alpha$  antibody (C-19; Santa Cruz Biotechnology Inc., Santa Cruz, CA, USA) or normal goat immunoglobulin G (IgG) (AB-108-C; R&D Systems, Minneapolis, USA) at 4°C overnight while rotating. Immunocomplexes were then incubated on a rotating platform for 3 h with protein A-sepharose at 4°C, washed in NetGel buffer (150 mM NaCl; 50 mM Tris-HCl pH 7.5; 1 mM EDTA; 0.1% NP-40; 0.25% gelatin), eluted and denatured in Laemmli buffer. Proteins from immunoprecipitation were resolved on sodium dodecyl sulfate polyacrylamide gel electrophoresis (SDS-PAGE) and transferred to nitrocellulose membrane

(Bio-Rad Laboratories, Hercules, CA). For immunoblotting, the following primary antibodies were used: rabbit polyclonal  $\alpha$ -HNF1 $\alpha$  (NBP1-33596, 1:2000; Novus Biologicals) and rabbit polyclonal  $\alpha$ -CBP (451, 1:1000; Santa Cruz Biotechnology, Santa Cruz, CA). Immune complexes were detected with horseradish peroxidase-conjugated species-specific secondary antiserum (Bio-Rad Laboratories, Hercules, CA), followed by enhanced chemiluminescence reaction (Bio-Rad Laboratories Inc., Hercules, CA, USA).

## Two-Dimensional Gel Electrophoresis

Two-dimensional gel electrophoresis (2-DE) was performed using IPGphor II (GE Healthcare) as previously described (Cozzolino et al., 2013). In brief, proteins (90  $\mu$ g) from nuclear extracts were precipitated with 100% acetone and then loaded on pH 3–10 IPG strips (IPGs) and electrofocused at 15,000 V/h at a maximum voltage of 5,000 V. The second-dimension separation was performed at a constant current of 50 mA for 2 h. Proteins were transferred to nitrocellulose membranes (Protran Nitrocellulose Transfer Membrane, Schleicher & Schuell, BD Biosciences), and Western blot was performed as described above with mouse monoclonal anti-Myc-Tag antibody (9B11, 1:1,000; Cell Signaling Technologies Inc. Danvers, USA).

## Statistical Analysis

Statistical significance was determined using paired one-tailed Student's *t*-test or one-sample Student's *t*-test. A *p* < 0.05 was considered statistically significant (\**p* < 0.05; \*\**p* < 0.01; \*\*\**p* < 0.001).

## RESULTS

### TGF $\beta$ Early Impairs HNF1 $\alpha$ Functional Activity

It has previously reported that TGF $\beta$  is able to interfere with the activity of the hepatocyte differentiation master gene HNF4 $\alpha$ , negatively controlling both gene expression and protein function (Santangelo et al., 2011; Cozzolino et al., 2013; Battistelli et al., 2017). These findings had seriously questioned the possibility of using HNF4 $\alpha$  as therapeutic molecule. In order to verify the possibility to use alternatively HNF1 $\alpha$  as MET inducer in a TGF $\beta$ -rich microenvironment, we explored the effect of this cytokine on the HNF1 $\alpha$  protein function.

To this aim, we utilized liver cell lines, already described in our laboratory, as models of hepatocytes at different stages of differentiation (Amicone et al., 1997; Bellovino et al., 1998; Grassi et al., 2015) and able to undergo EMT upon TGF $\beta$  treatment (Grassi et al., 2015; De Santis Puzzon et al., 2016). The first evidence of an additional level of HNF1 $\alpha$  negative control induced by TGF $\beta$  came from a time course analysis of HNF1 $\alpha$ -dependent gene expression regulation in hepatocytes treated with the cytokine.

**Figure 1A** shows that, as expected, TGF $\beta$  induced a significant and early transcriptional downregulation of HNF1 $\alpha$  (at 3 h of treatment) and of its target genes *HNF4 $\alpha$*  (at 6 h of treatment),

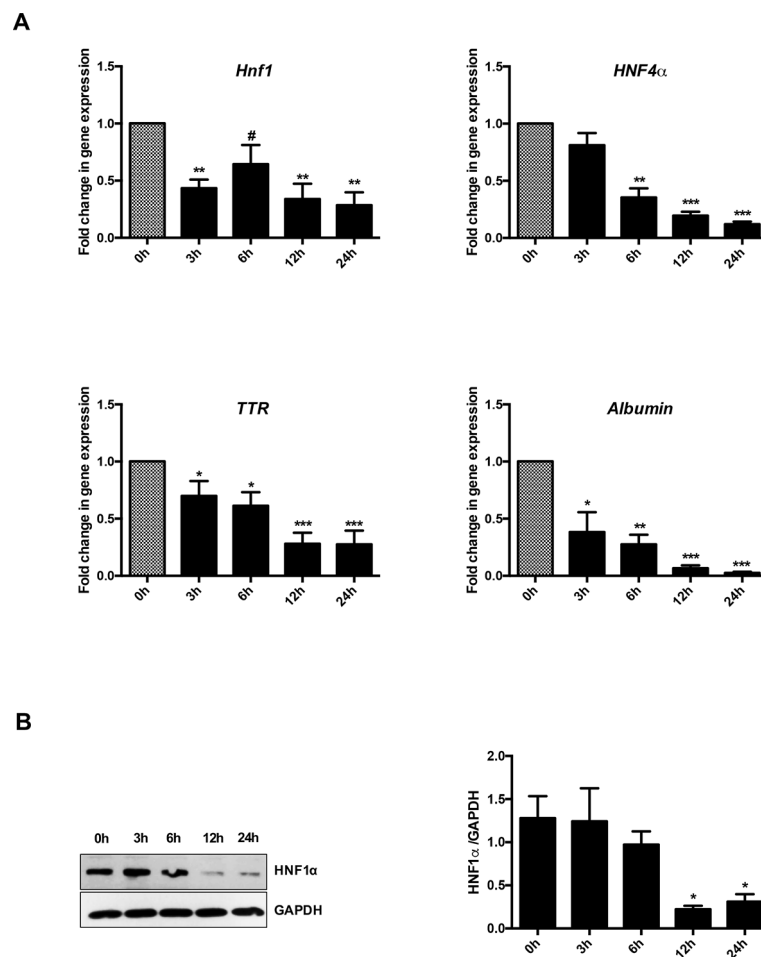


**FIGURE 1 |** Analysis of HNF1 $\alpha$  transcriptional activity in hepatocytes following transforming growth factor  $\beta$  (TGF $\beta$ ) treatment. **(A)** Gene expression analysis by RT-qPCR of HNF1 $\alpha$  and the indicated target genes in hepatocytes in a time-course experiment following TGF $\beta$  treatment. qPCR data, obtained in triplicate and normalized to the ribosomal RNA 18S, are expressed as fold change in gene expression in TGF $\beta$ -treated versus untreated cells (arbitrary value = 1) (\* $p$  < 0.06). The mean  $\pm$  SEM of three independent experiments is shown. The observed differences in gene expression are statistically significant (\* $p$  < 0.05; \*\* $p$  < 0.01; \*\*\* $p$  < 0.001). **(B)** Western blot analysis for HNF1 $\alpha$  in protein extracts from one of the experiments shown in **(A)**.  $\alpha$ -Glyceraldehyde 3-phosphate dehydrogenase was used as loading control. Densitometric analysis of WB data from three independent experiments is shown.

*Albumin* and *Transferrin* (TTR) (at 3 h of treatment). Notably, the downregulation of the target genes occurred when the reduction in the HNF1 $\alpha$  protein was not yet observable (Figure 1B), thus suggesting a functional inactivation of HNF1 $\alpha$  protein by TGF $\beta$  that precedes the effects of the transcriptional downregulation of its own gene.

To formally prove the posttranslational control of HNF1 $\alpha$  by TGF $\beta$ , we constitutively expressed an exogenous HNF1 $\alpha$  in a not fully differentiated hepatocyte cell line and in Ras-transformed hepatocytes (Cuzzolino et al., 2013).

HNF1 $\alpha$  target gene expression (*Albumin* and *TTR*), markedly induced by the exogenous HNF1 $\alpha$ , was significantly reduced by TGF $\beta$  in both cell lines (Figure 2A and Supplementary Figure S1A), while the ectopic HNF1 $\alpha$  protein level (Supplementary Figure S1B) and its nuclear localization (Figure 2B) were not modified. Furthermore, exogenous HNF1 $\alpha$  was not able to hamper the TGF $\beta$ -induced EMT,

as indicated by the transcriptional upregulation of *Snail* (Figure 2C), the downregulation and delocalization of E-cadherin (Figures 2C, D), and by the morphological transition (Figure 2B).

These data unveiled the dominance of TGF $\beta$  on HNF1 $\alpha$  overexpression, both in the regulation of target gene expression and in the induction of EMT, thus confirming its ability to negatively control HNF1 $\alpha$  at posttranscriptional level.

## TGF $\beta$ Does Not Affect DNA Binding Capacity of HNF1 $\alpha$

In an attempt to investigate the mechanisms involved in TGF $\beta$ -dependent HNF1 $\alpha$  inactivation, HNF1 $\alpha$  binding to regulatory sequences of its target genes *HNF4 $\alpha$*  and *Albumin* has been evaluated by a chromatin immunoprecipitation (ChIP) assay, at early time of TGF $\beta$  treatment. As shown in Figure 3A, the HNF1 $\alpha$  DNA binding activity was not affected by TGF $\beta$  even

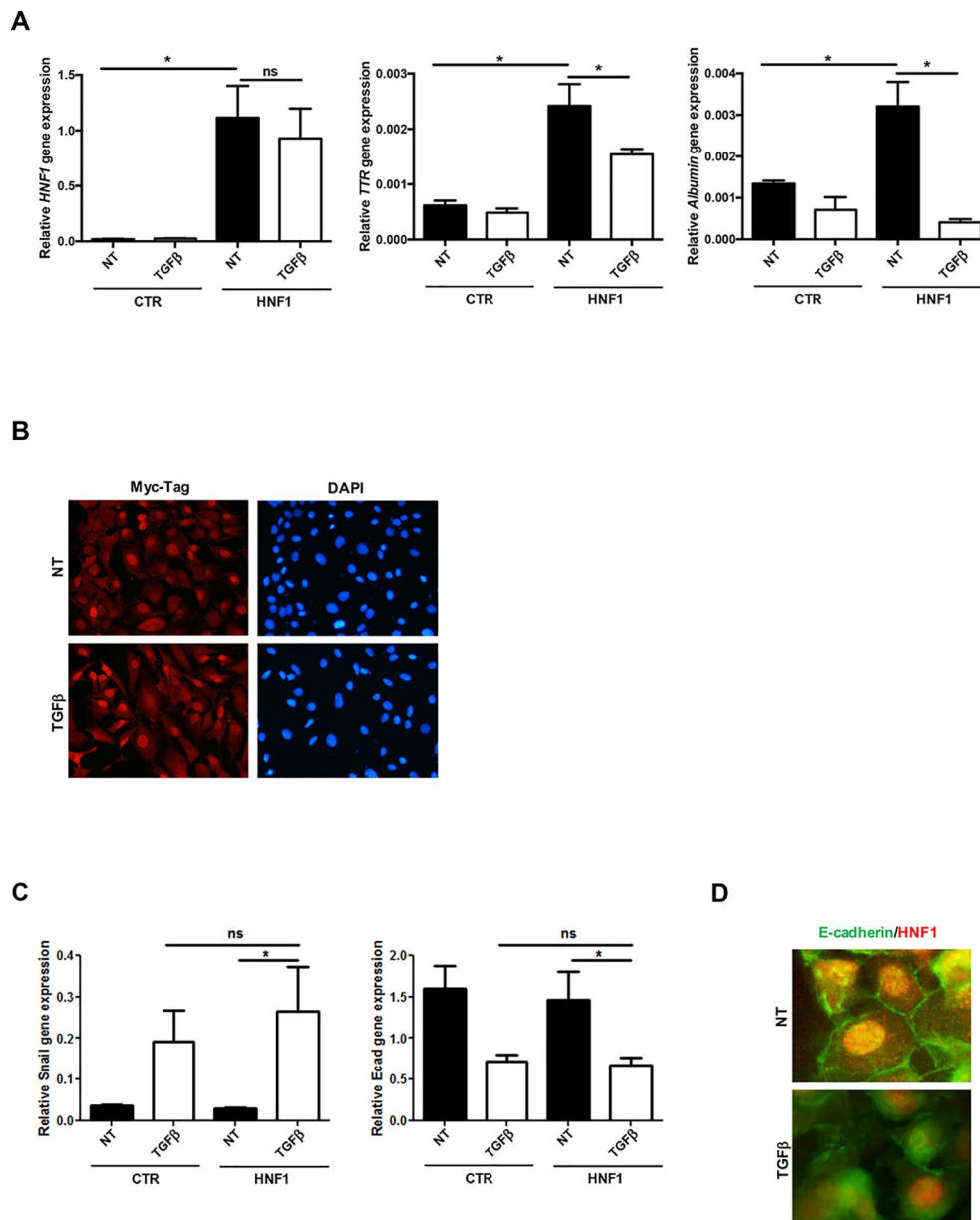


**FIGURE 2 |** TGF $\beta$  overrides HNF1 $\alpha$  constitutive expression. **(A)** Analysis of constitutively expressed HNF1 $\alpha$  activity following TGF $\beta$  treatment. RT-qPCR analysis for the indicated genes in hepatocytes, transiently transfected with pLCPX-HNF1 $\alpha$ <sup>Myc</sup> (HNF1) or the empty vector (CTR), treated with 4 ng/ml TGF $\beta$  for 24 h or left untreated (NT). qPCR data, obtained in triplicate and normalized to the housekeeping gene RPL34, are expressed as relative gene expression. The mean  $\pm$  SEM of three independent experiments is shown. Statistically significant differences are reported (\* $p$  < 0.05; ns, not significant). **(B)** Immunofluorescence analysis of hepatocytes transfected and treated as in **(A)**. Cells were stained with anti-MycTag antibody (red) and 4',6-diamidino-2-phenylindole (nuclei, blue). Magnification 10 $\times$ . **(C)** Analysis of EMT-related gene expression by RT-qPCR in hepatocytes, transiently transfected with pLCPX-HNF1 $\alpha$ <sup>Myc</sup> (HNF1) or the empty vector (CTR), treated with TGF $\beta$  for 24 h or left untreated (NT). qPCR data, obtained in triplicate and normalized to the housekeeping gene RPL34, are expressed as relative gene expression. The mean  $\pm$  SEM of three independent experiments is shown. Statistically significant differences are reported (\* $p$  < 0.05; ns, not significant). **(D)** Immunofluorescence analysis of hepatocytes transfected and treated as in **(C)**. Cells were stained with anti-E-cadherin (green) or anti-HNF1 $\alpha$  antibody (red). Magnification 20 $\times$ .

after 5 h of treatment. Later time points were not analyzed since endogenous HNF1 $\alpha$  was transcriptionally downregulated upon TGF $\beta$  treatment, as reported above.

However, and coherently with transcriptional data, the chromatin regions around the HNF1 $\alpha$  binding site showed, at early time points after TGF $\beta$  treatment, a significant

downregulation of the histone H3 acetylation, one of the main transcriptional activating chromatin modifications (**Figure 3B**).

Further evidence of the maintenance of HNF1 $\alpha$  binding capacity in TGF $\beta$ -treated cells have been obtained by EMSA experiments. As shown in **Figure 3C**, the HNF1 $\alpha$ /DNA complexes

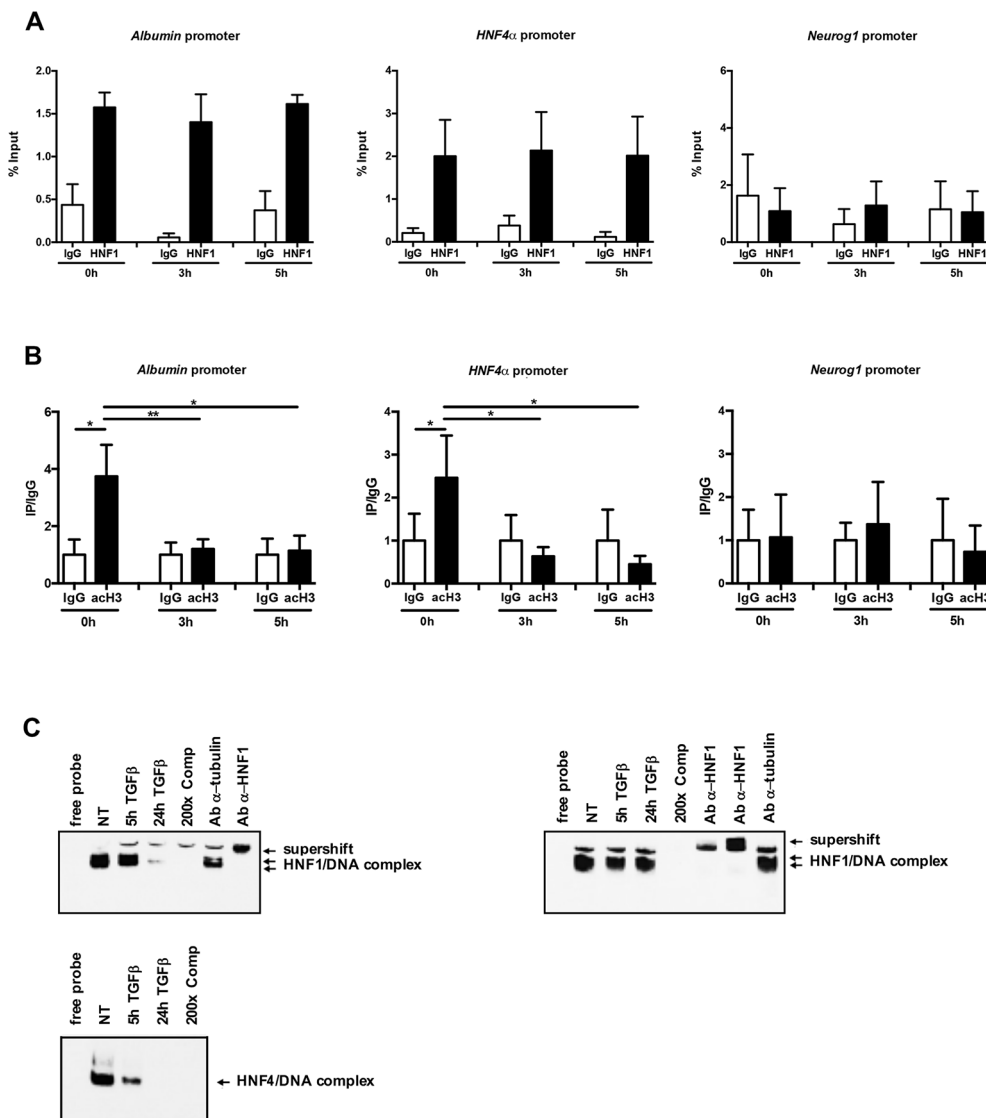


**FIGURE 3 | (A)** HNF1 $\alpha$  DNA binding activity after TGF $\beta$  treatment. qPCR analysis of chromatin immunoprecipitated from hepatocytes with anti-HNF1 $\alpha$  antibody was performed. HNF1 $\alpha$  consensus regions embedded in the indicated HNF1 $\alpha$  target gene promoters were analyzed. A HNF1 $\alpha$  nonbound region of *Neurogenin 1* promoter was utilized as negative control. Data are normalized to total chromatin input and background (control immunoprecipitation with IgG) and expressed as % input. Mean  $\pm$  SEM of qPCR data obtained in triplicate from three independent experiments are reported. **(B)** Analysis of acetyl histone H3 by chromatin immunoprecipitation assay in untreated and TGF $\beta$ -treated hepatocytes. qPCR analysis of chromatin immunoprecipitated from hepatocytes with anti-acetyl H3 antibody was performed. HNF1 $\alpha$  consensus regions embedded in the indicated HNF1 $\alpha$  target gene promoters were analyzed. A HNF1 $\alpha$  nonbound region of *Neurogenin 1* promoter was utilized as negative control. Data are normalized to total chromatin input and background (control immunoprecipitation with IgG) and expressed as (Ip/IgG) % input. The mean  $\pm$  SEM of qPCR data obtained in triplicate from five independent experiments are reported. \* $p < 0.05$ , \*\* $p < 0.01$ . **(C)** Electrophoretic mobility shift assay (EMSA) assays. Nuclear extracts from untreated (NT) or TGF $\beta$ -treated (for 5 or 24 h) parental (left, upper panel) or HNF1 $\alpha$ -overexpressing hepatocytes (right, upper panel) were analyzed for the binding to HNF1 $\alpha$  consensus site within the murine HNF4 $\alpha$  promoter. The presence of the HNF1 $\alpha$  protein in the protein/DNA complexes was revealed by the band supershift obtained with the addition of two different anti-HNF1 $\alpha$  antibodies. A 200-fold excess of unlabeled oligonucleotide and the antitubulin antibody were added to the untreated extracts to test the binding specificity. As control, HNF4 $\alpha$  DNA binding activity to its consensus site within the ApoC3 promoter was analyzed by EMSA in the same extracts (lower panel).

were observed and maintained until 5 h of TGF $\beta$  treatment (when the endogenous protein is still expressed, as shown in **Figure 1B**) in untreated parental hepatocytes and until 24 h of treatment in hepatocytes constitutively expressing HNF1 $\alpha$ , thus confirming that the mechanism involved in the HNF1 $\alpha$  inactivation does not impact on its DNA binding ability. On the contrary, and as

expected, in the same extracts, the binding of endogenous HNF4 $\alpha$  on its own consensus site within the promoter of *ApoC3* gene, was lost at early time points (5 h) of TGF $\beta$  treatment (**Figure 3C**, lower panel).

Overall, these data showed that TGF $\beta$ -induced functional inactivation of HNF1 $\alpha$  does not depend on the loss of its DNA



binding, but rather to the impairment of its ability to drive transcription activating chromatin modifications.

## TGF $\beta$ Induces HNF1 $\alpha$ Functional Inactivation Interfering With the Recruitment of CBP/p300 Acetyltransferases

The correlation between the TGF $\beta$ -induced HNF1 $\alpha$  functional inactivation and the loss of histone acetylation at its specific binding sites prompted us to investigate on the possible interference of TGF $\beta$  with the recruitment of histone acetyltransferase on the HNF1 $\alpha$  target gene promoters. It has been previously shown that HNF1 $\alpha$  interacts with the histone acetyltransferases CBP/p300 on target gene promoters (Ban et al., 2002; Dohda et al., 2004) and that the HNF1 $\alpha$ -dependent nucleosome hyperacetylation is required for the activation of tissue-specific target genes (Parrizas et al., 2001). Thus, we analyzed by ChIP the effects of the TGF $\beta$  treatment on the CBP/p300 occupancy of HNF1 $\alpha$  binding sites embedded in *Albumin* and *HNF4 $\alpha$*  gene promoters. Our results demonstrated the presence of CBP/p300 in the untreated sample and, interestingly, the early displacement of these proteins upon TGF $\beta$  treatment (Figure 4A).

To investigate on the mechanism involved in the lack of histone acetyltransferase recruitment on DNA, the physical interaction between CBP/p300 and HNF1 $\alpha$  has been evaluated in a coimmunoprecipitation assay, in the absence or in the presence of TGF $\beta$  (at 5 h of treatment). As shown in Figure 4B, the antibody specifically recognizing HNF1 $\alpha$  was able to immunoprecipitate CBP/p300 acetyltransferase in untreated hepatocytes, while the TGF $\beta$  treatment early reduces this protein–protein interaction. Notably, the total amount of CBP/p300 was not affected by TGF $\beta$  treatment.

Overall, these findings indicate that the loss of physical interaction between CBP/p300 and HNF1 $\alpha$ , with consequent displacement of the acetyl-transferase activity from the regulatory regions of HNF1 $\alpha$  target genes, represents the first step of TGF $\beta$ -induced HNF1 $\alpha$  inactivation, contributing to the onset of EMT in hepatocytes.

## TGF $\beta$ Induces PTMs of HNF1 $\alpha$ Protein

Our previous report unveiled that TGF $\beta$  induces a modification of HNF4 $\alpha$  phosphorylation profile responsible for protein functional inactivation (Cozzolino et al., 2013). Thus, in the attempt to further investigate on the mechanism responsible for the reduced interaction between HNF1 $\alpha$  and CBP/p300, we analyzed the effect of TGF $\beta$  on HNF1 $\alpha$  PTM profile. To this aim, we performed a two-dimensional gel electrophoresis with nuclear extracts from untreated and TGF $\beta$ -treated hepatocytes (3 h), ectopically expressing HNF1 $\alpha^{\text{Myc}}$ , followed by Western blot with a Myc-Tag-specific antibody. As shown in Figure 4C, TGF $\beta$  strongly affects the PTM pattern on HNF1 $\alpha$  protein. In particular, new specific “spot trains,” compatible with multiple phosphorylation/dephosphorylation events, and probably

revealing intermediate isoforms, were observed. Some of these modifications might account for the observed altered interaction of HNF1 $\alpha$  with CBP/p300, even if we cannot exclude the presence of additional PTMs nor the involvement of additional mechanisms (e.g., modulation of cofactors induced by TGF $\beta$ ) that can affect protein complex formation.

## DISCUSSION

The major contribution of the present work has been to unveil a novel mechanism by which TGF $\beta$  early affects the trans-activating function of the MET master gene HNF1 $\alpha$  in triggering EMT process in hepatocytes.

The pleiotropic TGF $\beta$  cytokine has emerged as a pivotal player in hepatocarcinogenesis, taking part in the interplay between microenvironment and liver cells from initial liver injury and inflammation through fibro/cirrhosis to tumor onset, growth, and metastasization (Amicone and Marchetti, 2018). In particular, at late stage of hepatocarcinogenesis, the unbalanced level of the cytokine in the tumor niche can drive transformed hepatocytes towards an EMT and, ultimately, to the acquisition of migratory and invasive properties (Fabregat et al., 2016). Accordingly, in HCC patients, it has been observed that the constitutive activation of TGF $\beta$  signaling contributes to tumor progression and is associated with a poor prognosis (Lee et al., 2012).

One of the key events during the progression of hepatocellular carcinoma is the loss of expression of master genes of epithelial/hepatocyte differentiation, such as *HNF4 $\alpha$*  and *HNF1 $\alpha$* , that play a pivotal role in the restraint of inflammation, fibrosis, and EMT (Yue et al., 2010; Hatzia Apostolou et al., 2011; Pelletier et al., 2011; Santangelo et al., 2011; Qian et al., 2015).

Our previous data demonstrated the ability of TGF $\beta$  signaling to downregulate *HNF4 $\alpha$*  and *HNF1 $\alpha$*  gene expression through the Snail-mediated transcriptional repression and, even before the transcriptional control, to affect the HNF4 $\alpha$  activity by inhibiting its DNA binding capacity (Cozzolino et al., 2013). Results of this work demonstrated that TGF $\beta$  is able to early inactivate also HNF1 $\alpha$ , acting at posttranslational level.

These observations suggest that the use of HNF1 $\alpha$ , elsewhere proposed as therapeutic tool in the control of liver fibrosis and tumor development, could be ineffective in an *in vivo* TGF $\beta$ -containing microenvironment. On the other hand, the knowledge of the molecular basis of the TGF $\beta$ -induced HNF1 $\alpha$  inactivation results is necessary to design new therapeutic approaches based on the use of molecules resistant to the inactivating effect of the cytokine.

Here, we demonstrated that (i) the functional inactivation of HNF1 $\alpha$  protein by TGF $\beta$  precedes the effects of the transcriptional downregulation of its gene, (ii) TGF $\beta$  does not interfere with the HNF1 $\alpha$  DNA-binding capability or its subcellular localization but induces a local reduction of chromatin acetylation at the HNF1 $\alpha$  binding sites within target gene promoters, and (iii) TGF $\beta$  interferes with the recruitment of CBP/p300 acetyltransferases by HNF1 $\alpha$  on target gene promoters, which could be due to a change of PTMs on HNF1 $\alpha$  protein.

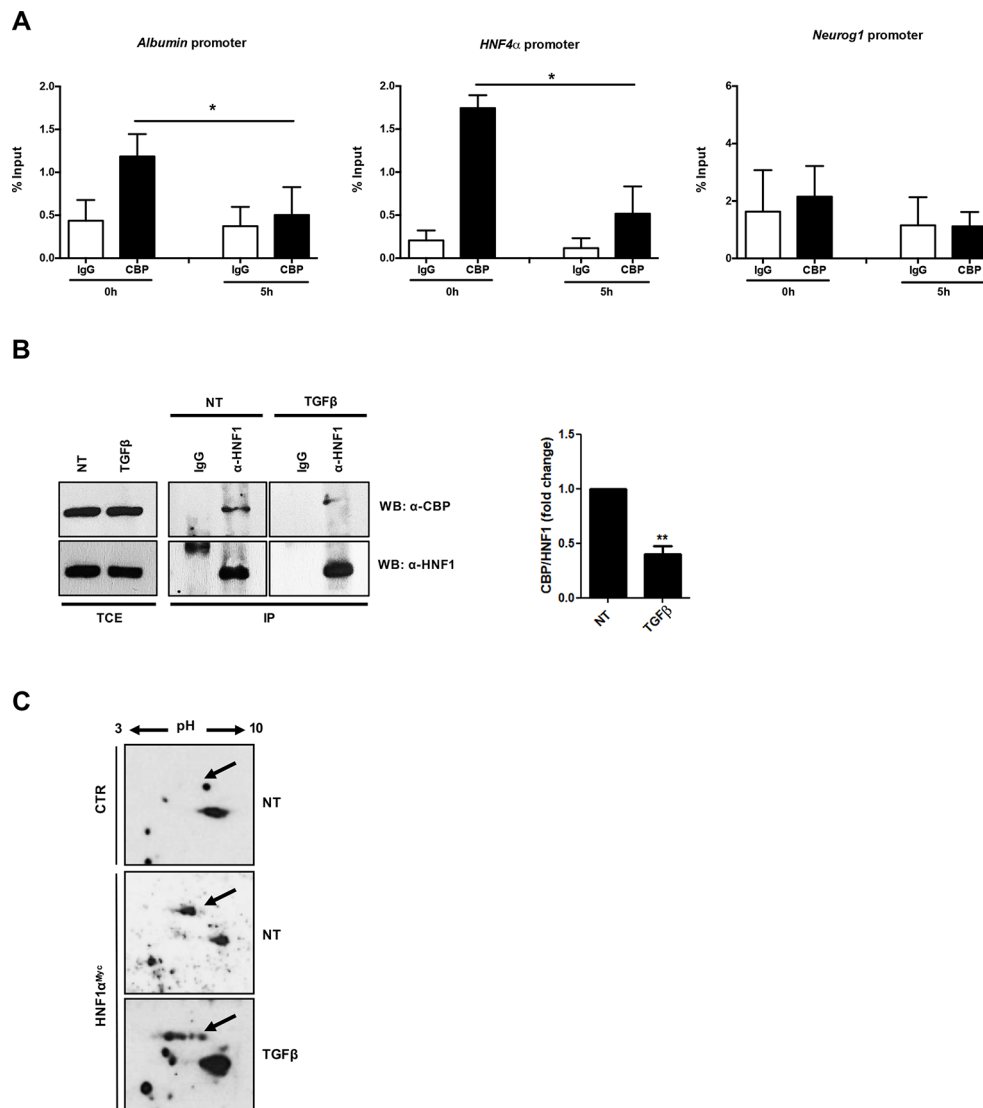


**FIGURE 4 | (A)** Analysis of CBP/p300 DNA binding activity after TGF $\beta$  treatment. qPCR analysis of chromatin immunoprecipitated with anti-CBP/p300 antibody from hepatocytes untreated or treated with TGF $\beta$  (for 5 h) was performed. HNF1 $\alpha$  consensus regions embedded in the indicated target gene promoters were analyzed. A HNF1 $\alpha$  nonbound region of *Neurogenin 1* promoter was utilized as negative control. Data are normalized to total chromatin input and background (control immunoprecipitation with IgG) and expressed as % input. Mean  $\pm$  SEM of qPCR data obtained in triplicate from three independent experiments are reported. **(B)** *In vivo* coimmunoprecipitation of HNF1 $\alpha$  and CBP/p300 in hepatocytes untreated or treated with TGF $\beta$  (for 5 h). Cells were lysed, immunoprecipitated with anti-HNF1 $\alpha$  antibody, and then analyzed by Western blotting with the indicated antibodies. As control, the immunoprecipitation with normal goat IgG was performed. TCE, total cell extracts. Densitometric analysis of WB data from three independent experiments is shown. **(C)** Analysis of HNF1 $\alpha$  protein PTMs following TGF $\beta$  treatment. Nuclear extracts from control hepatocytes (upper panel) and HNF1 $\alpha$ <sup>Myc</sup>-overexpressing hepatocytes treated for 3 h with TGF $\beta$  (lower panel) or left untreated (middle panel). Samples were separated by two-dimensional gel electrophoresis followed by Western blotting with anti-Myc-Tag antibody. HNF1 $\alpha$ -specific spots are indicated by the arrow. The appearance of multiple spots in TGF $\beta$ -treated hepatocytes can be observed. \*\*p < 0.05, \*\*\*p < 0.01.

To accomplish its functions on specific targets, HNF1 $\alpha$  often cooperates with coactivators or corepressor, including CBP/p300 acetyltransferases that play an important role in positively regulating transcription of hepatocyte-specific genes.

In general, p300 and CBP seem to act as transcriptional coactivators by bridging the activators to the basal transcriptional machinery and, through their histone acetyltransferase (HAT) activity, by modifying chromatin

structure to a locally open and transcriptionally active configuration (Chan and La Thangue, 2001).

HNF1 $\alpha$ /CBP and HNF1 $\alpha$ /p300 physical interactions have been previously reported (Soutoglou et al., 2000; Ban et al., 2002; Dohda et al., 2004). Furthermore, both CBP and p300 were found to interact with HNF1 $\alpha$  on the Albumin promoter and to cooperatively enhance its expression in primary hepatocytes (Dohda et al., 2004). The ability of HNF1 $\alpha$  to direct nucleosome hyper-acetylation to target genes is

fundamental for its transcriptional activity. A study carried out with *hnf1 $\alpha$* <sup>-/-</sup> mice models demonstrated that the organ-specific induction of different targets is strongly dependent on nucleosome acetylation (Parrizas et al., 2001). Our results confirmed the pivotal role of CBP/p300 as transcriptional coactivator of HNF1 $\alpha$  and indicated the impairment of the interaction between the two proteins as an effective and early mechanism utilized by TGF $\beta$  to neutralize the HNF1 $\alpha$  activity in the first phase of EMT process.

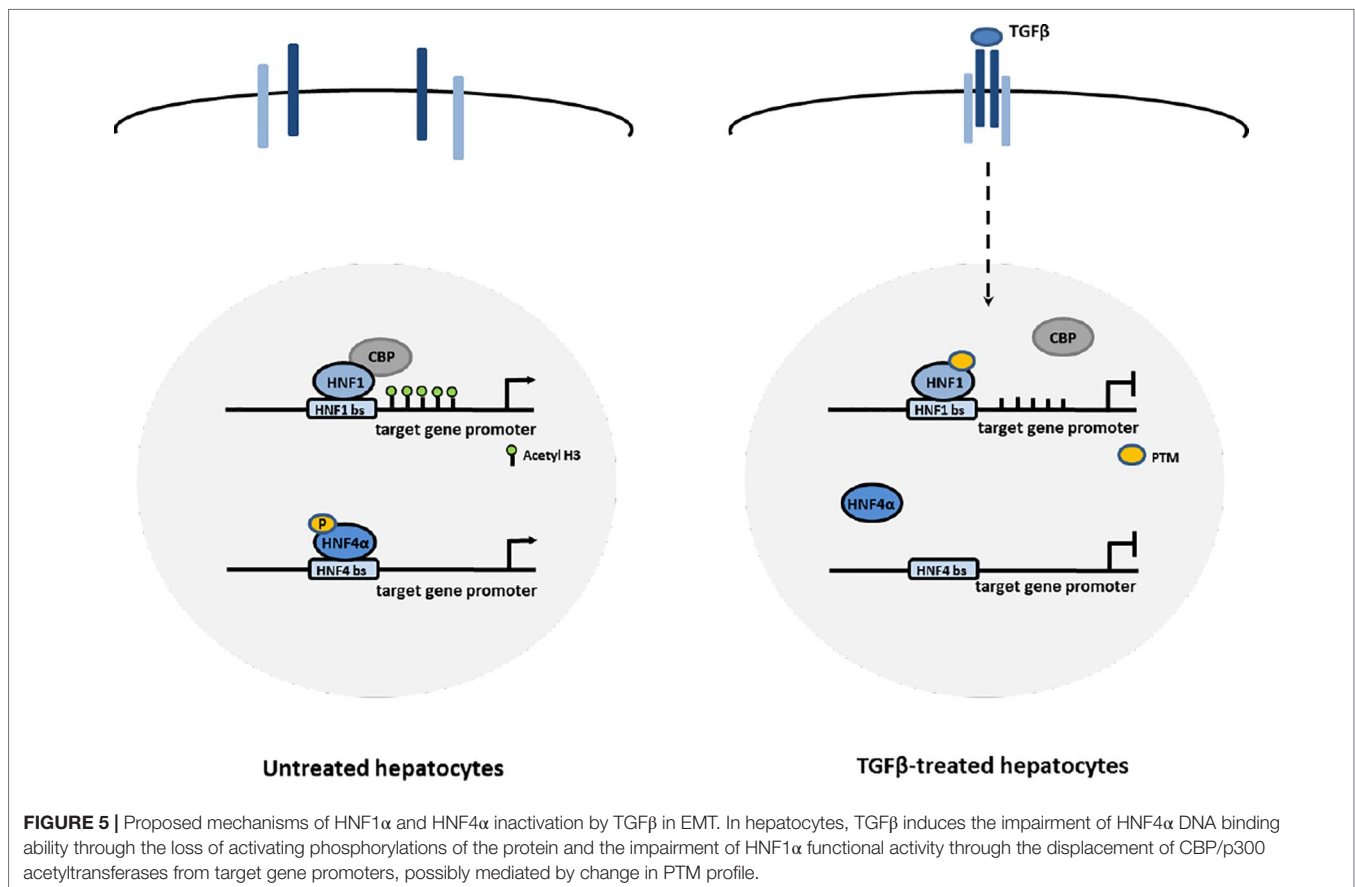
It has been described for some transcriptional factors known to recruit CBP and p300 on target genes the role of specific PTMs in mediating the physical protein-protein interaction (Chrivia et al., 1993; Wang et al., 2013). Previous proteomic studies on liver cells highlighted the presence of PTMs on HNF1 $\alpha$  protein. However, at present, there are only a few studies showing the role of these PTMs on its functional activity (Lim et al., 2002; Zhao et al., 2014; Kaci et al., 2018). Data obtained by 2-DE gel electrophoresis analysis suggest that the regulation of HNF1 $\alpha$ -CBP/p300 interaction by TGF $\beta$  could include HNF1 $\alpha$  posttranslational modifications. Further proteomic analysis will allow the identification of residues involved and their functional significance. We cannot exclude, in fact, that additional mechanisms could contribute to the impairment of HNF1 $\alpha$  activity by TGF $\beta$ .

The early neutralization of HNF1 $\alpha$  activity has great relevance in the induction of EMT process in hepatocyte.

In differentiated hepatocyte, in fact, it has been shown that HNF1 $\alpha$ , as well as HNF4 $\alpha$ , stably inhibits the expression of the EMT master gene *Snail* and, consequently, the mesenchymal program and that this control is mandatory for the maintenance of the differentiated phenotype (Santangelo et al., 2011; Battistelli et al., 2018). The late events involved in the TGF $\beta$ -dependent downregulation of both HNF1 $\alpha$  and HNF4 $\alpha$  have been previously characterized. Our previous works, indeed, described their transcriptional downregulation by TGF $\beta$  through the recruitment of *Snail* to HNF1 $\alpha$  and HNF4 $\alpha$  promoters with subsequent chromatin remodeling and transcriptional repression (Santangelo et al., 2011; Battistelli et al., 2017).

Thus, the early functional inhibition of HNF1 $\alpha$  and HNF4 $\alpha$  by TGF $\beta$  (even if through different mechanisms, as shown in **Figure 5**) could represent the first mechanism through which the expression of *Snail* and the mesenchymal program are released, and the EMT process is triggered.

In conclusion, the data presented here shed light on an early mechanism inhibiting HNF1 $\alpha$  function during the first step of EMT process in hepatocytes and, consequently, unveils a potential limitation of the use of HNF1 $\alpha$  as therapeutic tool for anti-EMT and antifibrosis molecular therapies in an *in vivo* TGF $\beta$ -containing microenvironment. Further characterization of the change in the HNF1 $\alpha$  PTM profile, induced by TGF $\beta$ , could allow the design of new therapeutic



approaches (i.e., mutant molecules resistant to the induction of these modifications) aimed to override the inactivating effect of the cytokine.

## DATA AVAILABILITY

The raw data supporting the conclusions of this manuscript will be made available by the authors, without undue reservation, to any qualified researcher.

## AUTHOR CONTRIBUTIONS

FB, MT, and AM contributed to the design of the research plan and to the interpretation of results. FB, CB, VN, CM, and AZ performed the experiments. CB and VN contributed to the analysis and representation of data. AM and LA wrote the

manuscript. MT and RS contributed to the critical revision of the manuscript. AM, LA, and MT revised the final draft of the manuscript. AM coordinated the experimental work. Financial support: MT, LA, AM.

## FUNDING

This study was supported by Sapienza University of Rome (Progetti di Ateneo: C26A15CL7B and RM118143646188C and by Associazione Italiana per la Ricerca sul Cancro (AIRC, IG 18843).

## SUPPLEMENTARY MATERIAL

The Supplementary Material for this article can be found online at: <https://www.frontiersin.org/articles/10.3389/fphar.2019.00942/full#supplementary-material>

## REFERENCES

- Amicone, L., and Marchetti, A. (2018). Microenvironment and tumor cells: two targets for new molecular therapies of hepatocellular carcinoma. *Transl. Gastroenterol. Hepatol.* 3, 24. doi: 10.21037/tgh.2018.04.05
- Amicone, L., Spagnoli, F. M., Spath, G., Giordano, S., Tommasini, C., Bernardini, S., et al. (1997). Transgenic expression in the liver of truncated Met blocks apoptosis and permits immortalization of hepatocytes. *EMBO J.* 16, 495–503. doi: 10.1093/emboj/16.3.495
- Amicone, L., Terradillos, O., Calvo, L., Costabile, B., Cicchini, C., Della Rocca, C., et al. (2002). Synergy between truncated c-Met (cyto-Met) and c-Myc in liver oncogenesis: importance of TGF-beta signalling in the control of liver homeostasis and transformation. *Oncogene* 21, 1335–1345. doi: 10.1038/sj.onc.1205199
- Ban, N., Yamada, Y., Someya, Y., Miyawaki, K., Ihara, Y., Hosokawa, M., et al. (2002). Hepatocyte nuclear factor-1alpha recruits the transcriptional co-activator p300 on the GLUT2 gene promoter. *Diabetes* 51, 1409–1418. doi: 10.2337/diabetes.51.5.1409
- Battistelli, C., Cicchini, C., Santangelo, L., Tramontano, A., Grassi, L., Gonzalez, F. J., et al. (2017). The Snail repressor recruits EZH2 to specific genomic sites through the enrollment of the lncRNA HOTAIR in epithelial-to-mesenchymal transition. *Oncogene* 36, 942–955. doi: 10.1038/ncr.2016.260
- Battistelli, C., Sabarese, G., Santangelo, L., Montaldo, C., Gonzalez, F. J., Tripodi, M., et al. (2018). The lncRNA HOTAIR transcription is controlled by HNF4alpha-induced chromatin topology modulation. *Cell. Death Differ.* 26(5):890–901. doi: 10.1038/s41418-018-0170-z
- Bellovino, D., Morimoto, T., Pisaniello, A., and Gaetani, S. (1998). *In vitro* and *in vivo* studies on transthyretin oligomerization. *Exp. Cell. Res.* 243, 101–112. doi: 10.1006/excr.1998.4137
- Chan, H. M., and La Thangue, N. B. (2001). p300/CBP proteins: HATs for transcriptional bridges and scaffolds. *J. Cell. Sci.* 114, 2363–2373.
- Chrivia, J. C., Kwok, R. P., Lamb, N., Hagiwara, M., Montminy, M. R., and Goodman, R. H. (1993). Phosphorylated CREB binds specifically to the nuclear protein CBP. *Nature* 365, 855–859. doi: 10.1038/365855a0
- Cicchini, C., Filippini, D., Coen, S., Marchetti, A., Cavallari, C., Laudadio, I., et al. (2006). Snail controls differentiation of hepatocytes by repressing HNF4alpha expression. *J. Cell. Physiol.* 209, 230–238. doi: 10.1002/jcp.20730
- Cozzolino, A. M., Alonzi, T., Santangelo, L., Mancone, C., Conti, B., Steindler, C., et al. (2013). TGFbeta overrides HNF4alpha tumor suppressing activity through GSK3beta inactivation: implication for hepatocellular carcinoma gene therapy. *J. Hepatol.* 58, 65–72. doi: 10.1016/j.jhep.2012.08.023
- Cozzolino, A. M., Noce, V., Battistelli, C., Marchetti, A., Grassi, G., Cicchini, C., et al. (2016). Modulating the substrate stiffness to manipulate differentiation of resident liver stem cells and to improve the differentiation state of hepatocytes. *Stem. Cells Int.* 2016, 5481493. doi: 10.1155/2016/5481493
- De Santis Puzzon, M., Cozzolino, A. M., Grassi, G., Bisceglia, F., Strippoli, R., Guarguaglini, G., et al. (2016). TGFbeta induces binucleation/polyploidization in hepatocytes through a Src-dependent cytokinesis failure. *PLoS One* 11, e0167158. doi: 10.1371/journal.pone.0167158
- Dohda, T., Kaneoka, H., Inayoshi, Y., Kamihira, M., Miyake, K., and Iijima, S. (2004). Transcriptional coactivators CBP and p300 cooperatively enhance HNF-1alpha-mediated expression of the albumin gene in hepatocytes. *J. Biochem.* 136, 313–319. doi: 10.1093/jb/mvh123
- Fabregat, I., Moreno-Caceres, J., Sanchez, A., Dooley, S., Dewidar, B., Giannelli, G., et al. (2016). TGF-beta signalling and liver disease. *FEBS J.* 283, 2219–2232. doi: 10.1111/febs.13665
- Grassi, G., DiCaprio, G., Santangelo, L., Fimia, G. M., Cozzolino, A. M., Komatsu, M., et al. (2015). Autophagy regulates hepatocyte identity and epithelial-to-mesenchymal and mesenchymal-to-epithelial transitions promoting Snail degradation. *Cell. Death Dis.* 6, e1880. doi: 10.1038/cddis.2015.249
- Hatziaepostolou, M., Polyarchou, C., Aggelidou, E., Drakaki, A., Poultides, G. A., Jaeger, S. A., et al. (2011). An HNF4alpha-miRNA inflammatory feedback circuit regulates hepatocellular oncogenesis. *Cell* 147, 1233–1247. doi: 10.1016/j.cell.2011.10.043
- Kaci, A., Keindl, M., Solheim, M. H., Njolstad, P. R., Bjorkhaug, L., and Aukrust, I. (2018). The E3 SUMO ligase PIASgamma is a novel interaction partner regulating the activity of diabetes associated hepatocyte nuclear factor-1alpha. *Sci. Rep.* 8, 12780. doi: 10.1038/s41598-018-29448-w
- Lazarevich, N. L., Cheremnova, O. A., Varga, E. V., Ovchinnikov, D. A., Kudrjavitseva, E. I., Morozova, O. V., et al. (2004). Progression of HCC in mice is associated with a downregulation in the expression of hepatocyte nuclear factors. *Hepatology* 39, 1038–1047. doi: 10.1002/hep.20155
- Lazarevich, N. L., Shavochkina, D. A., Fleishman, D. I., Kustova, I. F., Morozova, O. V., Chuchuev, E. S., et al. (2010). Deregulation of hepatocyte nuclear factor 4 (HNF4) as a marker of epithelial tumors progression. *Exp. Oncol.* 32, 167–171.
- Lee, D., Chung, Y. H., Kim, J. A., Lee, Y. S., Lee, D., Jang, M. K., et al. (2012). Transforming growth factor beta 1 overexpression is closely related to invasiveness of hepatocellular carcinoma. *Oncology* 82, 11–18. doi: 10.1159/000335605
- Lim, S., Jin, K., and Friedman, E. (2002). Mirk protein kinase is activated by MKK3 and functions as a transcriptional activator of HNF1alpha. *J. Biol. Chem.* 277, 25040–25046. doi: 10.1074/jbc.M203257200
- Marchetti, A., Bisceglia, F., Cozzolino, A. M., and Tripodi, M. (2015). New tools for molecular therapy of hepatocellular carcinoma. *Diseases* 3, 325–340. doi: 10.3390/diseases3040325



- Marchetti, A., Cicchini, C., Santangelo, L., Cozzolino, A. M., Costa, V., Tripodi, M., et al. (2013). Signaling networks controlling HCC onset and progression: influence of microenvironment and implications for cancer gene therapy. *J. Cancer Ther.* 4, 353–358. doi: 10.4236/jct.2013.42A042
- Ni, Q., Ding, K., Wang, K. Q., He, J., Yin, C., Shi, J., et al. (2017). Deletion of HNF1 $\alpha$  in hepatocytes results in fatty liver-related hepatocellular carcinoma in mice. *FEBS Lett.* 591, 1947–1957. doi: 10.1002/1873-3468.12689
- Ning, B. F., Ding, J., Yin, C., Zhong, W., Wu, K., Zeng, X., et al. (2010). Hepatocyte nuclear factor 4  $\alpha$  suppresses the development of hepatocellular carcinoma. *Cancer Res.* 70, 7640–7651. doi: 10.1158/0008-5472.CAN-10-0824
- Noce, V., Battistelli, C., Cozzolino, A. M., Consalvi, V., Cicchini, C., Strippoli, R., et al. (in press). YAP integrates the regulatory Snail/HNF4 $\alpha$  circuitry controlling epithelial/hepatocyte differentiation. *Cell. Death Dis.*
- Parrizas, M., Maestro, M. A., Boj, S. F., Paniagua, A., Casamitjana, R., Gomis, R., et al. (2001). Hepatic nuclear factor 1- $\alpha$  directs nucleosomal hyperacetylation to its tissue-specific transcriptional targets. *Mol. Cell. Biol.* 21, 3234–3243. doi: 10.1128/MCB.21.9.3234-3243.2001
- Pelletier, L., Rebouissou, S., Vignjevic, D., Bioulac-Sage, P., and Zucman-Rossi, J. (2011). HNF1 $\alpha$  inhibition triggers epithelial–mesenchymal transition in human liver cancer cell lines. *BMC Cancer* 11, 427. doi: 10.1186/1471-2407-11-427
- Qian, H., Deng, X., Huang, Z. W., Wei, J., Ding, C. H., Feng, R. X., et al. (2015). An HNF1 $\alpha$ -regulated feedback circuit modulates hepatic fibrogenesis via the crosstalk between hepatocytes and hepatic stellate cells. *Cell. Res.* 25, 930–945. doi: 10.1038/cr.2015.84
- Santangelo, L., Marchetti, A., Cicchini, C., Conigliaro, A., Conti, B., Mancone, C., et al. (2011). The stable repression of mesenchymal program is required for hepatocyte identity: a novel role for hepatocyte nuclear factor 4 $\alpha$ . *Hepatology* 53, 2063–2074. doi: 10.1002/hep.24280
- Song, G., Pacher, M., Balakrishnan, A., Yuan, Q., Tsay, H. C., Yang, D., et al. (2016). Direct reprogramming of hepatic myofibroblasts into hepatocytes *in vivo* attenuates liver fibrosis. *Cell. Stem. Cell.* 18, 797–808. doi: 10.1016/j.stem.2016.01.010
- Soutoglou, E., Papafotiou, G., Katrakili, N., and Talianidis, I. (2000). Transcriptional activation by hepatocyte nuclear factor-1 requires synergism between multiple coactivator proteins. *J. Biol. Chem.* 275, 12515–12520. doi: 10.1074/jbc.275.17.12515
- Wang, F., Marshall, C. B., and Ikura, M. (2013). Transcriptional/epigenetic regulator CBP/p300 in tumorigenesis: structural and functional versatility in target recognition. *Cell. Mol. Life Sci.* 70, 3989–4008. doi: 10.1007/s00018-012-1254-4
- Willson, J. S., Godwin, T. D., Wiggins, G. A., Guilford, P. J., and McCall, J. L. (2013). Primary hepatocellular neoplasms in a MODY3 family with a novel HNF1A germline mutation. *J. Hepatol.* 59, 904–907. doi: 10.1016/j.jhep.2013.05.024
- Xu, J., Lamouille, S., and Derynck, R. (2009). TGF- $\beta$ -induced epithelial to mesenchymal transition. *Cell. Res.* 19, 156. doi: 10.1038/cr.2009.5
- Yue, H. Y., Yin, C., Hou, J. L., Zeng, X., Chen, Y. X., Zhong, W., et al. (2010). Hepatocyte nuclear factor 4 $\alpha$  attenuates hepatic fibrosis in rats. *Gut* 59, 236–246. doi: 10.1136/gut.2008.174904
- Zavadil, J., and Bottinger, E. P. (2005). TGF- $\beta$  and epithelial-to-mesenchymal transitions. *Oncogene* 24, 5764–5774. doi: 10.1038/sj.onc.1208927
- Zeng, X., Lin, Y., Yin, C., Zhang, X., Ning, B. F., Zhang, Q., et al. (2011). Recombinant adenovirus carrying the hepatocyte nuclear factor-1 $\alpha$  gene inhibits hepatocellular carcinoma xenograft growth in mice. *Hepatology* 54, 2036–2047. doi: 10.1002/hep.24647
- Zhao, L., Chen, H., Zhan, Y. Q., Li, C. Y., Ge, C. H., Zhang, J. H., et al. (2014). Serine 249 phosphorylation by ATM protein kinase regulates hepatocyte nuclear factor-1 $\alpha$  transactivation. *Biochim. Biophys. Acta* 1839, 604–620. doi: 10.1016/j.bbarm.2014.05.001

**Conflict of Interest Statement:** The authors declare that the research was conducted in the absence of any commercial or financial relationships that could be construed as a potential conflict of interest.

Copyright © 2019 Bisceglia, Battistelli, Noce, Montaldo, Zammataro, Strippoli, Tripodi, Amicone and Marchetti. This is an open-access article distributed under the terms of the Creative Commons Attribution License (CC BY). The use, distribution or reproduction in other forums is permitted, provided the original author(s) and the copyright owner(s) are credited and that the original publication in this journal is cited, in accordance with accepted academic practice. No use, distribution or reproduction is permitted which does not comply with these terms.

# Advantages of publishing in Frontiers



## OPEN ACCESS

Articles are free to read  
for greatest visibility  
and readership



## FAST PUBLICATION

Around 90 days  
from submission  
to decision



## HIGH QUALITY PEER-REVIEW

Rigorous, collaborative,  
and constructive  
peer-review



## TRANSPARENT PEER-REVIEW

Editors and reviewers  
acknowledged by name  
on published articles

## Frontiers

Avenue du Tribunal-Fédéral 34  
1005 Lausanne | Switzerland

**Visit us:** [www.frontiersin.org](http://www.frontiersin.org)

**Contact us:** [info@frontiersin.org](mailto:info@frontiersin.org) | +41 21 510 17 00



## REPRODUCIBILITY OF RESEARCH

Support open data  
and methods to enhance  
research reproducibility



## DIGITAL PUBLISHING

Articles designed  
for optimal readership  
across devices



## FOLLOW US

@frontiersin



## IMPACT METRICS

Advanced article metrics  
track visibility across  
digital media



## EXTENSIVE PROMOTION

Marketing  
and promotion  
of impactful research



## LOOP RESEARCH NETWORK

Our network  
increases your  
article's readership